Glaciers, Ice Sheets, and Sea Level: Effect of a CO2-Induced Climatic Change (1985)

Pages
344

Size
8.5 x 10

ISBN
0309322405

Ad Hoc Committee on the Relationship between Land Ice and Sea Level; Committee on Glaciology; Polar Research Board; Commission on Physical Sciences, Mathematics, and Resources; National Research Council

Retreat of Rhône Glacier, Switzerland

1848

Aquarelle: H. Hogard

1970

Photo: M. Aellen

Glaciers, Ice Sheets, and Sea Level: Effects of a CO_2-Induced Climatic Change

Report of a Workshop
Held in Seattle, Washington, September 13-15, 1984

Ad Hoc Committee on the
Relationship between Land Ice and Sea Level
Committee on Glaciology
Polar Research Board
Commission on Physical Sciences, Mathematics, and Resources
National Research Council

NATIONAL ACADEMY PRESS
Washington, D.C. 1985

NOTICE: The project that is the subject of this report was approved by the Governing Board of the National Research Council, whose members are drawn from the councils of the National Academy of Sciences, the National Academy of Engineering, and the Institute of Medicine. The members of the committee responsible for this report were chosen for their special competences and with regard for appropriate balance.

This report has been reviewed by a group other than the authors according to procedures approved by a Report Review Committee consisting of members of the National Academy of Sciences, the National Academy of Engineering, and the Institute of Medicine.

The National Research Council was established by the National Academy of Sciences in 1916 to associate the broad community of science and technology with the Academy's purposes of furthering knowledge and of advising the federal government. The Council operates in accordance with general policies determined by the Academy under the authority of its congressional charter of 1863, which establishes the Academy as a private, nonprofit, self-governing membership corporation. The Council has become the principal operating agency of both the National Academy of Sciences and the National Academy of Engineering in the conduct of their services to the government, the public, and the scientific and engineering communities. It is administered jointly by both Academies and the Institute of Medicine. The National Academy of Engineering and the Institute of Medicine were established in 1964 and 1970, respectively, under the charter of the National Academy of Sciences.

Support for the conduct of this workshop and the preparation of this report was provided by the CO_2 Research Division of the Department of Energy under grant DE-FG01-84ER-60235.

Copies available in limited quantity from

Polar Research Board
2101 Costitution Avenue, N.W.
Washington, D.C. 20418

Printed in the United States of America

Ad Hoc Committee on the Relationship between Land Ice and Sea Level

Mark F. Meier, U.S. Geological Survey, Chairman
David G. Aubrey, Woods Hole Oceanographic Institution
Charles R. Bentley, University of Wisconsin
Wallace S. Broecker, Columbia University
James E. Hansen, Goddard Institute for Space Studies
W. Richard Peltier, University of Toronto
Richard C. J. Somerville, Scripps Institution of Oceanography

Staff
W. Timothy Hushen, Staff Director, Polar Research Board
Sherburne B. Abbott, Staff Officer
Thomas M. Usselman, Staff Officer

Committee on Glaciology

Mark F. Meier, U.S. Geological Survey, Chairman
Robert L. Brown, Montana State University
Jeff Dozier, University of California
William D. Hibler, U.S. Army Cold Regions Research and Engineering Laboratory
John Kreider, Arctec, Inc.
Ellen Stone Mosley-Thompson, Ohio State University
Thomas Osterkamp, University of Alaska
Charles R. Raymond, University of Washington
Richard C. J. Somerville, Climate Research Group, University of California, San Diego
Robert H. Thomas, NASA Headquarters

Ex-officio
Gary K. C. Clarke, Chairman, AGU Committee on Snow and Ice

Staff
W. Timothy Hushen, Staff Director
Sherburne B. Abbott, Staff Officer

Agency Liaison Representatives
Thomas J. Gross, CO_2 Research Division, Department of Energy
Bruce B. Hanshaw, U.S. Geological Survey
G. Leonard Johnson, Arctic Programs, Office of Naval Research
Ned A. Ostenso, National Oceanic and Atmospheric Administration
Peter E. Wilkniss, Division of Polar Programs, National Science Foundation

Polar Research Board

Charles R. Bentley, University of Wisconsin, Chairman
David Elliot, Ohio State University
W. Lawrence Gates, Oregon State University
Ronald L. Geer, Shell Oil Company
Ben C. Gerwick, Jr., University of California, Berkeley
Richard M. Goody, Harvard University
Arnold L. Gordon, Lamont-Doherty Geological Observatory
Philip L. Johnson, John E. Gray Institute, Lamar University
Arthur H. Lachenbruch, U.S. Geological Survey
Louis J. Lanzerotti, Bell Laboratories
Geoffrey Larminie, British Petroleum Company, Ltd.
Chester M. Pierce, Harvard University
John H. Steele, Woods Hole Oceanographic Institution
Ian Stirling, Canadian Wildlife Service
Cornelius W. Sullivan, University of Southern California
Gunter Weller, University of Alaska

Ex Officio
James H. Zumberge, U.S. Delegate to SCAR
Mark F. Meier, Chairman, Committee on Glaciology
Jerry Brown, Chairman, Committee on Permafrost

Staff
W. Timothy Hushen, Staff Director
Sherburne B. Abbott, Staff Officer

Agency Liaison Representatives
Thomas J. Gross, CO_2 Research Division, Department of Energy
Bruce B. Hanshaw, U.S. Geological Survey
G. Leonard Johnson, Arctic Programs, Office of Naval Research
Ned A. Ostenso, National Oceanic and Atmospheric Administration
Peter E. Wilkniss, Division of Polar Programs, National Science Foundation

Commission of Physical Sciences, Mathematics, and Resources

Herbert Friedman, National Research Council, Chairman
Thomas D. Barrow, Standard Oil Company (Retired)
Elkan R. Blout, Harvard Medical School
Bernard F. Burke, Massachusetts Institute of Technology
George F. Carrier, Harvard University
Herman Chernoff, Massachusetts Institute of Technology
Charles L. Drake, Dartmouth College
Mildred S. Dresselhaus, Massachusetts Institute of Technology
Joseph L. Fisher, Office of the Governor, Commonwealth of Virginia
James C. Fletcher, University of Pittsburgh
William A. Fowler, California Institute of Technology
Gerhart Friedlander, Brookhaven National Laboratory
Edward A. Frieman, Science Applications, Inc.
Edward D. Goldberg, Scripps Institution of Oceanography
Mary L. Good, UOP, Inc.
Thomas F. Malone, Saint Joseph College
Charles J. Mankin, Oklahoma Geological Survey
Walter H. Munk, University of California, San Diego
George E. Pake, Xerox Research Center
Robert E. Sievers, University of Colorado
Howard E. Simmons, Jr., E.I. du Pont de Nemours & Co., Inc.
Isadore M. Singer, Massachusetts Institute of Technology
John D. Spengler, Harvard School of Public Health
Hatten S. Yoder, Jr., Carnegie Institution of Washington

Staff
Raphael G. Kasper, Executive Director
Lawrence E. McCray, Associate Executive Director

Participants in the Workshop on Land Ice and Sea Level

M. F. Meier, U.S. Geological Survey, Workshop Chairman
C. S. Lingle, University of Colorado, Rapporteur
*W. Ambach, University of Innsbruck
D. G. Aubrey, Woods Hole Oceanographic Institution
R. G. Barry, University of Colorado
C. R. Bentley, University of Wisconsin
R. A. Bindschadler, NASA/Goddard Space Flight Center
W. F. Budd, University of Melbourne
R. L. Cameron, National Science Foundation
C. S. M. Doake, British Antarctic Survey
J. L. Fastook, University of Maine
T. J. Gross, Department of Energy
W. Haeberli, VAW/AHG, ETH-Zurich
J. E. Hansen, NASA/Goddard Institute for Space Studies
W. T. Hushen, National Research Council
S. S. Jacobs, Lamont-Doherty Geological Observatory
R. M. Koerner, Department of Energy, Mines and Resources
M. Kuhn, University of Innsbruck
E. L. Lewis, Institute of Ocean Sciences
O. Orheim, Norsk Polar Institute
W. R. Peltier, University of Toronto
U. Radok, University of Colorado
C. F. Raymond, University of Washington
N. Reeh, University of Copenhagen
D. Roemmich, University of California, San Diego
M. E. Schlesinger, Oregon State University
*J. H. Swift, University of California, San Diego
R. H. Thomas, NASA Headquarters
T. M. Usselman, National Research Council
R. S. Williams, Jr., U.S. Geological Survey

Local Participants

C. S. Brown
C. L. Driedger
A. J. Fountain
S. M. Hodge
E. G. Josberger
R. M. Krimmel
T. Pfeffer
S. C. Porter
L. A. Rasmussen
J. S. Walder

* Represented by written communication

Preface

The climate of the Earth is perpetually variable and changing. Uncertainties about future climate, compounded by concerns that the accumulation of carbon dioxide in the atmosphere and other by-products of human activities may bring about inadvertent changes of climate in future decades, place a premium on improved understanding and prediction of climate and its effects. It has been postulated that a significant rise of global sea level is expected to result from the melting of land ice and thermal expansion of the upper layer of the ocean due to climatic change by increasing CO_2 and other greenhouse gases in the atmosphere.

The uncertainties regarding how land ice and sea level will respond to a changing climate led the Committee on Glaciology to propose a workshop and subsequent report on the subject. Representatives of the CO_2 Division of the Department of Energy received this suggestion favorably. In addition, the plans for the workshop and report were discussed with the National Research Council's Board on Atmospheric Science and Climate, Marine Board, Board on Ocean Science and Policy, and Geophysics Study Committee.

The Polar Research Board established under its Committee on Glaciology a committee of seven individuals, including representatives of the disciplines of glaciology, geophysics, oceanography, geodesy, and climate modeling, to conduct a study on the relationships between terrestrial ice and sea-level change. The Committee held one meeting and a workshop, to which national and international experts were invited.

The workshop was held September 13-15, 1984, in Seattle, Washington. There were 30 invited participants and 10 local participants who attended and contributed to the workshop. The workshop examined the basic questions of how much water has been exchanged between land ice and ocean during the last century, what is happening now, and, given existing climate-modeling prediction, how much exchange can be expected in the next century. In addition, the evidence for exchange was examined and gaps in that evidence were identified. The report includes the 23 presentations made at the workshop, summarizes the workshop discussion, and presents the Committee's findings and recommendations.

Acknowledgments

The Committee wishes to acknowledge Craig S. Lingle (University of Colorado) for his role as rapporteur in drafting the proceedings of the workshop discussions.

The Committee also acknowledges with gratitude the support provides by the CO_2 Research Division of the Department of Energy, grant DE-FG01-84ER-60235, for the planning and conduct of the workshop.

Contents

1.
Executive Summary

The rising concentration of CO_2 and other greenhouse gases in the atmosphere is likely to produce a warmer climate in the future. One consequence of this might be an ensuing rise in sea level caused by the melting of ice on land and by volume expansion of ocean water. Uncertainties occur in all aspects of the problem of attempting to estimate sea-level rise.

In order to define our current knowledge of how much water is exchanged between land and sea, the Committee on Glaciology of the Polar Research Board convened a Workshop on the Interactions between Land Ice and the Oceans, in Seattle, Washington, September 13-15, 1984. This workshop builds on a workshop held in 1983 on the Environment of West Antarctica: Potential CO_2-Induced Changes. The Department of Energy supported both workshops. The focus of the 1984 Workshop was on defining what is known and what needs to be known about the contribution of ice melt to sea level at the present (defined as the past 100 years) and what that contribution is likely to be in the future (defined as the next 100 years) assuming that the climate will change significantly. Oceanographic, climatologic, geophysical, and glaciologic evidence was examined by invited experts. This report summarizes the consensus of the Workshop, mentions areas of uncertainty, and makes recommendations for research needed to reduce these uncertainties. The body of the report is followed by 23 signed attachments prepared by the invited experts.

The consensus of the Workshop is that sea level is rising, but the rate of rise is uncertain by a factor of 2; wastage of mountain glaciers and small ice caps contributes to this rise; probably very little if any sea-level change is caused by wastage of the Greenland Ice Sheet; and the Antarctic Ice Sheet is most likely growing, taking water out of the sea. The rate of change of mass of the ocean cannot be distinguished from zero. Whether the present rise in sea level can be adequately accounted for by just thermal expansion of ocean water is an open question. Future projections suggest that, in spite of increased precipitation, wastage of small glaciers and the Greenland Ice Sheet will add mass to the ocean; the resulting sea-level rise due to this cause likely will be a few tenths of a meter by the year 2100. The sea-level rise due to changes in Antarctica is more

uncertain; most likely it will be small, but a rise of an appreciable fraction of a meter by 2100 due to increased discharge of land ice to the sea is not beyond the realm of possibility.

Since the turn of the century, measurements of relative sea level suggest a global average rise of 1 to 3 mm/yr; however, the data coverage from the central ocean regions and the southern hemisphere is poor, and tectonic and isostatic disequilibrium effects have not been removed from most records. A preliminary calculation of the continuing adjustment of the Earth to the removal of the Laurentide and Fennoscandian ice sheets results in a corrected value of a little more than 1 mm/yr along the eastern U.S. coast. These corrected values still show considerable spatial variations of unknown cause. Ocean surface temperature appears to have risen by 0.6 $\pm$ 0.3°C since the turn of the century, but this result may be biased because of changing instrumentation and observation techniques. Those models that are currently used for computation of the increase in ocean volume due to thermal expansion generally do not incorporate the essential physics of deep-water formation and movement. The few observational data on changes of ocean temperature, salinity, and density structure during the last several decades show no statistically significant change except in local areas; a longer record is needed for firm conclusions. Atlantic water north of 50°N has slightly freshened since 1972, but this may be a temporary condition.

The glaciers and small ice caps of the world, excluding the ice sheets of Antarctica and Greenland, have, in general, been shrinking during the past 100 years (Table 1). However, the data set is temporally and spatially sparse. Most of the glacier wastage that contributes to sea-level rise is thought to be derived from the mountain ranges bordering the Gulf of Alaska, Central Asia, and the Patagonian ice caps, but these are areas with few observations. In some regions, even the area of glacier ice is poorly known.

TABLE 1 Estimated Mass Balance of Glaciers and Ice Sheets at the Present Time[a]

Ice Mass	Average Mass Balance (water equiv.) (m/yr)	Effect on Sea Level (mm/yr)	Report Section
Glaciers & small ice caps	-1.2 $\pm$ 0.7	+0.5 $\pm$ 0.3	3.3
Greenland Ice Sheet	0.02 $\pm$ 0.08	-0.1 $\pm$ 0.4	3.4
Antarctic Ice Sheet	0.02 $\pm$ 0.02	-0.6 $\pm$ 0.6	3.5

[a]Note: error limits represent approximate bounds of estimation and cannot be defined statistically.

Observations of present elevation changes of the Greenland Ice Sheet surface indicate thinning of the marginal zones and thickening of the central area. Accumulation rates are reasonably well known; ablation rates and their gradient with altitude are known only for a few sites in West Greenland; iceberg discharge has been measured for some outlet glaciers in West Greenland, and few estimates have been made along other coasts. Thus it is currently not possible to estimate reliably the exchange of mass between the Greenland Ice Sheet and the oceans, but most estimates suggest that gains and losses are about equal.

The present-day net balance of the Antarctic Ice Sheet is still not known precisely, but estimates have been improved over the past decade and most estimates suggest growth. The biggest uncertainties are in iceberg discharge, accumulation amounts in some regions, and rates of melting below the major ice shelves; also, few data exist on changes of the margin. The physics of the dynamic response of the ice sheets to variations in climate is known in general terms, but some processes are not well understood or have not yet been incorporated fully in numerical models. Major gaps in understanding concern basal sliding, the coupling of ice streams with the ice sheets in which they are embedded, and what determines the position of the seaward (calving) face of ice shelves. The present-day true polar wander and the nontidal acceleration of the Earth's rotation can be reproduced using modern models of the Earth's structure combined with a scenario for the loss of the Pleistocene ice sheets, without any need to assume present-day changes of ice-sheet volume, suggesting approximately zero mass balance for both the Antarctic and Greenland Ice Sheets.

In order to predict future changes in land ice due to a perturbed climate, climate models are required. Steady-state (asymptotic) models indicate, for a doubling of CO_2, a predicted average temperature rise of 2 to 4°C or possibly more. The global temperature rise is probably amplified at high latitudes. The major uncertainties result from the difficulty of parameterizing sea ice and predicting the effect of clouds on the perturbed climate. The physical basis for certain features predicted by the models is still not clear. Runoff, as opposed to melting, at the margins of the two existing ice sheets is not yet properly modeled. Predictions made by steady-state models incorporating a CO_2-perturbed climate show similarities in the global-scale distribution of climate variables, but the agreement is poor in regard to regional, longitudinal variations and in the higher latitudes and in the anticipated changes in precipitation. The time-dependent evolution of climate, driven by a changing CO_2 concentration, is extremely difficult to model, and many aspects are poorly understood.

Energy-balance models, as well as simple statistical, empirical models, exist that can be used to estimate the additional wastage (or growth) of glaciers and small ice caps in response to a perturbed climate. However, insufficient data exist to calibrate these models in most regions, the models are not easily linked to general circulation models, and glaciers in regions of monsoonal circulation are difficult to model. Mass-balance histories are often dominated by rare years of extremely negative balances, a further difficulty. Complete removal of the small glaciers of the world would cause a sea-level rise of 0.3 to 0.6 m.

Several ways exist for estimating the response of the ice sheets to a CO_2-perturbed climate. Estimates of the contribution to sea-level rise from the Greenland Ice Sheet are severely limited by lack of present-day data, as well as by lack of understanding of how the balance processes relate to large-scale climatic processes, how the infiltration/refreezing regimen would react to an increase in meltwater availability, and how iceberg calving would be affected.

Knowledge of ocean circulation near and under Antarctic ice shelves is limited. If a doubling of CO_2 in the atmosphere were to cause an increase in the temperature of circumpolar deep water of about 0.5°C, then a proportional increase might occur in the temperature of "warm" inflows onto the continental shelf. If the shelf circulation were to change so that circumpolar deep water intruded beneath all the ice shelves as freely as it does today beneath the George VI Ice Shelf, then the average ice-shelf melt might be raised from about 0.4 m/yr to as much as 3 m/yr. However, it is much more likely that the major ice shelves would continue to be protected, at least in part, by cold, high-salinity water that lies on the continental shelf.

In the case of the West Antarctic Ice Sheet, the situation is further complicated by the possibly delicate stability of the interaction between ice streams and ice shelves. If melting from the base of ice shelves were to increase markedly, the effect on ice streams could be far more important than the expected minor increase in surface melting and runoff. It is difficult to estimate rates because of uncertainties in knowledge of the heat transfer from the ocean to the ice shelves, the effect of ice-shelf thinning on the ice streams, and the mechanism of ice-shelf calving. On the other hand, increased accumulation due to a CO_2-enhanced atmosphere could contribute to sea-level fall.

Estimates of the contribution of glacial wastage to sea level for an atmosphere with a doubled concentration of CO_2 are given in Table 2.

For time scales longer than one century, the uncertainty in estimating potential changes in land ice and sea level increases significantly. The workshop participants did not attempt to make estimates beyond the year 2100, and the limits expressed in Table 2 should not be extrapolated beyond that year.

The workshop participants accept the importance of these general goals as essential to improvement in our ability to understand and predict sea-level change in the next century:

- Improve existing climate models especially in the treatment of clouds and sea ice, the simulation of high-latitude processes, and the development of time-dependent simulations.
- Determine the present-day global change in sea level more precisely.
- Determine to what extent the current rise in sea level is due to volume expansion of the ocean.

The following specific recommendations concern our ability to understand and predict the response of glaciers and ice sheets to an altered climate in the next century. These recommendations are all considered important to reducing uncertainties and are listed in order

TABLE 2 Estimates of the Contribution to Sea-Level Rise by Ice Wastage in a CO_2-Enhanced Environment[a]

Ice Mass	Annual Probable Contribution to Sea Level With Steady-State 2 x CO_2 Atmosphere (mm/yr)	Range of Estimated Contribution to Total Sea-Level Change to Year 2100 (m)	Report Section
Glaciers and small ice caps	2 to 5	0.1 to 0.3	4.2
Greenland Ice Sheet	1 to 4	0.1 to 0.3	4.3
Antarctic Ice Sheet	-3 to 10	-0.1 to 1 [b]	5.3

[a]For explanation of assumptions and scenarios involved, see Table 4. Note that thermal expansion of the oceans and other nonglacial processes that might cause additional sea-level rise are not included here.

[b] Values in the range of 0 to 0.3 m are considered most likely.

of decreasing priority based on amount of uncertainty that might be removed; priorities are assigned across the various disciplines. These recommendations are explained in greater detail in Section 6.3.

1. Southern Ocean Circulation near Antarctica (Sections 3.2, 5.2)

- Assess ocean heat transport across the continental shelf around Antarctica, especially in the Ross, Amundsen, Bellingshausen, and Weddell Sea sectors.
- Determine ocean circulation beneath the large ice shelves.
- Analyze how these conditions will change as a result of a CO_2-enhanced atmosphere.

2. Ocean/Ice Shelf Interactions (Sections 5.2 to 5.4)

- Measure present basal-melt rates and investigate their relationship to underlying ocean circulation.
- Investigate iceberg calving rates, and identify those factors that affect these rates and determine the seaward boundary of ice shelves.

3. Ice Streams (Section 5.3)

- Determine the factors controlling whether an ice stream flows in a rapid or slow mode.
- Compile a complete set of data on ice streams, including such items as their dimensions, slopes, and speeds.

4. Detection and Prediction of Future Changes (Sections 3.1-3.6, 4.1-4.3)

- **Measure changes in dimensions and discharge rates of glaciers and ice sheets.**
- **Determine changes in sea level and ocean temperature.**

2.
Introduction:
Relationship between Land Ice and Sea Level

A significant rise of global sea level is expected to result from the melting of land ice and thermal expansion of the upper layer of the ocean due to climatic change induced by increasing CO_2 and other greenhouse gases in the atmosphere. In the recently issued report, Changing Climate (NRC Carbon Dioxide Assessment Committee 1983), the National Research Council estimates that sea level will rise 70 cm over the next 100 years. The report Projecting Future Sea Level Rise (Environmental Protection Agency 1983) states that a global rise of between 144 and 217 cm by 2100 is most likely, but a global rise as low as 56 cm or as high as 345 cm by 2100 cannot be ruled out.

Land ice is likely to contribute to rising sea level for the following reasons. (1) Higher air temperatures will cause an increased rate of melting in the ablation areas of glaciers and ice sheets. (2) In addition, warming will probably cause ablation areas to expand as the equilibrium lines, which divide ablation from accumulation areas, retreat to higher elevations. Thus, the total areal extent of melting is likely to increase. However, some time will be required for ablation areas to expand, because increased melting above equilibrium lines may be accompanied by refreezing of much of this additional meltwater within the snow (Figure 1). (3) The Antarctic Ice Sheet, which now appears to be either in mass balance or gradually thickening, may begin to retreat in areas where it is resting on bedrock far below sea level. Such retreat, if it occurs, will not be due to surface melting but to increased melting from the bottom surfaces of the thick floating ice shelves that now buttress the grounded inland ice sheet in many places (Figure 2). Increased bottom melting, which may be caused by warmer ocean currents penetrating beneath the ice shelves, would probably cause grounding lines to retreat. Since retreat of grounding lines would be accompanied by thinning and accelerated discharge from the inland ice sheet, this would contribute to rising sea level.

Grounding lines are critical to the dynamics of marine ice sheets (large ice masses resting on bedrock far below sea level). Such ice sheets differ from terrestrial ice sheets, which tend to form steep terminal slopes at their margins. By contrast, marine ice sheets flatten out toward their seaward margins as buoyancy and subglacial-water effects enable the ice within their constituent ice streams (Figure 2) to move rapidly under the influence of small driving stresses. When the

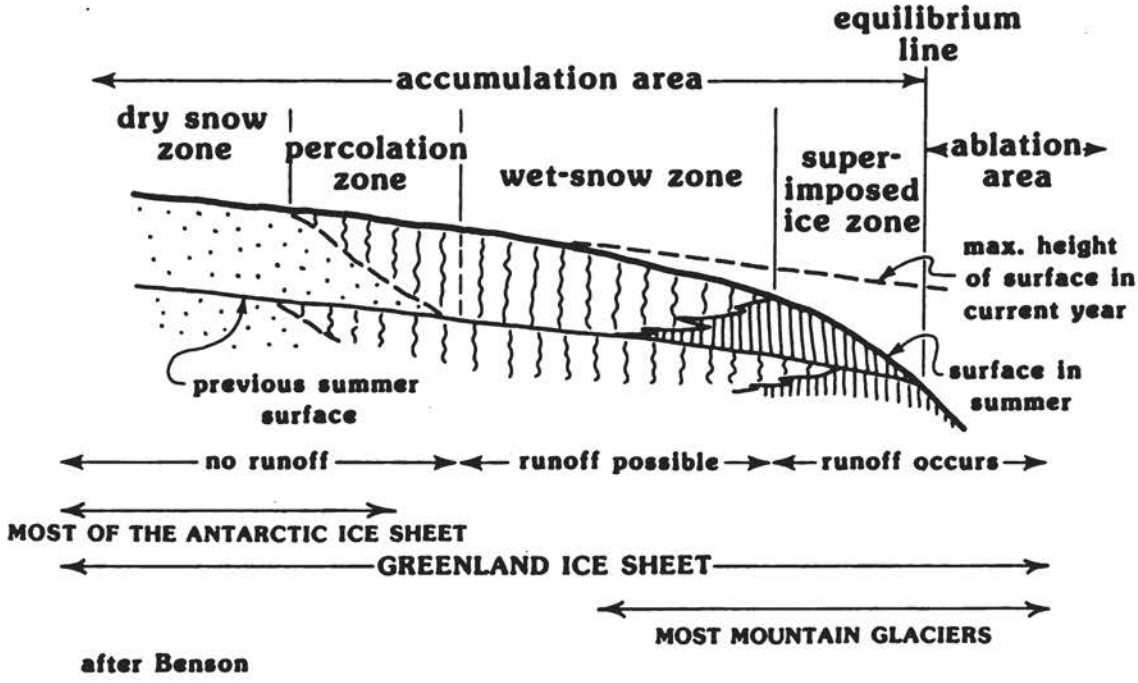

FIGURE 1 Section through snow and firn (old snow). At high altitudes (far from the coast), no surface melting occurs. At slightly lower altitudes, surface melting occurs but refreezes in that winter's cold snow layer. At lower altitudes, refrozen (superimposed) ice masses occur, and some subsequent melt of snow and superimposed ice may run off depending on the temperature of the underlying snow and ice mass. At the lowest altitudes (the ablation zone, below the equilibrium line), melting exceeds snow and ice accumulation and some or all of this meltwater runs off to the sea (modified from Benson 1962).

ice is no longer sufficiently thick to rest on bedrock, it floats. Seaward of this point, called the grounding line (or zone), it becomes a floating ice shelf. The true margin of a marine ice sheet is the seaward edge or calving front of the ice shelf, where icebergs detach (calve). Advance or retreat of the ice-shelf front depends on the rate of iceberg calving, which in itself cannot affect sea level because the ice shelf is already floating. However, since grounding lines are the seaward boundaries of thick grounded ice, retreat or advance of grounding lines does affect sea level. A grounding line tends to be metastable or unstable if the sea depth is greater than a critical depth, and the seafloor slopes down toward the ice-sheet interior. In this case, retreat--once initiated by an external event such as a thinning ice shelf--can become irreversible (Figure 2).

The immense East Antarctic Ice Sheet is grounded substantially below sea level in some areas, but the smaller ice sheet of West Antarctica is the only true marine ice sheet extant. The grounding lines around West Antarctica are 500 to 1200 m below sea level in many areas, which

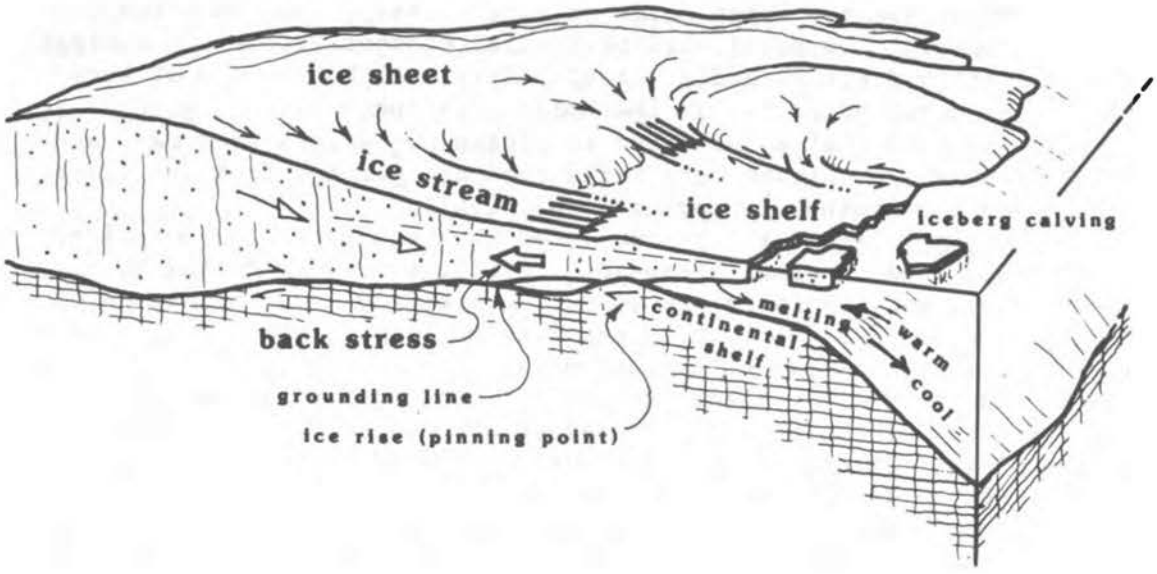

FIGURE 2 Sketch of a typical marine ice sheet, showing processes that control the flow of land ice to the sea. A backstress is exerted on an ice stream by the ice shelf owing to shear along pining points and lateral margins. Thinning of the ice shelf, caused by increased melt at its base or by accelerated calving and increased extension, causes a decrease in the backstress. This in turn causes accelerated discharge of land ice through ice streams to the sea.

is well below the critical depth. Stability appears to be maintained, however, by the buttressing influence of large floating ice shelves. Destabilization, accompanied by drastic retreat of this ice sheet during the next century, is not to be expected. However, if substantial warming occurs in the polar regions during the next 50 years, as suggested by atmospheric general circulation models, events may be set in motion during the next century that will lead to irreversible and drastic retreat of the West Antarctic Ice Sheet on a longer time scale. A drastic retreat of this ice sheet would cause mean global sea level to rise by as much as 5-6 m, and this would have far-reaching consequences, since a large fraction of the world population lives on low-lying coastal plains. However, population can adjust to change if the change is not too abrupt. The critical issue is the time scale: Will the drastic retreat of the West Antarctic Ice Sheet, if it occurs, take 100 years, 1000 years, or even longer?

The above factors, which are likely to contribute to rising sea level, may be counteracted to some degree by increased snowfall over Antarctica due to higher air temperatures. This may initially mitigate the effect of grounding-line retreat due to increased bottom melting beneath ice shelves, and it might possibly counterbalance or reverse the effect of grounding-line retreat on a longer time scale.

Recent studies of deep ice cores have shown rapid fluctuations in climate during the during the last glacial period (Dansgaard et al.

1982). These events, which occur on time scales of one to a few centuries, appear to be paralleled by similar changes in the CO_2 content of the entrapped air (Stauffer et al. 1984). Although none of these events has occurred so far in the Holocene (since the last glacial age), they do indicate that a mechanism involving CO_2 exists that can cause rapid switches in climate over large regions, perhaps from one quasi-stable mode to another (Broecker et al. 1985).

In Changing Climate it was concluded that estimates for both ice melting and ocean thermal expansion still have large uncertainty--at least 25 percent. This is due to our uncertainty over the causes of the current rise in sea level, our inability to predict whether changes in atmospheric circulation will cause more or less snow to fall on the ice sheets and the smaller glaciers, and our insufficient knowledge and understanding of the physical processes associated with the flux of heat to the ocean. Of even greater uncertainty is the potential drastic retreat of the West Antarctic Ice Sheet.

The recent reports Snow and Ice Research: An Assessment (NRC Committee on Glaciology 1983) and Environment of West Antarctica: Potential CO_2-Induced Changes (NRC Committee on Glaciology 1984) and a December 1983 workshop also examined the exchange of water between land ice and the oceans, especially as it relates to possible CO_2-induced climate change. It was apparent that much more information is needed to predict future sea-level change with any confidence. In view of the possible magnitude of change and the associated uncertainties, the Polar Research Board and its Committee on Glaciology concluded that an authoritative study is needed on the relationship between land ice and sea level, especially in view of existing climate-modeling predictions. This report presents the results of the ensuing workshop, which was held in Seattle, 13-15 September 1984. The group examined the basic questions of how much water has been exchanged between land ice and ocean during the last century, what is happening now, and, given existing climate-modeling predictions, how much exchange can be expected in the future.

The following specific questions were also examined:

I. What is the evidence for such exchange? (What do we know?)
   - A. Glaciological evidence (Greenland, Antarctica, other glaciers)
   - B. Oceanographic evidence (sea level, including thermal expansion, and salinity, temperature, and chemical changes possibly derived from glacier melt)
   - C. Geoidal evidence (length of day, polar wander, problems with assessing sea level)
   - D. Other evidence

II. What are the important gaps in the evidence or in our understanding of current processes. (What do we need to know to understand the present?)

III. What is likely to happen in the future, and what do we need to learn to have more confidence in predictions of the future?

This report presents the collective viewpoint of the national and international research community on the relationship between the volume of land ice and sea level. It includes a review of what is known of ocean volume changes during the last 100 years (Chapter 3), what land ice and ocean exchanges are likely to occur during the next century, and what we must learn to reduce the uncertainty of these estimates (Chapter 4), and a discussion of the possibility of the drastic retreat of the West Antarctic Ice Sheet (Chapter 5). The summary chapter includes an assessment of current information, assessment of unknowns and uncertainties, and identification of future research needs in priority order. The discussions found in Chapters 3, 4, and 5 are supported by the prepared statements of the workshop participants, which are included as attachments to this report.

3.
Sea-Level Changes during the Past 100 Years

Sea level appears to have risen 1 to 2 mm/yr and possibly 3 mm/yr in the past 100 years. Part of this rise may be due to thermal expansion of the oceans; the remainder has generally been attributed to melting of polar ice. However, studies of the current mass balance of the Antarctic Ice Sheet, which comprises about 85 percent of the total area of glacier ice on the Earth, suggest that a negative mass balance is not likely and that this ice sheet may be removing water from the world ocean. Recent estimates of the mass balance of the Greenland Ice Sheet (12 percent of the world's glacier ice area) suggest that it is close to balance. The remaining 3 percent of the Earth's glacier ice area (about 0.6 percent of the ice volume) may account for part of the unexplained rise in sea level.

In this chapter the evidence for ocean-volume changes during the past 100 years is examined. Measurements of relative sea level; oceanographic evidence of thermal expansion and freshwater input; and the contributions from glaciers and mountain ice fields, the Arctic ice caps, Greenland, and Antarctica are discussed.

Sea-level changes are recorded at tide gauges. The relative sea level (RSL) at a gauge may show long-term changes due to the vertical motion of the gauge, changes in the local density structure or circulation of the ocean, or changes in the global volume of the ocean. Changes in the ocean volume, termed eustatic changes, can be due to changes in the mass of the world ocean (caused, for instance, by the removal of ice mass from land) or by changes in the volume at constant mass of the world ocean (caused, for instance, by thermal expansion of ocean water). Changes in ocean volume without a change in mass are termed steric changes. The long-term vertical motion of tide gauges can be caused by many geologic processes; one of the most important is the continuing adjustment of the Earth to the loss of weight of the Pleistocene ice sheets (isostatic rebound). Also, the global record of relative sea level can be affected by changes in the volume of the ocean basin due to tectonic or sedimentary processes, without change in the mass or volume of the water; the effect of these processes is difficult to estimate. The long-term impact of man on the hydrologic cycle, through the depletion of groundwater reservoirs and the impoundment of water in reservoirs, is thought to have a negligible impact on ocean mass (Meier 1983).

3.1 RELATIVE SEA LEVEL

Measured Changes in Relative Sea Level

More than a dozen studies of global tide-gauge (sea-level) records indicate a rate of rise of relative sea level of between 1.0 and 2.0 mm/yr, or possibly up to 3.0 mm/yr, during the past century (see this volume, Attachment 1). A 1-2 mm/yr rate of rise is considered much more likely than a higher rate. The agreement of these independent analyses is remarkable considering the diversity of data bases and analysis techniques. The important conclusion is that relative sea level (RSL) appears to be rising globally, but the magnitude of rise and its cause are poorly known (Barnett 1983, 1984). On the U.S. east coast, the average rate of sea-level rise was significantly lower before 1934 than in the period following.

Estimates of RSL change are subject to substantial uncertainty. Present sea-level data are biased toward northern hemisphere measurements, and few data exist from mid-ocean. About 60 percent of the measurements are from the United States, Scandinavia, and Japan. Tectonic motion (Japan, U.S. West Coast) and isostatic adjustment (Scandinavia, U.S. East Coast) contaminate most available long-term tide-gauge records. The component of RSL change that is due to glacial isostatic adjustment can be estimated, but the contribution of meltwater input to the ocean is uncertain. The tectonic component of RSL change on mid-ocean islands cannot be predicted and subtracted out at present. Tide gauges are clearly needed in central ocean gyres, where there are now only two.

Instrumental stability is a major problem in measuring sea level. Most of the data were obtained with float gauges, which have a number of problems. Pressure sensors on the seafloor are not by themselves a substitute for tide gauges because they respond to factors other than sea-level change; fluctuations are caused, for example, by changes in the mean density of the water column. Noise problems also occur. However, modern statistical methods can be used to look for the low-frequency components of RSL change and to look at the phase lags between tide gauges in, for example, North and South America.

Regional tide-gauge studies and rigorous statistics of past RSL behavior will establish space and time scales of RSL change more clearly. Global averages depend on meaningful spatial averages from smaller regions, and these can be difficult to determine. Should the average of the measurements from 50 well-tended tide gauges in one area be weighed equally with measurements from one poorly tended station in another area? Most data before 1910 or 1920 are based on daily averages of four observations, and so are probably less reliable than more recent continuously recorded data, although the observation errors can be decreased by averaging over a sufficient number of days.

Areas that are geographically close can yield different RSL data because of tectonic motion. Data from China and Japan are contradictory, for instance, because China is much older and more stable geologically. Korean and Japanese sea-level data also differ considerably. Raw RSL data for the U.S. East Coast show different slopes or curves from three

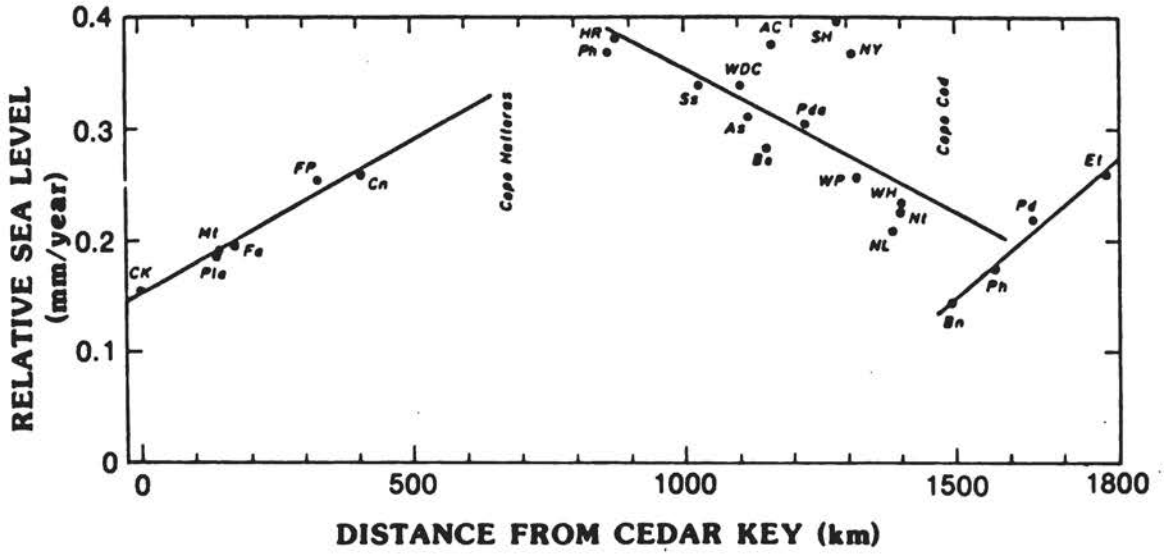

FIGURE 3 Mean annual relative sea-level changes during a 40-year period for U.S. East Coast stations, Cedar Key, Florida, to Eastport, Maine. Regression lines denote three main segments of the East Coast having different sea-level trends.

segments of the coast: south of Cape Hatteras, Cape Hatteras to Boston, and north of Boston (Figure 3). The variation in the curves becomes less, however, when the effect of isostatic rebound is removed. The adjusted data still show that sea level is rising.

Further advances in the estimation of global changes in RSL will require careful regional studies. RSL changes are a function of tectonic, glacial, isostatic, meteorological, oceanographic, and other factors; interdisciplinary studies are needed to separate the contributions of each. New geodetic positioning systems and other new instrumentation may make it possible to measure the vertical motion of each tide gauge. Improved statistical techniques must be developed for analyzing tide-gauge records and quantifying uncertainties. Where tide-gauge measurements are lacking or sparse, we must apply either prognostic models of forcing or best available estimates of forcing (tectonics, climate) to separate the contributions of the various causative agents. We must obtain regional and global baseline statistics so that 10, 20, or 30 years from now we can look for changes in rate of sea-level rise with some confidence.

Correction of Sea-Level Data for Continuing Isostatic Adjustment

Tide-gauge records can be corrected to remove the effects of glacio-isostatic disequilibrium by using an existing global and gravitationally self-consistent model (see this volume, Attachment 2). This model predicts the variation of relative sea level (RSL) anywhere on Earth subsequent to the loss of the Pleistocene ice sheets and is based on

viscoelastic field theory.

Radiocarbon-controlled RSL data going back 6000 to 7000 years were originally used to tune the model. RSL curves are computed, and the computed curve at each location is scaled so it passes through zero at the present time (i.e., present sea level is the datum at each location). The RSL curve can then be compared to dated emerged (or submerged) beaches at each of a large number of sites, and the parameters of the model are adjusted until a fit to the observations is achieved.

The Earth model is spherically symmetric, with no lateral heterogeneity of its physical properties. The elastic components of the structure are assumed fixed by the data of seismology. The only variable parameter in the Earth model is the viscosity, which is also assumed to be a function of radius only. The viscosity is assumed to be infinite in a thin layer near the Earth's surface, the surface lithosphere. Both the thickness of this layer and the variation of mantle viscosity with depth below the lithosphere have been inferred by fitting the observed RSL data.

The observed variations of RSL near the center of the regions that were once ice covered are relatively insensitive to lithospheric thickness and so may be employed to fix the mantle viscosity profile. Given the mantle viscosity profile, RSL data from sites near the ice-sheet margins and beyond may be employed to infer lithospheric thickness. The Laurentide and Fennoscandian ice sheets are of sufficient areal extent that the sensitivity in RSL response of the different regions to different components of the radial viscosity structure may be determined. Then the model may be employed to predict the expected RSL response at sites other than those employed to tune the model parameters.

The model may be used to predict the present-day variation of RSL due to the last deglaciation event at any site at which a tide gauge is located and was applied for this purpose to tide-gauge data for the U.S. East Coast (passive margin) and West Coast (active margin). The results [Figure 4(a)] demonstrate that about 30 percent of the observed rate of RSL rise at tide gauges along the U.S. East Coast was attributable to glacial isostatic adjustment. The average rate of rise of this region was about 1.1 to 1.2 mm/yr. There is no similar systematic deviation in the West Coast RSL data, which are widely scattered about a mean near zero, a result that is hardly surprising given the level of tectonic and anthropogenic activity in this region. Variations about the mean residual rate of RSL rise along the East Coast are extremely large, with the extremes being 0.8 mm/yr and 3 mm/yr, implying that the observations have been influenced by factors other than eustatic rise and glacio-isostatic adjustment.

3.2 EVIDENCE FROM THE OCEAN

Thermal Expansion of Ocean Water

The problems of the temporal variability of deep-ocean temperature and the relationship of temperature changes to changes in steric height (i.e., changes in volume at constant mass) and sea level can be

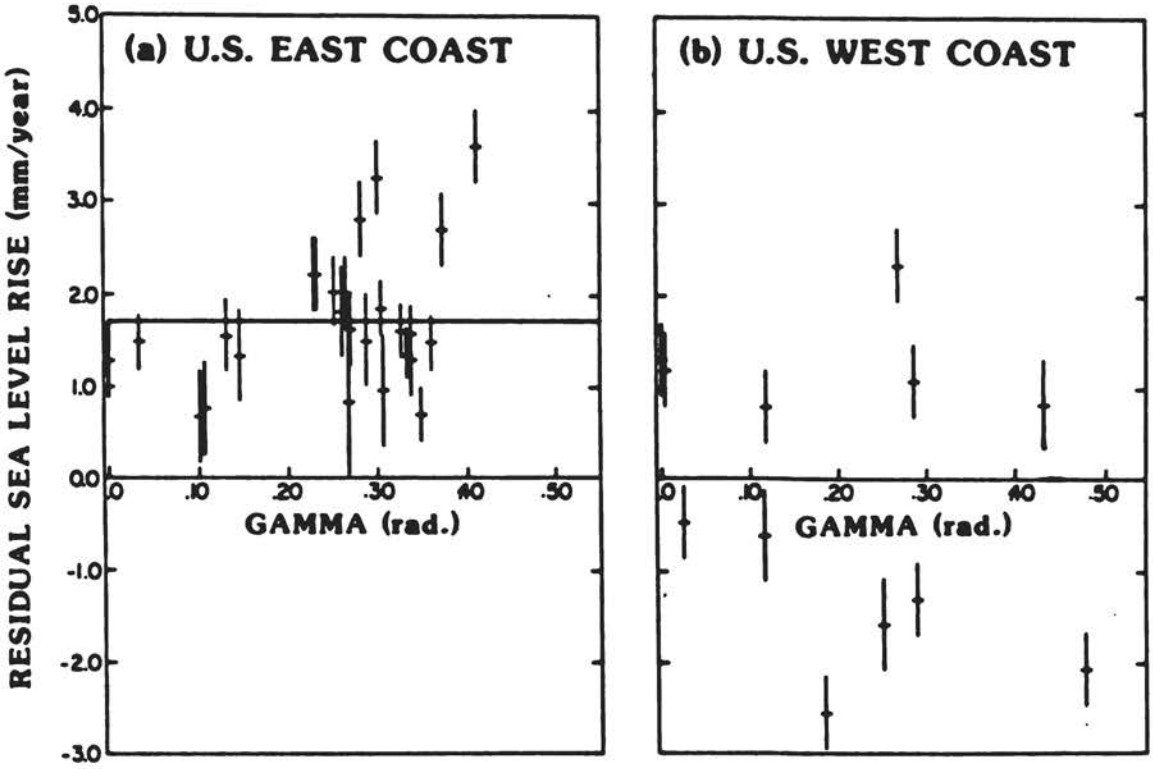

FIGURE 4 Preliminary results showing relative sea-level trends from tide-gauge data along the U.S. East (a) and West (b) Coasts in the period since 1940 corrected for isostatic adjustment effects. The horizontal scale is distance in radians from Key West, Florida (a), and San Diego, California (b). A clear trend is apparent in the corrected data for the East Coast, but not for the West. More refined calculations for the East Coast suggest that the trend is most likely in the range of 1.1 to 1.2 mm/yr.

addressed using data from the subtropical North Atlantic spanning several decades (see this volume, Attachment 3). This is the longest period for which high-quality hydrographic measurements are currently available. Data consist of a 27-year time series (Panuliris) from deep hydrographic stations near Bermuda, sea level at Bermuda, and two large-scale hydrographic surveys of the subtropical North Atlantic that were separated in time by 23 years. The purpose of concentrating on a single, relatively data-rich region was to obtain a nonaliased view of the scales of temporal variability that should be applicable elsewhere in the oceans. The following conclusions were reached:

(a) Although seasonal and interannual temperature fluctuations are concentrated in the upper ocean, decadal time-scale variations extend deep into the ocean (Figure 5). In the area studied, the upper 1000 m cooled by up to 0.5°C, and the interval from 1000 to 3000 m warmed by as much as 0.2°C.

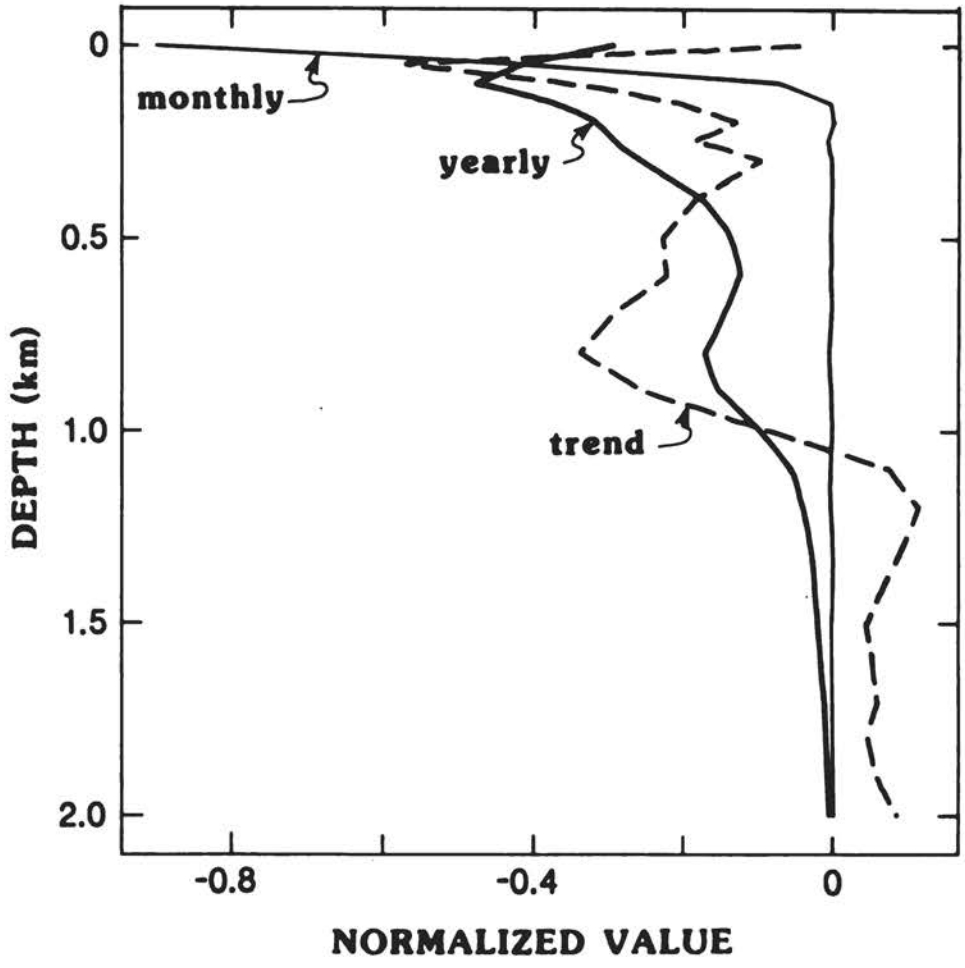

FIGURE 5 The first empirical orthogonal function (EOF) of the monthly mean profiles of steric height, the first EOF of the yearly anomaly profiles, and the linear trend in time of steric height over the period 1955-1981. All profiles are normalized. The first EOF is the shape with the smallest residuals, in a least-squares sense, for all the profiles in a given group. Data are from the 27-year Panuliris series, 32°10'N, 64°30'W (near Bermuda).

(b) The long-time-scale temperature changes resulted in changes in steric height that are closely related to sea-level variability. There is some suggestion that sea level is gradually rising relative to steric height (Figure 6), but the time series is still too short for a reliable conclusion. It will probably be necessary to extend the time series for an additional 20-30 years.

(c) Long-time-scale temperature changes are spatially variable on the scale of the oceanic gyres, particularly for depths in and above the main thermocline. Fluctuations in mid-ocean sea level may be quite independent of those at coastal stations, even over a period of 20 years or more. Although gyres tend to have some lower-frequency oscillations,

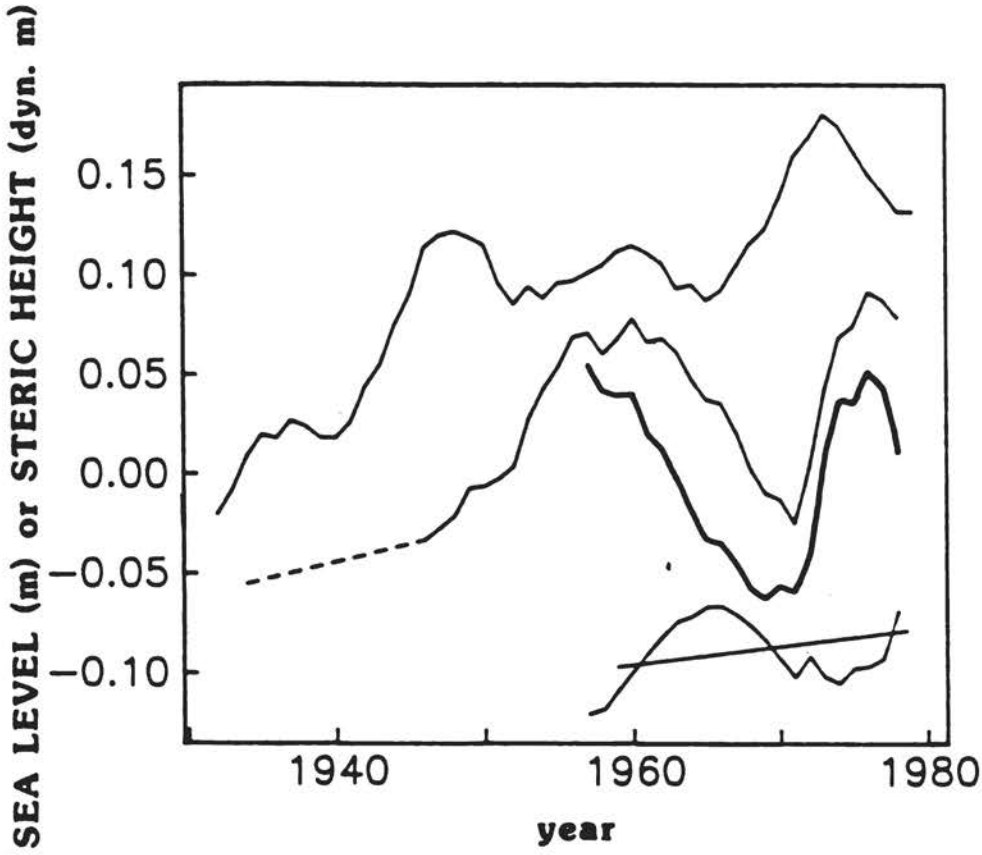

FIGURE 6 Five-year running means of, from top: Charleston sea level, Bermuda sea level, Panuliris steric height, and the residual of Panuliris steric height subtracted from Bermuda sea level. The beginning point of each curve is arbitrary. The straight line drawn through the bottom curve has an upward slope equivalent to a sea-level rise of 1 mm/yr.

aliasing cannot be responsible for the effects seen. For instance, the 4°C isotherm in some of the IGY north-south sections has a maximum depth at about 24°N. In 1981, the maximum depth of that isotherm was greater by 100 m. That change could not have been caused by a simple north-south translation of deep water.

The data do not necessarily indicate a reduction in the rate of deep-water formation; a reduction is seen in the census of deep water, but that indicates nothing definitive about the formation rate. The North Atlantic is the source of perhaps half of the deep water in the world ocean; the Southern Ocean is thought to make an approximately equal contribution. The data indicate that in the subtropical North Atlantic the upper 1000 m underwent a net contraction, but there was expansion in the depth range of 1000-3000 m. The amount of heat necessary to raise the temperature of the deep water a few tenths of a degree is actually very small compared with the amount of heat that the ocean

carries--on the order of 1 percent.

There is no evidence to rule out the possibility that thermal expansion of the deep water over the world ocean is responsible for the current rise in sea level. The long-term climatic signal may be in the deep ocean, and we are only seeing transient signals near the top. We must determine the minimum-depth water column that will yield long-term climatic information. At very few stations are measurements made deeper than 1000 m, and at still fewer are they made as deep as 4000 m.

The time series collected at the Bermuda station are very valuable, and it is important that they be continued. There are many other potential data sets that could be obtained by repeating a Pacific traverse, although a repeat at this time would not involve a particularly long time lag between measurements; two long sections were occupied across the South Pacific in 1967.

Possible Evidence of Deep-Water Freshening in the North Atlantic Ocean

The northern North Atlantic is a good location for examination of the deep ocean for evidence of recent changes in salinity (see this volume, Attachment 5). It is close to regions of deep-water mass formation and has been surveyed by expeditions 10-20 years apart. The northern North Atlantic plays a significant role in the ocean's contribution to climate response, because it can be thought of as one of the primary deep ventilators of the world ocean. Its deep-water components have been found to be closely tied to the winter sea surface, and so are potentially sensitive to environmental changes.

No changes were observed in the deep temperature and salinity fields during the period 1957 to 1972. In the 1970s, the surface layers of the northern North Atlantic freshened by about 0.1 o/oo; European oceanographers call this "the great 1970s salinity anomaly." A comparison of the deep-water salinities before and after the surface-water freshening showed that by 1981 deep-water salinities had changed throughout the northern North Atlantic. It is clear that the 1981 salinities were lower than their earlier counterparts. The deep freshening was about 0.02 o/oo. The overall cooling was about 0.15°C.

The surface-layer freshening in the 1970s propagated into the deep water because the downward penetration of the cooled water in the water-mass formation areas depends on its density not on its temperature or salinity alone. The net result of freshening of the surface water is colder, less-saline water for a given density, which produced the changes seen in the 1981 data. Since all the upper water north of 50°N freshened, perhaps there has been some increase in freshwater supply, or decrease in salty-water supply, since 1972. However, this may be a transient phenomena, and more years of observation will be required to define the cause of this apparent change.

The salinity changes cannot be interpreted in terms of a change in the height of the surface. The densities of the deep-water masses remained approximately the same, because there was a compensating temperature change. The deep water is both fresher and cooler. The specific volume of the deepest water observed during this period remained constant.

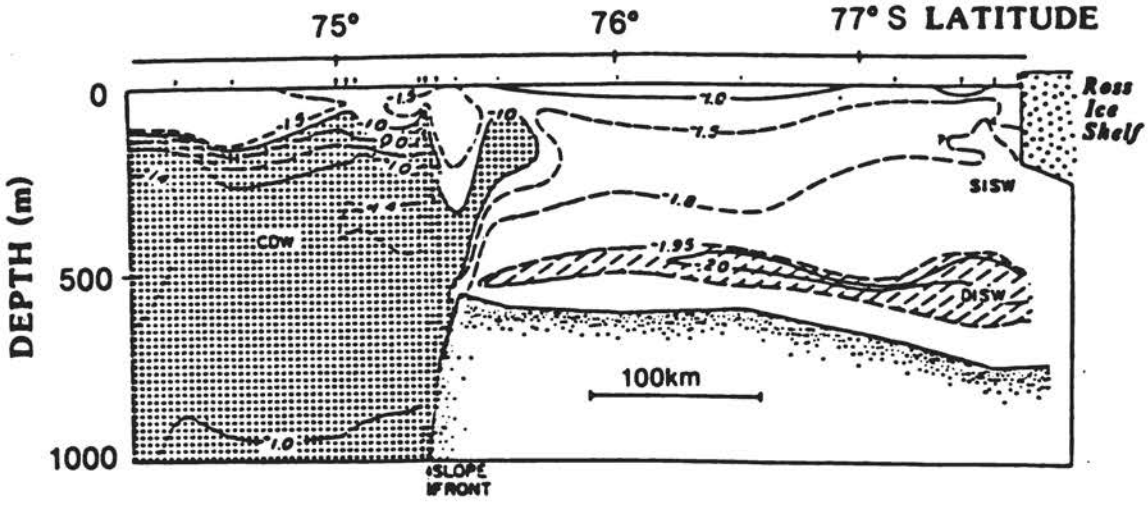

FIGURE 7 A December central 1976 temperature section through the primary Deep Ice Shelf Water (DISW) core in the Ross Sea. Ticks along the sea-level line indicate locations of vertical profiles. The DISW is at temperatures as much as 0.3°C lower than the sea-surface freezing point owing to heat lost in melting at the ice shelf base. Ice Shelf Water also has been observed on the continental shelf and slope in the Weddell Sea (Foldvik et al. 1985); it plays a significant role in bottom-water formation.

Variations in sea-ice formation could be responsible for salinity changes, but there are other possible causes as well. More information is needed before a conclusion can be drawn. If a change in the freshwater input is likely, the freshwater flux in the ocean rather than the water characteristics should be measured. The volume transports and the salinity contrast between the deep ocean and the surface must also be investigated.

Oceanographic Evidence of Freshwater Input to the Southern Ocean

Significant changes in salinity (>0.01 o/oo) and other chemical parameters have been observed in the deep waters of the southern oceans over time periods as short as one year (see this volume, Attachment 4).

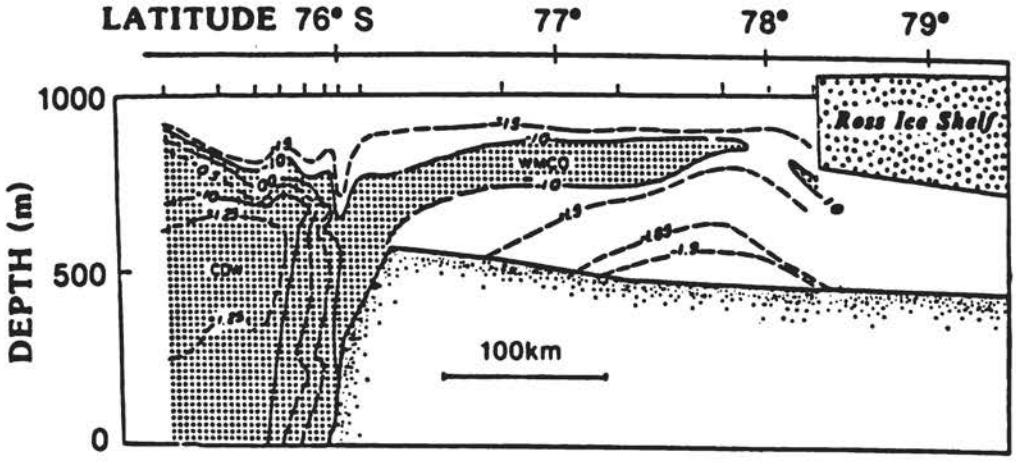

FIGURE 8 A December 1976 temperature section through the primary intrusion of warm water (WMCO) in the Ross Sea. Ticks along the sea-level line indicate locations of vertical profiles. This section, and the core of the warm-water intrusion, lies about 175 km east of the section shown in Figure 6. Derived from the Circumpolar Deep Water (CDW) north of the continental shelf, the WMCO inflow drops in temperature by about 2°C in crossing the slope front near 76°S. Year-long temperature measurements at the edge of the ice shelf indicate that portions of the WMCO there average more than 0.5°C above the in situ melting point.

These changes have been attributed to seasonality in the large-scale circulation, variability in the characteristics of bottom-water formation, and deep convection associated with the Weddell Sea Polynya (a large area that remains free of sea ice during some winters). Large salinity changes (0.05-0.10 o/oo) occur on decadal or shorter time scales throughout the water column on the Antarctic continental shelf but can be attributed to variability in sea-ice formation or residence time of water on the shelf. Glacial meltwater has been identified from temperature, salinity, and $\delta^{18}O$ observations in water beneath, and emerging from beneath, floating glacial ice (Figure 7). The heat necessary to melt the underside of an ice shelf comes from depression of the seawater freezing point with pressure and from intermediate-depth intrusions of relatively warm water onto the continental shelf and beneath the glacial ice (Figure 8). If the Antarctic Ice Sheet is in mass balance with a volume flux of 2000 km^3/yr and an iceberg calving rate of 1300 km^3/yr, then 700 km^3/yr of attached glacial ice melts directly into the shelf water. This corresponds to an average melting rate of 0.4 m/yr over the entire bottom surface area of all the floating ice shelves. Basal melting of the ice shelves lowers the $\delta^{18}O$ of shelf-water. Assuming that the melt-rate figure is correct, and taking into account the additional effects of freezing and precipitation, the oceanographic data suggest a 6-year residence time for water on the continental shelf. However, it is not at all certain that the Antarctic mass

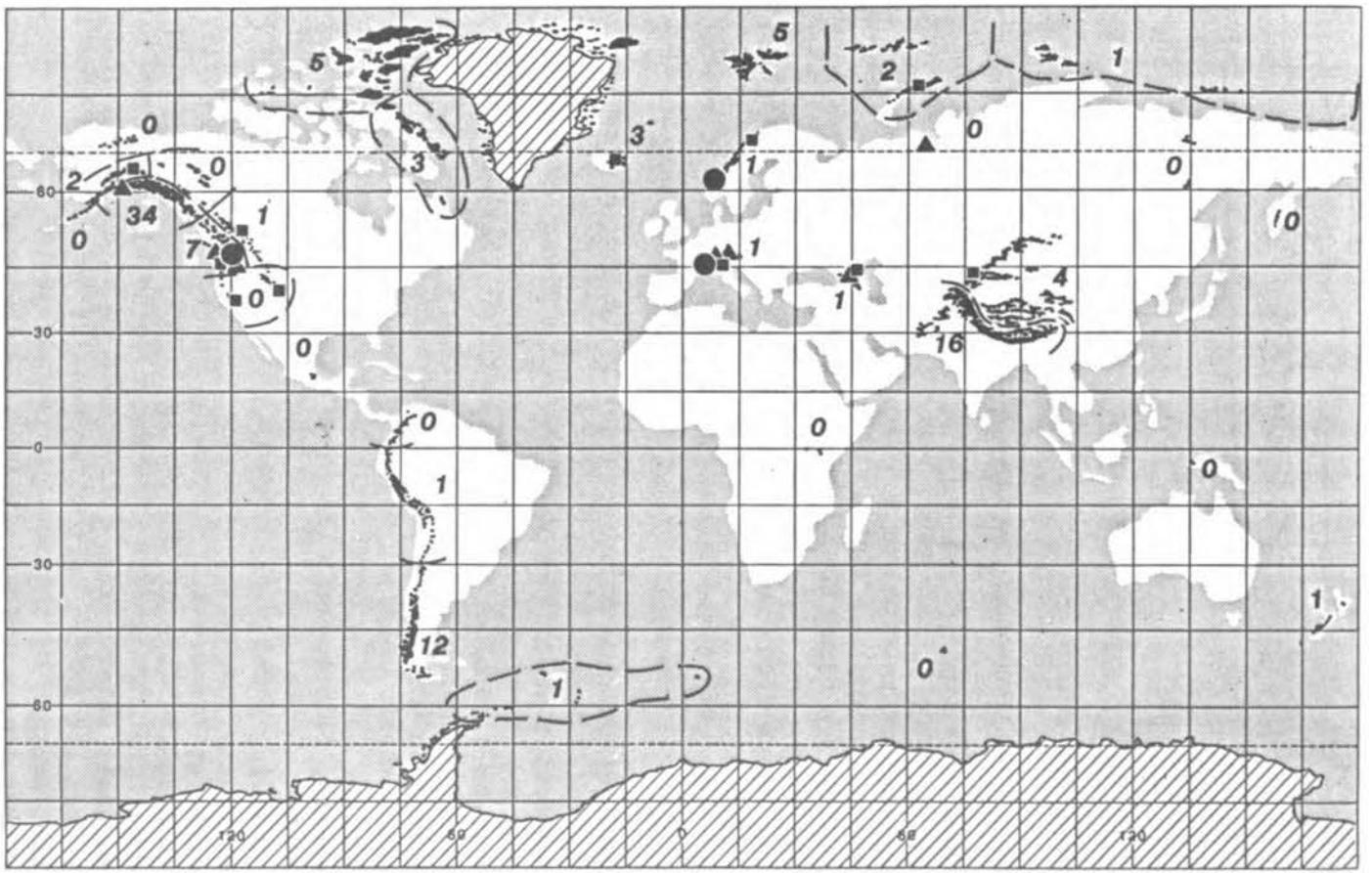

FIGURE 9 Locations of glaciers (black dots) exclusive of Antarctica and Greenland (areas with diagonal lining). Locations where long-term mass balance models are available are indicated by circles (models calibrated with long-term volume-change observations) or triangles (uncalibrated models). Squares indicate where other long-term volume-change data are available. Also shown, for each of 31 regions, is the percentage contribution of each region to the total volume of water transferred to the ocean from wastage of glaciers; 0 indicates less than 0.5 percent. Dashed lines separate regions.

balance is zero as assumed (see Section 3.5), nor are the mass input and calving fluxes well determined (e.g., see part of Section 3.5 on iceberg calving), so this estimate may require modification. There is little information available regarding short- or long-term variability in basal melting, basal freezing, or the residence time of shelf water.

3.3 CONTRIBUTION OF GLACIERS AND SMALL ICE CAPS TO SEA LEVEL

A Global Estimate

Observed long-term changes in glacier volume, and annual mass balance models, yield data on the transfer of water from glaciers, excluding those in Greenland and Antarctica, to the ocean (see this volume, Attachment 6). In general, these glaciers and small ice caps have been shrinking during the past 100 years. Shrinkage has been most pronounced among temperate and mid-latitude glaciers. Data on glacier mass balances are sparse, both temporally and spatially (Figure 9). An average change in glacier volume for the period 1900 to 1961 was calculated from the meager volume-change data and scaled to a global estimate by considering the intensity of the seasonal mass-balance fluxes. These data were used to calibrate the models to estimate the changing contribution of glaciers to sea level for the period 1884 to 1975.

The average rate of eustatic sea-level rise between 1900 and 1961 due to melting glaciers and small ice caps was found to be 0.46 ± 0.26 mm/yr, and the total rise was 0.28 ± 0.16 m (Meier 1984). Glaciers and small ice caps thus account for an important part of the observed sea-level rise.

More than a third of the calculated glacier contribution to rising sea level comes from the mountains bordering the Gulf of Alaska; the high mountains of Central Asia and the Patagonian Andes also make appreciable contributions. Analysis of these areas, especially the latter, has been hampered by a paucity of data.

Canadian Arctic Island Ice Caps

Measurements of mass balance on two small ice caps, a valley glacier, two large ice caps, and the Ward Hunt Ice Shelf for varying periods between 1959 and 1982 give a slightly negative glacier balance of 5 cm/yr (Figure 10) (see this volume, Attachment 7). Accumulation rates are approximately 20-25 cm/yr, and melt rates in the ablation zone range from 0 cm/yr at the equilibrium line to 100-200 cm/yr at sea level. Ice core records from the tops of the two large ice caps suggest that the mass-balance records refer to a period slightly cooler than the 1880-1980 average. A simple calculation suggests that a balance of -6 cm/yr may be applicable to the whole 100-year period for the Arctic Island ice caps.

Measurements of total vertical strain in three boreholes on Devon and North Ellesmere Ice Caps, thickness changes from repeated gravimetry on the Devon Ice Cap in the 1970s, and leveling at an ice-cap edge and across an outlet glacier of the same ice cap all suggest that the ice

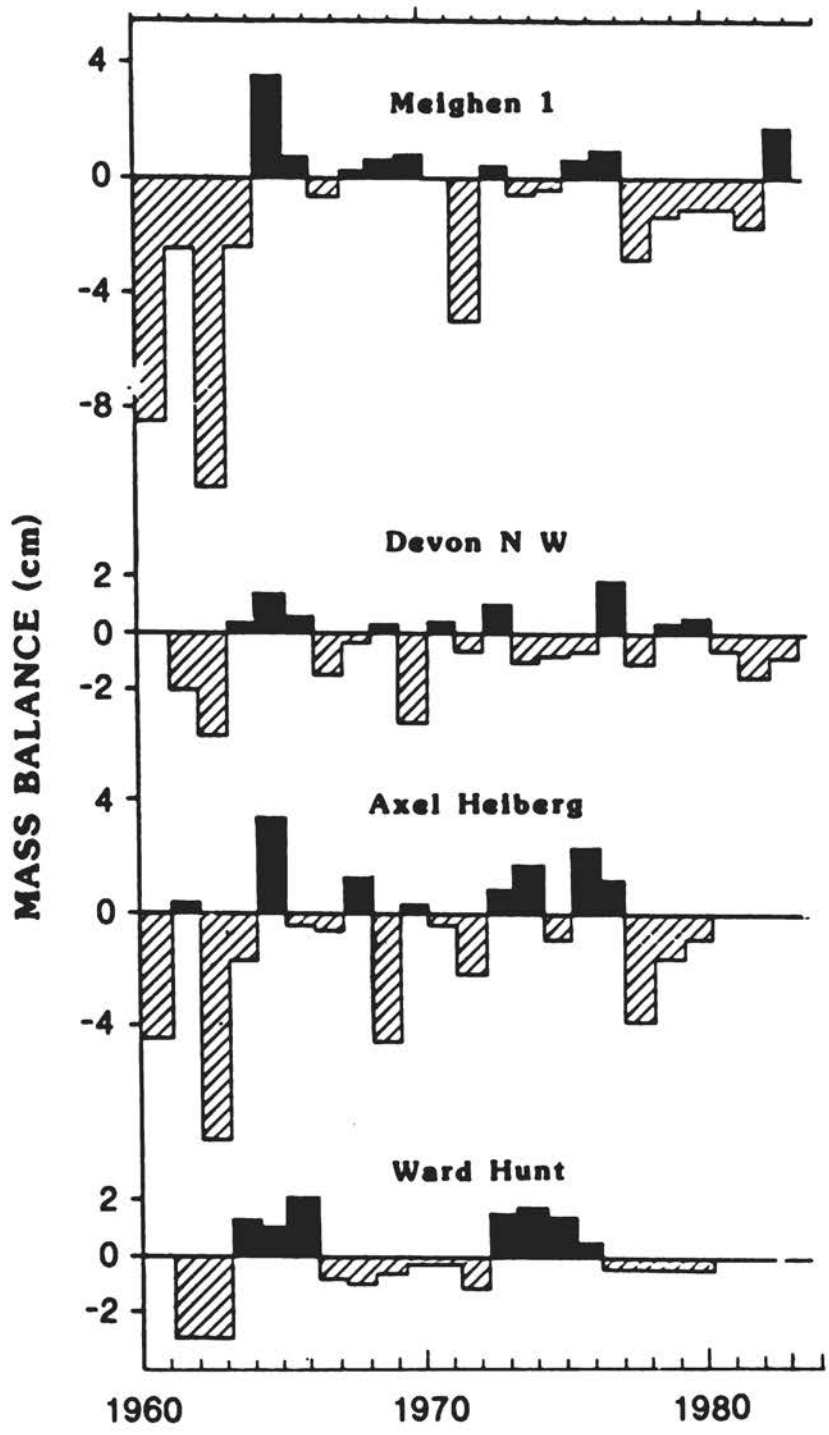

FIGURE 10 Mass balance of Meighen Ice Cap, northwest side of Devon Ice Cap, White Glacier on Axel Heiberg Island, and the Ward Hunt Ice Shelf on the Arctic Ocean coast of Ellesmere Island. Mass-balance fluctuations and the averages for the period of record are only a few centimeters of water equivalent per year.

caps are currently in an approximate steady-state condition. Comparison of aerial photography and satellite imagery taken in the 1950s and 1970s, respectively, show only very slight reductions in areas of the small ice caps and no detectable changes elsewhere. The various data sets are in agreement within the limits of the errors within each set.

A warm season increases the melt in the ablation area but has no effect on mass balance above the equilibrium line for ice caps in the Canadian Arctic, as the meltwater simply soaks into the firn and refreezes. A sustained warming of about 5°C, however, could remove much of the firn and cause a significant change in mass balance and runoff. The mean July temperature correlates well with melt rates, and so it would be desirable to estimate future melt rates in the Arctic as a function of the mean temperature during the warmest month.

3.4 CONTRIBUTION FROM GREENLAND

The mass balance of the Greenland Ice Sheet (Figure 11) can be estimated by the hydrological budget method; i.e., the time rate of change of the ice-sheet volume is the sum of input due to annual precipitation and loss due to annual melting and iceberg calving (see this volume, Attachment 8). Several estimates of the terms in this equation have been summarized by Weidick (1984):

Accumulation	500 ± 100 km^3/yr (water equivalent)
Melting	295 ± 100 km^3/yr (water equivalent)
Iceberg calving	205 ± 60 km^3/yr (water equivalent)

These estimates suggest that the Greenland Ice Sheet is not greatly out of balance with the present climate. However, the error limits show that the hydrological budget method cannot be used, at present, to draw a conclusion as to whether the ice sheet is growing or shrinking, nor is this method likely to provide an answer to the question in the near future.

Alternatively, direct measurements of the rate of thinning or thickening in specific areas can be extrapolated over the area of the entire ice sheet. Studies by several investigators at the Dye-3 borehole site show that the ice sheet is thickening there at a rate of 0.03 m/yr. Observations along the profile of the International Glaciological Expedition to Greenland (EGIG) indicate that surface elevations are increasing at an average rate of 0.085 m/yr in the accumulation zone of the west side of the ice divide, at latitude 70-72°N [Figure 12(a)] but are decreasing at an average rate of a few centimeters per year in the accumulation zone on the east side of the ice divide. However, observations along the same profile show that in the ablation zone, the West Greenland Ice Sheet surface is lowering at a rate of 0.2-0.3 m/yr at 70-72°N [Figure 12(b)]. This is in broad agreement with the 0.3-0.5 m/yr thinning rate inferred from geological data along the West Greenland margin.

It may be possible that the current thickening in central Greenland is due to the diminishing thickness of soft ice of Wisconsin

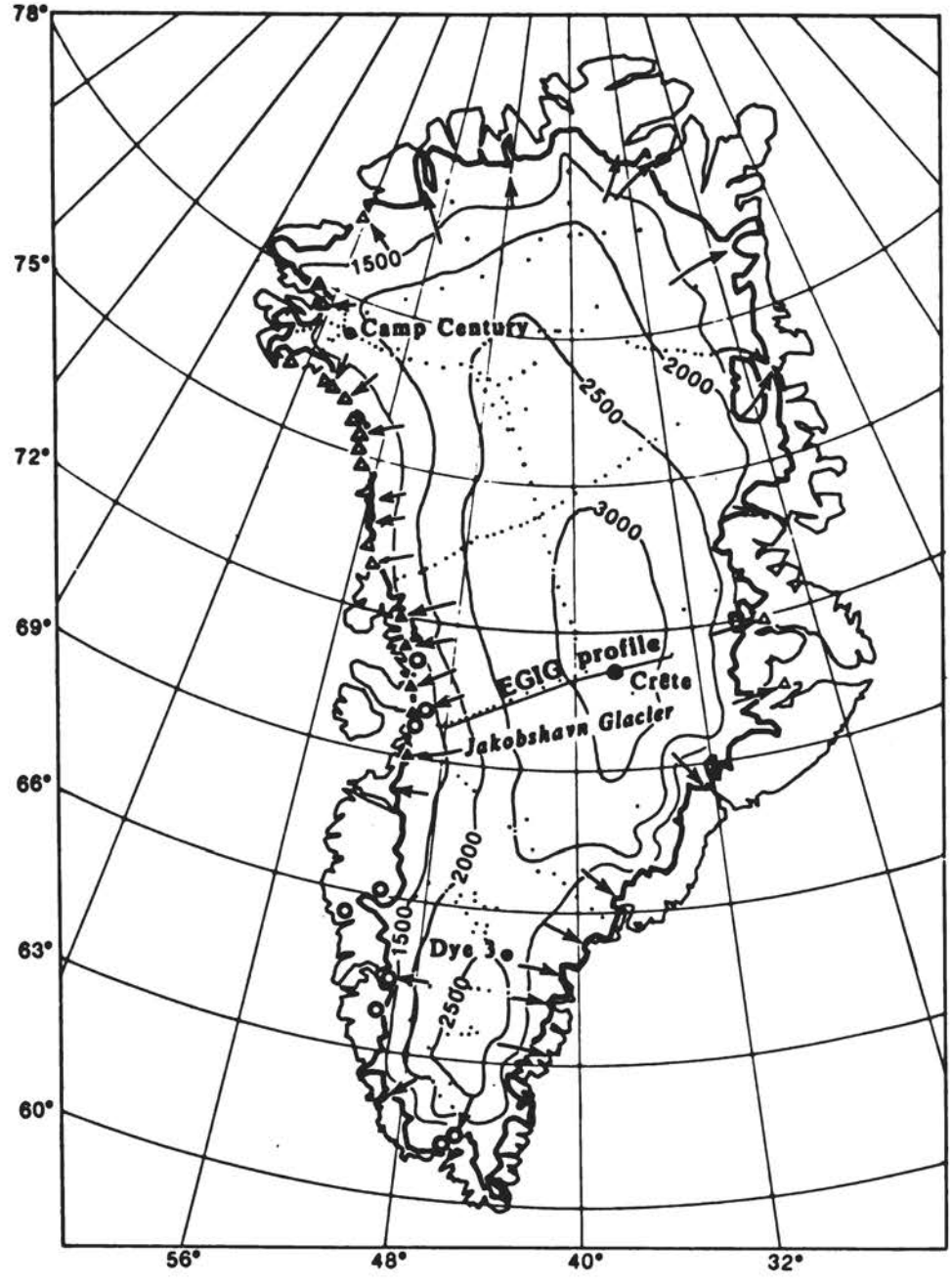

FIGURE 11 Surface topography in meters of the Greenland Ice Sheet. Border of the ice sheet indicated by heavy line. Major calving glaciers draining the ice sheet indicated by arrows, measurements of calving rates by solid triangles, and estimates or unpublished measurements of calving by open triangles. Modern ablation measurements indicated by open circles, and accumulation measurements by small dots. Large dots (Camp Century, Crete, and Dye 3) indicate deep core holes. The traverse profile of the International Glaciological Expedition to Greenland (EGIG) is also indicated (from Benson 1962; Radok et al. 1982; and this volume, Attachment 8).

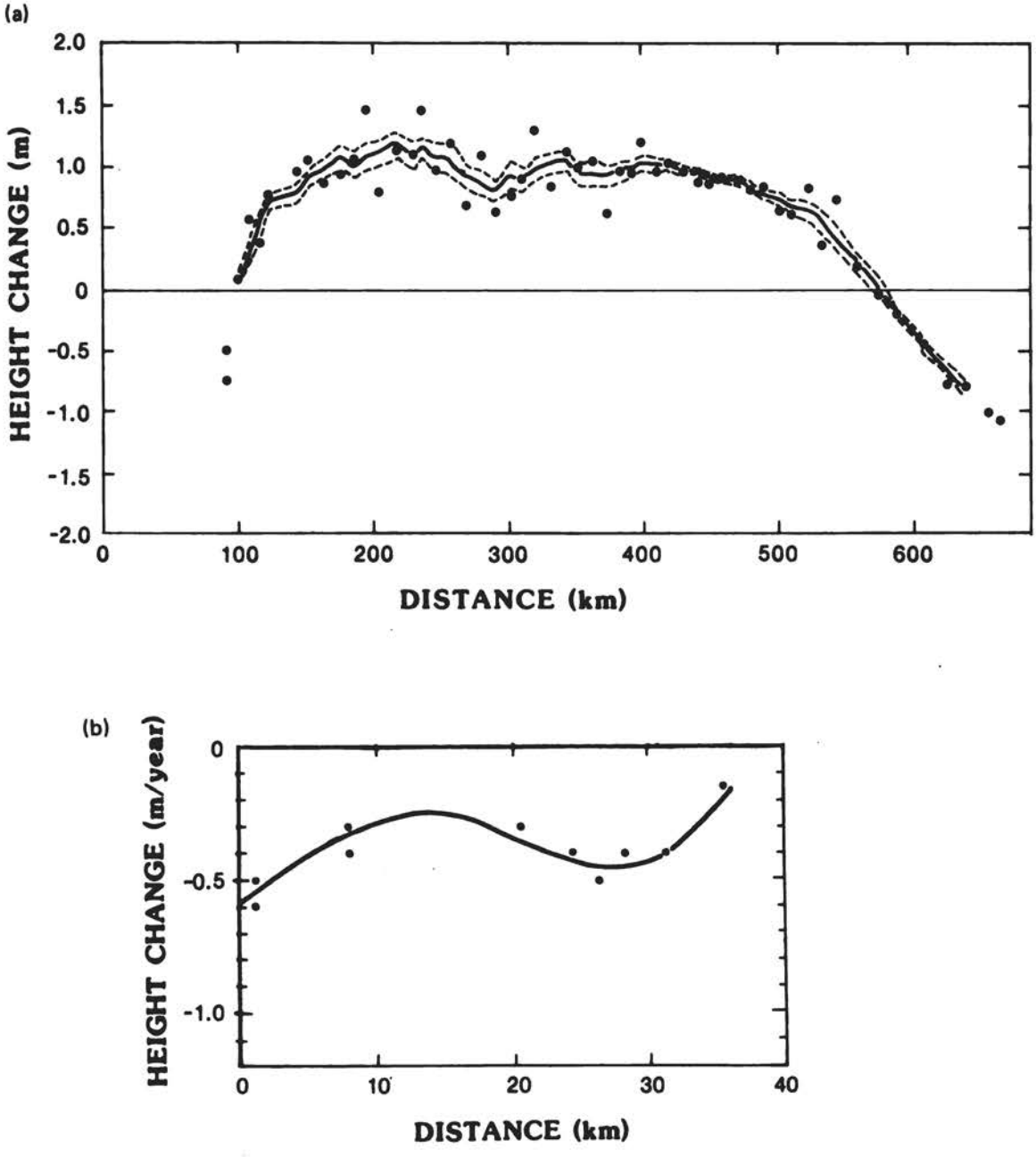

FIGURE 12 (a) Change in altitude of the surface of the accumulation area of the Greenland Ice Sheet along the EGIG Profile (Figure 11) for the period 1959-1968. Dots show measured values, the solid line is a 5-point running mean, and the dashed line shows error limits. Thickening is apparent except near the west (left) margin and in the east (right) (from Seckel 1977). (b) Rate of change in altitude of the surface of the ablation area at the west end of the EGIG profile, during 1948-1955. Solid line is a smooth curve through the observed points (dots). (from Bauer et al. 1968).

(Pleistocene) age in the deeper parts of the ice sheet. This suggestion needs to be checked with additional data from deep ice cores and through the use of dynamic models.

It is not possible at present to estimate reliably the exchange of mass between the Greenland Ice Sheet and the ocean, mostly owing to lack of observations in northern and eastern Greenland. Estimates of the total balance of the ice sheet based on an extrapolation of data from West Greenland to the entire ice sheet range from -110 km^3/yr to +270 km^3/yr (water equivalent). The corresponding rate of sea-level change is +0.3 to -0.7 mm/yr.

If the sparse observations of recent changes in the elevation of the ice-sheet surface are extrapolated to the entire ice sheet, thinning in the marginal area corresponding to a sea-level rise of about 0.2 to 0.3 mm/yr, and thickening in the accumulation area corresponding to a sea-level lowering of about 0.3 to 0.4 mm/yr, is indicated. The maximum expected annual variation due to the variability of net ablation from the Greenland Ice Sheet is 0.3 mm/yr.

3.5 CONTRIBUTION FROM ANTARCTICA

Antarctic Mass Balance--An Assessment

The estimate of Antarctic mass balance has improved over the last decade owing to increased coverage of accumulation and ice-flow measurements (see this volume, Attachment 9). With these measurements, estimates of the overall balance have tended to become closer to zero, ranging about -20 percent to +50 percent from a balance state. This is equivalent to a change in sea level ranging from a rise of 1.2 mm/yr to a fall of 3 mm/yr, respectively.

The maximum melt rate from the bottom of the Antarctic inland ice sheet is 3 mm/yr in areas where it is greatest, which makes a negligible contribution to rising sea level. The contribution to overall mass balance from basal melting beneath ice shelves is very uncertain. Under the Amery Ice Shelf (Figure 13) basal freezing appears to occur everywhere except close to the ice front. Slow basal freezing occurs under inland parts of the Ross Ice Shelf, and basal melting occurs closer to the ice front.

Other uncertainties in the Antarctic mass-balance estimates arise from lack of accumulation data over approximately one third of the continent and lack of outflow measurements around more than 50 percent of the coast. The problems involved are great, and the measurements are unlikely to be completed within the next decade. To determine the rate of thickening to within 15 percent accuracy from ground measurements, the average accumulation rate--probably about 0.15 m/yr--must be measured to better than 10 percent accuracy. An independent technique for determining net balance used direct measurement of surface elevation from satellite radar or laser altimetry combined with geodetic control (see this volume, Attachment 14).

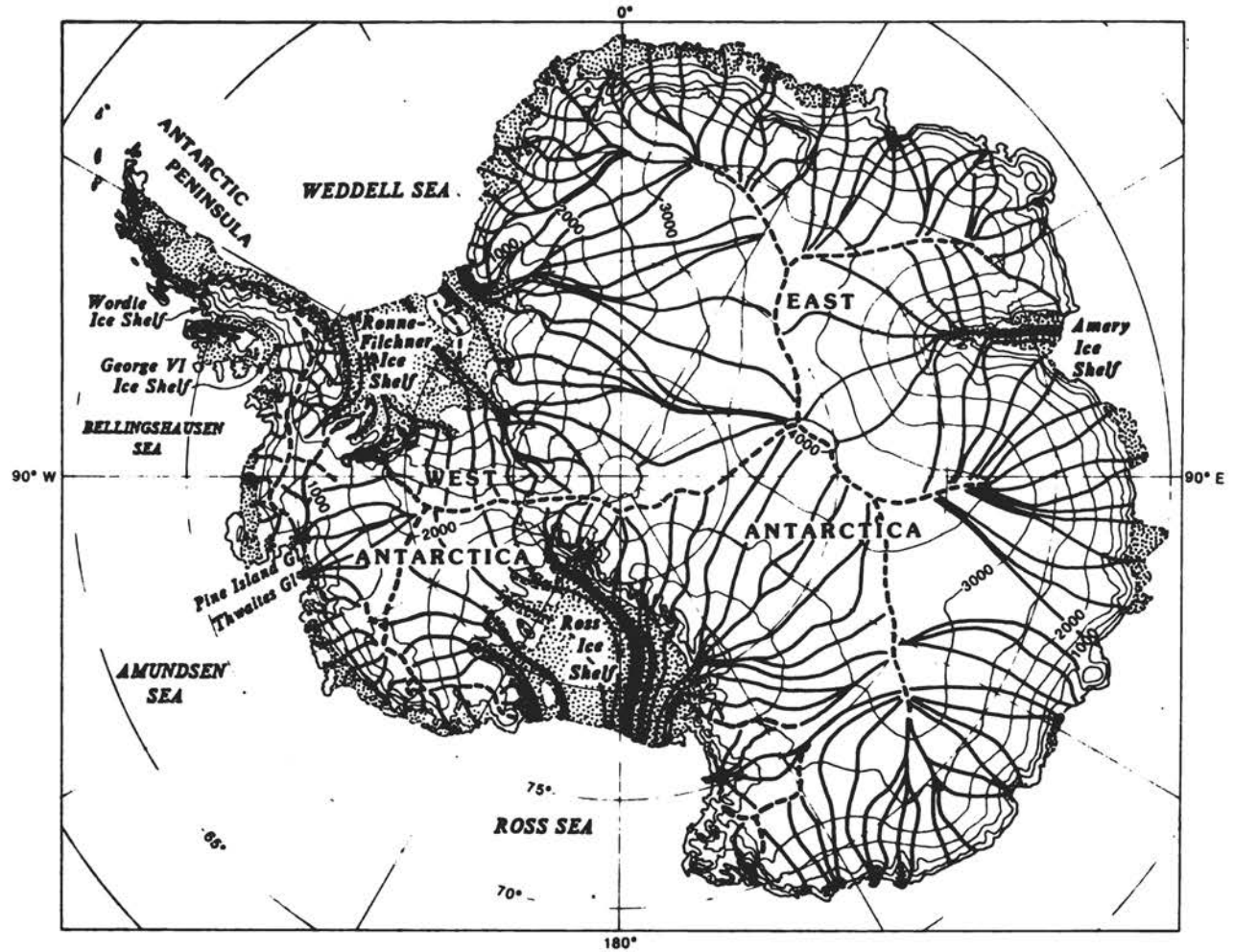

FIGURE 13 Surface topography (in meters) and flow directions (heavy lines) in Antarctica. Major ice divides are shown with dashed lines, and ice shelves are stippled. Note that most flow lines end in ice shelves; some others end in ice shelves that are too small for the scale of this map (from Drewry 1983).

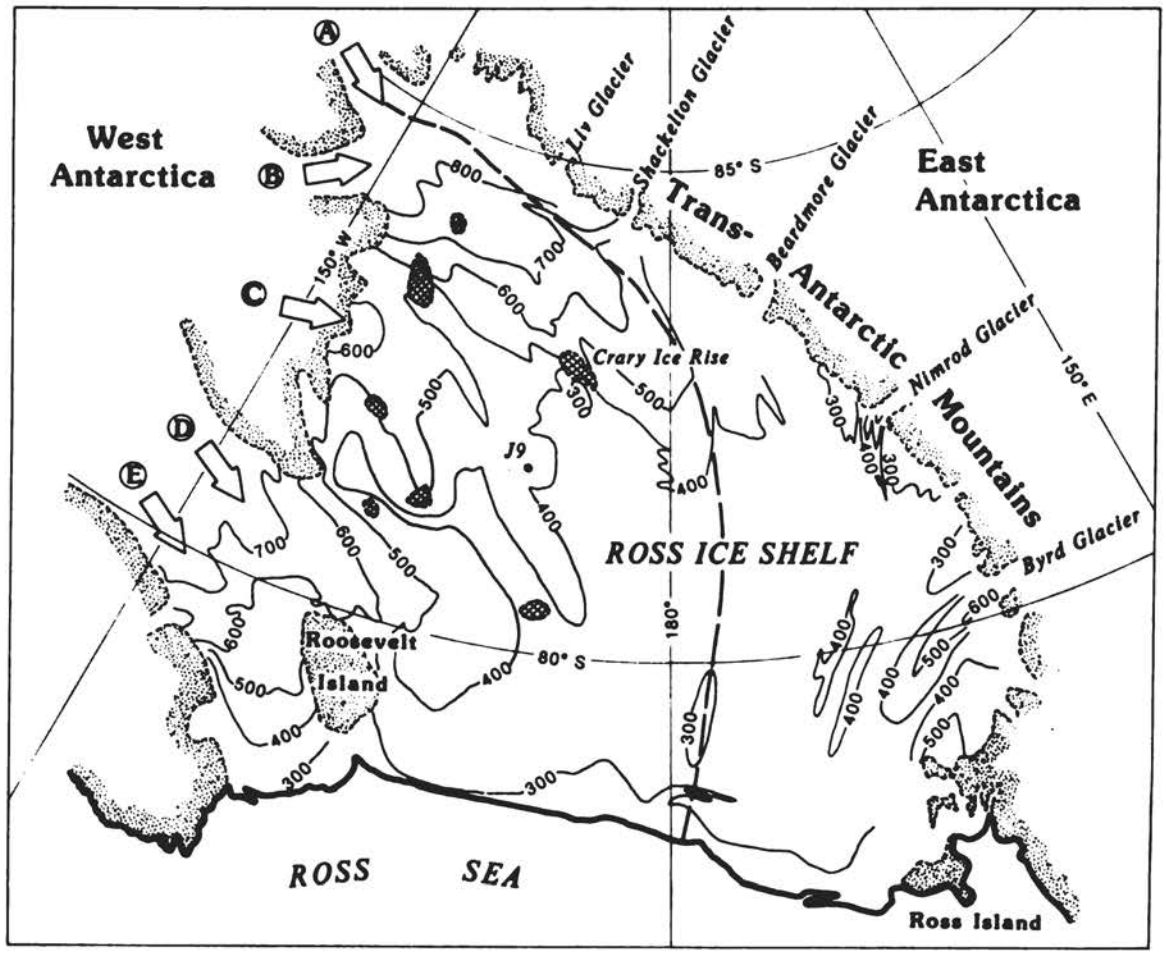

FIGURE 14 Thickness in meters of the Ross Ice Shelf. Island and major areas of grounded ice are stippled, and ice rises are cross hatched. Ice streams A through E are indicated by arrows. The dashed line separates ice derived from West Antarctica (left) from that derived from East Antarctica (right). J9 is the site of a drill hole through the ice shelf and measurements in the water column below.

West Antarctica, Ross Sea Sector

Extensive measurements made on the Ross Ice Shelf during the 1970s makes this sector one of the best known (see Figure 14). The ice thickness has been mapped in some detail, velocities of ice-shelf movement are known for the entire ice shelf from repeated satellite positioning combined with strain-rate observations, and surface mass balance rates are known from measurements of the depths to dated radioactive fallout horizons. From these data it is possible to make estimates of the sum of the rates of basal melting and change in thickness of the ice shelf (see this volume, Attachment 10). Calculations related to three flow bands within the part of the ice shelf fed by the West Antarctic inland

ice suggest that the mass balance of the ice shelf itself is not greatly different from zero but may be slightly positive (Thomas and Bentley, 1978; Jezek and Bentley, 1984). Similarly, study of the outflow from an East Antarctic outlet glacier (Nimrod Glacier) that can be traced across the ice shelf also yields a mass-balance estimate close to zero and suggests further that the basal melt rate must be low if the ice shelf is not thinning. On the other hand, comparisons of the mass fluxes into the ice sheet separately from East Antarctica and West Antarctica with the corresponding fluxes out near the ice-shelf front lead to the conclusion that basal melt rates of 0.1 to 0.2 m/yr beneath the main body of the ice shelf (excluding a hundred kilometer band near the ice front, wherein melt rates are high) are needed to maintain steady state. Thus even in this well-studied region the evidence is equivocal. Measurements that can ascertain basal melting rates and ice-shelf thickening rates separately are badly needed.

Another result of the Ross Ice Shelf studies is evidence that the ice shelf is capable of noticeable changes in its dynamics on a time scale of a century or two.

Antarctic Peninsula, Weddell Sea, and Amundsen Sea Sectors

The Antarctic Peninsula (Figure 13) has the warmest climate and highest snowfall in Antarctica; it receives 8 percent of the total accumulation while covering only 2.5 percent of the grounded ice area (see this volume, Attachment 11). However, even a gross change in the net accumulation would have only a small effect on sea level, and sea level would only rise about 0.5 m if all the ice in the peninsula were to melt. It is not feasible to give an accurate figure for the mass balance of the Antarctic Peninsula. Satellite images show that the Wordie and George VI Ice Shelves have diminished in recent years. Without data on grounding-line movement or ice velocity or thickness changes it is impossible to interpret the retreat in terms of ice-sheet shrinkage. Extreme limits of between 0 and 0.2 mm/yr could be placed on relative sea-level rise due to mass loss from the Antarctic Peninsula in the next 100 years.

The Filchner-Ronne Ice Shelves (Figure 15), which together make the largest ice shelf by volume, drain nearly one quarter of the Antarctic Ice Sheet to the Weddell Sea. The accumulation rate along the coast in the Weddell Sea sector is unusually high, about 0.40 m/yr, as indicated by pit stratigraphy. Radio-sounding measurements suggest strong bottom melting over most of these ice shelves, apart from the thin central area. Using estimates at the ice fronts of thickness, velocity, and total length gives the amount of ice expected to be lost by calving, in a steady-state condition. Combining this estimate with that of the ice input from the catchment area and the accumulation over the ice shelves themselves suggests an average basal melt rate for both ice shelves of about 1.0 m/yr. However, only one mass-flux measurement exists across the whole of that coast.

The thin ice in the center of Ronne Ice Shelf is the result of flow being impeded by a locally grounded area between Korff and Henry Ice Rises; thinning of the ice shelf by only a few meters would remove this

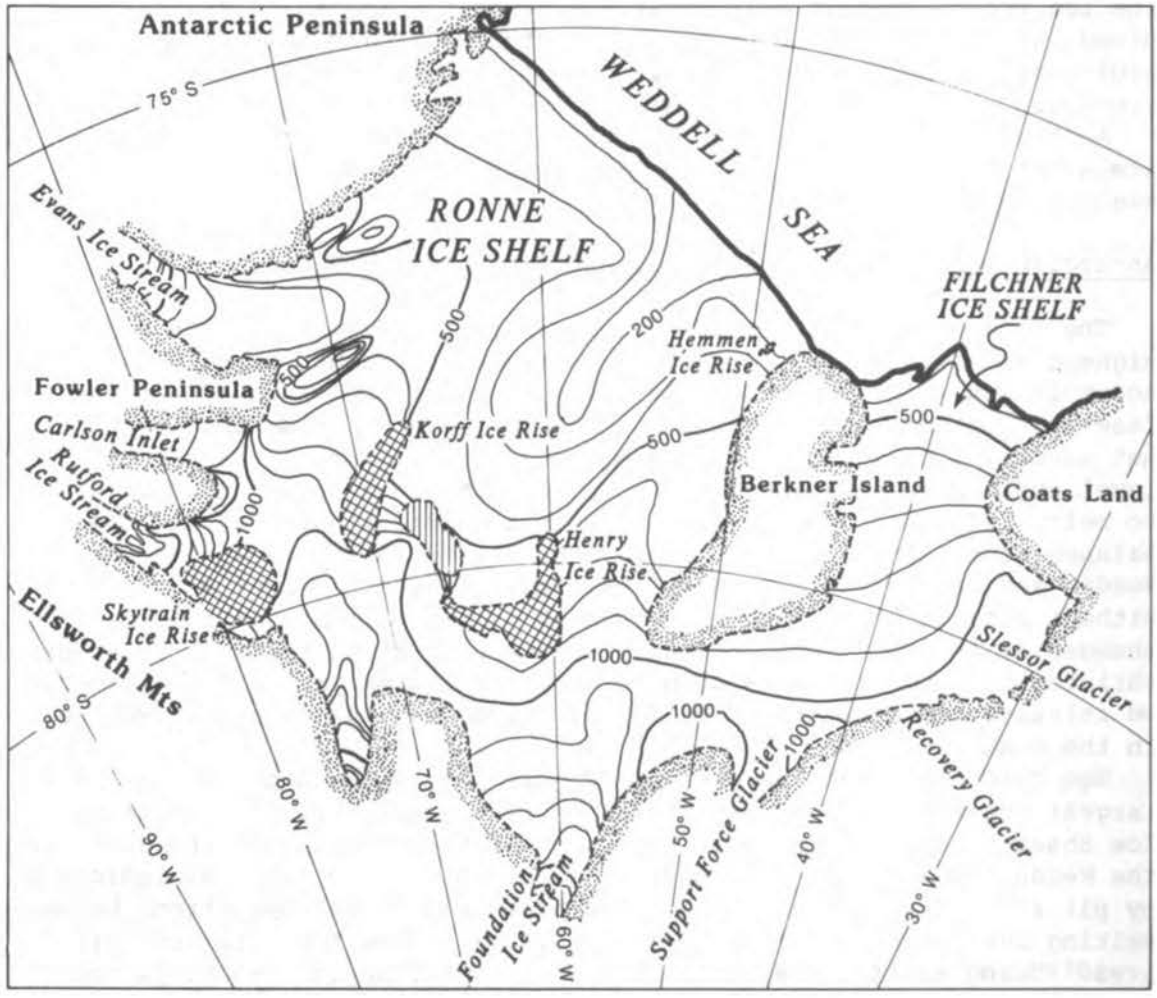

FIGURE 15 Thickness in meters of the Filchner-Ronne Ice Shelf. West Antarctica is to the left and south (below), East Antarctica is to the right. Islands and major areas of grounded ice are stippled, ice rises are cross hatched, and an area where the ice shelf is partially grounded is lined vertically.

restriction and reduce the backpressure on the inland ice sheet. Removal of this restraint might increase sea level by about 80 mm averaged over a period of about 500 years, i.e., at a rate of about 0.2 mm/yr. In total, sea level may increase by as much as 0.4 mm/yr owing to accelerated ice discharge in this region.

The Pine Island and Thwaites Glaciers may have potential for rapid ice-sheet disintegration. This conclusion is based on the belief that if sea level rises or if the ice thins then retreat of the grounding line could continue into the heart of the West Antarctic Ice Sheet unless stopped by a high step in the bedrock. On the other hand, radar sounding flights show that part of the present grounding line of the Pine Island Glacier appears to be held at the foot of a rock bar about 200 m high. Pine Island Glacier does not appear to be undergoing any extraordinary behavior. Mass-flux calculations over the catchment area appear to indicate a positive balance, with the total annual input of 86 ± 30 km^3 water equivalent exceeding the annual mass flux at the ice front of 25 ± 6 km^3 water equivalent by a large amount.

Iceberg Discharge

The extensive set of iceberg observations now becoming available indicates that the number of icebergs in the Southern Ocean and the rate of iceberg calving from Antarctica may have been underestimated (see this volume, Attachment 12). Also, most of the floating ice shelves are growing larger and storing progressively more ice, so the discharge rate from the grounded ice sheet is higher than can be deduced from the number of floating icebergs. Calving is very spasmodic; ice shelves grow for many years, then large pieces break off. With conservative estimates, the data suggest that the calving rate from Antarctica is more than 2×10^{15} kg/yr. The ongoing collection of iceberg statistics should, within a few years, provide a reasonably firm foundation for evaluating the calving rate, provided we can improve our understanding of the life expectancy, or residence time, of the Antarctic icebergs, now estimated at roughly 12 years near the coast and up to 20 years for grounded icebergs near floating glacier tongues. Estimates of iceberg lifetimes and the distribution of icebergs around the whole continent need to be defined more precisely before a calving rate can be stated with confidence.

Research Needs

From the foregoing it is clear that there are several research questions that badly need attention if better estimates of present-day Antarctic mass balance and predictions for the future are to be obtained. What are the factors that determine ice-stream flow with sliding? The most important regions to monitor, measure, and model can be delineated from our present knowledge of ice flux, and emphasis should be placed on these regions for further study. What is the role of the West Antarctic ice streams in the ice-sheet dynamics; how and why do they play that role? What is the basal mass balance under the ice shelves, and how can it be predicted from oceanogrpahic data? How

can changes in thickness of the ice shelves be measured separately from measurements of basal melting rates? What is the iceberg calving rate around the Antarctic at present, and how can the effect of a changing environment on the calving rate be determined? What are the time scales for variability in accumulation rate and iceberg discharge?

3.6 OTHER EVIDENCE

Evidence from Earth Rotation Data

Munk and Revelle (1952) argued that, on the basis of Earth rotation observations and data on true polar wander, some present-day melting of continental ice masses must be occurring. A more recent series of analyses is based on the assumption that subsequent to 6000 years before present, no further ice-mass disintegration occurred (see this volume, Attachment 2). Both the present-day expected polar wander (rate and direction) and the present-day rate of change of the length of day are modeled. The model correctly predicts both the true polar wander at the rate of 0.95×10^{-6} degrees/yr toward Hudson Bay that is shown by the International Latitude Service data and the nontidal acceleration of planetary rotation shown by ancient eclipse records and more recently by laser tracking of the LAGEOS satellite. The parameters of the model are fixed by comparing the model's relative sea level (RSL) and gravity-anomaly predictions to extensive RSL and gravity-anomaly data. When the model's Earth-rotation results are then compared with Earth-rotation data, the predictions agree well with the observations. It is not necessary to take into account additional tidal dissipation caused by submergence of the continental shelves during the past 10,000 to 20,000 years.

Further, the mantle viscosity profile required by the Earth-rotation data is compatible with that required by the free-air gravity and relative sea-level observations. Thus, present-day ice-sheet wastage is not required to fit the true polar wander data when a spherical-Earth model with a realistic radial viscoelastic structure is employed. This structure is of fundamental importance to the accurate prediction of true polar wander.

This model could conceivably be sensitive enough to rule out the possibility of a small rate of shrinkage of the polar ice sheets at the present time if all the other parameters were sufficiently well known. In its present form, the model does not rule out the possibility of some meltwater input to the ocean, but meltwater input is not required.

Global Land-Ice Monitoring

Standardized information about the distribution of and the variation in the Earth's ice cover is being gathered by the Temporary Technical Secretariat for the World Glacier Inventory and the Permanent Service on the Fluctuations of Glaciers (see this volume, Attachment 13). In 1986, the function of the Temporary Technical Secretariat will be assumed by the Permanent Service. A program is currently being designed

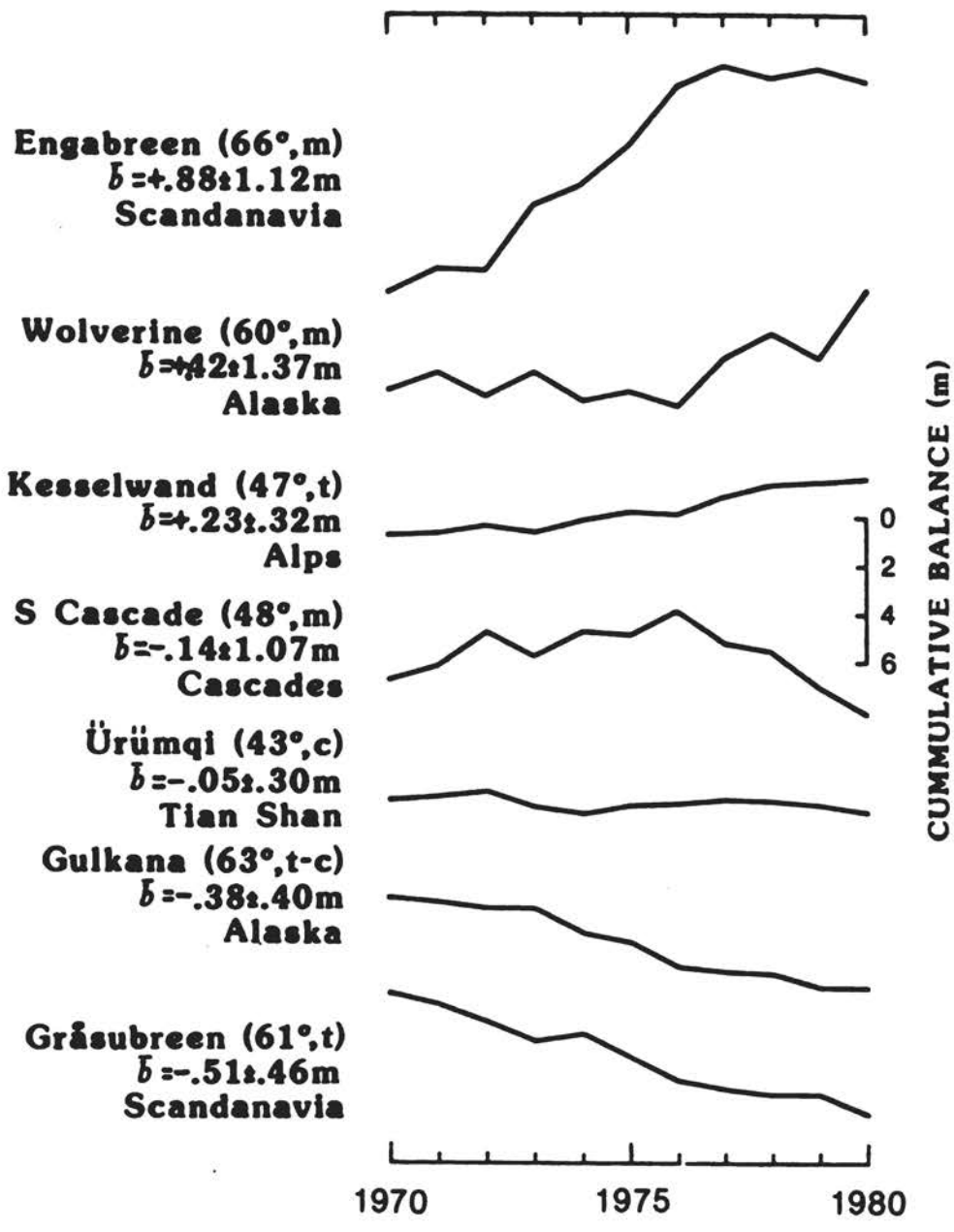

FIGURE 16 Cumulative mass balance of seven mountain glaciers in the northern hemisphere during 1970-1980. In parentheses are latitude and climatic environment (m, maritime; t, transitional; c, continental). Mean balance for period (b) is also given in meters of water equivalent per year. Glaciers in the same region (Scandinavia and Alaska) show disparate trends, apparently related in part to their climatic environment.

that includes (1) documentation at short intervals of mass-balance time series, (2) collection and publication of general fluctuation data, and (3) satellite observation of remote glaciers.

Mass-balance time series (Figure 16) are of primary importance for climate monitoring and hydrological assessments, and such information is being used to derive past and future contributions of mountain glaciers to sea-level changes. To infer the contribution to sea-level change from a given ice mass, it is necessary, in general, to measure its mass balance. In remote regions where sparse measurements must be extrapolated over large areas, large errors can be introduced. In such cases it is possible to construct a time series of data from individual poles or stakes. This eliminates some uncertainties but provides only limited information on long-term trends for the ice mass as a whole.

General fluctuation data including observations on glacier-length variation are basic to glaciological studies and paleoglaciological reconstruction. The lack of information about mass changes of the large polar ice sheets is still the most fundamental gap, which may eventually be closed by satellite altimetry. It is hoped that satellite observation of selected glaciers will extend the available information into less accessible areas and allow worldwide intercomparison of glacier fluctuations. A feasibility study is needed on monitoring the length of small glaciers by satellite imagery.

Present and near-future satellite remote-sensing technology already permits or soon will permit systematic, repetitive surveys to be accomplished of the world's large glaciers and ice sheets (Figure 17; see this volume, Attachment 14). Very-high resolution images such as those to be obtained by the SPOT satellite (10-m resolution) will yield enormous volumes of data, making it practical to study only selected representative areas and making it necessary to address problems of data handling and cost.

Determining the third dimension (altitude, thickness) of glaciers has been hampered by a lack of development of appropriate satellite remote sensors, although some success has been achieved with data from radar altimeters in determining elevations of ice shelves in Antarctica and the gently sloping parts of the Antarctic and Greenland Ice Sheets that lie at less than 72° of latitude. Recent work has established the feasibility of mapping margins of ice shelves from radar altimetry data. A working group at NASA is considering potential applications of synthetic-aperture radar to ice measurements. The next mission that could provide large quantities of data will be in the late 1980s on the Space Shuttle, the European ERS-1 satellite, and perhaps other satellites. If these satellites are going to be employed to collect glacier data, the geographical areas of interest must be defined very soon.

Evidence for Recent Changes in Snow Cover, Sea Ice, and Permafrost

Determination of the variability and trends in snow cover are needed to help in assessing the effects of CO_2-induced warming on the mass balance of glaciers and ice sheets (see this volume, Attachment 15). There is evidence of increased snowfall with higher winter temperatures in some regions, but the net effect of this is uncertain. Sea-ice

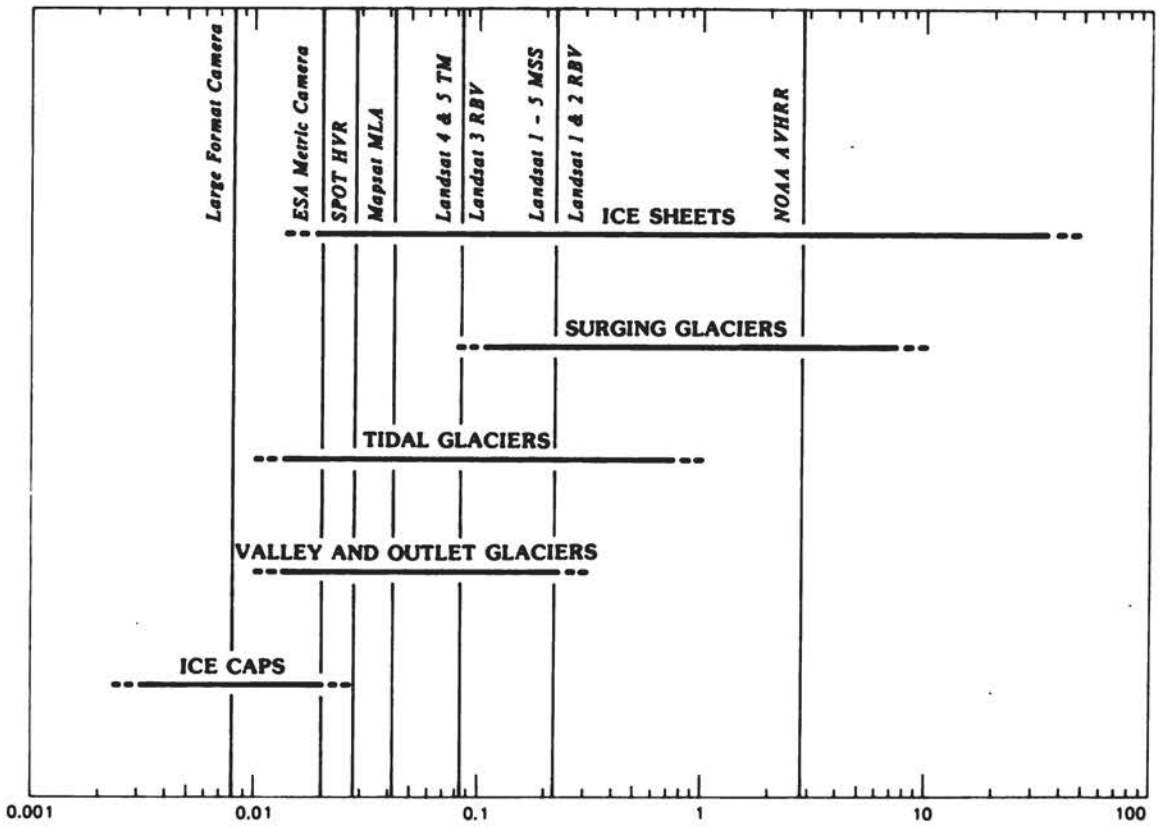

FIGURE 17 Graph showing the relationship between spatial resolution of existing and future imaging sensors (visible and infrared) on board various satellites and the approximate range of annual dynamic change of termini of different types of glaciers. The termini of ice sheets include ice shelves from which large tabular icebergs can calve off, producing large annual changes. Spatial resolution of a camera/film-filter system is given in meters per line pair. Spatial resolution for nonphotographic imaging sensors is taken to be 2.8 times the pixel resolution where a pixel is the dimension on the Earth's surface of a single picture element. ESA, European Space Agency; HRV, haute resolution visible (SPOT sensor); MLA, multispectral linear array; MSS, multispectral scanner (Landsat sensor); RBV, return beam vindicon (Landsat sensor); SPOT, Systeme Probatoire d'Observation de la Terre (French satellite); TM, thematic mapper (Landsat sensor); AVHRR, advanced very-high-resolution radiometer.

extent around Antarctica affects the snowfall on Antarctica and the ice shelf-oceanographic regime.

The observed annual maximum extent of northern hemisphere snow cover is 46 x 10^6 km^2 (standard deviation 2.5 x 10^6 km^2). The seasonal variation in snow-cover volume (water equivalent) is approximately 5 mm in sea-level equivalent, and the interannual variability is 1 mm.

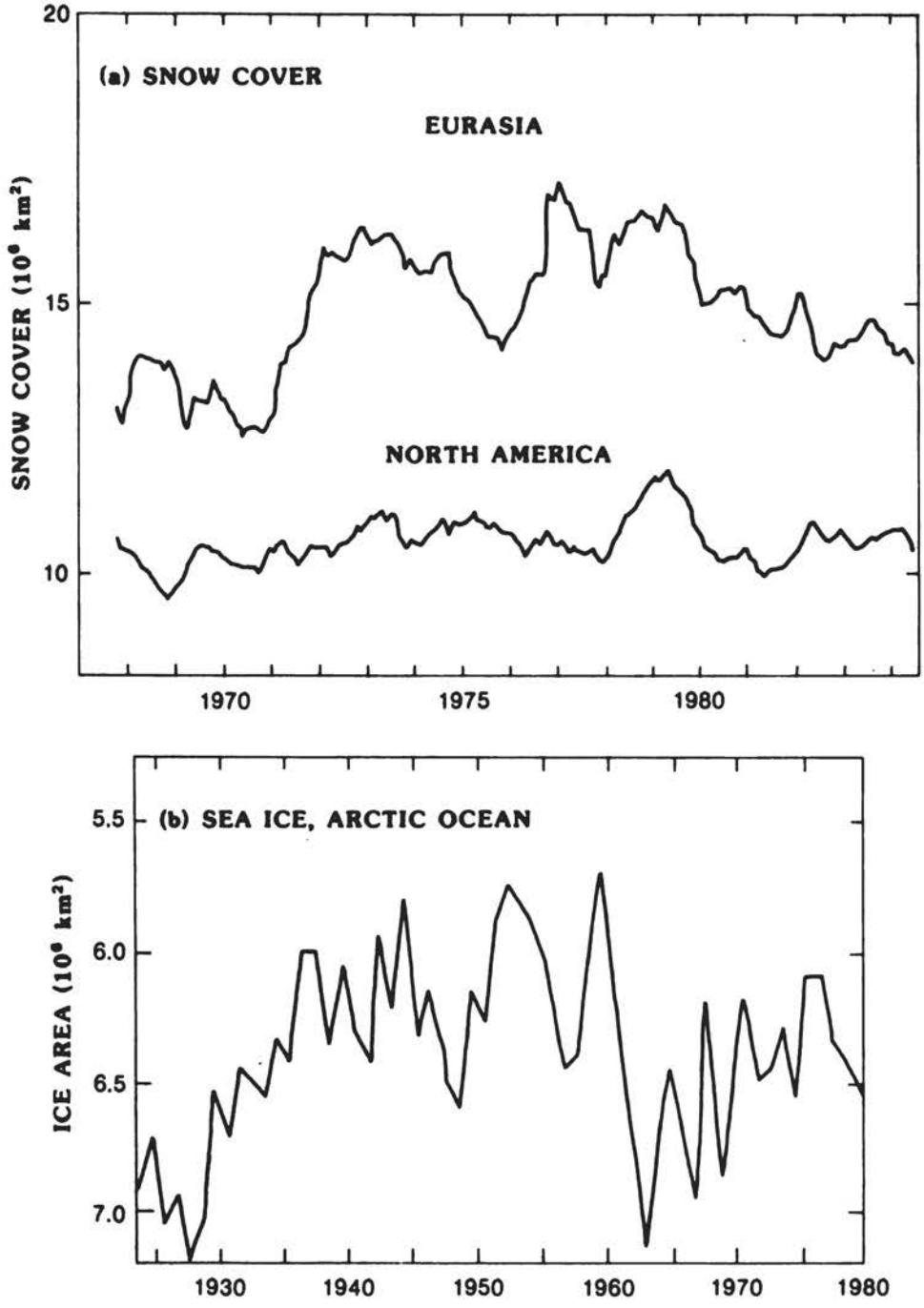

FIGURE 18 (a) Changing area of snow cover in Eurasia and North Amlrica, 1967-1984, smoothed using a 52-week running mean. Eurasia accounts for most of the variabilty, and no obvious long-term trend is apparent in either region (from M. Matson, unpublished). (b) Changing area of late August sea ice on the Arctic Ocean, 1924-1980. No obvious long-term trend is apparent, and the curve in the 1967-1980 interval shows little correlation with that in (a) (from Zhakharov 1981).

Eurasian snow cover dominates the variability in hemispheric extent [Figure 18(a)].

There are no evident recent trends in sea-ice extent in either hemisphere. Regional interannual ice anomalies, associated with atmospheric circulation anomalies, are large. For Arctic sea ice in late summer, there appears to be a fluctuation of $\pm 1 \times 10^6$ km^2 in extent associated with ± 1°C summer temperature anomalies (for 5-year running means). Fluctuations of Arctic ice extent for 1950-1980 show no apparent relationship with those of northern hemisphere snow cover [Figure 18(b)] or of Antarctic ice.

The water content of global permafrost is poorly known but may be on the order of 0.09 to 0.17 m equivalent global sea level. A ground-ice-melt contribution to the sea-level rise is unlikely to exceed a few millimeters over the next 100 years, in view of the partial melt anticipated for warming and the slow time response of ground ice.

Long-term monitoring of global sea ice and snow cover via passive microwave remote sensing is practical and essential. The feasibility of this technique for snow-cover mapping has been demonstrated but, so far, not routinely applied. Records of surface snow-cover observations also need to be compiled to augment the historical data base on variability and to serve as a calibration for the satellite data. Monitoring of changes in permafrost temperatures and improved information on permafrost extent, thickness, and ice content are also necessary to refine our estimates of warming impacts on this component of ice and snow on Earth.

4.
Probable Land-Ice and Ocean Exchanges during the next 100 Years, Exclusive of Antarctica

During the next 100 years, glaciers and ice caps (those ice masses other than the two large ice sheets) will probably make an increasing contribution to rising sea level. A larger contribution may come from increased ablation of the Greenland Ice Sheet, but attempts to make realistic estimates of this have been hampered by large uncertainty as to its present mass balance. In this chapter, predictions (derived from a general atmospheric circulation model) of increased ablation in marginal areas of the Greenland and Antarctic Ice Sheets are discussed, and the small glaciers in more temperate latitudes are considered. A program of measurements is suggested to reduce uncertainty regarding the present mass balance of the Greenland Ice Sheet, and a rough estimate of the likely contribution to rising sea level from Greenland is given. The more difficult question of the stability of the potentially unstable parts of the Antarctic Ice Sheet is discussed in Chapter 5.

4.1 PROBABLE CHANGES IN CLIMATE CAUSED BY INCREASING CO_2

Present global climate models have not been designed with the objective of examining sea-level response to global climate change. However, they can provide a preliminary evaluation of certain physical processes that are capable of contributing significantly to sea-level change and in this way help indicate the processes that should be studied more carefully (Hansen et al. 1983, 1984). Unfortunately, existing global climate models do not simulate the present climate at high latitudes, especially in Antarctica, very precisely, indicating that much improvement is needed before predictions of the future climate can be made with confidence (NRC Committee on Glaciology 1984).

Radiation-transfer calculations for steady-state models indicate that a doubling of CO_2 would produce a radiative forcing of about 4 W/m^2 (global average) and that, in the absence of any climate feedbacks, a global warming of 1.2-1.3°C would result. Global three-dimensional models that include climate feedback processes yield a global warming of 2-4°C, or possibly more, for doubled CO_2, indicating a net climate feedback factor of the order of 2. However, there is substantial uncertainty in our understanding and modeling of these feedbacks, which in the present models are due mainly to changes in atmospheric water vapor,

clouds, and sea-ice coverage. The effect of increasing concentrations of other radiatively active gases in the atmosphere will be to increase this warming further, perhaps by another 2-3°C (NRC Carbon Dioxide Assessment Committee 1983). Studies (NRC Climate Research Board 1979, 1982; NRC Carbon Dioxide Assessment Committee 1983) during the past several years give a best estimate for climate sensitivity of 3 $\pm$ 1.5°C for doubled CO_2, but it is not possible to exclude values somewhat outside this range.

Climate models and empirical data indicate that global surface warming will be amplified at high latitudes, especially in the northern hemisphere, perhaps by a factor of 2 or more, owing to the ice/snow albedo feedback and the greater atmospheric stability at high latitudes. Examination of the results of an existing doubled-CO_2 experiment suggest two processes that may contribute significantly to sea-level rise in the next century: (1) increased surface melt at the fringes of the ice sheets, principally in southern Greenland and some areas on the Antarctic coast, where ice losses may be balanced only partly by increased accumulation in the ice-sheet interiors; and (2) thermal expansion of ocean water due to higher air temperature. Climate models are not yet capable of predicting confidently the longitudinal distribution of climate change, as indicated by wide variations among different models. Time-dependent climate change will be extremely difficult to model reliably, because it will require realistic representation of the coupled atmosphere-ocean-sea ice system.

Principal improvements needed in the global climate models to obtain more realistic predictions of sea-level effects include (1) more accurate calculation of atmospheric transports of water vapor and sensible heat, which may require improved numerical schemes; (2) more realistic representation of clouds and sea ice; (3) more precise representation of surface topography, so that the ice surfaces occur at the proper elevations, which may require use of subgrid topographic variations in the models; (4) more accurate calculation of the albedo of snow and ice surfaces, including the changes in albedo accompanying surface melt and aging of snow; and (5) realistic representation of other aspects of ice and snow physics, including restriction of meltwater runoff to coastal ice slopes and firn that is saturated with meltwater. A critical requirement of the models is that they portray realistically the tracks, frequency, and intensity of storms that travel from the Antarctic Ocean onto the continent, since they are believed to be the principal mechanism for horizontal transport of water vapor and sensible heat to Antarctica.

4.2 EFFECT ON SMALL GLACIERS

Glaciers and ice caps smaller than about 10 to 100 km^2 react to changes in the climatic environment without entering the process as a feedback mechanism. This makes the description of their energy balance in terms of atmospheric variation meaningful, although an important term

in their mass balance, redistribution of snow by wind, generally defies analytical treatment.

For that period of the ablation season in which the snow and ice surface is melting, a particularly simple parameterization can be used to determine the change in altitude of the equilibrium line (see this volume, Attachment 16). This is, essentially, the ratio of the sum of the climatic disturbances to the sum of altitudinal derivatives of accumulation c, air temperature T, net radiation, and vapor pressure e.

For a scenario of $\delta T = +1°C$, $\delta c = 150$ mm/yr, $\delta e = +1$ hPa, and a change in cloudiness = +0.1, a rise in the equilibrium line of +190 m is predicted; this may increase to +230 m if the added accumulation is specified as having been deposited in winter exclusively. This example applies to conditions in the European Alps. The coefficients and derivatives used must be adapted for other climatic settings, e.g., maritime glaciers in the northwestern United States.

The temporal change in the mass balance can be analyzed similarly. If air temperature rises linearly with time, the glacial wastage (negative balance) increases to a maximum and then decreases as the glacier loses area. The maximum will occur in a few decades for small glaciers. Application of this model will require data on glacier area, length, and thickness as a function of altitude. Such data are now being compiled by the World Glacier Inventory and the Permanent Service on the Fluctuations of Glaciers (see this volume, Attachment 13).

Simple hydrometeorological (statistical, empirical) models, developed to extend mass-balance histories, also can be used to estimate the effect of rising temperature on the world's glaciers. For a temperature rise of 1.5 to 4.5°C, glacier wastage could produce a rise in sea level of 1.3 to 6.6 mm/yr, all other factors being held constant, with a rise in the range of 1.7 to 5.2 mm/yr considered more probable (Meier 1984). If the concentration of atmospheric CO_2 doubled in 100 years and if the rise in the annual meltwater contribution were linear, the probable contribution to sea level would be about 0.09 to 0.26 m.

Air temperature rose about 0.5°C from 1900 to 1961, and glacial wastage is estimated to have produced a 28-mm rise in sea level (Meier 1984). This suggests that a range of sea-level rise due to ice melt of 0.08 to 0.25 m in 100 years corresponds to a rise in air temperature in the range of 1.5 to 4.5°C, as has been suggested for the next century. The actual sea-level rise might be less because the area of glacier ice will have diminished. Also, increasing precipitation in many regions may largely offset the wastage.

Several major uncertainties arise in these simple predictions. One of the most important concerns is with the occasional years of extremely negative mass balances that often dominate balance histories; these rare events cannot be analyzed precisely because they are so unusual and therefore defy most statistical or empirical treatments, and they are difficult to study from a deterministic point of view because of limited data and inadequate knowledge. Another problem has to do with glaciers in areas affected by monsoonal circulation; minor changes in air temperature during the accumulation (summer) season determine the mass balance.

The total volume of the world's glaciers and ice caps, exclusive of the Greenland and Antarctic Ice Sheets, has been estimated in the range of 0.3 (Hollin and Barry 1979) to 0.6 m (Flint 1971) in sea-level equivalent. This is the upper limit to sea-level rise due to glacier wastage.

4.3 EFFECT ON THE GREENLAND ICE SHEET

A reasonable estimate of the range of possible sea-level change due to changes of the Greenland Ice Sheet is difficult to make, because no data on the present mass balance are available for large areas, especially in northern and eastern Greenland. This uncertainty in the present mass balance is illustrated by the fact that, of six estimates from different investigators, three are negative, and three are positive. Additional measurements (see this volume, Attachment 8) are needed to narrow the uncertainty of the present mass balance of the Greenland Ice Sheet and permit a more realistic projection of the contribution to rising sea level from this source during the next 100 years.

A synthetic-aperture radar satellite will be installed in a near-polar orbit toward the end of the 1980s. Its use over Greenland should be requested, because it would yield accurate data on the location of the equilibrium line. The Greenland Ice Sheet has a large ablation area and is thus a significant potential contributor of meltwater to the ocean if climatic warming causes an increase in the rate of ablation and an upward shift of the equilibrium line. Some of the additional meltwater will reach the ocean as runoff, but much of it will refreeze in the cold firn.

The increase in equilibrium-line elevation that is likely to be caused by climatic warming can be related to the altitudinal gradients of accumulation and the energy-balance components (see this volume, Attachment 17). The most important of these components are the change in the sensible heat flux over melting surfaces and the change in net radiation that is caused by a change in air temperature and cloudiness. Changes in albedo can be ignored because the altitudinal pattern of albedo follows the shift of the equilibrium line.

Accumulation and heat-balance measurements are required. Parameterization schemes established for other regions cannot be relied on to apply to the Greenland Ice Sheet. Sufficient data are available along the EGIG profile (Figure 11) and along the accumulation profiles measured by Benson (1962). These measurements were used by Ambach (1985) to compute the rate of increase of the equilibrium-line elevation with respect to air temperature, cloudiness, and accumulation rate. These three rates were found to be +77 m/°C of temperature, -4 m/0.1 of cloudiness, and -73 m/100 kg/m^2 of annual snow accumulation, respectively. These values suggest, for instance, a rise of about 500 m in the equilibrium-line altitude for a temperature rise of 6.5°C and an increase in precipitation of 10 percent. A similar rise in the equilibrium line, from approximately 1500 to 2000 m can be estimated using observed values of the lapse rate (gradient of temperature with altitude), corresponding

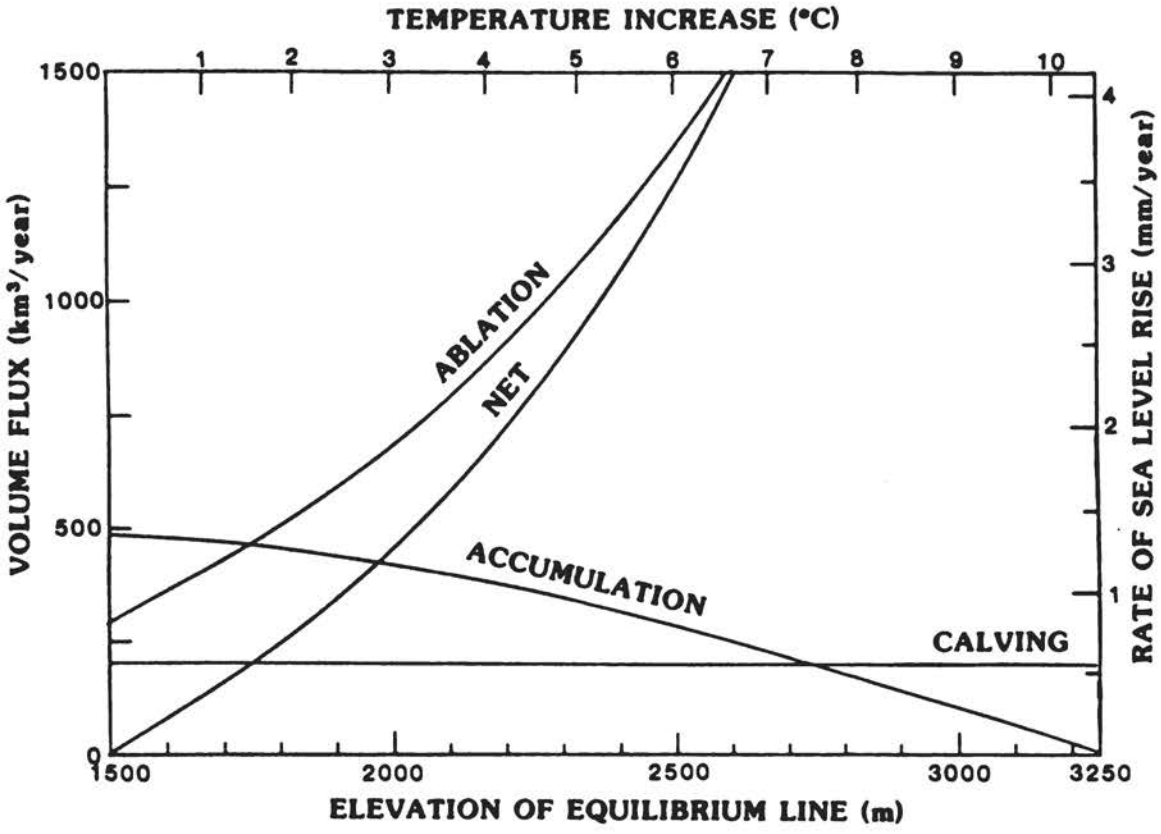

FIGURE 19 Magnitude of mass-balance volume fluxes versus elevation of the equilibrium line for a Greenland Ice Sheet model with constant calving. Secondary axes relate temperature increase to elevation of the equilibrium line (assuming the EGIG-line value of 0.6°/100 m) and rate of sea-level rise to volume flux.

to a somewhat lesser temperature change of 3 to 6°C (see this volume, Attachment 18). The difference in the temperature sensitivity of the equilibrium-line elevation according to the two methods is an indication of the uncertainty in the estimation process.

The relative increase in the melt rate likely to be caused by an upward shift of the equilibrium line from 1500 to 2000 m can also be calculated, assuming that no changes in the dynamics of the ice sheet occur. The upward shift will reduce the accumulation area, increase the ablation area, and force a shift from present approximate balance to one that is strongly negative. If it is assumed that the calving rate remains fixed, the new net mass balance will be about -460 km^3/yr (Figure 19). This converts to a rate of sea level rise of 1.3 mm/yr, if the increase in ablation runs off to the sea. It is unclear how much of the meltwater increase would be added to the ocean, however, because of refreezing within the firn layer and formation of superimposed ice. These processes should be incorporated in improved models for the prediction of the effect on sea level.

Over time, the ice sheet will adjust its shape to match the new climate. The accumulation area will thicken, the ablation area will thin, and the margin will retreat. In the next 100 years, little change in the flow dynamics is expected, although such change might be important for time scales of a 1000 years or more.

To estimate the total sea-level rise by the year 2100 produced by changes in the Greenland Ice Sheet, assume a scenario that there is no change in atmospheric warming from now to the year 2000, when the atmosphere warms at a rate that raises the equilibrium line 500 m by the year 2050 where it remains. The total change in sea level would be 0.10 m. For an extreme but highly unlikely case, with the equilibrium line raised 1000 m, the total rise would be 0.26 m. These numbers are maximum estimates and disregard the refreezing of meltwater in the cold firn.

5.
Probable Land-Ice and Ocean Exchanges during the Next 100 Years: Antarctica

The question of the stability of the West Antarctic Ice Sheet was raised by Mercer (1968, 1978) who pointed out that lake sediments and inactive solifluxion flows in Antarctica indicate summer temperatures that were 7 to 10°C higher sometime during the Pleistocene than at present. Mercer suggested that if a temperature rise of this magnitude occurred in the future, the Ross and Filchner-Ronne Ice Shelves would not survive. Citing earlier arguments by Hollin (1962) and Robin and Adie (1964, p. 116), Mercer hypothesized that destruction of the Ross and Filchner-Ronne Ice Shelves would be followed by rapid shrinkage of the West Antarctic Ice Sheet and that a previous disappearance of this ice sheet is the most likely reason that sea level was 6 m higher during the Sangamon interglacial about 120,000 years ago than at present. Subsequently, Hughes (1973) synthesized several lines of evidence suggesting that the West Antarctic Ice Sheet might be retreating at present, and Weertman (1974) demonstrated theoretically that a two-dimensional marine ice sheet terminating in an unbounded floating ice shelf would be unstable, if the depth at the grounding line exceeded a critical depth and the seabed sloped down toward the ice sheet interior. Such an ice sheet, Weertman argued, would either retreat until it vanished or expand until it reached the edge of the continental shelf. Although West Antarctica has received most of the attention, it should be noted that there are sections of the East Antarctic Ice Sheet that are also marine.

The questions of whether retreat is occurring now, if not, whether it is likely to begin at some point in the future, and in either case, how much time would be required for retreat to proceed to completion, have remained controversial. This chapter addresses these points, with emphasis on the question of how much retreat could be accomplished in the next century.

5.1 STATE OF KNOWLEDGE OF THE ENVIRONMENT OF WEST ANTARCTICA

The Committee on Glaciology organized a 1983 Workshop on Potential CO_2-Induced Changes in the Environment of West Antarctica (NRC Committee on Glaciology 1984), which was sponsored by the Department of Energy. The goal of the Workshop was to define a future environmental

scenario for the West Antarctic Ice Sheet, so that its contribution to sea-level changes could be estimated. However, the issue was raised as to whether even the present environment could be simulated properly, let alone a future one, and this required consideration of the quality of existing knowledge of the West Antarctic environment.

The basic climatology of the region consists of patchy and relatively short temperature records, most of them started during or since the IGY. Any trends in these data are as yet hidden by their natural variability. Precipitation presents special problems, being episodic and difficult to measure in the prevalent windy conditions. The general features of the climatological surface pressure field and the implied mean winds are well established, but changes from year to year are not. Conventional synoptic data for the ocean areas surrounding Antarctica exist only for the summers of 1955-1958 and for 1979. New information has come from satellite-observed cloud vortices, which define the main area of cyclogenesis and cyclolysis. Minor synoptic changes dominate the variability of regional climate and present a severe challenge for climate models to simulate.

The principal ice features that need to be considered are interannual changes in the extent of sea ice and melting at the base of the large ice shelves. The regional extent and concentration of the sea ice result from complex interactions with atmosphere and ocean and vary markedly from year to year. The sea-ice changes affect the production of water masses that control the extent of basal melting below the ice shelves, the major unknown in the mass and heat balances of the shelves. By contrast, the amount of surface melting can be assessed with the available climatic observations made on ice shelves in different latitudes; its effects are likely to be small.

Model simulations of the main climatic elements differ substantially from the best estimates of actual climatic conditions: modeled temperatures tend to be higher than those observed; and the Antarctic mean pressure trough is shallower than observed. These discrepancies may result from erroneous model treatments of the southern hemisphere storms, which in the simulations are less numerous than observed and do not form in the observed cyclogenetic regions.

In these circumstances the model predictions for higher CO_2 concentrations must be treated with caution. One major prerequisite for the realistic simulation of a CO_2-enhanced West Antarctica environment is an adequate representation of baroclinic eddies. Others are ocean models with sufficient resolution for simulating the production of key water masses and the transports in and across the Antarctic Circumpolar Current and a much fuller understanding of what goes on below the major ice shelves.

5.2 OCEANOGRAPHIC CONSIDERATIONS

The stability of marine ice sheets, such as the one occupying most of West Antarctica, depends on the back stress exerted on the land-based ice streams by the floating ice shelves (Figure 2). Thinning of the ice

shelves by melting would accelerate discharge of land ice to the sea. Although appreciable melting of the top surface of the ice shelves in the next century cannot be expected, increased melting at the undersurface of the shelves is possible. Whether it occurs depends on whether additional heat is transported by the ocean to the base of the ice shelves because of a CO_2-altered climate.

CO_2-Induced Warming of the Southern Ocean

The stability of the West Antarctic Ice Sheet thus could depend on the CO_2-induced warming of the Southern Ocean, particularly in the vicinity of the large ice shelves. To study this warming requires a simulation of CO_2-induced climatic change with a global coupled atmosphere-ocean general circulation model (GCM). Such coupled models are in their infancy, and one must consider their results as preliminary because they simulate the present climate imperfectly. In particular, the current sea-ice distribution in Antarctica is underestimated. One example of such a simulation is that recently performed with the Oregon State University (OSU) coupled GCM (see this volume, Attachment 19).

The atmospheric component of the OSU model is a two-layer primitive-equation GCM that predicts the atmospheric velocity, temperature, water vapor, and clouds; the pressure and temperature of the atmosphere at the Earth's surface; and the Earth's snow mass and soil water. The oceanic component is a six-layer primitive-equation GCM that predicts the velocity, temperature, and salinity of the ocean and the formation and melting of sea ice. Two 20-year simulations have been performed with the coupled atmosphere-ocean model that differ only in their prescribed "1 x CO_2" and "2 x CO_2" concentrations. Each simulation was started from the same initial conditions.

The distribution of the annual-mean zonal-mean temperatures according to the (2 x CO_2) - (1 x CO_2) models for year 16 shows that the atmospheric warming at the surface increases from the tropics to the subtropics, decreases toward the middle latitudes, and increases again toward the high latitudes [Figure 20(a)]. The warming increases with altitude in the tropics and subtropics and decreases with altitude elsewhere.

The oceanic surface warming increases from the tropics toward the mid-latitudes of both hemispheres and penetrates to a greater depth in the subtropics and mid-latitudes than in the equatorial region. The warming decreases with depth everywhere equatorward of 60° latitude in each hemisphere, and isotherms of warming extend from the subtropical surface water downward toward high latitudes. Particularly interesting features of the temperature change at depth are the maxima located near 65°N and 60°S in the 250-750 m ocean layer. In the south, the latter warming appears to extend into northern parts of the Ross, Amundsen, and Bellingshausen Seas, where temperature increases of more than 1°C are found 16 years after the CO_2 doubling [Figure 20(b)]. Further research is needed to determine the pathways and physical processes responsible for this apparent warming.

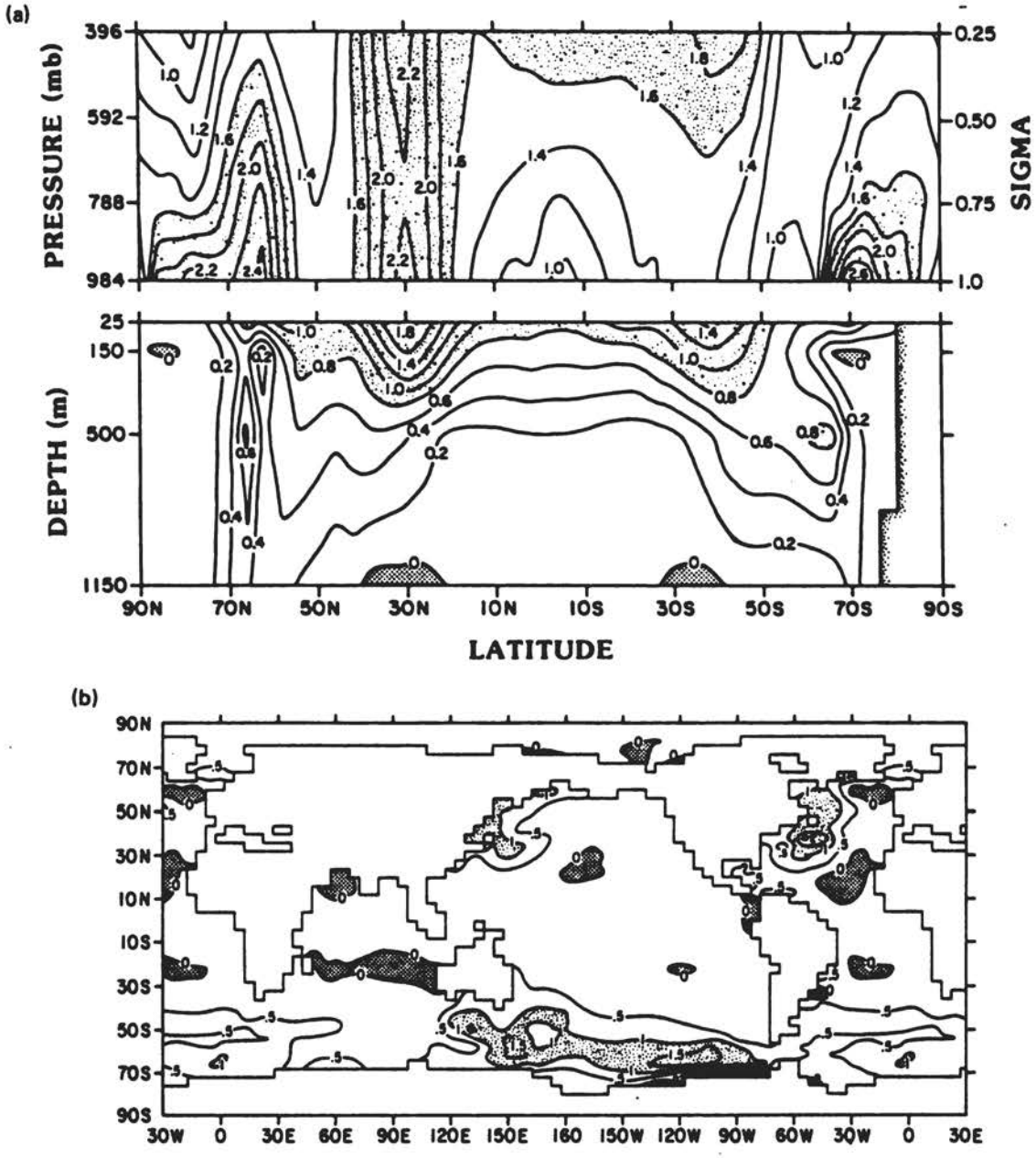

FIGURE 20 (a) Distribution of the difference between a doubled CO_2 environment in the annual-mean, zonal-mean temperatures (°C) of the atmosphere (above) and ocean (below) as a function of altitude and latitude. The sixteenth-year model simulation is shown. Atmospheric warming larger than 1.6°C is shown by light stipple, as is oceanic warming larger than 0.8°C, while oceanic cooling is indicated by heavy stipple. (b) Geographic distribution of the (2 x CO_2) - (1 x CO_2) difference in the annual-mean temperature (°C) of the 250-750 m ocean layer for year 16. Warming larger than 1°C is indicated by light stipple and cooling by heavy stipple.

Circulation on the Antarctic Continental Shelf

At present, a core of relatively warm water derived from Circumpolar Deep Water north of the Antarctic continental shelf is a primary source of heat for basal melting beneath the Ross Ice Shelf (see this volume, Attachment 4). The warm core has a summer cross section of about 100 km by 200 m and intrudes beneath the Ross Ice Shelf at a depth of 200 to 300 m near the calving front (Figure 7). With an average temperature 0.5°C above the in situ freezing point (Jacobs et al. 1979, 1985; Pillsbury and Jacobs 1985), this warm core water has the capacity to melt as much as 0.35 m/yr from the base of the ice shelf. Recirculation apparently returns some of the sensible heat in this warm core to the open Ross Sea, however, and the melting rate averaged over the entire bottom surface of the Ross Ice Shelf may be closer to 0.25 m/yr.

The oceanographic data and models are as yet insufficient to determine the basal mass balance with precision or to indicate whether the ocean-ice shelf system is now in a state of equilibrium. Even if a steady-state condition exists at present, future changes could occur if seawater circulating beneath the ice were to become warmer or transfer heat into the subice shelf cavities at a faster rate. This might occur if a warmer atmosphere resulted in a low-density cap of surface water on the Southern Ocean, less vertical heat flux, and a consequent deep-water temperature increase of up to 0.5°C (Gordon 1983). That would probably result in a proportional increase in water temperatures on the continental shelf, if the shelf-slope circulation did not change. In addition, some models indicate that a CO_2-warmed atmosphere might directly increase ocean temperatures by more than 1°C or more at ice-shelf depths and latitudes (Figure 8.3 in Revelle 1983).

A warmer atmosphere may also result in an altered continental shelf circulation in response to different wind patterns and reduced sea ice. At present, freezing of sea ice in the Ross Sea produces cold, high-salinity shelf water, which limits the intrusion of warmer Circumpolar Deep Water (CDW) beneath the Ross Ice Shelf. If the extent of winter sea ice in the Ross Sea in response to a 5°C warming were to decrease by about 50 percent, as modeled by Parkinson and Bindschadler (1984), the production of the buffering shelf water would be reduced, but whether there would be an increased basal melting is uncertain because the processes are too poorly understood. It is not even known why deep water now intrudes on to the continental shelf in some areas but not in others, let alone how the dynamics of shelf-slope exchanges might be altered in a warmer, fresher Southern Ocean.

Redistribution of ice beneath the ice shelves is also possible. Owing to the pressure dependence of the freezing point, an ice shelf gives rise to an ice pump (see this volume, Attachment 20). Ice is removed from the bottom of the ice shelf and deposited just beneath the contiguous sea ice; the rate of pumping is controlled by the rate of heat exchange possible through the melting boundary layer. Because of positive and negative buoyancy produced by ice melt and salt rejection on freezing, respectively, this pump produces vertical circulation of the seawater. A similar process may occur entirely beneath the ice shelf, if it has a varying draft; the process is enhanced strongly by a

current. While not altering the basal melt balance, this process could change the thickness profile and the mean temperature and thus the spreading rate of the ice shelf. It may also redistribute ice in the vicinity of critical pinning points where grounding occurs on submarine rises.

Despite the complications and uncertainties, it is possible to estimate the maximum melting rate beneath the Ross Ice Shelf that could be caused by a greatly increased intrusion of CDW across the continental shelf by noting that along the Bellingshausen Sea coast nearly undiluted CDW does intrude onto the continental shelf. This water, which is about 3°C above the in situ freezing temperature, causes basal melting rates on the order of 2 m/yr beneath the George VI Ice Shelf (Potter and Paren 1985). Basal melting of 2 m/yr thus could occur beneath the Ross Ice Shelf, if the continental shelf circulation were to change to allow undiluted CDW at its present-day temperature to flow beneath the shelves. Allowing further for a temperature increase in the CDW and direct warming near the shelves leads to an upper limit for increased basal melting of about 3 m/yr.

The atmospheric component of the OSU model is a two-layer primitive-continental shelf. This water, which is about 3°C above the in situ freezing temperature, causes basal melting rates on the order of 2 m/yr beneath the George VI Ice Shelf (Potter and Paren 1985). Basal melting of 2 m/yr thus could occur beneath the Ross Ice Shelf, if the continental shelf circulation were to change to allow undiluted CDW at its present-day temperature to flow beneath the shelves. Allowing further for a temperature increase in the CDW and direct warming near the shelves leads to an upper limit for increased basal melting of about 3 m/yr.

5.3 NUMERICAL MODELING OF ICE-STREAM FLOW

Modeling of Ice-Stream Flow with Basal Sliding

Numerical models can be used to explore the transient behavior of ice sheets and to estimate the time that it might take to make changes in their dimensions. Since most of the ice flux from West Antarctica is concentrated in a number of large ice streams, knowledge of ice-stream dynamics is critical to analysis of ice-sheet response. In many cases the ice streams are characterized by maximum downslope driving stress at a considerable distance inland from the grounding line. The zone of decreasing downslope driving stress from there to the grounding line is typically accompanied by a rapidly increasing speed ice movement. Before the ice streams can be modeled successfully, it is necessary to understand the dynamics of the high-speed ice flow under a small downslope gravitational driving stress.

The total amount of water beneath ice streams might be important. During the recent surge of Variegated Glacier in southeast Alaska, for example, the average thickness of the water layer across the entire width of the glacier was on the order of 0.1 m, not just a few millimeters (Kamb et al. 1985). The total volume of subglacial water that

was associated with fast sliding was thus large.

The temperate Columbia Glacier, Alaska, may offer a useful analog to an Antarctic ice stream. Flow of this glacier accelerated from less than 2 to more than 5 km/yr in 3 years as disintegration began and the terminus nearly went afloat. An exceptionally complete and detailed set of data is available (Fountain 1982; Meier et al. 1985a, 1985b; Rasmussen and Meier 1985).

One of the most prominent regions of ice-stream flow in the West Antarctic is the Ross Ice Shelf drainage basin. A large amount of basic geophysical data is now available for the Ross Ice Shelf. This extensive data set makes the region valuable for an analysis of the dynamics of the flow regime even though few data on observed flow velocities are yet available for the ice streams.

A preliminary analysis of the dynamics of this region by numerical modeling (Budd et al. 1984) showed that an important factor in the increasing velocities with decreasing basal shear stress is likely to be the decreasing normal stress as the grounding line is approached. It was also found that the basal thermal regime may play an important role in determining the velocity of the ice streams.

As a first attempt to examine the possible impact of basal temperatures on the ice-sliding rate, a simple temperature dependence was included in the ice-sliding law used by Budd et al. (1984), based on the experimental ice-sliding results of Barnes et al. (1971) and Budd et al. (1979). The sliding velocity was taken to be exponentially proportional to the temperature of the basal ice, directly proportional to the first power of the basal shear stress [because a first-power relationship provides a better fit to the inferred sliding velocity, when sliding is fast, than does a power-law relationship (Budd et al. 1984)] and inversely proportional to the square of the ice thickness in excess of buoyancy (Budd et al. 1985). The subglacial water pressure is taken into account in the basal sliding relationship by assuming, in effect, that it is given by the water pressure at the grounding line plus an additional pressure that is proportional to the depth of the bed below the grounding line. The effective normal stress on the bed at each point along the flow line is that which is caused by the thickness of the ice in excess of buoyancy. Near the grounding line, the longitudinal strain-rate profile is scaled by assuming a grounding-line strain rate that is within a range known to be typical.

When this sliding relation was incorporated in a three-dimensional steady-state model of the West Antarctic Ice Sheet, a clear enhancement of the sliding velocities within the major ice streams relative to the velocities of the neighboring ice was observed. Typically, the ice streams attained velocities of several hundred meters per year in the grounding zones, which is in broad agreement with the balance velocities and with velocities measured nearby on the Ross Ice Shelf (e.g., Thomas and MacAyeal 1982).

A time-dependent flow-line reconstruction model, with ice velocity specified by a combination of flow and sliding laws, can be used to investigate the formation of an ice stream in a region originally dominated by sheet flow (see this volume, Attachment 21). The evolution of this process can be determined on various time scales, showing changes

in the basal shear stress as the ice stream forms, as well as the changing mass outflow at the grounding line. Significant thinning occurs during the first 10 years only within 100 km of the grounding line (the region where the decoupling that leads to the development of an ice stream was explicitly defined). Response of the surface during the first 100 years extends about 50 km behind the head of the ice stream, but very little change in surface elevation occurs beyond this region. The elevation at the ice divide takes over 10,000 years to attain its equilibrium thickness.

Modeling of Ice Sheet Shrinkage through Acclerated Ice Stream Discharge

Three models that relate directly to shrinkage of the West Antarctic Ice Sheet through the mechanism of grounding line instability have been developed.

The first approach, by Fastook (1984, see also this volume, Attachment 21) was an attempt to calculate what might happen if the grounding line of Pine Island and Thwaites Glaciers, which empty in Pine Island Bay where there is now no ice shelf, were to retreat unstably. Fastook's emphasis was on producing a likely model rather than a most-rapid-retreat scenario, so he permitted an ice shelf to form in the embayment in front of the retreating grounding line. Surface lowering of the ice-sheet surface in the Pine Island Bay drainage basin led to destabilization of the ice streams flowing into the the Ross Ice Shelf (and presumably destabilization of those flowing into the other ice shelves also), so that their grounding lines then retreated. The process goes to completion, i.e., to disappearance of the West Antarctic inland ice, in about 6000 years. However, if an ice shelf is not allowed to form in the embayment, the grounding line retreats far into the interior in only a few hundred years. This model, like most others, points to the critical importance of the ice shelves.

A second model approach, by Lingle (1984; see also this volume, Attachment 23), applied his time-dependent numerical model of the dynamics of a polar ice stream grounded below sea level to Ice Stream E (Figure 14), one of the two most active ice streams draining the Ross Ice Sheet. Sensitivity tests showed the model ice stream to be sensitive principally to the backpressure from the ice shelf, changes in which are most likely to be caused by thickness of the ice shelf or in its average length from grounding line to ice front. The backpressure needed to hold the grounding line in dynamic equilibrium was found to be nearly equal to the actual back pressure mapped from field data by Thomas and MacAyeal (1982). This suggests that the grounding line of Ice Stream E is in fact close to dynamic equilibrium, neither retreating nor advancing rapidly, if the ice stream and its catchment area are approximately in mass balance as suggested by Rose (1979).

The likelihood of present-day stability was supported by perturbation studies. An assumed instantaneous 10 percent thinning of the ice shelf, with the position of the calving front kept stationary, resulted in a 33-km retreat of the grounding line during a 2000 model-year test period. Ten kilometers of retreat occurred during the initial 100-year period [Figure 21(a)]. Thinning of the ice sheet upglacier of the

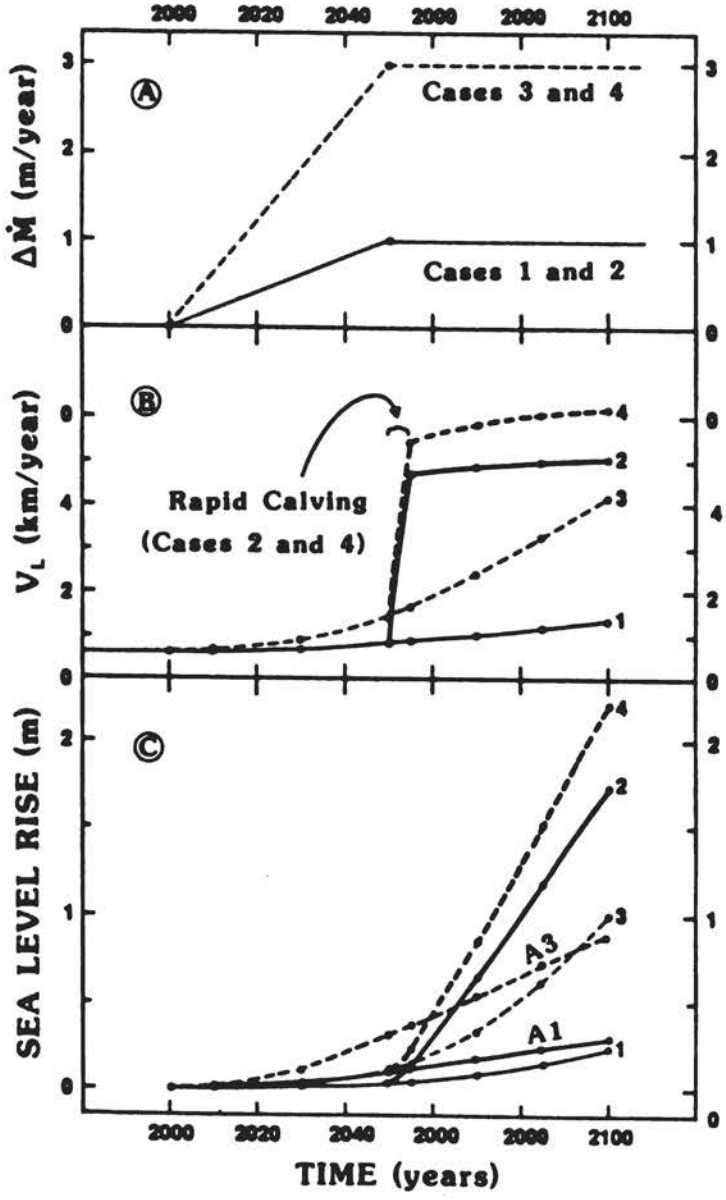

FIGURE 21 A typical Antarctic ice-drainage system. The ice stream pushes the ice shelf seaward past its margins and around grounded ice rises, and there is a compressive force (F_{is}) at the grounding line (X = L) between ice stream and ice shelf. This compressive force is transmitted for some distance (L) upstream of the grounding line, and there is an additional force (F_s) due to shear between the ice stream and its sides and bed. In a steady state, the weight-induced spreading stress in the ice stream is balanced by the backstress due to F_s and F_{is}. If the compressive force F_{is} is reduced owing to thinning of the ice shelf or accelerated calving at the ice-shelf margin, or both, extending strain rate in the ice stream will be increased, and the integration of this over the distance L produces increased ice velocity V_L at the grounding line.

grounding line occurred during the first 500 years, when retreat of the grounding line was relatively rapid, but subsequently the rate of thinning decreased as the grounding line apparently approached a new position of equilibrium owing to increasing backpressure from the lengthening ice shelf. Restabilization was not complete; rather, the retreat rate was reduced to about 6 m/yr, and the ice discharge velocity returned approximately to the balance velocity after 2000 model years. This result (together with a similar one for a 10 percent increase in the thickness of the model ice shelf) suggests that the grounding lines of Antarctic ice streams are stable with respect to small perturbations, on the order of $\pm$10 percent or less, in the thickness or lengths of their buttressing ice shelves. Further investigation is needed, particularly because there is field evidence (Jezek 1984) indicating that the Ross Ice Shelf is subject to short-term fluctuations.

On the other hand, the assumption of an instantaneous 50 percent thinning of the ice shelf, again with the position of the calving front kept stationary, caused the grounding line of the model ice stream to retreat rapidly and irreversibly [Figure 21(b)]. Retreat proceeded essentially to completion in 660 years. Assuming Ice Stream E to be representative of the entire West Antarctic Ice Sheet, this suggests that disappearance of the entire ice sheet, following drastic thinning or frontal retreat of its ice shelves, might take 6 or 7 centuries. Based on these results, and assuming that the rate of melting from the base of the ice shelves increases to 1 m/yr in 2030 and is steady thereafter, Lingle (this volume, Attachment 23) calculates that the contribution of the West Antarctic Ice Sheet to sea-level rise by 2100 would be only 0.03 to 0.05 m.

A third model approach, by Thomas (this volume, Attachment 22), has taken this concept further by assuming various combinations of basal melt rates and positions of the Ross Ice Shelf front and then extrapolating to all of Antarctica. He uses the year 2000 as the beginning date for increased melting, because field data indicate that the Ross Ice Shelf is not thinning and may even be thickening near the grounding line at present, and presumably some time will be required to establish a thinning trend. Thereafter, the basal melt rate beneath the ice shelf is taken to increase linearly to either 1 m/yr or 3 m/yr by 2050, and the ice shelf calving front is assumed either to remain where it is today, or to retreat rapidly, in the 2050s, to a line linking the major ice rises. For one model, ice discharge into the ice shelves is assumed to increase sufficiently to replace ice lost by basal melting. In the second model, melting is assumed to thin and weaken the ice shelf, which results in acceleration of tributary ice streams. The acceleration was calculated by assessing the impact of diminishing backpressure from the ice shelf on the longitudinal strain rates in the modeled ice stream (Figure 22).

The calculations were applied specifically to Ice Stream B and the Ross Ice Shelf. Extrapolation to all of Antarctica was based on the assumption that the same time-dependent fractional increase in volume flux across the grounding line that evolved from the model for Ice Stream B applied to the whole ice sheet. This assumption is based on the fact that most of the discharge from both East and West Antarctica

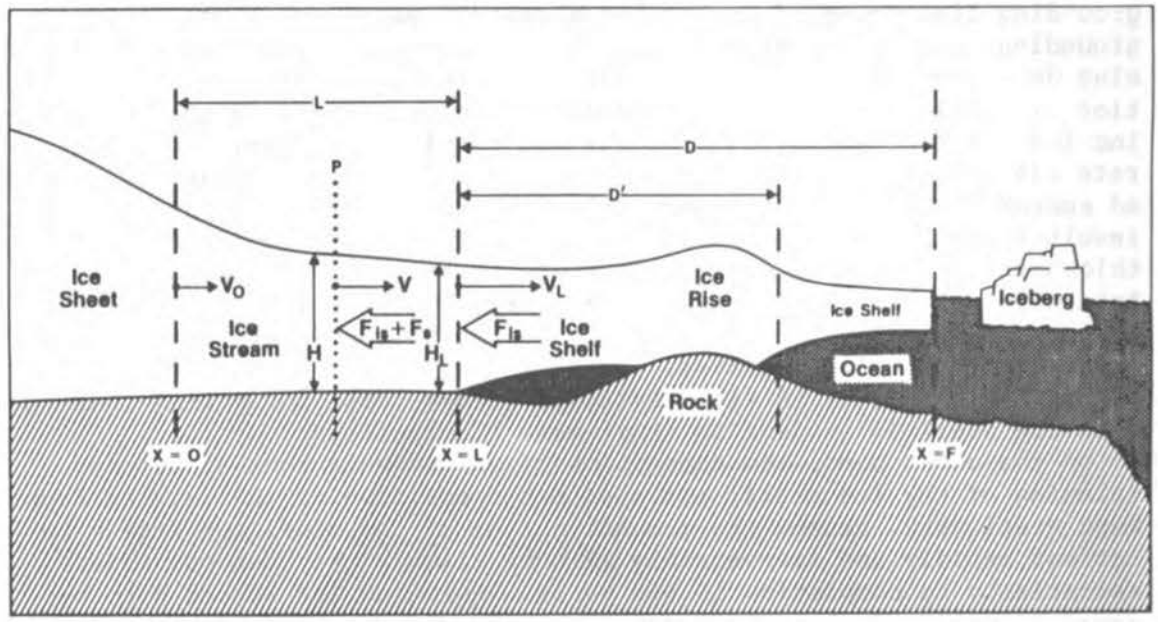

FIGURE 22 (a) Assumed enhanced ice-shelf basal-melt rates (M) due to CO_2-induced climatic warming during the next century. In cases 1 and 3, ice-shelf seaward fronts are assumed to remain in present-day positions. In cases 2 and 4, they are assumed to calve back in the 2050s to a line joining major ice rises (e.g., Crary Ice Rise in Figure 14). (b) Speed (V_L) of Ice Stream B at the grounding line calculated using model B for the four different melting and calving scenarios. (c) Sea-level rise due solely to increased ice discharge assuming all Antarctic outlet glaciers respond in the same way as Ice Stream B in Figure 4(b). Cases A1 and A3 depict sea-level rise derived using Model A, in which enhanced ice discharge exactly balances increased ice-shelf melting.

is through ice streams. Since most of the East Antarctic Ice Sheet is not marine in character, this is a rather extreme assumption, and certainly cannot be continued into times of drastic grounding-line retreat. Nevertheless, it is a useful model for ascertaining upper limits on the possible short-term response of the entire Antarctic Ice Sheet.

The model yields a wide range of estimated sea-level rise by the year 2100 (Figure 23), depending principally on the magnitude of the increased melting rate and the position of the ice-shelf front. Imposing reasonable limits on these parameters yields a range of 0.2-0.8 m, corresponding, respectively, to enhanced ice-shelf melting of 1-3 m/yr.

These numbers represent an upper limit to the response. There are at least three negative feedback mechanisms that have not been taken into account. First, the removal of the warmest ice from the base of the ice shelves by basal melting might stiffen them by decreasing their average temperature. Second, as the grounding lines retreat, the flow in the surrounding ice sheet would become more strongly convergent, thus decreasing the rate of thinning and slowing the retreat. Third, increasing velocities of the ice shelves themselves would probably cause

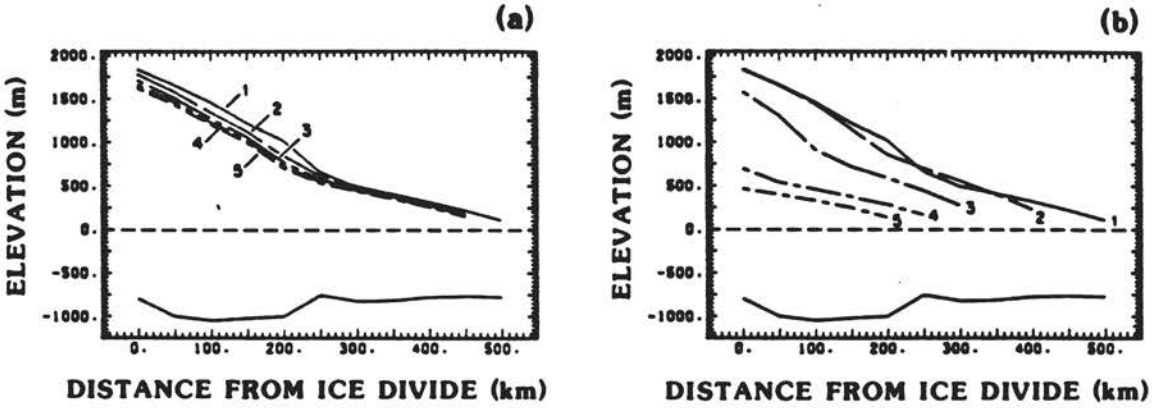

FIGURE 23 Thickness profiles for numerical models of Ice Stream E. (a) Model applied to the ice stream with backpressure at the grounding line decreased by 10 percent from equilibrium backpressure at start of run. This is equivalent to decreasing the mean ice shelf thickness by 10 percent from the mean thickness at equilibrium. The position of the calving front is assumed fixed. Profiles 1-5 are 0, 500, 1000, 1500, and 2000 years, respectively. Although the thickness becomes reduced, the ice stream reacts in a stable way to this small perturbation. (b) As above, except that the model is applied to the ice stream with backpressure at the grounding line decreased by 50 percent (at the start of the run) from equilibrium backpressure. This is equivalent to decreasing the mean ice-shelf thickness by 50 percent from the mean thickness at equilibrium. Profiles 1-5 are 0, 39, 251, 487, and 664 years, respectively. The ice stream reacts in an unstable way to this large perturbation.

increase in the lateral shear stresses along the sides of the ice shelves and around ice rises. This effect might be reduced, however, by softening of the ice owing to increased frictional warming.

The central role of backstress and hence of the lengths of the ice shelves, makes it essential to study the critical process of calving. A plane-strain finite-element analysis was used by Fastook (1984, see also this volume, Attachment 21) to model the stress distribution that occurs in an ice shelf or floating glacier terminus due to the unbalanced hydrostatic forces at the front. This mechanism for iceberg calving, which leads to a tension maximum at the top surface about one half an ice thickness back from the ice front, appears to be effective only in the presence of sufficient meltwater to keep the opening crevasse filled approximately to sea level. The possibility of bottom crevasses coinciding with top crevasses and leading to calving can be ruled out in all but a few special cases because bottom crevasses close as they move toward the ice front. The effect of ice fronts of different shapes (a submerged bulb and an undercut ice front) on the formation of surface crevasses is small. Since free meltwater is not to be expected by the year 2100 at the high latitudes in which the fronts of the Ross and Filchner-Ronne Ice Shelves lie, there is no clear mechanism for a rapid retreat of the ice margin.

It is clear, then, that we make no prediction of a rapid rise in sea level. It is possible that accelerated discharge of land ice from Antarctica will cause a modest rise in sea level in the next century. It is also possible that any accelerated discharge will be offset by increased snowfall on the continent, leading to a small contribution to sea-level change that could either be positive or negative.

6.
Summary and Recommendations

The rising concentration of CO_2 and other greenhouse gases in the atmosphere is likely to produce a warmer climate in the future. This, in turn, is expected to lead to a rise in sea level caused by the melting of ice on land and by volume expansion of ocean water. Attempts to estimate the probable sea-level rise are fraught with uncertainties in all aspects of the problem. The focus of this Workshop was to assess what is known and what needs to be known about the contribution of ice melt to the sea at the present (defined as the past 100 years) and what that contribution is likely to be in the future (defined as the next 100 years).

6.1 OCEAN VOLUME CHANGES DURING THE PAST 100 YEARS

Relative Sea Level

Since the turn of the century, global average sea level appears to have been rising; estimates of the rate range from about 1 to 3 mm/yr along most continental margins, but the data coverage from the central ocean regions and the southern hemisphere is poor. Tectonic and isostatic disequilibrium effects must be removed from the relative sea-level data to determine the eustatic component. Along some passive continental margins (e.g., eastern United States) it is possible to correct relative sea-level data approximately for the effect of the continuing adjustment of the Earth to the removal of the Laurentide and Fennoscandian ice sheets (glacio-isostatic rebound). The corrected value is a little more than 1 mm/yr along the eastern U.S. coast for the average sea level since the beginning of the century. The corrected values however, show considerable spatial variations (0.8 to 3 mm/yr) implying that other poorly defined tectonic or oceanographic effects are important. The rate of sea-level rise since the mid-1930s appears to be higher than before.

Volume Change Evidence from the Ocean

Ocean-surface temperature appears to have risen by $0.6 \pm 0.3°C$ since the turn of the century, but it is not yet certain whether the rise has

been the same as over land, partly because of bias introduced by changing instrumental and observational techniques. Models are available for the computation of the increase in ocean volume due to thermal expansion. However, the commonly used one-dimensional vertical advection-diffusion models do not reproduce the changes seen in those few areas where abundant data exist, nor do they reproduce the physics of the formation of deep water and its movement from high to low latitudes. Also, studies in data-rich areas suggest that changes in volume at constant mass (steric height) can show large spatial variations, indicating that sea-level changes along the coasts may be quite different from those in the mid-ocean gyres. The global data are inadequate for determining long-term trends in steric height. Estimates of the global rise in sea level due to thermal expansion during the past 30-40 years, using the simple models and assumed surface temperature changes, range from 0 to 0.7 mm/yr. As much as 1 mm/yr could also be caused by an expansion of deep water. In a data-rich area of the tropical North Atlantic the difference between changes in steric height and sea level (evidence of an addition of mass to the system) is about 0.5 to 1 mm/yr for the period 1955-1978, but shorter-period variations are larger than the long-term trend. In general, the observational data on changes of ocean temperature, salinity, and density structure during the past several decades are too few to demonstrate changes that are statistically significant, except in local areas.

Contribution from Glaciers and Small Ice Caps

The glaciers of the world, excluding the ice sheets of Antarctica and Greenland, have, in general, been shrinking during the past 100 years; shrinkage has been pronounced at mid-temperate latitudes (e.g., 0.37 m/yr in the Austrian Alps) and relatively minor in high latitudes (e.g., 0.06 m/yr in the Canadian Arctic). However, the data set is temporally and spatially sparse. An approximate correlation between net balance and balance amplitude makes it possible to estimate the global contribution to sea level. Most of this contribution is thought to be derived from the mountain ranges bordering the Gulf of Alaska, Central Asia, and the Patagonian ice caps, but these are areas with few observations. In some regions, even the area of glacier ice is poorly known.

Contributions from the Greenland and Antarctic Ice Sheets

Observations of present elevation changes of the Greenland Ice Sheet surface indicate thinning of the marginal zones and a thickening of the central area. Accumulation (precipitation) rates are reasonably well known for much of the ice sheet. Ablation rates and their gradient with altitude are known only for a few sites in West Greenland. The loss of ice by iceberg calving has been measured for some outlet glaciers in west Greenland; few estimates of calving have been made for the east, north, and northwest coasts. Thus it is not possible to estimate reliably the exchange of mass between the Greenland Ice Sheet and the

oceans, but most estimates suggest that gains and losses are approximately equal.

The present-day net balance of the Antarctic Ice Sheet also is not known precisely, but estimates have been improved over the last decade, and most estimates suggest growth. Perhaps the biggest uncertainty is in the iceberg discharge; also, accumulation data are lacking from about one third of the continent, the rates of melting below the major ice shelves are not well known, and few data exist on changes in the margin.

Evidence from Earth Rotation

The present-day true polar wander and the nontidal acceleration of the Earth's rotation can be reproduced using modern models of the Earth's radial viscoelastic structure combined with a realistic scenario for the loss of the Pleistocene ice sheets, without any need to assume present-day changes in volume of the ice sheets. This suggests approximately zero mass balance for both the Antarctic and Greenland Ice Sheets. The error limits in this estimate are not yet defined and await further calculation. Calculation of the effects of changes of other glaciers on the Earth's rotation rate might also yield useful conclusions.

Summary of Land Ice Contributions to Sea Level

Estimates of the present-day contribution of ice growth or wastage to sea-level change are summarized in Table 3.

TABLE 3 Estimated Mass Balance of Glaciers and Ice Sheets at the Present Time[a]

Ice Mass	Period of Observation (years)	Area (10^6 km^2)	Average Mass Balance (water equiv.) (m/yr)	Effect on Sea Level (mm/yr)	Report Section
Glaciers and small ice caps	1900-1960	0.54	-1.2 ± 0.7	$+0.5 \pm 0.3$	3.3
Greenland Ice Sheet	1929-1984[b]	1.73	$+0.02 \pm 0.08$[c]	-0.1 ± 0.4[c]	3.4
Antarctic Ice Sheet	1970-1984[d]	11.97	$+0.02 \pm 0.02$	-0.6 ± 0.6	3.5

[a] Note: Error limits represent approximate bounds of estimation and cannot be defined statistically.

[b] Observations scattered in both time and space.

[c] Combination of (a) historical estimates, (b) extrapolation of modern ablation data from West Greenland and accumulation data from Central Greenland, and (c) extrapolation of thickness change data from Central and West Greenland.

[d] Some observations taken earlier are included.

6.2 PROBABLE LAND ICE AND OCEAN EXCHANGES DURING THE NEXT 100 YEARS

Probable Changes in Climate Caused by Increasing CO_2

For steady-state models, radiation-transfer calculations indicate a radiative forcing of about 4 W/m^2 (global average) for a doubling of CO_2. When multiplied by a gain or feedback factor, this yields a predicted temperature rise of 2 to 4°C, or possibly more. The global temperature rise appears to be amplified at high latitudes according to current model results. The major uncertainties result from the difficulty of parameterizing sea ice and predicting the effect of clouds on the perturbed climate. The physical bases for some features of the model predictions are not obvious. Predictions of runoff, as opposed to melting, at the margins of the two existing ice sheets are not yet properly modeled. Predictions made by steady-state models show similarities in the global distribution of climate variables, but the agreement is poor in regard to longitudinal variations and in the higher latitudes. It is not yet certain why the different models produce these distributions. The time-dependent evolution of climate, driven by a changing CO_2 concentration through time, is extremely difficult to model and many aspects are poorly understood.

CO_2-Induced Warming of the Ocean

Coupled ocean-atmosphere general circulation models, still in the beginning stage of development, allow investigation of ocean warming in response to a doubled CO_2 atmosphere. One such model suggests that the warming decreases with depth equatorward of 60° latitude in each hemisphere, but near 65°N and 60°S shows interesting maxima at depths of 250-750 m. The southern edge of the latter temperature maximum is adjacent to some of the ice shelves of West Antarctica.

If the Antarctic Ice Sheet is supplying icebergs and meltwater to the Southern Ocean at a rate of 2000 km^3/yr, the mean residence time for water on the Antarctic continental shelf appears, according to one geochemical/oceanographic model, to be about 6 years, and the average melt rate at the base of all the ice shelves, 0.4 m/yr. If a doubling of CO_2 caused an increase in the temperature of circumpolar deep water of 0.5°C, as vertical heat-flux considerations suggest, and if that deep water were to intrude under all the ice shelves, then the average ice-shelf melt rate might increase to a value approaching 3 m/yr. However, this scenario contains major uncertainties, and improved understanding is needed.

Effect on Glaciers and Small Ice Caps

Energy-balance as well as simple statistical, empirical models exist that can provide estimations of the additional wastage (or growth) of glaciers (including small ice caps) in response to a perturbed climate. However, insufficient data exist to calibrate these models in many regions, the models are not easily linked to atmospheric general circulation models because the exchange processes that affect small glaciers

operate at subgrid scales, and it is difficult to model the mass balance of glaciers in areas of monsoonal circulation. Furthermore, mass-balance histories are often dominated by rare years of extremely negative balances; it is not well understood how to model these extreme events.
operate at subgrid scales, and it is difficult to model the mass balance of glaciers in areas of monsoonal circulation. Furthermore, mass-balance histories are often dominated by rare years of extremely negative balances; it is not well understood how to model these extreme events.

Insufficient data exist to calculate the maximum contribution to sea level owing to the complete removal of these glaciers because few thick-
Insufficient data exist to calculate the maximum contribution to sea level owing to the complete removal of these glaciers because few thick-ness measurements have been made on large mountain glaciers; estimates of the possible sea level range between 0.3 and 0.6 m.

Response of the Greenland and Antarctic Ice Sheets

The physics of the dynamic response of these ice sheets to variations in climate is known in general terms, but many aspects of the process are either not well understood or have not yet been incorporated fully in numerical models. A major problem is basal sliding; others include the mechanics of calving, the dynamics of ice streams, and the coupling of ice streams with the ice sheet. Also, models of the dynamic response probably should include adjustment of the ice sheets to the changing ratio of Pleistocene (soft) and Holocene (hard) ice. Another important influence on the temperature structure of the outer zones, especially of the Greenland Ice Sheet, is the percolation and refreezing of meltwater; although the physics is understood, few data exist for the calibration of models.

Several ways exist for making crude calculations of the response of the Greenland Ice Sheet to a CO_2-perturbed climate. Such calculations are severely limited by lack of present-day data, especially in east and north Greenland, as well as by lack of understanding of how the balance processes (both accumulation and ablation) relate to large-scale climatic processes, how the infiltration/refreezing regimen would react to an increase in meltwater availability, and how iceberg calving would be affected.

In the case of Antarctica, especially the West Antarctic Ice Sheet, the situation is further complicated by the possibly delicate stability of the ice stream/ice shelf interaction. Surface melting with runoff to the sea is unlikely to be significant in the next century. As already noted, melting from the base of ice shelves, induced by a warmer ocean, could increase markedly; this effect, through its influence on the feeding ice streams, could be important. Ice-shelf thinning and ice-stream acceleration can only evolve gradually with time, and it is difficult to estimate rates in view of our poor understanding of the rates at which heat can be delivered by the ocean to the ice shelves, the effect of ice-shelf thinning on the backstresses exerted on the ice streams, and ice-shelf calving. The ice streams may be relatively stable to small perturbations but not to large ones. Most general circulation models indicate that the precipitation over Antarctica will in-

crease; this effect will partly compensate for increased ice discharge.

Estimates of the contribution to sea level due to ice wastage in a CO_2-enhanced environment, and the scenarios on which they are based, are summarized in Table 4.

TABLE 4 Estimates of the Contribution to Sea-Level Rise by Ice Wastage in a CO_2-Enhanced Environment. Numbers in Parentheses Refer to Scenarios Given at Foot of Table[a]

Ice Mass	Annual Probable Contribution to Sea Level With Steady-State 2 x CO_2 Atmosphere (mm/yr)	Estimated Contribution to Total Sea-Level Change to Year 2100 Range (1) (m)	Report Section
Glaciers and small ice caps	2 to 5 (2)	0.1 (3) to 0.3 (4)	4.2
Greenland Ice Sheet	1 to 4 (5)	0.1 (6) to 0.3 (7)	4.3
Antarctic Ice Sheet	-3 to 10 (8)	-0.1 (9) to -1 (10)	5.3

[a]Note that thermal expansion of the oceans and other nonglacial processes might cause additional increments of sea-level rise.

(1) It is considered highly probable that the contribution to sea-level rise will not exceed these limits.

(2) Assuming rise in air temperature ΔT = 1.5 to 4.5°C, little increase in precipitation (accumulation).

(3) Linear increase with time in annual meltwater contribution due to ΔT = 1.5°C (or greater if partly compensated by increased accumulation) by 2085.

(4) As (3) except ΔT = 4.5°C, no increased accumulation, with the disappearance of much of the world's glaciers and ice caps.

(5) Ten percent increase in accumulation coupled with equilibrium-line altitude rise ΔELA = 500 to 1000 m, corresponding to ΔT = 6.5 to 13°C (this volume, Attachment 17) or ΔT = 3 to 6°C (this volume, Attachment 18), and with all the increased ablation running off to the ocean.

(6) Accumulation rate increased 10 percent 1985 < t < 2100. ELA and ablation rate at present value 1985 < t < 2000, ELA rises linearly with time 2000 < t < 2050, ELA held constant at 500 m 2050 < t < 2100, corresponding ΔT given in (5); all increased ablation runs off to ocean.

(7) As above except ΔELA = 1000 m.

(8) Increased accumulation (precipitation) but no increase in ice discharge (lower limit) to increased ice discharge but no increase in accumulation (upper limit).

(9) Increased accumulation with little increase in ice discharge.

(10) Melt rate at base of ice shelves same as present value (ΔM = 0) 1985 < t < 2000, ΔM rises linearly with time 2000 < t < 2050, ΔM = 3 m/yr 2050 < t < 2100, all ice above sea level in all of Antarctica affected in same way as Ice Streams B and E, little or no increased accumulation.

6.3 RECOMMENDATIONS FOR FURTHER RESEARCH

For time scales longer than one century, the uncertainty in estimating potential changes in land ice and sea level increases significantly. The workshop participants did not attempt to make estimates beyond the year 2100, and the limits expressed in Table 2 should not be extended beyond that year.

The workshop participants endorse the previous workshop report (NRC Committee on Glaciology 1984). That report presented a critical assessment of how well climate models simulate the present Antarctic environment and their ability to predict its future environment, as well as giving specific recommendations on how these predictions could be improved. Additional research is needed if the major uncertainties in our ability to predict the impact of a CO_2-enhanced climate on the world's land ice and oceans are to be reduced. This research includes general improvement in our ability to model atmospheric and oceanic circulation and to detect changes in mass and volume in the ocean and, in addition, some specific research tasks related to the response of the ice to the altered climate.

The workshop participants assume the importance of these general goals:

- Improve existing climate models by refining steady-state climate models, including improved parameterization of clouds and sea ice, more realistic modeling of topography and albedo to predict ice melt and runoff, and better understanding of why the models produce the sensitivity to CO_2 perturbations that they do. Especially important is modeling the time-dependent evolution of the ocean and the atmosphere as a coupled system, including the time evolution of CO_2 and trace-gas concentrations and the development of a time response function for the ocean-atmosphere system. (See Section 4.1)
- Determine the present-day global change in sea level more precisely, by establishing sea-level stations in strategic locations around the globe using interdisciplinary advice on siting; making regional studies of sea level to define regional tectonic, oceanographic, and isostatic sea-level signatures; improving statistical techniques for estimating global quantities from nonuniformly distributed and sampled sea-level records; and using contemporary glacio-isostatic rebound models to correct long-term tidal data including the determination of errors. (See Section 3.1)
- Determine to what extent the current rise in sea level is due to volume expansion of the ocean, by undertaking a program of high-quality observations of salinity and temperature in the different oceans to monitor long-term changes and developing improved understanding of vertical mixing processes in deep water. (See Section 3.2)

The following specific recommendations concern our ability to understand and predict the response of glaciers and ice sheets to an altered climate in the next century. These recommendations are all considered important to reducing uncertainties. The recommendations, but not the

tasks under each recommendation, are listed in order of decreasing priority based on amount of uncertainty that might be removed; these priorities are assigned across the various disciplines.

1. Southern Ocean Circulation Near Antarctica (Sections 3.2, 5.2)

- Assess ocean heat transport across the continental shelf around Antarctica, especially in the Ross, Amundsen, Bellingshausen, and Weddell Sea sectors.
- Determine ocean circulation beneath the large ice shelves.
- Analyze how these conditions will change as a result of a CO_2-enhanced atmosphere.

These tasks will require:

a. Large-scale oceanographic studies of the slope front region near the continental shelf break, particularly around West Antarctica, focused on the transports of water, salt, heat, and ice on and off the shelf, and ventilation of the deep ocean; better observations of sea-ice thickness and drift rates.

b. Numerical and analytical modeling of the oceanographic circulation on the Antarctic continental shelves, utilizing recent data; better coupling of global ocean circulation models with the continental-shelf region and better representation in all models of sea-ice formation and variability with climatic warming. The models of circulation on continental shelves should include storm conditions with katabatic wind forcing, particularly near the ice-sheet edge, buoyancy effects associated with increased freshwater supply, local increases or decreases in salinity, and water mass formation.

2. Ocean/Ice Shelf Interactions (Sections 5.2 to 5.4)

- Measure present basal-melt rates and investigate their relationship to underlying ocean circulation.
- Investigate iceberg calving rates, and identify those factors that affect these rates and determine the seaward boundary of ice shelves.

These tasks will require:

a. Observations near and beneath the ice shelves, focused on heat transfer from the boundary layer to the ice, the effect of bottom crevasses and bottom roughness on vertical mixing under the shelf, and monitoring key water masses such as high-salinity shelf water and the "warm" inflows. Drill holes, radio-echo sounding, and oceanographic observations will be required.

b. Mapping of the margins of the ice shelves repetitively, using satelliteborne imagers, to detect change and iceberg formation and movement; measurement of ice thickness, strain rate, and other variables near these margins; and the incorporation of these data in numerical models.

3. Ice Streams (Section 5.3)

- Determine the factors controlling whether an ice stream flows in a rapid or slow mode.
- Compile a complete set of data on ice streams, including such items as their dimensions, slopes, and speeds.

These tasks will require continued observation, theory, and modeling studies of basal sliding of glaciers and ice streams using data from deep ice cores and improvement in ice-dynamics models so that they incorporate realistic sliding laws as well as varying ice properties in addition to temperature and meltwater effects.

4. Detection and Prediction of Future Changes (Sections 3.1-3.6, 4.1-4.3)

- Changes in dimensions and discharge rates of glaciers and ice sheets.
- Changes in sea level and ocean temperature.

These tasks will require:

a. Using radar or laser altimetry from satellite platforms to extend topographic mapping of the ice surface to higher latitudes and utilizing repetitive surveys of surface altitude to measure the present rate of volume change. This latter task will require a more precise instrument (laser) than is currently available if it is to be accomplished in a few years; existing instruments (radar) will require several decades before yielding meaningful results. These instruments should be placed in a truly polar orbit.

b. Measuring the calving discharge of the outlet glaciers around the coast of Antarctica and along the east, north, and northwest coasts of Greenland, determining how the calving speed varies with time in these areas, and using these data to obtain a better understanding of how calving rates might be predicted.

c. Measuring the net balance as a function of altitude in the ablation zone of east and north Greenland, as well as the amount of runoff and the extent of the ablation zone, together with discerning how the ice melt and other balance components can be determined from synoptic meteorological data.

d. Developing and implementing a program of glacier mass-balance measurements in those areas of extensive glacier cover (especially in the mountains bordering the Gulf of Alaska and the Southern Andes); and completing the World Glacier Inventory, especially in these areas of extensive ice; and incorporating these results in an international data exchange program such as the proposed World Glacier Monitoring Service.

e. Exploring the link between glacier behavior and climate more extensively, especially in regard to how the regional synoptic conditions lead to a cumulative net balance, how subgrid scale processes can be incorporated in atmospheric circulation models, and investigating how the rare extremely negative net balances are caused.

f. Using modern radio-echo sounding techniques to measure the thickness of glaciers in regions of extensive ice cover, and using these data together with inventory results and glacier thickness models to calculate ice volumes.

g. Using contemporary models of glacio-isostatic disequilibrium in calculations of Earth rotation to define the present mass balance, and error limits, of the Antarctic and Greenland Ice Sheets; extending such calculations to the smaller ice masses so that the present trend in global ice melt can be better defined using an independent line of evidence.

References

Ambach, W., 1985. Climatic shift of the equilibrium line--Kuhn's concept applied to the Greenland Ice Cap. Annals of Glaciology, 6 (in press).

Barnes, P., D. Tabor, and J. C. F. Walker, 1971. The friction and creep of polycrystalline ice. Proceedings Royal Society of London, Ser. A, 324(1557), 127-155.

Barnett, T. P., 1983. Recent changes in sea level and their possible causes. Climatic Change, 5, 15-38.

Barnett, T. P., 1984. The estimation of "global" sea level change: A problem of uniqueness. Journal of Geophysical Research, 89(C5), 7980-7988.

Bauer, A., A. Ambach, and O. Schimpp, 1968. Mouvement et variation d'altitude de la zone d'ablation ouest de l'Indlandsis du Groenland entre 1948 et 1959. Meddr. Gronland, 174(1).

Benson, C. S., 1962. Stratigraphic studies in the snow and firn of the Greenland Ice Sheet, SIPRE Research Report 70.

Broecker, W. S., D. Peteet, and D. Rind, 1985. Does the ocean-atmosphere system have more than one stable mode of operation? Nature, 315(6014), 21-26.

Budd, W. F., P. L. Keage, and N. A. Blundy, 1979. Empirical studies of ice sliding. Journal of Glaciology, 25, 157-170.

Budd, W. F., D. Jenssen, and I. N. Smith, 1984. A three dimensional, time dependent model of the West Antarctic Ice Sheet. Annals of Glaciology, 5, 29-36.

Budd, W. F., D. Jenssen, and B. J. McInnes, 1985. Numerical modeling of ice stream flow with sliding. In T. H. Jacka (ed.), Australian Glaciological Research, 1982-1983, ANARE Research Notes Antarctic Division, Hobart (in press).

Dansgaard, W., H. Clausen, N. Gundestrup, C. Hammer, S. Johnsen, P. Kristensdottir, and N. Reeh, 1982. A new Greenland ice core. Science, 218(457a), 1273-1277.

Drewry, D. J., 1983. Antarctica: Glaciological and Geophysical Folio. Scott Polar Research Institute, Cambridge, England.

Environmental Protection Agency, 1983. Projecting Future Sea Level Rise. EPA 230-09-007, Washington, D.C., 121 pp.

Fastook, J. L., 1984. West Antarctica, the sea-level controlled marine instability: Past and future. In J. E. Hansen and T. Takahashi (eds.), Climate Processes and Climate Sensitivity, American Geophysical Union, pp. 275-287.

Flint, R. F., 1971. Glacial and Quaternary Geology. John Wiley and Sons, New York, 892 pp.

Foldvik, A., T. Gammelsrod, and T. Torresen, 1985. Circulation and water masses on the southern Weddell Sea shelf. In Oceanology of the Antarctic Continental Shelf, Antarctic Research Series, vol. 43, American Geophysical Union, Washington, D.C. (in press).

Fountain, A. G., 1982. Columbia Glacier photogrammetric altitude and velocity: Data set (1957-81). U.S. Geological Survey Open-File Report 82-756, 225 pp.

Gordon, A. L., 1983. Comments about the ocean role in the Antarctic glacial ice balance. In Proceedings: Carbon Dioxide Research Conference: Carbon Dioxide, Science and Consensus, Department of Energy, Washington, D.C., pp. IV.75-IV.85.

Hansen, J., G. Russell, D. Rind, P. Stone, A. Lacis, S. Lebedeff, R. Ruedy, and L. Travis, 1983. Efficient three-dimensional global models for climate studies: Models I and II. Monthly Weather Review, 111(4), 609-662.

Hansen, J., A. Lacis, D. Rind, and G. Russell, 1984. Climate sensitivity: Analysis of feedback mechanisms. In Climate Processes and Climate Sensitivity, American Geophysical Union, Washington, D.C.

Hollin, J. T., 1962. On the glacial history of Antarctica. Journal of Glaciology, 4, 273-295.

Hollin, J. T., and R. G. Barry, 1979. Empirical and theoretical evidence concerning the response of the Earth's ice and snow cover to a global temperature increase. Environment International, 2, 437-444.

Hughes, T., 1973. Is the West Antarctic ice sheet disintegrating? Journal of Geophysical Research, 78, 7884-7910.

Jacobs, S. S., A. L. Gordon, and J. L. Ardai, Jr., 1979. Circulation and melting beneath the Ross Ice Shelf. Science, 203, 439-443.

Jacobs, S. S., R. G. Fairbanks, and Y. Horibe, 1985. Origin and evolution of water masses near the Antarctic continental margin: Evidence from $H_2{}^{18}O/H_2{}^{16}O$ ratios in seawater. In Oceanology of the Antarctic Continental Shelf, Antarctic Research Series, vol. 43, American Geophysical Union, Washington, D.C. (in press).

Jezek, K. C., 1984. Recent changes in the dynamic condition of the Ross Ice Shelf, Antarctica. Journal of Geophysical Research, 89(B1), 409-416.

Jezek, K. C., and C. R. Bentley, 1984. A reconsideration of the mass balance of a portion of the Ross Ice Shelf. Journal of Glaciology, 30(106), 381-384.

Kamb, B., C. F. Raymond, W. D. Harrison, H. Engelhardt, K. A. Echelmeyer, N. Humphrey, M. M. Brugman, and T. Pfeffer, T., 1985. Glacier surge mechanism: 1982-1983 surge of Variegated Glacier, Alaska. Science, 227(4686), 469-479.

Lingle, C. S., 1984. A numerical model of interactions between a polar ice stream and the ocean: Application to ice stream E, West Antarctica. Journal of Geophysical Research, 89(C3), 3523-3549.

Meier, M. F., 1983. Snow and ice in a changing hydrological world. Hydrological Sciences Journal, 28(1), 3-22.

Meier, M. F., 1984. Contribution of small glaciers to global sea level. Science, 226(4681), 1418-1421.

Meier, M. F., L. A. Rasmussen, R. M. Krimmel, R. W. Olsen, and D. Frank, 1985a. Photogrammetric determination of surface altitude, terminus position, and ice velocity of Columbia Glacier, Alaska. U.S. Geological Survey Professional Paper 1258-F, 41 pp.

Meier, M. F., L. A. Rasmussen, and D. S. Miller, 1985b. Columbia Glacier in 1984: Disintegration underway. U.S. Geological Survey Open-File Report 85-81, 17 pp.

Mercer, J. H., 1968. Antarctic ice and Sangamon sea level. International Association of Hydrological Sciences Publication No. 79, pp. 217-225.

Mercer, J. H., 1978. West Antarctic ice sheet and CO_2 greenhouse effect: A threat of disaster? Nature, 271, 321-325.

Munk, W., and R. Revelle, 1952. Sea level and the rotation of the Earth. American Journal of Science, 250, 829-833.

NRC Carbon Dioxide Assessment Committee, 1983. Changing Climate. National Academy Press, Washington, D.C., 496 pp.

NRC Climate Research Board, 1979. Carbon Dioxide and Climate: A Scientific Assessment. National Academy of Sciences, Washington, D.C., 22 pp.

NRC Climate Research Board, 1982. Carbon Dioxide and Climate: A Second Assessment. National Academy Press, Washington, D.C., 72 pp.

NRC Committee on Glaciology, 1983. Snow and Ice Research, An Assessment. National Academy Press, Washington, D.C., 126 pp.

NRC Committee on Glaciology, 1984. Environment of West Antarctica: Potential CO_2-Induced Changes. National Academy Press, Washington, D.C., 236 pp.

Parkinson, C. L., and R. A. Bindschadler, 1984. Response of Antarctic sea ice to uniform atmospheric temperature increases. In J. E. Hansen and T. Takahashi (eds.), Climate Processes and Climate Sensitivity, American Geophysical Union, Washington, D.C., pp. 254-264.

Pillsbury, R. D., and S. Jacobs, 1985. Preliminary observations from long-term current meter moorings near the Ross Ice Shelf, Antarctica. In Oceanology of the Antarctic Continental Shelf, Antarctic Research Series, vol. 43, American Geophysical Union, Washington, D.C. (in press).

Potter, J., and J. Paren, 1985. Interaction between ice shelf and ocean in George VI Sound, Antarctica. In Oceanology of the Antarctic Continental Shelf, Antarctic Research Series, vol. 43, American Geophysical Union, Washington, D.C., (in press).

Radok, U., R. G. Barry, D. Jenssen, R. A. Keen, G. N. Kiladis, and B. McInnes, 1982. Climatic and physical characteristics of the Greenland ice sheet: Parts I and II. Cooperative Institute for Research in Environmental Sciences (CIRES), University of Colorado, Boulder.

Rasmussen, L. A., and M. F. Meier, 1985. Surface topography of the lower part of Columbia Glacier, Alaska 1974-1981. U.S. Geological Survey Professional Paper 1258-E, 63 pp.

Revelle, R. R., 1983. Probable future changes in sea level resulting from increased atmospheric carbon dioxide. In Changing Climate, National Academy Press, Washington, D.C., pp. 433-448.

Robin, G. de Q., and R. J. Adie, 1964. The ice cover. In R. Priestley, R. J. Adie, and G. de Q. Robin (eds.), Antarctic Research, Butterworths, London, pp. 100-117.

Rose, K. E., 1979. Characteristics of ice flow in Marie Byrd Land, Antarctica. Journal of Glaciology, 24, 63-75.

Seckel, H., 1977. Hohenanderungen im Gronlandischen Inlandeis zwischen 1959 und 1968. Meddelelser om Gronland, Bd. 187(4), Nyt Nordisk Forlag Arnold Busck, Kobenhavn.

Stauffer, B., H. Hofer, H. Oeschger, J. Schwander, and U. Siegenthaler, 1984. Atmospheric CO_2 concentrations during the last glaciation. Annals of Glaciology, 5, 160-164.

Thomas, R. H., and C. R. Bentley, 1978. The equilibrium state of the eastern half of the Ross Ice Shelf. Journal of Glaciology, 20, 509-518.

Thomas, R. H., and D. R. MacAyeal, 1982. Derived characteristics of the Ross Ice Shelf, Antarctica. Journal of Glaciology, 28, 397-412.

Weertman, J., 1974. Stability of the junction of an ice sheet and an ice shelf. Journal of Glaciology, 13, 3-11.

Weidick, A., 1984. Review of glacier changes in West Greenland. In Symposium on Climate and Paleoclimate of Lakes, Rivers, and Glaciers, Igles, Austria.

Zhakharov, V. F., 1981. L'dy Arktiki i sovremennyye prirodnyye protsessy (Ice of the Arctic and Present-Day Processes). Gidrometeoizdat, Leningrad, 136 pp.

Appendix: Workshop Presentations

ATTACHMENT 1

RECENT SEA LEVELS FROM TIDE GAUGES: PROBLEMS AND PROGNOSIS

D. G. Aubrey
Woods Hole Oceanographic Institution
Woods Hole, Massachusetts

INTRODUCTION

Changes in relative sea level play an important role in human affairs, with future increased importance if the anticipated global warming due to higher levels of atmospheric carbon dioxide causes significant melting of ice sheets. Throughout geologic history, relative sea level has been changing, on a full range of space and time scales. The rich spectra complicate the unraveling of recent relative sea-level trends, making prediction a complex task. Recent studies are helping to define the space and time scales of relative sea-level rise of the past century over the world's oceans, separating regional patterns of relative sea level from patterns, using tide-gauge records. We will test the hypothesis that rate of eustatic sea-level rise is increasing, or will increase in the near future, as a result of thermal expansion and addition of glacial meltwaters. Because of the nonuniform distribution of sea-level observations in both space and time, new statistical techniques beyond simple regressions have been developed and applied, resulting in definition of space and time scales of change with appropriate error estimates.

The complexity of space and time scales of relative sea-level change arises from many causes. The most important are tectonic, glacial rebound, and climatic causes; high-frequency oscillations also contribute to the complexity (e.g., Lisitzin 1974) of the space and time scales.

Under tectonic, we include effects arising from large-scale tectonics such as continental collision, cooling of new crust derived from oceanic spreading belts, and volcanism resulting from plate-boundary processes. Time scales of these processes are long (thousands of years and more), and space scales vary from tens to thousands of kilometers.

Glacial rebound represents the isostatic adjustment of formerly glaciated areas to lowered overburden due to glacial retreat. Space scales are hundreds to thousands of kilometers, and time scales are on the order of thousands of years. The uplift of Scandiavia following the most recent glaciation is an example of glacial rebound.

Climatic sea-level change is partly a response to heating or cooling of the upper oceans owing to changes in mean atmospheric temperatures and partly a reflection of increased water mass. Time scales are on

the order of tens of years and more, and space scales are global. These climatic effects may result from deglaciation, on one extreme, to shorter-term effects, such as the postulated rise due to increased atmospheric carbon dioxide (e.g., Mercer 1978). This sea-level pattern is partly a steric response, as the water volume increases because of heating. It is also partly due to increased water mass in the oceans, as glaciers advance or retreat because of changes in atmospheric temperatures and precipitation patterns.

Higher frequency sea-level changes include those due to seasonal heating/cooling, local meteorological conditions, and other processes. The El Nino-Southern Oscillation (ENSO) is an example of a lower-frequency atmospheric/oceanic interaction, with time scales of 1-10 years and spatial scales on the order of basin widths. ENSO can be an energetic part of some sea-level series. Not categorized are miscellaneous causes of relative sea-level change, including subsidence due to pore-fluid removal (such as in Galveston, Texas, or Long Beach, California). Subsidence due to higher sedimentation rates falls into this miscellaneous category, an example being the Mississippi River delta, which has more local impacts. Space scales of these processes generally are limited to hundreds of kilometers, with time scales ranging upward from tens of years. This superposition of space and time scales results in complex local relative sea-level time histories, requiring a battery of analysis techniques to separate individual effects.

The present paper concentrates on the past century of relative sea-level change because of the availability of precise tide-gauge records covering this period. The increased spatial coverage afforded by tide-gauge records, and their increased precision over alternate means of estimating sea-level rise (such as radiometric methods), make them useful for our intent of defining both regional and global space and time scales of sea-level variability. These stations are not without their drawbacks, however. Out of roughly 900 tide-gauge stations in the world (e.g., Lennon 1975-1978; Lutjeharms and Alheit 1983), approximately 90 percent are in the northern hemisphere. The three greatest densities of tide-gauge stations are in industrialized areas: the United States, northern Europe, and Japan. Lesser developed nations in Africa, South America, Central America, and southern Asia have only a few tide-gauge stations, most of which span short terms and have many record gaps; some have been discontinued. Thus, added to the number and variety of causes of relative sea-level change, we must deal with uneven spatial and temporal distribution of tide-gauge stations.

Previous work on extracting relative sea levels from tide-gauge information is extensive. Much of the earlier work was directed toward obtaining a single value representing the eustatic sea-level signature, reflecting Quaternary glacial processes and climatic effects. All faced the problems discussed earlier, with incomplete time and space coverage of sea-level data. In recent work, Emery (1980) chose to use the median value of rates of rise of relative sea levels to estimate eustatic changes. Gornitz et al. (1982) and Barnett (1982, 1983) subdivided the globe into units (14 and 11, respectively), within each of which a representative sea-level curve was derived, and then a global curve was obtained by equally weighting each of the various units. Equal

weighting of each unit prevented the added confidence derived from multiple sea-level records in some units. Selection of a representative sea-level curve also presented a problem, which influenced the results for the eustatic estimate. Barnett (1982) used eigenanalysis to examine global trends, which represented a useful advancement in examination of coherent sea-level phenomena.

Aubrey and Emery (1983) also applied eigenanalysis to examine the space and time scales of sea-level change along the U.S. coastlines. Rather than trying to estimate a single eustatic sea-level rate of rise, they defined the space and time scales of sea-level variability over the last half century. These could then be simplified to derive a mean rate of rise for the United States, if desired. The emphasis on defining spatial and teporal scales of change was a significant departure from previous work. Rather than modeling sea-level change with an a priori hypothesis of a eustatic signature, Aubrey and Emery (1983) defined the energetic space and time scales of change, which could then be model-tested later. This accords with the philosophy that a global response to some external cause of sea-level rise will not be uniform over the globe; rather there will be some spatial and temporal dependence on such a response. The term eustatic therefore implies space and time structure.

Most estimates of relative sea-level rise over the past century (Table 1.1) are between 10-15 mm/yr. Emery (1980) obtained a significantly higher value, for two primary reasons. First, he used data up to 1979, which would increase estimates of relative sea-level rise if relative sea-level rise were accelerating. Second, Emery's (1980) criterion for station selection was based on a statistical test that rejected rates whose standard deviation was greater than the estimate. Since this test is more stringent for stations with smaller rates of rise, it favored larger rates of rise. An improved error criterion would be to compare all rates of rise to a uniform deviation; for

TABLE 1.1 Estimates of Global Sea-Level Rise (after Barnett, 1982)

Authors	Rate (mm/yr)
Thorarinsson (1940)[a]	0.5
Gutenberg (1941)[a]	1.1 ± 0.8
Kuenen (1950)[a]	1.2 to 1.4
Lisitzin (1958)[a]	1.1 ± 0.4
Wexler (1961)[a]	1.2
Fairbridge and Krebs (1962)	1.2
Emery (1980)	3.0
Gornitz et al. (1982)	1.2
Barnett (1982)	1.5 ± 0.2
Barnett (1984)	2.3
Aubrey and Emery (unpublished)	0.3

[a]See Lisitzin (1974) for references.

instance, reject all stations whose rates of rise are uncertain within limits of 1 or 2 mm/yr. Aubrey and Emery (summitted) use such a criterion for studies of Japanese sea levels.

Finally, Barnett (1983, 1984) re-examined global sea levels, deriving an estimate of 2.3 mm/yr as a eustatic figure during the past 50 years. He expressed some reservation about whether the data merited further analysis to extract sea-level information. We believe that the sea-level scales can be defined better using improved statistical techniques.

RESULTS AND DISCUSSION

Using some sophisticated statistical techniques (see Aubrey and Emery, submitted), we have made progress in separating from tide-gauge records the various contributions to relative sea-level records. Rather than initiating a global analysis immediatley, regional studies have been undertaken to clarify more local sea-level behavior, distinguishing the signatures of the various geologic, isostatic, and oceanographic contributions to tide-gauge records. We present three examples of such regional studies to illustrate our success in identifying causes for sea-level fluctuations: a "stable" continental margin (the eastern United States), a technically active margin (Japan), and an isostatically adjusting margin (Fennoscandia).

United States sea levels were examined by Aubrey and Emergy (1983) to clarify the space and time structure of relative sea levels (spatial eigenfunctions 1 and 2). Figure 1.1 reveals some variabilty in the east coast sea levels and considerable variabilty in west coast sea levels. The west coast is considered tectonically active, while the east coast is generally regarded as a relatively stable margin. A closer examination of the east coast data (Figure 1.2) shows three major compartments, within each of which relative sea level exhibits a monotonic trend. From Cedar Keys, Florida, to Cape Hatteras, North Carolina, rate of relative sea-level rise steadily increases. From Cape Hatteras to Woods Hole, Massachusetts, rates of sea-level rise decrease, followed by further increase to the north. Although not shown on the figure because only U.S. stations were used, farther north into Canada, the rate of relative sea-level rise decreases and becomes negative, reflecting glacial rebound. This compartmentization of the U.S. east coast mirrors some poorly understood tectonic influence; if these compartments were not spatially resolved, then use of a few tide-gauge stations to derive a regional estimate would give a biased result. The time scales of relative sea-level behavior are depicted in the temporal eigenfunctions (Figure 1.3) and by spectra of these eigenfunctions (Figure 1.4). For sea levels along the U.S. east coast, the spectrum of motion reveals many time scales, including a dominant low-frequency motion, and broad periodicities of 6-10 years (poorly resolved because of the short record length and the small number of degrees of freedom of the estimate). Although not used for this purpose, in Aubrey and Emery (1983), these space and time scales permit decomposition of the sea-level signature into responses to different forcing functions. For instance, the

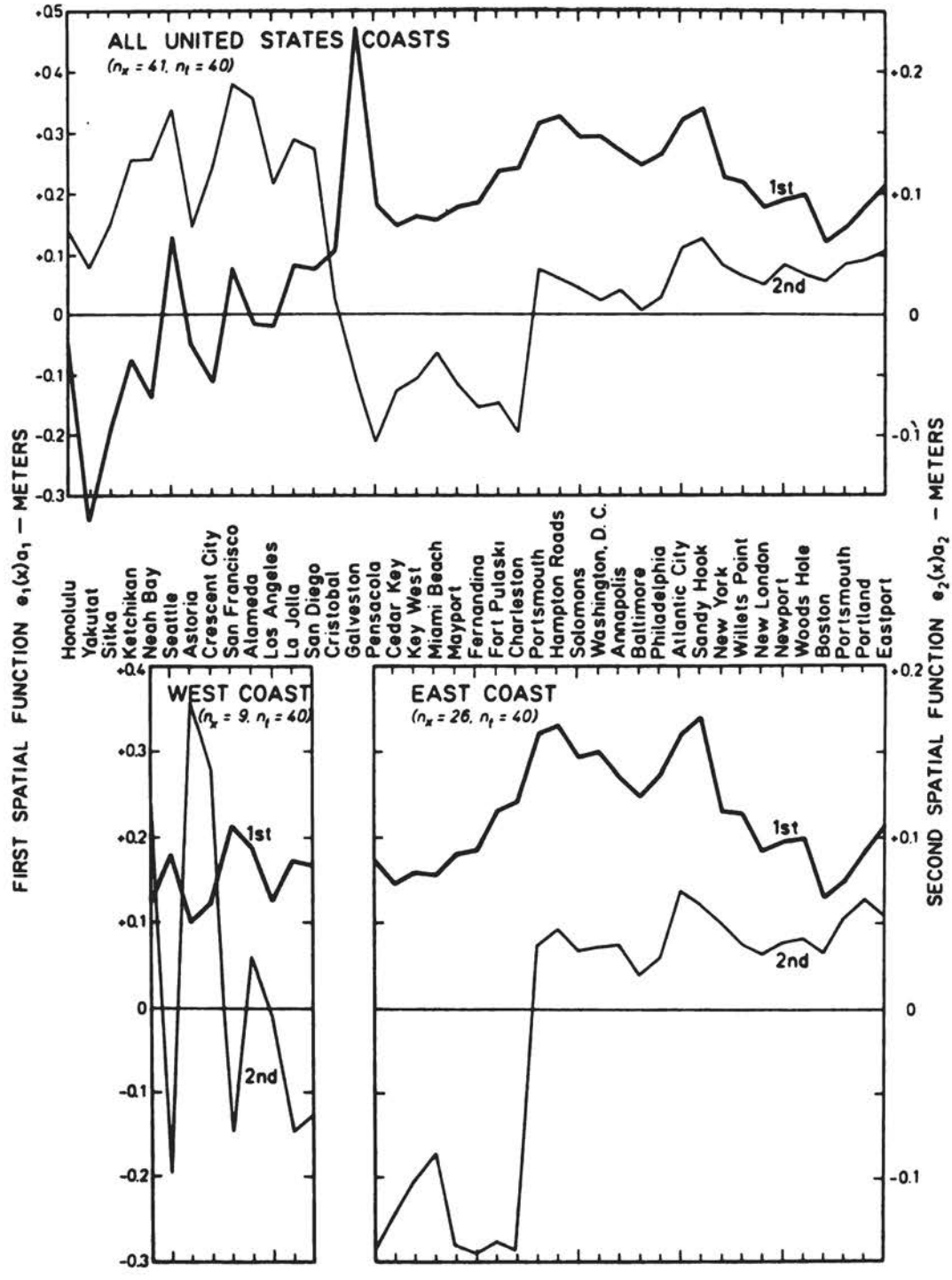

FIGURE 1.1 Spatial eigenfunctions for 41 stations having records of 40 years, with similar plots for 10 west-coast stations and 26 east-coast ones. First functions account for 65, 53, and 78 percent of total variations, and second functions for 10, 26, and 10 percent, respectively.

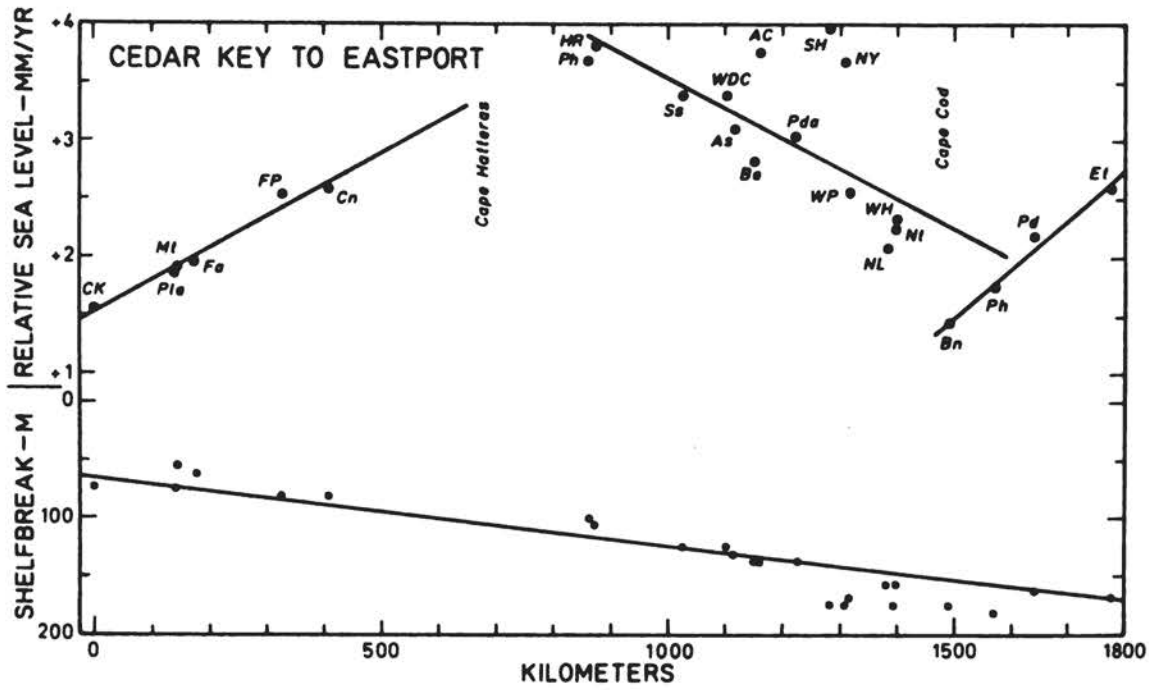

FIGURE 1.2 Mean annual relative sea-level changes during 40-year record from Figure 1.1 for east-coast stations. Regression lines denote three main segments of east coast having different sea-level trends; these trends are not reflected in depths to shelf break at points nearest each station.

higher frequencies reflect oceanographic factors, while low frequencies reflect tectonism, isostatic adjustment, and eustatic changes.

The coastline of Japan shows a complex history of sea levels (Aubrey and Emery submitted). Initially, because of the large density of sea-level stations in Japan, and because of its long-recognized tectonic activity, we were curious whether we could bring some order to interpretation of the land and ocean movements. We first performed a linear regression on each station in Japan exceeding 15 years in length (since we had previously observed that a 10-15 year cycle appeared in many Japanese sea-level records) and examined regional trends (Figure 1.5). Regression analysis, as discussed by Aubrey and Emery (1983), has severe drawbacks because of the direct comparison of dissimilar time periods and loss of definition of time scales of variability. In spite of these drawbacks, the regression analysis revealed a coherent trend of sea levels apparently related to the tectonics of the area and previously unpublished (Figure 1.6; Dambara 1971; Kato and Tsumura 1979; Aubrey and Emery submitted). Japan is an island arc with oceanic trenches to the east and south; to the east, the Japan Trench and Bonin Trench converge off southern Japan, while to the south, the short Nankei Trough apparently reflects relative movement between the two easterly trench segments (Figure 1.5). The regression trends appear to mirror the tectonism, in that the southeastern (Pacific) coast is submergent whereas

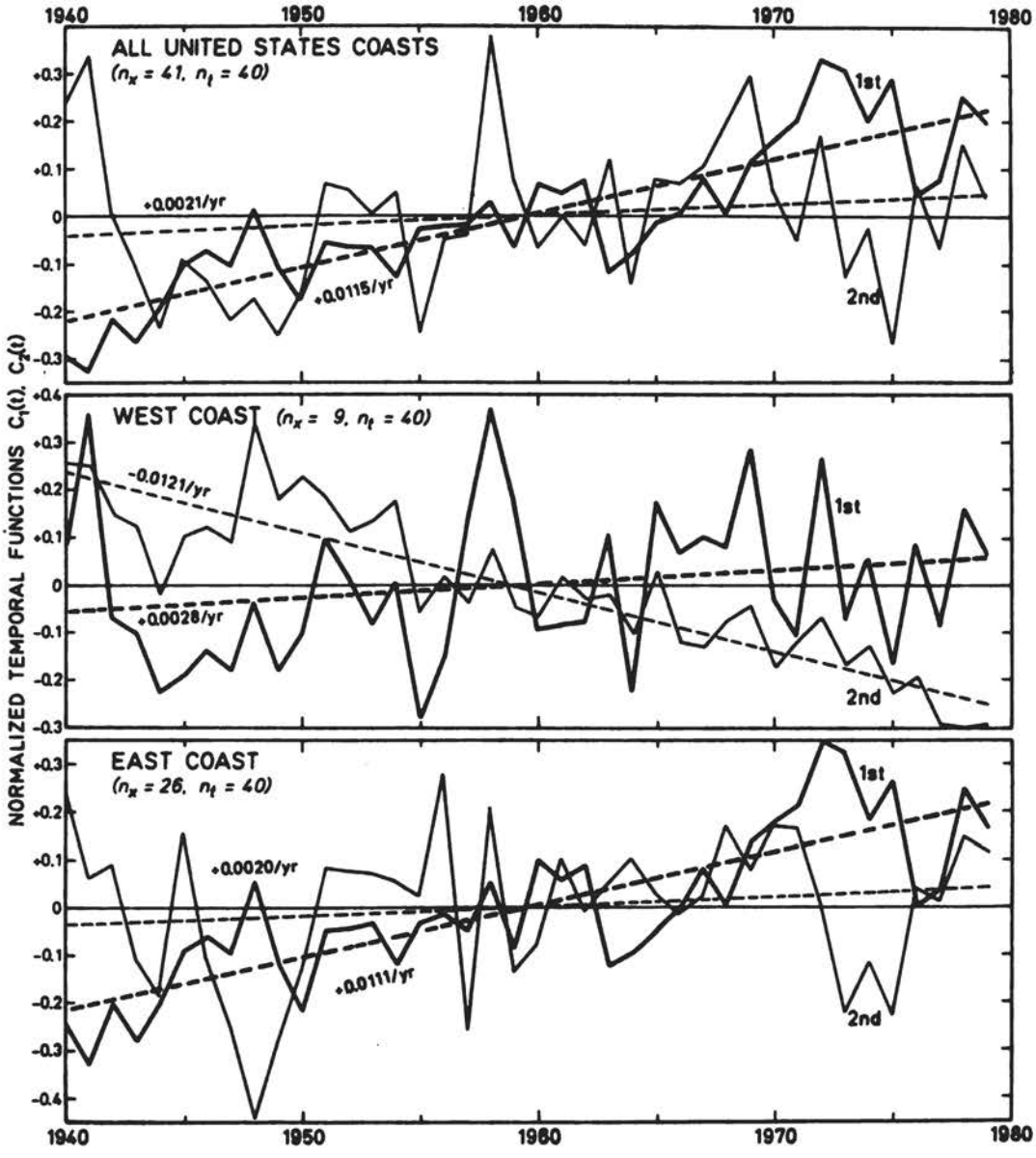

FIGURE 1.3. Temporal eigenfunctions for same stations of Figure 1.1. First functions account for 65, 53, and 78 percent of total variations, and second functions for 10, 26, and 10 percent, respectively. Linear trend for the first function must be weighted by corresponding spatial value to obtain local rate of sea-level rise.

the northwestern coast (Japan Sea) coast is emergent, apparently responding to frictional warping on the nonsubducting plate adjacent to the trench. In the southwestern part of Japan, a similar parallel but secondary warping indicates a second phase of subduction.

To examine these patterns further, eigenanalysis of all Japanese stations exceeding 15 years in length was performed, on both covariance

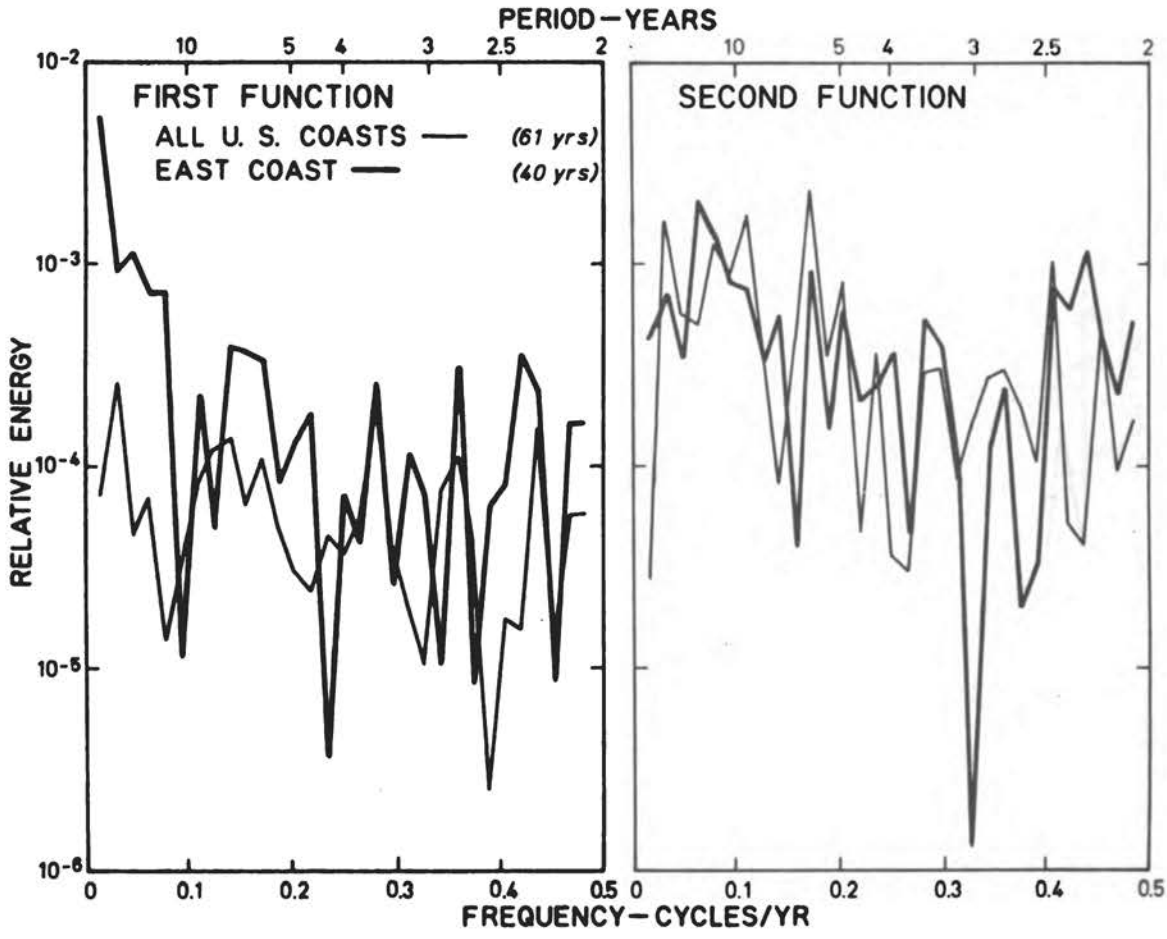

FIGURE 1.4 Spectra of first and second eigenfunctions for 12 U.S. stations for 61 years and for 26 east-coast stations for 40 years. Estimates have two degrees of freedom. Energy units are relative.

and correlation matrices (Figure 1.7). Results are similar to the regression case; the coastal change mirrors trench processes on the adjacent margins with warping of the nonsubducting plate. Spatial scales of motion are well defined, as are time scales (Figures 1.7 and 1.8). Dominant time scales include both low frequencies (reflecting tectonic and eustatic processses) and higher frequencies (reflecting oceanographic and climatic processes). Higher-frequency Japanese sea levels reflect the impact of Kuroshio meanders and correlate well with the Southern Oscillation Index (Aubrey and Emery submitted). Eigen-analysis efficiently represents the variabilty in the data, with the first few functions accounting for most of the data variabilty (Table 1.2). This example shows that even in a highly tectonic region, we can demonstrate local space and time scales of motion. In fact, this simple analysis has elucidated tectonic trends that have not been described previously.

FIGURE 1.5 Average annual vertical movement of land relative to sea level for the duration of 86 tide-gauge records in Japan having records longer than 10 years, plus eight stations for Korea to establish boundary positions. Rates are based on least-squares linear regressions, and they range from +6 to -24 mm/yr. Contours are at 2-mm/yr intervals. Stations are shown as solid dots.

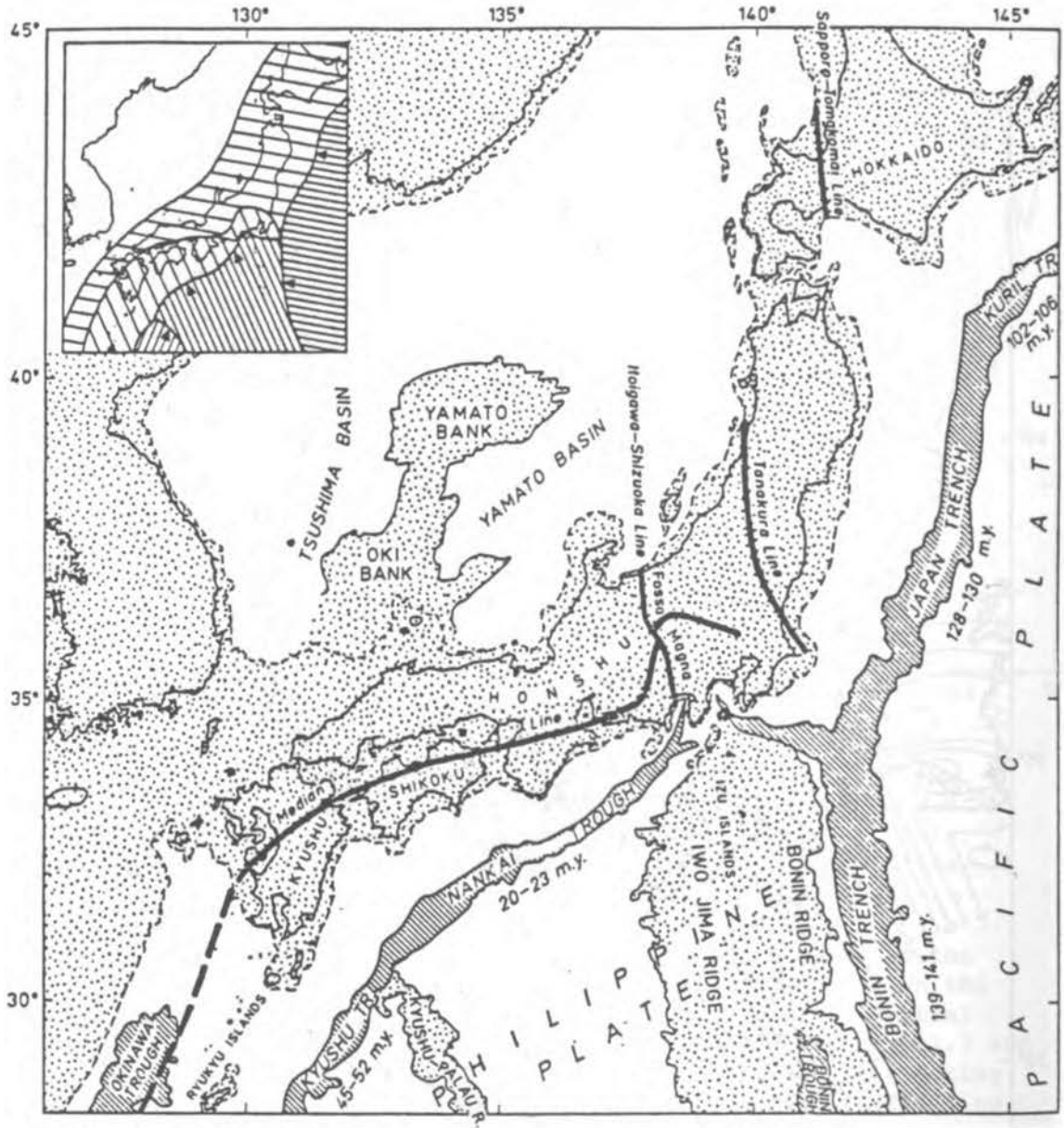

FIGURE 1.6 Tectonic trends on land and ocean floor. Topography modified from Boggs (1984) and others, major tectonic lines (faults) on land from Tanaka (1977), and ages of initial plate subduction from Hilde and Uyeda (1983). Insert shows oceanic plates, their present direction of movement, and the areas of overriding crust that have been structurally influenced by the subduction. Approximate shelf break (200-m contour)--dashed line; major positive elements--dotted; trenches and troughs--diagonal lines; plates--named with dates of initial subduction.

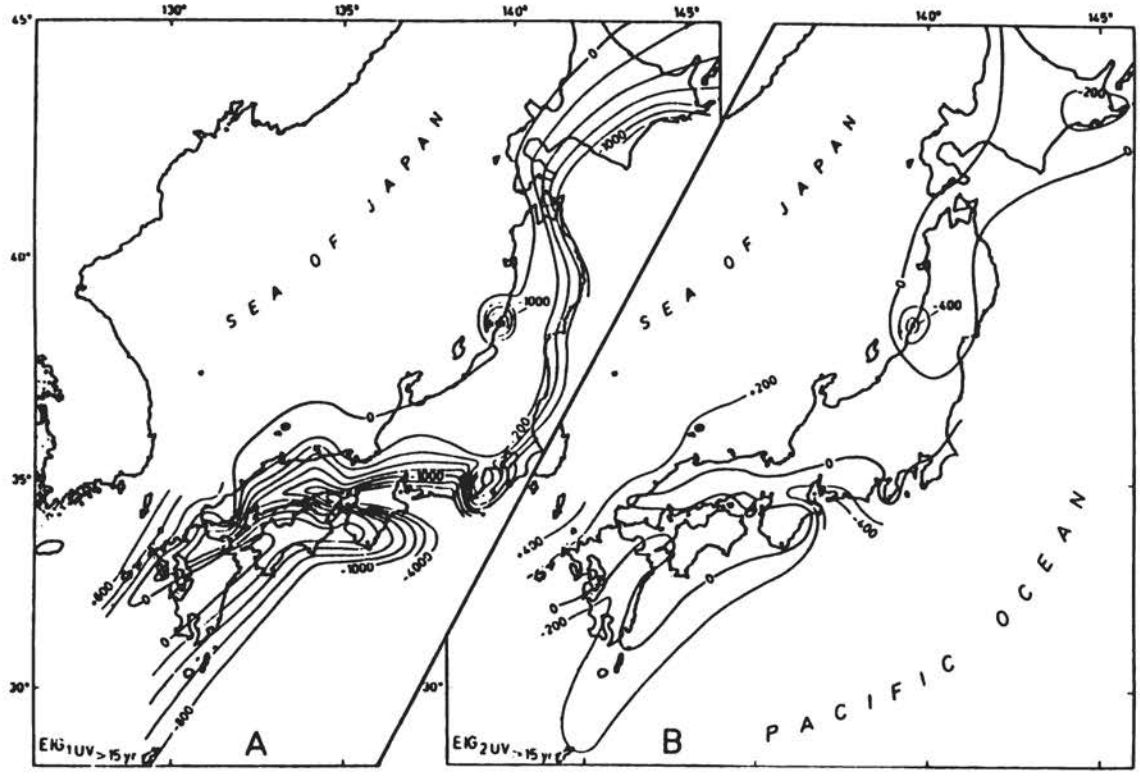

FIGURE 1.7 Spatial eigenfunctions for Japan in units of millimeters at 51 stations, each having unit variance and spanning at least 15 years. A, First function. Contours are at intervals of 200 units, with 4000-unit contour added. Multiplying this pattern by the temporal eigenfunction trend yields an estimate of sea-level rise in units of millimeters/year.

As a final example of regional studies, Fennoscandia is presented to represent the problems associated with an area with large isostatic sea-level signatures. Regression analysis (Figure 1.9) documents the influence of continued isostatic readjustment of the area, in qualitative accord with most, but not all, theories of glacial rebound (Clark et al. 1978; Mörner 1980; Peltier 1980). Eigenanalysis reveals much the same

TABLE 1.2 Eigenvalues for Japanese Sea Levels, 50-Year Sea-Level Analysis, True Variance

Eigenvalue Number	Percent of Variance Explained
1	82.7
2	4.2
3	3.3
4	2.5
5	1.7

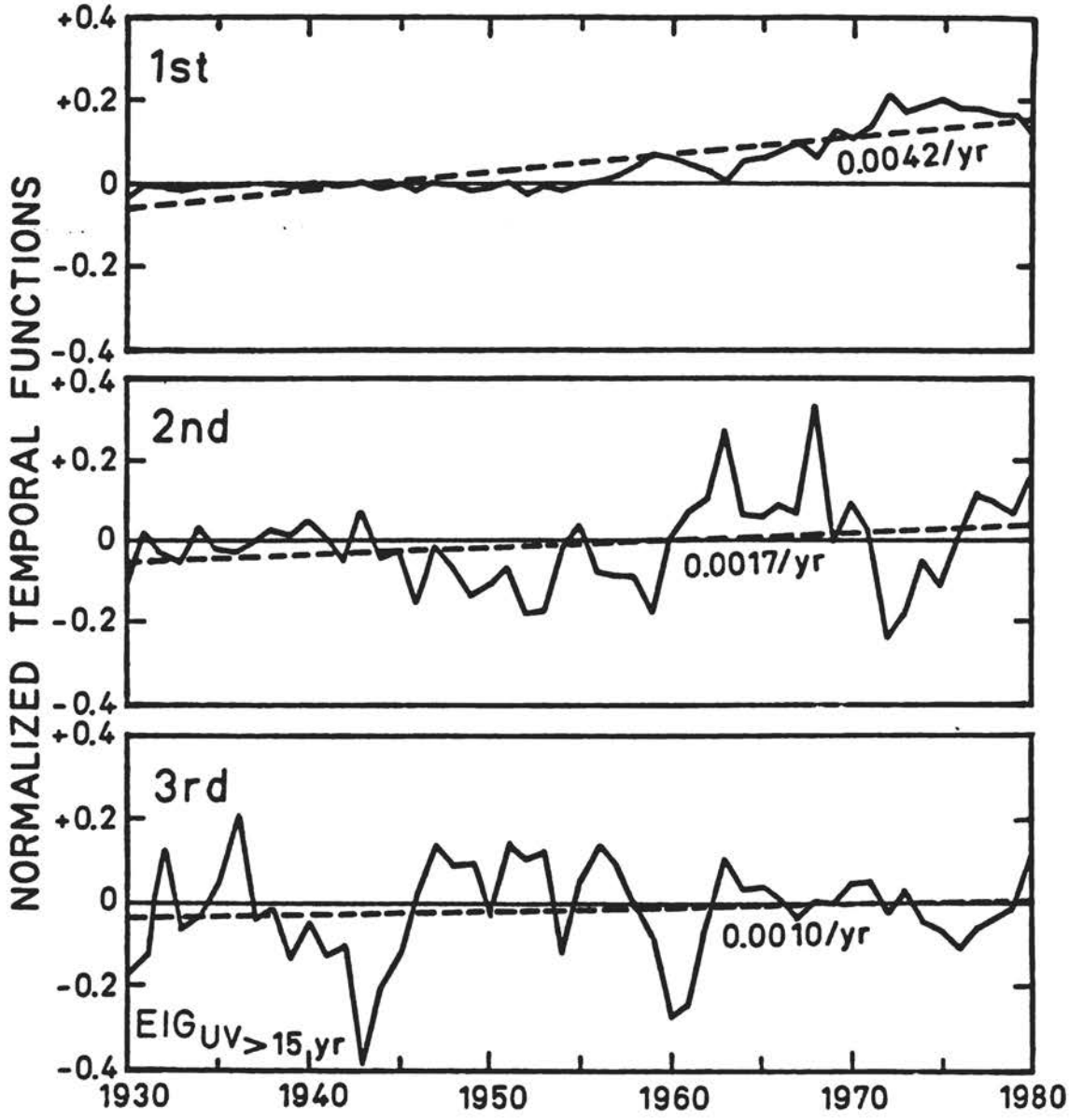

FIGURE 1.8 First, second, and third temporal eigenfunctions for same tide-gauge records used in Figure 1.7. Elevations are dimensionsless and normalized. These three functions account for 83, 4, and 3 percent, respectively, of total variations in records. Note that the best-fit straight line fails to follow the trend of data points, indicating an apparent increase in rate of movement of land or of sea level beginning about 1953 (see text for discussion).

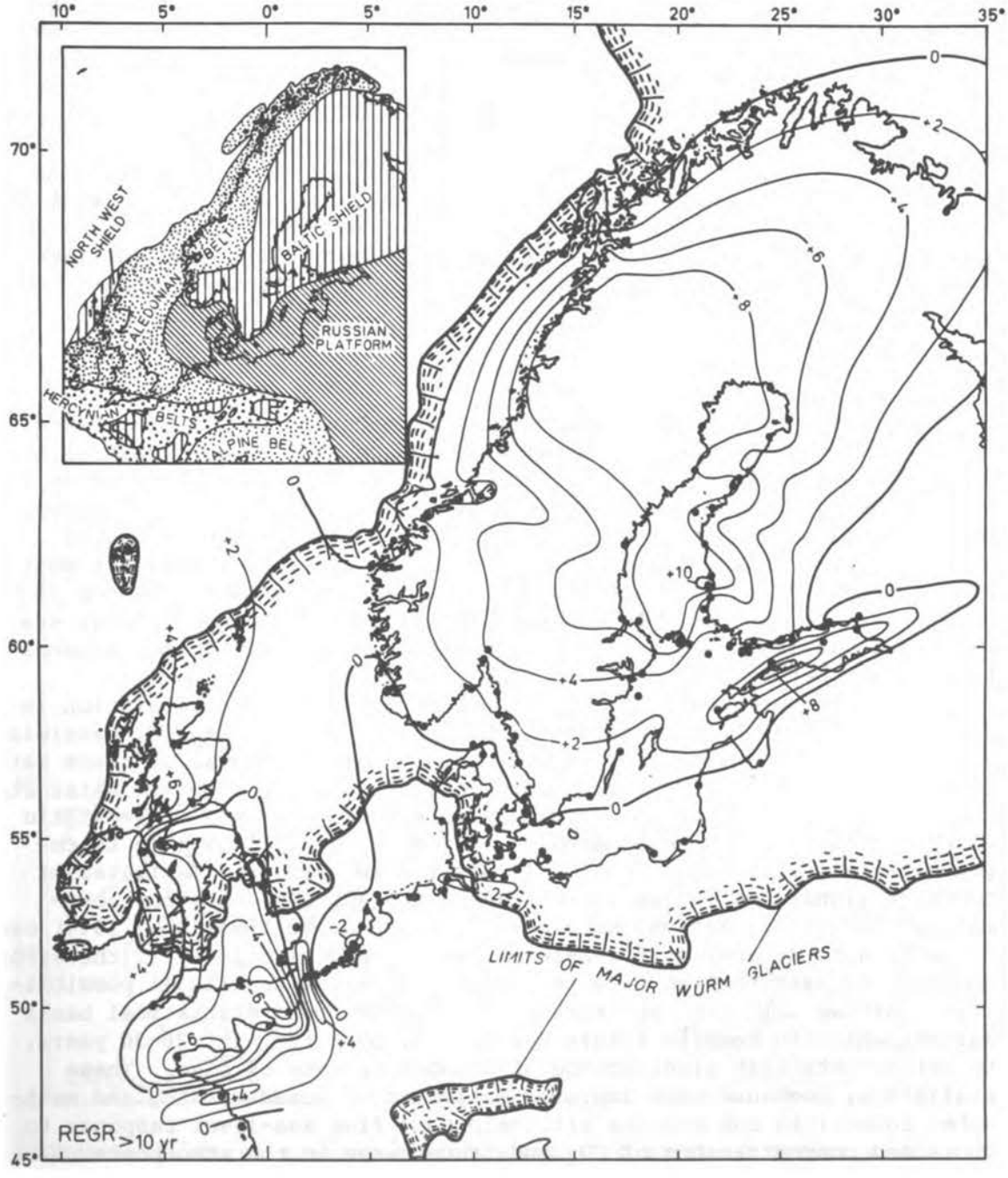

FIGURE 1.9 Mean annual uplift of Scandinavia and Scotland and downdrop of England and Brittany derived from least-squares regression analysis of 134 tide-gauge records having time spans longer than 10 years. Maximum extent of Würm glaciers is from Flint (1957, plate III). Insert shows tectonic provinces as compiled by Naylor and Mounteney (1975).

pattern of sea-level behavior, with slightly lowered maximum rates of land rise (Figures 1.10-1.12). Temporal behavior of relative sea level (Figure 1.10 inset) indicates a relative stability in the time history of sea-level rise, with some indication of change in rate of rise near 1924. The interpretation of this change in rate of rise is under investigation; we need to be certain that it is not a relic of the analysis procedure. Higher-frequency time behavior (second eigenfunction, Figure 1.10 inset) may be related to oceanographic factors, which have not yet been clarified. The spectra of the higher frequency sea-level variations are nearly flat, in contrast with previous regional studies in the United States, Japan, and the eastern Asian mainland. Note that the Gulf of Finland shows some evidence of tectonic behavior, perhaps unrelated to the isostatic uplift (Figures 1.9 and 1.12), near the intersection of the Baltic Shield and Russian Platform, Figure 1.8 inset).

PROGNOSIS

These three studies illustrate regional behavior that is sometimes difficult to isolate from eustatic signals and that severely biases our estimates of global sea levels. These three studies were in regions where density of tide-gauge stations allows us to define local trends. Unfortunately, most areas of the globe do not permit this degree of spatial resolution. Duration of observations are also shorter at most other places on the globe, reducing our ability to define time scales of sea levels. In order to make an intelligent estimate of global sea levels, including any eustatic components, we must define the regional trends much better than has been done previously.

What is the prognosis for being able to distinguish acceleration in rate of sea-level rise? Barnett (1984) made a strong case for pessimism in this regard, considering the poor signal-to-noise ratio in these data sets. We feel slightly more optimistic. If we can define and eliminate regional anomalies, and incorporate theoretical estimates of isostatic effects with empirical estimates of tectonics, we will be able to improve the signal-to-noise ratio of eustatic sea levels. Estimates of coherent global sea levels can be made, with appropriate error estimates. Robust regression techniques (e.g., Andrews 1974; Hogg 1974) can be applied to determine if sea-level rise is accelerating. If the error analyses suggest that we have no confidence in the results (a possibility), then we will have at least established a sound statistical basis against which to compare future sea levels, over the next 20-30 years, to better establish significance of changes in rate of rise. These statistics, combined with improved estimates of ocean warming and meltwater input into the oceans, will help to define sea-level response to increased concentrations of CO_2 and trace gases in the atmosphere.

How should we proceed with future sea-level research? Clearly, we need to increase our base of sea-level observations, particularly in mid-ocean years. Over the next few years, we must establish a larger, more uniform net of sea-level observatories. Because of their expense, they must be located with care and foresight. A working group consisting of geologists, tectonicists, isostatists, geodesists, physical

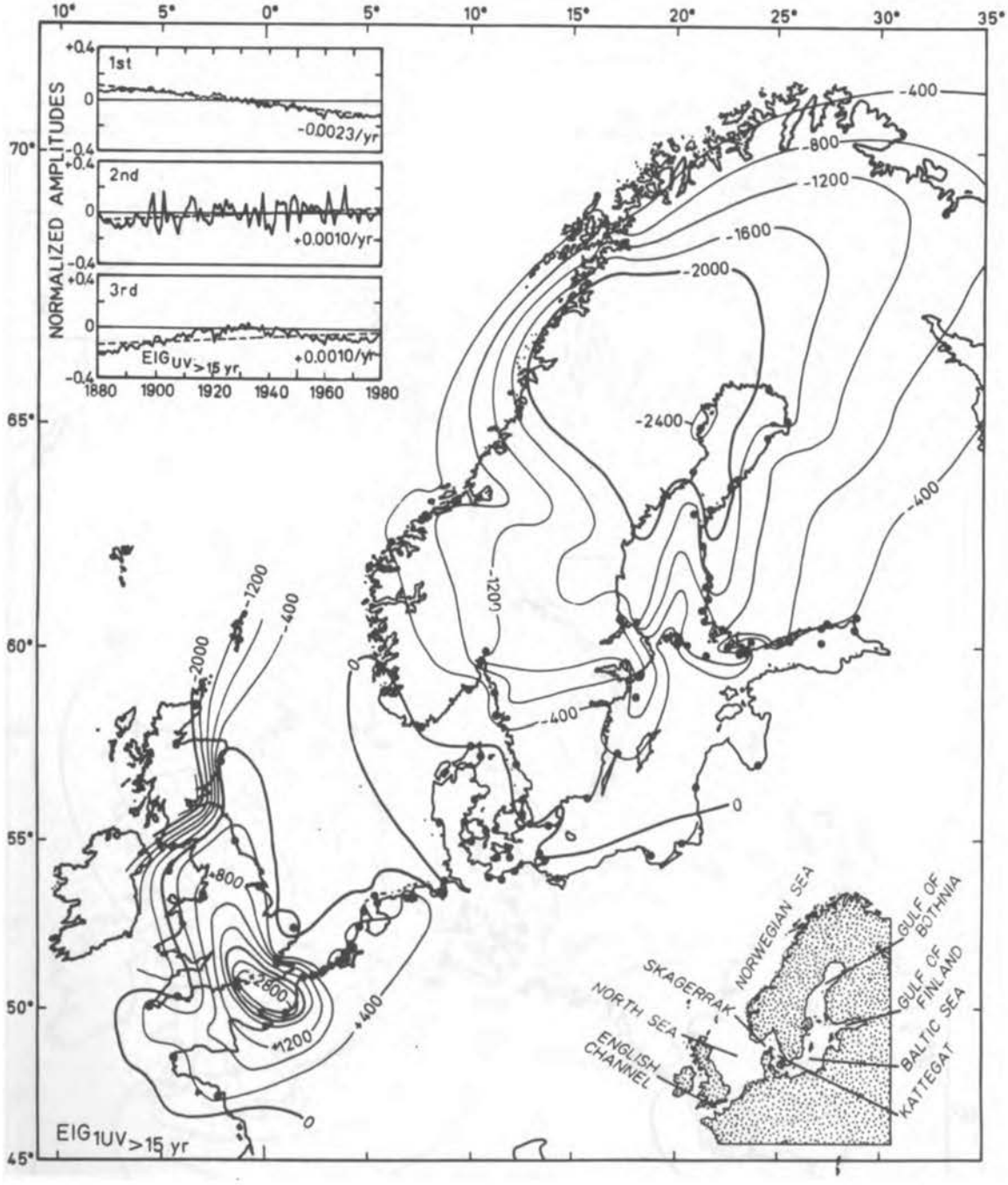

FIGURE 1.10 First spatial eigenfunction for northern Europe at intervals of 4000 units at 128 stations, each having unit variance and spanning at least 15 years. Insert at upper left has first three temporal functions for same stations and with elevations dimensionless and normalized; these functions account for 58, 13, and 6 percent, respectively, of total variation in records. Insert at lower right denotes water bodies mentioned in text.

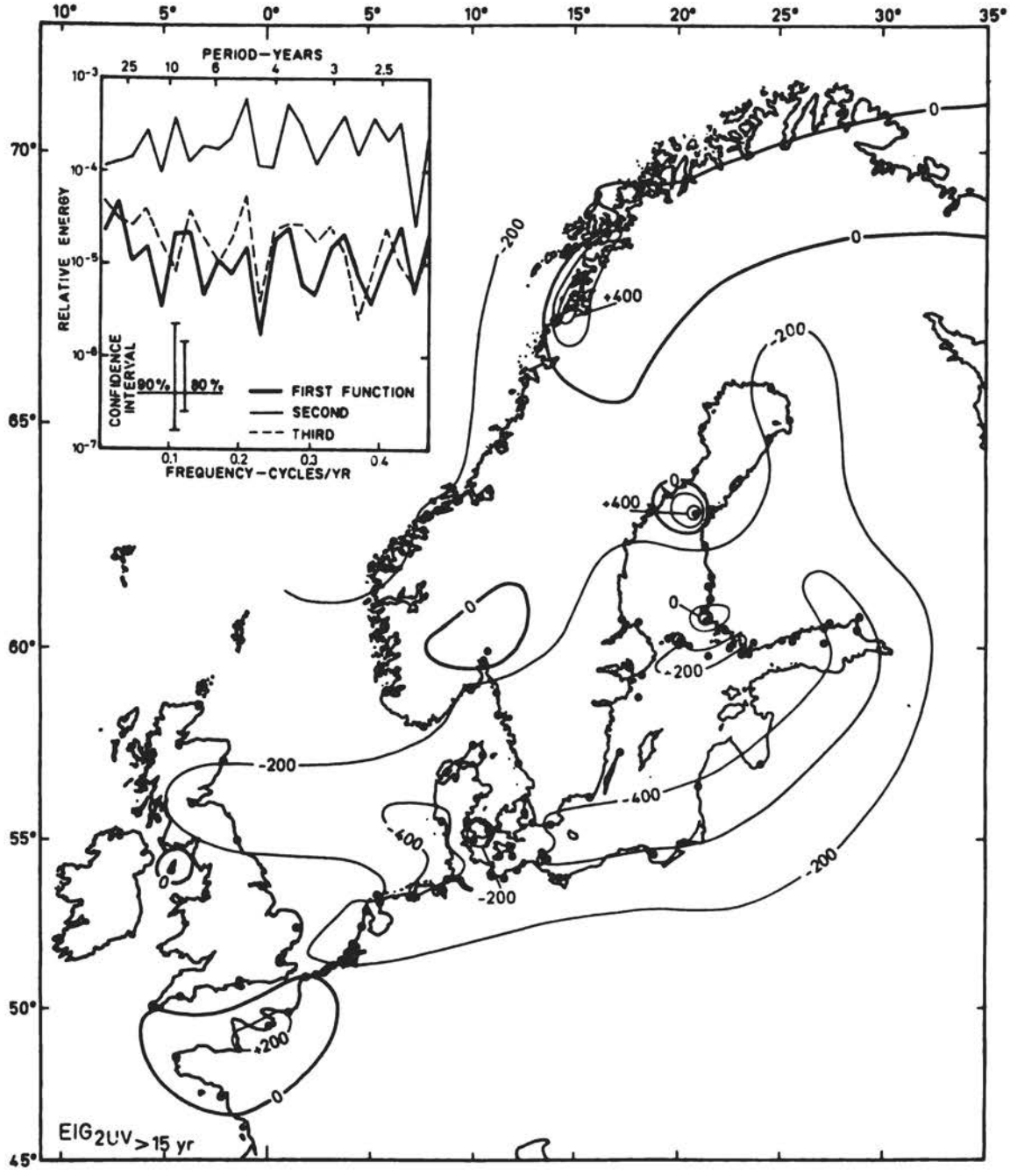

FIGURE 1.11 Second spatial eigenfunction for same stations used in Figure 1.10 at intevals of 200 units. Insert has spectra of first three temporal functions. Estimates have four degrees of freedom.

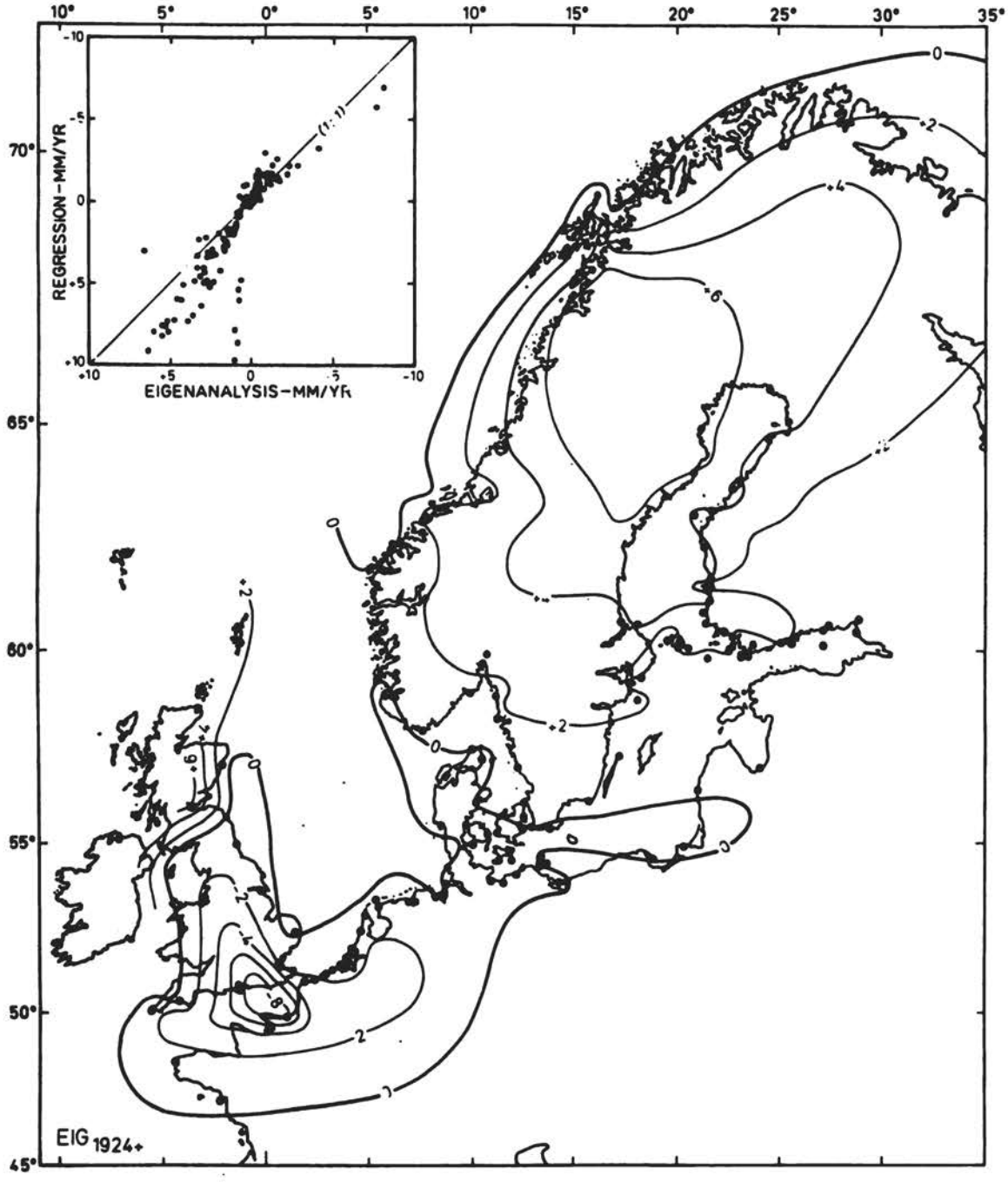

FIGURE 1.12 Mean annual vertical movement of land in northern Europe relative to sea level as constructed from eigenfunctions of Figures 1.10 and 1.11. Contours are in millimeters/year and are comparable with those of Figure 1.9 based on regression analysis.

oceanographers, climate modelers, glaciologists, and others should convene over the next year to establish a consensus on the placement of the next generation of sea-level gauges. Requirements of modelers, observationalists, and managers should all be included in this discussion, which should have global representation.

Accurate quantitative estimates of global eustasy have been elusive. Definition of changes in eustasy are possible only with improved observations, better statistical techniques, and diligence in research. The next few years should provide increased insight into causes and magnitude of sea-level variability, allowing us to access future measurements of relative sea-level rise with increased confidence.

ACKNOWLEDGMENTS

Contribution number 5845 Woods Hole Oceanographic Institution. This work was funded by the Woods Hole Oceanographic Institution's Coastal Research Center and the Department of Commerce, NOAA Office of Sea Grant under Grants No. NA 83-AA-D-00049 (R/B-54) and No. NA 80-AA-D-00077 (R/B-54). K. O. Emery commented on the manuscript and has been instrumental in all original research cited herein.

REFERENCES

Andrews, D. F., 1974. A robust method for multiple linear regression. Technometrics, 16, 523-531.

Aubrey, D. G., and K. O. Emery, 1983. Eigenanalysis of recent United States sea levels. Continental Shelf Research, 2, 21-33.

Aubrey, D. G., and K. O. Emery, submitted. Relative sea levels of Japan from tide-gauge records. Geological Society of America Bulletin.

Barnett, T. P., 1982. Recent changes in sea level and their possible causes. Climate Change, 5, 15-38.

Barnett, T. P., 1983. Some problems associated with the estimation of global sea level change. National Climate Program, U.S. Department of Commerce, NOAA, 39 pp.

Barnett, T. P., 1984. The estimation of "global" sea-level change: a problem of uniqueness. Journal of Geophysical Research, 89, 7980-7988.

Boggs, S., Jr., 1984. Quaternary sedimentation in the Japan arc-trench system. Geological Society of America Bulletin, 95, 669-685.

Clark, J. A., W. E. Farrell, and W. R. Peltier, 1978. Global changes of post-glacial sea level: A numerical calculation. Quaternary Research, 9, 265-287.

Dambara, T., 1971. Synthetic vertical movements in Japan during the recent 70 years. Bulletin of the Japanese Society of Geodesy, 17, 100-108.

Emery, K. O., 1980. Relative sea levels from tide-gauge records. Proceedings of the National Academy of Sciences, 77, 6968-6972.

Fairbridge, R., and O. Krebs, Jr. (1962). Sea level and the southern oscillation, Geophysical Journal, Royal Astronomical Society, 6, 532-545.

Flint, R. F., 1957. Glacial and Pleistocene Geology. John Wiley and Sons, Inc., New York, 553 pp.

Gornitz, V., S. Lebedeff, and J. Hansen, 1982. Global sea level trend in the past century. Science, 215, 1611-1614.

Hilde, T. W. C., and S. Uyeda (eds.), 1983. Geodynamics of the Western Pacific-Indonesian Region, American Geophysical Union, Washington, D.C.

Hogg, R. V., 1974. Adaptive robust estimation. Journal of the American Statistical Association, 69, 909-927.

Kato, T., and K. Tsumura, 1979. Vertical band movements in Japan as deduced from tidal records, (1951-1978). Bulletin of the Earthquake Research Institute, 54, 559-628.

Lennon, G. W., 1975-1978. Monthly and annual mean heights of sea level. Permanent Service for Mean Sea Level, Institute of Oceanographic Sciences, Merseyside, 3 volumes (looseleaf).

Lisitzin, E., 1974. Sea-Level Changes. Elsevier Scientific Publishing Company, New York, 286 pp.

Lutjeharms, J. R. E., and M. M. Alheit, 1983. Sea-level in the world ocean, volumes I-VII. National Research Institute for Oceanology, Council for Scientific and Industrial Research, CSIR Technical Report T/SEA 8303/1 - 8303/7.

Mercer, J. H., 1978. West Antarctic ice sheet and CO_2 greenhouse effect: A threat of disaster. Nature, 271, 321-325.

Mörner, N. A., 1980. The Fenno-Scandian uplift: Geological data and their geodynamical implication. In N. A. Mörner (ed.), Earth Rheology, Isostasy, and Eustasy, John Wiley and Sons, New York, pp. 251-284.

Naylor, D., and S. N. Mounteney, 1975. Geology of the North-West European Continental Shelf, Graham Trotman Dudley Publs., London, 162 pp.

Peltier, W. R., 1980. Ice sheets, oceans, and the earth's shape. In N. A. Mörner (ed.), Earth Rheology, Isostasy, and Eustasy, John Wiley and Sons, New York, pp. 45-63.

Tanaka, K., 1977. Outline of the geology of Japan. In K. Tanaka and T. Nozawa (eds.), Geology and Mineral Resources of Japan (3rd ed.), Geological Survey of Japan, vol. 1, pp. 2-16.

ATTACHMENT 2

CLIMATIC IMPLICATIONS OF ISOSTATIC ADJUSTMENT CONSTRAINTS ON CURRENT VARIATIONS OF EUSTATIC SEA LEVEL

W. R. Peltier
Department of Physics
University of Toronto

ABSTRACT

Two different types of geophysical data have recently been invoked to support the notion that the mass of water in the global ocean is increasing. These consist of local tide-gauge measurements of relative sea level and measurements of the wander of the Earth's pole of rotation with respect to the surface geography. This paper reviews recent analyses that demonstrate that the former data are significantly contaminated by ongoing changes of sea level forced by the melting of Würm-Wisconsin ice that occurred in the time interval 6-18 KBP. The latter observations, on the other hand, are entirely explicable as a response due to the same causative agency. These analyses therefore suggest that the rise in mean global sea level that appears to be required by the tide-gauge data may be steric in origin.

INTRODUCTION

In the recent geophysical literature considerable attention has been addressed to the question of whether a significant change in global climate has occurred during the past 100 years, that is, since the beginning of the industrial revolution. Indeed such change is expected owing to the increase in atmospheric CO_2 (and aerosol) load caused by the burning of fossil fuels, an increase that is now well documented. Because of the large intrinsic variability of annually averaged atmospheric temperature, it is not expected that this anthropogenically induced climatic amelioration would be directly detectable as yet, however, and there has been considerable interest in proxy records that might provide a clearer, if less direct, indication of the expected effect. One such class of proxy records that could potentially provide the desired information consists of data sensitive to variations of the mass of water in the global ocean. The idea that has motivated interest in such data is simply that a slight amelioration in global climate might be associated with a more significant warming in the polar regions and thus cause a detectable decrease in the mass bound in polar, or somewhat lower-latitude alpine, ice complexes. If the volume of continental ice <u>is</u> decreasing then there should be evidence of this in

several different oceanographic and geophysical data sets. The most obvious such data are those recorded on tide gauges, many of which have been installed for sufficient lengths of time (50 or more years) that any significant trend of relative sea level should be easily extracted. One less obvious type of data, which might be equally useful in establishing the existence of such an effect, consists of astronomical observations of fluctuations in the Earth's rotation. Because of the variations in the elements of the planetary inertia tensor that are forced by redistribution of the surface mass load during ice-sheet melting, both the length of day and the location of the rotation pole with respect to the surface geography should exhibit astronomically detectable changes. The latter data have the additional useful characteristic that they are only sensitive to the shift in surface mass load. On the other hand any sea-level trend observed in tide-gauge data is ambiguous in the sense that it might equally well be explained by invoking a change in water volume caused by thermal expansion or contraction as by a change in water mass.

In fact both of these types of data have recently been invoked in support of the notion that there is an increase of the mass of water in the global ocean currently taking place. Both Gornitz et al. (1982) and Barnett (1983) have interpreted a global array of tide-gauge-based relative-sea-level (rsl) measurements as revealing an ongoing increase of water volume. Best estimates of the expected steric (thermal expansion) contribution to this increase have been interpreted to suggest that this effect cannot entirely account for the observation. Meier (1984) argued on the basis of direct glaciological evidence that the small (alpine) glaciers of the world are the most likely source of at least part of the required meltwater. A significant problem with interpretation of rsl data from the global tide-gauge network is that the observations are significantly contaminated by isostatic adjustment effects (e.g., Peltier 1982). Although the melting of Würm-Wisconsin ice was complete by approximately 6000 years ago, relative sea level continues to change on this account because of the slow return to isostatic equilibrium, which is due to the high value of the viscosity of the Earth's mantle. In sites located in the regions immediately peripheral to the Laurentide and Fennoscandian ice sheets, relative sea level is rising at present owing to the decrease of local planetary radius caused by the viscous flow of material back into the regions that were once ice covered. This effect may be important since a large number of tide gauges are located in such regions (U.S. east coast, European west coast). One of the purposes of this paper is to discuss a method that has been developed that is suitable to filter isostatic adjustment effects from the tide-gauge data and thereby to reveal more clearly any residual effect that might exist. This analysis will be discussed in the next section of this paper.

The second class of data that has also been suggested as requiring some present-day disintegration of continental ice consists of the observed wander of the rotation pole toward eastern Canada at a rate near 0.95 degree per million years. The history of the position of the rotation pole has been recorded since the turn of the century by the International Latitude Service (ILS) (e.g., Vincente and Yumi 1969,

1978), and the polar wander revealed in it was interpreted by Munk and Revelle (1955) as requiring some current variation of the surface ice load. Recent analysis has demonstrated, however, that this interpretation of Munk and Revelle is incorrect. Arguments reviewed in the third section of this paper, establish rather conclusively that the observed wander of the rotation pole in the ILS path is entirely explicable as a memory of the planet of the last deglaciation event of the current ice age. Furthermore, the nontidal acceleration of the Earth's rotation, recently inferred on the basis of the orbit of the LAGEOS satellite, is also entirely explicable as a memory of the melting of Würm-Wisconsin ice (Peltier 1983). These data together appear to restrict severely the magnitude of any ongoing reduction of the volume of continental ice. The implications of isostatic adjustment contamination of both the tide-gauge data and Earth-rotation observations to the climate-change issue are discussed in the concluding section.

FILTERING THE TIDE-GAUGE DATA TO REMOVE ISOSTATIC ADJUSTMENT EFFECTS

Over the past decade, beginning with the paper by Peltier (1974), a complete gravitationally self-consistant model has been developed that is able to predict rather accurately the variation of relative sea level that should be observed anywhere on the Earth's structure due to ice sheet disintegration. A recent summary of this research will be found in Peltier (1982). To date the model has been exclusively employed to predict rsl changes due to the melting event that began 18,000 years ago and ended about 6000 years ago that saw the disappearance of large ice sheets from Canada and Fennoscandia and reduction of the ice in West Antarctica. By comparing the predictions of this model with the ^{14}C record of rsl change over the time since melting began, it has proven possible to infer the variation of effective planetary viscosity with depth. This parameter is a crucial ingredient in thermal convection models of the process of continental drift, and the inferred value of the mantle viscosity may be construed as verifying the validity of this convection hypothesis (Peltier 1985). Since the viscoelastic model does fit the ^{14}C record of deglaciation everywhere, it may be employed to predict the present-day rate of rsl variation anywhere where there is a tide gauge and thereby to filter from these "modern" oceanographic data the local effect due to present-day glacial isostatic disequilibrium. The way in which this analysis is done will be illustrated by considering sites from along the eastern seaboard of the continental United States shown on Figure 2.1.

The first step in the procedure is to establish accord between the predictions of the model and the ^{14}C record of rsl variations on the long time scale of these observations. A collection of such data published by Bloom (1967) from this region has recently been analyzed in Peltier (1984), who has argued that a good fit to them appears to require a lithospheric thickness somewhat in excess of 200 km if the mantle viscosity profile is fixed to a constant value of 10^{21} Pa s. The goodness of fit of this model to ^{14}C data from six sites along the U.S. east coast is illustrated by the comparisons in Table 2.1,

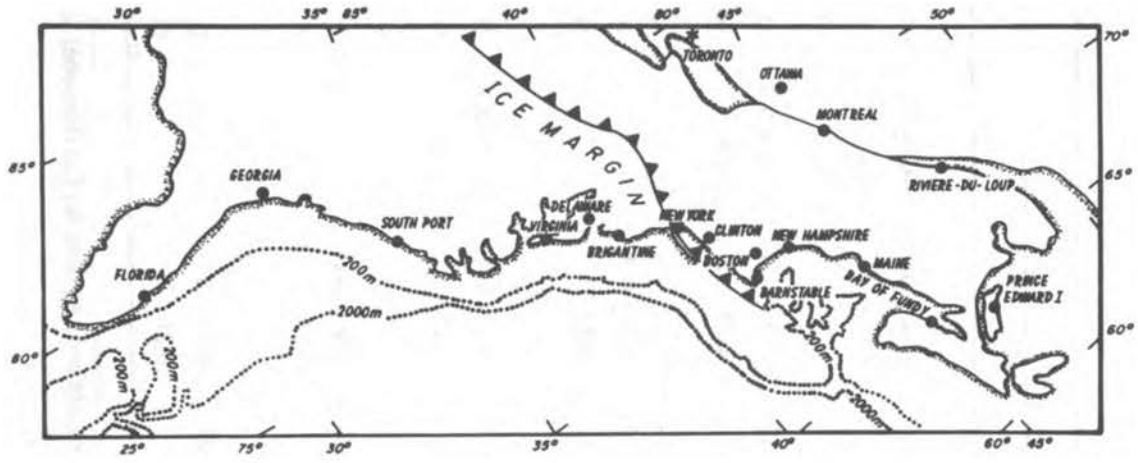

FIGURE 2.1 Sites along the U.S. east coast at which ^{14}C data exist that can be employed to fix the parameters of the viscoelastic model employed to filter the tide-gauge data.

which demonstrate that the model does explain the data rather well. We may therefore proceed to employ it to predict the rate of rsl rise that should be observed at any specific tide gauge along the coast and to subtract this prediction from any trend that may exist in the individual tide-gauge records. Barnett (1983) has shown that all tide gauges along this stretch of coast do in fact reveal a trend toward rising relative sea level as a function of time.

Figure 2.2(a) shows a preliminary plot of the residual (corrected) rsl trends at a larger number of east coast tide-gauge sites as a function of distance in radians from the site at Pensacola in Florida. Also shown in this figure as the horizontal line is the mean rate of rsl rise about which the residuals fluctuate. A more refined calculation suggests that the mean of the data corrected for isostatic adjustment effects is between 1.1 and 1.2 mm/yr. The average rate of submergence along the U.S. east coast due to this cause is near 0.8 mm/yr, so that the contamination is about 40 percent of the raw trends. For comparison purposes Figure 2.2(b) shows the corrected trends for tide-gauge sites along the U.S. west coast. Along this active continental margin there is no consistent signal revealed either before or after correction. This is hardly surprising given the intensity of tectonic activity in this region due to the presence of San Andreas transform fault. The east coast passive margin, however, provides a much more stable "float" for the inference of residual rsl variation, and the data from this region do seem to require that some process other than glacial isostatic adjustment is contributing to the observed submergence in this region at present. In attempting to understand what this effect is, it may be important to note that the tide-gauge data from almost all sites along this coast show that the local rates of sea-level rise decreased rather sharply after about 1940. This may be an important constraint on the candidate mechanisms that might be invoked to explain the observations. An additional constraint is that discussed in the next section.

TABLE 2.1 Observed and Predicted rsl (in meters) at Selected Eastern Seaboard Sites [a]

	Time, kyr								
Location	-8	-7	-6	-5	-4	-3	-2	-1	0
Southport									
Observed					-3.3 ± 0.5	-2.2 ± 0.4	-1.2 ± 0.2	-0.5 ± 0.1	0
Predicted					-2.26	-0.96	-0.30	-0.03	0
Virginia									
Observed	-22 ± 4	-17 ± 3	-13 ± 3	-10 ± 3	-7.0 ± 1.5	-3.0 ± 1.0	-0.5 ± 0.5	-0.4 ± 0.5	0
Predicted	-29.52	-21.70	-14.90	-9.63	-5.95	-3.45	-1.78	-0.68	0
New York									
Observed	-17.8 ± 3.0	-16.0 ± 2.4	-13.0 ± 2.2	-9.4 ± 1.5	-6.4 ± 0.6	-4.4 ± 0.5	-1.2 ± 0.3		0
Predicted	-22.48	-19.06	-14.45	-10.02	-6.56	-4.00	-0.88		0
Brigantine									
Observed				-10.5 ± 0.6	-7.5 ± 0.5	-5.2 ± 0.5	-3.0 ± 0.4	-1.4 ± 0.4	0
Predicted				-11.32	-7.79	-4.40	-2.36	-0.95	0
Clinton									
Observed		-10.2 ± 0.7	-8.4 ± 0.5	-6.7 ± 0.5	-4.7 ± 0.5	-3.4 ± 0.5	-1.0 ± 0.2		0
Predicted		-20.39	-15.5	-10.84	-7.16	-4.41	-0.94		0
Boston									
Observed				-9.0 ± 3.0	-6.0 ± 3.0	-2.5 ± 2.0	-0.5 ± 0.5		0
Predicted				-9.02	-6.03	-3.74	-0.84		0

[a] Calculations are based on the gravitationally self-consistent model with realistic ICE-2 melting chronology and an Earth model with a lithospheric thickness of 245 km and 1066B elastic structure.

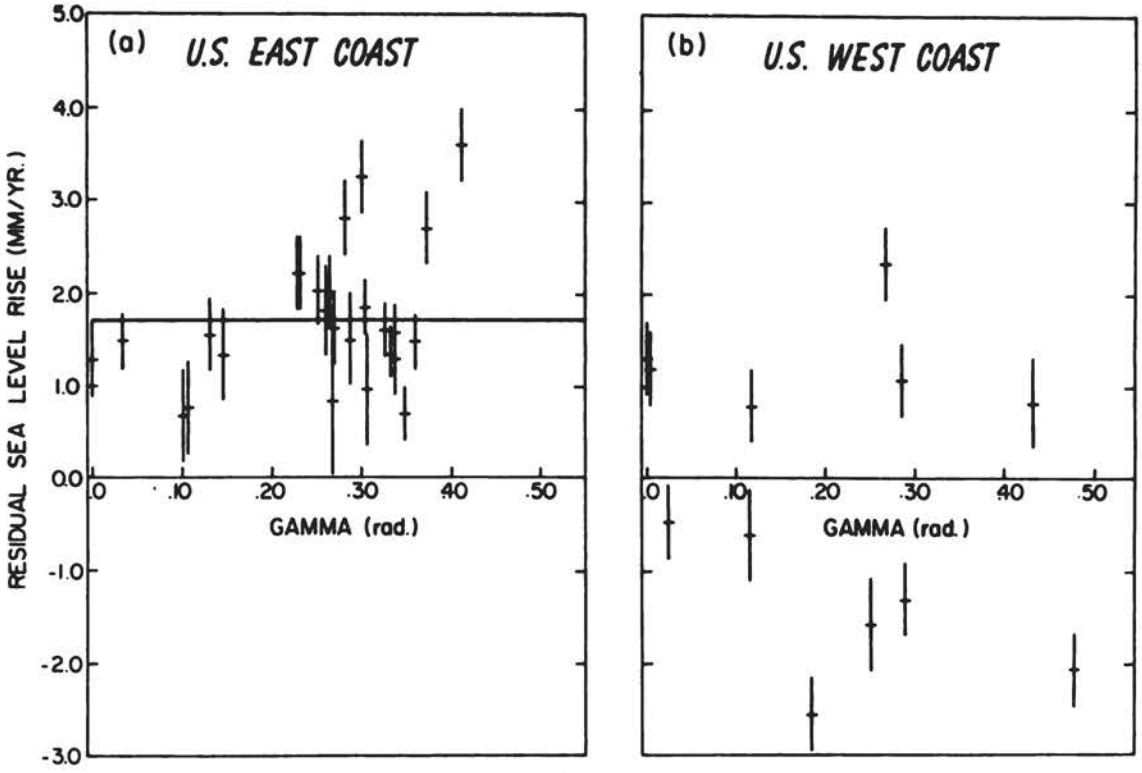

FIGURE 2.2 Relative sea-level trends from tide-gauge data along the U.S. east (a) and west (b) coasts in the period since 1940 corrected for isostatic adjustment effects.

EARTH ROTATION AND ICE-SHEET DISINTEGRATION

The ILS record of polar motion shown in Figure 2.3 is dominated by oscillatory variations of pole position due to the interference of the 12-month annual and 14-month Chandler wobbles. The interference between those two closely spaced frequencies explains the 7-year beat period in the record that may be extracted by visual inspection. Of more interest in the present context is the slow drift of the pole relative to the Conventional International Origin (CIO), upon which these oscillatory variations are superimposed. The direction of drift is shown on the inset polar projection of Figure 2.3 by the arrow that points roughly along the 76 degree west meridian. The rate of drift in this direction is 0.95 $\pm$ (0.05) degree per million years (e.g., Dickman 1977). In 1952 Munk and Revelle published a paper that purported to show that this observed true polar wander required that some ongoing change in surface mass load of the planet be currently taking place. They suggested that the required surface load forcing was due to mass loss from Greenland and/or Antarctica. The theoretical analysis on which this conclusion was based was predicated on the assumption that insofar as the rotational response to surface loading was concerned the planet could be

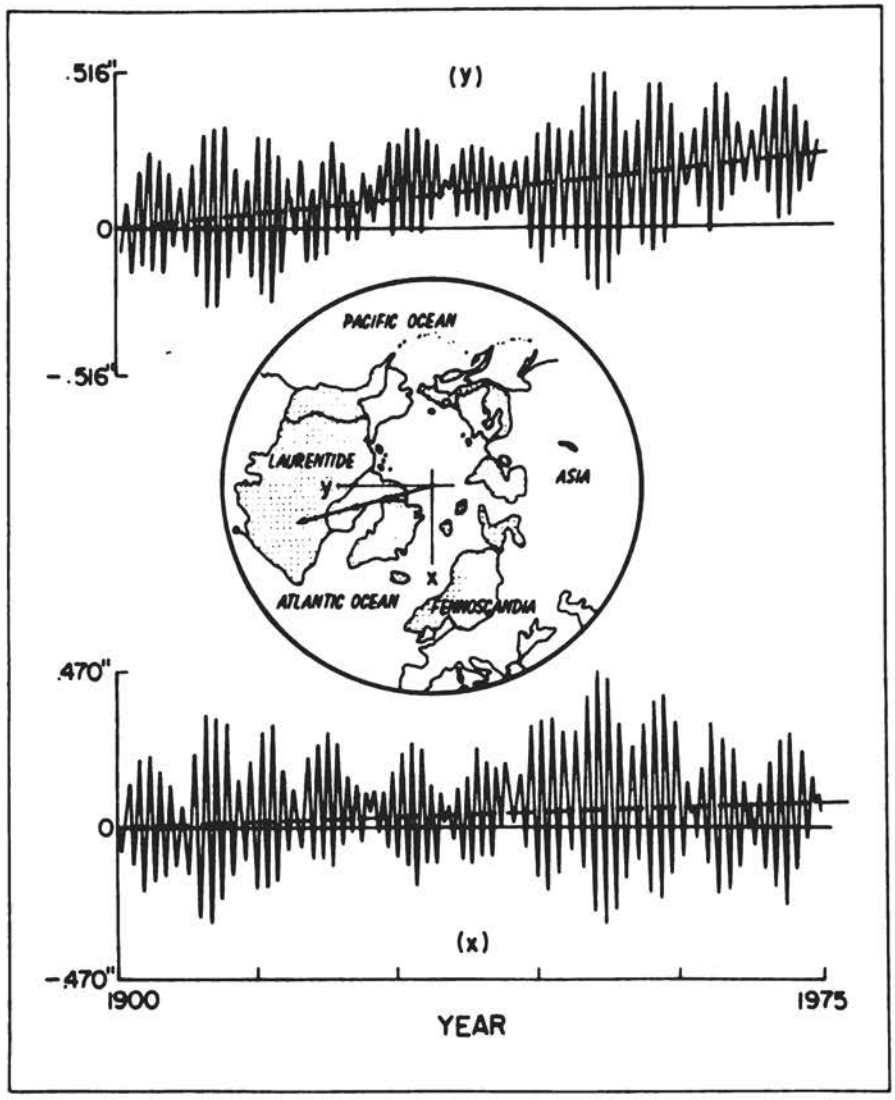

FIGURE 2.3 The ILS record of polar motion in the time period since 1900 relative to the conventional international origin (CIO).

assumed to be representable as a homogeneous viscoelastic sphere. A characteristic of the rotational response of such a model planet is that the centrifugal and isostatic adjustment contributions to the response exactly annihilate one another, the result being that no polar wander is predicted in circumstances in which the surface mass load is constant. To explain the drift observed in the pole path shown in Figure 2.3, Munk and Revelle were therefore obliged to invoke some time variation of surface load, and they pointed to the Greenland and/or Antarctic ice masses as being the likely cause. This idea has continued to play a role in the recent literature on sea level and climate change, where

it is suggested as providing additional evidence that the mass of water in the global ocean must be increasing.

Unfortunately this analysis of Munk and Revelle (1952) has recently been shown to be incorrect. The flaw in their argument that the observed polar wander requires a concurrent variation of the surface mass load is that the argument is based on the assumption that the homogeneous viscoelastic model of the Earth is an adequate model in terms of which to describe the rotational response to surface mass loading. In a recent sequence of papers (Peltier 1982, Peltier and Wu 1983, Wu and Peltier 1984) it has been clearly demonstrated that the internal viscoelastic layering of the real Earth has an extremely important effect on the rotational response to surface loading. In fact the effect is such as to break the symmetry on the basis of which the centrifugal and isostatic adjustment contributions to the rotational response are forced to cancel one another at all times during free relaxation of the homogeneous model. Layered viscoelastic models therefore process a finite "memory" in their rotational response to surface loading such that the pole continues to wander long after the surface load has ceased to vary. In terms of such realistic viscoelastic models it is therefore conceivable that the polar wander illustrated on Figure 2.3 could simply be a memory of the planet's response to the last deglaciation event of the current ice age. That this could be the case is also strongly suggested by the fact that the direction of polar wander is slightly to the east of the centroid of the Laurentide ice mass, an effect that is an expected consequence of the additional forcing due to the deglaciation of Fennoscandia.

Analysis in the three previously cited papers shows in fact that the observed direction and rate of polar wander in the ILS path are both predicted very nicely on the basis of the assumption that the only rotational forcing is that due to the 10^5 year periodic ice age cycle that has dominated the $\delta^{18}O$ record of continental ice volume fluctuations during the past 700,000 years of Earth history. The polar wander speed predicted for a sequence of models that differ only in the complexity of their internal viscoelastic layering is shown in Figure 2.4. The zero of time on the figure is taken coincident with the end of the last 10^5 year glaciation cycle, of which seven have been included in the assumed prehistory. As discussed in Wu and Peltier (1984) the ice sheets on Canada, Fennoscandia, and West Antarctica have all been included and have been approximated by spherical caps of appropriate mass that accrete water from and discharge meltwater to, ocean basins of realistic form. The temporal history of each cap is assumed fixed by the sawtooth approximation to the typical $\delta^{18}O$ record shown on Figure 2.5. Following the zero of time on Figure 2.4 there is no further variation of surface load.

The models for which the polar wander-speed predictions are shown in Figure 2.4 consist of a homogeneous model with a lithospheric of thickness $\bar{L}$ = 120 km (fixed for all models as indicated on the figure) designated LOF (no core), a model with a homogeneous mantle and a high-density invisid core (LOF), a model with one density discontinuity in an otherwise homogeneous mantle (L1F), and a model with two internal mantle density discontinuities (L2F). The models with internal mantle density

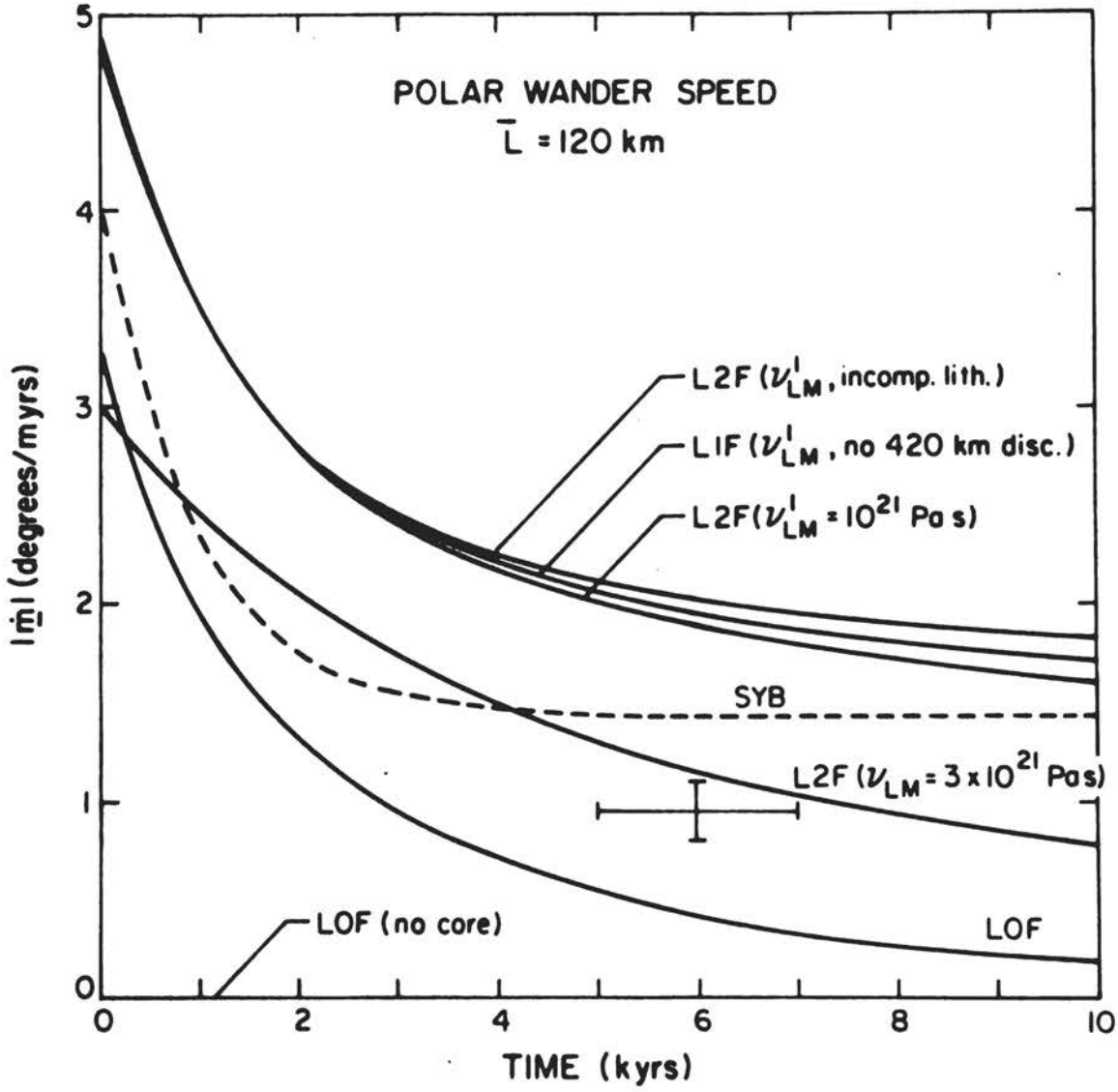

FIGURE 2.4 Polar wander-speed predictions for the viscoelastic models discussed in the text. The cross at t = 6 kyr is the observed secular drift extracted from the data shown in Figure 2.3.

discontinuities have these features located at 670-km depth (L1F) and 420-km depth (L2F). The magnitudes of the density contrasts in these models are close to those in the realistic model 1066B of Gilbert and Dziewonski (1975). Inspection of the various predictions shows first that essentially zero polar-wander speed is predicted for the homogeneous model (LOF no core) in accord with the analysis of Munk and Revelle (1952). However, as one adds structure to the interior of the model the speed prediction begins to depart very significantly from zero. The predictions are for models that have an upper-mantle viscosity of 10^{21} Pa s, and a good fit to the observations is clearly obtained by

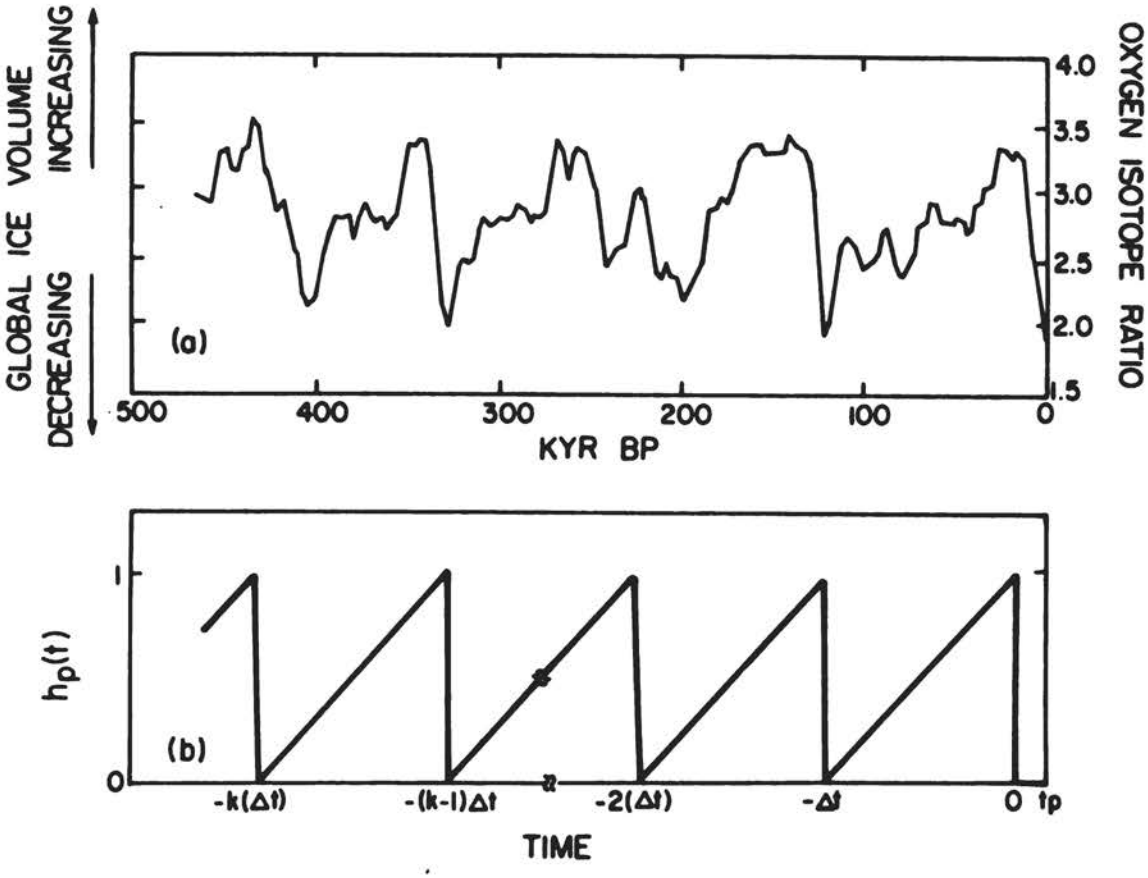

FIGURE 2.5 Sample $\delta^{18}O$ time series (upper) and sawtooth approximation (lower) employed to constrain the load cycle employed for the polar wander-speed predictions shown in Figure 2.4.

model L2F with a lower-mantle viscosity of 3×10^{21} Pa s. This same model has been shown to be compatible with most of the other data of glacial isostatic adjustment also. In particular, it has been shown to be compatible with the recently observed nontidal component of the acceleration of planetary rotation that has been extracted from the orbit of the LAGEOS satellite (Peltier 1983) and previously through the analysis of ancient eclipse data.

CONCLUSIONS

The influence of ongoing glacial isostatic adjustment in response to the melting of Würm-Wisconsin ice that began roughly 18,000 years ago and ended about 6000 years is a significant source of contamination of tide-gauge records of the variation of relative sea level. Before such data are invoked to constrain present-day variations of water volume, they should be decontaminated by removing isostatic adjustment effects using the gravitationally self-consistent model for rsl variations as a filter. An application of this technique to sea-level data from the

U.S. east coast shows that roughly 40 percent of the tide-gauge-inferred rsl rise is due to the glacial isostatic submergence of this coast. The residual could in principle be due either to an increase in the mass of water in the global ocean or to a steric effect.

The fact that the observed secular variations in the nontidal acceleration of planetary rotation and in the location of the rotation pole are both so well predicted on the basis of the assumption that no ongoing variation of surface mass load is occurring may be taken as strong evidence that the tide-gauge-inferred residual rate of rsl rise is predominantly steric in origin. These observations appear to be extremely sensitive to significant rates of change in the surface ice and water load. In fact, the two rotation effects are complimentary constraints in that the nontidal acceleration is particularly sensitive to ice melting near the rotation poles, whereas the polar wander is driven entirely by off-polar loading effects. Certainly the Munk and Revelle (1952) argument that the present-day observed polar wander requires a concurrent variation of surface-mass load is incorrect, however, since this is explicable on the basic of the hypothesis that it is entirely a consequence of previous load variations.

REFERENCES

Barnett, T. P., 1983. Recent changes in sea level and their possible causes. Climate Change, 5, 15-38.

Bloom, A. L., 1967. Pleistocene shorelines: A new test of isostasy. Geological Society of America Bulletin, 78, 477-1493.

Dickman, S. R., 1977. Secular trend of the Earth's rotation pole: Consideration of motion of the latitude observatories. Geophysics Journal Royal Astronomical Society, 57, 41-50.

Gilbert, F., and A. M. Dziewonski, (1975). An application of normal mode theory to the retrieval of structural parameters and source mechanisms from seismic spectra. Philosophical Transactions Royal Society of London, Series A278, 187-269.

Gornitz, V., S. Lebedeff, and J. Hansen, 1982. Global sea level trend in the past century. Science, 215, 1611-1614.

Meier, M. F., 1984. Contribution of small glaciers to global sea level. Science, 226, 1418-1421.

Munk, W., and R. Revelle, 1952. Sea level and the rotation of the Earth, American Journal of Science, 250, 829-833.

Munk, W., and R. Revelle, 1955. Evidence from the rotation of the Earth, Annals of Geophysics, 11, 104-108.

Peltier, W. R., 1974. The impulse response of a Maxwell Earth. Reviews of Geophysics and Space Physics, 12, 649-669.

Peltier, W. R., 1982. Dynamics of the ice age Earth. Advances in Geophysics, 24, 1-146.

Peltier, W. R., 1983. Constraint on deep mantle viscosity from LAGEOS acceleration data. Nature, 304, 434-436.

Peltier, W. R., 1984. The thickness of the continental lithosphere. Journal of Geophysical Research, 89, 303-316.

Peltier, W. R., 1985. Mantle convection and viscoelasticity. Annual Reviews of Fluid Mechanics, 17, 561-608.

Peltier, W. R., and P. Wu, 1983. Continental lithospheric thickness and deglaciation induced true polar wander. Geophysical Research Letters, 10, 181-184.

Vincente, R. O., and S. Yumi, 1969. Co-ordinates of the pole (1899-1968), referred to the conventional international origin. Publications International Latitude Observatory, Mizusawa, 7, 41-50.

Vincente, R. O., and S. Yumi, 1978. Revised values (1941-1961) of the coordinates of the pole referred to the CIO. Publications International Latitude Observatory, Mizusawa, 7, 109-112.

Wu, P., and W. R. Peltier, 1984. Pleistocene deglaciation and the Earth's rotation: A new analysis. Geophysics Journal Royal Astronomical Society, 76, 753-792.

ATTACHMENT 3

Sea Level and the Thermal Variability of the Ocean

D. Roemmich
Scripps Institution of Oceanography

INTRODUCTION

This study focuses on changes in the volume of the ocean at constant mass and the relationship of these steric changes with sea level. It has been shown previously that steric height changes dominate sea-level variability on seasonal and interannual time scales (e.g., Shaw and Donn, 1964; Schroeder and Stommel, 1969; Reid and Mantayla, 1976). But how do specific volume changes compare to sea-level variations over periods of decades or longer? Can the secular trends observed in many sea-level records be attributed to steric expansion and contraction of the water column? Is there some residual sea-level rise that cannot be due to steric expansion?

Barnett (1983) found that the global hydrographic data base is inadequate for determining long-term trends in steric height. He considered pairs of stations from nearly the same location and the same month of the year, but separated in time by more than 30 years. In each of 11 regions of the world ocean, between 1 and 68 pairs were found. But the standard deviation of the difference in steric height of the sea surface relative to 1000 db was very large (20 dynamic centimeters in several regions), and none of the areas had a statistically significant trend. Relative to the "noise" consisting of mesoscale eddies and other energetic low-frequency phenomena, a hypothetical signal of order 1 dynamic centimeter per 10 years is small. The sampling problem is formidable.

The approach used here was to concentrate on a single relatively data-rich region, the subtropical North Atlantic, rather than to seek a global solution. The objective was to discover how much variability in steric height is contained in time scales of decades or longer and to determine what vertical and horizontal scales of variability correspond to these long-term changes. These are essential to answer the questions of how long the ocean must be sampled at a single location, and how many locations must be sampled and to what depths in order to determine the relationship of steric height to the long-term trend in sea level.

BERMUDA SEA LEVEL AND THE PANULIRIS DATA

The longest regular time series of deep hydrographic stations is the Panuliris series (32°10'N, 64°30'W) near Bermuda (Figure 3.1). This

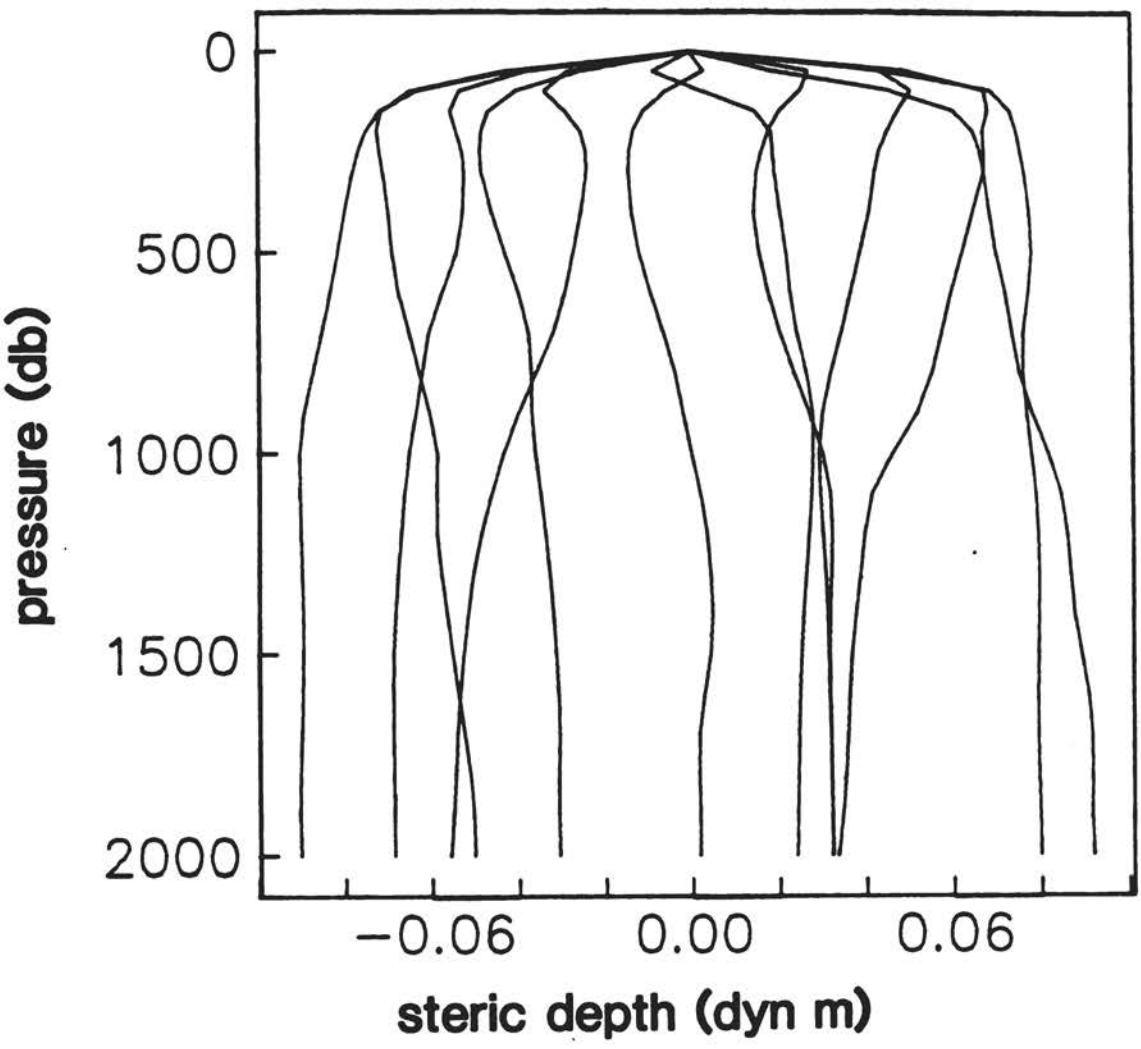

FIGURE 3.1 Monthly mean values of steric depth at the Panuliris station, averaged over 1954-1981, with the average over all months removed. Steric depth is the integral of specific volume from the ocean surface down to the pressure level indicated on the ordinate.

program of measurements was initiated by Henry Stommel and carried out by the Bermuda Biological Station beginning in 1954. Weather permitting, and barring occasional other problems, two casts per month were made at a location where the water depth is about 3000 m. Nearly all casts extend to 2000 m and many to 2500 m or deeper. From 1954 to 1981, 392 casts were made to depths greater than 2000 m. The time series is not long for our purposes, and its limited depth precludes a study of the abyssal water, but it is all that we have.

A number of investigators have studied the Panuliris data, sometimes in combination with Bermuda sea level. Shaw and Donn (1964) compared monthly means of sea-level data (corrected for atmospheric pressure

variations) with monthly means of the steric height of the sea surface relative to 2000 db and found them to be indistinguishable. Schroeder and Stommel (1969) noted that this seasonal signal was mainly confined to the upper 200 db and was due to local buoyancy fluxes across the sea surface. They also found that there were year-to-year variations in steric height that were also mirrored in the sea-level record and attributed these variations to vertical motion of the main thermocline. Wunsch (1972) considered 8 years of data, computing spectra of steric height and sea level. He found that the steric height spectrum tapered off at periods longer than a year, an incorrect inference that probably resulted from the shortness of the record length available at that time. Pocklington (1972) constructed time series of temperature at a number of standard depths using data from 1955 to 1969. He observed a trend of decreasing temperature down to 400 m with a suggestion that it continued to decrease as deep as 800 m. Below this there was no apparent trend. Frankignoul (1981) compared temperature at 10 standard levels in the first 12 years of Panuliris data with temperature in the next 12 years. He too found a temperature decrease down to 1000 m with a slight increase at 1600 and 2000 m. [The text and Table 1 of Frankignoul (1981) appear to reverse the sign of the changes, but they are given correctly in his Figure 2.]

Here, 27 years of Panuliris data will be used for two purposes. First, it will be shown that in contrast to seasonal and interannual variations, which are confined to the upper 1000 m, a significant 27-year trend in the data extends down to the level of the deepest observations. Then, this trend in time will be compared to a large space-scale temperature difference between two deep hydrographic surveys, each of which covered the subtropical North Atlantic at the same two latitudes.

All the Panuliris casts were sorted by month and year and interpolated to 24 standard depths that were 50 m apart down to 300 m and then 100 m apart down to 2000 m. Casts in a given month were averaged over all years to estimate a mean annual cycle. Then, for each cast the monthly mean (over all years) was subtracted in order to remove the annual cycle, and all casts in a year were averaged to estimate a mean anomaly for the year. We are interested in seeing how, on different time scales, the variability extends to different depths. Figure 3.1 shows steric depth for each of the 12 monthly mean profiles. By steric depth, we mean that the specific volume anomaly is integrated downward from the ocean surface to the pressure level indicated by the ordinate. It can be seen that the month-to-month changes in specific volume are large in the upper 200 m and small below this. Figure 3.2 is of steric depth for the 26 yearly anomalies. The year-to-year changes in steric depth are slightly larger in magnitude than the annual cycle and clearly are distributed over a much greater depth range. This depth difference is summarized by examining empirical orthogonal functions (EOFs) of the specific volume profiles. The first EOF is, by definition, a best-fitting shape, in a least-squares sense, to all the profiles in a group. Figure 3.3 shows the first EOF for the annual cycle of specific volume variations and the first EOF for the yearly anomalies. The much greater depth range of the yearly anomalies is apparent. The secondary maximum

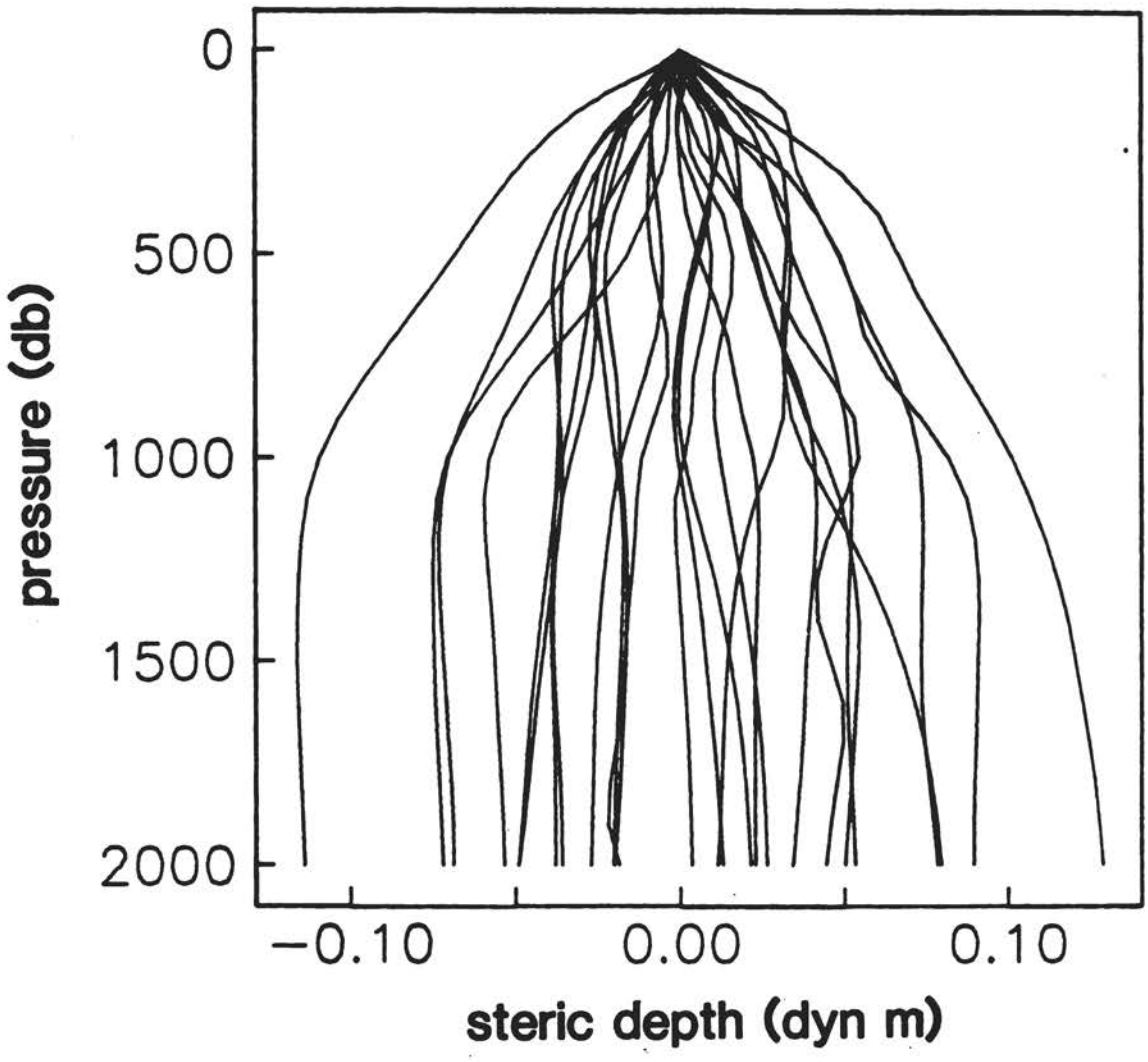

FIGURE 3.2 Yearly anomalies in steric depth (monthly mean values removed) at the Panuliris station for the years from 1955 to 1981.

in the yearly anomalies at 800 m is in the main thermocline. These EOFs describe 90 percent and 62 percent of the total variance in the profiles of the annual cycle and the yearly anomalies in specific volume, respectively.

But our main interest is in longer time scales. The yearly temperature anomalies were smoothed with a 5-year running mean filter and are displayed in Figure 3.4. Successive standard levels are offset from one another by 0.25°C. In and above the thermocline, down to 1000 m, one can see decreasing temperature between 1957 and 1970, as described by Pocklington (1972). However, the temperature then began to rise again, reaching a maximum in 1975-1977 that was still generally cooler than the initial values. Below 1000 m, the pattern is qualitatively different. In the deep levels, the O(20-year) oscillation seen above is not appar-

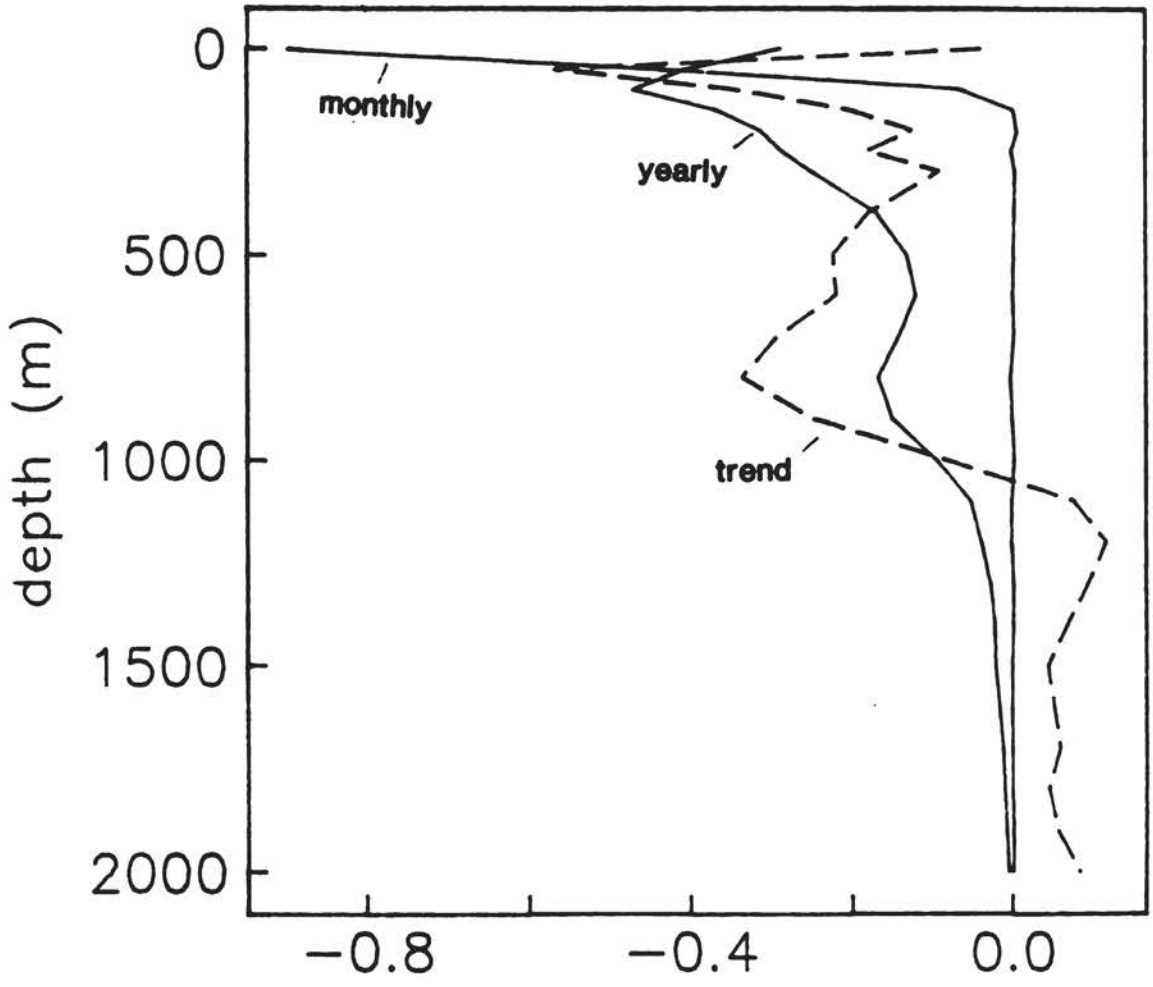

FIGURE 3.3 The first empirical orthogonal function of the monthly mean profiles of steric depth and the first EOF of the yearly anomaly profiles, normalized to have unit length. The third profile is of the linear trend in time of steric depth over the period 1955-1981, also normalized to unit length.

ent. Rather, there is a more regular rise amounting to between 0.1 and 0.2°C. The long time-scale variations below 1500 m appear not to be coupled to those in the thermocline.

In order to extract the longest time scale in the Panuliris data, a linear trend in specific volume over 26 years was computed at each standard depth. For comparison purposes, the trends were normalized in the same way as the EOFs and are plotted in Figure 3.3. The pattern is similar to the EOF of yearly anomalies in that it has a maximum in the main thermocline. An important difference though is that the trend does not become negligibly small below 1000 m. Rather it extends to the deepest levels sampled and to some undetermined depth beyond, with a change in sign at about 1000 m. In viewing the trends in relation to

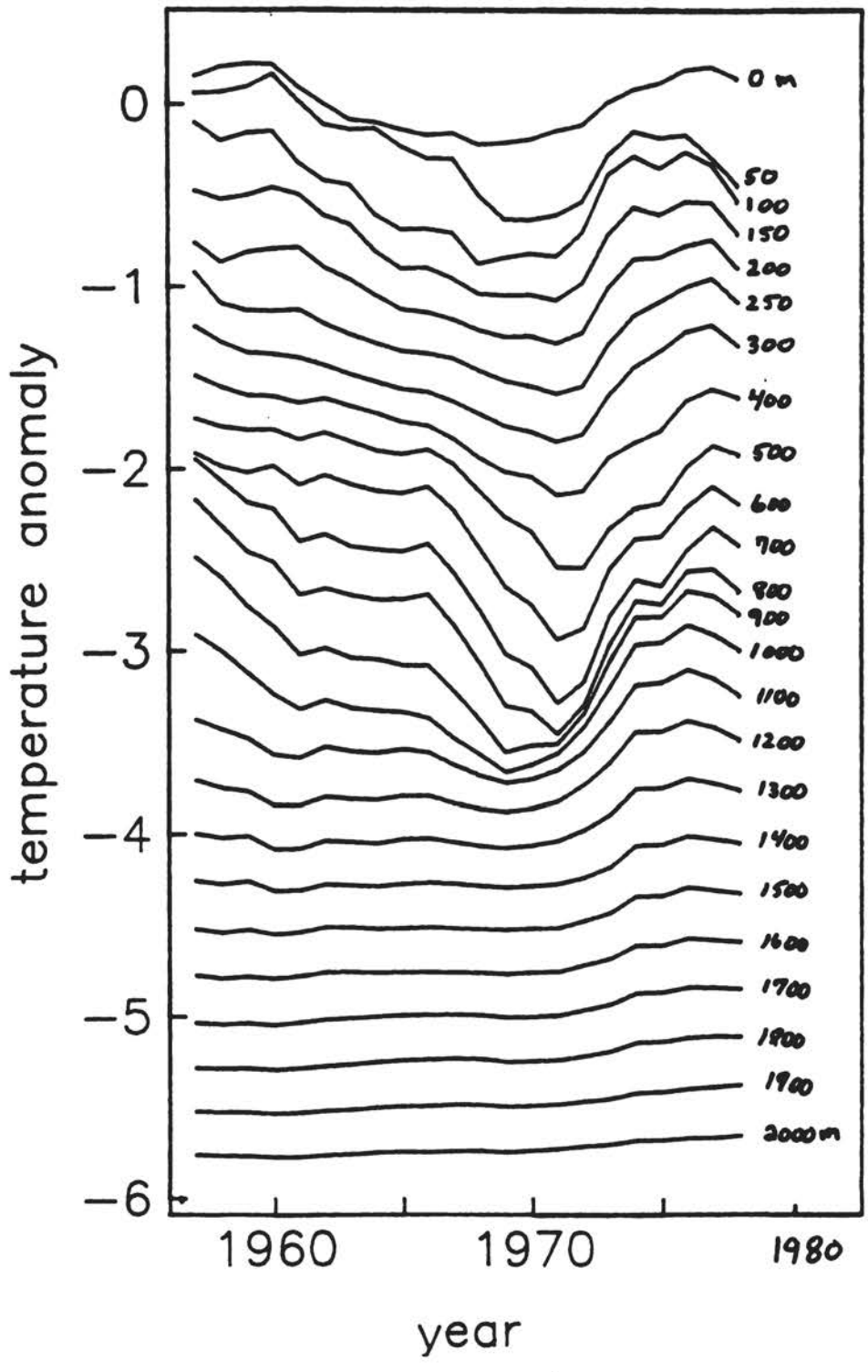

FIGURE 3.4 The 5-year running mean of temperature anomaly at the Panuliris station at 24 standard depths. Standard depths are offset by 0.25°C.

the running mean values in Figure 3.4, it is clear that the oscillations are as large or larger than the apparent trend and that the apparent trend in another 25 years of data could be quite different.

The trends observed at the Panuliris station are presumably not strictly local, and one would like to know the spatial extent of the signal. For this purpose, we compare the Panuliris trends to two large space-scale surveys separated in time by 22 years. As part of the International Geophysical Year (IGY) hydrographic survey, transatlantic sections were occupied along latitudes 36°15' from the United States to Spain and 24°30'N from Morocco to the Bahamas. With very similar ship tracks, these sections were repeated by the R/V Atlantis II in 1981. The two IGY sections have a total of 99 hydrographic stations, whereas the 1981 sections, made with a continuously profiling conductivity-temperature-depth recorder (CTD), have 191 stations to the ocean bottom. Large-scale differences in water-mass volumes were discussed by Roemmich and Wunsch (1984).

Here, we examine the average temperature difference as a function of depth along that part of the 36°N section that is east of the Gulf Stream and west of the mid-Atlantic ridge. This difference is shown in Figure 3.5, together with the linear trend in temperature in the Panuliris data, expressed on the same time frame. The standard error of the linear trend is shown by the error bars. Although there are differences in detail, these two profiles of temperature difference are remarkably similar considering that one is the difference between two large space-scale surveys and the other is a trend in time at a single point. They show a cooling trend, or uplifting of isotherms, down to the base of the thermocline at about 1000 m and a warming or downward displacement below. In the large space-scale surveys the warming extended down to a depth of about 3000 m. Moreover, a similar pattern existed along 36°N east of the mid-Atlantic ridge and along 24°N for the width of the ocean. At 24°N, the cooling was in a more restricted layer down to only 500 m with warming from 500 to 3000 m (Roemmich and Wunsch, 1984). Just as the thermocline showed more structure than the deep water in the time domain, there also appears to be greater spatial variability in the 22-year difference above 1000 m than in the deep water (see Roemmich and Wunsch, 1984, for maps of temperature difference). The existence of both the Panuliris time series and the two large space-scale surveys allows us to confirm that the secular trends in the Panuliris data are indicative of change over much of the subtropical gyre.

Of central importance here is the relationship between the apparent trends in specific volume and sea level. In Figure 3.6, the 5-year running mean of Bermuda sea level is shown together with that of the Panuliris steric height of the sea surface relative to 2000 db. For reference, we also show sea level at Charleston, South Carolina. It is at nearly the same latitude as Bermuda, and the record there is typical of the U.S. east coast. The correlation of Bermuda sea level and Panuliris steric height is very high: the correlation coefficient is about 0.9 for the unsmoothed yearly values. Charleston sea level, on the other hand, does not show the fall and rise that is associated with the thermocline variations at Bermuda (Figure 3.4) but rather has a more steady rise. If the Charleston record is detrended, then the residual

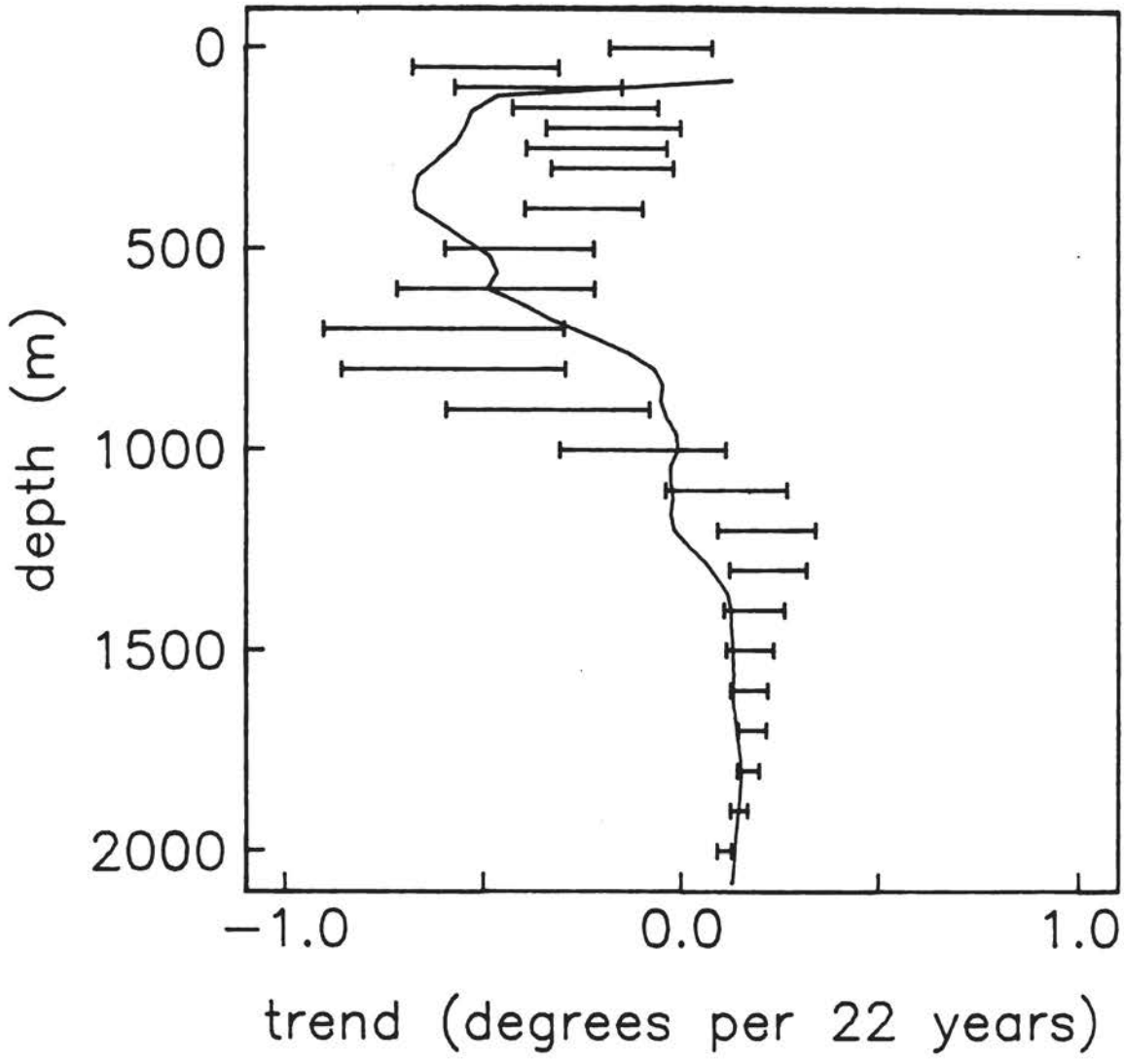

FIGURE 3.5 The smooth curve expresses the temperature difference between the IGY (1959) and 1981 surveys along 36°N west of the mid-Atlantic ridge and east of the Gulf Stream. A positive value indicates that the ocean was warmer in 1981. The horizontal bars show the linear trend of temperature in time, with the standard error of the estimate, at the Panuliris station.

has substantially less variance than the Bermuda record. The base of the thermocline slopes sharply upward across the Gulf Stream from east to west. The 7°C isotherm, found at about 1000 m in the Sargasso Sea is at around 200 m shoreward of the Gulf Stream. If all water above 7°C was cooled by a uniform amount, the effect on sea level would be 5 times as great on the offshore side of the Gulf Stream. Thus, the lower sea-level variance at the coast may be explained by a lower sensitivity to temperature fluctuations in the thermocline. An interesting question,

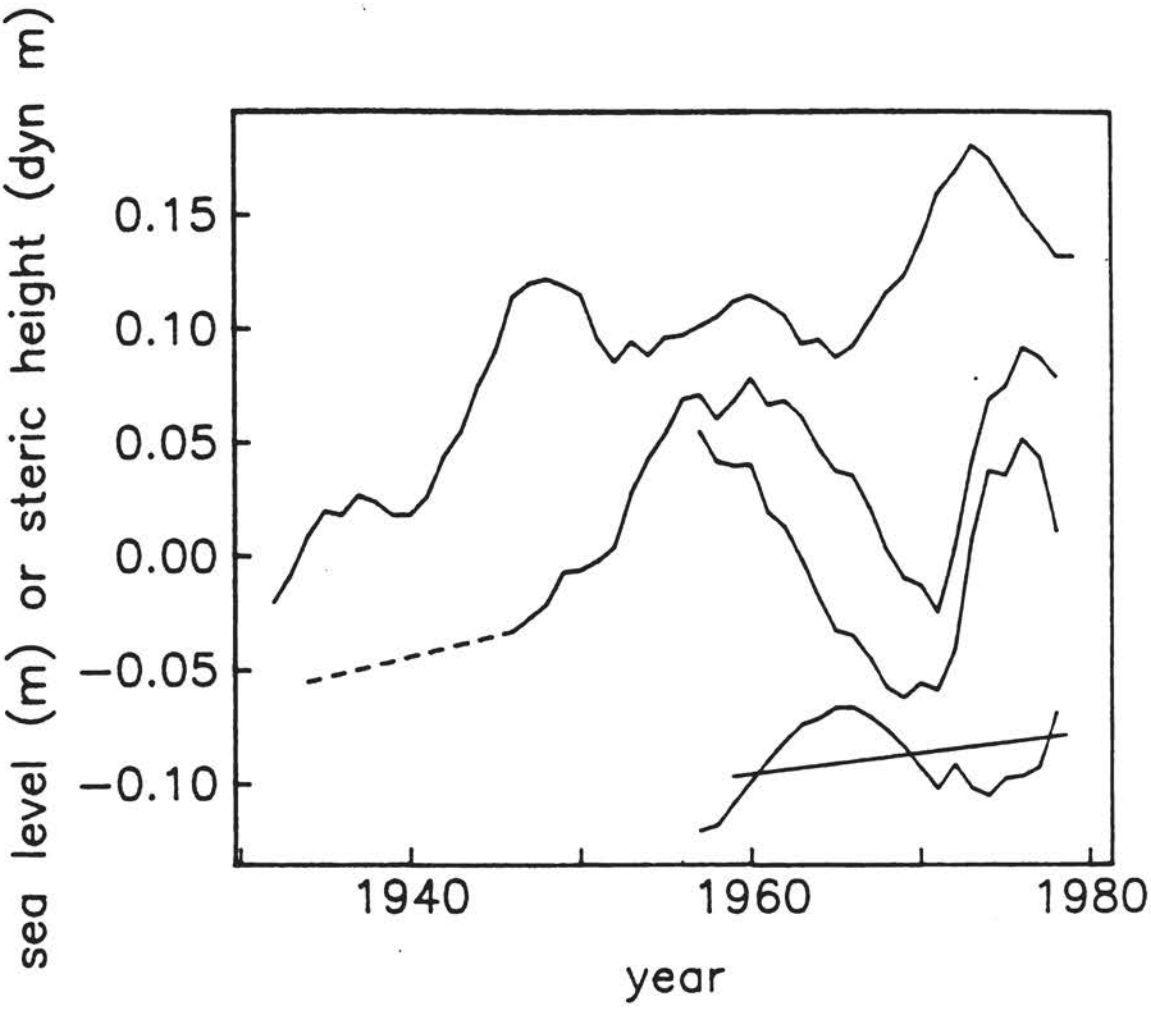

FIGURE 3.6 From top to bottom, 5-year running means of Charleston sea level, Bermuda sea level, Panuliris steric height (0/2000 db), and residual of steric height subtracted from sea level. The height of each curve is arbitrary. The straight line drawn through the bottom curve has an upward slope of 1 dyn cm per decade.

which we believe cannot be answered by the present data base, is whether all or part of the sea-level rise observed along the eastern U.S. can be attributed to the subthermocline warming seen throughout the subtropical North Atlantic.

A power-density spectrum of Bermuda sea level was computed using monthly mean values from 1955 to 1978. The high-frequency end is undoubteldy affected by aliasing, but here we are concerned only with the longest periods. A comparable series of monthly steric height of the sea surface relative to 2000 db was obtained by interpolating the Panuliris data, also from 1955 to 1978. The two spectra are displayed together in Figure 3.7. They are indistinguishable at periods of a year

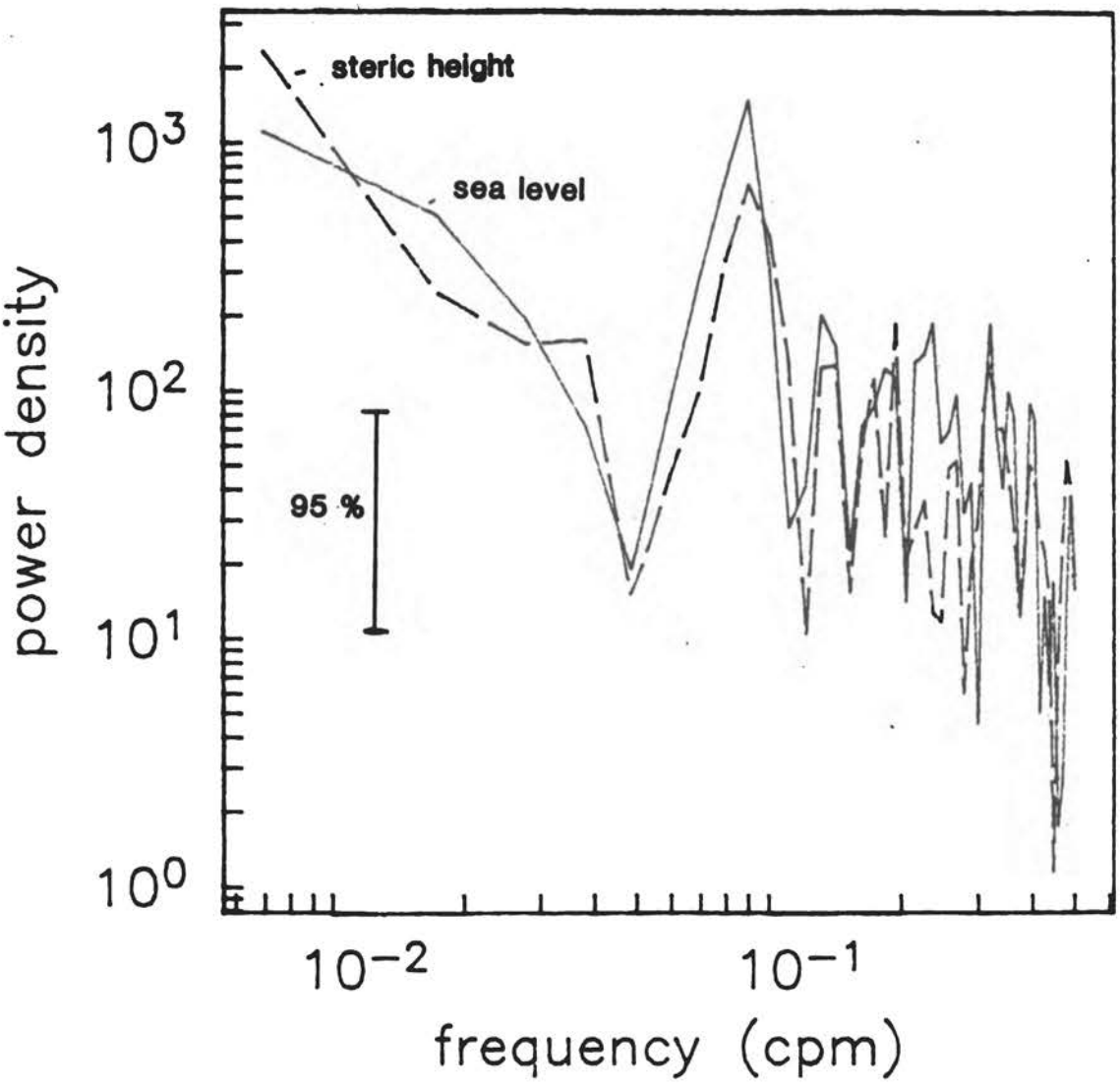

FIGURE 3.7 Power density spectra band averaged over three frequency bands of Bermuda sea level and Panuliris steric height (0/2000 db).

and longer. Indeed the only appearance of a difference is in a band from about 3 to 5 months, where the sea-level spectrum appears elevated. A prominent annual signal is seen in both records. In the lowest-frequency bands, both spectra slope more steeply than (frequency)$^{-1}$, indicating that the energy density per unit log frequency increases with increasing period.

As another way of illustrating this point, consider the difference of steric height (0/2000 db) subtracted from sea level. That is shown, again as a 5-year running mean, at the bottom of Figure 3.6. Time variations in this difference amount to a few centimeters. For reference, a line sloping upward at 1 cm per decade is also shown. There is an apparent trend, indicating a rise in sea level relative to steric

height. But the 0(10-year) variations are larger than the apparent trend. Further, data from the 1981 and IGY surveys of the subtropical Atlantic suggest that if the warming from 2000 to 3000 db were considered, the apparent trend in the sea-level residual would be approximately halved. This is obviously not the end of the story. Several decades more of Bermuda sea level together with steric height are required in order to see if the upward trend in sea level, which is the overall Bermuda record (1933-1980) but not in the 1954-1980 segment overlapping the Panuliris observations, is re-established. If so, the question is whether the rise is accounted for by an increase in steric height or whether there is a residual rise in sea level not attributable to steric expansion.

DISCUSSON

A principal lesson of the extensive North Atlantic data sets is that steric height variations occur over such a variety of space and time scales that the problem of even defining a global trend, let alone observing it, is a difficult one. In the 27 years of overlapping steric height and sea-level data at Bermuda, there was no evidence of a "spectral gap" that would allow separation of the time scale spanned by the data from a much longer time scale that would appear as a trend. Rather, the sea-level and steric-height spectra were equally red in the lowest-frequency bands. An encouraging sign is that longer 50-year sea-level records such as the Charleston record in Figure 3.6 (for which there is no accompanying steric-height time series) do show evidence of such a gap. That is, the 15-cm trend over 50 years is greater than the 5 cm fluctuations over 10 to 20 years at that location. The expectation then is that about 50 years of sea level together with steric height at Bermuda would resolve the question of whether the sea-level trend is accompanied by a trend in steric height (at that location).

Steric changes in the water column on time scales of a decade and longer are not confined to or concentrated in the upper ocean. In the subtropical North Atlantic such changes extend to depths of at least 3000 m. Maxima in temperature change appeared in the thermoscline at depths of from 300 to 700 m and below the thermocline at about 1800 m. For observational programs, the large vertical extent of the signal means that the entire depth of the ocean should be sampled. The Panuliris data are not sufficiently deep, though this deficiency can be made up by a few ancillary deep measurements elsewhere. For climate modeling studies, it is clear that the commonly used one-dimensional vertical advection-diffusion models not only miss the essential physics of the problem but cannot even mimic the observed patterns of change. Critical processes are air-sea interactions at middle and high latitudes, which determine volume and composition of the mid-depth and deep-water masses and the spreading of those waters to lower latitudes.

Temperature variations had a somewhat different character in and above the thermocline than in the deep water. The thermocline fluctuations had greater variance in the time domain than the deeper changes and also more variability around the subtropical gyre. Over 27 years,

the thermocline fluctuations made a greater contribution to steric height change than the deep changes, but on a longer time scale it is not clear whether mid-depth or deep variations would dominate. The thermocline comes to the surface along the northern rim of the subtropical gyre, and these waters are therefore subject to atmospheric forcing relatively near to the area of our study. The deep water is farther removed from contact with the atmosphere, which can account for the more gradual changes and larger spatial scale of the deep signal.

REFERENCES

Barnett, T., 1983. Long-term changes in dynamic height, Journal of Geophysical Research, 88, 9547-9552.

Frankignoul, C., 1981. Low-frequency temperture fluctuations off Bermuda, Journal of Geophysical Research, 86, 6522-6528.

Pocklington, R., 1972. Secular changes in the ocean off Bermuda, Journal of Geophysical Research, 77, 6604-6607.

Reid, J., and A. Mantayla, 1976. The effect of geostrophic flow upon coastal sea elevations in the northern North Pacific Ocean, Journal of Geophysical Research, 81, 3100-3110.

Roemmich, D., and C. Wunsch (1984). Apparent changes in the climatic state of the deep North Atlantic Ocean, Nature, 307, 447-450.

Schroeder, E., and H. Stommel (1969). How representative is the series of monthly mean conditions off Bermuda? In Progress in Oceanography 5, 31-40.

Shaw, D., and W. Donn (1964). Sea level variations at Iceland and Bermuda, Journal of Marine Research, 22, 111-122.

Wunsch, C. (1972). Bermuda sea level in relation to tides, weather, and baroclinic fluctuations, Reviews of Geophysics and Space Physics, 10, 1-49.

ATTACHMENT 4

OCEANOGRAPHIC EVIDENCE FOR LAND ICE/OCEAN INTERACTIONS IN THE SOUTHERN OCEAN

Stanley S. Jacobs
Lamont-Doherty Geological Observatory
of Columbia University

SALINITY CHANGES IN THE DEEP OCEAN

There is ample evidence that subsurface water masses in the Southern Ocean undergo salinity changes with time, but few of these evolutions have any direct relationship to land ice. For example, Rochford (1965) showed that SCOR-UNESCO "calibration" stations in the Southeast Indian Ocean experienced apparent seasonal fluctuations on the order of 0.02 per mil in the deep salinity maximum. Closer to Antarctica, Gordon (1978) attributed a 3000-m-deep freshening of 0.005 to 0.03 per mil between 1973 and 1977 to convective overturning associated with the giant Weddell Polynya. Foster and Middleton (1979) demonstrated an increase of 0.02 per mil between 1975 and 1976 in the salinity of bottom water flowing out of the Weddell Sea and ascribed this to year-to-year changes in atmospheric conditions that affect the rate of sea-ice formation. Their transects show similar salinity alterations in the overlying deep water, which may be recovering from the polynya events of the mid-1970s, encountering variability in its resupply of Circumpolar Deep Water or displaying the effects of other mixing and circulation changes unrelated to glacial ice.

DATA QUALITY

The 0.02 per mil salinity changes noted above are of the same magnitude as reported climatic freshening of the deep North Atlantic over the past two decades (Brewer et al. 1983) and about a factor of 10 greater than the potential accuracy of salinity (conductivity) measurements. It should be mentioned, however, that the reference standard water has varied by nearly 0.01 per mil over the same time period (Mantyla 1980), and there are several other factors that can and do degrade the precision of shipboard salinity determinations. Furthermore, oceanographic data quality problems tend to increase with the age of the observations. Gordon (1982) demonstrated a cooling of Weddell Deep Water starting in the mid-1950s but could not use the accompanying salinity data back to 1912 (A. L. Gordon, Lamont-Doherty Geological Observatory, personal communication, 1984).

SALINITY CHANGES ON THE CONTINENTAL SHELF

Large salinity changes have been observed on the Antarctic continental shelf over the past two decades. From the Lamont data (open symbols) in Figure 4.1, it could be argued that the High Salinity Shelf Water (HSSW) near Ross Island has decreased by at least 0.05 per mil in salinity since 1968. If that decrease were due to melting of the Ross Ice Shelf, it would correspond to a melt rate of 7 cm/yr, averaged over

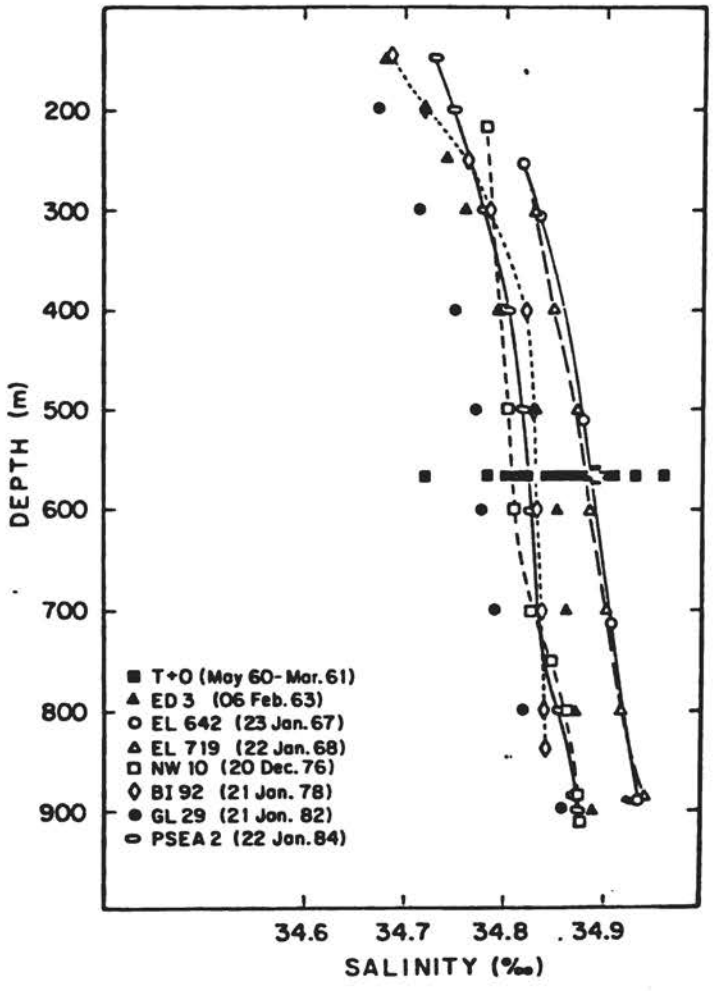

FIGURE 4.1 Salinity measurements from 1960 through 1984 in High Salinity Shelf Water in the Ross Sea. Corresponding temperature measurements are all near the sea-surface freezing point (about -1.85 to -1.95°C). The vertical profiles were taken within a half-circle of 15-km radius centered near 77°15'S, 168°22'E, just north of Ross Island. The time-series observations at 565 m were taken through an ice hole in McMurdo Sound. Data from Tressler and Ommundsen (1962), Countryman and Gsell (1966), Jacobs et al. (1982, and other reports), and Biggs and Amos (1983).

the entire ice shelf base. HSSW does melt the shelf ice and serve some other interesting functions, but its thermohaline properties are primarily set by sea-surface freezing, as attested by its homogeneous temperature near the 1-atm freezing point (Jacobs et al. 1970, 1985). With no change in other parameters a salinity decrease of 0.05 per mil in HSSW would correspond to about 1 m less sea ice in one year, or 12 cm less over the 1968-1976 period. The first value is unlikely, but the latter is within the noise level of known annual sea-ice variability, although the Ross Sea sector does not appear to show a decrease over the time interval (Figure 5 in Zwally et al. 1983). Seasonal cycles within the HSSW are also large, as demonstrated by the solid squares in Figure 4.1, representing salinity measurements at 3-week intervals throughout the year in McMurdo Sound. The variability in residence time for water on the continental shelf is not known.

ICE-SHELF WATER: THE PRIMARY EVIDENCE FOR GLACIAL MELTING

While variability in sea ice can mask a freshening signal, even near large blocks of melting continental ice, it can be demonstrated that the boundary layers directly beneath ice shelves are strongly influenced by basal meltwater (Jacobs et al. 1979a, 1985; Potter and Paren 1985). Probably the most striking examples of glacial melting that reach the open ocean are the "Deep" Ice Shelf Waters in some temperature sections

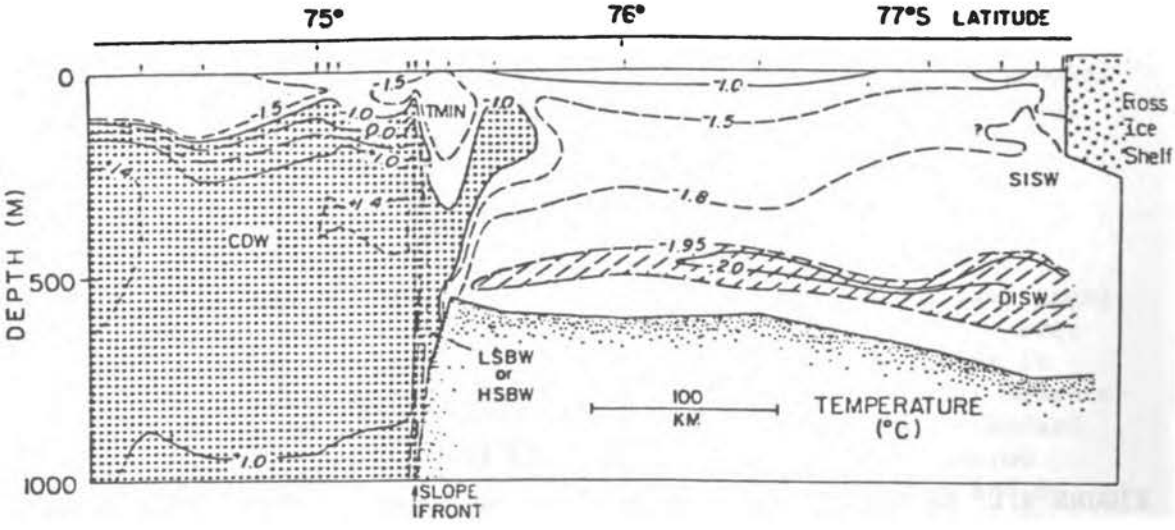

FIGURE 4.2 A December 1976 temperature section through the primary Deep Ice Shelf Water core in the Ross Sea, after Jacobs et al. (1979b). This water is at temperatures as much as 0.3°C below the sea-surface freezing point, owing to heat loss in melting at the ice-shelf base. Ice Shelf Water has been observed on the continental slope in the Weddell Sea (Foldvik, as reported in Killworth 1983) and plays a significant role in "bottom"-water formation.

along and perpendicular to the Antarctic ice shelves (Jacobs et al. 1970; 1979b; Carmack and Foster 1976; Foldvik et al. 1985). These features (e.g., Figure 4.2) result primarily from basal melting by HSSW (Jacobs et al. 1979a), particularly in the interior regions of the sub-ice-shelf cavities (MacAyeal 1984). In the Ross Sea the overflow is about 0.15 per mil fresher than the average HSSW and, during a 7-month period in 1978, set to the northeast at a mean velocity of 1.4 cm/sec. MacAyeal (1984) has argued that since HSSW is constrained to the sea-surface freezing temperature, this mode of basal melting would be relatively insensitive to climate change. However, the volume of HSSW may influence basal melting by "warm" intrusions at intermediate depths.

"WARM" CORES: THE PRIMARY HEAT SOURCES FOR GLACIAL MELTING

The vulnerability of basal ice to the intrusion of relatively "warm" water underneath may be illustrated by the order-of-magnitude differences between estimated melting rates for several ice shelves. Jacobs et al. (1985) identified a "Shallow" Ice Shelf Water that results from glacial ice melting into a "warm" inflow (WMCO), derived from Circumpolar Deep Water (CDW) north of the Ross Sea continental shelf (Figure 4.3). Year-long current and temperature measurements in this WMCO near the Ross Ice Shelf (Pillsbury et al. 1985) show mean flows to the south and west around 5 cm/sec Given average dimensions of 200 m by 100 km and an average temperature 0.5°C above the <u>in situ</u> freezing point (Jacobs et al. 1979a), this WMCO could melt as much as 35 cm/yr off the ice-shelf base if recirculation did not return some of the sensible heat to the open Ross Sea.

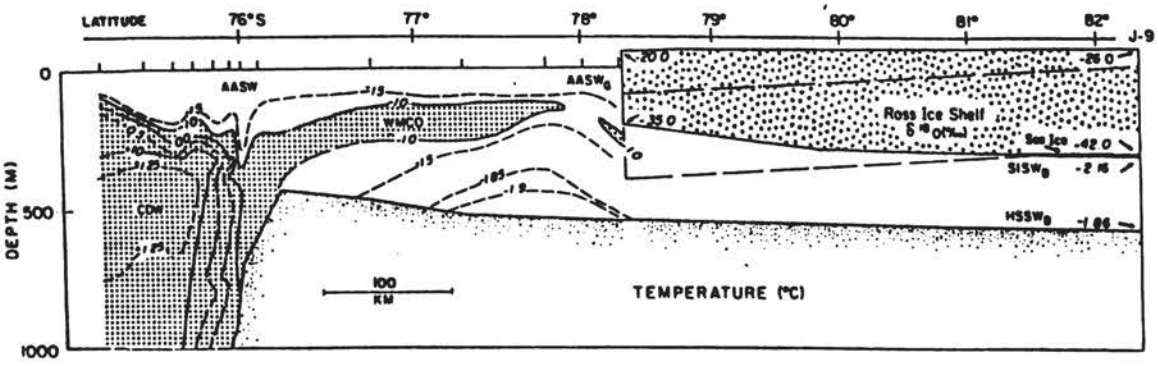

FIGURE 4.3 A December 1976 temperature section through the primary intrusion of "warm" water (WMCO) in the Ross Sea, after Jacobs et al. (1985). Derived from the Circumpolar Deep Water north of the continental shelf, the temperature of this inflow drops by about 2°C in crossing the slope front. Year-long temperature measurements at the Barrier indicate that it may average more than 0.5°C above the freezing temperature there (Pillsbury et al., 1985).

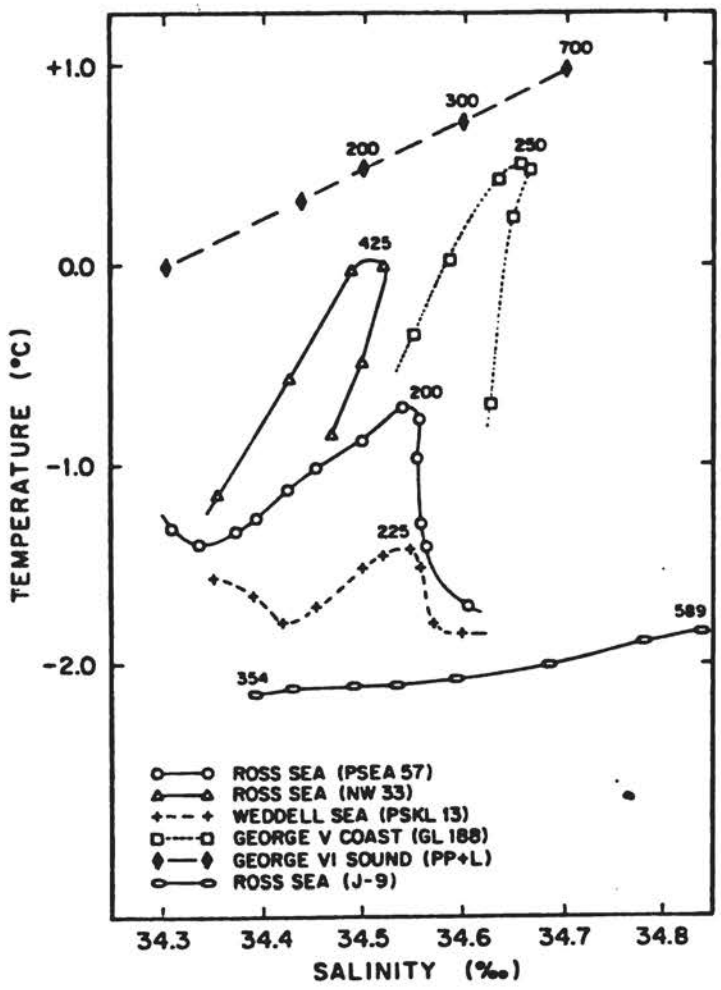

FIGURE 4.4 Temperature/salinity diagram illustrating the range of thermohaline properties of several "warm" intrusions onto the Antarctic continental shelf. Observations taken beneath the ice shelf at "J-9," several hundred kilometers south of the Ross Barrier, are shown for comparison. Data from Gammelsrod and Slotsvik (1981), Jacobs and Haines (1982), and Paren et al. (1983).

Intrusions of "warm" water onto the Antarctic continental shelf display a considerable range of thermohaline characteristics (Figure 4.4). Of particular note is the Amundsen-Bellingshausen coastline where nearly undiluted CDW appears to intrude onto the continental shelf and beneath the ice shelves. This water is about 3°C above the in situ freezing temperature of the glacial ice and leads to basal melt rates on the order of 2 m/yr (Hughes, 1983; Potter and Paren, 1985). It may be of interest to explore pontential links between this ocean heat transport, the hypothesized recent disappearance of grounded or floating continental ice from this glaciologically unstable sector of the continent (Kellogg et al. 1982; Fastook 1984), and estimates of higher CDW temperatures in a CO_2-warmed future (Gordon 1983; Schlesinger, this volume,

Attachment 19). Dense shelf water may now limit access by CDW and its WMCO derivatives to restricted portions of the Antarctic coastline (Jacobs et al. 1985). However, relatively small changes in sea ice production might alter the HSSW salinity and volume (Figure 4.1), which in turn could influence the continental shelf circulation.

GEOCHEMICAL EVIDENCE FOR ATMOSPHERE/ICE/OCEAN INTERACTIONS

Glacial ice spikes the seawater into which it melts with a low ^{18}O tracer that can be related to the melting rate and the residence time of shelf water. Water on the Ross Sea continental shelf has an average $\delta^{18}O$ content that is about 0.2 o/oo lower than its source water offshore owing to the combined impacts of glacial meltwater, sea ice freezing, and precipitation (Figure 4.5). The line that crosses the horizontal bar in Figure 4.5 at a residence time of 6.2 years corresponds to a mass balance condition for the ice sheet, with 2000 km^3/yr attrition, 65 percent of which is lost in icebergs and 35 percent in melting of the attached glacial ice. Allowing for some iceberg melting over the continental shelf, this is equivalent to average net melting under all the ice shelves of about 0.4 m/yr (Jacobs et al. 1985). Shelf-water residence times that fall within the range of the solid bar in Figure 4.5 are consistent with most independent calculations of "bottom"-water formation rates, but the higher rates are not closely coupled to mass transport on and off the shelf. Tracers like chlorofluoromethanes (Freons) could help to refine estimates of shelf-water residence time (Trumbore et al. 1984). The residence time of surface and shelf water and the ventilation time of the deep ocean in the Antarctic are critical factors in the effectiveness of this region as a CO_2 sink for the atmosphere. Representative samples of Antarctic shelf and deep waters are now being processed for key parameters in the carbon cycle (e.g., Takahashi et al. 1984).

THE ICEBERG CONNECTION

Bentley (1984) has postulated that a disintegrating West Antarctic ice sheet might be slowed by several factors, including the presence of pack ice and the sluggishness of ocean currents in moving icebergs away from the calving bays. However, except for localized regions of fast ice, the sea ice that forms at the coastline probably drifts away from it continually during the long winter season (Wordie 1921; e.g., Gill 1973). Icebergs would tend to move with the pack, or through it under the influence of subsurface currents, as shown by trajectories on the weekly Antarctic ice charts generated by the NAVY-NOAA Joint Ice Center. The subsurface currents are energetic, with measured speeds up to 55 cm/sec and mean northerly drifts at some locations (Jacobs et al. 1979a; Jacobs and Haines 1982; Pillsbury and Jacobs 1985). Icebergs go aground on submarine rises, move to the west along the continental margin (Tchernia and Jeannin 1980), and probably recirculate within existing ocean and shelf gyres. Their melt rates during these exercises will

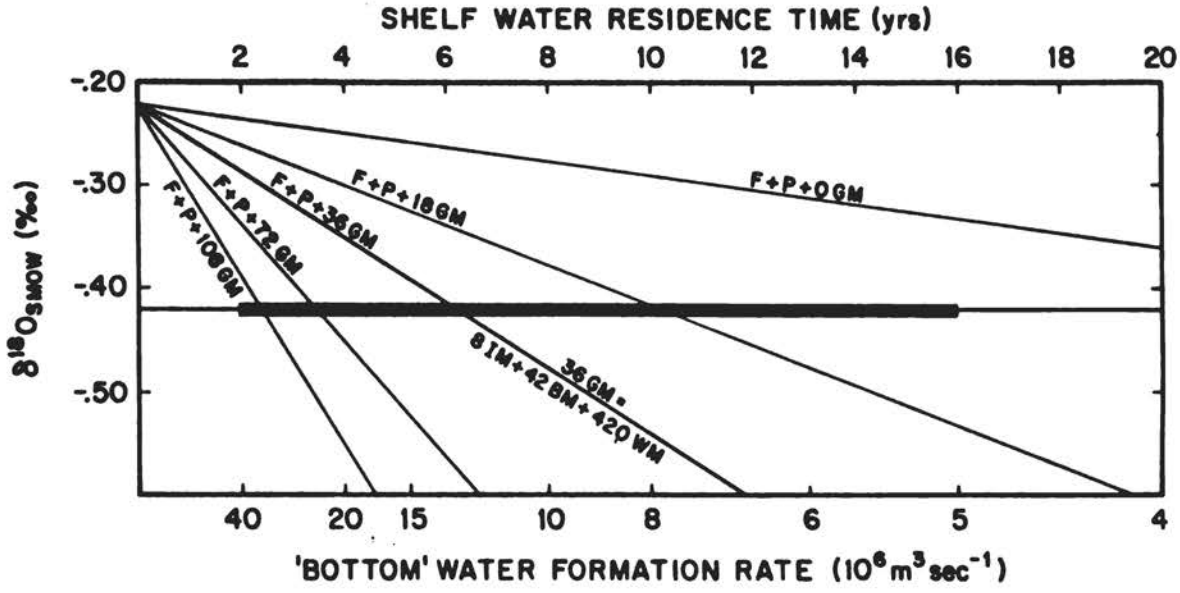

FIGURE 4.5 Relationship between shelf-water $\delta^{18}O$ content, residence time, and glacial melt rates (cm/yr) for the circumpolar continental shelf. The $\delta^{18}O$ content of shelf water is decreased by net sea-ice freezing (F = 1 m/yr), precipitation minus evaporation (P = 15 cm/yr), and glacial meltwater (GM, variable). GM includes basal melting (BM), wall melting (WM), and iceberg melting (IM) averaged over the continental shelf area. After Jacobs et al. (1985).

increase whenever the ice draft extends down into the CDW or "warm" inflows on the continental shelves.

The ocean budgets that relate to ice-shelf mass balance could be improved considerably if we had better information on the formation, thickness, drift, and decay of sea ice and icebergs. In this regard, it may be worth noting that most accounts of Antarctic icebergs attribute their origins to the large ice shelves. However, observations incidental to our oceanographic work suggest relatively little recent calving of the Ross Barrier. Assuming the two recent positions in Figure 4.6 are accurate, the Ross Ice Shelf has advanced over 15 km in the past two decades, i.e., about what would be expected from its estimated northward rate of motion during this period (SPRI/NSF charts). At an average thickness of 250 m, the northward advance between 1962 and 1983 represents a volume of ice roughly equivalent to 1.5 times the annual accumulation on Antarctica. The earlier barrier positions, after David (1914), suggest a short-term (10-yr) instability and a long-term (100-yr) stability in its location.

CIRCULATION UNDER THE ICE SHELVES

Present-day circulation underneath the Antarctic ice shelves has been inferred from a variety of remote data. Summer oceanographic observa-

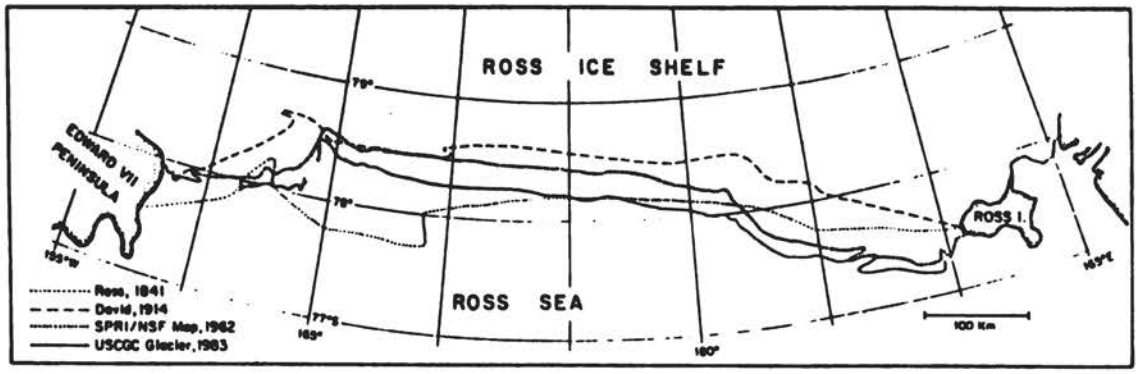

FIGURE 4.6 Four determinations of the Ross Barrier position between 1841 and 1983. The two early positions are from David (1914). The shaded area between the two recent positions, assuming a thickness of 250 m, represents over 3000 km^3 of ice.

tions near the northern edges of the ice have shown probable regions of seawater inflow and outflow and have provided information on likely property changes beneath the ice (Jacobs et al. 1970, 1979a, 1985; Carmack and Foster 1976; Gammelsrod and Slotsvik 1981; Potter and Paren 1985). Instruments moored year-round near the Ross Barrier (Jacobs and Haines 1982; Pillsbury and Jacobs 1985) or lowered through holes in the sea ice (Tressler and Ommundsen 1962) have revealed seasonal thermohaline changes and energetic deep currents. Regions of probable basal melting and freezing have been identified by radio echo-sounding from aircraft (Neal 1979; Robin et al. 1983).

Beneath the ice, direct current observations showed a strong tidal circulation, with speeds over 15 cm/sec, in a water column stratified by basal melting (Jacobs et al. 1979a; Jacobs and Haines 1982). Geochemical measurements suggest a short residence time for seawater beneath the ice (Michel et al. 1979; Trumbore et al. 1984), in agreement with observed biological activity, which must depend on a continuing supply of food to the sub-ice region (Bruchhausen et al. 1979). Cores through the ice shelves have confirmed that sea-ice layers exist at the bases in some locations (Zotikov et al. 1980; Morgan 1972). Large bottom crevasses (Clough 1975) are likely sites of concentrated freezing and brine drainage. Modelers of the sub-ice shelf circulation have considered the roles of tidal mixing and rectification, melt-water plumes (MacAyeal 1984, 1985), and the probable transfers of heat and salt (Wexler 1960; Gade 1979).

Net basal melting under the Antarctic ice shelves appears to be a significant factor in the mass balance of the ice sheet. The oceanographic data and models are as yet insufficient, however, to determine the basal mass balance with any precision or to indicate whether the ocean-ice shelf system is now in a state of equilibrium. Even if a steady-state condition exists at present, future changes could occur if seawater circulating beneath the ice becomes warmer or transfers heat into the sub-ice cavities at a faster rate. This might occur if a warmer atmosphere resulted in a low-density cap of surface water on the

Southern Ocean, less vertical heat flux, and a consequent deep-water temperature increase of up to 0.5°C (Gordon 1983). That would probably result in a proportional increase in water temperatures on the continental shelf, even if the shelf-slope circulation did not change. Some models indicate that a CO_2-warmed atmosphere might directly increase ocean temperatures by more than 1°C at ice-shelf depths and latitudes (Figure 8.3 in Revelle 1983). A warmer atmosphere may also result in an altered continental shelf circulation in response to different wind patterns and less (?) sea ice. Presumably, less sea ice would result in less dense shelf water, potentially exposing the ice-shelf base to warmer deep water over greater areas. It is not known why "warm" water now intrudes onto the continental shelf in some areas but not in others, nor how the dynamics of shelf-slope exchanges might be altered in a warmer and fresher Southern Ocean.

Freezing and melting under the floating ice shelves will only have an impact on sea level if those processes indirectly change the volume of grounded ice. At present, the sub-ice-shelf circulation and temperature field is such that the pressure-dependent freezing temperatures may cause ice to be melted in one location and redeposited elsewhere on the ice-shelf base. While not altering the basal mass balance, this process could change the ice thickness profile and its mean temperature and flow rate. It may also redistribute ice in the vicinity of critical pinning points where grounding occurs on submarine rises. Transporting more heat beneath the ice may not increase the melting rate if, at the same time, the circulation slows and the water column becomes more highly stratified. It might, however, alter the melting locations, which could be of equal importance. We often overlook many of the positive and negative feedbacks. A warmer ocean may well increase basal melting, assuming that bottom-water formation rates increase to dispose of the cold meltwater; but a warmer ocean is also likely to experience increased evaporation, perhaps leading to increased accumulation on the ice sheet that would balance wastage at the margins.

RECOMMENDATIONS FOR FUTURE RESEARCH

1. Interdisciplinary oceanographic studies of the slope front region near the continental shelf break. The focus should be on understanding the year-round transport of water, heat, salt, and ice on and off the shelf and the significance of this region in ventilation of the deep ocean. Particular attention should be directed to the critical and practically unsampled Amundsen-Bellingshausen sector.
2. Direct measurements of ocean properties near and under the ice shelves. The objectives should be to understand the ocean-to-ice heat transfer, the oceanographic role of bottom crevasses, and the effectiveness of "supercooling relief" (Lewis, this volume, Attachment 20) in redistributing ice on the base of an ice shelf.
3. Long-term monitoring of potentially sensitive water masses, such as the "warm" inflows and the High Salinity Shelf Water, in conjunction with relevant cryospheric and atmospheric parameters. The objective should be to understand the production mechanisms of these waters and

determine how their spatial and temporal variabilities relate to various climatic factors. Bottom moorings, drifters, and repeated shipboard water sampling will be needed.

4. Modeling of the ocean circulation on and near the Antarctic continental shelves and beneath the ice shelves. The emphasis should be on better coupled shelf circulation and global ocean circulation models, fully coupled dynamic/thermodynamic ice models (e.g., Hibler 1984), and realistic representations of atmospheric driving and air-sea exchanges. See also MacAyeal (1983) and Semtner (1983).

5. Direct measurements of sea-ice formation, concentrations, drift, and melting and of leads and polynyas in the sea ice (e.g., Cavalieri and Martin 1985; Kurtz and Bromwich 1985; Zwally et al. 1985). The objectives should be to provide high-quality ground-truth observations for calibrating satellite imagery and model studies and quantitative information on brine drainage over the continental shelf and slope.

6. Satellite monitoring of the ice-sheet elevations and perimeter and of the calving and movement of all medium and large icebergs (e.g., Orheim, this volume, Attachment 12; Holdsworth 1985). This information is needed to improve estimates of ice-sheet mass balance and to refine calculations of shelf-water residence time.

ACKNOWLEDGMENTS

The author's current Southern Ocean work is supported by the National Science Foundation under grant DPP-81-19863, with supplemental support provided by the Department of Energy through Interagency Agreement DE-AI01-84ER60201.

REFERENCES

Baumgartner, A. and E. Reichel, 1975. The World Water Balance: Mean Annual Global, Continental and Maritime Precipitation, Evaporation and Run-Off, Elsevier, New York, 179 pp.

Bentley, C. R., 1984. Some aspects of the cryosphere and its role in climatic change. In J. Hansen and T. Takahashi (eds.), Climate Processes and Climate Sensitivity, Geophysical Monograph 29, Ewing Volume 5, American Geophysical Union, Washington, D.C., pp. 207-220.

Biggs, D. C., and A. F. Amos, 1983. Oceanographic data from the southwestern Ross Sea, January 1982: STD and nutrient chemistry programs. Texas A&M Univ., Ref. 83-3-T.

Brewer, P. G., W. S. Broecker, W. J. Jenkins, P. B. Rhines, C. G. Rooth, J. H. Swift, T. Takahashi, and R. T. Williams, 1983. A climatic freshening of the deep Atlantic north of 50°N over the past 20 years. Science, 222, 1237-1239.

Bruchhausen, P. M., J. A. Raymond, S. S. Jacobs, A. L. DeVries, E. M. Thorndike, and H. H. Dewitt, 1979. Fish, crustaceans, and the sea floor under the Ross Ice Shelf. Science, 203, 449-450.

Carmack, E. C., and T. D. Foster, 1976. Circulation and distribution of oceanographic properties near the Filchner Ice Shelf, Deep-Sea

Research, 22, 77-90.
Cavalieri, D., and S. Martin, 1985. A passive microwave study of polynyas along the Antarctic Wilkes Land Coast. In Oceanology of the Antarctic Continental Shelf, Ant. Res. Ser., Vol. 43 (in press).
Clough, J. W., 1975. Bottom crevasses in the Ross Ice Shelf, Journal of Glaciology, 15(73), 457-458.
Countryman, K. A., and W. L. Gsell, 1966. Operations Deep Freeze 63 and 64, Summer Oceanographic features of the Ross Sea. U.S. Navy Hydrog. Off., TR-190, 193 pp.
David, T. W. E., 1914. Antarctica and some of its problems, The Geographic Journal, XLIII(6), 605-630.
Fastook, J. L., 1984. West Antarctica, the sea-level controlled marine instability: Past and future. In J. Hansen and T. Takahashi (eds.), Climate Processes and Climate Sensitivity, Geophysical Monograph 29, M. Ewing Volume 5, American Geophysical Union, Washington, D.C., pp. 275-287.
Foldvik, A., T. Gammelsrod, and T. Torresen, 1985. Circulation and water masses on the Southern Weddell Sea Shelf. In Oceanology of the Antarctic Continental Shelf, Ant. Res. Ser., vol. 43, American Geophysical Union, Washington, D.C. (in press).
Foster, T. D. and J. H. Middleton, 1979. Variability in the bottom water of the Weddell Sea. Deep-Sea Research, 26A, 743-762.
Gade, H. G., 1979. Melting of ice in sea water: A primitive model with application to the Antarctic ice shelf and icebergs. Journal of Physical Oceanography, 9(1), 189-198.
Gammelsrod, T., and N. Slotsvik, 1981. Hydrographic and current measurements in the southern Weddell Sea 1979/80. Polarforschung, 51(1), 101-111.
Gill, A. E., 1973. Circulation and bottom water production in the Weddell Sea, Deep-Sea Research, 20, 111-140.
Gordon, A. L., 1978. Deep Antarctic convection west of Maud Rise. Journal of Physical Oceanography, 8(4), 600-612.
Gordon, A. L., 1982. Weddell Deep Water variability. Journal of Marine Research, 40, Suppl., 199-217.
Gordon, A. L., 1983. Comments about the ocean role in the Antarctic glacial ice balance. In Proceedings Carbon Dioxide Research Conference: Carbon Dioxide, Science and Concensus, 19-23 Sept. 1982, Berkeley Springs, W. Va.
Hibler, W. D., III, 1984. The role of sea ice dynamics in modeling CO_2 increases. In J. Hansen and T. Takahashi (eds.), Climate Processes and Climate Sensitivity, Geophysical Monograph 29, Ewing Volume 5, American Geophysical Union, Washington, D.C., pp. 238-253.
Holdsworth, G., 1985. Some effects of ocean currents and wave motion on the dynamics of floating glacier tongues. In Oceanology of the Antarctic Continental Shelf, Ant. Res. Ser., vol. 43, American Geophysical Union, Washington, D.C. (in press).
Hughes, T., 1983. The stability of the West Antarctic Ice Sheet: What has happened and what will happen. In Proceedings Carbon Dioxide Research Conference: Carbon Dioxide, Science and Concensus, 19-23 Sept. 1982, Berkeley Springs, W. Va.
Jacobs, S. S., and W. E. Haines, 1982. Ross Ice Shelf Project

Oceanographic Data, 1976-79, Tech. Rept. L-DGO 82-1, 505 pp.

Jacobs, S. S., A. F. Amos, and P. M. Bruchhausen, 1970. Ross Sea oceanography and Antarctic bottom water formation, Deep-Sea Research, 17, 935-962.

Jacobs, S. S., A. L. Gordon, and J. L. Ardai, 1979a. Circulation and melting beneath the Ross Ice Shelf. Science, 203, 439-442.

Jacobs, S. S., A. L. Gordon, and A. F. Amos, 1979b. Effect of glacial ice melting on the Antarctic Surface Water. Nature, 177(5696), 469-471.

Jacobs, S. S., R. G. Fairbanks, and Y. Horibe, 1985. Origin and evolution of water masses near the Antarctic Continental margin: Evidence from $H_2{}^{18}O/H_2{}^{16}O$ ratios. In Oceanology of the Antarctic Continental Shelf, Ant. Res. Ser., vol. 43 (in press).

Kellogg, T. B., D. E. Kellogg, and J. B. Anderson, 1982. Preliminary results of microfossil analyses of Amundsen Sea sediment cores, Antarctic Journal of the United States, XVII(5), 125-126.

Killworth, P., 1983. Deep convection in the world ocean, Reviews of Geophysics and Space Physics, 21(1), 1-26.

Kurtz, D., and D. Bromwich, 1985. A recurring, atmospherically-forced polynya in Terra Nova Bay. In Oceanology of the Antarctic Continental Shelf, Ant. Res. Ser., vol. 43, American Geophysical Union, Washington, D.C. (in press).

MacAyeal, D. R., 1983. Potential effect of CO_2 warming on sub-ice shelf circulation and basal melting. In: Environment of W. Antarctica: Potential CO_2-Induced Changes, Report of a Workshop, Madison, Wis., 5-7 July 1983, National Academy Press, Washington, D.C., pp. 212-221.

MacAyeal, D. R., 1984. Thermohaline circulation below the Ross Ice Shelf: A consequence of tidally induced vertical mixing and basal melting. Journal of Geophysical Research, 89(C1), 597-606.

MacAyeal, D. R., 1985. Evolution of tidally triggered meltwater plumes below ice shelves. In Oceanology of the Antarctic Continental Shelf, Ant. Res. Ser., vol. 43, American Geophysical Union, Washington, D.C. (in press).

Mantyla, A. W., 1980. Electrical conductivity comparisons of standard seawater batches P29 to P84. Deep-Sea Research, 27A, 837-846.

Michel, R. L., T. W. Linick, and P. M. Williams, 1979. Tritium and carbon-14 distributions in seawater from under the Ross Ice Shelf Project ice hole. Science, 203, 445-446.

Morgan, V. I., 1972. Oxygen, isotope evidence for bottom freezing on the Amery Ice Shelf. Nature, 238, 393-394.

Neal, C. S., 1979. The dynamics of the Ross Ice Shelf revealed by radio echo-sounding, Journal of Glaciology, 24(90), 295-307.

Paren, J. G., J. R. Potter, and J. Loynes, 1983. Using oxygen isotope tracers to determine the ocean circulation under an ice shelf. IUGG Symposium: Applications of stable isotopes to problems in climatology and oceanography, Hamburg.

Pillsbury, R. D., and S. Jacobs, 1985. Preliminary observations from long-termcurrent meter moorings near the Ross Ice Shelf, Antarctica. In Oceanology of the Antarctic Continental Shelf, Ant. Res. Ser., vol. 43, American Geophysical Union, Washington, D.C. (in press).

Pillsbury R. D., D. Root, J. Simkins, and J. Bottero, 1985. A compilation of observations from moored current meters: Currents, temperature, salinity and pressure in the Ross Sea, February 1983-January 1984. In Oceanology of the Antarctic Continental Shelf, Ant. Res. Ser., vol. 43, American Geophysical Union, Washington, D.C. (in press).

Potter, J. R., and J. G. Paren, 1985. Interaction between ice shelf and ocean in George VI Sound, Antarctica. In Oceanology of the Antarctic Continental Shelf, Ant. Res. Ser., vol. 43, American Geophysical Union, Washington, D.C. (in press)

Revelle, R. R., 1983. Probable future changes in sea level resulting from increased atmospheric carbon dioxide. In Changing Climate, Report of the CO_2 Assessment Committee, National Academy Press, Washington, D.C., pp. 433-438.

Robin, G. deQ., C. S. M. Doake, H. Kohnen, R. D. Crabtree, S. R. Jordan, and D. Moller, 1983. Regime of the Filchner-Ronne Ice Shelves, Antarctica. Nature, 302(5909), 582-586.

Rochford, D. J., 1965. Rapid changes in the characteristics of the deep salinity maximum of the South-East Indian Ocean. Australian Journal of Marine and Freshwater Research, 16, 129-149.

Semtner, A. J., Jr., 1983. Modeling the oceanic environment of West Antarctic, including CO_2-induced changes. In: Environment of W. Antarctica: Potential CO_2-Induced Changes, Report of a Workshop, Madison, Wis., 5-7 July 1983, National Academy Press, Washington, D.C., pp. 212-221.

Takahashi, T., W. S. Broecker, J. Goddard, J. White, B. N. Opdyke, S.C. Sutherland, and J. Olafson, 1984. Seasonal study of the CO_2 and tracer distributions in the high latitude North and South Atlantic Oceans. Prog. Rept. to Exxon Res. and Eng. Co.

Tchernia, P., and P. F. Jeannin, 1980. Observations of the Antarctica East Wind Drift using tabular icebergs tracked by satellite Nimbus F (1975-1977). Deep-Sea Research, 27(6A), 467-474.

Tressler, W. L., and A. M. Ommundsen, 1962. Seasonal oceanographic studies in McMurdo Sound, Antarctica. U.S. Navy Hydrog. Office, TR-125, 141 pp.

Trumbore, S., S. S. Jacobs, and W. Smethie Jr., 1984. Distribution of chloroflouromethanes (F-11 and F-12) in the Ross Sea. EOS, 65(45), 915.

Wexler, H., 1960. Heating and melting of floating ice shelves. Journal of Glaciology, 3, 626-645.

Wordie, J. M., 1921. The Ross Sea drift of the Aurora in 1915-1916. Geographic Journal London, 58, 219-224.

Zotikov, I. A., V. S. Zagorodnov, and J. V. Raikovsky, 1980. Core drilling through the Ross Ice Shelf (Ant.) confirmed basal freezing. Science, 207, 1463-1465.

Zwally, H. J., C. L. Parkinson, and J. C. Comiso, 1983. Variability of Antarctic Sea ice and changes in carbon dioxide. Science, 222, 1005-1012.

Zwally, H. J., J. C. Conniso, and A. L. Gordon, 1985. Antarctic offshore polynyas and oceanographic effects. In Oceanology of the Antarctic Continental Shelf, Ant. Res. Ser., vol. 43, American Geophysical Union, Washington, D.C. (in press).

ATTACHMENT 5

A FEW COMMENTS ON A RECENT DEEP-WATER FRESHENING

James H. Swift
Scripps Institution of Oceanography
La Jolla, California

Until recently there has been virtually no modern-day evidence of any large-scale alteration in deep-ocean salinity. Of course, we have not been accumulating high-precision deep salinity data long, but nonetheless the concept of a "steady-state ocean" has been broadened by tradition to include the deep temperature and salinity fields. Small variations in deep-water salinity have been observed in the western North Atlantic, particularly on the often-run Woods Hole to Bermuda section, but these have been so near the noise level that they have not yet received wider attention.

The GEOSECS (Geochemical Ocean Sections) program provided sparse, large-scale coverage of the North Atlantic in 1972. While the deep GEOSECS temperatures and salinities were similar to those from past expeditions, the GEOSECS data did show new features, notably a deep tongue of tritium-enriched water extending southward from Denmark Strait. The presence of the deep tritium signal showed that the bottom layers in the northwest Atlantic clearly responded on a time scale of 10 years or less to the injection of tritium into the atmosphere by thermonuclear testing.

Indeed, in general the best location to examine the deep ocean for evidence of recent changes is the northern North Atlantic: it is close to the deep-water mass formation regions and has been surveyed by expeditions 10-20 years apart.

The apparent sensitivity of the deep northwest Atlantic on 10-year (or less) time scales added immediate interest to the data gathered in 1981--9 years after GEOSECS--by the Transient Tracers in the Ocean North Atlantic Study (TTO/NAS). A total of 250 high-quality hydrographic/geochemical stations were occupied north of 17°N, a region covered by only 43 stations during GEOSECS. The TTO track provided some basin-scale sections, thus giving adequate coverage and facilitating comparison with other data from different years. Early reports in the summer and fall of 1981 from TTO/NAS indicated detectable changes in deep-ocean properties in the northern North Atlantic during the 9 years following GEOSECS. Brewer et al. (1983) have outlined the essentials of the new observations: a shift toward colder, fresher deep water in the northern North Atlantic and a larger freshening in the upper layers there.

The northern North Atlantic plays a significant role in the ocean's contribution to climate response, because it can be thought of as the

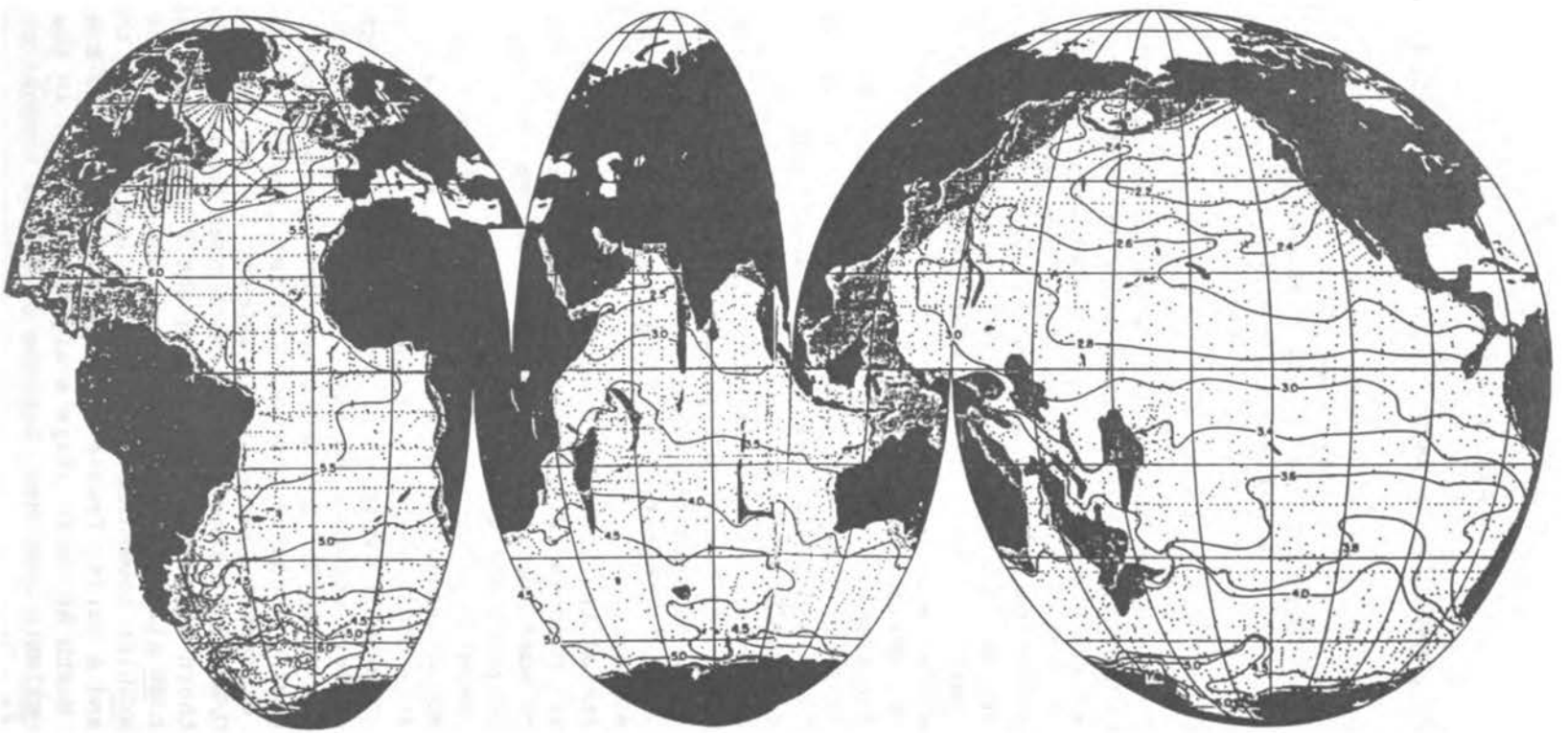

FIGURE 5.1 Dissolved oxygen (ml/l) on an isopycnal that lies near 2000 m over much of the World Ocean (nominally σ_2 = 37.0 when in the depth range 1500 to 2500 m). From Reid (1981).

primary deep ventilator of the World Ocean. In Figure 5.1 recently ventilated, or oxygenated, deep water can be seen spreading from the North Atlantic into the other oceans. Part of these high waters derive from dense outflows to the North Atlantic from the Greenland, Iceland, and Norwegian seas and part from processes within or over the deep northern basins of the Atlantic.

We can examine the northern sources by following a long section around the northern North Atlantic (Figure 5.2), following the western boundary undercurrent. Note that the section and the undercurrent cut through a fracture zone in the mid-ocean ridge. This section passes near the overflows and the deep-water formation zone in the Labrador Sea.

The sections in Figure 5.3 start in the Iceland-Scotland overflow on the right, go through the Charlie-Gibbs Fracture Zone and up to the northern Irminger and Labrador seas in the middle, then around the Grand Banks on the left. There is a great deal of information in these sections--here I will discuss only a few of the features.

The middle section shows salinity versus density (referred to 2000 db), not depth, and only in the denser portions of the water column. Because the Labrador Sea data are from winter cruises, the density of the sea surface shows up there. The bottom contour is bottom density, and it shows the contributions of dense water from the two main overflows.

There are differences in the salinities and final densities of the overflows. The Iceland-Scotland overflow mixes with much warmer, saltier, and less dense water and forms a relatively high-salinity deep layer, underneath lower-salinity Labrador Sea water. The Denmark Strait overflow is a little fresher to begin with and mixes mostly with the layers immediately above, which are not so different. Thus the Denmark Strait overflow retains its relatively low salinity and high density and forms the bottom water in the northwest Atlantic.

The bottom section shows dissolved oxygen versus density, along the same path. The three northern North Atlantic Deep Water sources are shown by the sources of relatively well-oxygenated water in the Labrador Sea, the Denmark Strait overflow, and the Iceland-Scotland overflow.

The relatively well-oxygenated deep layer spreading south around the Grand Banks shows the propagation of the younger, overflow-derived deep waters southward via the western boundary undercurrent.

One of the results of this data analysis was that these deep-water components are closely tied to the winter sea surface and so are potentially sensitive to environmental changes. But during the 1957-1972 period emphasized in Figure 5.3, no such changes were observed in the deep temperature and salinity fields.

But in the 1970s, the surface layers of the northern North Atlantic freshened, by about 0.1 o/oo. European oceanographers call this "the great 1970s salinity anomaly." This section was well-enough reoccupied in 1981 to compare the deep-water salinities before and after the surface-water freshening.

By 1981 deep-water salinities had changed throughout the northern North Atlantic. Figure 5.4 shows the salinity versus density section from Figure 5.3, and the same section in 1981, contoured for the same

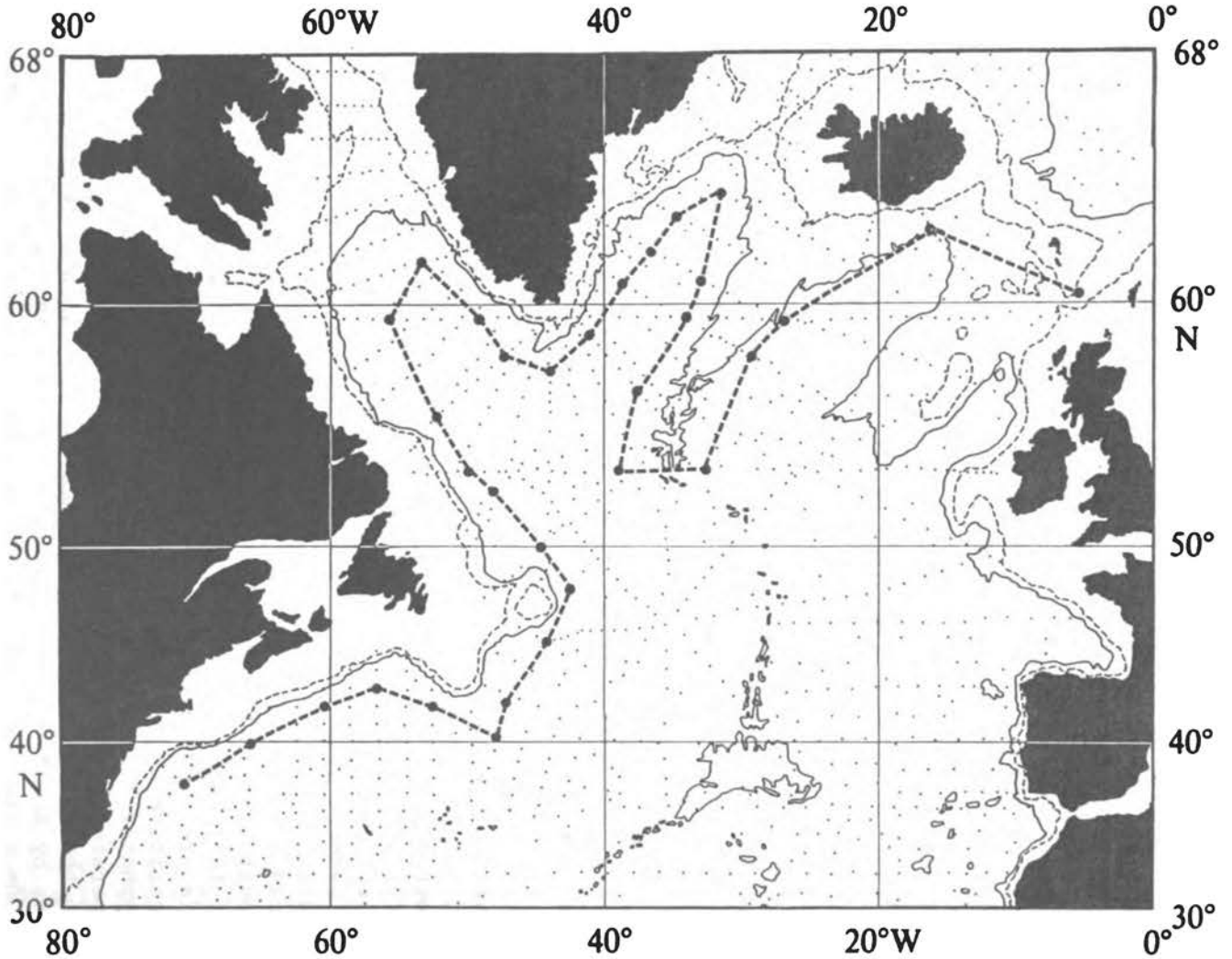

FIGURE 5.2 Map showing path of the section shown in Figures 3 and 4. The 500-m and 2000-m isobaths are shown.

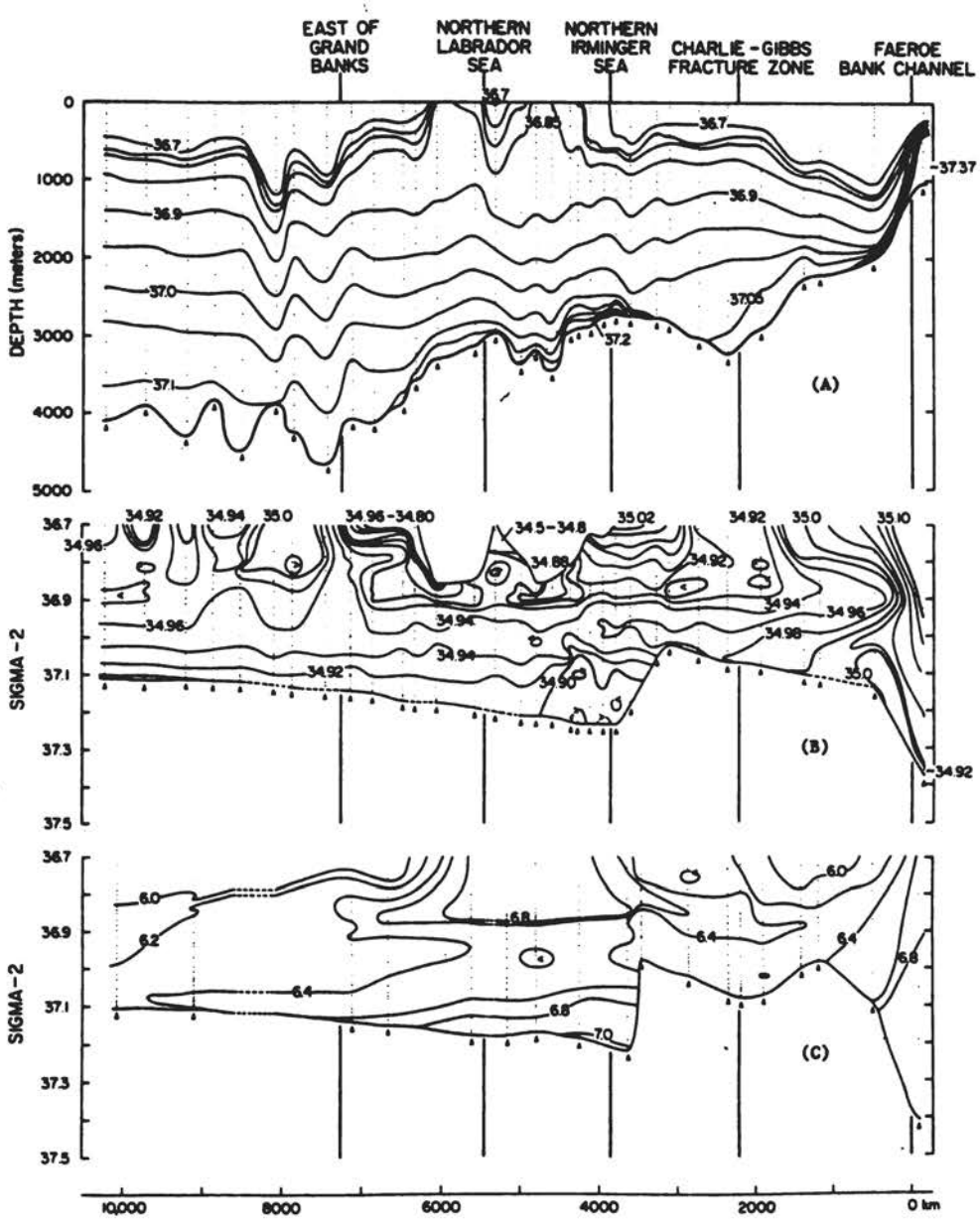

FIGURE 5.3 Vertical section from the Faeroe-Shetland Channel to the eastern U.S. continental margin of (A) σ_2 versus depth, (B) salinity ($x10^3$) versus σ_2, and (C) dissolved oxygen ($x10^3$) versus σ_2. Sections (A) and (B) are drawn from a composite of historical data (Chain 1960 and 1972, Crawford 1960 and 1965, Erika Dan 1962, Atlantis 1964, Hudson 1967, and Knorr 1972 and 1976) along the long, winding path shown in Figure 5.2. The only post-1972 data in (A) and (B) are from a single Knorr 1976 station in the Faeroe-Shetland Channel. Section (C) is drawn from April-October 1981 TTO/NAS data along a nearly identical path (see Swift, 1984a). Section (A) is contoured only for $\sigma_2 > 36.7$, and (B) and (C) show properties only where $\sigma_2 \geq 36.7$. The contour intervals are (A) 0.05 kg/m^3, (B) 0.02×10^{-3} (for $S \geq 34.8 \times 10^{-3}$), and (C) 0.2×10^{-3}. From Swift (1984b).

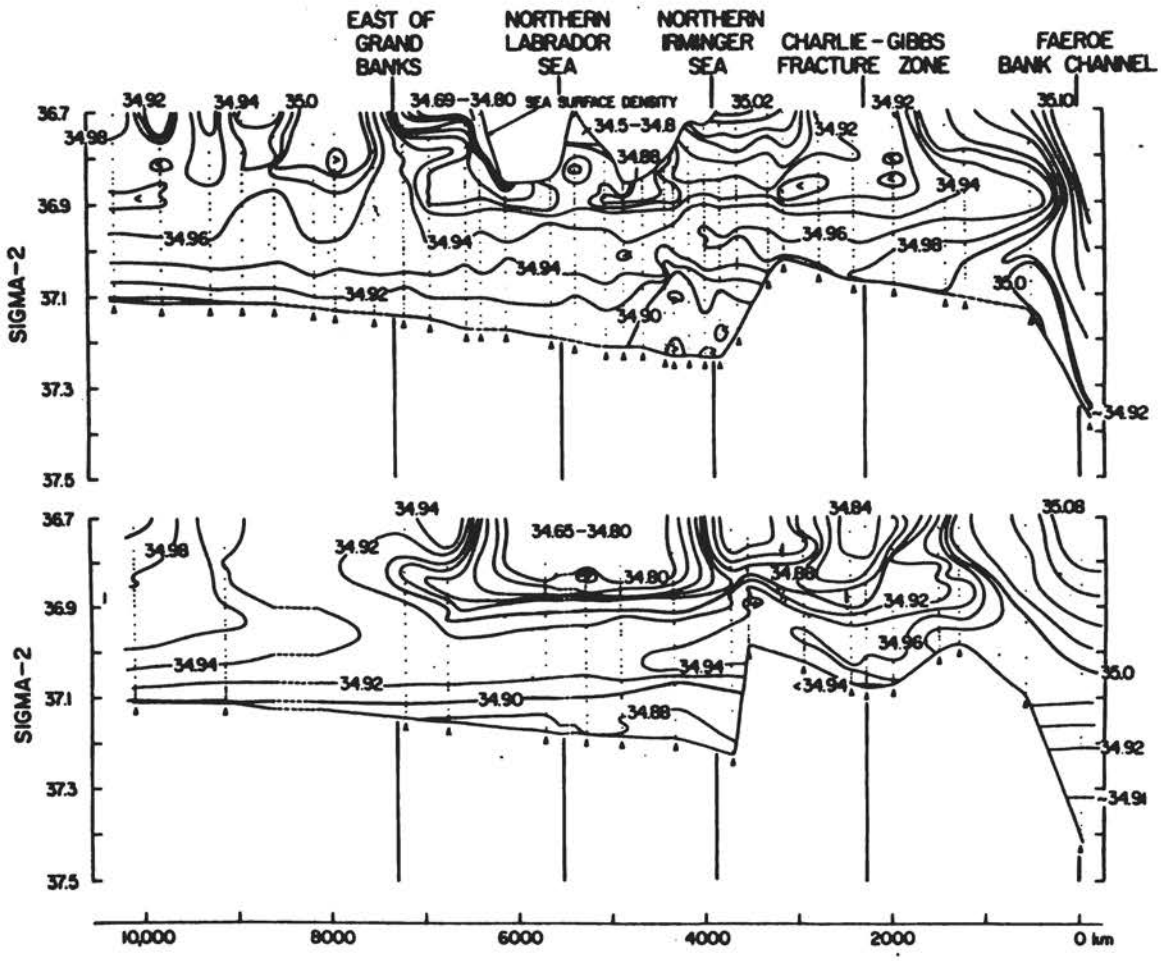

FIGURE 5.4 Sections of salinity ($x10^3$) versus σ_2 on a long, winding path from the Faeroe Bank Channel to the waters off the U.S. east coast (location shown in Figure 5.2). The upper section is from Figure 5.3, and the lower section is drawn from April-October 1981 TTO/NAS data. The only post-1972 data in the upper section are from a single Knorr 1976 station in the Faeroe-Shetland Channel. From Swift (1984a).

ranges, and it is clear that the 1981 salinities were lower than their earliest counterparts. The deep freshening was about 0.02 o/oo, and, since densities in each layer are about the same, we can see there was also an overall cooling, which in this case was about 0.15°C.

Figure 5.5 shows this deep temperature-salinity shift at one location, in this case northeast of the Grand Banks. Four deep stations from 1960 to 1972 showed virtually the same potential temperature-salinity correlation, at least for the deep waters colder than 3°C or so. But the 1981 station at this location shows noticeably colder, fresher water--the changes are four standard deviations above the noise level. These changes occurred in virtually every deep-water layer in the northern North Atlantic, north of 50°N.

The surface-layer freshening in the 1970s propagated into the deep

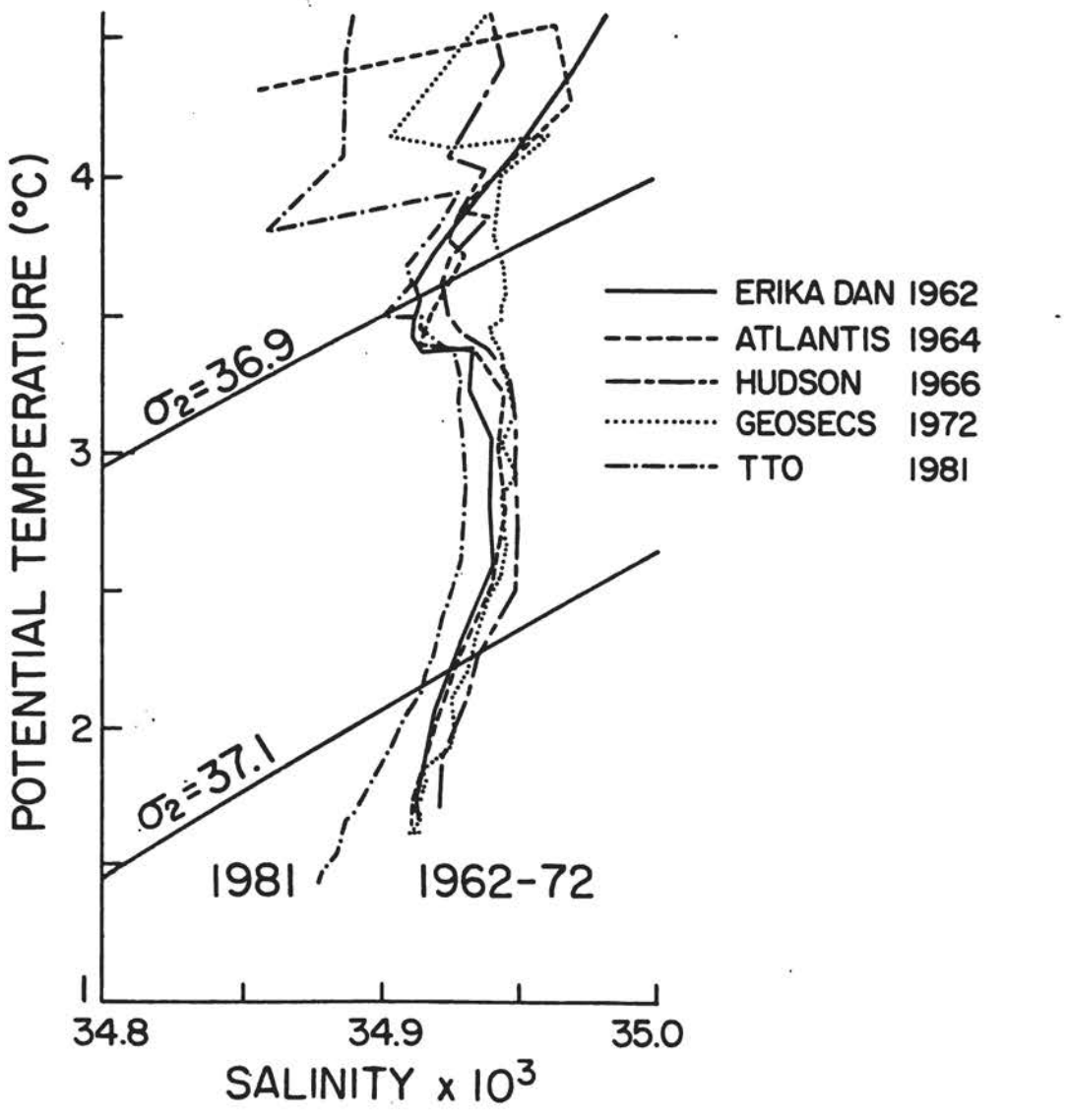

FIGURE 5.5 Potential temperature-salinity correlations below 4.5°C for four stations from 1962-1972 and from TTO/NAS (1981), all from a location NE of the Grand Banks extending to about 3500 m. From Swift (1984a).

water because in winter in the water mass formation areas the downward penetration of the cooled water depends on its density not its temperature or salinity alone. The net result of a freshening of the surface water is to produce colder, less saline water for a given density. This produced the changes seen in the 1981 data.

The origin of the low salinities is an interesting puzzle. Figure 5.6 shows surface salinities before the salinity shift. The formation of dense waters in the Labrador and Greenland seas owes much to the salty water carried north at this and deeper levels. But much fresher

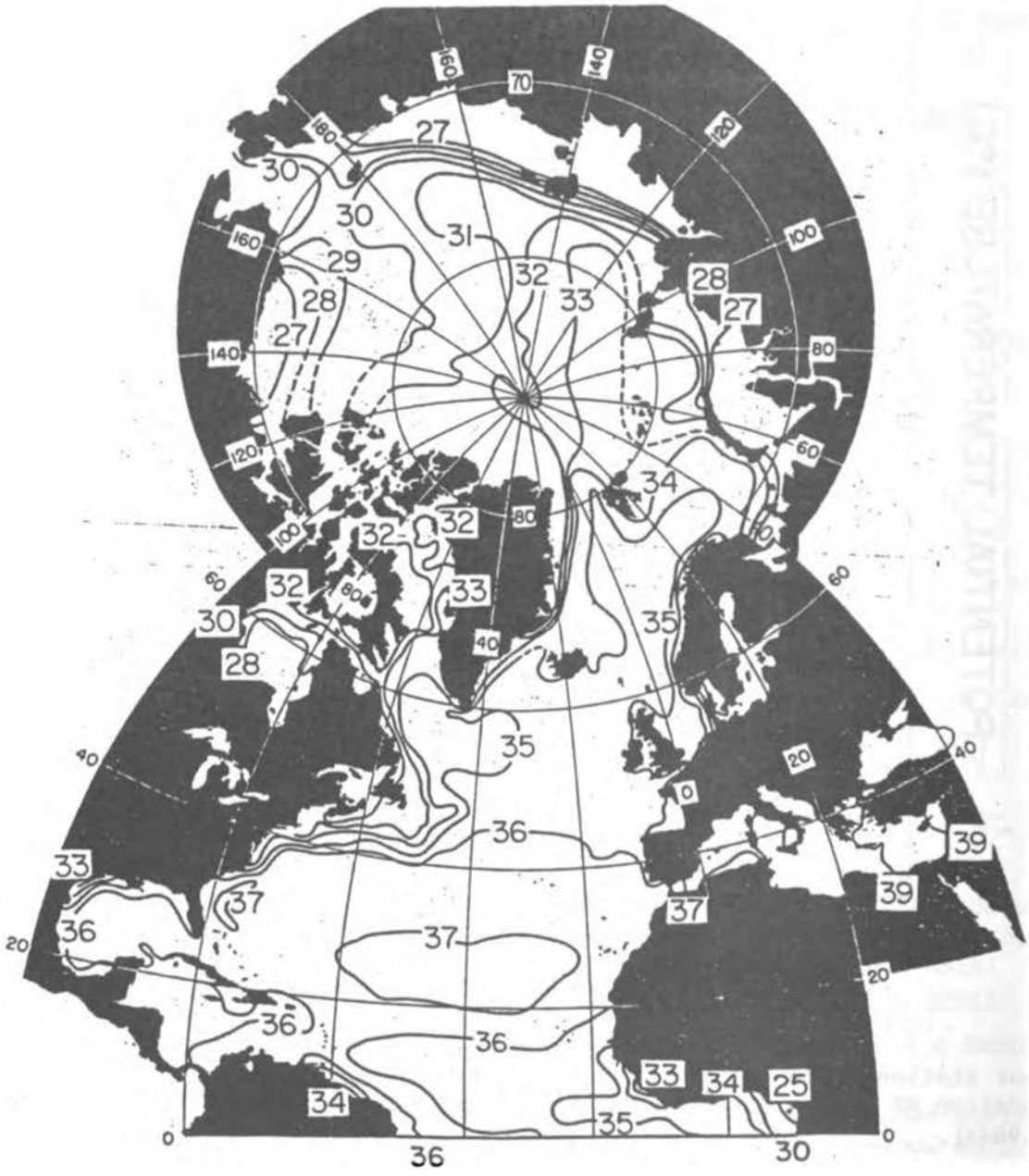

FIGURE 5.6 Salinity ($x10^3$) at the sea surface. From Reid (1979).

water is plentiful along the boundaries. At first, I supposed that some shift in forcing in the 1970s allowed the fresh boundary waters to penetrate seaward into the deep gyres where the deep waters are formed. But we can see in Figure 5.6 that the freshwaters do not just flow south out of the northern North Atlantic--they are in fact mostly incorporated into the gyres by the time they reach the Grand Banks. If during the 1970s the freshwaters had simply spread away from the boundaries in the

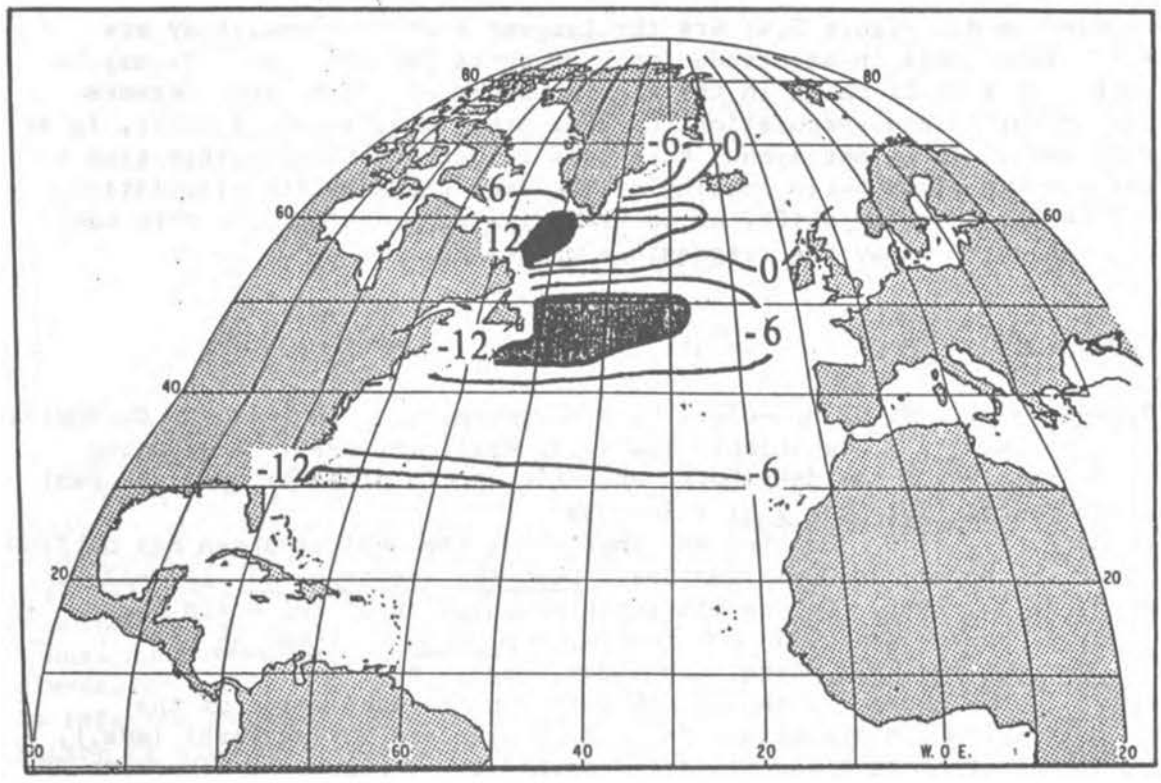

FIGURE 5.7 Change in integrated Sverdrup transport, average from 1973-1981 minus 1955-1972. The transports were calculated from multi-year average sea level pressures on a 5° grid. Data from the Scripps Institution of Oceanography Climate Research Group. Owing to a minor computational error, the values shown are not in Sverdrups, but in nontraditional units. The average changes were 30 percent of the 1955-1972 base period.

north and were mixed into the deeper layers, then some areas of the far northeastern Atlantic might be expected to increase in salinity, lacking the accustomed supply of freshwater from the west.

But since all the upper waters north of 50°N freshened, perhaps there has been some increase in freshwater supply, or decrease in salty water supply, since 1972.

There have indeed been interesting long-term changes in the atmospheric circulation consistent with this. Figure 5.7 shows the difference of average wind-driven transport in the period 1973-1981 minus that from 1955-1972. The changes are an average of about 30 percent of the mean at each grid point and so may be significant. The negative values indicate a greater southward interior surface transport in recent years. Since the greatest negative values occur over the North Atlantic Drift, I wonder if the high salts there might have been swept southward, partially shutting down the supply of salty water to the northeast Atlantic, and hence to the Labrador and Norwegian-Greenland seas.

But we should remember that although these deep-water salinity

changes (e.g., Figure 5.4) are the largest ever observed, they are still very small in magnitude (only 20 parts per million). It may be that only a small shift in the sinking zones of the balance between precipitation and evaporation, or some other similar small shift, is at work here. In either event, this does illustrate the possible ties to large-scale atmospheric forcing of the deep thermohaline circulation, making the salinity shift, as we trace its propagation, one more tool with which to study the responsible processes.

REFERENCES

Brewer, P. G., W. S. Broecker, W. J. Jenkins, P. B. Rhines, C. G. Rooth, J. H. Swift, T. Takahashi, and R. T. Williams, 1983. A climatic freshening of the deep North Atlantic (north of 50°N) over the past 20 years. Science, 222, 1237-1239.

Reid, J. L., 1979. On the contribution of the Mediterranean Sea outflow to the Norwegian-Greenland Sea. Deep-Sea Research, 26, 1199-1223.

Reid, J. L., 1981. On the mid-depth circulation of the World Ocean. In B. A. Warren and C. Wunsch (eds.), Evolution of Physical Oceanography, MIT Press, Cambridge, Mass., pp. 70-111.

Swift, J.H., 1984a. A recent θ-S shift in the deep water of the northern North Atlantic. In J. E. Hansen and T. Takahashi (eds.), Climate Processes and Climate Sensitivity, Geophysical Monograph 29 (Ewing Volume 5), American Geophysical Union, Washington, D.C., pp. 39-47.

Swift, J. H., 1984b. The circulation of the Denmark Strait and Iceland-Scotland overflow waters in the North Atlantic. Deep-Sea Research, 31.

ATTACHMENT 6

MASS BALANCE OF THE GLACIERS AND SMALL ICE CAPS OF THE WORLD

Mark F. Meier
U.S. Geological Survey
Tacoma, Washington

Most of the glaciers of the world have been shrinking since the turn of the century. Could this wastage account, in part, for the observed rise in sea level? Thorarinsson (1940), in a comprehensive and seminal analysis, attempted to answer this question without the benefit of good maps or sufficient data. Many more data are now available, but major gaps still exist. In this paper existing modern data are analyzed, and a method for extending the results to a global basis based on the annual mass exchange is suggested. This paper summarizes part of the discussion and results presented by Meier (1984), to which the reader is referred for more detail. A new section on the geographical distribution of glacier balances is included here. Data from the ice sheets of Antarctica and Greenland and the small glaciers that border them are not included in this discussion.

Observational data on glacier fluctuations include measurements of advance or retreat, mass-balance histories derived from snow pits and ice cores, volume (surface altitude) changes, directly measured annual and seasonal mass balances, and mass-balance sequences extended by use of numerical models. The first two types are, unfortunately, virtually impossible to use to infer long-term changes in ice mass. Advance/retreat data do not provide volume change information and can be misleading in sign. Stratigraphic measurements of balances in pits and cores taken at single locations in the accumulation area are insufficient to infer the mass change of the entire glacier. Measurements of mass balance, made on the glacier surface, provide directly applicable but short-term results.

This analysis is based mainly on published long-term volume change data, together with extended mass-balance histories developed from models. The balance models are based on statistical relations between meteorological and hydrological data and measurements of mass balance; some models were calibrated or verified with long-term volume change results. This calibration is possible because the long-term volume change (in cubic meters of water equivalent) is equal to the sum over this time of the specific annual or net balance (in meters of water equivalent) for each year multiplied by the total glacier area (in square meters) for that year. The calibration is important because the statistical relations between meteorological and hydrological variables (e.g., precipitation, temperature, runoff) and balance components (e.g.,

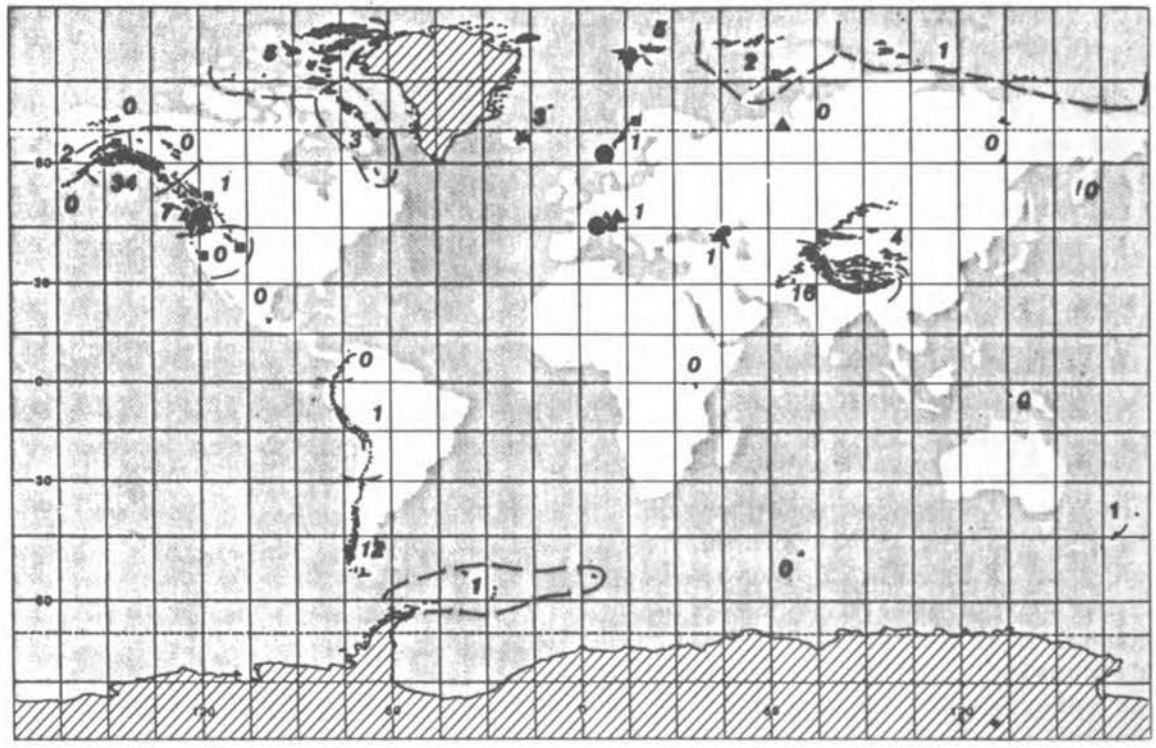

FIGURE 6.1 Location of glaciers (black dots) exclusive of Antarctica and Greenland (areas with diagonal lining). Locations where long-term mass-balance model results are available are indicated by circles (models calibrated with long-term volume change observations) or triangles (uncalibrated models). Squares indicate where other long-term volume-change data are available. Also shown, for each of 31 regions, is the percentage contribution of each region to the total volume of water transferred to the ocean from glacier wastage; 0 indicates less than 0.5 percent. Dashed line separates regions.

accumulation, melt) may not be stationary over long time intervals.

Glacier balance and volume change data for periods of record exceeding 50 years were found for 25 glaciers (Table 6.1, Figure 6.1) from reports of the Permanent Service on the Fluctuations of Glaciers [IASH (ICSI)--Unesco 1967, 1973, 1977) and other sources. The mean period of record for those glaciers is from 1900.5 to 1961.7. The balance model sequences were pruned to the interval 1900-1961 to make the data set more homogenous. The unweighted average of these 25 mean balances is -0.40 m/yr (water equivalent) $\pm$ 0.25 (standard deviation); the mean of the 13 regional averages is -0.34 $\pm$ 0.20 m/yr; and the mean of the regional averages weighted by quality of the data is -0.38 $\pm$ 0.20 m/year (Table 6.1).

The 25 glaciers with long-term data make up a biased sample of the world's glaciers: all but one are between 38° and 69°N latitude; none are at low latitudes or in the southern hemisphere (Figure 6.1). Thus

TABLE 6.1 Long-Term Balance Data

Region	No. of Glaciers	Method*
Brooks Range, U.S.	1	a
Alaska Range, U.S.	1	b
Kenai Mts., U.S.	1	a
Cascades, U.S.	3	b, d, e,
Rocky Mts., Canada	1	b
Rocky Mts., and Sierra Nevada, U.S.	2	a, b
Iceland	1	c
Novaya Zemlya, USSR	1	D
Scandanavia	2	b, e
Alps	8	b(5), c, e(2)
Caucasus, USSR	2	b, d
Ural Mts., USSR	1	d
Tien Shan, USSR	1	d

* a, Estimate of long-term volume change; b, measured long-term volume change; c, estimate of long-term volume change for all glaciers in region; d, uncalibrated HM model; e, HM model calibrated with long-term volume change.

	Average Balance	Average Amplitude	Balance/Amplitude Ratio
Mean of regional averages	-0.34(0.20)		-0.21(0.13)
Weighted mean	-0.38(0.20)		-0.23(0.13)
Range	-0.71 to +0.02	0.50 to 3.20	-0.50 to +0.02
Correlation coefficient		0.55	

Figures in parentheses are standard deviations.

a method is needed to relate these results to an estimate of the mass balance of the whole Earth's cover of glaciers.

The suggestion has been made (Meier 1984) that the magnitude of the long-term balance may be related to the magnitude of the seasonal mass fluxes (accumulation and ablation) and that this may be used as a scaling factor to derive global estimates. The annual mass balance b and the balance amplitude a are here defined as

$$b = b_w + b_s,$$
$$a = (b_w - b_s)/2,$$

where b_w is the winter balance and b_s (normally negative) is the summer balance. Winter and summer balances are used instead of annual accumulation and ablation, respectively, which are rarely measured. Values of the annual amplitude can be calculated for most of the world's glacier areas from data reported since 1965 and can be estimated for other areas because they are primarily functions of the climatological regime. The annual amplitudes are highest at temperate to sub-Arctic (and sub-Antarctic) latitudes, lowest near the poles, and also decrease with increasing continentality (Figure 6.2).

The 1900-1961 data summarized in Table 6.1 are averaged by region and then scaled to a global average in terms of sea-level change by

$$h(1961) - h(1900) = -\frac{1}{J}\left[\sum_{j=1}^{J}\frac{\bar{b}_j}{a_j}\right]\left[\sum_{k=1}^{K}(a_k\bar{G}_k)\right]A^{-1}$$

where h is the sea-level equivalent of global glacier balance (without consideration of elastic, plastic, or thermal compensation of ocean or Earth), $\bar{b}_j$ is the average balance change in the jth region for the period 1900-1961, (J = 13, Table 6.1), a_j is the annual amplitude

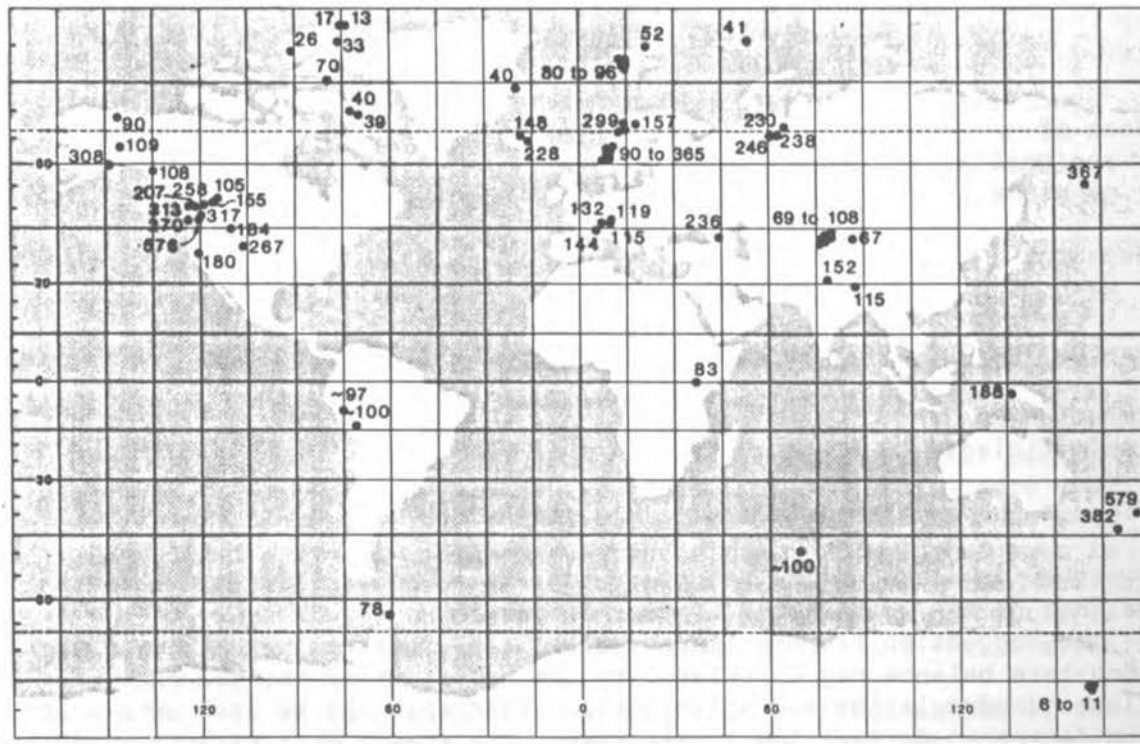

FIGURE 6.2 Location and values of annual amplitude data. Values are in centimeters/year (water equivalent). Contours of annual amplitude are inferred on climatological grounds in areas of few data.

associated with the $\bar{b}_j$, $\bar{G}_k$ is the 1900-1961 average of the area of glacial ice in the kth region of the world (K = 31), a_k is the average annual amplitude associated with each $\bar{G}_k$, and A is the area of the world's ocean. Numerical data for each of the 31 regions are tabulated in Meier (1984).

This scaling procedure assumes a relation between $\bar{b}$ and a. For the 13 regional averages, the correlation coefficient between the two quantities is -0.55 (Table 6.1). Thus, the implied relation is only crudely supported by the data. Obviously, large amounts of thinning or thickening (large $|b|$) are impossible in regions where the balance amplitude is small, but the converse is not necessarily true. Koerner (this volume, Attachment 7) suggests that the average balance of the Devon Island Ice Cap, representative of small ice caps in Arctic Canada, is about -0.05 m/yr; the analysis here estimates a balance of -0.06 m/yr. Other estimation difficulties are discussed in Meier (1984).

The scaled results suggest that the wastage of the world's glaciers and small ice caps contributed 0.46 $\pm$ 0.26 mm/yr to the 61-yr rise in sea level. The effect of the assumption about scaling by annual amplitude can be seen by examining two extreme cases: no scaling yields a global sea-level change of 0.57 mm/yr; assuming that no change has occurred in high latitudes (>70°) yields a sea-level change of 0.36 mm/yr. Both extreme values lie within the estimated error limits of the scaled result. Recent calculations of the effect of this glacial wastage on the Earth's rotation rate and polar motion suggest that this large amount of wastage may not be compatible with observations of rotation rate and polar motion (Yoder and Ivins 1985; W. R. Peltier, University of Toronto, personal communication). However, these calculations may not be definitive because zero change was assumed for the Greenland and Antarctic Ice Sheets.

Figure 6.1 shows that more than a third of the calculated glacier contribution to sea level comes from the mountains bordering the Gulf of Alaska; also, the high mountains of Central Asia and the Patagonian Andes make appreciable contributions. Along the Alaskan coast these glaciers constitute a "line source" of freshwater discharge on the order of 2×10^4 m^3/s, which is comparable with the discharge of the entire Mississippi River system (Royer, 1982). This result stems from the fact that these regions combine large areas of ice with high rates of accumulation and ablation and, therefore, high possible rates of wastage. By way of contrast, areas with small annual amplitude and large ice area (e.g., Canadian Arctic) or large annual amplitude and small ice area (e.g., Washington State, New Zealand) are much less important in terms of impact on global sea level, now and in the immediate future. Unfortunately, the three most important regions are also regions of meager observatonal data; almost nothing is known about the mass balance of the Patagonian Ice Cap.

The present-day contribution to global sea level, 0.46 $\pm$ 0.26 mm/yr, represents between one fourth and one half of the observed rise (1 to 2 mm/yr). In the future, with a CO_2-enhanced atmosphere, the absolute contribution from glaciers will probably rise because increased ice melt due to higher air temperature is likely to overpower the more modest--but more uncertain--increases in precipitation in glacierized areas.

Meier (1984) estimates that a rise of air temperature of 1.5 to 4.5°C, other conditions remaining the same, could lead to a rate of glacier wastage equivalent to 1.7 to 5.2 mm/yr of sea-level rise and perhaps a total rise in the next century of 0.08 to 0.25 m. However, these are only crude estimates; refinement is needed. The total volume of the world's glaciers has been estimated at 0.30 to 0.60 m in sea-level equivalent.

REFERENCES

IASH (ICSI)--Unesco, 1967, 1973, 1977. Fluctuations of Glaciers. IASH (ICSI)--Unesco, Paris, v. 1, 1967; v. 2, 1973; v. 3, 1977.

Meier, M. F., 1984. The contribution of small glaciers to global sea level. Science, 226, 1418-1421.

Royer, T. C., 1982. Coastal fresh water discharge in the northeast Pacific, Journal of Geophysical Research, 87(C3), 2017-2021.

Thorarinson, S., 1940. Present glacier shrinkage, and eustatic changes in sea level. Geografiska Annaler, 22, 131-159.

Yoder, C. F., and E. R. Ivins, 1985. Changes in Earth's gravity field from Pleistocene deglaciation and present-day glacier melting. EOS, 66(18), 245.

ATTACHMENT 7

CANADIAN ARCTIC ISLANDS: GLACIER MASS BALANCE AND GLOBAL SEA LEVEL

R. M. Koerner
Polar Continental Shelf Project
Energy, Mines & Resources, Canada

INTRODUCTION

The Canadian Arctic Island glaciers (Figure 7.1) cover 108,600 km^2, which is 0.7 percent of the world's and 5 percent of the northern hemisphere's ice cover. It is the largest concentration of ice outside of Antarctica and Greenland. The glaciers can be divided into three basic types.

A. Dynamic ice caps and their outlet glaciers compose the greater part of the ice cover. The largest ice caps are about 20,000 km^2 in area with thicknesses commonly ranging between 300 and 800 m (Koerner 1977). Velocities vary seasonally on the outlet glaciers owing to the presence of meltwater at the bed (Iken 1974) but mean annual values of 30 m/yr are common.

B. The smaller ice caps (less than 90 km^2) are stagnant and are mostly located on plateaus 500-800 m above sea level. From their geometry they appear to vary in thickness between 20 and 60 m. The best studied of these, Meighen Ice Cap, showed a thickness of 121 m in a borehole at its highest point (Koerner and Paterson 1974). However, this ice cap is unusual in many respects, for example, it lies at an elevation of only 130-250 m above sea level; it will be discussed later.

C. Ice Shelves are located along the north coast of Ellesmere Island, bordering the Arctic Ocean. The Ward Hunt Ice Shelf is the most extensive and measures 50 km x 10 km with a thickness of 40 m.

Routine mass-balance measurements have been made on at least one of each of the above types of ice mass in the past two decades. They will be discussed later.

GLACIAL HISTORY

Various ice core studies (e.g., Paterson et al. 1977; Fisher et al. 1983) indicate that the larger Canadian ice caps began their growth at least as early as the beginning of the last ice age. Thus the ice cores from Devon and Agassiz Ice Caps include ice from the last ice age. They also show evidence of the warmth of the Hypsithermal 5000 years ago and

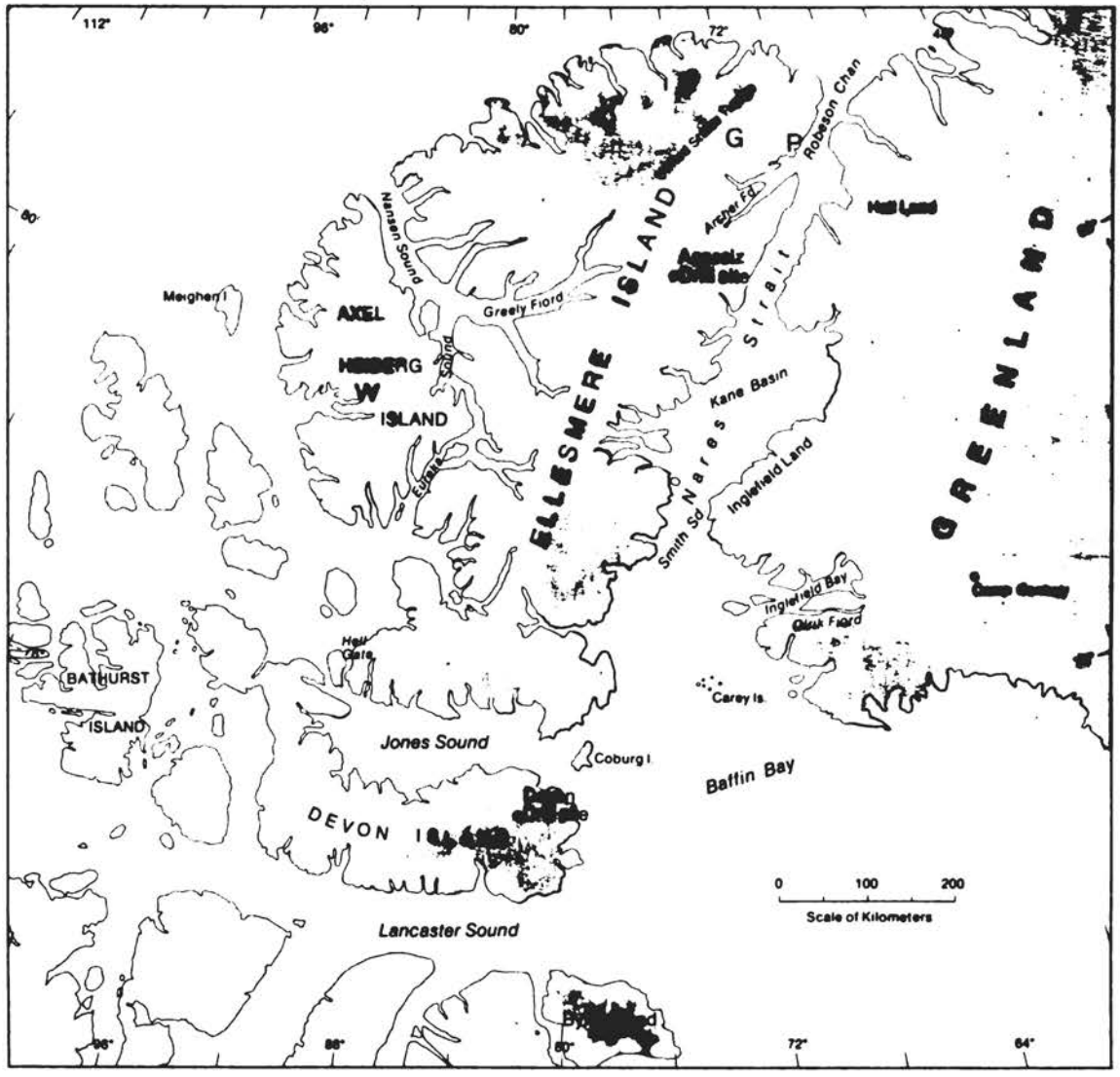

FIGURE 7.1 Canadian Arctic Island Ice Caps. G, Gilman Glacier; P, ice cap above St. Patrick Bay (both locations are on Northern Ellesmere Island to the east of the main ice cap); W, White Glacier on Axel Heiberg Island. The shaded areas represent ice-covered areas.

the short cold period that began about 350 years ago and ended early this century. The last part of these records is important in placing the short mass-balance records of the past 20-30 years in context and allowing calculations to be made of the past 200 years of mass balance. The stagnant ice caps and the ice shelves are all less than 4500 years old (Koerner and Paterson 1974; Lyons and Mielke 1973). Recent Work (Koerner, unpublished) suggests that the size of the stagnant ice caps may be proportional to their age so that the smallest are remnants of the most recent cold period.

ACCUMULATION AND ABLATION

Quite detailed studies have been made of the snow accumulation rate over the Canadian High Arctic (Koerner 1979; Woo et al. 1983). The highest accumulation rates are found along the ice cap slopes facing Baffin Bay (Figure 7.1), where they reach over 500 kg m^{-2} yr^{-1}. However, the most common accumulation rate lies between 150 and 300 kg m^{-2} yr^{-1}.

While ablation measurements have been made on many glaciers (e.g., Adams 1966; Müller and Kesler 1969) the regional variation of ablation is much more poorly known than that of accumulation largely because records of the latter are preserved above the firn line. Ablation shows the usual inverse relationship with altitude but only a very weak one with latitude (Koerner 1979). One to three meters of ice melts from the glacier surfaces near sea level each summer. The equilibrium line varies between 500 m altitude on the Baffin Bay glacier slopes to a more common value of about 1300 m elsewhere. In 9 years out of 10 melting occurs right to the tops of the ice caps, where just a few millimeters of snow may melt and refreeze within the firn/snow pack.

MASS BALANCE

Stake Measurements

Routine mass-balance measurements have been made on some of the ice caps and glaciers since the late 1950s and the early 1960s (Table 7.1). Data from the most continuous records are shown and referenced in Figure 7.2. For the 22-year period between 1961 and 1983 the overall balance on the High Arctic ice caps has been slightly negative, with a specific balance of -130.0 kg m^{-2} yr^{-1} on Meighen Ice Cap and -53.1 kg m^{-2} yr^{-1} on the northwest side of Devon Ice Cap. Mass-balance measurements on the northern part of Agassiz Ice Cap made since 1977 suggest that its balance follows quite closely that of Devon Ice Cap. Six years of mass-balance measurements on other parts of Devon Ice Cap (Koerner 1970) showed that its northwest sector, where routine measurements are now made annually, is representative of the whole ice cap in terms of annual balance. On its southeast part very high accumulation rates push the equilibrium line 200-600 m lower than elsewhere. However, slightly higher ablation rates and larger areas in the ablation zone effect similar mass balances to the rest of the ice cap (Koerner 1970). Because the larger ice caps cover a much greater area than the stagnant ones the Devon Ice Cap mass-balance values will be considered representative of the Arctic Island ice-covered areas.

Area Changes

One of the most common methods used to detect aerial changes of glaciers with time is to use photographic records to compare glacier snout, or ice-cap edge positions, from one period to another. In a preliminary study of this kind, aerial photographs from the 1950s have

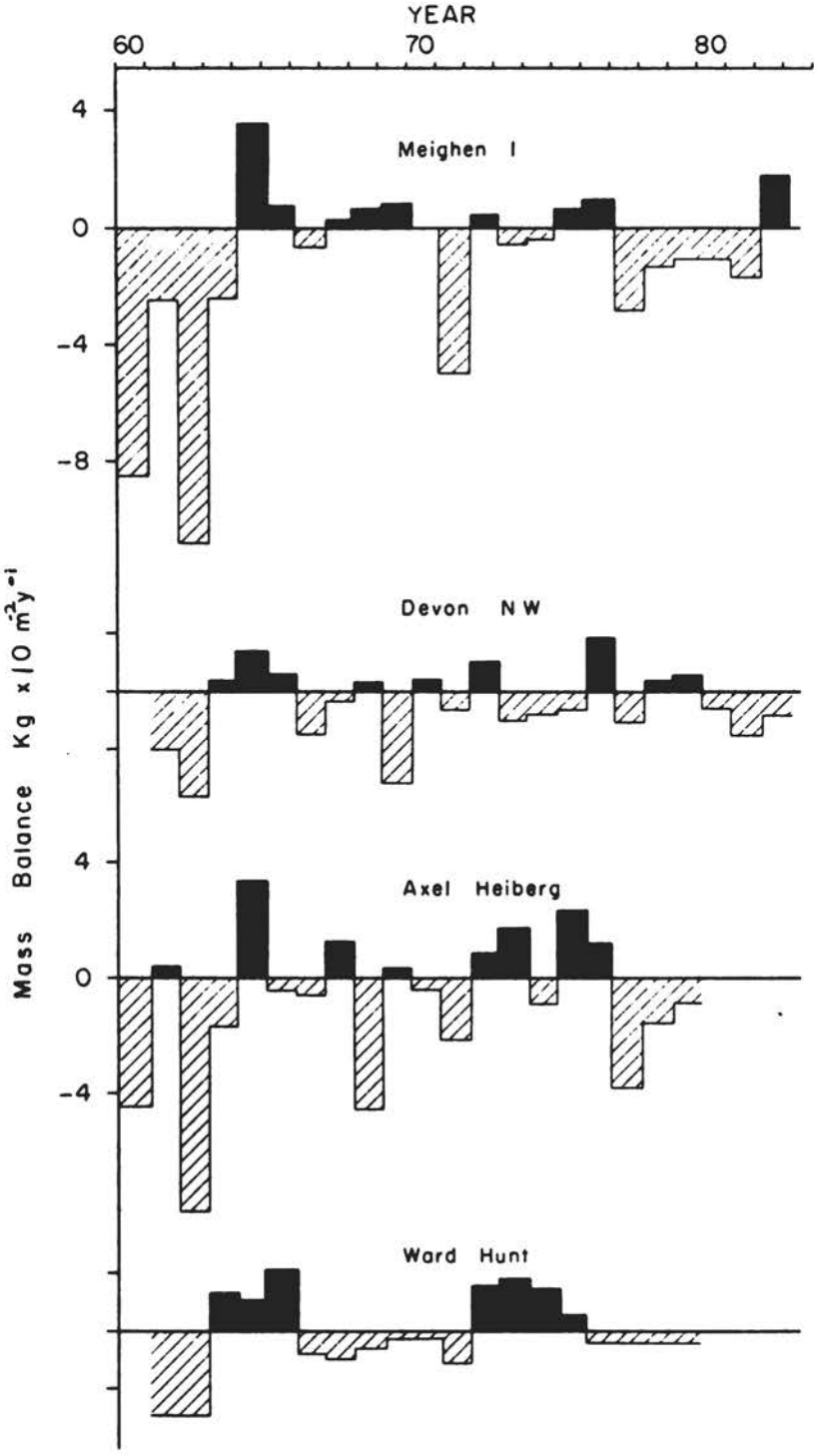

FIGURE 7.2 Mass balance of Meighen Ice Cap, Northwest side of Devon Ice Cap, White Glacier on Axel Heiberg Island, and the Ward Hunt Ice Shelf on the Arctic Ocean coast of Ellesmere Island.

TABLE 7.1 Measurements of Mass Balance, Canadian Arctic Islands

Location	Period of Measurement	Reference	Organization
Devon Ice Cap	1961-	Koerner (1970)	PCSP
Agassiz Ice Cap	1977-	--	PCSP
Meighen Ice Cap	1959-	Arnold (1965) Paterson (1969)	PCSP
Melville S. Ice Cap	1964-	--	PCSP
Ward Hunt Ice Shelf	1961-	Hattersley-Smith and Serson (1973)	Various
St. Patrick Bay	1972	Bradley and England (1978)	Univ. Mass.
White Glacier	1959-	Arnold (1981)	Trent Univ.

NOTE: All the above ice caps or glaciers have been the subject of mass-balance studies that were continuing in 1983. Those on Melville Island and above St. Patrick Bay have been measured intermittently. Other areas of glacier mass-balance measurement have not been included if the network has been abandoned.

been compared with either aerial photographs or Landsat satellite imagery taken in the 1970s.

Few changes have been found, with the exception of retreat of the edges of some stagnant ice caps. For example, between 1950 and 1960 Meighen Ice Cap suffered a 6 percent reduction in area; some former nunataks are now part of the ice-free land at the edge of the ice cap, and a new 700-m-long nunatak has appeared near its northern edge since the 1950s. These changes are characteristic of a stagnant ice cap with a slightly negative balance. However, stake measurements show that while the edge has retreated the central parts have been thickening. For the 1960-1982 period along one stake profile the surface has been lowered at a mean rate of 100 mm/yr near the edge, but ice at the center has thickened at a mean rate of 90-100 mm/yr.

The overall conclusion from this preliminary study is that over the past 20-30 years a slightly negative balance (measured using the stake method) has effected only a very slight glacier edge retreat, which cannot be readily detected from photographic comparisons on all but the smaller, stagnant, ice caps. Additionally, one can say that all the larger ice caps must have been close to a steady state for a long period of time as their edge positions seem to be so stable.

Thickness Changes

Thickness changes of glaciers can be detected by various methods and an attempt made to evaluate the results in terms of mass balance. Some of those methods have been used in the Canadian High Arctic by Arnold (1968, 1981) and the Polar Continental Shelf Project (unpublished).

Leveling profiles have been surveyed in two areas of the ablation zone on Devon Ice Cap. The first was made across Sverdrup Glacier at 400 m above sea level (Figure 7.1) in 1965 and again in 1975. No significant changes in glacier elevation over this 10-year period could be found. Similar results were obtained from leveling traverses made in 1969 and 1971 at the northwest edge of the Devon Ice Cap, although the changes that might be expected over a 2-year period there are less than the standard error of the measurements. Arnold (1968), using traditional survey methods, measured an average surface lowering for 1957-1967 in the ablation zone of Gilman Glacier (Figure 7.1) of 0.17 m/yr. Using photogrammetric methods he also found a lowering of 0.83 m/yr near the terminus of White Glacier (Arnold 1981).

Measurements at about the elevation of the 1961-1982 equilibrium line on the northwest side of the Devon Island Ice Cap have shown slightly positive strain rates there. Positive strain rates at the equilibrium line indicate that the glacier there is out of phase with present climate such that over the last 20 years the balance must have been slightly more negative than usual. However, it is almost impossible to define how long a period "usual" refers to.

In the accumulation zone, repeated measurements of the length of surface-to-bedrock boreholes at the top of Devon and Agassiz Ice Caps have not shown any significant changes in thickness in recent years. Repeated gravity measurements on Devon Ice Cap confirmed the results there. Arnold (1968), using traditional survey methods, found no changes in elevation in the accumulation zone above Gilman Glazier (Figure 7.1) for the 1957-1967 period.

The combined evidence indicates that during the 1960s and 1970s the mass balance of the Canadian High Arctic glaciers has been slightly negative. The unchanging surface elevation of the tops of two of the ice caps and lower down in the accumulation zone of another, suggests that accumulation rates have not changed significantly for a period substantially longer than the period of our mass-balance measurements. Consequently, the slightly negative balance must be due to a slight increase in summer melting rates. While results from the two leveling profiles in the ablation zone of Devon Ice Cap do not support this conclusion, the measurements of Arnold (1968, 1981) in the ablation zones of two glaciers, the edge retreat of the small ice caps, and the strain rate evidence from the northwest side of the Devon Ice Cap do.

1882-1982 MASS BALANCE AND THE NEXT 100 YEARS

Figure 7.3 shows the oxygen-18 record for the 1870-1972 period. If we ignore for the moment that an oxygen isotope record of this kind represents air temperatures during periods of snowfall, we see that the

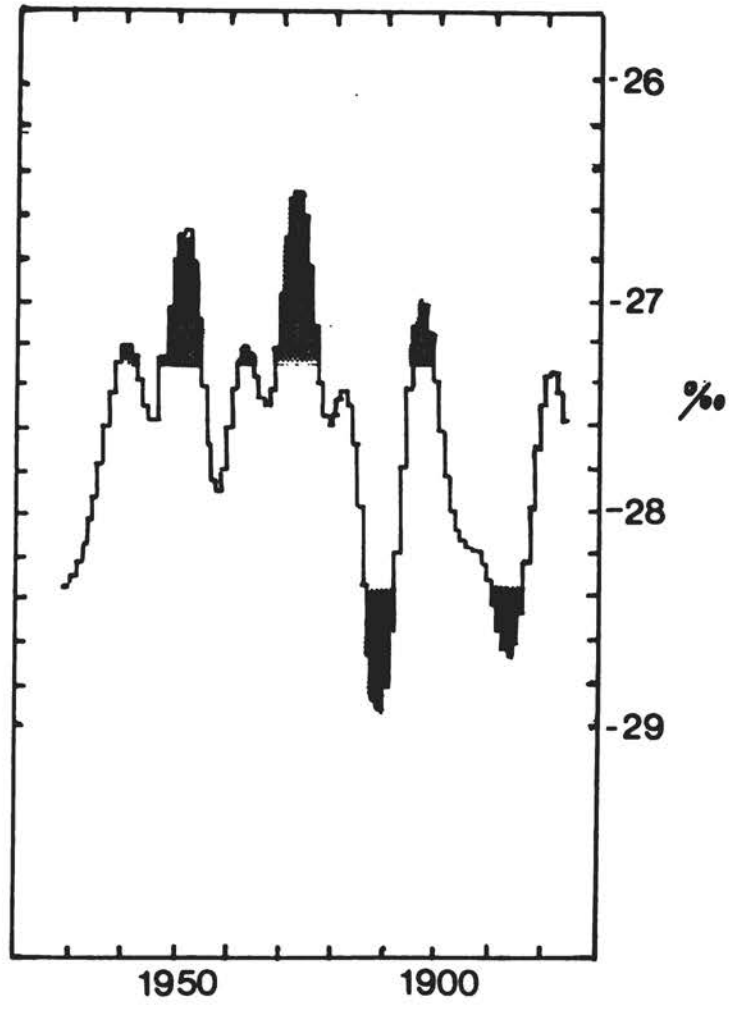

FIGURE 7.3 Oxygen-isotope values from the top of Devon Ice Cap. The shaded portions of the bargraph represent periods between 1880 and 1973 that had "warmer" or "colder" isotope values than those from the period 1961-1973, which is part of the period during which mass balance measurements discussed in the text were made.

period when mass-balance measurements were made on the Canadian ice caps is slightly cooler than the 100-year mean. Figure 7.2 shows that the first two or three years of mass balance measurements were made in the warm period of the 1930s and 1950s. Therefore, because the data are not adequate for anything other than a rough estimate, a range of mass balance has been calculated using the most negative balance for the 1960-1983 period and also the average value; a more positive value is not likely to be realistic.

The values are listed in Table 7.2 and show that in terms of sea level change the Canadian High Arctic ice caps have contributed very little. This is essentially the conclusion that Meier (1984) arrived

TABLE 7.2 Sea-Level Rise Resulting from a Negative Mass Balance on the Canadian Arctic Island Ice Caps

Negative Balance ($kg\ m^{-2}\ yr^{-1}$)	Ice Loss from Glaciers (km^3/yr)	Sea-Level Rise (mm/100 yr)	Remarks
52.6	5	1.5	1961-1981 mean
359.0	38	10.7	Most neg. balance (1961-1962)

NOTE: Measurements from the northwest side of Devon Ice Cap.

at in his consideration that the main contribution to sea-level change is from those glaciers at lower latitudes with much higher accumulation and ablation rates.

Turning to the next 100 years we should realize that calculating the effect on mass balance of increasing CO_2 levels still entails a lot of guess work. A range of higher temperatures have been forecast. However, to make a reasonably accurate prediction of future mass balance, the effects of increased CO_2 on synoptic weather patterns is needed (see, for example, Alt 1978, 1979).

It is now clear that the warm pulse of the 1930s and 1950s was not due to an anthropogenic effect. A statistical time-series analysis based on a few hundred years of oxygen-isotope and melt-series data from cores (Fisher and Koerner 1983) "forecasted" the warm period of this century and also suggested that, anthropogenic effects apart, there will be a slight cooling over the next 50 years of about 0.5-1.0°C; the summers will cool slightly more than this. On top of this uncertain prediction we have another based on the CO_2 effect. At this stage one can say little more than that the more negative balances for the 1960-1983 period will become more common if the CO_2 models are correct. Thus we might take the most negative estimate for the <u>past</u> 100 years as a reasonable forecast for the <u>next</u> 100 years (Table 7.2). However, one must emphasize that a more accurate forecast will have to wait until we know how synoptic weather patterns will change in our area. We should remember though that even if all the Canadian High Arctic ice caps melt completely global sea level will only rise by 60-120 mm.

REFERENCES

Adams, W. P., 1966. Ablation and run-off on the White Glacier, Axel Heiberg Island, Canadian Arctic Archipelago. Axel Heiberg Island Research Reports, Glaciology No.1, McGill University, Montreal, 77 pp.

Alt, B. T., 1978. Synoptic climate controls of mass balance variations on Devon Island Ice Cap, Arctic and Alpine Research, 10(1), 61-80.

Alt, B. T., 1979. Investigation of summer synoptic climate controls on the mass balance of Meighen Ice Cap. Atmosphere-Ocean, 3, 181-199.

Arnold, K. C., 1965. Aspects of the glaciology of Meighen Island, Northwest Territories, Canada. Journal of Glaciology, 5(6), 399-410.

Arnold, K. C., 1968. Determination of changes of surface height 1957-1967, of the Gilman Glacier, Northern Ellesmere Island, Canada. M.A. Thesis, McGill University, Montreal, 74 pp.

Arnold, K. C., 1981. Ice ablation measured by stakes and terrestrial photogrammetry--A comparison on the lower part of the White Glacier. Axel Heiberg Island Research Reports, Glaciology No. 2, pp. 98.

Bradley, R. S., and J. England, 1978. Recent climatic fluctuations of the Canadian High Arctic and their significance for glaciology. Arctic and Alpine Research, 10(4), 715-731.

Fisher, D. A., and R. M. Koerner, 1983. Ice-core study: A climatic link between the past, present and future. In C. R. Harington (ed.), Syllogous Vol. 49, Climate Change in Canada 3, National Museums of Natural Sciences, Ottawa, pp. 50-69.

Fisher, D. A., R. M. Koerner, W. S. B. Paterson, W. Dansgaard, N. Gundestrup, and N. Reeh, 1983. Effect of wind scouring on climatic records from ice-core oxygen-isotope profiles. Nature, 301(5897), 205-209.

Hattersley-Smith, G., and H. Serson, 1973. Reconnaissance of a small ice cap near St. Patrick Bay, Robeson Channel, Northern Ellesmere Island, Canada. Journal of Glaciology, 12(66), 417-421.

Iken, A., 1974. Velocity fluctuations of an Arctic valley glacier. A study of the White Glacier, Axel Heiberg Island. Axel Heiberg Island Research Reports, Glaciology No. 5, McGill University, Montreal, 116 pp.

Koerner, R. M., 1970. The mass balance of the Devon Island Ice Cap, Journal of Glaciology, 9(57), 325-336.

Koerner, R. M., 1977. Ice thickness measurements and their implications with respect to past and present ice volumes in the Canadian High Arctic Ice Caps. Canadian Journal of Earth Sciences, 14(12), 2697-2705.

Koerner, R. M., 1979. Accumulation, ablation and oxygen isotope variations on the Queen Elizabeth Island Ice Caps, Canada. Journal of Glaciology, 22(86), 25-41.

Koerner, R. M., and W. S. B. Paterson, 1974. Analysis of a core through the Meighen Ice Cap, Arctic Canada, and its paleoclimatic implications. Quaternary Research, 4, 253-263.

Lyons, J. B., and J. E. Mielke, 1973. Holocene history of a portion of northernmost Ellesmere Island. Arctic, 26, 314-323.

Meier, M. F., 1984. Contribution of small glaciers to global sea level. Science, 226, 1418-1421.

Müller, F., and C. M. Kesler, 1969. Errors in short-term ablation measurements on melting ice surfaces. Journal of Glaciology, 8(52), 91-105.

Paterson, W. S. B., 1969. The Meighen Ice Cap, Arctic Canada: Accumulation, ablation and flow. Journal of Glaciology, 8(54), 341-352.

Paterson, W. S. B., R. M. Koerner, D. A. Fisher, S. J. Johnsen, H. R. Clausen, W. Dansgaard, P. Bucher, and H. Oschger, 1977. An oxygen isotope climatic record from the Devon Island Ice Cap, Arctic Canada. Nature, 266(3602), 308-511.

Woo, M. K., R. Herron, P. Marsh, and R. Stoer, 1983. Comparison of weather station snowfall with winter snow accumulation in High Arctic Basins. Atmosphere-Ocean, 21(3), 312-325.

ATTACHMENT 8

GREENLAND ICE-SHEET MASS BALANCE AND SEA-LEVEL CHANGE

Niels Reeh
Department of Physical Glaciology
Geophysical Institute
Copenhagen, Denmark

INTRODUCTION

The aim of this paper is to review what we currently know about the mass balance of the Greenland ice sheet. Observations will be reviewed that allow estimates of the balance of the ice sheet locally and as a whole. In conclusion, a discussion is given of the potentials and limitations of observational efforts in relation to improving our knowledge of the present and near-future transfer of mass between the Greenland Ice Sheet and the oceans.

MASS BALANCE OF THE ICE SHEET AS A WHOLE

The Mass-Balance Equation

The mass-balance equation, which expresses the law of mass conservation for a glacier or ice sheet, may be written:

$$\partial V/\partial t = Q_P - Q_M - Q_C, \qquad (8.1)$$

where V is the glacier volume, t is time, Q_P is the annual precipitation, and Q_M and Q_C are the annual volume losses by melting and calving of icebergs, respectively. All volumes are expressed in terms of water equivalents. The change of mass (volume) of an ice sheet can be determined by observing either the left-hand side of Eq. (8.1) (observations of surface elevation changes) or by summing observations of the three terms on the right-hand side (the hydrological budget method). We shall first deal with the budget method.

The Budget Method

For the Greenland Ice Sheet, the accumulation and ablation areas constitute 1,440,000 km^2 and 290,000 km^2, i.e., 84 percent and 16 percent respectively, of the total ice-sheet area. The volume of the Greenland Ice Sheet has been estimated at 2,400,000 km^3 of water equivalent (Holtzscherer and Bauer 1954), whereas the volume of the local glaciers has been given by Weidick (1975) as no more than 100,000 km^3.

Slightly different estimates have been obtained in other studies. Radok et al. (1982), for example, applying a different map basis and incorporating ice thickness observations obtained by radio-echo soundings, give the total area of the ice sheet as 1,670,000 km^2 and the ice volume as 2,740,000 km^3 of water equivalent.

Disregarding that a small fraction of this volume is positioned below present sea level, the volume corresponds to a potential sea-level rise of 7.4 m.

Several estimates have been made for the actual gain, loss, and total balance of the Greenland Ice Sheet. In terms of cubic kilometers of water equvalent, accumulation is 500 $\pm$ 100, melting is 295 $\pm$ 100, and calf ice is 205 $\pm$ 60 (Weidick 1984).

The estimates show that the Greenland Ice Sheet is believed not to be greatly out of balance under the present climatic conditions but also that our present knowledge of the terms on the right-hand side of Eq. (8.1) is insufficient to permit a mass-balance estimate that is accurate enough to be useful in assessing the present transfer of mass between the Greenland Ice Sheet and the oceans. In the following, the Q_P, Q_M, and Q_C terms of Eq. (8.1) will be considered in more detail.

Precipitation-Distribution in Greenland (Q_P)

Figure 8.1 shows the actual distribution of precipitation over Greenland. The map is based on accumulation rate data for the ice sheet, obtained by firn stratigraphic methods (pit studies, ice corings) and precipitation records from coastal stations. Previous compilations (e.g., Mock 1967 and Radok et al. 1982) are compared with the results obtained by the Greenland Ice Sheet Program (Langway et al. 1985), which has supplied new information in particular as regards the southern Greenland Ice Sheet (Reeh and Clausen in preparation). The main difference between Figure 8.1 and previous maps (e.g., Mock 1967) is that the accumulation rate over the southwestern slope of the ice sheet between 65°N and 69°N shown in Figure 8.1 is only about 50 percent of the corresponding values given by Mock.

Even though there are still large areas of the Greenland Ice Sheet that are not covered by accumulation rate observations, the Q_P term is currently the best known of the three terms on the right-hand side of Eq. (8.1).

Melting From the Greenland Ice Sheet (Q_M)

Estimates of the mean net balance (net ablation) over the ablation area of the Greenland Ice Sheet ranges between 107 and 130 g cm^{-2} yr^{-1} [see Table 4.7 in Radok et al. (1982)]. These estimates are based mainly on scattered observations from the ablation zone in west Greenland, i.e., on the observations by Loewe (1933) around 71°N for the years 1929-1931 and those of Bauer around 69.5°N for the year 1958-1959 (Ambach, 1979).

In 1979 the Geological Survey of Greenland (GGU) initiated systematic observations of ablation at several locations of the ice-sheet margin and on local glaciers in west Greenland (Hojmark Thomsen 1984b), see Figure 8.2. The GGU observations from the ice margin are plotted in Figure 8.3(a) together with the above-mentioned older data. Apparently,

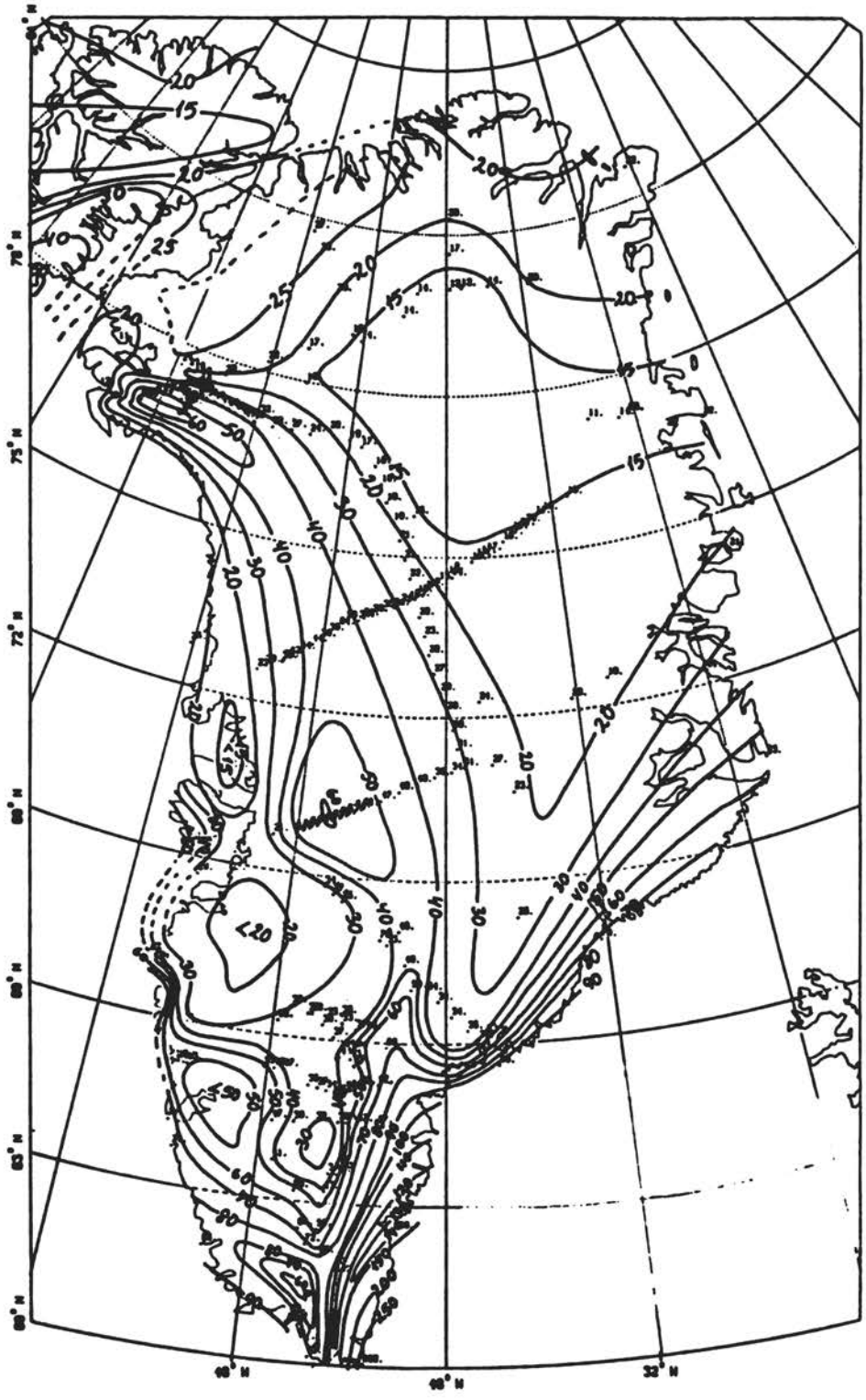

FIGURE 8.1 Distribution of precipitation in Greenland (g cm^{-2} yr^{-1}). Compiled by N. Reeh, 1984.

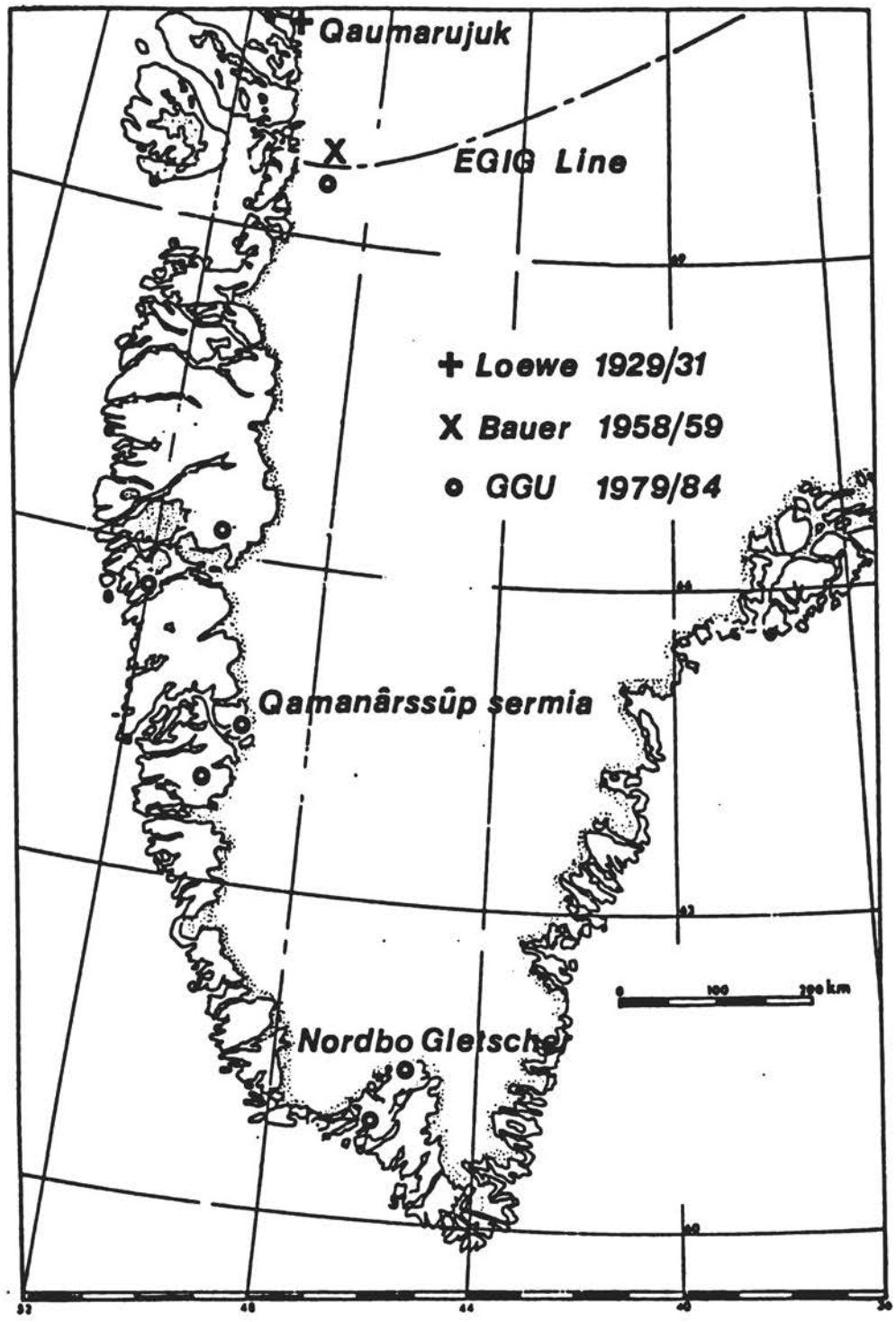

FIGURE 8.2 Locations for ablation-rate studies in west Greenland. Not all GGU (the Geological Survey of Greenland) locations have been observed throughout the entire period 1979-1984. Also some locations have now been abandoned.

to judge from this figure, there is no systematic latitudinal variation of the ablation rate along the west Greenland ice margin. However, the curves in the figure represent at most a few years of mass-balance observations for different periods. As illustrated by Figures 8.3(b) and 8.3(c), the mass-balance/elevation relationship can vary greatly from one year to another. This clearly demonstrates that previous estimates of the ablation from the Greenland Ice Sheet based on only a few years of observations at very few locations should be taken with reservation. Using a straight-line approximation to all the ablation-rate data shown in Figure 8.3, for example, results in an average ablation rate of 165 g cm^{-2} yr^{-1} obtained by Weidick and Olesen (1978) for the same area, but applying only the ablation observations before 1979. The only practical way to overcome the problem is to supplement the ablation observations with ablation models designed to predict ablation rates on the basis of observed meteorological data (Braithwaite 1980).

An important feature to be considered in such models is the refreezing of meltwater in the firn layers of the upper low-inclination areas of the ablation zone of the ice sheet.

A few results obtained by means of Braithwaite's (1980) ablation model are shown in Figures 8.4(a) and 8.4(b). Figure 8.4(a) shows calculated annual ablation rates in west Greenland as a function of latitude and altitude for the period 1965-1974. The calculations--as pointed out by Braithwaite himself--can be criticized for neglecting important effects such as heating of the air as it moves inland; nevertheless, they suggest a strong latitudinal gradient of the ablation rate, particularly for the lower altitudes.

Figure 8.4(b) illustrates the calculated year-to-year variations in equilibrium-line altitude around 69.5°N in west Greenland, which can be used as a measure of ablation variations. On the assumption that the shown variations are typical for the entire west Greenland Ice Sheet margin, and that the ablation rate-elevation gradient is constant from one year to another, as suggested by Figures 8.3(b) and 8.3(c), the variation in equilibrium line altitude can be converted to variations in total annual ablation in west Greenland. This suggests a year-to-year variability of the total ablation of up to 35 km^3 water equivalent per year.

Even the most sophisticated ablation model, however, cannot make up for the lack of observations of ablation rates in east and north Greenland, where even the elevation of the equilibrium line (the line of zero net-balance) is poorly known.

In conclusion, whereas our knowledge of the ablation of the west Greenland ice margin has been greatly improved in the last few years owing to the GGU ice margin program, and probably, when combined with ablation models, will allow reasonably accurate estimates of the ablation in the period of time covered by systematic meteorological observations (i.e., since the end of the last century), it is currently not possible to give qualified estimates of the total ablation from the Greenland Ice Sheet mainly for lack of data from east and north Greenland. Even though precise statements cannot be given, actual ablation rates in east Greenland are probably lower than has been previously

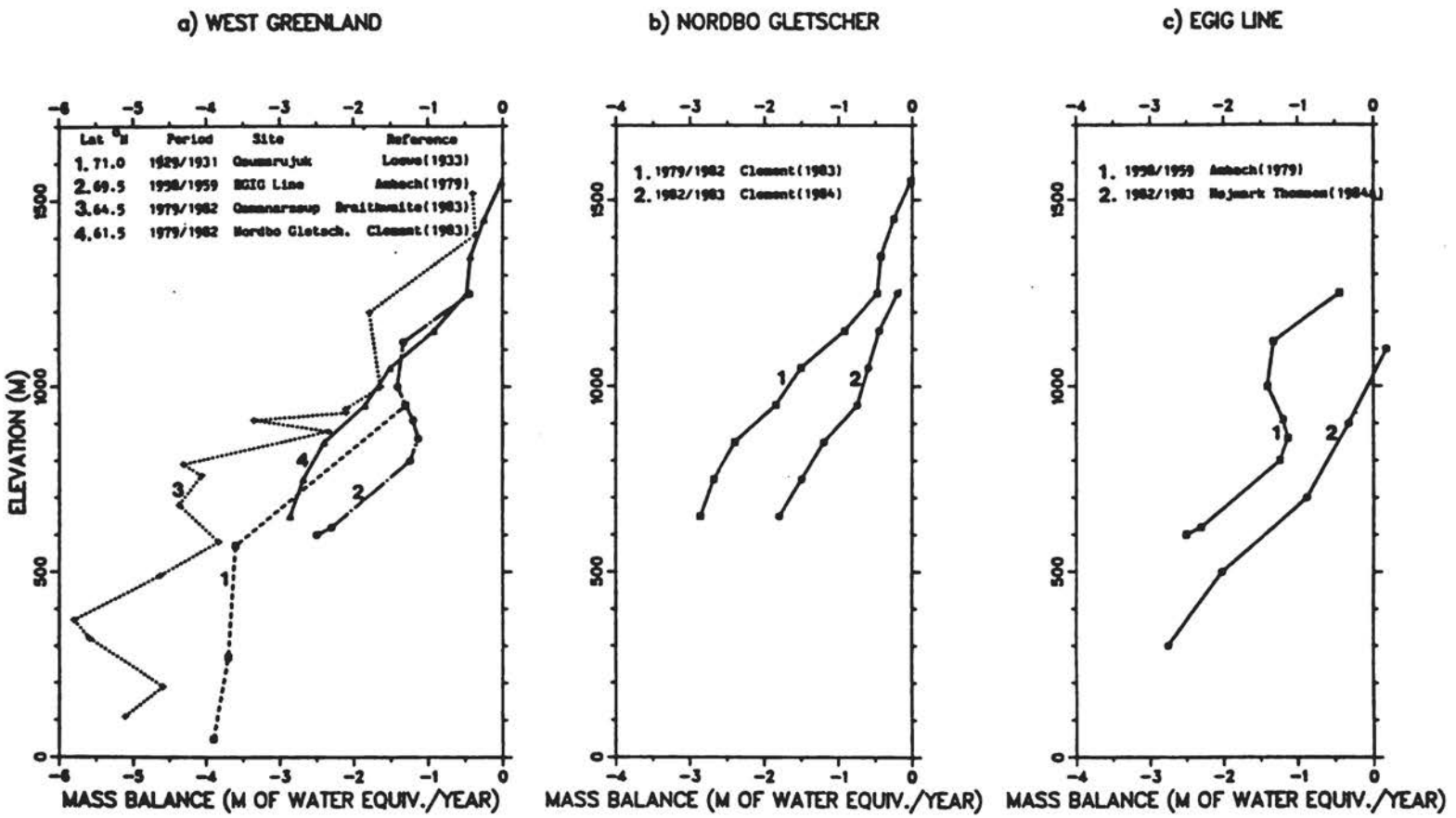

FIGURE 8.3 Mass-balance observations in the ablation zone of the west Greenland Ice Sheet.

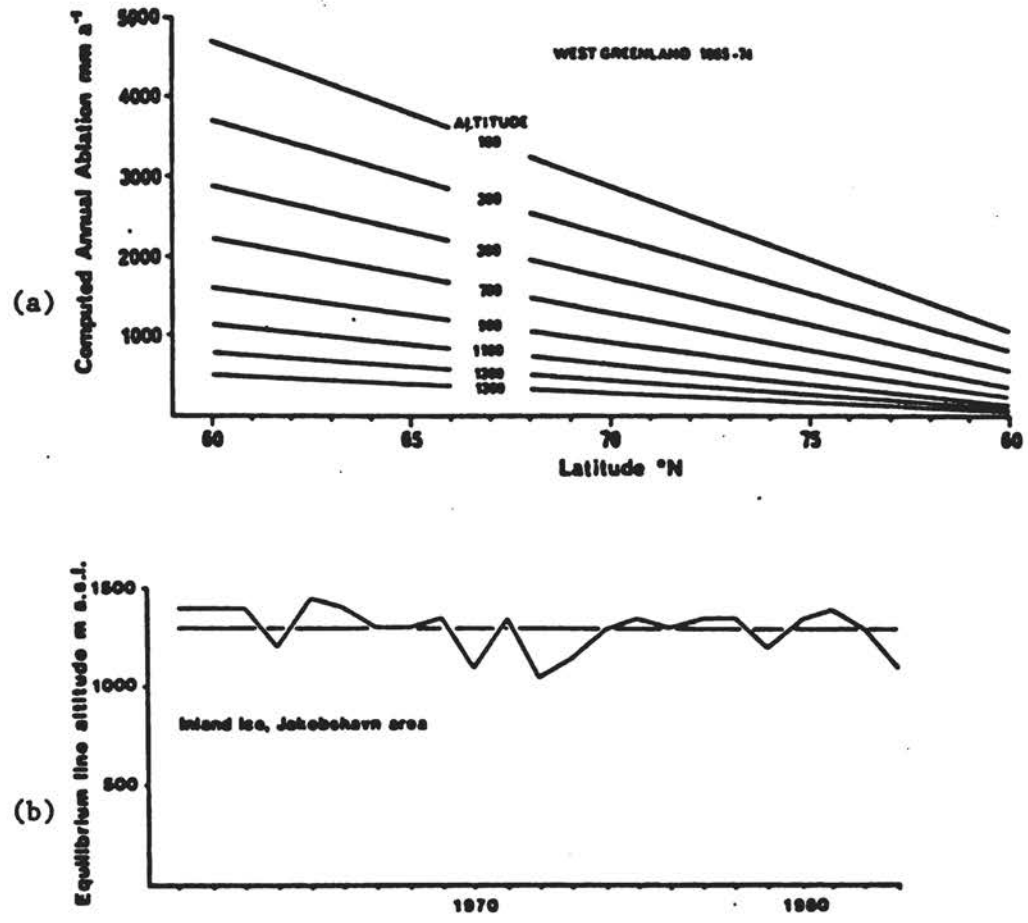

FIGURE 8.4 (a) Computed annual ablation for 1965-1974 in west Greenland in millimeters per year. From Braithwaite (1980). (b) Calculated variations in equilibrium-line altitude on the Inland Ice, Jakobshavn area, 1961-1983. The straight line indicates the 1961-1983 mean value. From Braithwaite and Hojmark Thomsen (1984).

estimated, in southern east Greenland owing to neglect of the large precipitation over the ice sheet margin (see Figure 8.1) and in central east Greenland owing to high elevations of the ice sheet margin, and a consequent restricted extension of the ablation zone.

Loss by Calving of Icebergs (Q_C)

The most extensive studies of iceberg discharge from the Greenland Ice Sheet are those of Bauer et al. (1968b) and Carbonnell and Bauer (1968), who determined the calving flux from the outflow glaciers calving into Disko Bugt and Umanak Fjord, west Greenland, by means of repeated areal photography. The results of these two studies deviate by about 10 percent (90 km^3 of ice per year in 1957 and 102 km^3 of ice per year in 1964).

Weidick and Olesen (1978), based on the investigations mentioned above and scattered information about calving glaciers in southwest

Greenland, estimated the total calf-ice production from west Greenland glaciers between 60°N and 71°N to be 97 km^3 of water per year. Few observations of calving rates for north and east Greenland have been made. Olesen and Reeh (1969) gave the calf-ice production from the northern part of the Scoresby Sund region as 11 km^3 of ice per year. For the southern part of Scoresby Sund, the calving flux based on observations in 1972 has been estimated at 6.5 km^3 of ice per year (Olesen and Reeh, unpublished). For northwest, north, and the major part of east Greenland, calving fluxes are entirely based on estimates and consequently have little weight when attempting to assess the total mass balance of the Greenland Ice Sheet. To give an impression of the proportion of the calf-ice production that is solely based on estimates, Figure 8.5 shows inferred calf-ice production from various sectors of the Greenland Ice Sheet, based on the assumption that the ice sheet is currently in balance with the accumulation-rate distribution shown in Figure 8.1 and assuming ablation rates as indicated in Figure 8.5. It appears that out of an estimated total calving flux of 310 km^3 of ice/year only about 45 percent, i.e., 130 km^3 of ice/year, is based on observed calving front ice velocities and thicknesses. As is the case with ablation, this demonstrates that a reliable estimate of the total calving flux from the Greenland Ice Sheet cannot be obtained at present owing to insufficient observation coverage, in particular for northwest, north, and east Greenland.

Observations of Surface Elevation Change

Direct observations of the change of surface elevation of the Greenland Ice Sheet have been made by Bauer et al. (1968a) for the period 1948-1959 and by Seckel (1977) for the period 1959-1968. The observations of Bauer et al. (1968a) cover the main part of the ablation zone of the EGIG line, i.e., the west Greenland Ice Sheet margin around 69.5°N, whereas Seckel's (1977) measurements cover the total section along the EGIG profile, see Figure 8.2. Both investigations show a lowering of the ice-sheet surface in the ablation zone, which on average amounts to 0.3 and 0.24 m of ice/year, respectively, see Figures 8.6(a) and 8.6(b). On the contrary Seckel's observations in the accumulation zone of the Greenland Ice Sheet at 70-72°N indicate an increase of the ice-sheet surface elevation, which on average has a magnitude of 0.085 m of ice/year as far as the west-facing slopes are concerned [Figure 8.6(b)]. For the east-facing slopes, however, the observations indicate a decrease of surface elevation on the order of a few centimeters/year. The results for the ablation zone agree with an observed average thinning rate of 0.3-0.5 m of ice/year, derived at various sites along the west Greenland ice margin by comparing trimline elevations corresponding to the ice-sheet extension around 1880 to present glacier surface elevations (Hojmark Thomsen, 1983), see Figure 8.7. Also the general retreat in this century of the ice margin in west Greenland (see, e.g., Weidick 1968; Weidick and Hojmark Thomsen 1983), illustrated in Figure 8.8, may be taken as evidence for a present thinning of the marginal zone of the west Greenland Ice Sheet.

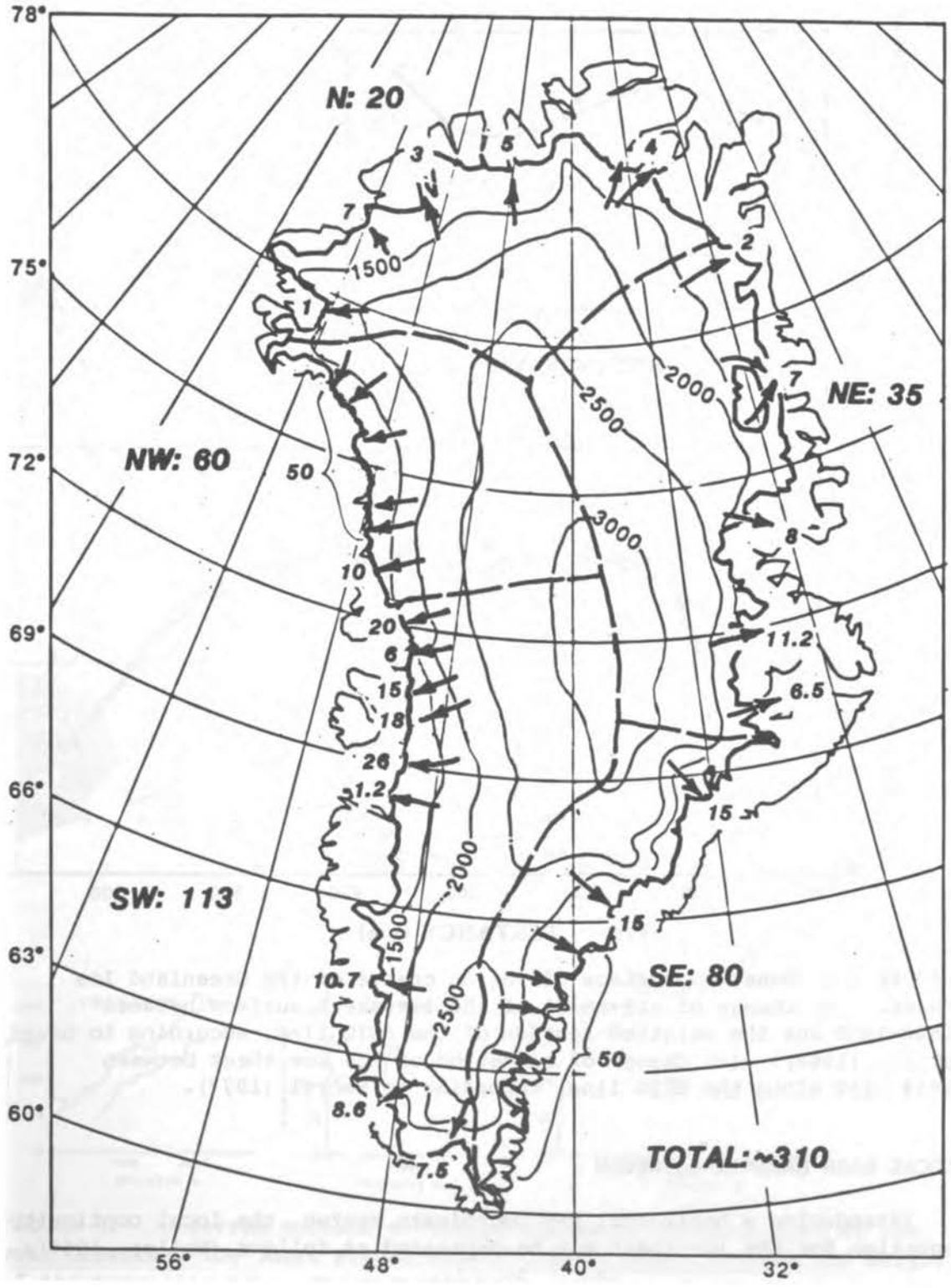

FIGURE 8.5 Estimated calf-ice discharge from Greenland Ice Sheet in cubic kilometers of water equivalent per year, based on balanced-state assumption. N. Reeh, 1984.

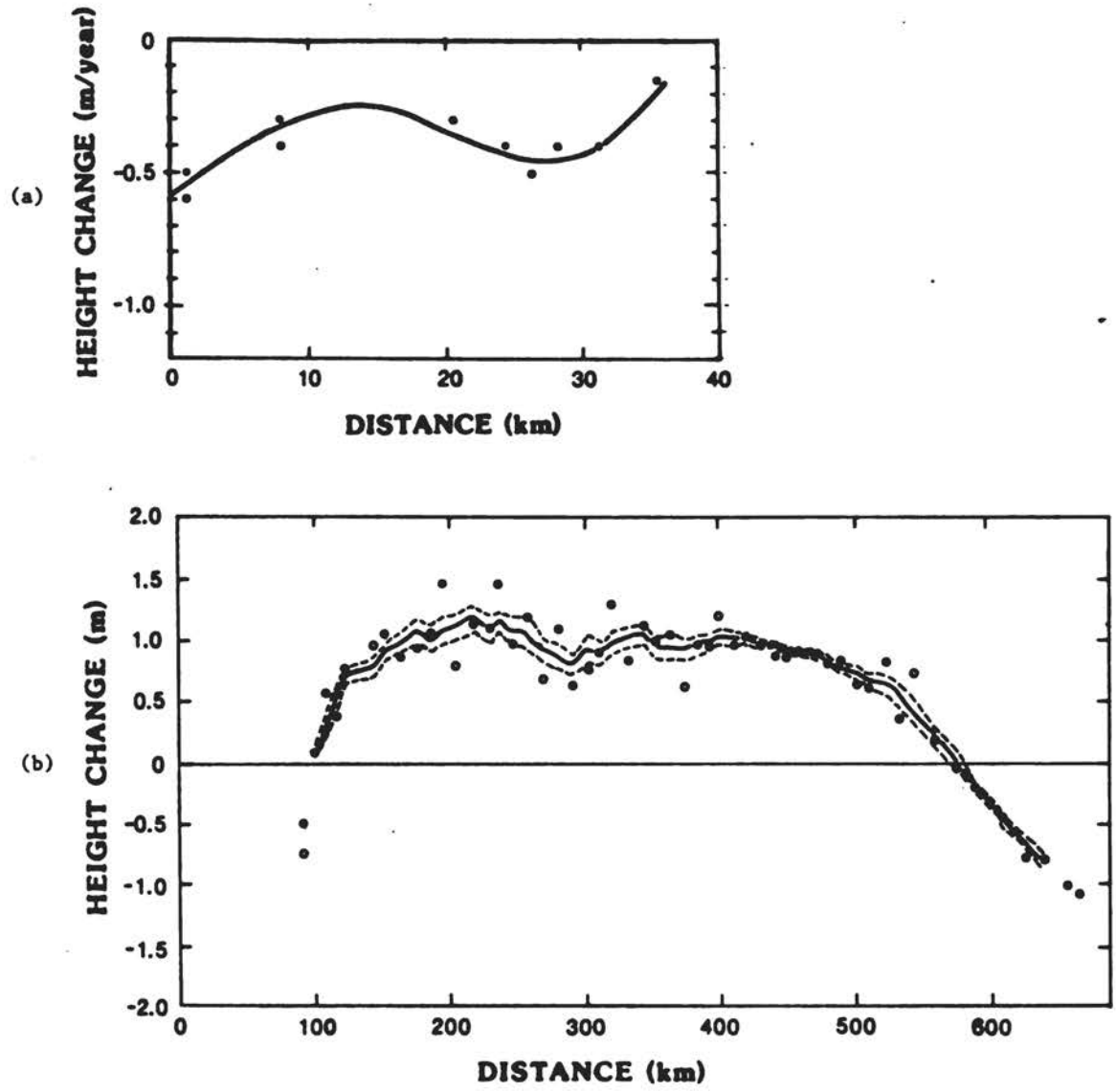

FIGURE 8.6 Observed surface elevation change of the Greenland Ice Sheet. (a) Change of elevation of the ice-sheet surface between 1948-1959 for the ablation section of the EGIG line, according to Bauer et al. (1968). (b) Change of elevation of the ice sheet between 1959-1968 along the EGIG line, according to Seckel (1977).

LOCAL MASS BALANCE EQUATION

Introducing a horizontal x-y coordinate system, the local continuity equation for the ice sheet may be expressed as follows (Mellor, 1968):

$$\partial H/\partial t = a - H\left(\frac{\partial u_m}{\partial x} + \frac{\partial v_m}{\partial y}\right) - u_m \frac{\partial H}{\partial x} - v_m \frac{\partial H}{\partial y}, \qquad (8.2)$$

where H is ice thickness (in meters of ice equivalent), t is time, a is

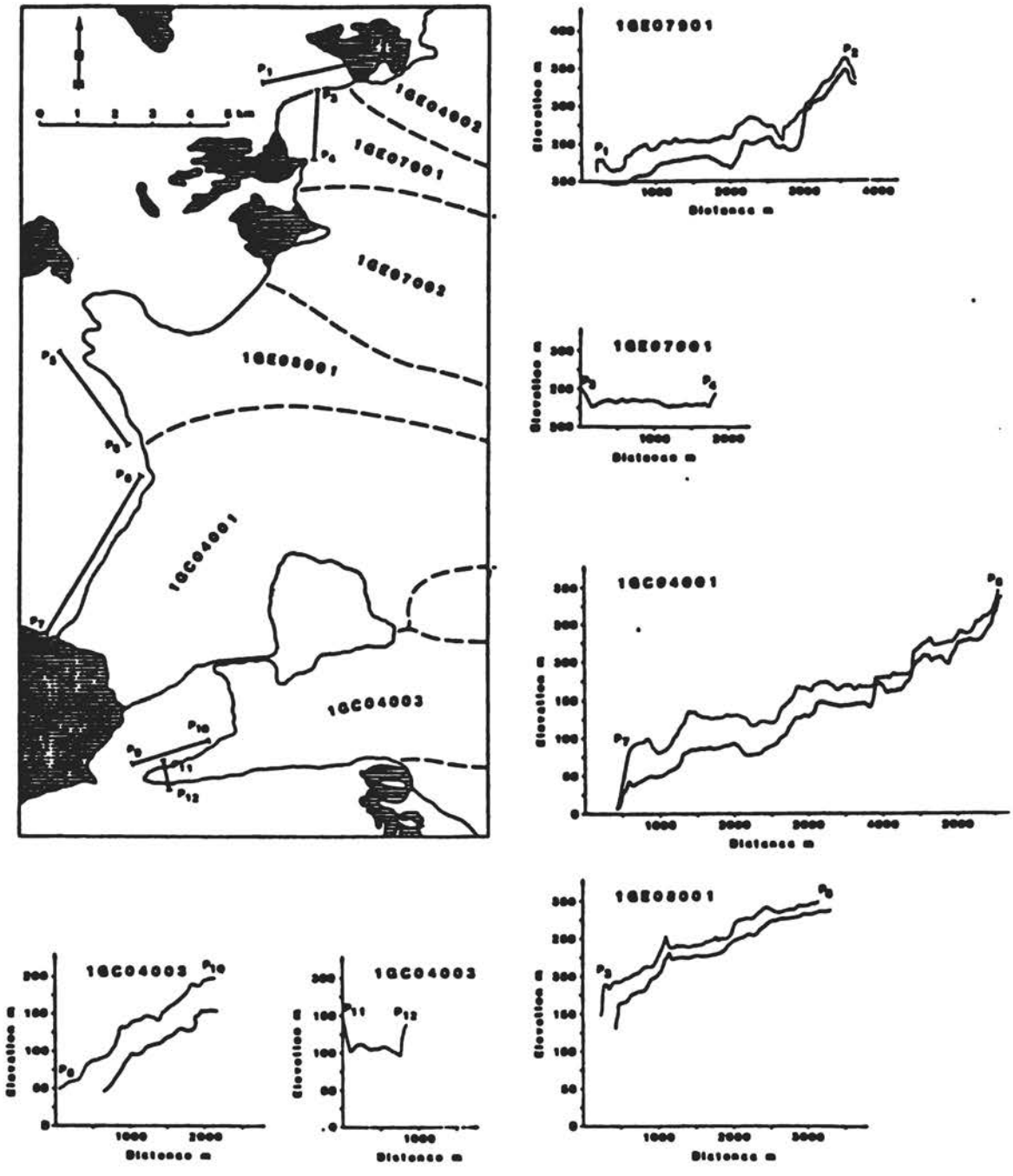

FIGURE 8.7 Observed surface elevation change of marginal zone of the west Greenland Ice Sheet around 69.5°N. Upper profiles show the height of the trim-line zone, corresponding to extension of the glaciers around 1880. Lower profiles show the height of the ice margin in 1959. From Hojmark Thomsen (1983).

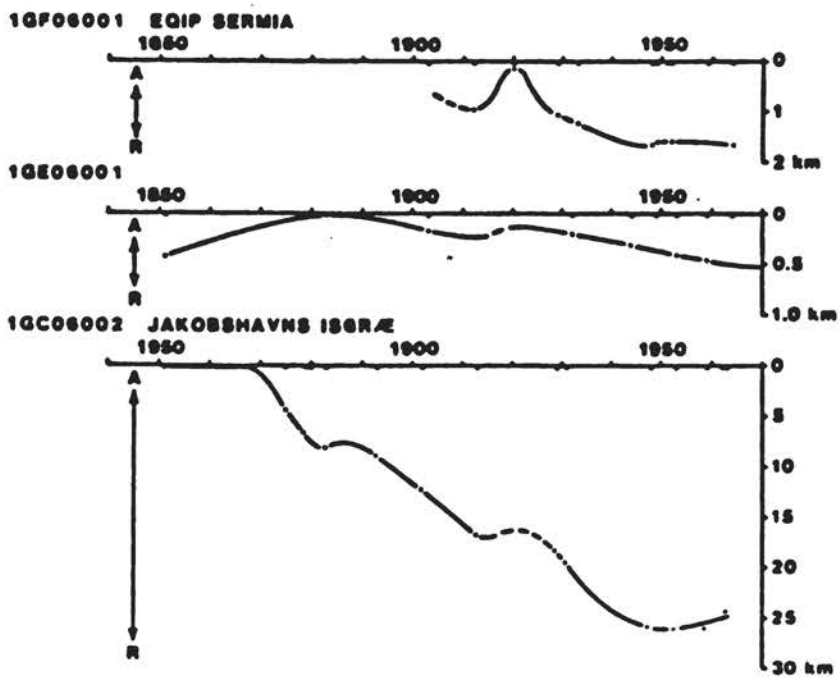

FIGURE 8.8 Change in position of front of lobes from the Inland Ice margin in Disko Bugt. 1GE08001 is a land-based lobe. The two other lobes are calf-ice-producing and situated, respectively, north and south of lobe 1GE08001. From Weidick and Højmark Thomsen (1983).

accumulation rate (meters of ice equivalent per year), and u_m and v_m are horizontal ice-flow velocities in the x and y directions, respectively, averaged over the ice thickness.

It is assumed that the depth-density profile is constant in time and space and that the ice is frozen to the bed so that there is no mass loss or gain at the bottom of the ice sheet. If we further assume that the x axis is in the direction of flow and that the shape of the horizontal velocity profile does not change along the flowline, Eq. (8.2) can be rewritten in terms of the surface velocity and surface strain rates:

$$\partial H/\partial t = a - \frac{1}{f}\left[H\left(\frac{\partial u_s}{\partial x} + \frac{\partial u_s}{\partial y}\right) + u_s \frac{\partial H}{\partial x}\right], \qquad (8.3)$$

where index s indicates a value at the surface and $f = u_s/u_m$ is the shape factor of the horizontal velocity profile, which is assumed not to vary along the flow line, as already mentioned.

Equation (8.3) has been used to estimate the local balance at several locations on the Greenland Ice Sheet (Shumsky 1965; Mellor 1968; Mock 1976) and recently by Reeh and Gundestrup (submitted) who applied the method to the ice sheet in south Greenland near the Dye 3 deep hole.

The older estimates indicate large unbalances of the Greenland Ice Sheet (up to more than 1 m/yr), in some cases positive, in others negative. For example Mellor (1968) estimated that the Dye 3 area has a positive balance of 1 m/yr. However, this large value is based on

application of an unrealistically large value of the surface velocity (50 m/yr) and a numerically far too large transverse strain-rate value of -5.0×10^{-4} yr^{-1}.

Generally the previous mass-balance estimates suffer from lack of precise data and/or neglect of the difference between surface and average values, i.e., precise knowledge of the velocity profile shape factor f. A reliable estimate of this factor is made possible by the down borehole inclinometry of the deep hole at Dye 3 (Gundestrup and Hansen in press). Combining the results of these investigations with those obtained by the upstream glaciological program (Whillans et al. 1984; Overgard and Gundestrup 1985; Reeh et al. 1985), the rate of change of surface elevation at Dye 3 is estimated to be $\partial H/\partial t = 0.03$ m/yr, with 95 percent confidence limits of -0.03 m/yr $< \partial H/\partial t < +0.09$ m/yr.

Also the previous estimate by Mock (1976) of the balance of the ice sheet at Crête in central Greenland was reviewed by Reeh and Gundestrup, who concluded that Mock's estimate of -0.25 m/yr is likely too low. Applying a value of the shape factor f = 1.6, which is not an unrealistic value at Crête (Reeh et al. 1978; Raymond 1984) (positioned at an ice divide), will change $\partial H/\partial t$ to a positive value of +0.05 m/year in accordance with the observation by Seckel (1977) referred to in the previous section.

As concluded by Reeh and Gundestrup, it seems as if only their results from Dye 3 and the observations reported by Seckel (1977) are accurate enough to allow conclusions as regards the present mass balance of the central regions of the Greenland Ice Sheet. Both studies indicate thickening rates on the order of 5-10 cm/yr. However, this result should not induce somebody to conclude that the Greenland Ice Sheet as a whole is currently gaining mass. As previously mentioned, observations from the ice sheet margin in west Greenland indicate that, in general, this part of the ice sheet is currently thinning and receding. Whether the likely gain in the central parts of the ice sheet or the loss in the western marginal areas is the larger cannot be determined on the basis of the data available.

Moreover, an even greater uncertainty concerning the mass balance of the total Greenland Ice Sheet arises from the fact that few mass-balance observations have been made in the eastern and northern parts of the ice sheet.

DISCUSSIONS AND CONCLUSIONS

The Budget Method

It is currently not possible by means of the hydrological budget method to estimate reliably the transfer of mass between the Greenland Ice Sheet and the oceans, mainly because of lack of observations of ablation rates and calving fluxes in north and east Greenland. However, to collect the necessary data will require several years of field investigations at several localities in logistically rather inaccessible areas and, therefore, would require a major logistic and scientific

effort. Moreover, even though such efforts were offered, no safe guarantees could be given that the goal (i.e., accurately assessing the present mass balance of the Greenland Ice Sheet) would be achieved.

Therefore, even though important new information about the balance of the Greenland Ice Sheet can be, and should be, obtained by evaluating existing data (for example, determining positions and changes of positions of the snow line and the calving fronts of the outlet glaciers from the north and east Greenland Ice Sheet by satellite imagery), it is concluded that the hydrological budget method should not be considered a potential method for providing the answer to the important question of whether the Greenland Ice Sheet as a whole is currently losing or gaining mass.

Observation of Surface Elevation Change

The available observations of surface elevation changes of the Greenland Ice Sheet are restricted to the marginal areas in west Greenland, where a thinning is documented to have taken place since the end of the last century and in general is continuing at present, and to the central part of the ice sheet at 70-72°N, where the ice sheet seems to thicken on the west-facing slopes and to thin on the east-facing slopes. Whether the gain in the central areas or the loss in the western marginal areas is the larger cannot be determined with the data available. However, as a means of studying the state of balance of the Greenland Ice Sheet, observations of surface elevation change provide a method with a large potential. For the marginal areas of the ice sheet, repeated air-photogrammetric surveys seem to be feasible (Andreasen et al. 1982; Højmark Thomsen 1983), whereas repeated accurate profiling, e.g., by means of airborne satellite-tracked laser is a potential method to be used in the interior regions of the ice sheet.

Local Mass-Balance Method

The Dye 3 study (Reeh and Gundestrup, submitted) indicates that this method is also a potential method for obtaining reliable information about the balance of the Greenland Ice Sheet. Apart from the ratio between surface and mean velocities (which requires inclinometer measurements in deep boreholes, but alternatively can be derived from ice-flow model calculations), the quantities to be observed (i.e., accumulation rate, surface velocity, surface strain rates, surface slope, and ice thickness profile) can be obtained by surface programs.

Mass Exchange between the Greenland Ice Sheet and the Ocean

Even though it is not possible at present to give a qualified estimate of the actual contribution from the Greenland Ice Sheet to sea-level change (even the sign of the contribution is currently unknown), a few illustrative numbers can be calculated. For example, extrapolating the observed average thinning rate of about 0.3 m/yr for the ablation area of the west Greenland Ice Sheet to the total ablation area,

results in a mass loss corresponding to a sea-level rise of 0.2-0.3 mm/yr. On the other hand, extrapolating the observed thickening rate of about 0.1 m/yr for the interior regions in south and central Greenland to the total accumulation area of the ice sheet, results in a mass gain corresponding to a sea-level lowering of about 0.4 mm/yr. Finally, the year-to-year variability of the total ablation deduced in a previous section for west Greenland, corresponds to a year-to-year variability of sea-level change of about 0.1 mm/yr.

REFERENCES

Ambach, W., 1979. Zur Nettoeisablation in einem Höenprofil am Grönländischen Inlandeis. Polarforschung, 49(11), 55-62.

Andreasen, J. O., N. Tvis Knudsen, and J. T. Moller, 1982. Glaciological investigations at Qamanarssup sermia, Field Report 1980. Gronlands Geol. Unders. Gletscher-hydrol. Meddr. 82/4, Kobenhavn.

Bauer, A., A. Ambach, and O. Schimpp, 1968a. Mouvement et variation d'altitude de la zone d'ablation ouest de l'Indlandsis du Groenland entre 1948 et 1959. Meddelelser om Gronland, 174(1).

Bauer, A., M. Baussart, M. Carbonnell, P. Kasser, P. Perroud, and A. Renaud, 1968b. Missions aériennes de reconnaissance au Groenland 1957-1958. Observations aériennes, détermination des vitesses des glaciers vêlant dans Disko Bugt et Umanak Fjord. Meddelelser om Gronland, 173(3).

Braithwaite, R. J., 1980. Regional modelling of ablation in West Greenland, GGU rapport no. 98.

Braithwaite, R. J., 1983. Glaciological investigations at Qamanarssuo sermia, interim report 1982 and appendix tables. Gronlands Geol. Unders., Gletscher-hydrol. Meddr. 83/4, Kobenhavn.

Braithwaite, R. J., and H. Hojmark Thomsen, 1984. Runoff conditions at Paakitsup Akuliarusersua, Jakobshavn estimated by modelling. Gronlands Geol. Unders., Gletscher-hydrol. Meddr. 84/3, Kobenhavn.

Carbonnell, M., and A. Bauer, 1968. Exploitation des couvertures photo-graphiques répétées du front des glaciers vêlant dans Disko Bugt et Umanak Fjord Juin-Juillet 1964. Meddelelser om Gronland, 173(5).

Clement, P., 1983. Glaciologiske undersogelser i Johan Dahl Land 1982. Gronlands Geol. Unders., Gletscher-hydrol. Meddr. 83/1, Kobenhavn.

Clement, P., 1984. Glaciological activities in Johan Dahl area, south Greenland, as a basis for mapping hydropower potential. The Geological Survey of Greenland, Report no. 120, Kobenhavn, pp. 113-121.

Gundestrup, N. S., and B. L. Hansen, in press. Borehole survey at Dye 3, South Greenland. Journal of Glaciology.

Hojmark Thomsen, H., 1983. Glaciologiske undersogelser ved Pâkitsup Ilordlia 1982 Ilulissat/Jakobshavn. Gronlands Geol. Unders., Gletscher-hydrol. Meddr. 83/3, Kobenhavn.

Hojmark Thomsen, H., 1984a. Glaciologiske undersogelser i Disko Bugt omradet 1983. Gronlands Geol. Unders., Gletscher-hydrol. Meddr. 84/1, Kobenhavn.

Hojmark Thomsen, H., 1984b. Sammenfattende aktivitetsrapport for det glaciologiske delprogram for vandkraftprojektet bynaere bassiner 1982/1984. Gronlands Geol. Unders., Gletscher-hydrol. Meddr. 84/4, Kobenhavn.

Holtzscherer, J. J., and A. Bauer, 1954. Contribution a la connaissance de l'Inlandsis du Groenland. Publication No. 39 de l'Association Internationale d'Hydrologie, pp. 244-296.

Langway, C. C., Jr., W. Dansgaard, and H. Oeschger (eds.), 1985. Proceedings of the Symposium on GISP 1971-1981. American Geophysical Union, Washington, D.C.

Loewe, F., 1933. Die Schneepegelbeobachtungen. In K. Wegner (ed.), Wissen-Schaftliche Ergebnisse der Deutschen Gronland-Expedition Alfred Wegner 1929 und 1939/31, Vol 1, pp. 153-161.

Mellor, M., 1968. The Greenland mass balance: Flux divergence considerations, Publication no. 79 de l'Association Internationale d'Hydrologie Scientifique, Gentbrugge (Belgique), pp. 275-281.

Mock, S. J., 1967. Calculated patterns of accumulation on the Greenland Ice Sheet. Journal of Glaciology, 6, 795-803.

Mock, S. J., 1976. Geodetic positions of borehole sites of the Greenland Ice Sheet Program. CRREL report 76-41, Corps of Engineers, U.S. Army, Hanover, New Hampshire.

Olesen, O. B., and N. Reeh, 1969. Preliminary report on glacier observations in Nordvestfjord, East Greenland, i Gronlands Geol. Unders. Rapport no. 21, 41-53.

Overgaard, S., and N. S. Gundestrup, 1985. Bedrock topography of the Greenland Ice Sheet in the Dye 3 area. In C. C. Langway, Jr., W. Dansgaard, and H. Oeschger (eds.), Proceedings of the Symposium on GISP 1971-1981. American Geophysical Union, Washington, D.C.

Radok, U., R. G. Barry, D. Jenssen, R. A. Keen, G. N. Kiladis, and B. McInnes, 1982. Climatic and Physical Characteristics of the Greenland Ice Sheet. CIRES, University of Colorado, Boulder.

Raymond, C. F., 1984. Deformation in the vicinity of ice divides. Journal of Glaciology, 29(103), 357-373.

Reeh, N., and N. S. Gundestrup, submitted. Mass balance of the Greenland ice sheet at Dye 3. Journal of Glaciology.

Reeh, N., H. B. Clausen, W. Dansgaard, C. U. Hammer, and S. J. Johnsen, 1978. Secular trends of accumulation rates of three Greenland stations. Journal of Glaciology, 20(20), 27-30.

Reeh, N., S. J. Johnsen, and D. Dahl-Jensen, 1985. Dating the Dye 3 deep ice core by flow model calculations. In C. C. Langway, Jr., W. Dansgaard, and H. Oeschger (eds.), Proceedings of the Symposium on GISP 1971-1981. American Geophysical Union, Washington, D.C.

Seckel, H., 1977. Höhenänderungen im Grönländischen Inlandeis zwischen 1959 and 1968. Meddelelser om Gronland, 187(4).

Shumsky, P. A., 1965. Variation in the mass of the ice cap in central Greenland. Doklady Akad. Nauk SSSR, 162(16), 320-322.

Weidick, A., 1968. Observations on some Holocene glacier fluctuations in west Greenland, Meddelelser om Gronland, 165(2).

Weidick, A., 1975. A review of Quaternary Investigations in Greenland. Institute of Polar Studies, The Ohio State University, Rep. 55.

Weidick, A., 1984. Review of glacier changes in west Greenland. Symposium on Climate and Paleoclimate of Lakes, Rivers and Glaciers, Igles, Austria.

Weidick, A., and H. Hojmark Thomsen, 1983. Lokalgletschere og Indlandsisens rand i forbindelse med udnyttelse af vandkraft i bynaere bassiner. Gronlands Geol. Unders., Gletscher-hydrol. Meddr. 83/2.

Weidick, A., and O. Olesen, 1978. Hydrologiske Bassiner i Vestgronland. Gronlands Geologiske Undersogelse, Oster Voldgade 10, DK-1350 Kobenhavn K.

Whillans, I. M., K. C. Jezek, A. R. Drew, and N. Gundestrup, 1984. Ice flow leading to the deep corehole at Dye 3, Greenland. Annals of Glaciology, 5, 185-190.

ATTACHMENT 9

THE STATE OF BALANCE OF THE ANTARCTIC ICE SHEET AN UPDATED ASSESSMENT 1984

W. F. Budd and I. N. Smith
Meteorology Department
University of Melbourne

PROBLEMS WITH THE EARLY ASSESSMENT

Many of the early assessments of the mass balance of the Antarctic concluded that the net budget appeared to be positive by an amount possibly up to about 100 percent of the mass input, cf., Mellor (1959), Loewe (1967), Bardin and Suzetova (1967). At that time one of the large unknowns that was thought could contribute to greater loss and therefore a closer state of balance was the possible existence of large melt rates under the large ice shelves. The subsequent studies of the Amery Ice Shelf (Thomas and MacAyeal 1982) have shown that large net losses do not occur there and significant basal growth occurs far inland of the front.

A second source of error in the early estimates was the lack of direct measurements of outflow glacier velocities or ice thickness and the consequent use of analogy arguments to estimate the total flux based on the few observed glaciers. Outlet glacier speeds typically vary from 200 to 2000 m/yr, and thicknesses from 200 to 2000 m. Consequently large errors can easily arise in the estimates when data are lacking.

The third major source of error was the sparcity of data on net accumulation over the interior of the Antarctic, particularly over central East Antarctica. The combination of the uncertainties in the mass influx and outflux resulted in a total possible error of about $\pm$100 percent of the gross influx.

MORE RECENT DATA AND REGIONAL ASSESSMENTS

Since the mid-1960s a number of regional studies have concentrated on the balance of individual drainage basins, which together provide a much better understanding of the total balance, e.g., Giovinetto (1970), Allison (1979), Whillans (1979), Young (1979), Morgan and Jacka (1981), and Kotlyakov et al. (1983).

The traverse into the interior and the longer-term data from the inland stations have resulted in more recent net accumulation estimates lower (by up to a factor of 2) than the earlier estimates. This has been clearly brought out by the more recent net accumulation compilations of Bull (1972), Kotlyakov et al. (1974), and Budd and Smith (1982), compared with the earlier maps of Bentley et al. (1964) or the

Soviet Atlas, Bakayev (ed.) (1966).

A method of assessing the balance over the Antarctic ice sheet by a direct comparison of observed and computed "balance velocities" was indicated by Budd et al. (1984). Again their computation of balance velocities used higher accumulations from a modified version of the Soviet Atlas accumulation map, and as a consequence those balance velocities could not be expected to be too high.

A NEW COMPUTATION OF BALANCE VELOCITY AND FLUXES

Sufficient new data are now available to warrant a new computation of balance velocities and balance volume or mass flux. Surface elevation and ice thickness have been compiled and presented in map form by the Scott Polar Research Institute (SPRI) Map Folio [Drewry (ed.) 1983]. Accumulation data since the compilation of Kotlyakov et al. (1974) have accrued from the Ross Ice Shelf region (Clausen et al. 1979) and East Antarctica (Budd and Young 1979; Young 1979; Young et al. 1982). These data were used in a new compilation by Budd and Smith (1982). Since then additional information has come from East Antarctic traverses by Australia and the Soviet Union, cf., Kotlyakov et al. (1983) and Jones (1984). These new data have now been used together with a compilation in preparation by D. J. Drewry (personal communication) to prepare the new balance velocity map.

The whole Antaractic surface and ice thickness was digitized from the SPRI maps and interpolated to a 20-km-spacing square grid. A similar procedure was used for the net accumulation. The balance ice volume flux and balance velocity over the grid were then computed using a new technique devised by W. F. Budd and I. N. Smith (University of Melbourne, unpublished) for use specifically with grid-point data since the program does not require the derivation of flowlines. The results, as shown in Figure 9.1, indicate much more detailed variation than the map of Budd et al. (1971), which was based on a broad 200-km-spacing data field. The new velocities tend also to be somewhat lower than the earlier ones in the interior and at the coast capture more clearly the channeling of the ice flow into the high-speed outlet glaciers and ice streams. The large ice shelves are not well protrayed owing to the lack of elevation detail available and the flat terrain. In general, however, the pattern of balance velocities corresponds quite well to the recognized major glacier outflow regions. It remains to compare the magnitudes of the balance velocities with the available observations.

OBSERVED ANTARCTIC ICE VELOCITIES

A compilation of observed Antarctic ice velocities was compared with the early balance velocity map in the presentation by Budd (1979). Although this compilation is still unpublished it has become recognized that the pattern of observed velocities show considerable similarity to the balance velocities. Since that time additional observed velocities have become available including Enderby Land Glaciers (Morgan and Jacka

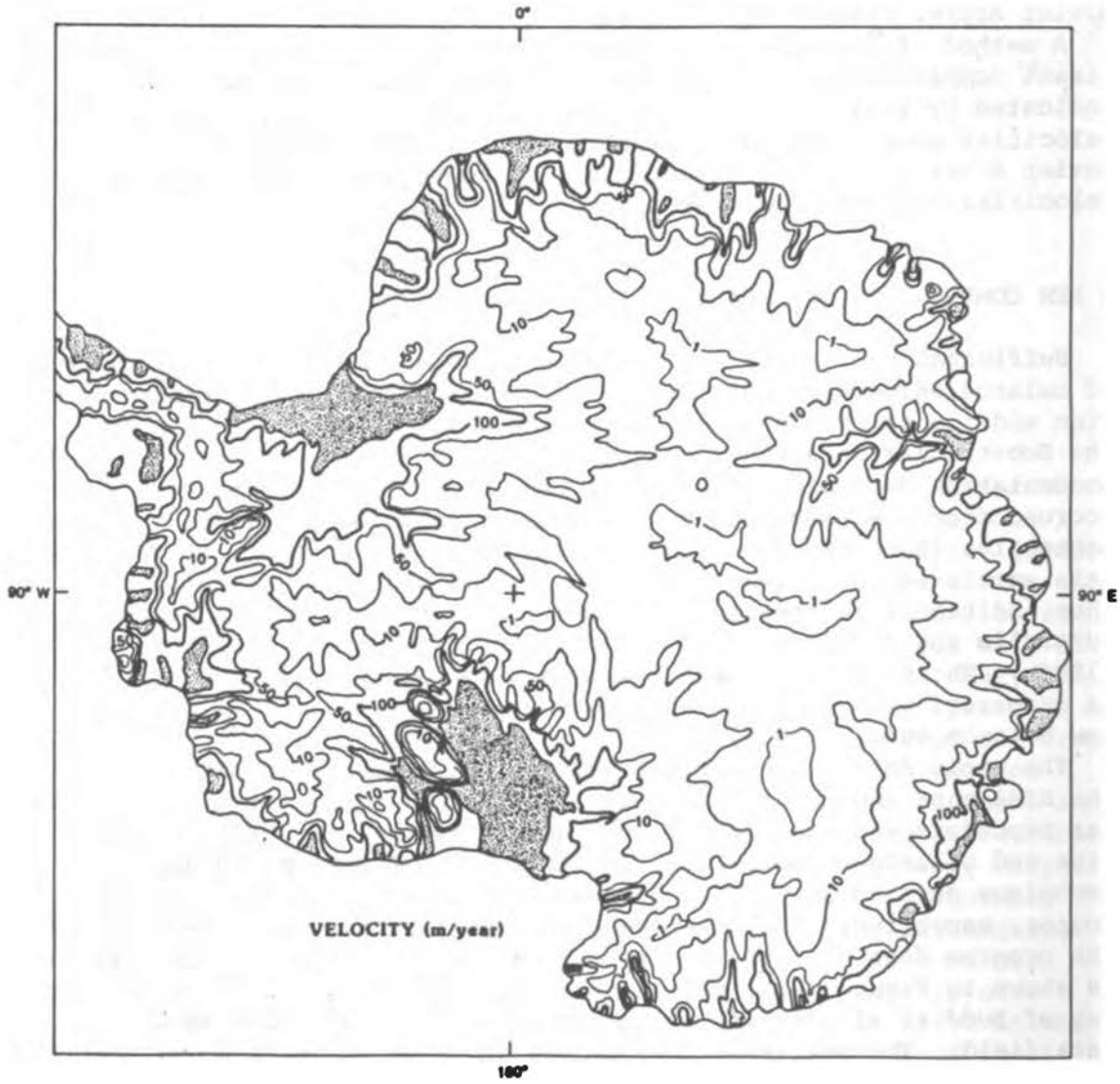

FIGURE 9.1 Computed balance velocity distribution for the Antarctic ice sheet representing the average velocity through a vertical column as required to keep the ice sheet in steady-state balance with an accumulation distribution as given by Budd and Smith (1982) and ice thickness from Drewry (1983). The calculations were made using a 20-km-resolution grid over the area.

1981), Foss Ice Shelf (Thomas and MacAyeal 1982), south of Casey towards Vostok (Sheehy unpublished), east of Casey toward Dumont d'Urville (Jones 1984), west of Casey toward Mirny (Medhurst 1984), and Dome C to Pioneerskaya (Hamley 1984).

The updated compilation is shown with the earlier balance velocity map in Figure 9.2. It should be noted that the balance velocities represent a mean through the vertical column and should therefore be expected to be less than the observed surface velocities. Many of the

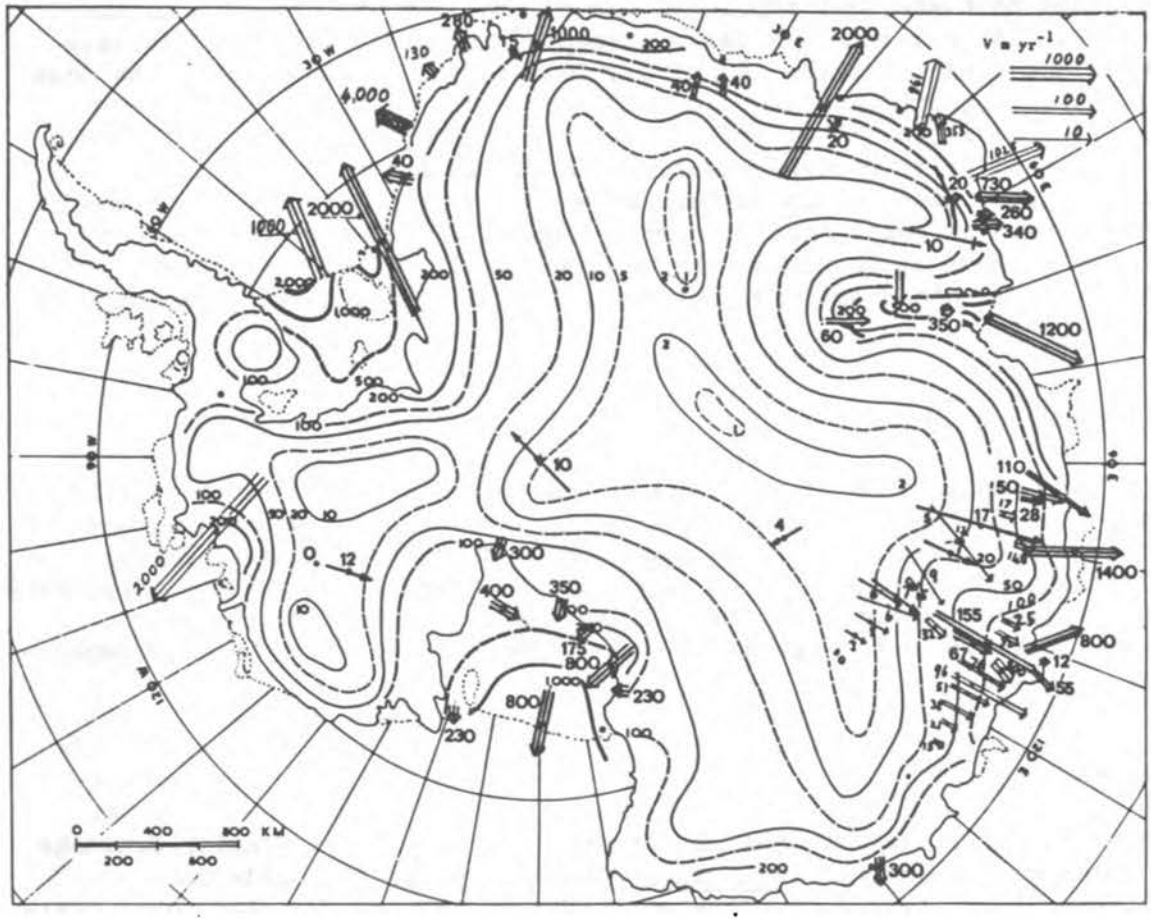

FIGURE 9.2 The earlier balance velocity distribution map of Budd et al. (1971) based on a 200-km-resolution system is shown with vectors depicting observed surface velocities superimposed. It should be noted that the balance velocities represent vertical column averages and should be less than surface velocities for steady-state balance. Comparison with Figure 9.1 suggests that the observed velocities in the interior may not be far from balance.

observed velocities are too closely spaced so that only the major features or averages of such groups are shown. By comparison with Figure 9.1 it can be seen that the new computed balance velocities tend to have the contours displaced further coastward in East Antarctica. A general appraisal with the observed velocities and computed velocities shows similar magnitudes that are more in line with a $\pm$25 percent rather than a factor-of-2 difference.

For more limited regions where it is possible to carry out more precise comparisons, the state of balance appears to be even closer than $\pm$25 percent, e.g., West Antarctic Ross Ice Shelf basin (Budd et al. 1984; Kotlyakov et al. 1983; Jones 1984) and Enderby Land (Morgan and Jacka 1981).

A further use of the balance velocities map is to highlight those

regions that are most important for the balance assessment. Already around East Antarctica a large number of the most important glaciers have now been measured. A systematic integral of flow around the coast is still required.

In summary the total influx over the Antarctic ice sheet of about 2×10^3 km/yr is probably nearly balanced by the outflow with a discrepancy most likely in the range of 0 to +20 percent. In terms of sea level the total Antarctic mass flux of 2×10^3 km/yr represents about 6 mm/yr of sea-level change. A net gain of 0 to 20 percent therefore represents a net decrease contribution to sea level of about 0 to 1.2 mm/yr.

ACKNOWLEDGMENT

The computations on a 20-km grid covering Antarctica form a joint project of the Meteorology Department, University of Melbourne, with the Cooperative Institute for Research and Enviornmental Sciences (CIRES) of the University of Colorado at Boulder. The work is supported by a grant to CIRES from the U.S. National Oceanic and Atmospheric Administration and by contract DOE-AC02-84ER60197 with the U.S. Department of Energy.

REFERENCES

Allison, I. F., 1979. The mass budget of the Lambert Glacier drainage basin, Antarctica. Journal of Glaciology, 22(87), 223-235.

Bardin, V. I., and I. A. Suzetova, 1967. Basic morphometric characteristics for Antarctica and budget of the Antarctic ice cover. JARE Scientific Reports, Special Issue No. 1, pp. 92-100.

Bakayev, U. G. (ed.), 1966. Soviet Antarctic Expedition Atlas of Antarctica. Main Administrations of Geodesy and Cartography of the Ministry of Geology, USSR.

Bentley, C. R., et al., 1964. Physical Characteristics of the Antarctic Ice Sheet. Antarctic Map Folio Series 2, American Geographical Society, New York.

Budd, W. F., 1979. Review of the dynamics of ice masses (unpublished paper presented at the IGS Symposium on the Dynamics of Ice Masses).

Budd, W. F., and I. N. Smith, 1981. The growth and retreat of ice sheets in response to orbital radiation changes. International Association of Hydrological Sciences Publication 131 (Symposium at Canberra 1979 - Sea Level, Ice and Climatic Change), pp. 369-409.

Budd, W. F., and I. N. Smith, 1982. Large-scale numerical modelling of the Antarctic ice sheet. Annals of Glaciology, 3, 42-49.

Budd, W. F., and N. W. Young, 1979. Results from the I.A.G.P. flowline study inland of Casey, Wilkes Land, Antarctica. Journal of Glaciology, 24(90), 89-101.

Budd, W. F., D. Jenssen, and U. Radok, 1971. Derived physical characteristics of the Antarctic Ice Sheet. ANARE Interim Reports Ser. A (IV) Glaciology (Publication 120).

Budd, W. F., M. Corry, and T. H. Jacka, 1982. Results from the Amery Ice Shelf Project. Annals of Glaciology, 3, 36-41.

Budd, W. F., D. Jenssen, and I. N. Smith, 1984. A three-dimensional time-dependent model of the West Antarctic ice sheet. Annals of Glaciology, 5 (in press).

Bull, C., 1972. Snow accmulation in Antarctica. In L. O. Quam (ed.) Research in the Antarctic, American Association for the Advancement of Science, Washington, D.C., pp. 367-421.

Clausen, et al., 1979. Surface accumulation on Ross Ice Shelf. Antarctic Journal of the United States, 14(5), 68-72.

Drewry, D. J. (ed.), 1983. Antarctica: Glaciological and Geophysical Folio. Scott Polar Research Institute, Cambridge.

Giovinetto, M. B., 1970. The Antarctic ice sheet and its probable bi-modal response to climate. International Association of Hydrological Sciences Publication 86, pp. 347-358.

Hamley, T., 1984. Glaciological measurements on the 1983-84 Soviet traverse from Mirny to dome C. Australian Glaciological Research 1982-1983, Antarctic Division Hobart (in press).

Jones, D., 1984. Glaciological measurements in eastern Wilkes Land Antarctica. Australian Glaciological Research, 1982-1983, Antarctic Division Hobart (in press).

Kotlyakov, V. MN., et al., 1974. Novaya karta pitaniya lednikovogo pokrova Antartidy (New map of the accumulation on the Antarctic ice sheet). Materialy Glyatriologicheskikh Issledovaniy. Khronika. Obsuzhdeniya, 24, 248-255.

Kotlyakov, V. MN., B. M. Dyurgerov, and P. A. Korolyev, 1983. Accumulation and mass balance of the large ice-catchment basin in East Antarctica. Data of Glaciological Studies, Chronicle Discussion No. 47, Academy of Sciences, USSR, pp. 49-61.

Loewe, F., 1967. The water budget in Antarctica. JARE Scientific Reports, Special Issue No. 1, pp. 101-110.

Medhurst, T. G., 1984. Glaciological measurements in Western Wilkes Land, Antarctica. Australian Glaciological Research 1982-83, Antarctic Division Hobart (in press).

Mellor, M., 1959. Mass balance studies in Antarctica. Journal of Glaciology, 3(26), 522-533.

Morgan, V. I., and T. H. Jacka, 1981. Mass balance studies in East Antarctica. International Association of Hydrological Sciences Publication 131 (Symposium at Canberra 1979 - Sea Level, Ice and Climatic Change), pp. 253-260.

Thomas, R. H., and D. R. MacAyeal, 1982. Derived characteristics of the Ross Ice Shelf, Antarctica. Journal of Glaciology, 28(100), 397-412.

Whillans, I. M., 1979. Ice flow along the Byrd Station strain network, Antarctica. Journal of Glaciology, 24(90), 15-28.

Young, N. W., 1979. Measured velocities of interior East Antarctica and the state of mass balance within the I.A.G.P. area. Journal of Glaciology, 24(90), 77-87.

Young, N. W., et al., 1982. Accumulation distribution in the I.A.G.P. area Antarctica: 90°E-150°E. Annals of Glaciology, 3, 333-338.

ATTACHMENT 10

GLACIOLOGICAL EVIDENCE: THE ROSS SEA SECTOR

Charles R. Bentley
Geophysical and Polar Research Center
University of Wisconsin-Madison
Madison, Wisconsin

THE ROSS EMBAYMENT

The Ross Ice Shelf Geophysical and Glaciological Survey (RIGGS) (Bentley 1984; Robertson et al. 1982), together with airborne radar sounding in West Antarctica (Rose 1979) and shipboard echo sounding in the Ross Sea (Hayes and Davey 1975), has made it possible to draw a subglacial and submarine topographic map of the entire "Ross Embayment" (Figure 10.1) (Albert et al. 1978; Bentley and Jezek 1982). The unbroken continuity of the subglacial and submarine topography across the West Antarctic ice sheet grounding line shows that the position of the grounding line is largely determined by ice-sheet dynamics and the heights of sea level and is, therefore, easily subject to change in time. In fact, we believe that its position has varied greatly in the past and that it could be moving now.

Because depths to ocean bottom were measured on a 55-km grid, small, isolated rises in the ocean floor easily could be missed. After combining evidence from the distribution of bottom crevasses found by analysis of radar data, from ice and water layer thicknesses, and from surface crevassing, Jezek and Bentley (1983) concluded that there are six additional sites of grounded ice (besides Roosevelt Island and Crary Ice Rise) on the ice shelf--all in the grid western sector and generally associated with known areas of shallow water (Figure 10.2). It is widely believed that areas of grounded ice may play a central role in stabilizing the ice sheet by acting as "pinning points" in the ice shelf.

THE ROSS ICE SHELF--ICE THICKNESS

Most of the shelf, as shown by a map of ice thickness compiled using RIGGS data (Bentley et al. 1979) (Figure 10.3), is characterized by broad intrusions of thick ice that reflect the tremendous volume of ice entering the shelf from the ice streams and outlet glaciers. Particularly

---

This is contribution number 427 of the Geophysical and Polar Research Center, University of Wisconsin-Madison.

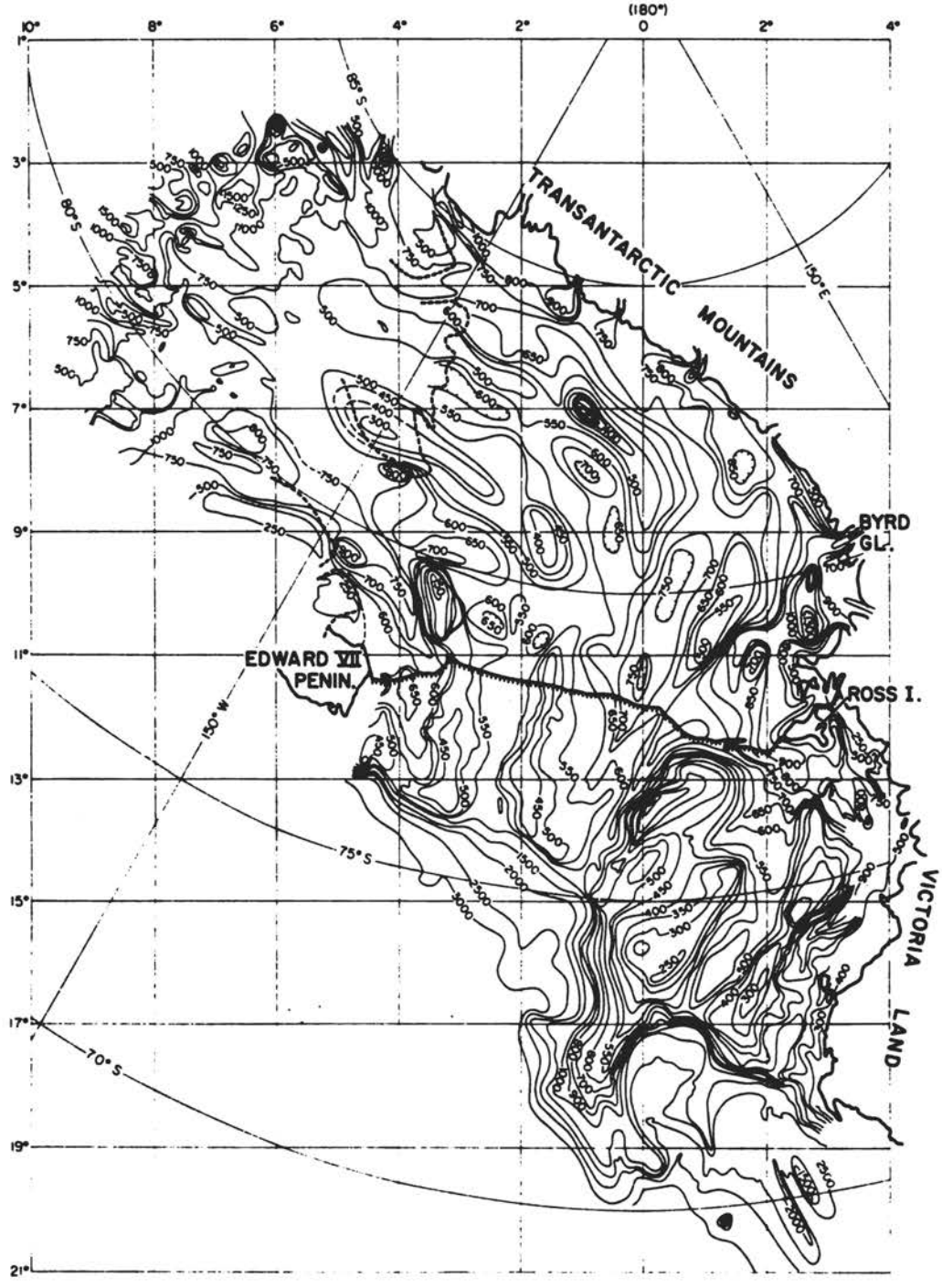

FIGURE 10.1 Submarine topography of the Ross Embayment (from Bentley and Jezek 1982). The contour interval changes from 50 m in the Ross Sea and under the Ross Ice Shelf to 250 m beneath the West Antarctic inland ice. This map, and also all succeeding maps except Figure 10.6, shows "grid" coordinates: a rectangular system with meridians parallel to the Greenwich meridian (north toward Greenwich) and its origin ($L = 0°$, $\lambda = 0°$) at the South Pole.

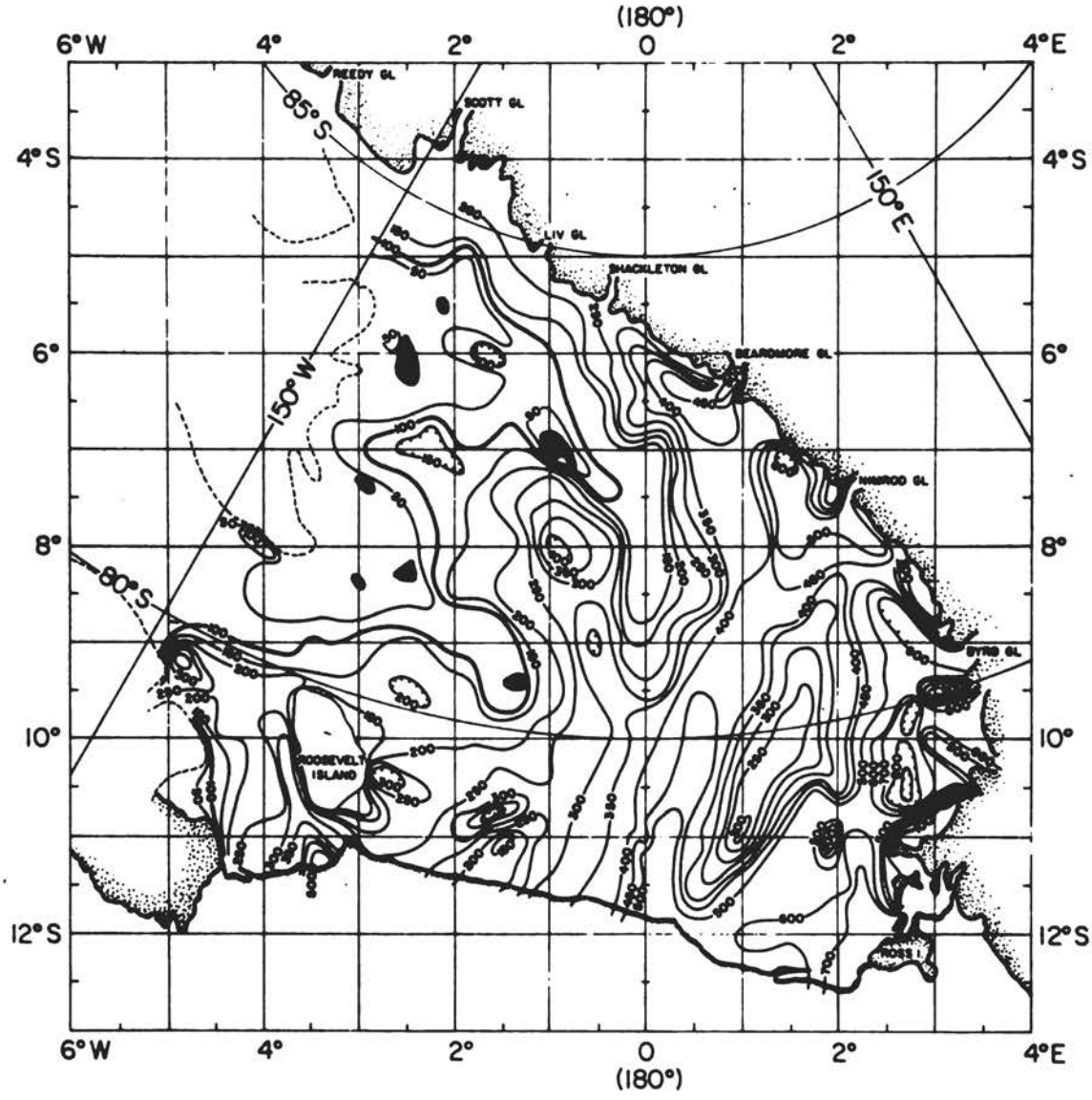

FIGURE 10.2 Water-layer thickness contours and the locations of areas of grounded ice (solid black areas) from RIGGS data. The contour interval is 50 m.

striking are the lobes associated with the Ice Streams B and D and with Byrd Glacier. Crary Ice Rise, centrally located on the ice shelf (grid position: 7°S, 1°W), forms an obstruction to ice flow that causes severe changes in ice thickness. The grid eastern flank of the ice rise is wrapped by a thick finger of ice that may result from the damming effect that the ice rise has on upstream ice but that also may be interpreted as evidence for a more grid easterly position of the grounding line on this flank of the ice rise some time in the recent past. The damming effect is also manifest in the pronounced minimum in ice thickness in

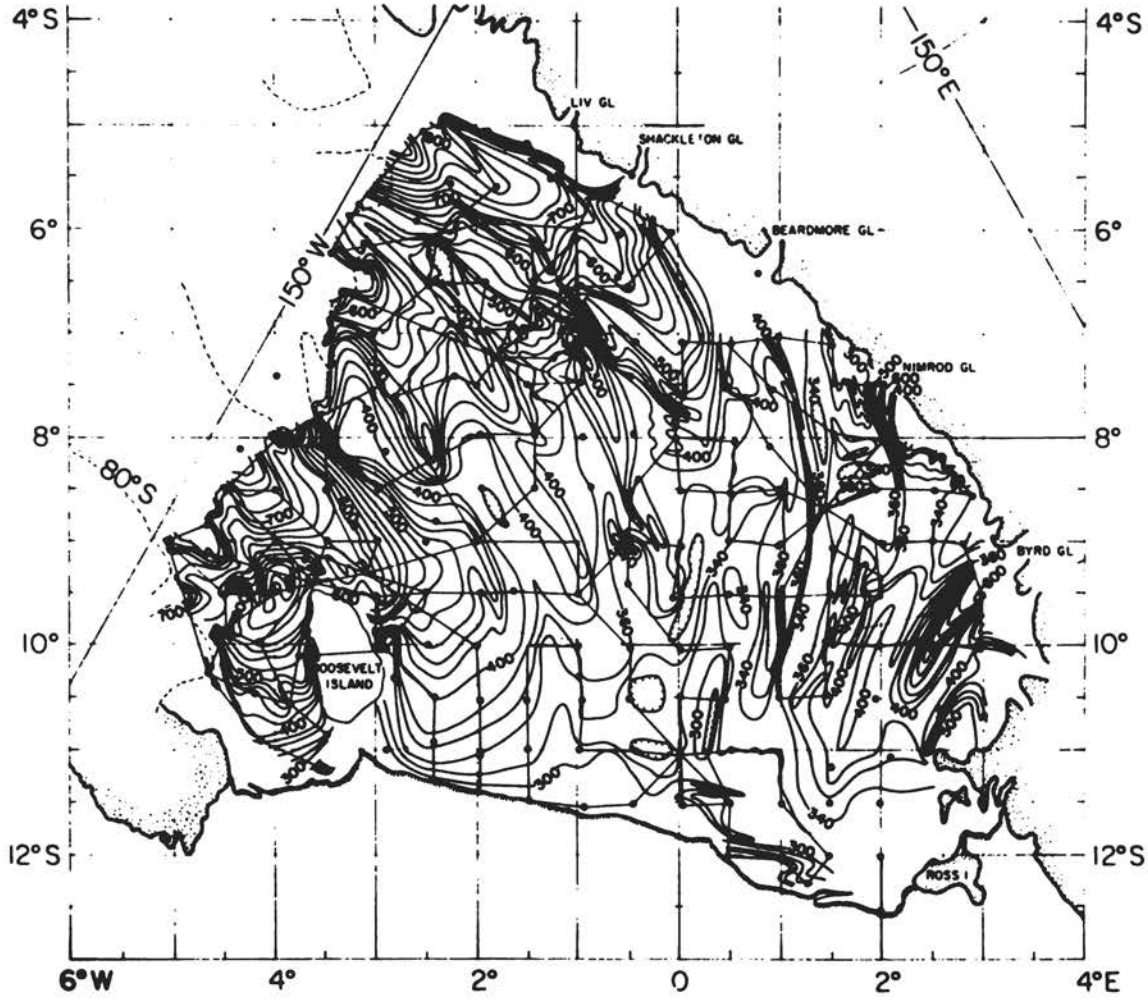

FIGURE 10.3 Ice thickness map produced from radar sounding data collected during RIGGS. Flight lines and surface stations (solid circles) are shown (Bentley et al. 1979). The contour interval is 20 m.

the lee of the ice rise, i.e., directly downstream. Contours upstream of Roosevelt Island are convoluted and contain anomalous closed minima, suggesting considerable "turbulence" as Ice Streams D and E are deflected around the island. There are several other relative maxima and minima. The entire grid eastern part of the shelf is characterized by convoluted ice thickness patterns. We believe that some of the complexities arise from disequilibrium conditions in the ice shelf.

ICE FLOW AND MASS BALANCE

Repeated position location by navigational satellite, carried out by U.S. Geological Survey personnel and compiled by Thomas et al. (1984)

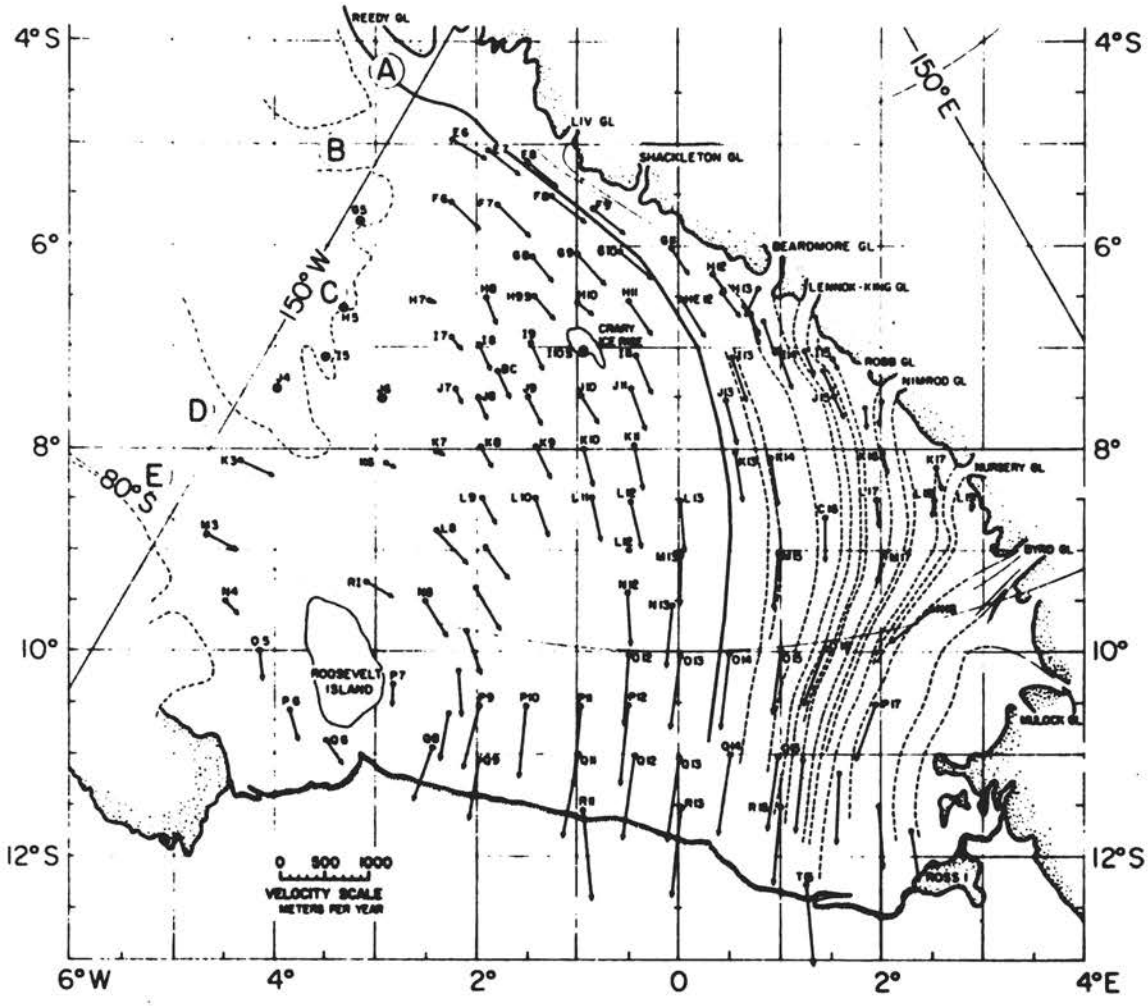

FIGURE 10.4 Velocity vectors determined from Doppler satellite tracking data (arrows) and flow lines based on variations in radar echo strength (dashed lines). The heavy line in the central part of the map represents the boundary between East and West Antarctic ice. The dotted lines show the output gate and lateral boundaries (one extrapolated) of Thomas and Bentley's (1978a) flow band MNOPQR. The solid line from Ross Island to the dotted line is the portion of the RISS (Dorrer et al. 1969) line used in the mass-balance calculations of this paper.

yields a straightforward map of the present-day velocity vectors on the ice shelf (Figure 10.4). The agreement with previous data from the Ross Ice Shelf Survey (RISS) (Dorrer et al. 1969) is excellent, and the association with ice-stream and outlet-glacier input is well defined, except for Ice Stream C, where the coverage is sparse and the evidence inconclusive. Some glaciologists believe that Ice Stream C is now inactive but that it flowed much more actively in the past.

Flow lines have been mapped in the grid eastern sector of the ice shelf by Bentley et al. (1979), using the RIGGS airborne data (Figure

10.4), and by Neal (1979), who worked with the airborne radar data from the U.S.-U.K. program. They have drawn flow lines by correlating changes in the amplitude of bottom reflections between flight lines--for instance, the ice emerging from East Antarctic glaciers generally produces a strong reflection, whereas the reflections off the bottom of the ice between outlet glaciers are poor. Neal suggested that these reduced signal strengths are associated with brine percolated into the firn from upwardly penetrating bottom crevasses; however, there is also evidence to suggest that there is absorption and scattering taking place in the deeper ice as well. The pattern of bright and dark bands is easily correlated between flight lines and can be used to infer the direction of ice flow, since there is good correspondence between the radar reflection bands and velocity vector data in the grid eastern sector of the ice shelf (Figure 10.4).

The agreement between the two sets of data shows conclusively that there have been no major changes in the flow directions on the ice shelf over the 1500-year residence time of East Antarctic glacier ice in its passage across the Ross Ice Shelf to the Ross Sea. That rules out such drastic phenomena as surges of the inland ice into and through the ice shelf, or complete disappearance of the ice shelf, for the last millenium and a half (Bentley 1981).

Mapping flow lines on the basis of correlatable radar reflectors is not so straightforward in the western sector. Although there are some features that can be traced down the ice shelf (Neal 1979; Jezek 1984), Jezek (1984) showed that they do not correspond to modern flow lines determined from measured velocities. Instead, there is indication that these tracks are records of ice-flow changes, a point that is discussed further below.

Using the technique of measuring the depth to dated radioactive fallout horizons, Clausen et al. (1979) determined the surface mass balance over most of the ice shelf (Figure 10.5). From measured velocities, strain rates, accumulation rates, and ice thicknesses, Thomas and Bentley (1978a) calculated the mass balance in three flow bands located in the grid western half of the ice shelf. A positive sum of ice-shelf thickening and bottom melting (it is not possible from the available data to distinguish between the two) of 0.15 ± 0.06 m of ice per year was found near Roosevelt Island--an area that may experience significant basal melting. Near the RISP drill site, the figure was approximately 0--since the bottom balance rate there is probably small, this suggests that the ice shelf is near equilibrium in that region. The mass balance calculations in the third flow band, upstream of Crary Ice Rise, which showed ice-shelf thickening, had to be reconsidered because one of the newly discovered (or, in this case, rediscovered) ice rises falls within the flow band. Jezek and Bentley (1984) reported two new calculations in this area, one taking the ice rise into account and the other avoiding it, that indicate a mass balance not significantly different from zero, but with a considerable uncertainty. On the other hand, calculations on the temperature profile at J9 (MacAyeal and Thomas 1979) support the idea of ice-shelf thickening upstream of Crary Ice Rise.

The flow-line map makes it possible to make separate balance analyses for the ice shelf corresponding to ice input from East and West Antarc-

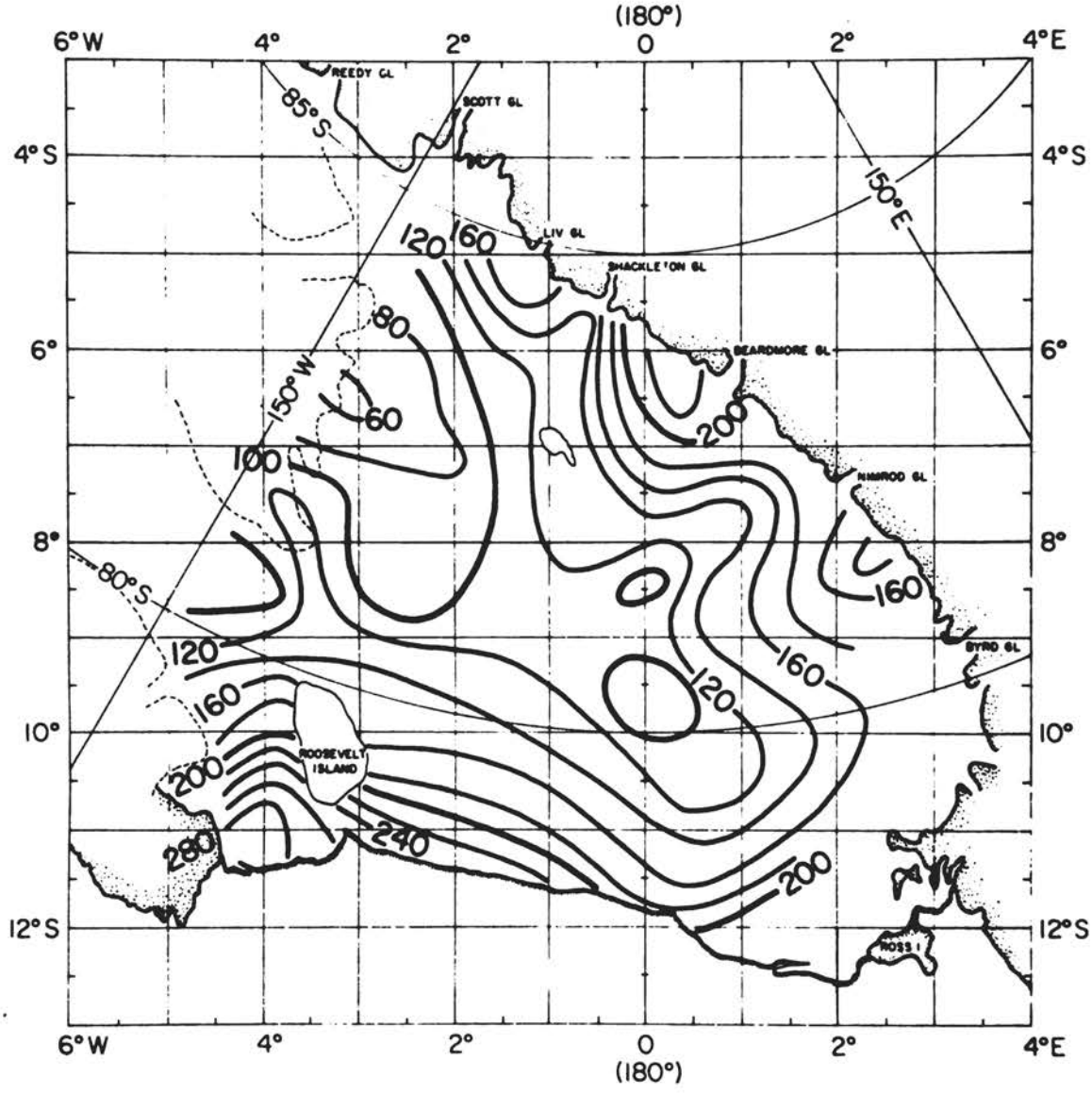

FIGURE 10.5 Surface mass-balance rates (in mm/yr of water equivalent) from RIGGS, based on depths to dated radioactive fallout horizons (Clausen et al. 1979) and measured accumulation at stakes (Thomas et al. 1984). The contour interval is 20 mm/yr.

tica. The flow line that marks the grid western boundary of ice from Reedy Glacier has been chosen as the boundary between East Antarctic and West Antarctic flow.

East Antarctic Input

This analysis extends that of Giovinetto et al. (1966) with a major improvement in the accuracy with which the East Antarctic discharge is known. Uncertainty in the outflow from Byrd Glacier was responsible for virtually the entire 30 percent error in the total mass flux cited by Giovinetto et al. (1966). The primary source of error was the necessity for calculating the ice thicknesses from surface elevations. The ice thickness is now known accurately from radar sounding (P. Calkin, cited by Hughes 1975) on the section across which Swithinbank (1963) measured surface velocities; the mass flux is 17.8 ± 1.8 km^3/yr [the tabulated value in Giovinetto et al. (1966) was 16.3 ± 10.6 km^3/yr].

The ice discharge through most of the other major outlet glaciers (Scott, Amundsen, Beardmore, Nimrod, and Mulock Glaciers) has been taken unchanged from the tabulation in Giovinetto et al. (1966). Estimates for Shackleton and Reedy Glaciers, on which no velocity measurements have been made, were obtained by interpolation and extrapolation from an arbitrary, ad hoc plot (of the ratio of the measured mass flux to the width at the mouth versus distance along the Transantarctic Mountain front) for the other outlet glaciers. The contribution to the mass input from smaller outlet glaciers and from cirque and piedmont glaciers has also been taken from Giovinetto et al. (1966), with a 10 percent increase to correct for the extension of the section to Reedy Glacier. The total mass flux into the ice shelf across the Transantarctic Mountains, calculated in this way, is $(51 \pm 4) \times 10^{12}$ kg/yr.

The other major input term is that of mass accumulation on the surface of the ice shelf, which was calculated by planimeter from the map shown in Figure 10.5. The total mass input so calculated is 23×10^{12} kg/yr, which corresponds to a mean accumulation rate of 140 kg m^{-2} yr^{-1} over the area of 160,000 km^2.

The error in the mass input at the surface was taken to be $\pm 5 \times 10^{12}$ kg/yr, or about 20 percent. This is a conservative estimate, since it is the same percentage as that found for all Antarctica by Giovinetto (1964) in his thorough analysis of errors, even though both the error in individual measurements and the error due to temporal variability are substantially less in the radioactive-fallout method of Clausen et al. (1979) than in the pit-and-stake method to which Giovinetto's (1964) analysis applied.

The output perimeter for the grid eastern section was taken along the RISS line (Figure 10.4). The flux through that perimeter was calculated to be $(55 \pm 6) \times 10^{12}$ kg/yr (61 ± 6 km^3/yr), using velocities from Dorrer et al. (1969) and ice thicknesses determined from the RIGGS ice thickness map between Ross Ice Shelf Survey station R5 (grid coordinates 11.7°S, 2.3°E) and the western limit of the flow band and including a flux of 1 km^3/yr grid east of RISS station R5, as calculated by Giovinetto and Zumberge (1968). Since the outflow perimeter was 75 km or more back from the front of the ice shelf, the region near

the ice front where melting at the underside of the ice shelf is known to be large (Crary 1961; Giovinetto and Zumberge 1968) was excluded. Consequently, no a priori estimate of bottom melt has been included.

The standard error in the outflow has been estimated at ±10 percent, again a conservative figure, since the errors in mean ice thickness, and the length of the outflow perimeter are both about 5 percent, and the error in the movement rates is less than 1 percent (Giovinetto and Zumberge 1968).

The total mass input, $(74 \pm 6) \times 10^{12}$ kg/yr, and output, $(55 \pm 6) \times 10^{12}$ kg/yr, differ significantly at the 95 percent confidence level. The difference is $(19 \pm 8) \times 10^{12}$ kg/yr, or 26 ± 11 percent of the input. [This is about 40 percent as large as the difference $(48 \pm 29 \times 10^{12}$ kg/yr) between mass input and output calculated by Giovinetto et al. (1966) for the whole East Antarctic drainage system feeding into the Ross Ice Shelf through the Transantarctic Mountains.] The implication, then, is that the ice is currently flowing into the ice shelf at a rate faster than it is flowing out. The difference is equivalant to a mean of 130 ± 50 mm/yr as the sum of the rates of increase in ice thickness and bottom melting rate for the grid eastern ice shelf. This means that if the ice shelf is in steady state, the average basal melting rate behind the output perimeter must be (130 ± 50) mm/yr. If the melting rate is less, the ice shelf must be thickening correspondingly.

West Antarctic Input

For the portion of the Ross Ice Shelf fed from West Antarctica, there is no complete measurement of mass input by glacial flow. However, we can compare the total mass accumultion rate on the West Antarctic drainage basin and Ross Ice Shelf with the outflow, using recent evidence. The map of accumulation rate on the ice shelf (Figure 10.5) shows a large central region of accumulation rates less than 120 kg m^{-2} yr^{-1}. By extrapolating this region through the adjacent portion of West Antarctica, where there are no data, to connect with a similar accumulation minimum grid northeast of Byrd Station (see map in Bentley et al. 1964), an accumulation map for the whole drainage basin has been drawn (Figure 10.6). This leads to a mass input $(150 \pm 30) \times 10^{12}$ kg/yr, corresponding to an average accumulation rate of 125 ± 25 kg m^{-2} yr^{-1} over the area of 1.2×10^{6} km^2. An error estimate of ±20 percent has been adopted, as previously explained.

The mass flux out was calculated as follows. From the boundary line dividing East Antarctic and West Antarctic outflow along the RISS track (Dorrer et al. 1969) to the flow line that forss the grid eastern limit of flow band MNOPQR in Thomas and Bentley (1978a) (Figure 10.4), an average ice thickness of 325 m was taken from the RIGGS ice thickness map, and a mean velocity of 872 m/yr was calculated from the RISS work (Dorrer et al. 1969). The cross-sectional length is 235 km. This leads to a flux of 60×10^{12} kg/yr. The outflow from the Thomas and Bentley (1978a) flow band is 41 km^3/yr corresponding to 37×10^{12} kg/yr. There remains a small section between Edward VII Peninsula and the grid western side of Thomas and Bentley (1978a) flow band (Figure 10.4); here estimates of 300 m/yr for the velocity, 340 m for the ice

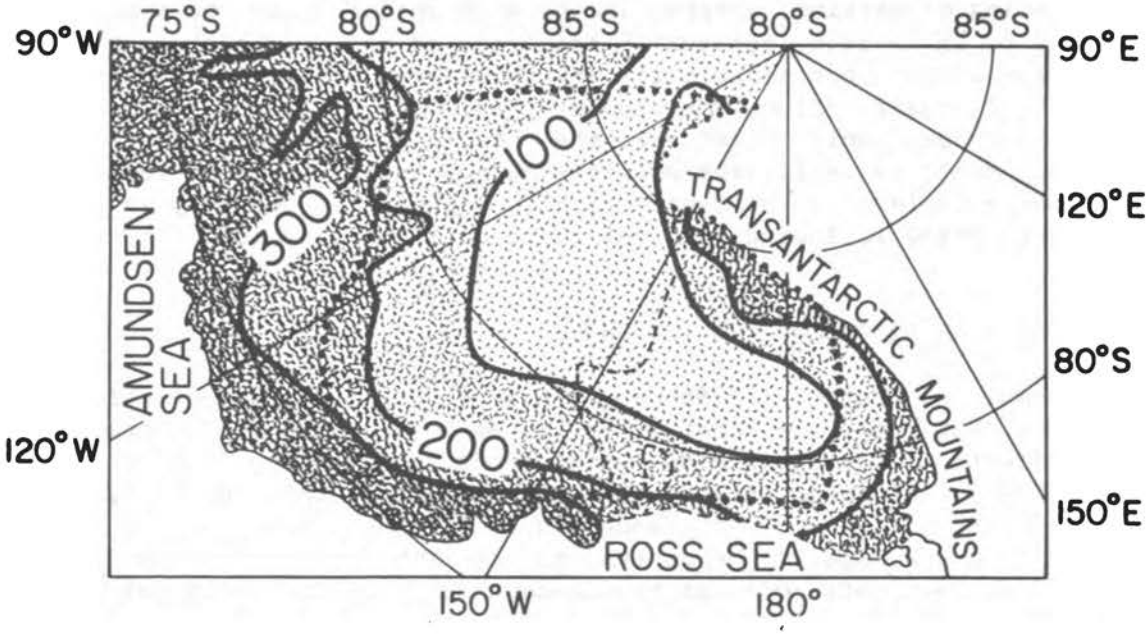

FIGURE 10.6 Surface balance rate (mm/yr) West Antarctic/Ross Ice Shelf system.

thickness, and 46 km for the cross-sectional length lead to a mass flux out of 4×10^{12} kg/yr. Adopting an error of ±10 percent, as on the grid eastern part of the ice shelf, leads to a total output estimate of $(101 \pm 10) \times 10^{12}$ kg/yr. The input and output are thus not significantly different at the 95 percent confidence level. However, since the errors were conservatively chosen, the implication of a real difference is again strong. The excess, $(49 \pm 32) \times 10^{12}$ kg/yr, is (33 ± 21) percent of the input, or a mean of 0.20 m/yr for the thickening-plus-melt rate for the grid western portion of the shelf. For steady state to exist without bottom melting, the mean accumulation rate over the whole drainage system would have to be less than 90 kg m^{-2} yr^{-1} (90 mm equivalent water thickness per year), a figure that is unacceptably low.

There is an important difference in the nature of the flux differences in the two cases discussed. For the grid western ice shelf, the input is calculated entirely from snow accumulation rates <u>within the past 25 years</u>. The response time of the glacial system to a varying input is certainly much larger than 25 years, so the excess input could simply reflect a snowfall in the past few decades that is 33 ± 21 percent larger than the long-term mean. For the grid eastern ice shelf, on the other hand, the snowfall input is only 30 percent of the total input, so the flux difference nearly equals the accumulation rate--the long-term mean accumulation rate would have to be nearly zero to yield balance. Thus, the evidence for real <u>dynamical</u> imbalance and/or bottom melt is stronger in the grid east than in the grid west, even granted a <u>mass</u> imbalance in both areas.

It should be noted further that a positive flux difference in the grid eastern sector means directly that the ice shelf itself is either

thickening or melting, whereas in the grid western part there might simply be an average increase in thickness of the ice in the entire drainage system, not necessarily any thickening or melting of the Ross Ice Shelf itself. Since the studies previously mentioned (Thomas and Bentley 1978a) imply indeed that the thickening-plus-melting rate for the ice shelf is small, the positive mass balance, if it is real, would suggest a buildup of the West Antarctic inland ice, possibly in a recovery phase following a former surge of the inland ice.

TEMPORAL VARIATIONS OF THE ICE SHELF

Thomas and Bentley (1978b) and Lingle (1984) modeled the retreat of the West Antarctic ice sheet after the Holocene maximum. Incorporating the effects of sea-level rise, which tends to force the grounding line to retreat, and shear stress along the margins of the ice shelf, which tend to inhibit retreat, the modeling shows that retreat of the ice sheet from the edge of the continental shelf began about 15,000 years before present (BP) and that the present-day Ross Ice Shelf was largely established by about 7000 yr BP. An important result of these calculations is that buttressing of the inland ice sheet by the bounded ice shelf probably prevented a much deeper penetration of the grounding line into the interior of West Antarctica, perhaps reducing the entire marine portion of the inland ice to an ice shelf or removing it altogether. Interpretation of the isostatic gravity anomalies in the Ross Embayment (Greischar and Bentley 1980) supports the history of ice-sheet retreat deduced from the modeling studies. Long-wavelength isostatic gravity anomalies show a clear trend of increasingly negative values from about 0 near Ross Island to -15 mgal near the Siple Coast (Bentley et al. 1982), which is consistent with incomplete rebound from a former crustal depression resulting from glacial loading and a relative maximum over the central part of the ice shelf, which implies early crustal unloading in an area where, according to the model results, the grounding line first retreated. Greischar and Bentley (1980) calculated that, in the absence of changes in the ice sheet from other causes, isostatic uplift will cause a readvance of the grounding line at rates of 25-200 m/yr, eventually reaching a position running roughly from Roosevelt Island to Beardmore Glacier.

On a shorter time scale, there is evidence suggesting that the state of the ice shelf varies considerably over periods of several hundred years. Bentley (1981) observed both transverse and longitudinal variations (i.e., variations along a flow line) in basal reflectivity and signal strengths from internal layers as recorded on radar sounding of a section of the ice shelf comprising ice flowing from a group of valley glaciers between Beardmore and Nimrod Glaciers (Figure 10.7). Correlation between individual glacier bands was good enough to yield a striking pattern of large variations in reflection characteristics every few centuries for some 1400 years. Although he proposed no specific causal mechanism for these variations, Bentley (1981) suggested that they are related to fluctuations in the grounding lines of the valley glaciers induced by climatic changes. This idea is supported by a correspondence

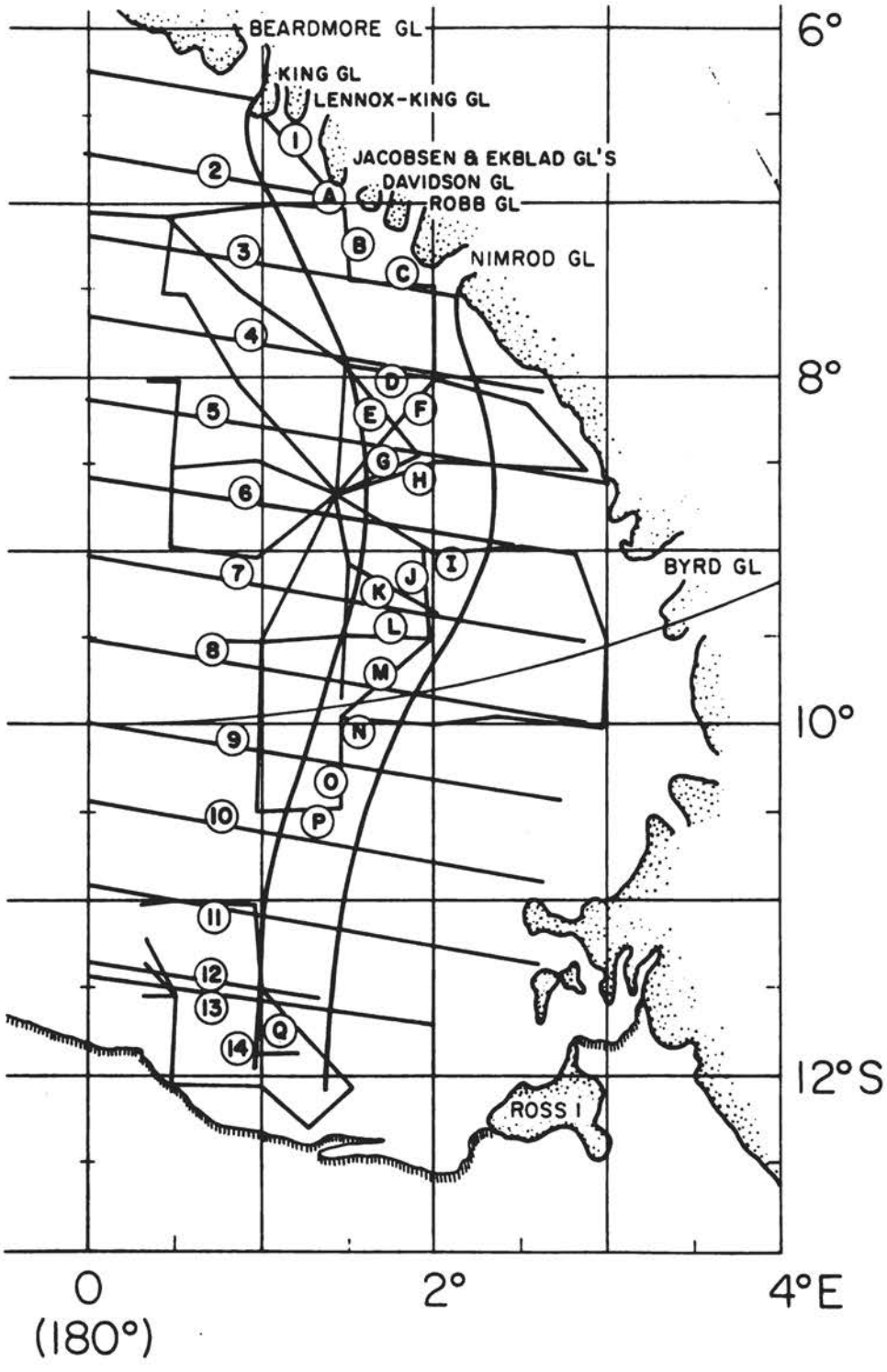

FIGURE 10.7 Map of grid eastern portion of the Ross Ice Shelf, showing the relationship of flight lines to the Transantarctic Mountain glaciers and the ice-shelf flow band. The numbered and lettered lines denote NSF/SPRI/TUD and RIGGS flights, respectively.

between the glacial variations with time and oxygen isotope ratios in ice cores from Byrd Station (Johnsen et al. 1972) and Dome C (Lorius et al. 1979)(Figure 10.8). Unfortunately, the glacial record for the last 200 years is missing, owing to poorly known velocities close to the mouths of the alpine glacier.

The flow band from Nimrod Glacier itself, however, shows no significant deviations from zero for the thickening-plus-melting rate (Figure 10.9). The most likely interpretation of this is that the rates of thickening and of bottom melting are separately small and that neither has changed much over the last 1500 years. If so, and if Nimrod Glacier is typical of East Antarctic outlet glaciers cutting the Transantarctic Mountains, then the implication is that the mass flux of East Antarctic inland ice into the Ross Ice Shelf has been steady over that period of time. Furthermore, since the conditions controlling bottom balance rates are unlikely to be related to the flow bands (except perhaps close to the glacier mouths), it is reasonable to conclude that the bottom balance rates over a much more extensive area of the ice shelf, determined by the subglacial oceanic circulation pattern, have probably remained little changed over the last fifteen centuries.

The small thickening-plus-melting rate for the Nimrod Glacier flow band contrasts with the large positive value for the whole grid eastern part of the ice shelf. If both numbers are correct, then different parts of the shelf must behave differently. One might speculate, for example, that the thick ice of the Byrd Glacier flow band is undergoing particularly strong melting.

If one examines the fluxes in the alpine glacier bands, very large relative changes can be seen--up to a factor of 10 for one of them (Figure 10.9). The flux changes are not coherent between glacier bands, nor are their changes large enough in total volume to affect the overall picture for the ice shelf. Nevertheless, the alpine glacier variations do show that large local changes, presumably climatically controlled, can take place on time scales on the order of centuries.

Further evidence of recent changes in the ice shelf comes from an analysis by Jezek (1984) of reflectors in the ice shelf downstream of Crary Ice Rise. Although the nature of the reflectors has not been determined, they can be traced downstream across the ice shelf. These tracks were found to cut across the flow lines drawn on the basis of present-day velocities (Figure 10.10). Jezek (1984) interpreted this as a lateral migration of the source of the reflector, which he believes to be the grid eastern margin of Crary Ice Rise, in the sense of an areally shrinking ice rise, with the most rapid change occurring about 400 years ago. That the fluctuations in the ice shelf are regionally controlled is suggested by the additional observation of a discrepancy between a reflector track near the Siple Coast and the associated velocity vectors. A steady-state ice shelf for the last 200 years is implied by the parallelism of the reflector tracks and velocity vectors near the sources of the reflectors both at Crary Ice Rise and on the Siple Coast.

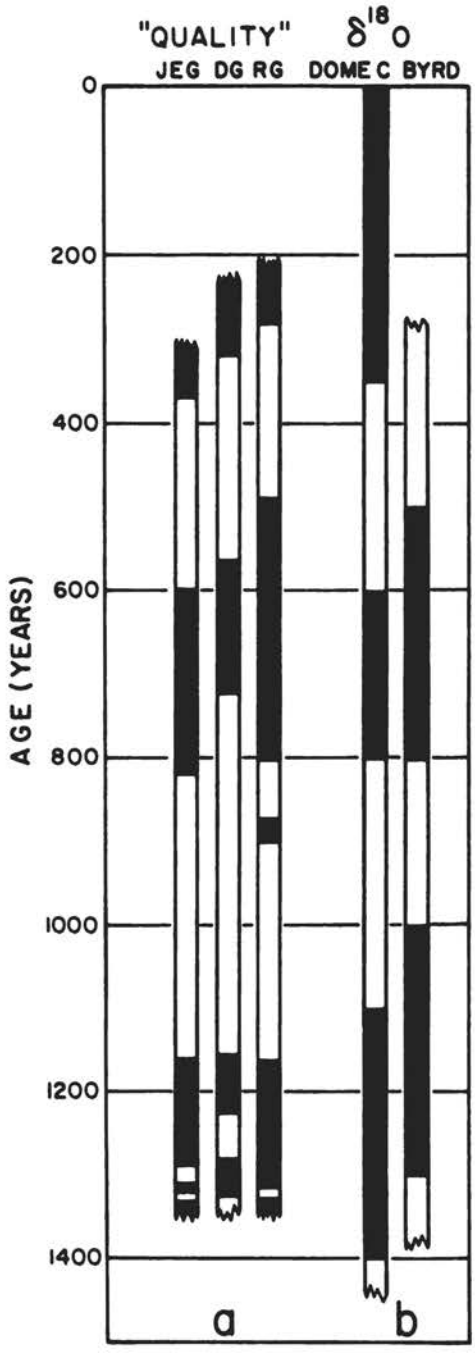

FIGURE 10.8 (a) "Quality" versus residence time on the ice shelf for the bands corresponding to Jacobsen and Ekblad glaciers (JEG), Davidson Glacier (DG), and Robb Glacier (RG). Black sections have high "quality," as defined in Bentley (1981), compared with that in white sections. (b) Oxygen isotope ratios versus age in drill holes at Dome C (East Antarctica) and Byrd Station (West Antarctica). Black sections correspond to relatively high $\delta^{18}O$ values (algebraically), i.e., warmer temperatures; white sections to relatively low $\delta^{18}O$ values.

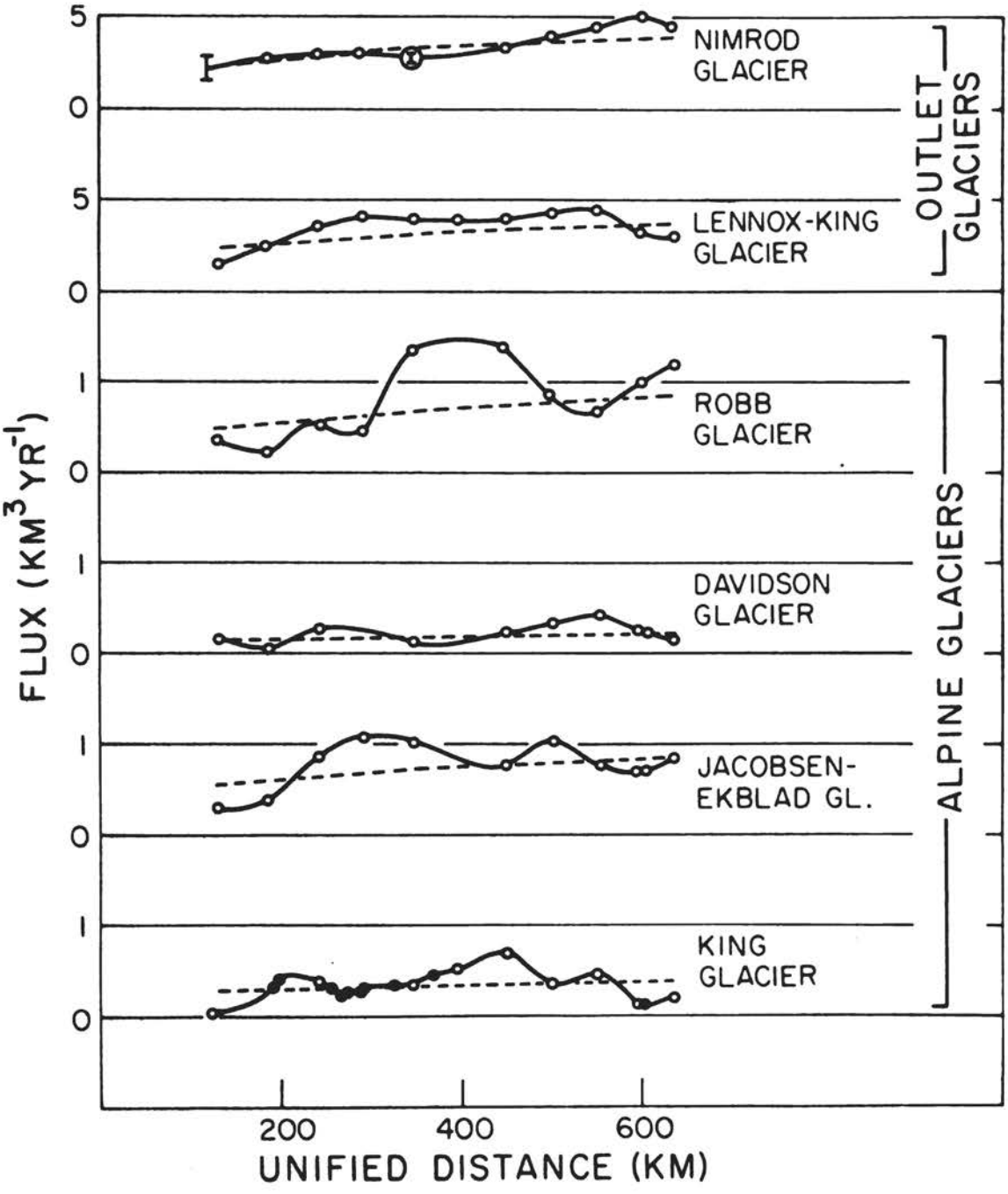

FIGURE 10.9 Fluxes from the glaciers feeding the band delineated in Figure 10.7. Note the different flux scales for the outlet and alpine glaciers. The "unified distance" is a scale with an adjustable zero point chosen to make the plotted distances approximately equivalent to the same residence time on the ice shelf for each glacier band.

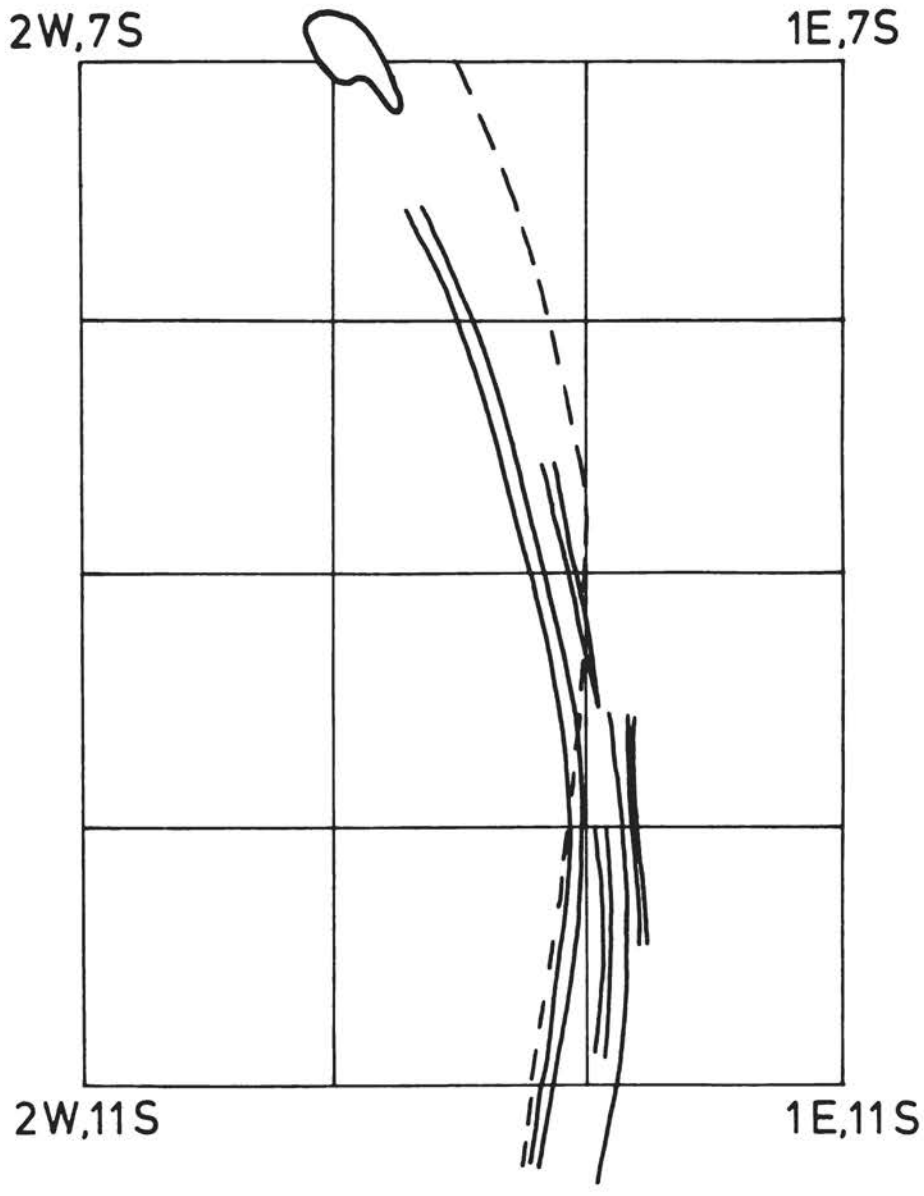

FIGURE 10.10 Debris tracks (heavy lines) and a flow line (dashed line) based on the velocity vectors downstream of Crary Ice Rise.

CONCLUSIONS

1. The Ross Sea drainage system of the West Antarctic Ice Sheet is probably gaining mass at present.
2. The grid western Ross Ice Shelf is now in, or close to, steady state, and has been over the last two centuries.
3. The Ross Ice Shelf is capable of noticeable changes in its dynamics on a century time scale.

4. The fluxes from Transantarctic alpine glaciers show changes as large as an order of magnitude with pseudoperiods of a few centuries, but the flux from at least one outlet glacier (Nimrod) appears to have been steady for the last millenium and a half.
5. The apparent contradiction between the input-outflow difference for the entire East Antarctic-fed part of the Ross Ice Shelf, which is significantly positive, and that for the Nimrod Glacier flow band, which is close to zero, suggests that melting rates or thickening rates (or both) vary strongly across the ice shelf.

REFERENCES

Albert, D. G., C. R. Bentley, and L. L. Greischar, 1978. Submarine topography of the Ross Embayment from the continental shelf to the Byrd Subglacial Basin (abstract). Transactions American Geophysical Union, 59(4), 30.

Bentley, C. R., 1981. Variations in valley glacier activity in the Transantarctic Mountains as indicated by associated flow bands in the Ross Ice Shelf. In Sea Level, Ice and Climatic Change, International Association of Hydrological Sciences Publication No. 131, pp. 247-251.

Bentley, C. R., 1984. The Ross Ice Shelf Geophysical and Glaciological Survey (RIGGS): Introduction and summary of measurements performed. Antarctic Research Series, vol. 42, American Geophysical Union, Washington, D.C., pp. 1-20.

Bentley, C. R., and K. C. Jezek, 1982. RISS, RISP and RIGGS: Post-IGY glaciological investigations of the Ross Ice Shelf in the U.S. programme. Journal of the Royal Society of New Zealand, 11(4), 355-372.

Bentley, C. R., R. L. Cameron, C. Bull, K. Kojima, and A. J. Gow, 1964. Physical characteristics of the Antarctic ice sheet. Antarctic Map Folio No. 2, American Geographical Society, New York.

Bentley, C. R., J. W. Clough, K. C. Jezek, and S. Shabtaie, 1979. Ice thickness patterns and the dynamics of the Ross Ice Shelf. Journal of Glaciology, 24(90), 287-294.

Bentley, C. R., J. D. Robertson, and L. L. Greischar, 1982. Isostatic gravity anomalies on the Ross Ice Shelf, Antarctica. In C. Craddock (ed.), Antarctic Geosciences, University of Wisconsin Press, pp. 1077-1081.

Clausen, H. B., W. Dansgaard, J. O. Nielsen, and J. W. Clough, 1979. Surface accumulation on Ross Ice Shelf. Antarctic Journal of the U.S., XIV(5), 68-72.

Crary, A. P., 1961. Glaciological studies at Little America Station, Antarctica, 1957 and 1958. IGY Glaciological Report Series, no. 5. IGY World Data Center A, Glaciology, American Geographical Society, New York.

Dorrer, E., W. Hoffman, and W. Seufert, 1969. Geodetic results of the Ross Ice Shelf survey expeditions, 1962-1963 and 1965 and 1966. Journal of Glaciology, 8(52), 67-90.

Giovinetto, M., 1964. The drainage systems of Antarctica: Accumulation. In M. Mellor (ed.), Antarctic Snow and Ice Studies, Antarctic Research Series, No. 2, American Geophysical Union, Washington, D.C., pp. 127-155.

Giovinetto, M., and J. H. Zumberge, 1968. The ice regime of the eastern part of the Ross Ice Shelf drainage systems. International Association of Hydrological Sciences Publication No. 79 (IUGG/IASH General Assembly, Berne, 1967), pp. 255-265.

Giovinetto, M. B., E. S. Robinson, and C. W. M. Swithinbank, 1966. The regime of the western part of the Ross Ice Shelf drainage system. Journal of Glaciology, 6(43), 55-68.

Greischar, L. L., and C. R. Bentley, 1980. Isostatic equilibrium grounding line between the West Antarctic ice sheet and the Ross Ice Shelf. Nature, 283(5748), 651-654.

Hayes, D. E., and F. J. Davey, 1975. A geophysical study of the Ross Sea, Antarctica. Initial Reports of the DSDP 28, pp. 887-907.

Hughes, T. J., 1975. The West Antarctic ice sheet: Instability, disintegration, and initiation of ice ages. Reviews of Geophysics and Space Physics, 13(4), 502-526.

Jezek, K. C., 1984. Recent changes in the dynamic condition of the Ross Ice Shelf, Antarctica. Journal of Geophysical Research, 89(B1) 409-416.

Jezek, K. C., and C. R. Bentley, 1983. Field studies of bottom crevasses in the Ross Ice Shelf, Antarctica. Journal of Glaciology, 29(101), 118-126.

Jezek, K. C., and C. R. Bentley, 1984. A reconsideration of the mass balance of a portion of the Ross Ice Shelf. Journal of Glaciology, 30(106), 381-384.

Johnsen, S. J., W. Dansgaard, H. B. Clausen, and C. C. Langway, Jr., 1972. Oxygen isotope profiles through the Antarctic and Greenland ice sheets. Nature, 235(5339), 429-434.

Lingle, C. S., 1984. A numerical model of interactions between a polar ice stream and the ocean: Application to Ice Stream E, West Antarctica. Journal of Geophysical Research, 89(C3), 3523-3549.

Lorius, C., L. Merlivat, J. Jouzel, and M. Pourchet, 1979. A 30,000-yr isotope climatic record from Antarctic ice. Nature, 280, 644-648.

MacAyeal, D. R., and R. H. Thomas, 1979. Ross Ice Shelf temperatures support a history of ice-shelf thickening. Nature, 282, 703-705.

Neal, C. S., 1979. Dynamics of the Ross Ice Shelf as revealed by radio echo sounding. Journal of Glaciology, 24(90), 295-307.

Robertson, J. D., C. R. Bentley, J. W. Clough, and L. L. Greischar, 1982. Sea bottom topography and crustal structure below the Ross Ice Shelf, Antarctica. In C. Craddock (ed.), Antarctic Geoscience, University of Wisconsin Press, pp. 1083-1090.

Rose, K. E., 1979. Characteristics of ice flow in Marie Byrd Land, Antarctica. Journal of Glaciology, 24(90), 63-75.

Swithinbank, C. W. M., 1963. Ice movement of valley glaciers flowing into the Ross Ice Shelf, Antarctica. Science, 141(3580), 523-524.

Thomas, R. H., and C. R. Bentley, 1978a. The equilibrium state of the eastern half of the Ross Ice Shelf. Journal of Glaciology, 20(84), 509-518.

Thomas, R. H., and C. R. Bentley, 1978b. A model for Holocene retreat of the West Antarctic ice sheet. Quaternary Research, 10, 150-170.

Thomas, R. H., D. R. MacAyeal, and D. H. Eilers, 1984. Glaciological studies on the Ross Ice Shelf, Antarctica, 1973-78. Antarctic Research Series, vol. 42, American Geophysical Union, Washington, D.C., pp. 21-53.

ATTACHMENT 11

ANTARCTIC MASS BALANCE: GLACIOLOGICAL EVIDENCE FROM ANTARCTIC PENINSULA AND WEDDELL SEA SECTOR

C. S. M. Doake
British Antarctic Survey

INTRODUCTION

Stretching northward to within 1000 km of South America, the Antarctic Peninsula is the closest part of Antarctica to any other continent and reaches to the lowest latitudes. The climate is generally the warmest in Antarctica, and the peninsula has the highest snowfall. With mountain peaks more than 2000 m high along most of its 1500 km length, the peninsula acts as a topographic barrier separating the atmospheric circulation patterns over the Pacific Ocean to the west from those over the Weddell Sea to the east. Two distinct climatic regimes can be recognized, with a divide close to the eastern escarpment of the peninsula. Temperatures are up to 7°C lower on the Weddell Sea side, where the temperature regime is dominated by extensive sea ice. The Weddell Sea contains the most persistent sea ice, which in summer can account for half the total amount around Antarctica.

Ice shelves fringe the coast of the Antarctic Peninsula, but whereas on the Weddell Sea side the Larsen Ice Shelf reaches almost to the northern extremity of the peninsula at 64°S, on the western side ice shelves extend only as far north as 67°S. The apparent existence of the ice shelves close to their climatic limit and the recent retreat of their ice fronts suggests that they should react sensitively to changes in atmospheric or oceanic temperatures or to shifts in accumulation patterns.

Much of both the East and West Antarctic ice sheets drain into the Ronne-Filchner Ice Shelves, which together make the largest ice shelf by volume and which form the southern boundary of the Weddell Sea. Cold water produced by melting on the underside of the ice shelf flows into the Weddell Sea where mixing with saline waters released by sea-ice formation helps to create Antarctic Bottom Water. A lobe of thin ice in the center of the Ronne Ice Shelf is the result of flow being impeded by a locally grounded area between Korff and Henry ice rises; thinning of the ice shelf by only a few meters would remove this restriction and reduce the restraint on the inland ice sheet.

On the sub-Antarctic island of South Georgia, evidence of glacial retreat over the past hundred years can be recognized from terminal moraines.

MASS BALANCE

The total area of grounded ice in Antarctica is about 12 x 10^6 km^2 (Drewry et al. 1982). Recent estimates of accumulation rates have been made using emissivity values mapped at 31 GHz by the NIMBUS-6 satellite's scanning microwave spectrometer (SCAMS) (Rotman et al. 1982). By combining these data with the generalized map of Antarctic surface elevations (Revelle 1983), the resulting estimates of net accumulation over Antarctica, split into ten regions (Figure 11.1) are shown in Table 11.1. Five isohydropleths have been used, giving six categories for accumulation in each region. The drainage basins for the Ronne, Filchner, Amery, and Ross Ice Shelves were taken from selected ice flow lines on the surface elevation map of the Scott Polar Research Institute Antarctic folio series [Drewry (ed.) 1983]. The total accumulation over the Antarctic Peninsula has also been calculated using measured values of accumulation rate at various sites (R. Frolich, personal communication). The measurements were made using different techniques, including oxygen-isotope layering, ß-activity, shallow seismic refraction studies, and snow stakes. There are sufficient values to construct curves of accumulation against altitude for different regions and to sum the accumulation within every 500-m contour interval. The total accumulation is given in Table 11.1. Table 11.2 shows that nearly one quarter of the Antarctic ice sheet flows into the Ronne-Filchner Ice Shelves, and almost one quarter of the total accumulation for Antarctica falls over the Antarctic Peninsula and catchment areas, which eventually connect with the Weddell Sea. The high accumulation rate over the Antarctic Peninsula means that it receives 8 percent of the total accumulation while covering only 2.5 percent of the grounded ice area. However, even a gross change in the net accumulation would have a small effect on sea level: the volume of the net annual accumulation for the peninsula of about 226 km^3 of water equivalent corresponds to removing an average of only 0.6 mm from the surface of the world's ocean. Sea level would rise on average by 0.5 m if all the grounded ice in the peninsula (about 180 x 10^3 km^3) were to melt. The figure in Table 11.1 for total accumulation in Antarctica of 2685 km^3 is higher than some earlier estimates, largely because of the high accumulation rates determined from the satellite data at 77-79°S, 20°W-40°E, and 73-76°S, 60-90°W; areas comprising almost 20 percent of the total (Rotman et al. 1982). Data from stable isotope ratios and ß-activity profiles taken in the Antarctic Peninsula confirm the satellite-derived accumulation rates there (Peel and Clausen 1982), but near the coast around East Antarctica there is more uncertainty about the values.

There are great uncertainties about how much ice is lost each year because of lack of measurements of ice thickness and velocity around the periphery of the ice sheet. It is not feasible to give an accurate figure for the mass balance of the Antarctic Peninsula, and other evidence has to be examined to decide whether the ice sheet there is shrinking or growing.

TABLE 11.1 Accumulation (km^3 water equivalent) over Ground Ice in Various Catchment Areas

Region[a]	Accumulation (cm)							
	5	5-10	10-20	20-30	30-40	40	Total	% of Total
Antarctic Peninsula	--	--	--	--	--	226	226	8.4
Ronne Ice Shelf, WA	--	0	5	10	37	181	233	8.7
Ronne Ice Shelf, EA	17	21	5	1	2	--	46	1.7
Filchner Ice Shelf, EA	42	38	24	50	24	9	187	7.0
30°W - Amery	--	6	34	48	143	339	570	21.2
Amery	8	46	60	23	70	--	207	7.7
Amery-Ross	1	45	82	234	277	32	671	25.0
Ross Ice Shelf, EA	50	49	--	--	--	--	99	3.7
Ross Ice Shelf, WA	--	17	49	32	16	7	121	4.5
West Antarctica	--	--	--	--	60	265	325	12.1
Total	118	222	259	398	629	1059	2685	
% of Total	4.4	8.3	9.6	14.8	23.5	39.4		

Average accumulation = 0.22 m

[a]WA, West Antarctica; EA, East Antarctica)

TABLE 11.2 Characteristics of Selected Drainage Basins

Region	Area		Accumulation	
	10^6 km^2	%	km^3	%
Ronne-Filchner Ice Shelves	3.0	24.2	466	17.4
Ross Ice Shelf	2.4	19.3	222	8.3
Antarctic Peninsula	0.3	2.4	226	8.4

ICE-FRONT MOVEMENT

Since the advent of satellite pictures, it has been possible to measure retreat of ice fronts around the Antarctic Peninsula (Doake 1982). Figure 11.2 shows how the Wordie and George VI Ice Shelves have diminished. However, without data on either grounding-line movement or of ice velocity or thickness changes it is not possible to interpret the breakback unambiguously in terms of ice-sheet disintegration. Despite the impressive development of fracture patterns on Wordie Ice Shelf, there does not appear to have been any change in the position of the grounding line; however, early LANDSAT images are difficult to interpret in this region, and no firm conclusions can be drawn. At the southern end of the George VI Ice Shelf there is an area of thin ice and partially sea-ice covered polynya around the Eklund Islands. Reports from travelers 30 years ago suggest that there may have been substantial changes in this area since then, but these suggestions have been difficult to confirm. Retreat of the Larsen Ice Shelf on the northeast corner of the peninsula has been documented and appears to be more than would be expected from episodic calving of icebergs. Again, there are

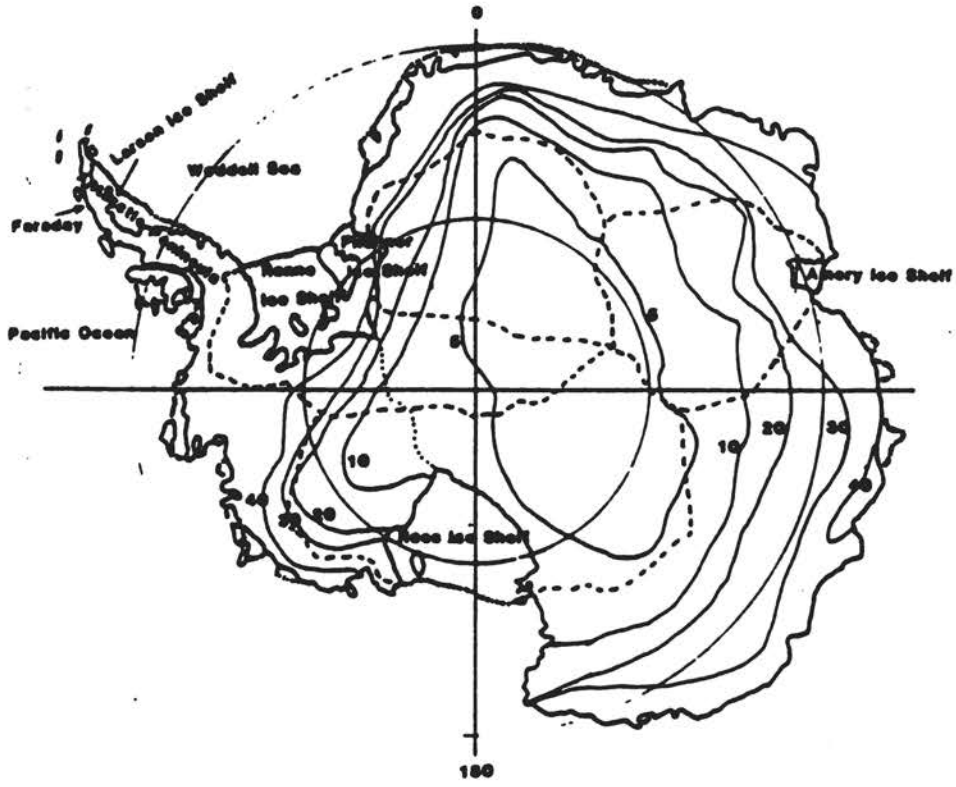

FIGURE 11.1 Isohydropleths (in units of centimeters of water equivalent) over the grounded-ice area of Antarctica (extrapolated from Rotman et al. 1982). Dashed lines indicate catchment areas.

no other measurements of ice thickness or velocity that could be used to help to interpret the ice-front movement.

By way of contrast, the position of Halley station on Brunt Ice Shelf in the eastern Weddell Sea (Figure 11.3) has been accurately measured by a number of techniques since the International Geophysical Year. A recent analysis of the data showed that in about 1972 the velocity of that part of the ice shelf doubled from about 400 to 700 m/yr over a period of about a year and has been almost steady since then (Simmons and Rouse 1985). The position of the ice front has remained practically constant, small pieces being continually eroded with no large icebergs being formed. It appears that the movement of Brunt Ice Shelf may be affected by the complex conditions created by curving past McDonald Ice Rumples and being partially driven by Stancomb-Wills Ice Stream to the north. Conditions do not seem to have altered substantially at the grounding line, where blocks break off periodically and become separate from the inland ice. To the extent that Brunt Ice Shelf appears to consist of large icebergs welded together by accumulation on sea ice, it would seem to be untypical as an Antarctic ice shelf. However, there is no evidence that the sudden increase in velocity at Halley was due to an increase in velocity across the grounding line.

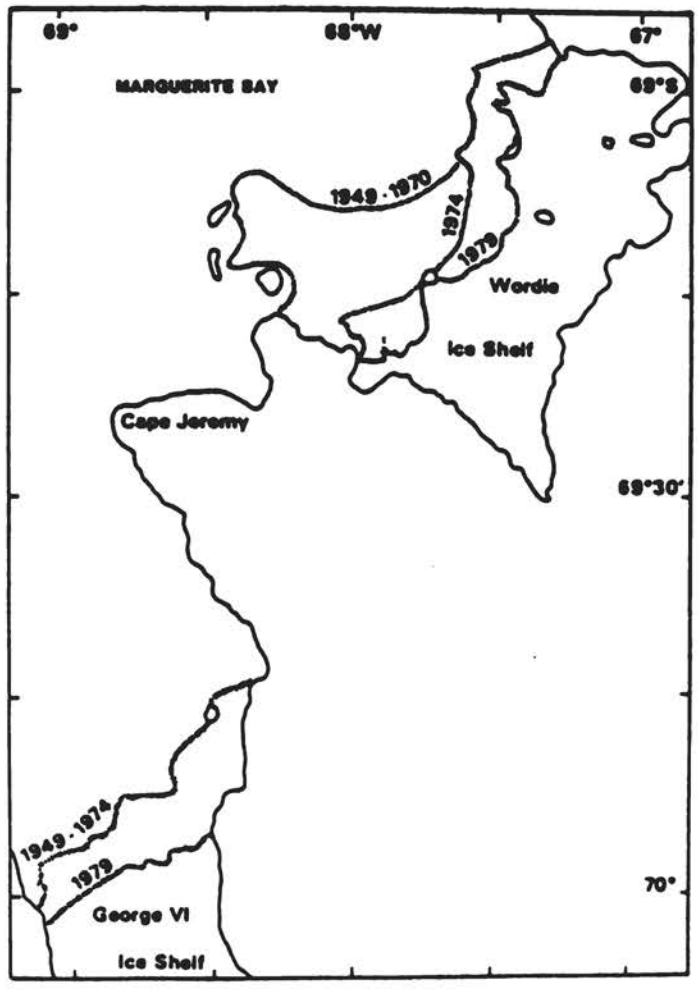

FIGURE 11.2 Receding ice-front positions of Wordie and George VI Ice Shelves.

Recent observations of the shape of the northern ice front of the George VI Ice Shelf suggest that the forward velocity can vary substantially from place to place. Velocities increase from about 100 m/yr on the eastern side to about 700 m/yr on the west (J. R. Potter, personal communication). Although the change in velocity across the ice front may not be completely uniform, the overall pivotal behavior is reminiscent of the movement of Brunt Ice Shelf near Halley.

OCEANOGRAPHY

The physical and chemical properties of the sea under an ice shelf affect the bottom melting or freezing rate. Both the flow of the ice shelf and the final properties of the seawater depend on this interaction, yet it remains one of the least understood of the processes that determine the mass balance of the ice sheet. Measurements of current,

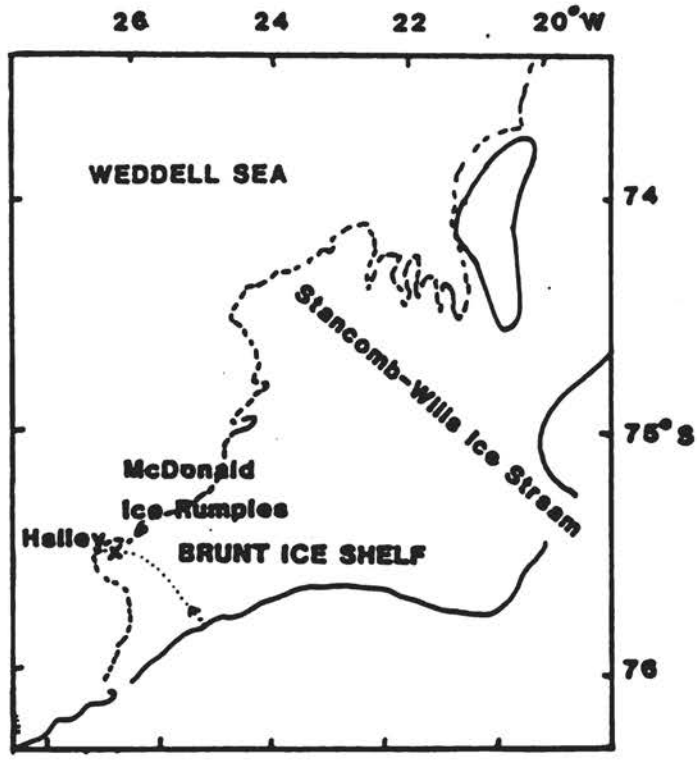

FIGURE 11.3 Map of Brunt Ice Shelf. Dotted line indicates approximate flow line through Halley.

temperature, salinity, and oxygen-isotope ratio with depth have been made at both the northern and southern ends of George VI Sound (Potter and Paren in press). Very slack flow characterizes most of the channel cross section. Temperature against salinity plots for the northern ice front show a linear behavior (Figure 11.4), in accord with a simple process of a closed two-component system in which freshwater ice melts in warm seawater of fixed temperature, salinity, and oxygen-isotope ratio. More complicated plots from the southern ice front suggest that more water components are involved, where the temperature of all but the deepest water is colder than at the northern ice front. Data from elsewhere such as the Ross and Weddell Seas cannot be interpreted so clearly. The accumulation over the catchment area for the George VI Ice Shelf can be calculated accurately, allowing estimates to be made of both the average melt rate and the mean isotope ratio of the melt, assuming steady state. The estimated average melt rate, of around 2 m/yr (Table 11.3), agrees within error limits with the observed currents at the northern ice front. It also falls well within the range of melt rates deduced from measurements on the surface of the ice shelf of ice flow and deformation (Bishop and Walton 1981). Assuming that the relationship between isotope ratio and temperature/altitude observed today has remained unchanged, the mean isotope ratio of the melt, calculated from extrapolating a plot of salinity versus isotope ratio to zero salinity, agrees well with the value expected if there has been no

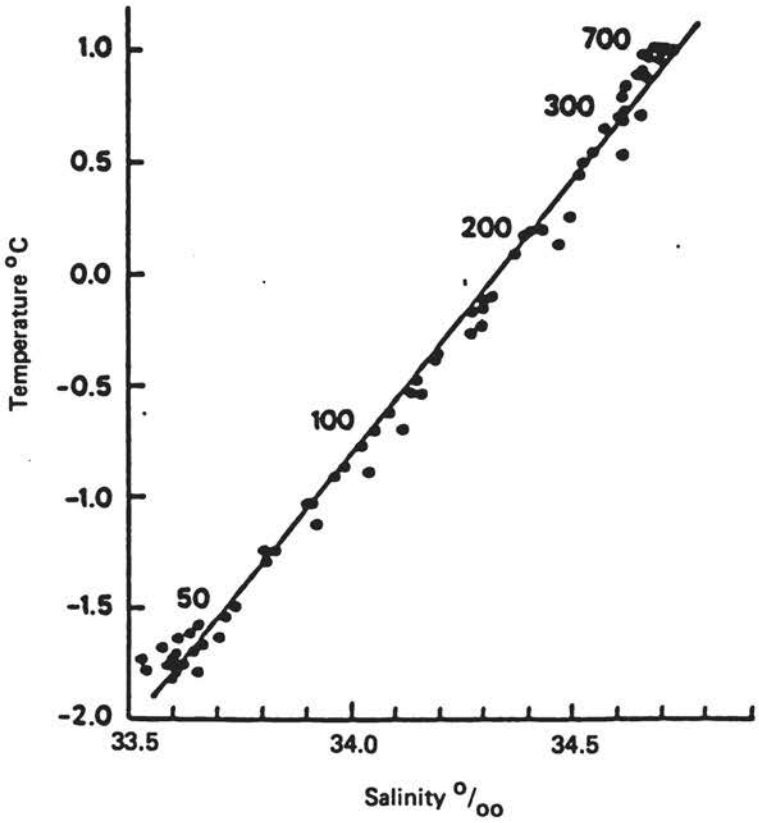

FIGURE 11.4 Temperature-salinity relationship for five sites in George VI Sound. Numbers against the data points indicate depth in meters.

TABLE 11.3 Bottom Melting Rates for Selected Ice Shelves

	Ice Front				Input (km^3/yr)				Melt
	Length	Thick.	Vel.	Calving			Melt	Area	Rate
Ice Shelf	(km)	(km)	(km/yr)	km^3/yr	Inland	Shelf	(km^3/yr)	$10^3 km^2$	(m/yr)
Ross	600	0.25	1.0	150	222	105	177	526	0.3
Ronne	500	0.25	1.1	138	279	190	331	380	0.9
Filchner	180	0.35	1.3	82	187	47	152	93	1.6
Roone and Filchner	--	--	--	220	466	237	483	473	1.0
George VI	--	--	--	4	42	11	49	25	2.0

dramatic change in the altitude distribution of the snow surface in the catchment area over the past few thousand years.

RONNE-FILCHNER ICE SHELVES

Together, the Ronne-Filchner Ice Shelves drain about three-million square kilometers of the Antarctic ice sheet, both East and West. Most of the ice discharged from the inland ice sheet into the ice shelves flows through ice streams. Long-base-length hydrostatic tiltmeters have

been used on Rutford Ice Stream to locate the position of the grounding line accurately, in order to monitor possible changes in the future (Stephenson and Doake 1982). Recently, a rumpled area between Korff and Henry ice rises has been surveyed (Figure 11.5). Large-amplitude surface relief indicates that the ice is grounded, although not strongly enough to form an ice rise. Combining measurements of surface elevation and ice thickness (Figure 11.6) shows that grounding across the rumples has thickened the ice by between 10 and 30 m above that required for it to float (A. M. Smith, personal communication). Downstream of the rumples a lobe of thin ice, around 200 m thick, stretches to the ice front. Restraint across the grounded area reduces the forward velocity, probably to between 10-100 m/yr, effectively blocking flow between the ice rises. The major ice streams draining East and West Antarctica are diverted to the east of Henry Ice Rise and to the west of Korff Ice Rise, respectively. Further study is needed to find out if the rumpled area is an ephemeral feature or whether it plays a critical role in determining the outflow from the ice sheet.

Radio echo measurements indicate strong bottom melting over most of the Ronne-Filchner Ice Shelves apart from the thin central area (Robin et al. 1983). Using estimates at the ice fronts of thickness, velocity, and total length gives the amount of ice expected to be lost by calving when averaged over a period of several years and assuming that the mean position of the ice front remains constant. Combining this estimate with that of the ice input from the catchment area and the accumulation over the ice shelves themselves suggests that the average melt rate for both ice shelves must be around 1.0 m/yr. A similar calculation for Ross Ice Shelf suggests an average melt rate of 0.3 m/yr (Table 11.3). For these three ice shelves the total amount of ice lost by bottom melting could be twice that estimated for all ice shelves given in other attempts to calculate the mass balance (Bardin and Suyetova 1967; Kotlyakov et al. 1978). This gives an indication of the certainty surrounding mass-balance calculations.

ANTARCTIC PENINSULA

Retreat of the ice margin has been observed at a few sites on the west coast of the peninsula in recent years, mainly at occupied stations. It is uncertain to what extent this phenomenon is due to cultural effects, such as increased albedo because of deposition of dirt of various forms. Along the west coast of the peninsula, most sites for stations are chosen on bare rock, so that by definition they are in a zero net accumulation zone. The few accumulation measurements that have been made in the northern part of the peninsula suggest that accumulation initially increases quickly with altitude near the coast. A small shift in the position of the equilibrium line would give an exaggerated effect on the nearly stagnant ice ramps that have been seen to retreat, without necessarily causing any significant change in the overall balance.

The pattern of melt rates deduced over the George VI Ice Shelf from surface measurements of ice movement and deformation (Bishop and Walton

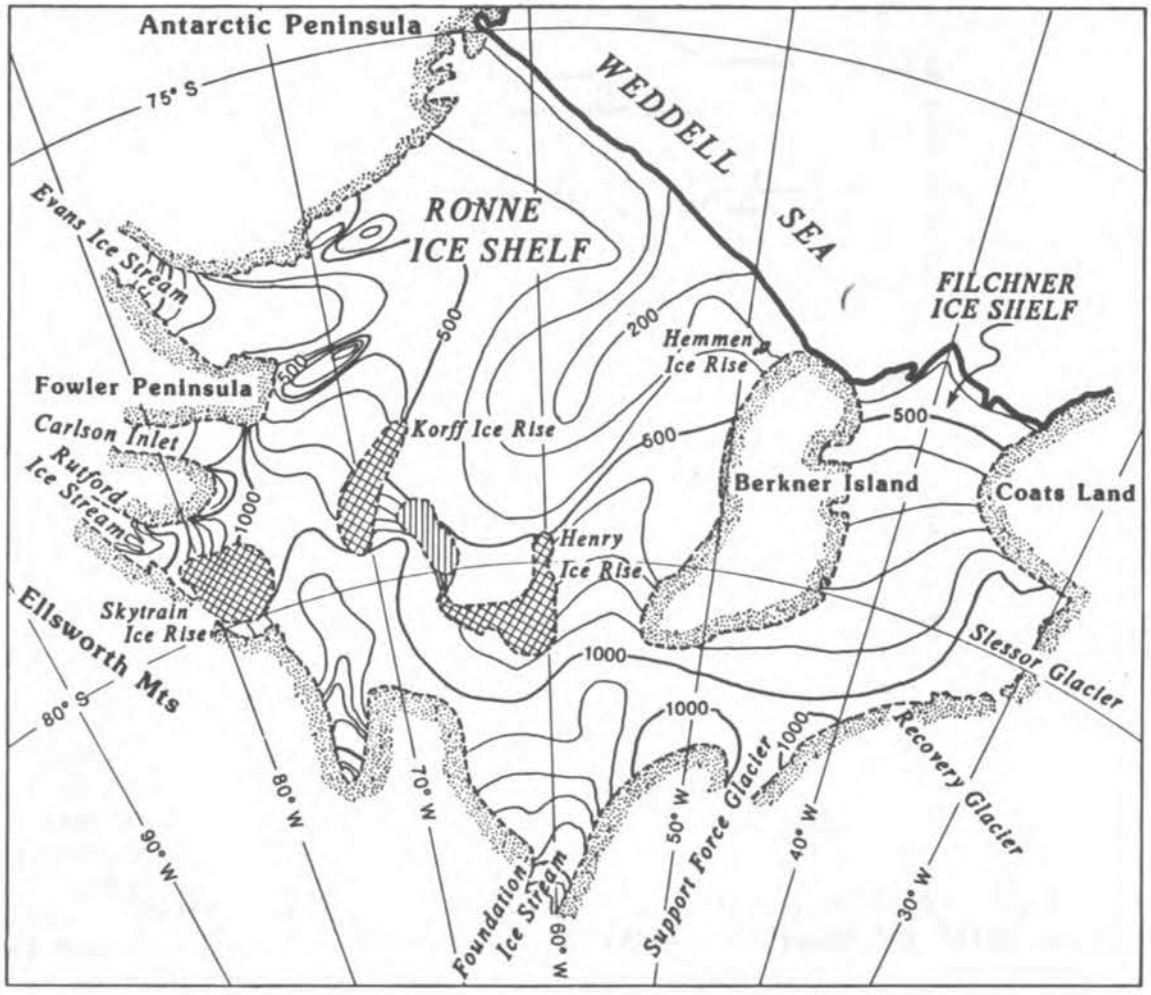

FIGURE 11.5 Ice thickness contours for Ronne-Filchner Ice Shelves.

1981) suggest either that bottom melting is highly variable or that there is a time dependence to the flow distribution. There is no reason to suppose that oceanographic conditions are so inhomogeneous that they could be responsible for the variability, and it seems more reasonable that the complex interaction between all the glaciers feeding the ice shelf can transmit disturbing influence over large distances. Phase-sensitive radio echo sounding should be accurate enough to confirm whether ice thickness is changing with time.

A direct measure of changing ice volume, apart from satellite altimetry, is to measure a surface profile between two fixed rock stations. A 2-km line across a snowfield in the peninsula showed no significant change over the period 1975-1980.

A 19-yr-long tidal record from Faraday station on Argentine Islands shows that there has not been any increase in mean sea level (J. C. Farman, personal communication). A slight fall might be possible, although masked by noise. Gravitational attraction by the ice sheet

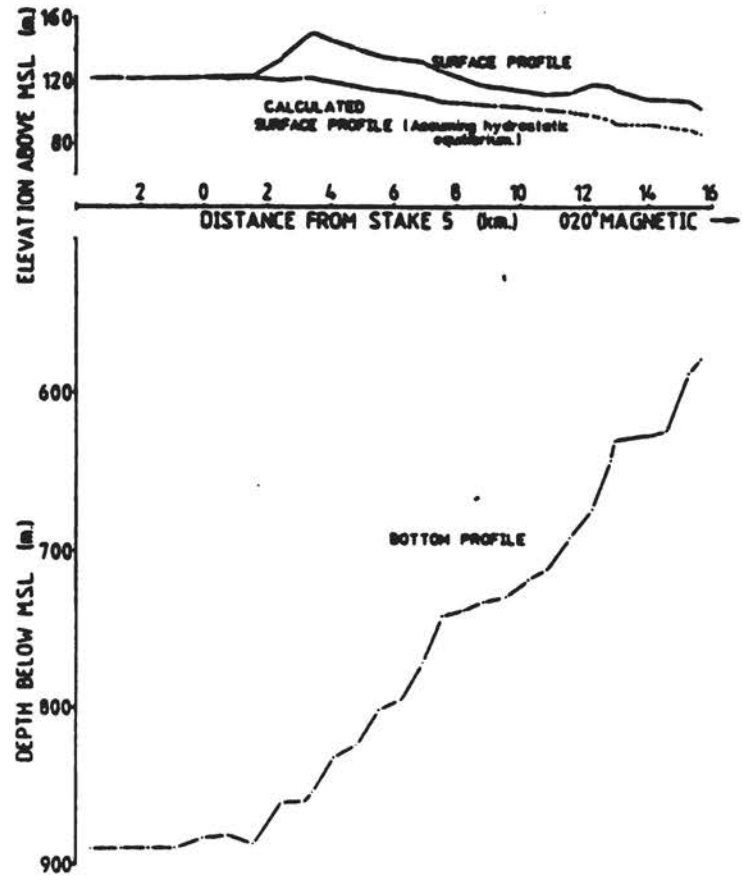

FIGURE 11.6 Surface elevation and bottom profile of ice rumples between Korff and Henry ice rises, Ronne Ice Shelf.

acts in such a way that a decrease in ice volume would lead to a local fall in sea level close to Antarctica. This change could be concealed by other factors, but the tidal data might be taken as indicating that at least there has been no net increase in ice mass over the past two decades.

PINE ISLAND GLACIER

Pine Island Glacier has been suggested as the area showing possibly the greatest potential for rapid ice-sheet disintegration (Stuiver et al. 1981). This conclusion is based on the belief that if sea level rises or if the ice thins then retreat of the grounding line will continue into the heart of the West Antarctic ice sheet until stopped by a high step in the bedrock. Two ratio echo sounding flights in February 1981 crossed Pine Island Glacier (Crabtree and Doake 1982). These data showed that Pine Island Glacier floats on the sea for about 90 km and that the present grounding line appears to be held at the foot of a rock bar about 200 m high. Landsat images have been used to determine the

velocity of the ice front. Using both velocity and thickness data, a simple ice shelf model shows that Pine Island Glacier does not appear to be undergoing any extraordinary behavior. However, this can not be taken as evidence for either that the glacier is necessarily in an equilibrium state now or that it may not in the future suddenly retreat. Mass-flux calculations over the catchment area appear to indicate a positive balance, with the total annual input of 86 $\pm$ 30 km^3 water equivalent exceeding the annual mass flux at the ice front of 25 $\pm$ 6 km^3 water equivalent by a considerable amount. The mass-balance figures are based on sparse data, but the inference of a positive balance is similar to that made for other drainage basins of major outlet glaciers in East Antarctica.

CLIMATIC TRENDS

Meteorological records have been kept since the beginning of the century in the Antarctic Peninsula region. A slight warming has been apparent from the 1940s until the mid-1970s. There is a good correlation between oxygen isotope ratios in a core from the southern Antarctic Peninsula and temperatures recorded at Faraday, 700 km north (D. A. Peel, personal communication). The deepest hole drilled in the peninsula so far has recovered ice 500 years old on James Ross Island (Aristarain et al. 1983).

Retreat of glaciers on South Georgia, which lies just within the Antarctic convergence, has left annual terminal moraines. They document almost continual recession over the past hundred years, with a period of readvance in the 1920s and 1930s (R. J. Timmis, personal communication). Hodges Glacier, South Georgia, was intensively studied as part of the International Hydrological Decade program and also showed continual wastage since the 1950s. This century mass balance correlates well with mean annual air temperature and with percentage of depressions passing to the north of the island.

Sea-ice extent has only been estimated consistently and accurately since satellite observation became possible. There has been no significant long-term trend over the past 10 years (Zwally et al. 1983). However, records from whaling stations show that much greater northerly limits have been achieved this century, with South Georgia being surrounded at times. The connection between sea-ice cover and ice-sheet mass balance is unknown.

CONCLUSION

There is no definitive evidence of significant changes in mass balance in the Antarctic Peninsula or the Weddell Sea area. What data there are suggest a net mass loss rather than gain, but no quantitative estimates can be made.

A change in climate could affect either component of the mass balance--accumulation or ablation. The volume of the total annual accumulation of around 2500 km^3 corresponds to removing an average of almost

7 mm from the surface of the sea. There is great uncertainty in the accumulation figure, and nothing is known about any probable annual variability. However, trends over time scales of the order of decades could give an immediate effect on sea level while being of too short term to start affecting the processes that regulate the discharge, and hence ablation, of ice. Because of the known local variability of accumulation with position, it could be difficult to make sufficient shallow-core measurements to determine statistically significant trends. However, the problem would seem to focus attention on near-surface processes.

Deeper-seated processes influence the flow of ice. An increase in mass loss implies more ice, or its melt, reaching the sea either through ice streams feeding ice shelves or by calving at ice cliffs along the coastline. Once afloat, further melting does not affect sea level although there may be a reaction on the flow of inland ice. In order to determine the influence of climatic change on ablation, it seems necessary to concentrate on factors controlling ice flux across grounding lines. Some of the aspects involved would be ice streams--sliding velocity, marginal crevassing, and side-wall shear; ice shelves--bottom melting, restraint from side-wall shear and ice rise pinning, and calving.

The most direct way of determining changes in ice volume over periods of a few years or decades appears to be by satellite altimetry. Because each drainage basin is likely to react in a different way to changes in climate, and because within a single basin there may be conflicting evidence of change, it is necessary to gather an overall picture. However, areas showing greatest activity are probably those near the margin and characterized by the highest surface slopes. Thus, an altimeter is required that is capable of the necessary accuracy over the steepest slopes expected to be found.

ACKNOWLEDGMENTS

I would like to thank all my colleagues at BAS who have so kindly and generously helped in many ways to prepare this contribution to the workshop.

REFERENCES

Aristarain, A., J. Jouzel, and M. Pourchet, 1983. A 500 year isotope record in James Ross Island snow (Antarctic Peninsula). Abstract IUGG, XVIII, IAMAP, Hamburg.

Bardin, V. I., and I. A. Suyetova, 1967. Basic morphometric characteristics for Antarctica and budget of the Antarctic ice cover. Japanese Antarctic Research Expedition Scientific Reports. Special Issue No. 1, 92-100.

Bishop, J. F., and J. L. W. Walton, 1981. Bottom melting under George VI Ice Shelf, Antarctica. Journal of Glaciology, 27(97), 429-447.

Crabtree, R. D., and C. S. M. Doake, 1982. Pine Island Glacier and its drainage basin: Results from radio echo sounding. Annals of Glaciology, 3, 65-70.

Doake, C. S. M., 1982. State of balance of the ice sheet in the Antarctic Peninsula. Annals of Glaciology, 3, 77-82.

Drewry, D. J. (ed.), 1983. The Surface of the Antarctic Ice Sheet, Sheet 2 of Antarctica: Glaciological and Geophysical Folio. Scott Polar Research Institute, Cambridge.

Drewry, D. J., S. R. Jordan, and E. Jankowski, 1982. Measured properties of the Antarctic ice sheet: Surface configuration, ice thickness, volume and bedrock characteristics. Annals of Glaciology, 3, 83-91.

Kotlyakov, V. M., K. S. Losev, and I. A. Loseva, 1978. The ice budget of Antarctica. Polar Geography, 2(4), 251-262.

Peel, D. A., and H. B. Clausen, 1982. Oxygen-isotope and total beta-radioactivity measurements of 10 m ice cores from the Antarctic Peninsula. Journal of Glaciology, 28(98), 43-55.

Potter, J. R., and J. G. Paren, in press. Interaction between ice shelf and ocean in George VI Sound, Antarctica. Antarctic Research Series, Vol. 43, Oceanology of the Antarctic Continental Shelf.

Revelle, R. R., 1983. Probable future changes in sea level resulting from increased atmospheric carbon dioxide. Changing Climate, National Academy Press, Washington, D.C., pp. 433-448.

Robin, G. de Q., C. S. M. Doake, M. Kohnen, R. D. Crabtree, S. R. Jordan, and and D. Moller, 1983. Regime of the Ronne-Filchner Ice Shelves, Antarctica. Nature, 302(5909), 582-586.

Rotman, S. R., A. D. Fisher, and D. H. Staelin, 1982. Inversion for physical characteristics of snow using passive radiometric observations. Journal of Glaciology, 28(98), 179-185.

Simmons, D. A., and J. R. Rouse, 1985. Accelerating flow of the Brunt Ice Shelf, Antarctica. Journal of Glaciology, 30, 377-380.

Stephenson, S. N., and C. S. M. Doake, 1982. Dynamic behaviour of Rutford Ice Stream. Annals of Glaciology, 3, 295-299.

Stuiver, M., G. H. Denton, T. J. Hughes, and J. L. Fastook, 1981. History of the marine ice sheet in West Antarctica during the last glaciation: A working hypothesis. In G. H. Denton and T. J. Hughes (eds.), The Last Great Ice Sheets. Wiley-Interscience, New York, pp. 319-436.

Zwally, H. J., C. L. Parkinson, and J. C. Comiso, 1983. Variability of Antarctic sea ice and CO_2 change. Science, 220(4601), 1005-1012.

ATTACHMENT 12

ICEBERG DISCHARGE AND THE MASS BALANCE OF ANTARCTICA

Olav Orheim
Norsk Polarinstitutt
Oslo, Norway

INTRODUCTION

Evaluation of the mass balance of Antarctica requires knowledge of input and losses. A number of studies have investigated the mass balance of limited areas or sectors of Antarctica, e.g., Giovinetto and Robinson (1966) and ongoing studies under IAGP. However, such studies cover only part of the Antarctic circumference. Numerous studies have also been published concerning the mass balance for the whole continent. The input--or net accumulation--for Antarctica is probably about 2×10^{15} kg/yr, and several recent estimates have converged around this value following improved data coverage across the continent. Our knowledge of the systematic accumulation pattern over the continent is now so good that the error in this value is probably less than 20 percent. There seems also to be near-consensus among various authors that the total mass balance of Antarctica is positive, even though there are large variations in the estimate of the mass loss (Bull 1971).

The mass loss is mainly in the form of iceberg calving and basal melting. The Ross Ice Shelf Project and other studies in recent years (e.g., D. R. MacAyeal, University of Chicago, unpublished) have led to improved understanding of the melting under the ice shelves, which is perhaps around 0.2×10^{15} kg/yr. There are probably large uncertainties in this figure.

The annual calving rate was estimated by Mellor (1961) as 0.6×10^{15} kg/yr and by Suyetova (1966) as 1×10^{15} kg/yr, with most other estimates between these two figures. However, estimates as high as $2\text{-}3 \times 10^{15}$ kg/yr have also been made (Loser 1973). The uncertainty in the calving loss is probably considerably higher than the combination of all other uncertainties in the total mass balance.

The first large data set on icebergs in the southern ocean has now become available through international cooperation. In this paper I give the first comprehensive presentation of these data, which include more than 30,000 icebergs classified by size, and show that this data set indicates that the rate of iceberg calving from Antarctica has been underestimated.

TABLE 12.1 Iceberg Data on File at Norsk Polarinstitutt

Year	Classified by size	Unclassified	Total
Before 1981	1,924	2,925	4,849
1981-1982	5,062	737	5,799
1982-1983	8,855	2,950	11,805
1983-1984	17,890	3,645	21,535
	33,731	10,257	43,988

THE ICEBERG DATA

Only very limited Antarctic iceberg data were available before 1980. The most comprehensive sets published by various Soviet authors covered 1663 bergs. Orheim (1980) published size statistics on 2119 bergs observed on the Norwegian Antarctic Research Expedition (NARE) 1978-1979 and showed that former statistics seemed to be biased in favor of larger bergs. Some Australian data was also available from many years of observations (e.g., Budd et al. 1980), but there was clearly a need for more extensive field observations.

In 1981 I therefore proposed, through the SCAR Working Group on Glaciology, to organize the systematic collection of iceberg statistics, and we have since then regularly distributed standard forms to all ships going to Antarctica. On these forms the icebergs are recorded in four length classes: 10-50 m, 50-200 m, 200-500 m, and 500-1000 m, and those over 1000 m length are described individually. The number of participating ships has increased greatly from the start in 1981-1982 (Table 12.1), and practically all ships to Antarctica took part in the collection during the 1983-1984 season. All data are put on file at Norsk Polarinstitutt, and we return to each participating nation printed copies of their data and plots of all data received. We also provide on request the data for any particular area and in general can provide selected data in any manageable form to those who take part. We believe that this collection of data has a value larger than the sum of its parts and that it should be made attractive to those providing raw data. The data set is growing rapdily and includes now more than 3000 separate observations. Table 12.1 shows the status on 9 September 1984, when it included data on 44,000 bergs, of which over 33,000 were classified by size. More data were still being received and processed for 1983-1984.

The number of classified icebergs observed in recent years are shown in Table 12.2. It should be noted that some observers have not recorded icebergs in the smallest size category, and our experience indicates also that there will be a tendency to overestimate the size when based on radar observations alone. Some compensation has been done for the latter, but this only affects a small fraction of the large icebergs.

The mean volumes are computed for each size are shown in Table 12.3. The volumes of the bergs greater than 1000 m are computed as the products of the observed lengths, widths, and freeboard x 7. Not all records include data on all three dimensions, and occasionally bergs

TABLE 12.2 Classified Icebergs

Year	Number	%	Size (m)	Unit volume (10^6 m^3)	Total volume (10^9 m^3)
	970	50.4	10-50	0.015	0.0
	624	32.4	50-200	0.96	10.6
1977-1981	177	9.2	200-500	17.92	3.2
	97	5.0	500-1000	112.5	6.3
	56	2.9	>1000	Measured individually	368.1
	1,924			Total volume	378.2
	1,863	36.8	10-50	0.015	0.0
	2,346	46.3	50-200	0.96	9.3
1981-1982	662	13.1	200-500	17.92	11.9
	146	2.9	500-1000	112.5	16.4
	45	0.9	> 1000	Measured individually	314.5
	5,062			Total volume	345.1
	2,575	29.1	10-50	0.015	0.0
	2,823	31.9	50-200	0.96	2.7
1982-1983	2,265	25.6	200-500	17.92	40.6
	853	9.6	500-1000	112.5	96.0
	339	3.8	>1000	Measured individually	130.2
	8,855			Total volume	269.5
	6,345	35.5	10-50	0.015	0.1
	5,277	28.5	50-200	0.96	5.1
1983-1984	3,747	20.9	200-500	17.92	67.1
	1,898	10.6	500-1000	112.5	213.5
	623	3.5	>1000	Measured individually	263.9
	17,890			Total volume	549.6

	Size (m)	Number	%	Total volume ($10^9 m^3$)
All Years	10-50	11,753	34.8	0.2
	50-200	11,070	32.8	10.7
	200-500	6,851	20.3	122.8
	500-1000	2,994	8.9	332.2
	>1000	1,063	3.2	1,076.7
		33,731		1,542.6

may be recorded as greater than 1000 m without size information. The following dimensions are used where information is not recorded: length = 1000 m; width = 0.75 x length; and thickness = 300 m.

The choice of the numbers 7 x freeboard, or 300 m, for the thickness is based on the limited thickness observations available, which also show the somewhat unexpected result that for the large icebergs there

TABLE 12.3 Calculated Volume of Classified Bergs

Size class (m)	Length (m)	Width (m)	Thickness (m)	Volume (10^6 m^3)
10-50	30	25	20	0.015
50-200	120	100	80	0.96
200-500	320	280	200	17.92
500-1000	750	600	250	112.5
> 1000	Measured individually			

is no correlation between thickness and horizontal dimensions. In reality many icebergs are not right-angled parallepiped in shape, but our observations show that this is a good approximation for most of the larger bergs.

TOTAL ICEBERGS IN THE SOUTHERN OCEAN

To determine the total number of icebergs in the Southern Ocean requires evaluation of (a) the presence of repeated observations and (b) which fraction of the relevant ocean area has been observed.

(a) Repeated observations can be present within the records from one ship or between records from different cruises. The observations are normally made at 6-hour intervals at each ship. This means that the observing circles, whether by radar or visual, will not normally overlap. A typical observer elevation of 20 m will give a maximum radius of observation to an iceberg of 30 m freeboard = 21 nautical miles, i.e., there will be no overlap of observation at velocities of 7 knots or higher. The data have been corrected in cases of repeated observations from slower-moving or stationary ships.

It is more difficult to avoid repeated observations from two ships traversing the same area, or from one ship revisiting the area. Considerable care is taken to eliminate from the files multiple recordings of icebergs greater than 1000 m. This has been done even when the observations are made from different ships because the large bergs are usually well described and unique within a limited area. It is not possible to avoid multiple recording of smaller bergs if two ships pass the same area close in time, but such instances are not frequent, and this will not be a large error in the total mass of icebergs. Indeed, this will not introduce <u>any</u> error in computed total icebergs in the Antarctic ocean provided the iceberg distribution is representative.

(b) The total area of observing circles has been computed for each season based on the data for the elevation of the observing platform(s) on the ships and taking the iceberg freeboard as 30 m. Often the records include information on visibility, which is then used for the visual observations. Our experience indicates that the real observed area is commonly less than this computed theoretical area. However, using this computed area we find that the <u>maximum</u> ocean area south that has been observed in various years is shown in Table 12.4. The fraction is based on the Southern Ocean area south of the Antarctic Convergence,

TABLE 12.4 Maximum Ocean Area Observed

Year	Observed Area (10^6 km^2)	Fraction of Southern Ocean	Total Numbers of Bergs 10 m	Total Ice Volume (10^{12} m^3)	Total Ice Mass (10^{15} kg)
1981-1983	1.9	1/19	340,000	12.0	9.6
1983-1984	2.4	1/15	330,000	8.5	6.8
All years	5 (?)	1/7	325,000	11.4	9.1

which equals 37 x 10^6 km^2. The total numbers are computed using the data from Table 12.2, and the mass is based on density of 800 kg/m^3.

ANNUAL ICEBERG PRODUCTION

To estimate annual iceberg production requires evaluation of the residence time of the bergs, i.e., their "life expectancy." Drift measurements (Tchernia 1977; Tchernia and Jeannin 1980; Vinje 1980) show that an iceberg from 50°E, which follows the coastal current, will take less than 1 year to reach the southern Weddell Sea and then 2 to 3 years to move north into the westwind drift. Some bergs do not drift into the Weddell Sea, and these take less than 1 year to reach the westwind drift. Icebergs starting further east seem to drift less far along the coast before moving north away from the coast.

Several authors have estimated the half-life of the icebergs starting from the continent (e.g., Budd et al. 1980; Orheim 1980; Kristensen unpublished), and the consensus seem to be that the half-life is 2 to 5 years for bergs near the Antarctic coast and about 1 year for those that have drifted northward from the continent and into the westwind drift. Our monitoring of bergs that have reached the Antarctic Convergence indicate a half life of less than a year once the bergs have reached these warmer waters.

An "average" half-life of bergs south of the Antarctic Convergence seems to be 2 to 4 years. Combining a 4-year half-life with the above iceberg observations leads to an mean annual calving rate from Antarctica of 2.3 x 10^{15} kg, i.e., a larger loss than the net accumulation of 2 x 10^{15} kg.

The three main objectives that can be raised to this conclusion are the following:

(1) The iceberg data collected so far are not representative in time or space, especially that iceberg concentration is lower in the less-studied Pacific sector;

(2) The fraction of the observed ocean is taken to be too small; and

(3) The half-life is larger than hitherto assumed, or we should use a longer half-life because most observations are near the continent.

Clearly adjustments can be made to all the valuers and assumptions used here for 2 and 3. For example, we could consider the data as representative only for the ocean south of 60°S, which, for comparison, covers 20 x 10^6 km. The results are also clearly sensitive to the observations of unusually large bergs, which may be overrepresented in the early data. However, we must choose both to consider the data unrepresentative, combined with an unlikely choice of assumptions, to arrive at the commonly used low calving rate of 0.6 x 10^{15} kg. Continuation of the iceberg registration program should clarify these questions.

At present state of knowledge I conclude that the international collection of iceberg statistics indicates that the rate of iceberg calving from Antarctica is 3 to 4 times higher than the commonly accepted value and that the present mass balance of Antarctica may be negative.

REFERENCES

Budd, W. F., T. H. Jacka, and V. I. Morgan, 1980. Antarctic iceberg melt rates derived from size distribution and movement rates. Annals of Glaciology, 1, 103-112.

Bull, C., 1971. Snow accumulation in Antarctica. In Research in the Antarctic, American Association for the Advancement of Science, Washington, D.C., pp. 367-421.

Giovinetto, M. B., and E. S. Robinson, 1966. The regime of the western part of the Ross Ice Shelf drainage system. Journal of Glaciology, 6, 55-68.

Kristensen, E. G. M., unpublished. Antarctic tabular icebergs in ocean waves. Ph.D. Thesis, University of Cambridge, 229 pp.

Loser, K. S., 1973. Estimation of run-off from Antarctic and Greenland ice sheets. In Symposium on the Hydrology of Glaciers, IASH Publication 95, pp. 253-254.

Mellor, M., 1961. The Antarctic Ice Sheet. Cold Regions Science and Engineering Report, I, 50 pp.

Orheim, O., 1980. Physical characteristics and life-expectancy of tabular Antarctic icebergs. Annals of Glaciology, 1, 11-18.

Suyetova, I. A., 1966. The dimensions of Antarctica. Polar Record, 13(84), 344-347.

Tchernia, P., 1977. Etude de la derive antarctique Est-Quest au moyen d'icebergs suivis par la satellite Eole. In M. Dunbar (ed.), The Polar Oceans, Proceedings of the Polar Oceans Conference, Montreal, pp. 107-120.

Tchernia, P., and P. F. Jeannin, 1980. Observations on the Antarctic east wind drift using tabular icebergs tracked by satellite NIMBUS F (1975-1977). Deep-Sea Research, 27(6A), 467-474.

Vinje, T. E., 1980. Some satellite-tracked iceberg drifts in the Antarctic. Annals of Glaciology, 1, 83-87.

ATTACHMENT 13

GLOBAL LAND-ICE MONITORING: PRESENT STATUS AND FUTURE PERSPECTIVES

Wilfried Haeberli
Permanent Service on the Fluctuations of Glaciers
FAGS/ICSU and VAW/ETHZ, ETH-Zentrum
Zurich, Switzerland

INTRODUCTION

Efforts to monitor land ice on a global scale date back to the past century (Forel and Du Pasquier 1896). The original goal of this undertaking was to monitor and to analyze changes in climate by regularly observing the variations of existing glaciers. In recent years, renewed attention has been given to the possibility of drastic future changes within the cryosphere due to CO_2-induced warming. The need for careful observation of permafrost and its thermal stability is now recognized (Osterkamp 1984), and the collection of glacier fluctuation data on an international level is currently being redesigned.

The Permanent Service on the Fluctuations of Glaciers and the Temporary Technical Secretariat for the World Glacier Inventory are the two international services that collect, process, and publish standardized glacier data. It is planned to merge these two services in the near future and to form a new world glacier monitoring program. This paper briefly summarizes the background to this development and gives some perspectives for the future.

HISTORICAL BACKGROUND AND PRESENT STATUS

The International Commission on Glaciers summarized worldwide glacier observations in annual reports between 1895 and 1913, and at reduced frequency in the time period 1914-1959. Its successor, the International Commission on Snow and Ice (ICSI) of the International Association of Hydrological Sciences (IAHS) established, in 1967, the Permanent Service on the Fluctuations of Glaciers (PSFG) as one of the services of the Federation of Astronomical and Geophysical Services of the International Council of Scientific Unions (FAGS/ICSU). This resulted in the publication of three volumes containing glacier fluctuation data: (Vol. I: 1959-1965, Kasser 1967; Vol. II: 1965-1970, Kasser 1973; Vol. III: 1970-1975, Müller 1977). Preparation of Vol. IV (Fluctuations of Glaciers 1975-1980) is now under way, and publication is planned for 1985.

Following recommendations by the "Comite Special de l'Annee Geophysique Internaionale" in 1955 and by the Coordinating Council of the

International Hydrological Decade (1965-1974), a working group of ICSI produced a "Guide for the Compilation and Assemblage of Data for a World Inventory of Perennial Snow and Ice Masses" published by UNESCO/IAHS in 1970. After a corresponding resolution was passed by ICSI/IAHS, together with financial support from UNEP, UNESCO, and some member states, the Temporary Technical Secretariat for the World Glacier Inventory (TTS/WGI) started operations in 1976. The WGI, as a global undertaking, will terminate in 1985.

PSFG publications contain standardized data about changes in length, mass, and volume of glaciers. Figure 13.1 illustrates an example from the Swiss Alps. The curve of cumulative balances clearly shows the spectacular mass losses that occurred around the middle of the twentieth century, something that appears to be quite typical for most parts of the world. The reaction of glacier tongues to this development very much depends on the size of the glacier. Small cirque glaciers flow under low stresses; their altitudinal range is smaller than year-to-year variations of the equilibrium line position. Variation in glacier length, therefore, is a direct reflection of the position of the equilibrium line and of the mass balance during the corresponding year, rather than a consequence of complex dynamic reactions due to changes in ice flow. Advance and retreat of medium-sized mountain glaciers are expressions of a dynamic response to balance changes that have accumulated over periods of the order of a decade. With a time lag of a few years, Trient glacier, for instance, markedly advanced around 1890, 1920, and in recent years, as a reaction to positive mass balances. Aletsch glacier is the longest valley glacier in the Alps. Its dynamic response to balance changes is slow and takes place with considerable time lag. Only secular variations show up in fluctuations of its length. The examples in Figure 13.1 demonstrate that measurements of length variation of glaciers furnish information about balance and climatic changes of different frequencies and that the strength of the signal thereby obtained is approximately inversely proportional to the frequency of the recorded variation.

The World Glacier Inventory is a snapshot of ice conditions on Earth during the second half of this century. Detailed regional inventories contain information about the location, surface area, width, length, orientation, elevation, and morphological characteristics of single ice bodies (Müller et al. 1976). Figure 13.2 is an example of a computer plot that can be derived from such data. Glacier elevation is related to the abundance of precipitation (cf., Ahlmann 1933; Kerschner in press). Low values for the equilibrium line altitude, or the mean glacier elevation, or the median glacier elevation indicate the existence of abundant precipitation, of maritime-type glaciers, and of increased runoff in meltwater streams. In regions with elevated glaciers, precipitation and runoff are reduced and continental-type glaciers are encountered. Such information as represented in Figure 13.2 can be used for hydrological assessments (Kotlyakow and Krenke 1982), as well as for climatological comparison of glaciers (see below). Preliminary glacier inventories will contain less detail, but interpretation of satellite imagery should at least furnish data about the glacierized area in all parts of the world (Scherler 1983). Graphs and tables in the final WGI

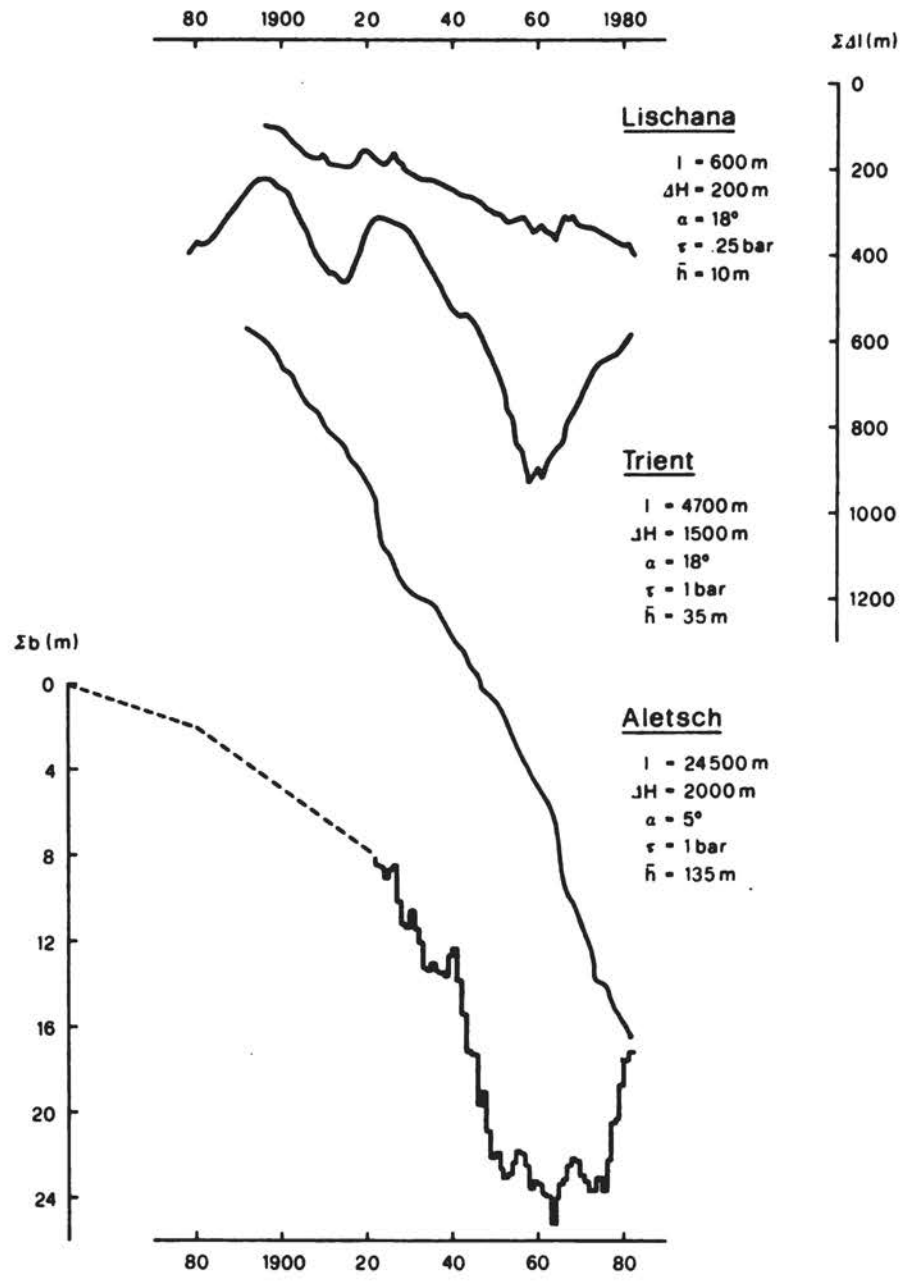

FIGURE 13.1 Cumulative mass balance (Σb) of Aletsch glaciers and cumulative length chances ($\Sigma \Delta \ell$) of a cirque glacier (Lischana), a steep mountain glacier (Trient), and a flat valley glacier (Aletsch) in the Swiss Alps during the past 100 years. Mass balance of the glaciers in the Aletsch region is determined by hydrological measurements combined with repeated large-scale mapping (Kasser et al. 1982). ℓ, length; ΔH, altitudinal extent; α, overall surface inclination; $\bar{\tau}$, average basal shear stress; $\bar{h}$, mean thickness of the glaciers. $\bar{\tau}$ and $\bar{h}$ are estimated from data given by Müller et al. (1976) and Maisch and Haeberli (1982).

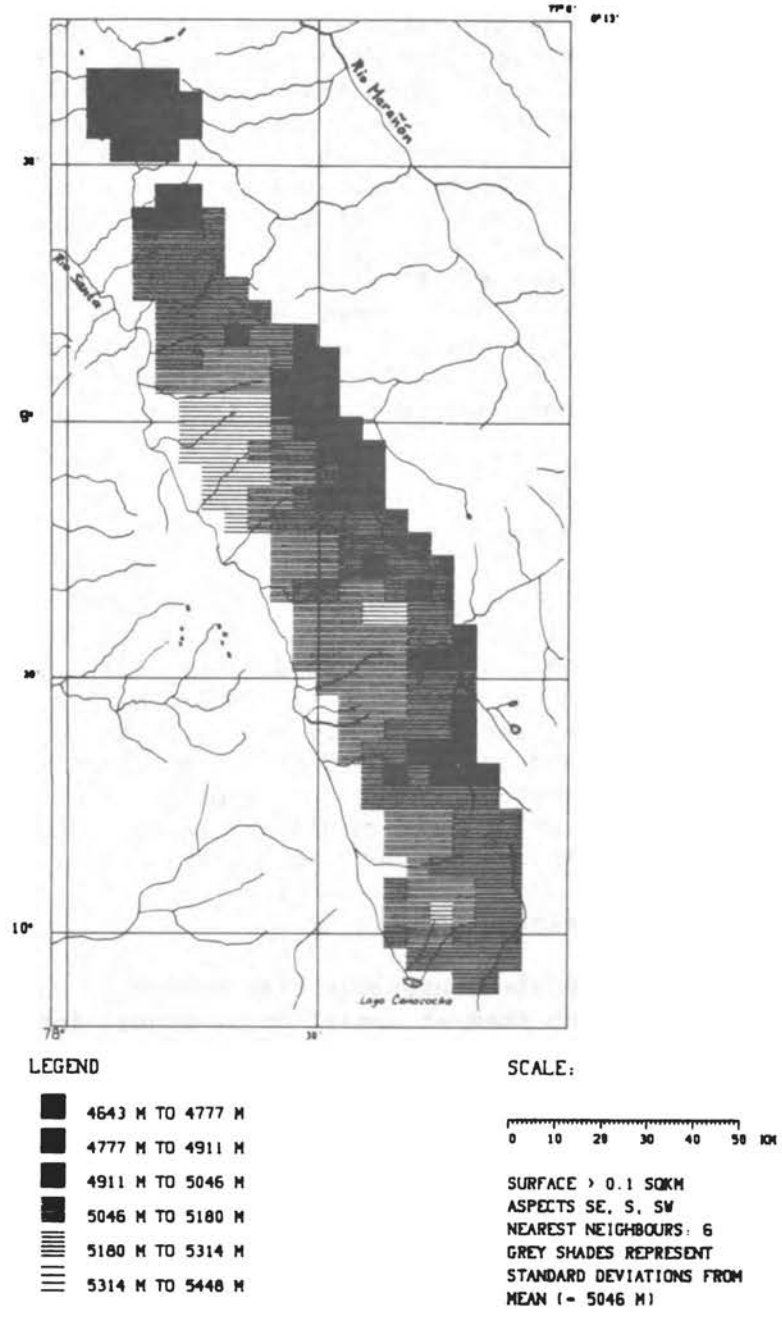

FIGURE 13.2 Median glacier elevations in the Cordillera Blanca (Peru). Only glaciers with surface areas >0.1 km^2 and exposed to SE, S, SW are considered. Computer plot provided by K. Scherler (TTS/WGI, Zürich). publication will indicate what geographical information is available for the glaciers in each region.

The data described above are being used for many scientific and practical purposes. The worldwide retreat of glacier tongues is still one of the most reliable indicators to the phenomenon that the energy balance at the Earth's surface has changed markedly on a global scale over the last 100 years. Progress in the parametrization of climate-glacier relationships (e.g., Kuhn 1981) has allowed paleoglaciological and paleoclimatological reconstructions to be made (e.g., Kruss 1983; Haeberli and Penz in press), which show remarkably good agreement with direct observations or computer experiments using global circulation models (e.g., Manabe and Broccoli 1984). Forecasting future glacier behavior has become a task of increasing importance in several parts of the world (Bindschadler 1980; Shi et al. 1980; Rasmussen and Meier 1982) and is always based on some type of glacier fluctuation data. Assessing the influence of glacier variations on runoff is essential for the design of hydroelectric power schemes in mountain regions, for irrigation projects in semiarid areas in many parts of the world, and for estimating the effect of glacier melt on sea-level variations (Meier 1984). Information contained in regional inventories is thereby of great practical use.

PERSPECTIVES OF FUTURE GLACIER MONITORING

For future world glacier monitoring, it is planned to combine the tasks of the two existing services, and thereby collect available standardized glacier fluctuation data and update preliminary regional inventories for applications in a variety of fields, such as glaciology, climatology, hydrology, and Quaternary geology. The future program should be so designed as to (1) speed up the documentation of representative mass-balance studies, (2) provide a better overview of the more numerous observations on changes in glacier length, and (3) reach global coverage by using statellite imagery for remote areas.

Time Series of Mass-Balance Studies

It is planned to update continuous time series of mass-balance measurements and to publish them at annual or bi-annual intervals. Two main problems exist: (1) judging how representatative the observations are and (2) keeping long-term observations running or even extending the measurements to as yet undocumented regions.

How spatially representative glacier fluctuation data are in general depends on the time period considered and the climatological aspects involved. Appropriate stratification of glacier data and selection of reference glaciers require a classification of glaciers with respect to climate and glacier size, the two main factors influencing the processes of mass exchange at the surface of and within perennial ice bodies. The size aspect is less important for mass-balance data because balance observations are usually carried out, for practical reasons, on relatively small mountain glaciers. The limited number of observed glaciers (around 50) only warrants the use of a simple climatological classification; it seems to be most appropriate to combine latitudinal categories

(tropical, temperate, and polar zones) with a scheme of maritime, transitional, and continental-type climates. Figure 13.3 illustrates this scheme, which is mainly based on the experiences of Russian and Chinese authors (Shumskii 1964; Shi and Li 1981; cf., Haeberli 1983). Maritime-type glaciers are found in regions where the annual precipitation is higher than about 2000 m. The mean annual air temperature at the equilibrium line is above -2°C. Balance gradients are high (1 m/100 m and more), mass exchange with the atmosphere (accumulation and ablation) is intense, and mass turnover within the mostly temperate ice bodies is high. Continental-type glaciers are fed by annual precipitation, which remains below 500 mm. The equilibrium line is at altitudes where the mean annual air temperature is around -10°C or lower. Balance gradients are small (0.1 m/100 m and less, if not disturbed by local winds on small glaciers), and mass turnover within the mostly cold glaciers is low. Such glaciers often end within the zone of continuous permafrost

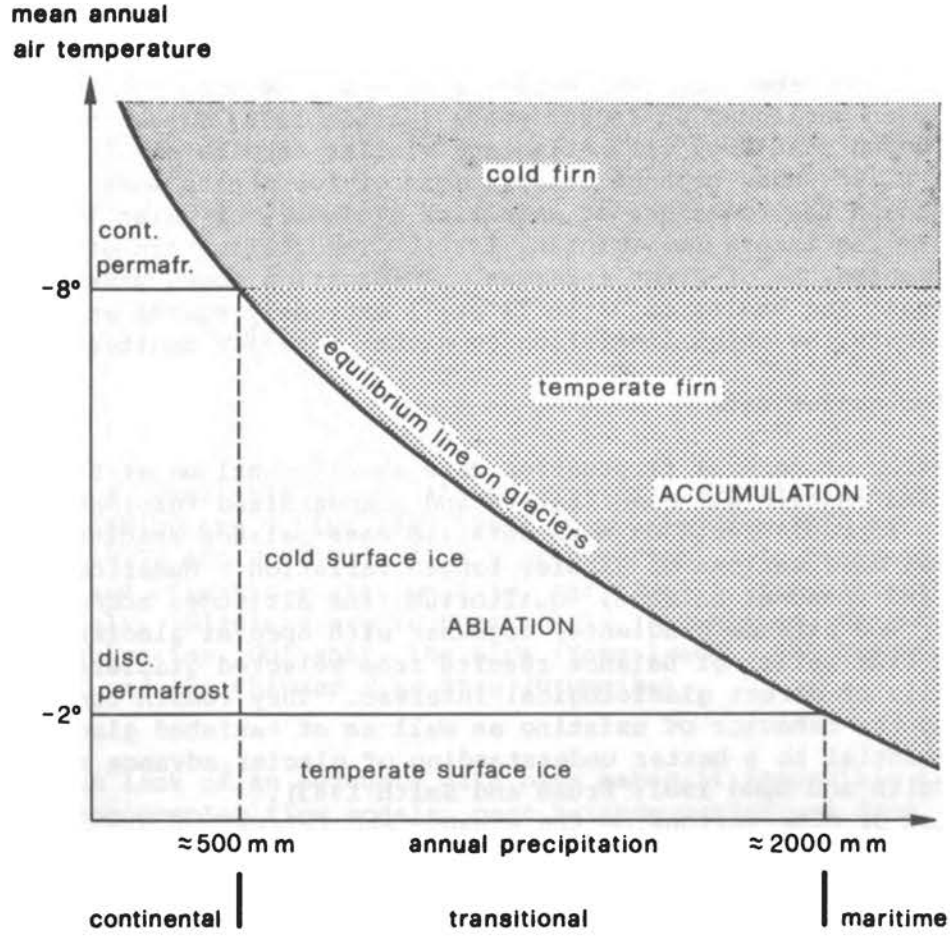

FIGURE 13.3 Scheme illustrating the structure of the cryosphere as a function of temperature and precipitation and serving as a basis for a rough climatological classification of glaciers.

and have reduced mass exchange with the atmosphere. Many mountain glaciers are in between these two categories and may therefore be called transitional or subcontinental.

Figure 13.4 summarizes the balance variations of seven glaciers in the northern hemisphere during 1970-1980. Strongly positive balances were observed for high-latitude, maritime-type glaciers, whereas the mass of transitional (and continental?)-type glaciers at these latitudes steadily decreased. This trend is confirmed by studies on neighboring glaciers, and it seems to have continued after 1980 (Haakensen 1984; Mayo and Trabant 1984; Weller 1984). It may possibly indicate that the increased precipitation that accompanies a general temperature rise in polar regions predominantly affects the margins of mountain chains. At lower latitudes, the general tendency is less clear.

It is of fundamental importance that long-term mass-balance observations be continued. Reduced stake networks need not necessarly mean reduced quality of reported data. The linear balance model for single glaciers, as proposed and discussed by Lliboutry (1974), is a useful tool for cost saving and long-term monitoring of glacier mass balance and can also be applied when investigating how geographically representative local observations are (Reynaud 1980). Most interesting reconstructions of mass-balance time series reaching back into the past century have been published in recent years (Martin 1978; Tangborn 1980), and it is hoped that they will stimulate similar studies on other glaciers. Direct mass-balance observations of ice sheets would become feasible should the technique of satellite altimetry of polar ice be available in the future (Swithinbank 1980). The realization of this would, of course, be of great interest. Information about mass changes of the largest ice bodies on Earth is still extremely sparse and, up to now, represents the chief limitation to global land-ice monitoring.

General Fluctuation Data

Publication of general fluctuation data should continue at 5-year intervals and contain all quantitative and standardized information available. Emphasis rests on more detailed mass-balance results and on the numerous observations of glacier length variation. Numerical values of annual and seasonal balance, equilibrium line altitude, accumulation area ratio, and balance gradients, together with special glacier maps, complement time series of balance results from selected glaciers and are primarily of direct glaciological interest. They remain fundamental to modeling the behavior of existing as well as of vanished glaciers and are essential to a better understanding of glacier advance and retreat (Smith and Budd 1981; Kruss and Smith 1983).

The value of observations on the advance and retreat of glacier tongues should not be underestimated. Beyond its practical use in densely populated mountain regions, especially the Alps, such information remains an irreplaceable tool for extending the information from balance studies, both in space and back in time (e.g., Hastenrath 1984); the measuring technique is simple and can easily be applied everywhere. Futhermore, past glacier advances can be reconstructed on the basis of historical records and field evidence (cf., Figure 13.5). In many

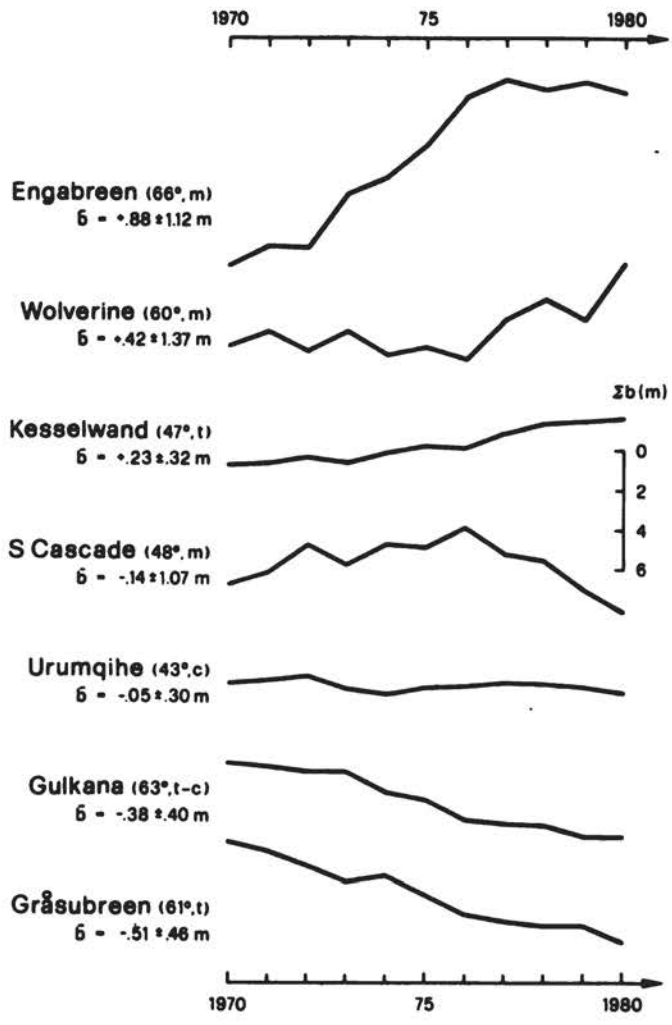

FIGURE 13.4 Cumulative mass balance (Σb) of seven glaciers in the northern hemisphere during 1970-1980. Data are from PSFG Vol. III (Müller, 1977) and PSFG Vol. IV (in preparation). In brackets are latitude and climatic environment (m, maritime; t, transitional; c, continental). Glaciers are in Scandinavia (Engahbreen, Grasubreen), Alaska (Wolverine, Gulkana), the Alps (Kesselwand), the Cascades (South Cascade), and the Chinese Tian Shan (Urumqihe).

cases, the lack of an adequate data base makes it impossible to derive, by applying complex flow models, past balance variations from such reconstructions. However, much simpler methods may help to calculate approximate figures. Thickness changes can be estimated from glacier length variations by assuming that the product of mean ice depth and surface gradient (i.e., the basal shear stress averaged over the whole glacier length) remains nearly constant ($\pm$ a few percent) in time. Calculated thickness changes then have to be extrapolated for the whole glacier surface by taking the variation of surface area versus altitude

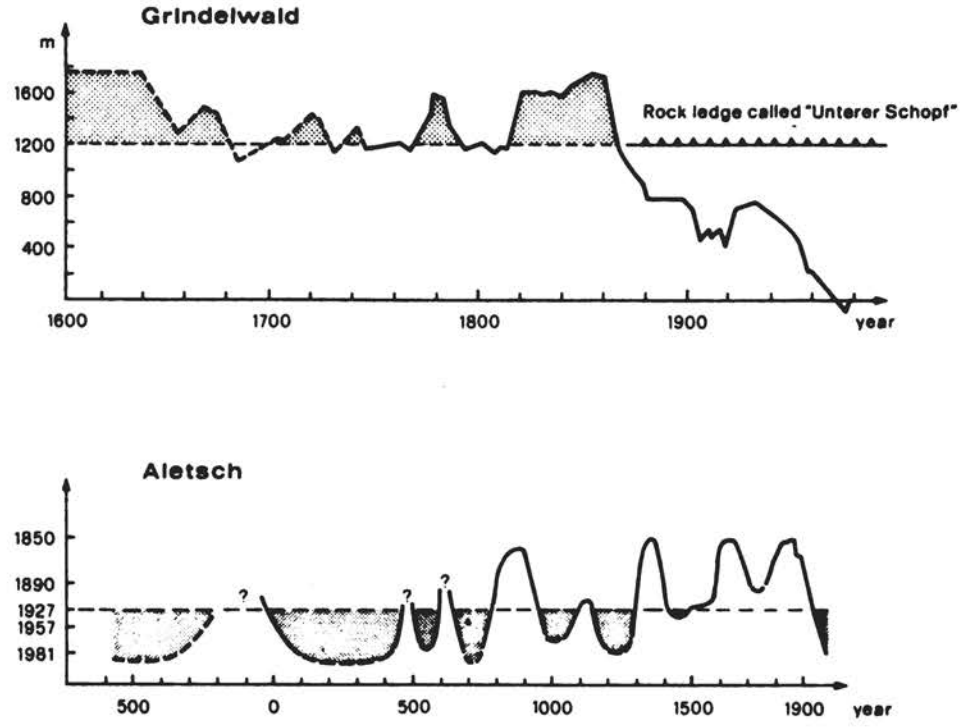

FIGURE 13.5 History of glacier length variations of two glaciers in the Swiss Alps. Reconstruction is based on analysis of direct measurements, historical sources, tree-ring information, ^{14}C-dating, and detailed mapping of morainic deposit. The Lower Grindelwald glacier is a steep mountain glacier that reacts to balance changes over time periods on the order of about a decade, whereas the Great Aletsch glacier, a flat valley glacier, shows secular variations only. The ordinate represents the distance from an arbitrarily chosen point in the case of the Grindelwald glacier and the historical positions of the ice front along the central flow line in 1850, 1890, 1927, 1957, and 1981 in the case of the Aletsch glacier. Note that the time scale is different in the two graphs. Simplified after Zumbühl (1980, Grindelwald) and Holzhauser (1983, Aletsch).

into account, or they have to be calibrated using actually measured values. The latter technique has been used for Aletsch glacier to reconstruct trends of cumulative balances back into the nineteenth century (Figure 13.1). The fact that the front of this glacier is currently retreating, despite the most recent mass gains, indicates that the glacier tongue does not yet receive increased influx of ice from the higher parts of the glacier--a result of the fact that balance and length changes are usually nonsynchronous. Moreover, it means that mass balance is not simply "uncoupled" from the dynamic response and, hence, from the size of a glacier. On the basis of kinematic wave theory (Weertman and Birchfield 1983), the time lag between balance and length changes of Aletsch glacier can be estimated to be on the

order of decades, and time periods of corresponding length should be considered only when simple ("steady-state") approaches are used.

Smaller glaciers, which adjust more quickly to changes in climatic conditions, should be considered for monitoring variations of higher frequency. This implies that worldwide intercomparison of glacier length variations can only be reasonably undertaken if glaciers of comparable size and similar morphological characteristics are chosen for interpretation. The required stratification of the relatively large sample (500-1000) of regularly observed glaciers involves geometrical parameters that are related to the transfer of mass within the investigated ice bodies. The main parameters are the length (or surface area), which defines the travel distance for waves and other forms of down-glacier energy dissipation (Lliboutry and Reynaud 1981), and the basal shear stress, which is related to glacier flow by ice deformation and sliding at the bed. The mean basal shear stress of a glacier is the key parameter to dynamic ice-flow considerations as well as to reconstructions of vanished glaciers. It is a reflection of the mass turnover within a given glacier. Because mass turnover depends on the mass exchange at the surface, i.e., the rate of balance change with altitude (activity index, Meier 1961), the mean basal shear stress is in some way connected to the balance gradient (continentality) and to the altitudinal extent of a glacier. This concept (Figure 13.6) is based on geometrical data from Ice Age glaciers and deserves refinement using modern thickness determinations, such as radio-echo soundings (e.g., Sverrisson et al. 1980; Dowdeswell et al. 1984). It involves the idea that small glaciers and glaciers in regions of low precipitation (continental-type glaciers) may flow under low stresses and, hence, may react less intensively to climatic perturbations than large glaciers and glaciers in a maritime enviornment (cf., Xie 1982). In fact, the geometrical parameters that define the mean basal shear stress of a glacier (altitudinal extent, length, surface gradient, cross-sectional shape, ice depth) appear to be most suitable for a geometrical (kinematic) classification of glaciers. Appropriate categories of reference glaciers, however, still have to be selected by analyzing the topographical information reported for the observed glaciers and by comparing this information with glacier inventory data.

Satellite Observations of Remote Glaciers

Regularly observed glaciers are not evenly distributed over all the glacerized regions of the world. This problem should, at least partially, be overcome by the use of satellite imagery. The possibilities and limitations of such a program are related to the technical aspects of satellite imagery as well as to the characteristics of glacier variations.

Since 1972, Landsat imagery has enabled repeated planimetric determination of glacier extension all over the world at latitudes lower than about 80° to be made. Well-known limiting factors are clouds, snow cover, shadows of mountains, debris cover, and pixel resolution. Problems related to clouds and snow can be avoided by frequently repeated coverage, but nevertheless strongly reduce the number of

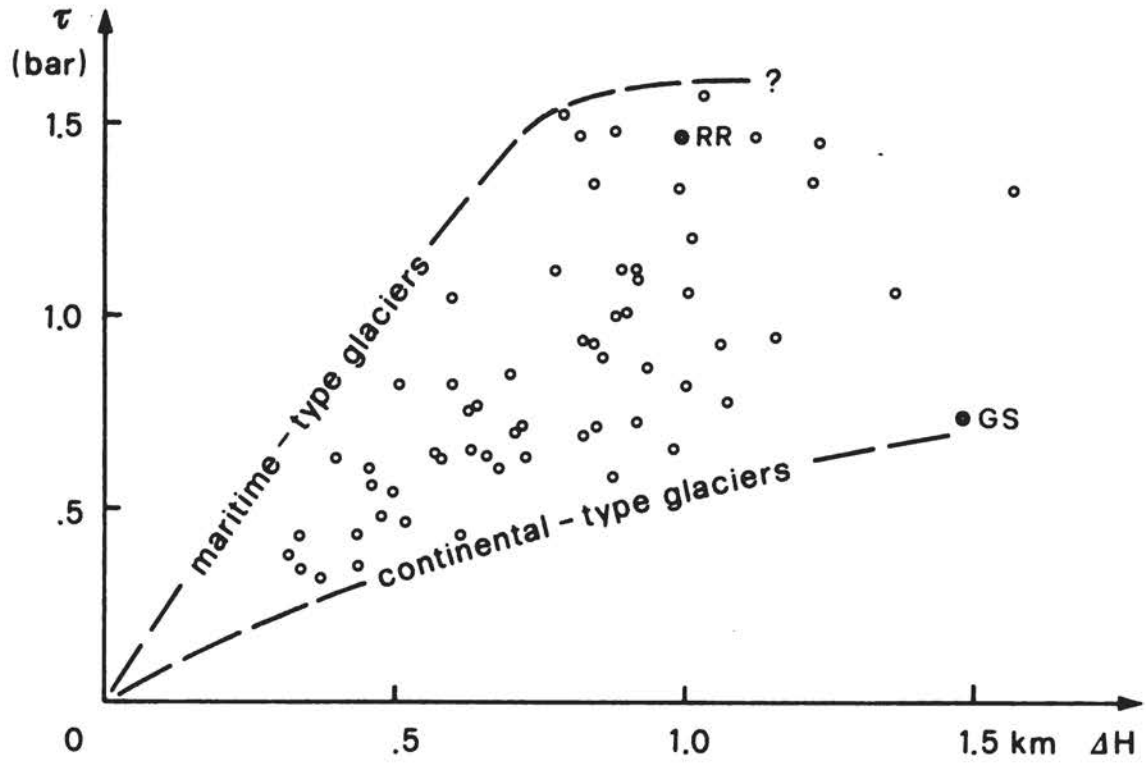

FIGURE 13.6 Average basal shear stress ($\bar{\tau}$) of mountain glaciers as a function of their altitudinal extent and climatic environment. Data are from reconstructions of Ice Age glaciers in the Alps (Maisch and Haeberli, 1982). RR, present-day Rhone glacier (thickness measured by radio-echo sounding); GS, late-glacial (Gschnitz) valley glacier.

usable images. Mountain shadows can make it impossible to study small glaciers or glacier tongues in deep valleys. Thick debris cover hides the lowermost parts of many mountain glaciers (Figure 13.7). It delays the adjustment of glacier length to climate warming and, hence, can strongly reduce the possibility of interpreting glacier length measurements in a simple or straightforward way. Pixel resolution of early Landsat MSS imagery was on the order of 80 m, but it was improved with Landsat 3-RBV and Landsat 4-TM to around 30 m. SPOT imagery, which will seemingly replace the Landsat series in the late 1980s, is planned to have a resolution of about 10 m.

Despite the obvious existing possibilities, application of satellite imagery for monitoring glacier changes has, so far, not been examined and used systematically (Howarth 1983; Williams 1983). The most easily recognized variations are the drastic changes of front positions during glacier surges and during periods of instabilty of retreating tidal glaciers (Krimmel and Meier 1975). These phenomena are of great glaciological interest, but their relation to climate is not well understood. Within the framework of climate monitoring, it is therefore appropriate to also observe length changes of "undisturbed" glaciers. The best

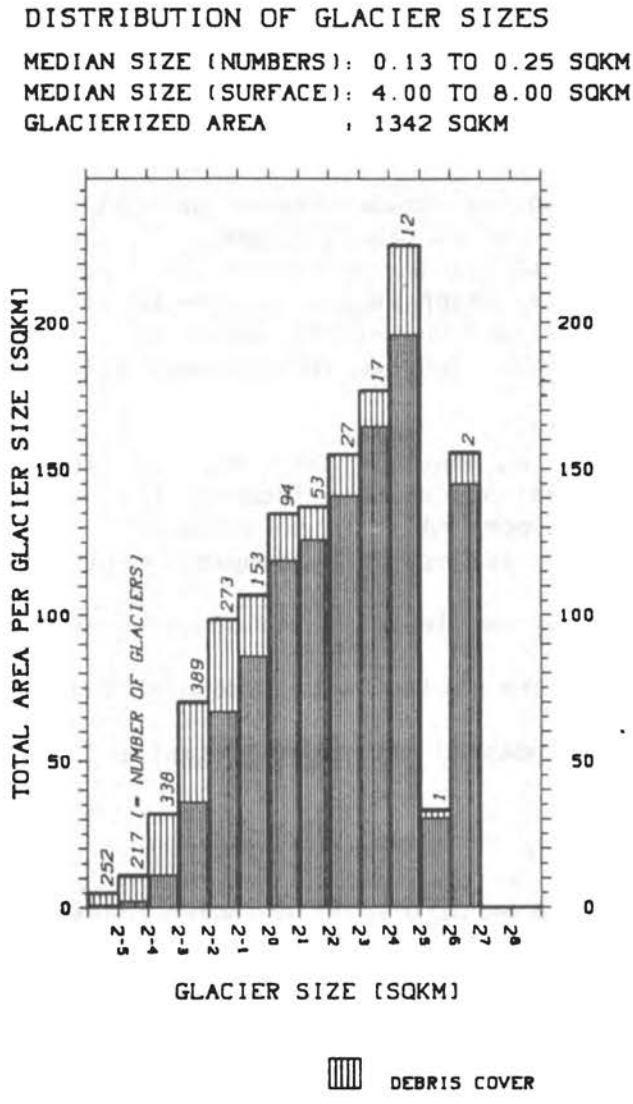

FIGURE 13.7 Distribution of glacier sizes and debris-covered areas for glaciers in the Swiss Alps. Note that the relative amount of debris-covered ice increases with decreasing glacier size. Computer plot provided by K. Scherler (TTS/WGI, Zürich).

approach may be to study, in each region, groups of glaciers with varying sizes and, hence, with varying time lags between balance and length changes. Interpretation with respect to balance variations of various frequencies could be based on empirically determined relationships (time lags) between balance and length changes. Recording fluctuations of very small glaciers is especially delicate and requires an appropriate combination of ground resolution and time interval to be considered. To design a suitable program, it is necessary to investigate its technical feasibility and to select groups of glaciers in a number of

"reference areas" that have to be defined on the basis of climatological considerations and statistical information from the World Glacier Inventory.

CONCLUSIONS AND RECOMMENDED PROGRAM

Future glacier monitoring should combine the tasks of the Permanent Service on the Fluctuations of Glaciers and of the Temporary Technical Secretariat for the World Glacier Inventory of collecting and publishing standardized information, which is then usable by glaciologists, climatologists, hydrologists, and Quaternary geologists. It is planned to start a corresponding joint program in 1986, which is to include the following activities:

1. Establishment of an annual or bi-annual publication series containing selected mass-balance results (running time series);
2. Investigation of possibilities to summarize glacier fluctuation data (classification of glaciers, intercomparison of glacier length variations);
3. Feasibility study and installation of satellite observations in selected remote areas;
4. Continuation of the publication of general fluctuation data at 5-year intervals;
5. Completion and updating of regional glacier inventories.

REFERENCES

Ahlmann, H. W., 1933. Present glaciation round the Norwegian Sea. Geografiska Annaler, XV(1), 316-348.

Bindschadler, R. 1980. The predicted behavior of Griesgletscher, Wallis, Switzerland, and its possible threat to a nearby dam. Zeitschrift für Gletscherkunde und Glazialgeologie, 16(1), 45-59.

Dowdeswell, J. A., D. J. Drewry, O. Liestöl, and O. Orheim, 1984. Radio echo-sounding of Spitzbergen glaciers: Problems in the interpretation of layer and bottom returns. Journal of Glaciology, 30(104), 16-21.

Forel, F.-A., and L. Du Pasquier, 1896. Les variations periodiques des glaciers, Ier rapport. Archives des Sciences Physicques et Naturelles, II, 129-147.

Haakensen, N., 1984. Glasiologiske Undersokelser i Norge 1981. Rapport 1-84, Norges Vassdrags- og Elektrisitetsvesen, Oslo, 79 pp.

Haeberli, W., 1983. Permafrost-glacier relationship in the Swiss Alps--today and in the past. In Permafrost: Fourth International Conference, Proceedings, National Academy Press, Washington, D.C., pp. 415-420.

Haeberli, W. and U. Penz, in press. An attempt to reconstruct glaciological and climatological characteristics of 18 ka BP Ice Age glaciers in and around the Swiss Alps. Zeitschrift für

Gletscherkunde und Glazialgeologie, Symposium on Climate and Paleoclimate of Lakes, Rivers and Glaciers.

Hastenrath, S., 1984. The Glaciers of the Equatorial East Africa. Riedel, Dordrecht, 353 pp.

Holzhauser, H., 1983. Die Geschichte des Grossen Aletschgletschers während der letzten 2500 Jahre. Bulletin Murithienne, 101, 113-134.

Howarth, P. J., 1983. Evaluation of Landsat digital data for providing glaciological information, Final report. Unpublished. Nat. Hydrology Research Inst., Inland Waters Directorate, Environment Canada, Ottawa, Ontario, 43 pp.

Kasser, P., 1967. Fluctuations of Glaciers 1959-1965. IAHS and UNESCO, Paris.

Kasser, P., 1973. Fluctuations of Glaciers 1965-1970. IAHS and UNESCO, Paris.

Kasser, P., M. Aellen, and H. Siegenthaler, 1982. Die Gletscher der Schweizer Alpen 1973/74 und 1974/75. Bericht, Glaziologisches Jahrbuch der Gletscherkommission der SNG. 159 pp.

Kerschner, H., in press. Quantitative paleoclimatic inferences from late glacial snowline, timberline and rock-glacier data, Tyrolean Alps, Austria. Zeitschrift für Gletscherkunde und Glazialgeological, Symposium on Climate and Paleoclimate of Lakes, Rivers and Glaciers.

Kotlyakow, V. M., and A. N. Krenke, 1982. Investigations of hydrological conditions of alpine regions by glaciological methods. In Hydrological Aspects of Alpine and High Mountain Areas, IAHS Publication No. 138, pp. 31-42.

Krimmel, R. M., and M. F. Meier, 1975. Glacier applications of ERTS images. Journal of Glaciology, 15(73), 391-402.

Kruss, P., 1983. Climate change in East Africa: A numerical simulation from the 100 years of terminus record at Lewis glacier, Mount Kenya. Zeitschrift für Gletscherkunde und Glazialgeologie, 19(1), 43.

Kruss, P. D., and I. N. Smith, 1983. Numerical modelling of the Vernagtferner and its fluctuations. Zeitschrift für Gletscherkunde und Glazialgeologie, 18(1), 93-106.

Kuhn, M. 1981. Climate and glaciers. In Sea Level, Ice, and Climatic Change (Proceedings of the Canberra Symposium, Dec. 1979) IAHS publ. No. 131, pp. 3-20.

Lliboutry, L., 1974. Multivariate statistical analysis of glacier annual balances. Journal of Glaciology, 13(69), 371-392.

Lliboutry, L., and L. Reynaud, 1981. "Global dynamics" of a temperate valley glacier, Mer de Glace, and past velocities deduced from Forbes' bands. Journal of Glaciology, 27(96), 207-226.

Maisch, M., and W. Haeberli, 1982. Interpretation geometrischer Parameter von Spaetglazial-Gletschern im Gebiet Mittelbuenden, Schweizer Alpen. Physische Geographie, 1, 111-126.

Manabe, S., and A. J. Broccoli, 1984. Ice-age climate and continental ice sheets: Some experiments with a general circulation model. Annals of Glaciology, 5, 100-105.

Martin, S., 1978. Analyse et reconstitution de la serie des bilans annuels du Glacier de Sarennes, sa relation avec les fluctuation du

niveau de trois glacier du Massif du Mont-Blanc (Bossons, Argentiere, Mer de Glace). Zeitschrift für Gletscherkunde und Glazialgologie, 13(1/2), 127-153.

Mayo, L. R., and D. C. Trabant, 1984. Observed and predicted effects of climate change on Wolverine Glacier, Southern Alaska. In Proceedings of a Conference: "The Potential Effects of Carbon Dioxide-Induced Climatic Changes in Alaska, University of Alaska-Fairbanks, Misc. Publ. 83-1, pp. 114-123.

Meier, M. F., 1961. Mass budget of South Cascade Glacier, 1957-1960. U.S. Geological Survey Professional Paper 424B, 206-211.

Meier, M. F., 1984. Contribution of small glaciers to global sea level. Science, 226, 1418-1421.

Müller, F., 1977. Fluctuations of Glaciers 1970-1975. ICSI/IAHS and UNESCO, Paris.

Müller, F., T. Caflisch, and G. Müller, 1976. Firn und Eis der Schweizer Alpen, Gletscherinventar. Geographisches Institut der ETH Zürich, Publ. Nr. 57, 174 pp.

Osterkamp, T. E., 1984. Potential impact of a warmer climate on permafrost in Alaska. In Proceedings of a Conference: "The Potential Effects of Carbon Dioxide-Induced Climatic Changes in Alaska, University of Alaska-Fairbanks, Misc. Publ. 83-1, pp. 106-113.

Rasmussen, L. A., and M. F. Meier, 1982. Continuity equation model of the drastic retreat of Columbia Glacier, Alaska. U.S. Geological Survey Professional Paper 1258-A, 23 pp.

Reynaud, L., 1980. Can the linear balance model be extended to the whole Alps? In World Glacier Inventory, Proceedings of the Reider-Alp Workshop, September 1978. IAHS-AISH Publ. no. 126, pp. 273-284.

Scherler, K. E., 1983. Guidelines for preliminary glacier inventories. Department of Geography, Swiss Federal Instiutute of Technology, ETH, Zürich. 16 pp.

Shi, Y., and Li, J., 1981. Glaciological research of the Qinghai-Xizang Plateau in China. In Proceedings of Symposium on Qinghai-Xizang (Tibet) Plateau, Beijing, China, pp. 1589-1597.

Shi, Y., W. Wang, and X. Zhang, 1980. Forecasting the change of the Batura glacier this and the next centuries (in Chinese, English abstract). Lanzhou Institute or Glaciology and Cryopedology, pp. 191-207.

Shumskii, P. A., 1964. Principles of Structural Glaciology, Dover Publ., New York, 497 pp.

Smith, I. N., and W. F. Budd, 1981. The derivation of past climate changes from observed changes of glaciers. In Sea Level, Ice and Climatic Change, Proceedings of the Canberra Symposium, December 1979. IAHS Publ. No. 131, pp. 31-52.

Sverrisson, M., A. E. Johannesson, and H. Björnsson, 1980. Radio-echo equipment for depth sounding of temperate glaciers. Journal of Glaciology, 25(93), 477-486.

Swithinbank, C. 1980. The problem of a glacier inventory of Antarctic. In World Glacier Inventory, Proceedings of the Riederalp Workshop, September 1978, IAHS-AISH Publ. no. 126, 229-236.

Tangborn, W. 1980. Two models for estimating climate-glacier relationship in the North Cascades, Washington, U.S.A. Journal of Glaciology, 25(91), 3-21.

Weertman, J., and G. E. Birchfield, 1983. Basal water film, basal water pressure, and velocity of traveling waves on glaciers. Journal of Glaciology, 29(101), 20-27.

Weller, G., 1984. A monitoring strategy to detect carbon dioxide-induced climatic changes in the polar regions. In Proceedings of a Conference: "The Potential Effects of Carbon Dioxide-Induced Climatic Changes in Alaska, University of Alaska-Fairbanks, Misc. Publ. 83-1, pp. 23-30.

Williams, R. S., Jr., 1983. Remote sensing of glaciers. In Manual of Remote Sensing, Vol. II, 2nd ed.. American Society of Photogrammetry, Falls Church, Va.

Xie, Z., 1982. Primary researches on coefficient of stability of glaciers. InProceedings of the Symposium on Glaciology and Cryopedology. Geographical Society of China, Lanzhou Institute of Glaciology and Cryopedology, Academia Sinica, pp. 37-45 (in Chinese).

Zumbühl, H. J., 1980. Die Schwankungen der Grindelwaldgletscher in den historischen Bild- und Schriftquellen des 12. bis 19 Jahrhundpart Ein Beitrag zur Gletschergeschichte und Erforschung des Alpenraums. Denkschriften der Schweizerischen Naturforschenden Gesell, XCII, Zürich.

ATTACHMENT 14

MONITORING THE AREA AND VOLUME OF ICE CAPS AND ICE SHEETS: PRESENT AND FUTURE OPPORTUNITIES USING SATELLITE REMOTE-SENSING TECHNOLOGY

Richard S. Williams, Jr.
U.S. Geological Survey
Reston, Virginia

INTRODUCTION

Ice is present on our planet in a variety of forms and locations: as ice crystals in the atmosphere; as snow cover on land, on glaciers, and on sea ice; as sea ice; as ground ice (seasonal or permafrost); and as glacier ice. Each of these distributions of ice is an element of the hydrologic cycle (global water budget), an element that, for short or long periods of time, becomes static in the dynamic hydrologic cycle (Meier 1983). Meier (1980) provided an excellent review of the use of remote-sensing technology, from spacecraft and aircraft, to determine remotely various physical characteristics of these various elements of the cryosphere. Depending on the latitude and topographic elevation (that is, local climate), snow cover may persist for days, weeks, or months. Sea-ice cover is highly variable on a seasonal and annual basis. Ground ice may be seasonal in temperate latitudes or more long lived (and deeper in extent) in polar or high-mountain regions. With regard to long-term variations in sea level, however, glaciers, because of their great volume, are the single most important component of the cryosphere; glacier ice is also the second largest reservoir of water on our planet (Meier 1983, 1984). Glaciers have varying response times to climatic change depending on their area, volume, and geographic location--generally decades for valley and outlet glaciers, centuries for ice caps, and millennia for ice sheets.

An excellent review of traditional methods of measuring areal and volumetric changes of glaciers and compiling glacier inventories is given by Haeberli (this volume, Attachment 13). Considerable field effort has been expended in determining areal fluctuations and mass balance of selected glaciers; mountain glaciers have been the type most studied in this way by glaciologists (Wallén 1981; Meier 1984; Haeberli, this volume, Attachment 13). Because the Greenland and Antarctic ice sheets account for 99.3 percent of the volume of glacier ice on Earth, and polar and subpolar ice caps and ice fields account for much of the remaining 0.7 percent, a means for remotely measuring volumetric changes in ice sheets and ice caps is needed to assess directly the contribution of change in volume of glacier ice to sea-level variation.

Sensors now carried by Earth-orbiting satellites provide the means for the remote determination of areal changes in ice sheets and ice

caps; planned sensors for future satellites will provide the means for the accurate remote determination of surface elevation of ice sheets and ice caps, although some preliminary ice-sheet elevation measurements have already been accomplished by means of satelliteborne radar altimeters and more are planned (McIntyre and Drewry 1984).

The important scientific and practical objective of determining the present volume of glacier ice on our planet and its flux with time can eventually be realized through the application of existing remote-sensing technology and technology to be available during the next decade. The measurement of the volumetric fluctuation of glaciers can be used as a global "early-warning" system of changes in climate. Significant melting of polar ice caps and ice sheets would cause a rise in sea level that would have serious economic effects on low-lying coastal areas and fixed-port facilities (Allison 1981; Hoffman et al. 1983; Revelle 1983).

MONITORING AREAL AND VOLUMETRIC CHANGES OF GLACIERS

The mass balance equation of an ice sheet or glacier can be written as (Reeh, this volume, Attachment 8):

$$dv/dt = Q_p - Q_m - Q_c,$$

where v is volume of a glacier, t is time, Q_p is the annual precipitation (water equivalent), Q_m is the annual loss in volume due to melting and runoff, and Q_c is the loss in volume caused by calving of icebergs (where the margin of the glacier terminates in a lake or the ocean). As noted by Reeh, the change in mass of a glacier can be determined by direct measurement of volumetric changes or by measuring the total annual precipitation and the amount of melting and calving of icebergs. Only about 50 glaciers worldwide have regular direct measurements made of their mass balance, and Meier (1984) was able to find data on volume change for only 25 glaciers over a more than 50-year interval.

Direct mass-balance studies of glaciers require field observations and measurements; calculation of volume, change on the basis of change in area, and thickness can be carried out by remote-sensing technology. The calculation of absolute volume of a glacier requires measurement of the glacier's areal dimensions, surface topography, and thickness; however a change in volume (dv/dt) can be calculated from changes in absolute elevation of the surface of the glacier without knowledge of the absolute volume.

Terrestrial and aerial photographs have long been used to document the position of glacier termini and to measure the areal extent of glaciers and ice caps. The five spacecraft in the Landsat series (launched in 1972, 1975, 1978, 1982, and 1984), enabled glaciologists to measure repetitively the areal extent of glacier ice on a worldwide basis. Imaging sensors on satellites are especially well suited to measuring changes in the areal extent of ice caps (Williams 1983b) and ice sheets and to monitoring dynamic changes of glaciers (Figure 14.1).

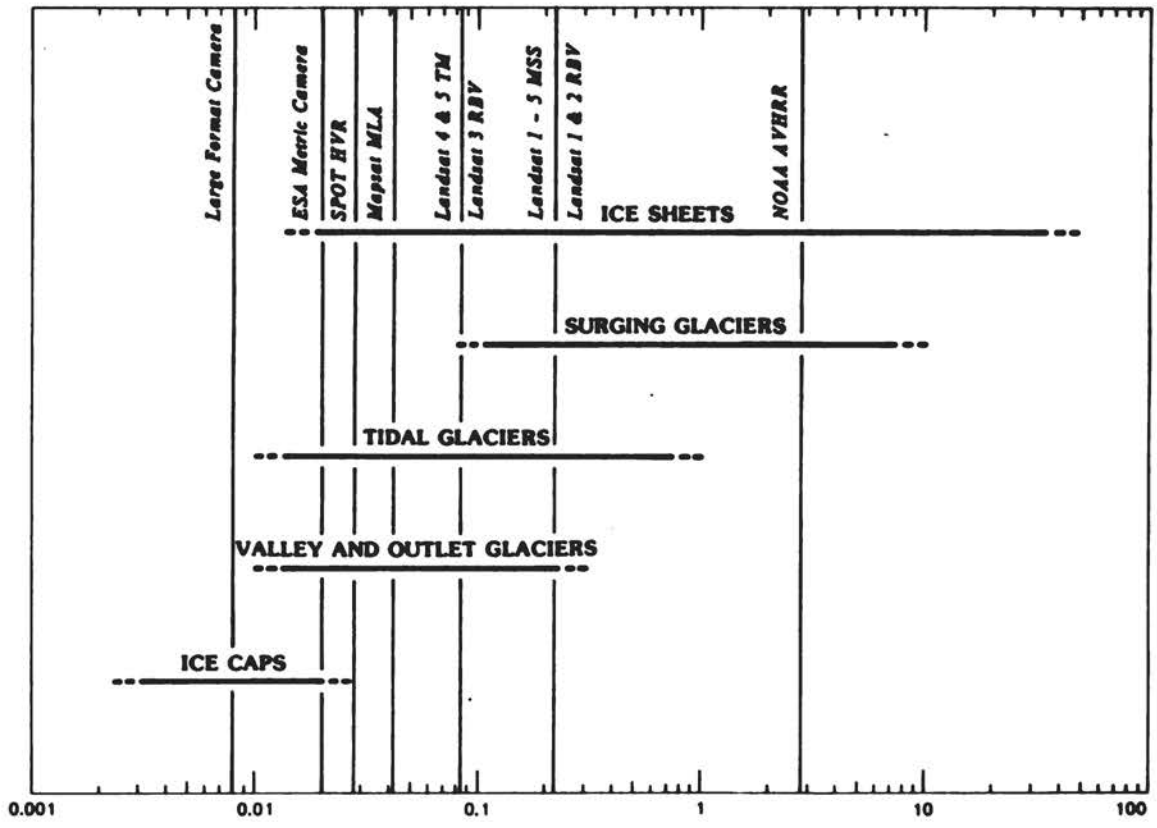

FIGURE 14.1 Graph showing the relationship between spatial resolution of existing and future imaging sensors (visible and infrared) onboard various satellites and the approximate range of annual dynamic change of termini of different types of glaciers. Termini of ice sheets includes ice shelves from which large tabular icebergs can calve off, producing large annual changes. Spatial resolution of a camera/film-filter system is given in meters per line pair. Spatial resolution for nonphotographic imaging sensors is taken to be 2.8 times the pixel resolution where a pixel is the dimension on the Earth's surface of a single picture element. ESA, Eropean Space Agency; HRV, haute resolution visible (SPOT sensor); MLA, multispectral linear array; MSS, multispectral scanner (Landsat sensor); RBV, return beam vindicon (Landsat sensor); SPOT, Systems Probatoire d'Observation de la Terre (French satellite); TM, thermatic mapper (Landsat sensor); AVHRR, advanced-very-high-resolution radiometer.

Monoscopic imagery provides two-dimensional (x, y) information about the areal extent of glaciers. Landsat images have provided a means for delineating the areal extent of ice sheets and ice caps (Björnsson 1980; Williams 1983b); for determining the changing position of the termini of valley, outlet, and tidal glaciers (Krimmel and Meier 1975), and the margins of ice sheets and ice shelves [Swithinbank et al. 1976; Colvill

1977; Swithinbank and Lane 1977; Drewry (ed.) 1983]; and for measuring the average speed of flow of some glaciers, by a time-lapse method of sequential images, in Iceland (Williams et al. 1974, 1975, 1979) and in Antarctica (Williams et al. 1982).

Determination of the third dimension (z) of glaciers has been hampered by a lack of appropriate satellite remote sensors, although some success has been achieved by using data from Seasat and GEOS radar altimeters to determine the elevations of ice shelves in Antarctica and of the gently sloping parts of the Antarctic and Greenland ice sheets at latitudes not greater than 72° south and north (Brooks et al. 1978, 1983; Zwally et al. 1983). Recent work by Thomas et al. (1983) established the feasibility of mapping margins of ice shelves from radar-altimetry data.

The physical characteristics of valley, tidal, and outlet glaciers and small ice caps can be determined through a combination of direct and remote measurement techniques. Aerial photographs and Landsat images provide information about the areal of a glacier. Repetitive aerial photographs and Landsat images provide a "time-lapse" look at dynamic glaciological phenomena, enabling scientists to observe the advance or recession of glacier termini during surge conditions (Williams et al. 1974, 1979); to monitor iceberg production from Jakobshavns Isbrae, West Greenland (Stove et al. 1984); to infer dynamics of flow of outlet glaciers in Antarctica (McIntyre 1983, in press); to observe the pattern of change in thickness through time (Rasmussen and Meier 1985); to measure velocity fluctuations (Meier et al. 1985) and velocity of terminus (Meier et al. 1978; Williams et al. 1982); and to determine position of the firn line (Williams 1983a; Ostrem 1975). Photogrammetric analysis of steroscopic aerial photographs, together with sufficient geodetic control on the ground, permits the compilation of accurate topographic maps of the surface morphology of glaciers (Kasser 1967, 1973; Müller 1977; Meier et al. 1978).

Theoretically, accurate topographic maps of glaciers can be prepared from steroscopic images and photographs acquired from an orbiting spacecraft (Doyle 1983; Colvocoresses 1984), but a specially designed mapping satellite, such as Mapsat, a satellite system designed by the U.S. Geological Survey (Itek Optical Systems 1981; Colvocoresses 1982), will be needed to achieve systematic repetitive 1:50,000-scale or smaller topographic maps, having a 20-m contour interval, on a global basis. The Mapsat concept has recently been accepted by the International Society for Photogrammetry and Remote Sensing, which has termed it the Orbital Mapping System (OMS) (Colvocoresses, 1984). The U.S. Large Format Camera (LFC), flown for the first time on the October 1984 Space Shuttle (STS Mission 41-G) was specifically designed for photogrammetrically accurate mapping of the Earth's surface (Doyle 1983). Preliminary results from photogrammetric analysis of high-resolution (8-m resolution per line pair) black-and-white LFC photographs (stereopairs) confirmed that 1:50,000-scale topographic maps, having 20-m contour intervals, can be prepared (F. J. Doyle, U.S. Geological Survey, personal communication, 1984). The French SPOT Satellite, to be orbited in 1985, may also have a limited capability for topographic mapping.

TABLE 14.1 Present and Future Capability for Acquiring Physical Characteristics of Glaciers from Satellite Sensors[a]

Glaciological Parameter	Capability	Satellite	Sensor	Remarks
Glacier area	Present	Landsat	MSS, RBV, TM	TM images are expected to provide more precise information
Surface Topography	Present (ice sheets only)	Seasat, GEOS, Geosat	Radar altimeter	Large areal footprint; altimeter loses lock-in areas of irregular topography, accuracies to ±1 m. Orbital inclination limits coverage to area between 72° north and south latitudes only. The future ERS-1 radar altimeter will reach latitudes of 82°.
Change in surface topography (traverse)	Future	High-inclination polar-orbiting satellites	Laser altimeter coupled with precise geodetic positioning	Small footprint; will enable precise surface-elevation (±1-10 cm) and $\partial v/\partial t$ of glaciers. Systematic repetitive coverage needed.
Surface topography	Present	Space Shuttle	LFC, ESA metric camera	Limited geographic nonsystematic coverage.
(contour map)	Future	High-inclination polar-orbiting satellite (Mapsat)	Stereoscopic multi-spectral linear array (MLA) 3 scanners, coupled with precise geodetic positioning	Systematic, global coverage of multispectral stereoscopic imagery. 1:50,000-scale maps of glaciers at 20-m contour interval (already achieved with Large Format Camera photgraphs).
Firn limit	Present	Landsat	MSS, TM	TM images should provide more accurate delineation.
Termini fluctuation (including surge behavior)	Present	Landsat	MSS, TM	TM images should provide more accurate measurements of fluctuation.
Velocity of termini	Present	Landsat	MSS, TM	TM images will enable more supraglacial features to be identified, therby permitting more average velocity measurements of glacier termini.
Terminal moraines	Present (?) Future	Landsat Mapsat, SPOT	TM, Spectroscopic MLA, HRV	TM may provide needed inflormation. Stereoscopic images are probably needed to recognize and map terminal moraines.

[a] ERS, European Remote Sensing satellite; ESA, European Space Administration; GEOS, Geodetic Earth Observatory Satellite; HRV, haute resolution visible (SPOT sensor); LFC, Large Format Camera; MLA, multispectral linear array; MSS multispectral scanner (Landsat 1-5 sensor); RBV, return beam vidicon (Landsat 1-3 sensor); SPOT, Système Probatoire de la Terre (French satellite); TM, thematic mapper (Landsat 4 and 5 sensor).

Although the measurement of relative elevation (contour intervals of 1 m) of parts of the Antarctic and Greenland ice sheets has already been achieved from data acquired by radar altimeters on Seasat and GEOS, laser altimeters on future polar-orbiting satellites are needed to achieve elevation accuracies of a few centimeters (Bufton et al. 1981; Zwally et al. 1981). Such dedicated future satellites are the key element in determining volumetric changes in glaciers on a regional and global basis (Swithinbank 1983, in press; National Research Council 1983). However, such accuracies are meaningless unless the elevations are precisely located geodetically. Satellites that combine precise geodetic position with precise elevation data are essential.

Information about the absolute thickness of glaciers, however, must be obtained either by drilling through the glacier or by using geophysical methods, such as seismic, gravimetric, or radio-echo sounding devices. Nowadays, radio-echo sounding is the preferred method, either by surface (Watts and England 1976) or airborne (Drewry 1981) traverses.

Remote-sensing technology is an important element in the measurement of the areal extent, topographic configuration, and thickness of glaciers and in the monitoring of changes in all of these physical characteristics. Although selected glaciers have been surveyed and monitored over long periods (greater than 50 years) (Meier 1984), most of the world's glaciers have not been studied scientifically. Most glacierized areas are inadequately mapped (Southard and MacDonald 1974; Swithinbank 1980, in press) and have limited aerial photographic coverage. Present and near-future satellite remote-sensing technology already permits (Ferrigno and Williams 1980; Williams and Ferrigno 1981) or will permit (Swithinbank 1983, in press) systematic repetitive surveys of the world's glaciers (Table 14.1; Haeberli, this volume, Attachment 13). Areal measurements of glaciers obtained from satellite images, when combined with geodetically precise elevation data acquired by satelliteborne laser altimeters, will, in conjunction with accurate attitude-reference systems on such satellites and accurate ephemeris data from the Global Positioning Satellite (GPS) system, permit quantitative measurements of change in volume or glacier ice over time at precise geographic locations. These measurements, in turn, will permit an assessment of the actual contribution of the melting of glacier ice to the secular rise in sea level.

REFERENCES

Allison, I. (ed.), 1981. Sea Level, Ice, and Climatic Change, Proceedings of the symposium (7-8 December 1979) held during the 17th General Assembly of the International Union of Geodesy and Geophysics, Canberra, Australia. International Association of Hydrological Sciences Publication No. 131, 471 pp.

Björnsson, H., 1980. The surface area of glaciers in Iceland. Jökull, 28, 31.

Brooks, R. L., W. J. Campbell, R. O. Ramseier, H. R. Stanley, and H. J. Zwally, 1978. Ice sheet topography by satellite altimetry. Nature, 274(5671), 539-543.

Brooks, R. L., R. S. Williams, Jr., J. C. Ferrigno, and W. B. Krabill, 1983. Amery ice shelf topography from satellite radar altimetry. In R. L. Oliver, P. R. James, and J. B. Jago (eds.), Antarctic Earth Science--Proceedings of the Fourth International Symposium on Antarctic Earth Sciences (16-20 August 1982). University of Adelaide, South Australia, Australian Academy of Science, Canberra, pp. 441-445.

Bufton, J. L., J. E. Robinson, M. D. Femiano, and F. S. Flatow, 1981. Satellite laser altimetry for measurement of ice-sheet topography. International Geoscience and Remote Sensing Symposium, June 8-10, 1981, Washington, D.C., Digest, v. 2, pp. 1003-1011.

Colvill, A. J., 1977. Movement of Antarctic ice fronts measured from satellite imagery. Polar Record, 18(15), 390-394.

Colvocoresses, A. P., 1982. An automated mapping satellite system (Mapsat). Photogrammetric Engineering and Remote Sensing, 48(10), 1585-1591.

Colvocoresses, A. P. (chairman), 1984. Acquisition and Processing of Space Data for Mapping Purposes. Report of the Committee of Working Group IV/3, International Society for Photogrammetry and Remote Sensing, 35 pp.

Doyle, F. J., 1983. Surveying and mapping with space data. In Papers of the Corten Retirement Symposium. International Institute for Aerial Survey and Earth Sciences (ITC), Enchede, Netherlands, 17 pp.

Drewry, D. J., 1981. Radio echo-sounding of ice masses--principles and applications. In A. P. Cracknell (ed.), Remote Sensing in Meteorology, Oceanography, and Hydrology, Elelis Horwood, Ltd., Chichester, England, pp. 270-284.

Drewry, D. J. (ed.), 1983. Antarctica--Glaciological and Geophysical Folio. Scott Polar Research Institute, Cambridge University, Cambridge, England, unpaginated.

Ferrigno, J. G., and R. S. Williams, Jr., 1980. Satellite image atlas of glaciers. In World Glacier Inventory, Proceedings of the Riederalp (Switzerland) Workshop. International Association of Hydrological Sciences Publication No. 126, pp. 333-341.

Hoffman, J. S., D. Keyes, and J. G. Titus, 1983. Projecting Future Sea Level Rise. Methodology, Estimates to the Year 2100, and Research Needs. Office of Policy and Resource Management, U.S. Environmental Protection Agency, Washington, D.C., revised second edition, 121 pp.

Itek Optical Systems, 1981. Conceptual design of an automated mapping system (Mapstak). Final technical reprot to the U.S. Geological Survey, Itek Report No. 81-8449A-1 (12 January 1981).

Kasser, P., 1967. Fluctuations of Glaciers 1959-1965. International Association of Scientific Hydrology, UNESCO, Paris, 52 pp.

Kasser, P., 1973. Fluctuations of Glaciers 1965-1970. International Association of Hydrological Sciences, UNESCO, Paris, 357 pp.

Krimmel, R. M., and M. F. Meier, 1975. Glacier applications of ERTS images. Journal of Glaciology, 15(73), 391-402.

McIntyre, N. F., 1983. The topography and flow of the Antarctic ice sheet. Ph.D. dissertation, Cambridge University, Cambridge, England, 198 pp.

McIntyre, N. F., in press, The dynamics of ice sheet outlets. Journal of Glaciology.

McIntyre, N. F. and D. J. Drewry, 1984. Modelling ice-sheet surfaces for ERS-1's radar altimeter. ESA Journal, 8(3), 261-274.

Meier, M. F., 1980. Remote sensing of snow and ice. Bulletin of the Hydrological Sciences, 25(3), 307-330.

Meier, M. F., 1983. Snow and ice in a changing hydrological world: Hydrological Sciences Journal, 28(1), 3-22.

Meier, M. F., 1984. Contribution of small glaciers to global sea level. Science, 226(4681), 1418-1421.

Meier, M. F., A. Post, C. S. Brown, D. Frank, S. M. Hodge, L. R. Mayo, L. A. Rasmussen, E. A. Senear, W. G. Sikonia, D. C. Trabant, and R. D. Watts, 1978. Columbia Glacier progress report. U.S. Geological Survey Open-File Report 78-264, 78 pp.

Meier, M. F., L. A. Rasmussen, R. M. Krimmel, R. M. Olsen, and D. Frank, 1985. Photogrammetric determination of surface altitude, terminus position, and ice velocity of Columbia Glacier, Alaska. In Studies of Columbia Glacier, Alaska, U.S. Geological Survey Professional Paper 1258-F, 41 pp.

Müller, F., 1977. Fluctuations of Glaciers 1970-1975. International Association of Hydrological Sciences, UNESCO, Paris, 269 pp.

National Research Council, 1983. Snow and Ice Research: An Assessment. Polar Research Board, National Academy Press, Washington, D.C., 126 pp.

Ostrem, G., 1975. ERTS data in glaciology--an effort to monitor glacier mass balance from satellite imagery. Journal of Glaciology, 15(73), 403-414.

Rasmussen, L. A., and M. F. Meier, 1985. Surface topography of the lower part of Columbia Glacier, Alaska, 1974-81. In Studies of Columbia Glacier, Alaska, U.S. Geological Survey Professional Paper 1258-E, 62 pp.

Revelle, R. R., 1983. Probable future changes in sea level resulting from increased atmospheric carbon dioxide. In Changing Climate, National Academy Press, Washington, D.C., pp. 433-448.

Southard, R. B., and W. R. MacDonald, 1974. The cartographic and scientific application of ERTSW-1 imagery in polar regions. Journal of Research (U.S. Geological Survey), 2(4), 385-394.

Stove, G. C., K. Green, R. V. Birnie, G. Davison, L. Bagot, M. Palmer, G. Kearn, P. F. S. Ritchie, and D. E. Sugden, 1984. Monitoring iceberg production from West Greenland tidewater glaciers using Landsat data--results from the AGRISPINE experiment for the Jakobshavns Isbrae, Macaulay Institute for Soil Research, Craigiebuckler, Aberdeen, Scotland, and the National Remote Sensing Centre, Space and New Concepts Department, Royal Aircraft Establishment, Farnborough, Hampshire, England, 32 pp.

Swithinbank, C., 1980. The problem of a glacier inventory of Antarctica. In World Glacier Inventory, Proceedings of the Riederalp (Switzerland) Workshop. International Association of the Hydrological Sciences Publication No. 126, pp. 229-236.

Swithinbank, C., 1983. Towards an inventory of the great ice sheets. Geografiska Annaler, 65A(3-4), 289-294.

Swithinbank, C., in press. A distant look at the cryosphere. In Proceedings of 25th Meeting of the Committee on Space Research (COSPAR), Symposium 4.

Swithinbank, C., and C. Lane, 1977. Antarctic mapping from satellite imagery. In R. E. Peel, L. F. Curtis, and E. C. Barrett (eds.), Proceedings of the 28th Symposium of the Coston Research Society, Remote Sensing of the Terrestrial Enviornment, University of Bristol, Butterworth Publishing Co., London, pp. 212-221.

Swithinbank, C., C. Doake, and R. Crabtree, 1976. Major changes in the map of Antarctica. Polar Record, 18(114), 295-299.

Thomas, R. H., T. V. Martin, and H. J. Zwally, 1983. Mapping ice-sheet margins from radar altimetry data. Annals of Glaciology, 4, 283-288.

Wallén, C. C., 1981. Monitoring the world's glaciers--the present situation. Geografiska Annaler, 63A(3-4), 197-200.

Watts, R. D., and A. W. England, 1976. Radio-echo sounding of temperate glaciers: Ice properties and sounder design criteria. Journal of Glaciology, 17(75), 39-48.

Williams, R. S., Jr., 1983a, Remote sensing of glaciers: Geological applications. In R. N. Colwell (ed.), Manual of Remote Sensing, Second Edition. American Society of Photogrammetry, Falls Church, Virginia, pp. 1852-1866.

Williams, R. S., Jr., 1983b. Satellite glaciology of Iceland. Jökull, 33, 3-12.

Williams, R. S., Jr., and J. G. Ferrigno, 1981, Satellite image atlas of Earth's glaciers. In M. Deutsch, D. R. Wiesnet, and A. Rango (eds.), Satellite Hydrology. American Water Resources Association, Minneapolis, Minnesota, pp. 173-182.

Williams, R. S., Jr., A. Bödvarsson, S. Fridriksson, G. Palmason, S. Rist, H. Sigtryggsson, K. Saemundsson, S. Thorarinsson, and I. Thorsteinsson, 1974. Environmental studies of Iceland with ERTS-1 imagery. In Ninth International Symposium on Remote Sensing of Environment, Environmental Research Institute of Michigan, Ann Arbor, Michigan, pp. 31-81.

Williams, R. S., Jr., A. Bödvarsson, S. Rist, K. Saemundsson, and S. Thorarinsson, 1975. Glaciological studies in Iceland with ERTS-1 imagery. Journal of Glaciology, 15(73), 465-466.

Williams, R. S., Jr., S. Thorarinsson, H. Björnsson, and G. Gudmundsson, 1979. Dynamics of Iceland ice caps and glaciers. Journal of Glaciology, 24(90), 505-507.

Williams, R. S., Jr., J. G. Ferrigno, T. M. Kent, and J. W. Schoonmaker, Jr., 1982. Landsat images and mosaics of Antarctica for mapping and glaciological studies. Annals of Glaciology, 3, 321-326.

Zwally, H. J., R. H. Thomas, and R. A. Bindschadler, 1981. Ice-sheet dynamics by laser altimetry. U.S. National Aeronautics and Space Administration Technical Memorandum 82128, 11 pp.

Zwally, H. J., R. A. Bindschadler, A. C. Brenner, T. V. Martin, and R. H. Thomas, 1983. Surface elevation contours of Greenland and Antarctic ice sheets. Journal of Geophysical Research, 88(C3), 1589-1596.

ATTACHMENT 15

SNOW COVER, SEA ICE, AND PERMAFROST

R. G. Barry
CIRES, University of Colorado
Boulder, Colorado

SIGNIFICANCE

Information on the temporal and spatial variability of snow cover and sea-ice extent is needed to enable possible global trends in these variables to be detected. Less readily determined, but similarly important, are the depth of snow cover and sea-ice thickness and age structure. Decreases in snow and ice extent are anticipated in response to CO_2-induced global warming, especially as this warming would be amplified several times in high latitudes. The time scale of response for snow cover would be 1-10 yr, and sea ice about 10 yr. However, there is evidence of increased snowfall amount with higher winter temperatures in some high-latitude regions, although the net effect of this is uncertain. Furthermore, sea-ice extent around Antarctica has an influence on the amount of snowfall on the ice sheet and the ice shelves and there are additional possible interactions between ice-extent concentration and the ice shelf-oceanographic regime. These have been little explored up to now.

Permafrost extent and thickness will also diminish in response to a CO_2-induced warming on a longer-term scale (about 10^2-10^3 yr). Any ground-ice melt would be of global significance in terms of the contribution to sea level.

OBSERVATIONS

Comprehensive global information on snow cover and sea-ice extent has only become available through the use of satellite remote sensing since the late 1960s; reliable data sets in digital form exist in each case from about 1972-1973 (Dewey and Heim 1981; Barry et al. 1984; Sturman and Anderson 1984). For individual ocean areas, or countries, "historical" observations of sea-ice extent and snow cover provide longer time series, but many problems arise with such records, and care is necessary in utilizing them in climatic analysis.

Surface observations of snow cover (or sea-ice extent) are generally point observations, and there are differences in reporting procedures in different countries. Although regional data compilations do exist, they vary in accuracy in time and spatial coverage in ways that are

Table 15.1 Snow and Ice Components (Modified from Hollin and Barry, 1979)

	Area (10^6 km^2)	Ice Volume (10^6 km^3)	Sea-Level Equivalent[a] (m)
Land ice: East Antarctica[b]	9.86	25.92	64.8
West Antarctica[c]	2.34	3.40	8.5
Greenland	1.7	3.0	7.6
Small ice caps and mountain glaciers	0.54	0.12	0.3
Permafrost (excluding Antarctica):			
Continuous	7.6	0.03 to	0.08 to
Discontinuous	17.3	0.7	0.17
Sea ice: Arctic[d]			
Late February	14.0	0.05	
Late August	7.0	0.02	
Antarctic[e]			
September	18.4	0.06	
February	3.6	0.01	
Land Snow Cover[f]			
N. Hemisphere			
Early February	46.3	0.002	
Late August	3.7		
S. Hemisphere			
Late July	0.85		
Early May	0.07		

[a] 400,000 km^3 of ice is equivalent to 1 m global sea level.

[b] Grounded ice sheet, excluding peripheral, floating ice shelves (which do not affect sea level). The shelves have a total area of 1.62 x 10^6 km^2 and a volume of 0.79 x 10^6 km^3 (Drewry and Heim 1983).

[c] Including the Antarctic Peninsula.

[d] Excluding the Sea of Okhotsk, the Baltic Sea, and the Gulf of St. Lawrence (Walsh and Johnson 1979). Maximum ice extents in these areas are 0.7 million, 0.4 million, and 0.2 million km^2, respectively.

[e] Actual ice area excluding open water (Zwally et al., 1983). Ice extent ranges between 4 million and 20 million km^2.

[f] Snow cover includes that on land ice but excludes snow-covered sea ice (Dewey and Heim, 1981).

usually not specified. These problems are illustrated for sea-ice data by Barry (1985). Permafrost thickness is incompletely known and the actual ice volume only crudely estimated.

General evaluations of the utility of snow cover, sea/lake ice, and permafrost for possible early detection of CO_2-induced climatic effects are given elsewhere (Barry 1984, in press).

VARIABILITY AND TRENDS

Table 15.1 summarizes the seasonal extremes of hemisphere snow cover and sea-ice extent. Northern hemisphere snow cover and Antarctic sea ice are the dominant seasonal components.

The variabiity of northern hemisphere snow cover for 1967-1984 is shown in Figure 15.1 (M. Matson, personal communication, 1984); the data are smoothed by a 12-month running mean. Eurasian snow cover dominates the interannual variability in hemispheric extent. Converted to snow cover volume (water equivalent), the seasonal variation is approximately 5 mm of sea-level equivalent and the interannual variability is 1 mm. There is no evidence of any long-term trend in snow cover area.

There is also no clear indication of long-term trends in sea-ice extent in either hemisphere. Various studies show that interannual ice anomalies on a regional scale, which are associated with corresponding anomalies in atmospheric circulation, are large (Walsh and Johnson 1979; Cavalieri and Parkinson 1981; Zwally et al. 1983). Kukla and Gavin (1981) reported a decrease in sea ice in the South Atlantic sector between the 1930s and the 1970s, but the significance of this on a hemispheric scale is uncertain. Soviet estimates of Arctic sea-ice extent in late summer, 1950-1980, show a fluctuation of approximatley $\pm$1°C June-August temperature anomalies over the polar cap 65-85°N, for 5-year running means of each series (see Figure 15.2). During the period of ice retreat, the atmosphere is known to "force" the ice over lags of several months (Walsh and Johnson 1979). Corresponding records of summer ice area and temperature from 1924 are virtually uncorrelated; this suggests either that one or both data sets are unreliable or that some unknown, perhaps oceanic process, affected the earlier Arctic ice regime. The fluctuations of Arctic ice over the 1970-1980 period show no apparent relationship with those of northern hemisphere snow cover.

Several studies of borehole temperature profiles in Alaskan permafrost indicate a warming effect of about 2°C over the last 100 years (Lachenbruch et al. 1982), and there are various qualitative indications of thawing and permafrost retreat. The ice content of global permafrost is poorly known, but estimates of the potential contribution to sea level are of the order of 0.08 to 0.17 mm (Barry in press). However, the contribution to sea-level rise over the next 100 years is unlikely to exceed a few millimeters, in view of the fractional melt anticipated for warming and the slow responsed time of ground ice to changes in surface air temperature.

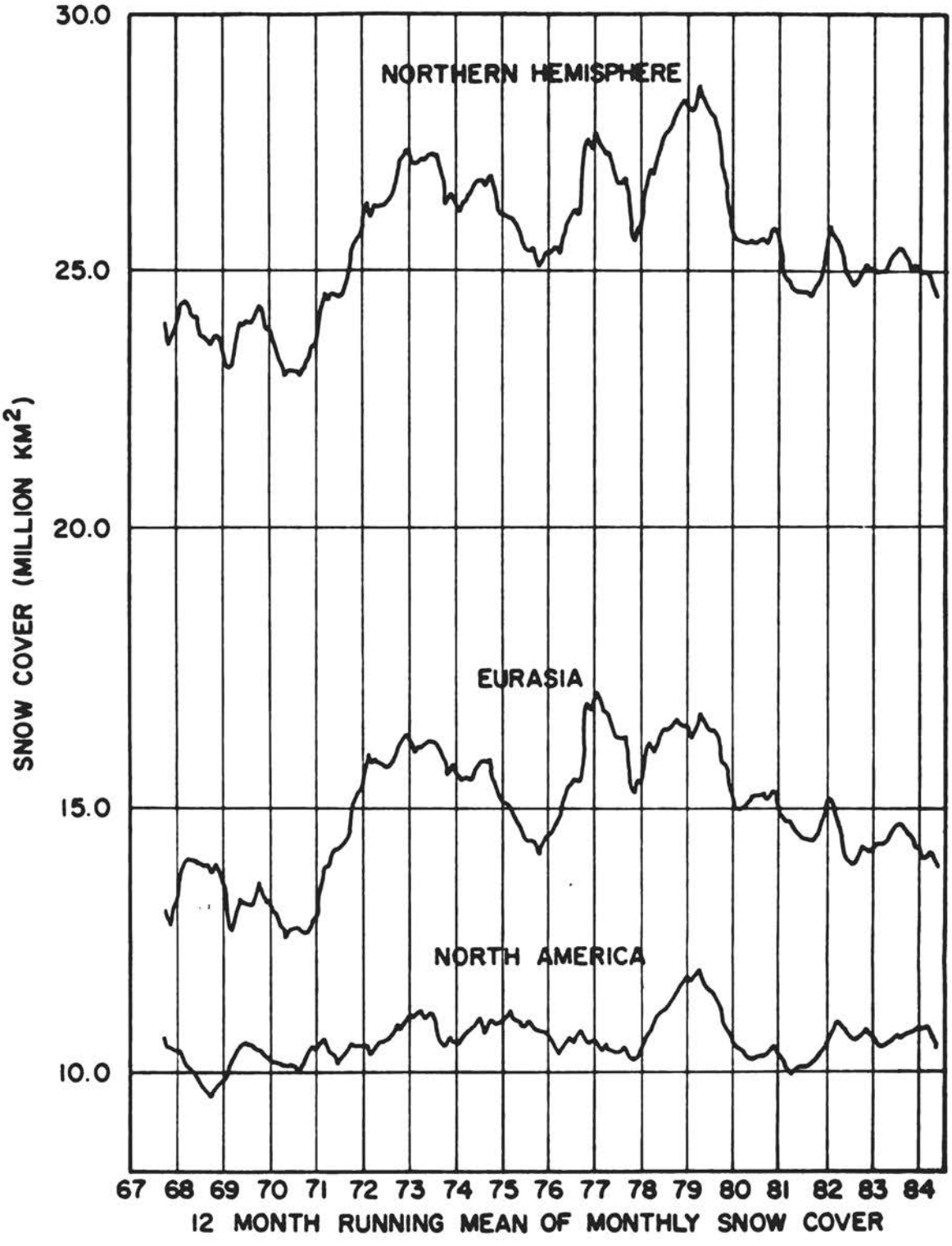

FIGURE 15.1 Trends of snow cover in the northern hemisphere, Eurasia, and North America, 1967-1984, smoothed via a 52-week running mean (M. Matson, unpublished).

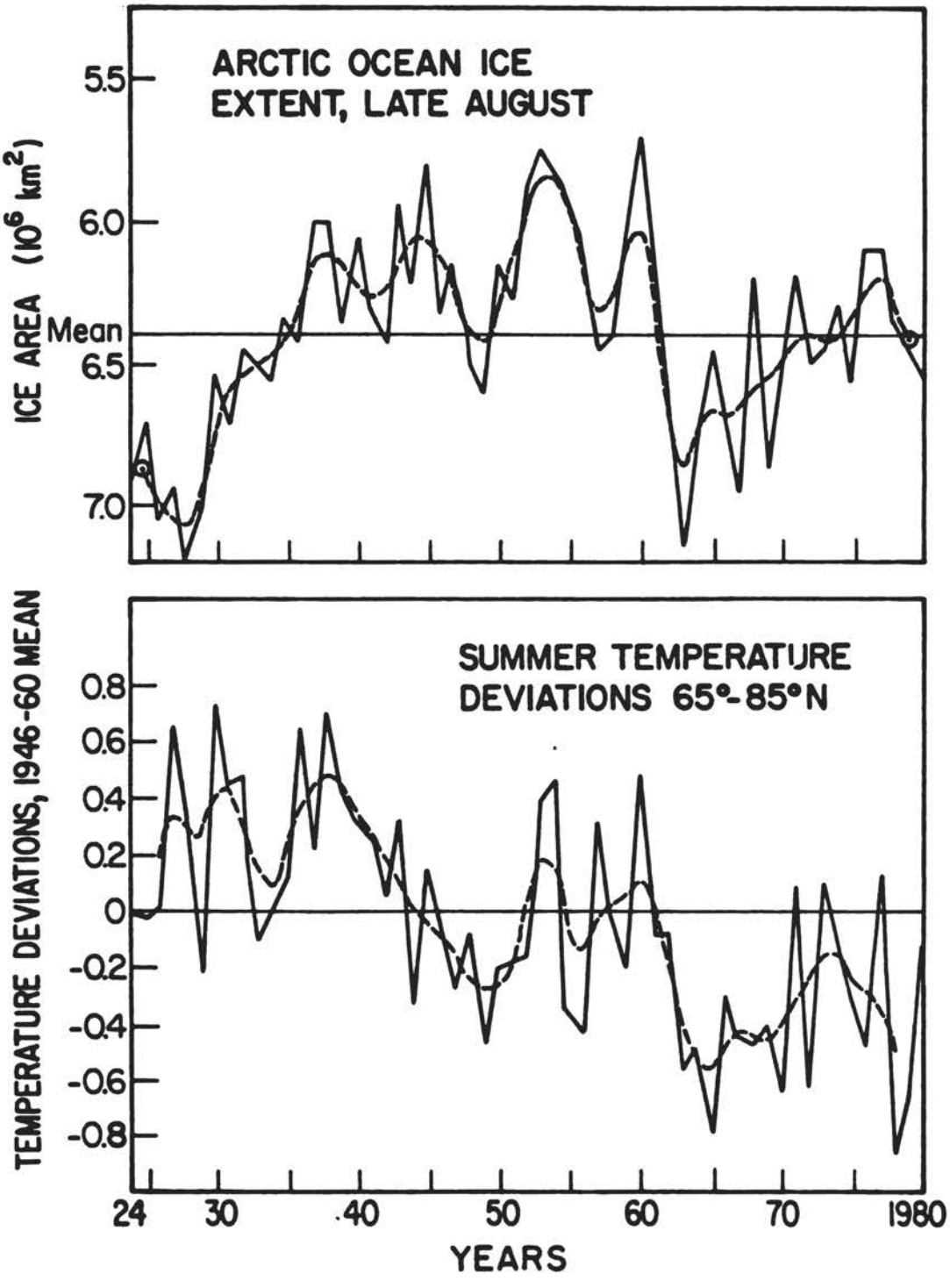

FIGURE 15.2 Arctic Ocean ice extent in late August, 1924-1980, and summer temperature departures from the 1946-1960 mean for latitudes 65-85°N. Dashed line denotes 5-year binomially weighted running mean (from Barry 1983).

INTERACTIONS BETWEEN SNOW COVER, SEA ICE, AND LAND ICE

Projections of the mass-balance response of land ice to possible CO_2-induced climate change must take account of potential interactions between the various components of the climate system. Two such interactions are of relevance here. According to Limbert (1984) accumulation in the coastal areas of Antarctica may increase during a warming. The Wolverine Glacier in southern Alaska thickened during 1976 and 1981, a period of warmer and more snowy winters (Mayo and Trabant 1984). Consequently a global warming (which in any case would not be uniformly distributed) would undoubtedly give rise to a complex spatial pattern of land-ice growth/thinning. Temperature-snowfall relationships have received little systematic attention from both observational and modeling standpoints.

The second potential interaction concerns the relationship between sea-ice extent and cyclonic activity, which gives snowfall in Antarctica. A shrinkage of the sea-ice cover would facilitate greater penetration of moist airflows into Antarctica. This effect could strengthen the above-noted tendency for increased snowfall to accompany a warming.

Other possible interactions involve the role of sea-ice cover in reducing wave action along the ice shelf margins at the present time. This factor remains to be considered quantitatively in assessments of possible rates of ice-shelf calving.

OBSERVATIONAL AND RESEARCH NEEDS

The observational record of global snow cover and ice is short so that their natural variability and trends are poorly specified on decadal and longer time scales. Long-term monitoring via passive microwave remote sensing is practical and essential. The feasibility of this technique for mapping snow-cover extent has been demonstrated but, so far, not routinely applied. Records of surface snow-cover depth and water equivalent also need compiling to augment the historical data base and to serve as a calibration for the satellite data. Sea-ice extent can now be mapped routinely, even in the presence of cloud cover or darkness, but information on ice concentration, age, and thickness is inadequate. Combined remote sensing, sonar, and field measurements are necessary to define the ice mass balance and its fluctuations. Monitoring of changes in permafrost temperatures with depth and improved information of permafrost extent, thickness, and ice content are also necessary to refine our estimates of the potential impacts of climatic perturbations.

REFERENCES

Barry, R. G., 1983. Arctic Ocean ice and climate: Perspectives on a century of polar research. Annals, Association of American Geographers, 73, 485-501.

Barry, R. G., 1984. Possible CO_2-induced warming effects on the cryosphere. In N. A. Mörner and W. Karlen (eds.), Climatic Changes on a Yearly to Millenial Basis, Reidel Publishing Co., Dordrecht, pp. 571-604.

Barry, R. G., 1985. The sea ice data base. In N. Untersteiner (ed.), The Geophysics of Sea Ice, Plenum Press, New York, in press.

Barry, R. G., in press. The cryosphere and climatic change. In M. C. MacCracken and F. Luther (eds.), Detection of CO_2-Induced Climatic Change, Department of Energy, Washington, D.C.

Barry, R. G., A. Henderson-Sellers, and K. P. Shine, 1984. Climate sensitivity and the marginal cryosphere. In J. E. Hansen and T. Takahasi, (eds.), Climate Processes and Climate Sensitivity, Geophysical Monograph, 29, American Geophysical Union, Washington, D.C., pp. 221-237.

Cavalieri, D. J., and C. L. Parkinson, 1981. Large variations in observed Antarctic sea ice extent and associated atmospheric circulation. Monthly Weather Review, 109, 2323-2336.

Dewey, K. F., and R. J. Heim, 1981. Satellite observations of variations in northern hemisphere seasonal snow cover. NOAA Technical Report, NESS 87, Washington, D.C.

Kukla, G. J., and J. Gavin, 1981. Summer ice and carbon dioxide. Science, 214, 497-503.

Lachenbruch, A. H., J. H. Sass, V. B. Marshall, and T. H. Moses, 1982. Permafrost, heat flow, the geothermal regime at Prudhoe Bay. Journal of Geophysical Research, 87, 9301-9316.

Limbert, D. W. S., 1984. West Antarctic temperatures, regional differences, and the nominal length of summer and winter seasons. In Environment of West Antarctica: Potential CO_2-Induced Changes, Polar Research Board, National Academy Press, Washington, D.C., pp. 114-139.

Mayo, L. R., and D. C. Trabant, 1984. Observed and predicted effects of climate change on Wolverine Glacier, Southern Alaska. In J. H. McBeath (ed.), The Potential Effects of Carbon Dioxide-Induced Climatic Changes in Alaska, University of Alaska-Fairbanks, School of Agriculture and Land Resources Management, Misc. Pub. 83-1: 114-123.

Sturman, A. P., and M. R. Anderson, 1984. A comparison of Antarctic sea ice data sets and inferred trends in ice area. Journal of Climate and Applied Meteorology, in press.

Walsh, J. E., and C. M. Johnson, 1979. Interannual atmospheric variability andassociated fluctuations in Arctic sea-ice extent. Journal of Geophysical Research, 84, 6915-6928.

Zwally, H. J., C. L. Parkinson, and J. C. Comiso, 1983. Variability of Antarctic sea ice and changes in carbon dioxide. Science, 220, 1005-1012.

ATTACHMENT 16

REACTIONS OF MID-LATITUDE GLACIER MASS BALANCE TO PREDICTED CLIMATIC CHANGES

M. Kuhn
Innsbruck University

SPECIFICATIONS

When investigating the possible contribution of mountain glaciers to the river runoff into the ocean and to an increase in sea level following conceivable climatic changes one needs to further specify the terms involved in the problem, or to set a scenario that fits the topic of this paper. A number of existing models are discussed in this volume. In this context, climatic changes in mid-latitudes mean a warming of about 4.0°C mean annual temperature in 100 years, possibly associated with it a minor increase in mean annual cloudiness and in precipitation.

Mid-latitude glaciers shall be understood to have a mean annual ice temperature of 0°C in the majority of their mass and a terminus above sea level so that calving and grounding line problems can be disregarded, and it is supposed that they have clearly distinguishable accumulation and ablation areas. Within these constraints, they may be further distinguished according to respective climatic characteristics, e.g., into maritime, continental, and monsoonal types. Without much difficulty, the following considerations may be applied to subtropical, arid zone glaciers as well.

Contrary to polar-ice fields, mid-latitude mountain glaciers do not influence the general circulation or large-scale climate. While their existence modifies local wind systems and changes the annual course of river runoff, their presence or absence at the end of the summer season is of little effect compared to the interannual variability of the seasonal snow cover of the mid-latitudes.

Although on a global scale feedback between atmosphere and mid-latitude mountain glaciers is negligible, the boundary layer above the thermal admittance of the glacier is modified by the persistence of a 0°C surface throughout the summer. These effects, however, can be covered by the transfer coefficients of the energy-balance equations.

Finally, the restriction to mass balance deserves further comment. In a strict sense, it will always be the entire physical system of a glacier that reacts to a climatic change, e.g., its mass, length, width, temperature, water content, and velocity. The system components are responsible for establishing a new steady state or equilibrium following a given climatic forcing, but energy and mass balance are the interface through which climatic change is transmitted into the glacier system,

which will adapt to it according to the given topography and the dynamic properties of the ice.

The water output of a glacier is not a linear response to climatic change. We are not even sure that the system (climate input/water output) is transitive, i.e., whether a given climatic forcing and given initial conditions will always, or in all glaciers, result in the same reaction (Meier 1983). For this reason the present discussion will be restricted to the climate/ice interface, i.e., to local mass energy balances, and the method chosen is that of linearization of individual components.

A SIMPLE ALGORITHM

One example for the method mentioned above has been given previously (Kuhn 1981). It has linked cumulative accumulation c with temperature T and radiation R as parameters of the energy balance. Some of the difficulties enumerated above have been avoided by simply considering the system on an annual basis at the equilibrium line, where the reaction is nearly immediate since no mass transport is involved. At the equilibrium line altitude h, accumulation equals ablation (c = a) and ablation can be parameterized by air temperature T and net radiation R:

$$a = f(T, R). \tag{16.1}$$

A climatic fluctuation in any of these three variables (δc, δT, δR) is compensated by the altitudinal gradients ($\partial c/\partial z$ measured along the glacier surface) such that equilibrium is established at the new altitude, $h + \delta h$. Using the latent heat of melting, L = 335 kJ/kg, and the duration of melting for converting between mass and energy terms, δh can be expressed as

$$\delta h = \frac{-\delta c + \frac{\tau}{L}\left(\delta R + \alpha \delta T\right)}{\frac{\partial c}{\partial z} + \frac{\tau}{L}\left(\frac{\partial R}{\partial z} + \alpha \frac{\partial T}{\partial z}\right)}, \tag{16.2}$$

where α is the heat-transfer coefficient according to

$$H = -\alpha(T - T_0), \tag{16.3}$$

with T_0 the surface temperature and H the turbulent flux of sensible heat. T is the air temperature of the free atmosphere at the same level, e.g., that extrapolated from a valley station. The equation given above can be summarized by

$$\delta h = \Sigma \delta q_i / \Sigma(\partial q_i/\partial z), \tag{16.4}$$

where the q_i are annual totals expressed uniformly in either energy or mass units.

Three points of interest have to be mentioned:

1. δh can be caused by individual δq_i or by a combination of them.
2. The formalism given above treats the variables (R, c, T) as if they were independent. In nature they will most likely be interrelated, hence a combination of influences will prevail.
3. Depending on climate, other parameters than (R, c, T) may be selected for q_i, above all, a term representing heat flux.

NUMERICAL EXAMPLES

In Table 16.1 examples are given for the δh ensuing from various possible components of a climatic disturbance, δq_i. In this case the constants and vertical derivatives appearing in Eq. (16.2)-(16.4) are valid for alpine conditions, and the δq_i are specified. If units of mass balance are chosen, $\Sigma \partial q_i/\partial z$ equals the vertical balance gradient, which is dominated by a component due to $\partial T/\partial z = -0.006°C/m$ in most climatic regions. The second contribution to the balance gradient is associated with $\partial c/\partial z$, the accumulation gradient. Even though this has a lesser magnitude, it is more variable from one climatic region to the other than the former, being large under maritime and small under continental conditions.

The scenario for Table 16.1 is made up by the following δq_i:

- a doubling of CO_2
- a temperature increase of 4°C
- an increase of water-vapor pressure of 1 hPa
- an increase of cloudiness by one tenth
- and an accumulation increase of 100 kg/m^2 per year
- of this additional accumulation five snowfall events are assumed to occur during summer, increasing albedo from 0.4 to 0.8 for each one day.

Several CO_2 models predict negligible changles in cloudiness and precipitation. Modest changes of these are included in Table 16.1 to demonstrate their effect in principle. For α a value of 1.6 MJ m^{-2} d^{-1} $°C^{-1}$ was used, and τ was set equal to 100 days. For $\Sigma \partial q_i/\partial z = \partial b/\partial z$ the value of +10 kg m^{-2} yr^{-1}/m was taken from central alpine observations.

PRACTICAL APPLICATION

The value of δh thus determined establishes the position of the new accumulation area for a given topography. This accumulation area has a size S_c and a mean specific balance b_c. If, after a climatic change, the glacier reaches a new steady state

$$S_c b_c = S_a b_a, \qquad (16.5)$$

i.e., the annual net accumulation has to flow across the new equilibrium

TABLE 16.1 Changes of Energy Fluxes (δq_i), Associated Annual Mass Balance Changes (δb_i), and Changes of Equilibrium-Line Altitude (δh) Following a Doubling of CO_2 (see Text for Inputs)[a]

Climatic Disturbances	δq_i (MJ m^{-2} d^{-1})	δb_i (kg m^{-2} yr^{-1})	δh_i (m)
δq_s (T)	+ 6.00	-1790	+ 180
δL (T)	+ 1.40	- 420	+ 40
δL (CO_2)	+ 0.35	- 100	+ 10
δL (w)	+ 0.82	- 240	+ 25
δG (w)	- 0.63	+ 190	- 20
δG (r)	- 0.30	+ 90	- 10
δq_l (e)	+ 1.70	- 510	+ 50
δc	- 0.33	+ 100	- 10
Total effect	9.01	-2680	+ 265
Effect of T and CO_2 alone	7.75	-2310	+ 230

[a]Energy fluxes concerned:
global radiation G
atmospheric downward radiation L
sensible heat q_s
latent heat (condensation) q_l

line each year and waste in the new ablation area, S_a, by net ablation, b_a.

Thus, knowing δh and $\partial b/\partial z$ and having a suitable ice-dynamics model, the reaction of a glacier to a changed climate can be predicted. The prediction algorithm presented here does not use absolute values of the energy and mass balance components but only its temporal and altitudinal derivatives, which is a decisive advantage when treating unmeasured glaciers.

For a large individual ice mass such as the Greenland ice sheet, the shift of the equilibrium line can be used as input in an ice-dynamics model in order to determine the new equilibrium shape and thus total mass loss contributing to sea-level change.

For a large number of mountain glaciers this procedure would be impractical. A mountain group such as the Alps contains several thousand glaciers of varying sizes, aspects, slopes, and shapes. For some regions, glacier inventories exist, as reported by Haeberli (this volume, Attachment 13), which list these parameters and their statistics. In the most general case such as the Andes or Himalayas, only the total area and the mean equilibrium line altitude can be estimated.

As long as this ice covered area S remains unchanged it is sufficient to know the disturbance of mean specific balance δb_a of the ablation area S_a. If the extent of S_a is not known, the ratio $S_a/S = 0.4$ is an approximation found valid in many individual glaciers. Thus, the additional, CO_2-induced meltwater production per year is

$$M = S_a \delta b_a = 0.4\, S \delta b_a. \qquad (16.6)$$

Values of δb_a and its components are given in the example of Table 16.1. The balance disturbance δb corresponds to Meier's (1962) budget imbalance and appears also in the linear balance model of Lliboutry (1974), see also Reynaud (1980).

However, there remain two basic difficulties: (1) S_a will shrink at a rate determined by the spatial change of ice thickness, and (2) the contribution of CO_2-induced meltwater to annual runoff will cease once a new equilibrium position is reached. Thus even under the most simplified conditions the new equilibrium needs to be specified.

To help this situation, two premises or educated guesses are required: (1) a representative profile of ice thickness, or an area/volume function, and (2) the area/height distribution from which the accumulation area can be fitted to the new equilibrium-line altitude. Since even an elaborate glacier inventory will furnish only the latter, it is proposed here to assume that area/volume and area/height data from one model-sized glacier are representative for the entire collective. Under these circumstances the total melt or mass loss can be determined as the difference between two equilibrium states.

THE TEMPORAL EVOLUTION

In the climate scenario of ever increasing CO_2 concentrations, air temperature will not reach a steady level so that glaciers after CO_2 doubling will not reach a new equilibrium in the sense of the discussion above but will continue to adjust to the changing climatic forcing.

In order to assess the amount of water annually taken out of glacial storage and added to the ocean, let us make some gross simplifications about the climatic change and glacier response. (1) Suppose that temperature increases linearly by 0.04 K/yr and that (2) the corresponding ablation, according to Table 16.1 increases by 0.0267 m/yr, (3) let all glaciers have rectangular shapes of constant width W and length r so that the decrease of ablation area is

$$\partial S_a/\partial t = W \partial r/\partial t, \qquad (16.7)$$

and (4) let the glacier tongues have the longitudinal cross section of a wedge of angle α and let their thickness be constant over W.

When an annual lowering (mass balance) of the surface, b, increasing by $\partial b/\partial t = -0.027$ m/yr the size change becomes thus

$$\partial S_a/\partial t = W \partial r/\partial t = W \frac{\delta b(t)}{\tan \alpha} \qquad (16.8)$$

or

$$S_a(t) = S_a(0) + W \frac{\delta b(t)}{\tan \alpha}. \qquad (16.9)$$

The annual contribution to sea-level rise will be

$$M(t) = S_a(t)\,\delta b(t), \tag{16.10}$$

$$M(t) = S_a(0)\,\delta b(t) + \frac{W}{\tan\alpha}[\delta b(t)]^2, \tag{16.11}$$

so that with

$$\partial M = S_a(0)\,\delta b(t) + \frac{W}{\tan\alpha}\,2\delta b(t)\,(\partial b/\partial t) \tag{16.12}$$

and with

$$\delta b(t) = b_1 t \tag{16.13}$$

a maximum will be reached at

$$t_{max} = -\frac{S_a(0)}{2W}\,\frac{\tan\alpha}{b_1}, \tag{16.14}$$

if $b_1 < 0$ is given in units of length/time.

CONCLUSIONS

According to most models, a CO_2-induced warming would be of the order of 0.04°C/yr. This warming, if continued at a constant rate over 100 years, would be followed by a raise of the equilibrium line of mid-latitude mountain glaciers of 2-3 m/yr. This raise is forced by the disturbance of a number of climatic variables among which δt, δc, and δe are the most important ones. It is controlled by the altitudinal gradients of mass and energy balance components, notably by that of accumulation that is more variable from one climatic region to another than the vertical temperature gradient.

While adjusting to the new climatic setting, mid-latitude glaciers will waste ice at a rate that will come to a maximum within a few decades, depending on the size range of the glaciers.

In order to give reliable estimates and predictions, better statistics of the area/number, area/altitude, and area/volume or length/thickness spectra is required. The data banks of existing regional glacier inventories, which are the prime source for such information, will be enlarged and further evaluated by the newly established World Glacier Monitoring Service.

The mid-latitude glaciers will continue to contribute significantly to sea-level rise as they are the ice masses closest to decay conditions at present; but with the extensive melting considered here, their number will drastically decrease in the coming 100 years.

REFERENCES

Kuhn, M., 1981. Climate and glaciers. In Proceedings of the Canberra

Symposium on Sea Level, Ice and Climatic Change. International Association of Hydrological Science Publication No. 131, pp. 3-20.

Lliboutry, L., 1974. Multivariate statistical analysis of glacier annual balances. Journal of Glaciology, 4, 252-263.

Meier, M. F., 1962. Proposed definitions for glacier mass budget terms. Journal of Hydrological Sciences, 28, 3-22.

Meier, M. F., 1983. Snow and ice in a changing hydrological world. Journal of Hydrological Sciences, 28(1), 3-22.

Reynaud, L., 1980. Can the linear balance model be extended to the whole Alps? International Association of Hydrological Science Publication No. 126, pp. 273-284.

ATTACHMENT 17

THE SHIFT OF EQUILIBRIUM-LINE ALTITUDE ON THE GREENLAND ICE SHEET FOLLOWING CLIMATIC CHANGES

W. Ambach and M. Kuhn
Innsbruck University

INTRODUCTION

When considering the various possible sources of climatically induced ice melt one has to focus attention on those ice masses that have large ablation areas in the present climatic situation. Apart from mountain glaciers this is definitely the case on the Greenland Ice Sheet. Possible changes in the extent of this ablation area are directly related to the shift of the equilibrium line.

EQUILIBRIUM LINE AND HEAT BALANCE

The condition defining the equilibrium line, i.e., accumulation equals ablation, can be linked to climatic variables: accumulation is proportional to precipitation and is modified by snow drift, and ablation is determined by the energy balance of the surface, for which temperature, albedo, and cloudiness are the most decisive climatic variables. Disturbances in these variables lead to a shift of the equilibrium line by δh to an altitude that is determined also by the altitudinal gradients of accumulation and energy balance components. This shift can be modeled as follows:

$$\delta h = \frac{\Sigma \delta q_i}{\Sigma \delta q_i \, \partial z} , \qquad (17.1)$$

where the q_i are the mass or energy balance components to uniform units of either mass or energy fluxes (see also Kuhn, this volume, Attachment 16).

Of the variables involved, the most important are the change in sensible heat flux $\delta q_s = \alpha \delta T_a$ over melting surfaces (where T_a is the air temperature and a the bulk heat-transfer coefficient), and the change in net radiation $\delta q_r = \alpha' \delta T_a + \beta \delta w$, which is caused by a change in temperature δT_a and cloudiness w (α', β are factors of proportionality). Changes in albedo can be ignored as the altitudinal pattern of albedo follows the shift of the equilibrium line.

Among the gradients, $\partial c/\partial z$ (c = snow accumulation) deserves the greatest attention since it is the one that changes most between different climatic regions. It is clear from Eq. (17.1) that a small positive

value of $\Delta \partial q_i / \partial z$ amplifies the reaction of h to a climatic disturbance and that large positive values damp the shift of the equilibrium line.

A PRACTICAL APPROACH

For the application of Eq. (17.1) accumulation and heat--alance measurements are required as the use of parametrization schemes established for other climatic regions should not be accepted for the Greenalnd Ice Sheet without proof.

The only area of Greenland that offers sufficient data of the required variables is the area of the EGIG activities and of the accumulation profiles across Greenland measured by Benson (1962). Heat-balance measurements in the EGIG profile, which are analyzed with respect to heat-balance modeling have been published by Ambach (1985a).

Based on these data the equilibrium line shift was computed for the EGIG profile (Ambach 1985b). Considering only disturbances δT_a, δw, and δc and taking into account the formation of superimposed ice the following results were established:

$$\delta h / \delta T_a = + 77 \text{ m } K^{-1} \quad (\text{with } \delta w = 0, \delta c = 0), \tag{17.2}$$

$$\delta h / \delta w = - 4 \text{ m per 1/10 of cloudiness } (\delta T_a = 0, \delta c = 0), \tag{17.3}$$

$$\delta h / \delta c = - 73 \text{ m per 100 kg/m}^2 \text{ of snow accumulation } (\delta T_a = 0, \delta w = 0). \tag{17.4}$$

The application of these coefficients to the CO_2 scenario is left to the reader.

When these results are applied to other regions of Greenland the varying magnitude of the accumulation gradient has to be taken into account. Benson's accumulation profiles show a regional variable accumulation pattern in which there even exist certain zones with negative altitudinal accumulation gradients. This is important, for instance, in the Thule area where the present-day equilibrium line is situated only little below the altitude at which accumulation starts to decrease with ablation. Should the equilibrium line be shifted to that altitude, a further shift into the region of negative accumulation gradient would be enlarged by a factor of 2-3 (Ambach and Kuhn, 1985). However, it is not clear whether this peculiar accumulation pattern would persist in a changed climate.

CONCLUSIONS

The required estimate of the possible contributions of increased melting to global sea-level rise will be demonstrated for a 100-m shift of equilibrium line in the EGIG profile, where the surface slope is 1:100. Here, $a\delta h = 100$ m causes an increase of ablation area S_a within a parallel stripe by 27 percent. With the reasonable assumption that the mean ablation gradient remains constant there follows a change of

the mean specific ablation δa of 27 percent so that the relative increase of melt following $\delta h = 100$ m becomes

$$\frac{\delta M}{M} = \frac{\delta S_a}{S_a} + \frac{\delta \bar{a}}{\bar{a}} + \frac{\delta \bar{a} \delta S_a}{\bar{a} S_a} = 0.61. \qquad (17.5)$$

In this formulation no dynamic reactions of the ice mass are considered. The shift of the equilibrium line follows instantaneously the climatic disturbances, even year by year. The question of which part of the meltwater surplus generated by the climatic warming can be accepted as a loss of mass is open. It is obvious that the formation of superimposed ice above the present-day position of the equilibrium line plays an important role for this question, which needs to be discussed with greater details (see Kuhn and Ambach, this volume, Attachment 16). Finally, with the restrictions accepted in the evaluation, the concept can be applied also in other regions of the Greenland Ice Sheet provided the input data for the modeling are known.

REFERENCES

Ambach, W., 1985a. Characteristics of the heat balance of the Greenland Ice Sheet for modelling. Journal of Glaciology, 30, 3-12.

Ambach, W., 1985b. Climatic shift of the equilibrium line--Kuhn's concept applied to the Greenland Ice Cap. Annals of Glaciology, 6.

Ambach, W. and M. Kuhn, 1985. Accumulation gradients in the EGIG-Profile and some implications for modelling. Zeitschrift für Gletscherkunde und Glazialgeologie, 21.

Benson, C. S., 1962. Stratigraphic studies in the snow and firn of the Greenland Ice Sheet. SIPRE Research Report, 70.

ATTACHMENT 18

CONTRIBUTION OF THE GREENLAND ICE CAP TO CHANGING SEA LEVEL: PRESENT AND FUTURE

Robert A. Bindschadler
NASA/Goddard Space Flight Center

ABSTRACT

A static, two-dimensional flowline model is developed to predict the response of the net mass balance of the Greenland Ice Cap to warmer climates. An average accumulation is assumed along with a linear decrease of ablation with altitude and a calving term that is either constant or simply related to surface ablation. Warmer climates are parameterized by a rise in the equilibrium line. Cases of rises in the equilibrium line of 500 m and 1000 m are calculated. Using an observed value of the lapse rate, these cases correspond to approximate increases in surface temperature of 3 and 6°C. Net mass balances for these cases are -461 km^3/yr and -1259 km^3/yr, respectively, compared with a present net balance of near zero. The respective rates of sea-level rise are 1.3 mm/yr and 3.5 mm/yr.

PRESENT BEHAVIOR

Calculations of the mass balance of the Greenland Ice Cap are usually divided into three terms: accumulation, ablation or surface melting, and calving. Because of the size of this ice cap, precise measurements of any of these terms are difficult, but some estimates have been made based on the available data. Table 18.1 summarizes an average of five published estimates. These estimates indicate that the Greenland Ice Cap is at present very near mass balance. Dividing the net mass balance by the area of the ocean surface, 362×10^6 km^2 (Flint 1971, p. 84), results in a figure that represents the present change in sea level due to the Greenland Ice Cap mass balance: -0.03 ± 0.10 mm/yr (minus indicating a drop in sea level).

SIMPLE MODEL OF GREENLAND ICE CAP

To predict how the Greenland Ice Cap would respond to a change in climate, a simple two-dimensional model is constructed, which typifies a single flowline within the ice cap (Figure 18.1). Assuming that ice behaves as a plastic material, Orowan and Perutz (1949) showed with a

TABLE 18.1 Estimates of Mass Balance of the Greenland Ice Sheet (from Ambach 1982)

Accumulation:	500+	81 km^3/yr
Ablation:	-290±	26 km^3/yr
Calving:	-200±	28 km^3/yr
Net	10±	51 km^3/yr

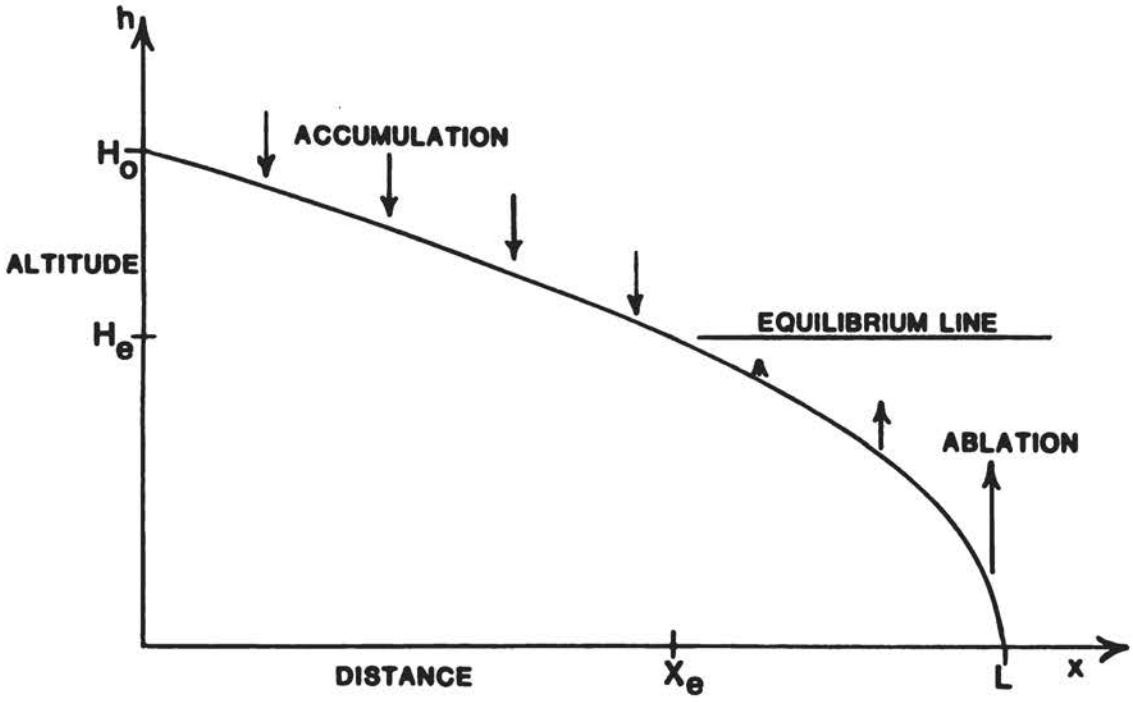

FIGURE 18.1 Schematic diagram of ice-cap flowline showing axes and representative position of equilibrium line.

balance of forces argument that the central elevation of the ice cap, H, and the length of the ice, L, are related by

$$H^2/L = 2\tau/\rho g, \tag{18.1}$$

where τ is the plastic yield stress and ρ and g are the density of ice and gravitational acceleration, respectively. Equilibrium of the ice sheet requires that the elevation profile along a flowline will be a parabola of the form

$$h(x) = H(1 - x/L)^{1/2}, \tag{18.2}$$

where x is the position from the center along the flow axis and h is the elevation at any point. To fit the present climatology of Greenland to the model, Benson's (1962) figure of an average accumulation rate a = 0.35 m/yr (water equivalent) is used. For ablation, a model of a linear increase in ablation rate with decreasing altitude is used:

$$\dot{b} = \dot{d}b/dh\ (H_e - h), \tag{18.3}$$

where $\dot{b}$ is the ablation rate and H_e is the equilibrium-line altitude (i.e., that point x_e where annual accumulation equals annual ablation and $\dot{b} = 0$). Using an average value (for 72°N) from Braithwaite (1980, Figure 5), $\dot{d}b/dh$ = 2.3 m/yr per 1500 m elevation = 0.00153/yr. The present-day equilibrium line is at an average elevation of 1500 m relative to sea level (Ambach 1982).

To complete the model, calving must be included. The appropriate units for this term are volume of ice calved per unit time per unit width, which are applied at x = L. The approximte perimeter of the ice cap is 5000 km so calving flux per unit width C = 200/5000 km^2/yr = 0.04 km^2/yr.

The mass balance terms per unit width can now be written:

$$\text{Accumulation:}\quad A = \int_0^{x_e} \dot{a}\,d\zeta, \tag{18.4}$$

$$\text{Ablation:}\quad M = \int_{x_e}^{L} [H_e - h(\zeta)\,d\zeta, \tag{18.5}$$

and

$$\text{Calving:}\quad C = 0.04\ \text{km/yr}. \tag{18.6}$$

For a net mass balance of zero,

$$A = M + C \tag{18.7}$$

or

$$\dot{a}\left(L - \frac{H_e^2}{k}\right) = \frac{1}{3}\frac{\dot{d}b}{dh}\left(\frac{H_e^3}{k}\right) + C, \tag{18.8}$$

where

$$k = 2\tau/\rho g. \tag{18.9}$$

Using the values given above for $\dot{a}$, $\dot{d}b/dh$, H_e, and C, and using H = 3250 m with respect to sea level, ρ = 0.9 g/cm^3, and g = 980 cm/sec^2, Eqs. (18.1), (18.8), and (18.9) can be solved for L and τ:

$$k = 355\ \text{km}$$
$$\tau = 1.3\ \text{bar}.$$

Multiplying the values of A and M by the 5000-km perimeter of Greenland used earlier produces values of 488 km^3/yr for the accumulation flux and 289 km^3/yr for the ablation flux, a very close fit to the published estimates given earlier. The major difference is that we have forced net mass balance by Eq. (18.7).

For convenience, Eq. (18.8) can be rearranged to

$$L = \frac{1}{k} H_e^2 + \frac{1}{3} \frac{1}{\dot{a}k} \frac{db}{dh} H_e^3 + \frac{c}{\dot{a}} \quad , \tag{18.10}$$

where on the right-hand side the first term is the length of the ablation zone and the second and third terms are the length of the accumulation zone. It is important to remember that this development greatly simplifies the geometry of the ice cap. Nevertheless, it does a reasonably good job of simulating the extent and position of the accumulation and ablation zones and is useful in examining the possible response of Greenland to climate change.

STATIC RESPONSE TO CLIMATE CHANGE

A canonical scenario for predicting climate change is to double the amount of CO_2 in the atmosphere, say from 300 ppm to 600 ppm. This case has been investigated with many global circulation models with the general result of a mean atmopsheric warming of 2 to 3.5°C with a larger increase in the polar regions (Schlesinger 1984). The GISS model (Hansen et al. 1984) predicts a rise in surface temperatures of 4°C in southern Greeland to 6°C in northern Greenland with a 10 percent increase in accumulation rates over the ice cap. A warmer climate would obviously increase the melting at the margins of the ice cap and raise the elevation of the equilibrium line. This rise of the equilibrium line can be calculated, in principle, by using measured values of the surface temperature gradient versus altitude. In practice, it must be cautioned that this technique may break down for large changes in surface temperature. Two values of this gradient are available in the literature:

(1) 0.6°/100-m elevation (EGIG line 70°N - 71°N; see Ambach 1982),
(2) 1.12°C/100-m elevation (Camp Century, 76.5°N; Benson, 1962).

R. G. Barry (University of Colorado, personal communication) pointed out that the Camp Century figure may be artificially high owing to its proximity to the coast, while the EGIG value is much closer to typical values of the atmospheric lapse rate. Uncertainty in this figure makes difficult a direct correlation of the effects of atmospheric warming to a rise in equilibrium-line elevation. A rise in the equilibrium line of 500 m would correspond to a temperature increase of 3°C if only the EGIG line value is used, but 5.6°C if the Camp Century value is used. Further, Ambach and Kuhn (this volume, Attachment 17), who examined each term of the heat balance separately at the snow surface, suggest that a 500-m rise in the equilibrium line would correspond to a 6.5°C rise in atmospheric temperature. Therefore two cases of warmer climate

TABLE 18.2 Changes in Mass-Balance Terms with Climate

Term	Present Climate	Warm Case I	Warm Case II
H_e	1500 m	2000 m	2500 m
x_e	279 km	220 km	145 km
Ablation rate at margin	2.3 m/yr	3.1 m/yr	3.8 m/yr
Accumulation flux	488 km^3/yr	424 km^3/yr	279 km^3/yr
Ablation flux	289 km^3/yr	685 km^3/yr	1338 km^3/yr
Calving flux	200 km^3/yr	200 km^3/yr	200 km^3/yr
Net mass balance	-1 km^3/yr	-461 km^3/yr	-1259 km^3/yr
Rate of sea-level rise	0	1.3 mm/yr	3.5 mm/yr

will be examined quantitatively: Case I will correspond to a conservative rise of 500 m in the elevation of the equilibrium line, while Case II will use a 1000-m rise of the equilibrium line. The "doubled-CO_2" atmosphere should fall somewhere between these two cases.

By assuming that the value of db/dh does not change and accumulation rates increase by 10 percent, the model can be used to calculate the changes in the mass-balance terms for these two cases (Table 18.2). As can be seen from Table 18.2, the net mass balance would become strongly negative for the warmer climate cases. Both the accumulation and ablation fluxes contribute to the mass loss; the decrease in accumulation area outweighs the 10 percent increase in accumulation rate, while the ablation area increases as well as the average ablation rate. Figure 18.2 presents the size of the mass-balanced terms for any change in equilibrium line. In this figure the effect of accelerating ablation for a warming climate is clearly seen. What can also be seen is the decrease in accumulation flux that occurs as the climate warms. Once the equilibrium line exceeds 3250 m, the entire ice cap becomes an ablation zone and disappearance of the ice cap is assured. The net mass balance in this extreme is -3139 km^3/yr or 8.7 mm/yr in sea-level rise. Using the EGIG-line value of surface temperature gradient (0.6°C/100 m), this case would require an average rise in surface temperature over the ice cap of 10.2°C. This value is about twice the final polar warming predicted by general circulation models (GCMs) for "doubled-CO_2" atmospheres but is roughly equivalent to polar warming for a "quadrupled-CO_2" atmosphere.

The few transient experiments that have been done indicate that the response time for this magnitude of atmospheric warming is a few decades (J. Hansen, Goddard Institute for Space Studies, personal communication; M. Schlesinger, Oregon State University, personal communication). The ice cap on the other hand, will respond much more slowly. An estimate of the characteristic response time of the ice cap can be calculated by the time it would take a kinematic wave to travel the length of the cap. In equilibrium, the maximum velocity is at the equilibrium line and is equal to the $\dot{a}x_e/H_e$ = 65 m/yr. In general, the kinematic wave velocity is about 4 times the ice velocity, and the response time is

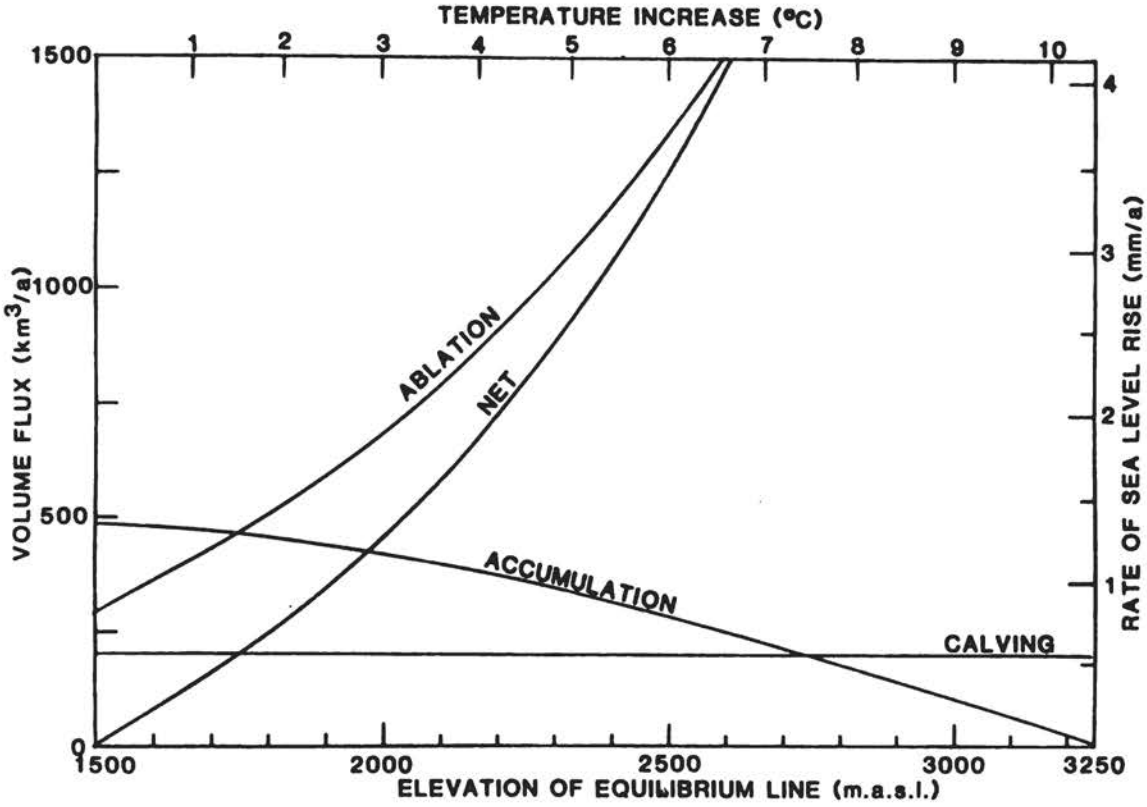

FIGURE 18.2 Magnitude of mass-balance terms versus elevation of equilibrium line for Greenland model with constant calving. Secondary axes relate temperature increase to elevation of equilibrium line (assuming EGIG-line value of 0.6°/100 m) and rate of sea-level rise to volume flux.

355 km/4 x 65 m/yr = 1365 yr. Therefore, the climate would have equilibrated long before the ice cap would have had time to equilibrate. This fact justifies the static treatment just completed.

If any dynamic response of the ice cap is neglected for the moment, the changes in the ice cap's geometry over a 100-year period following the atmospheric warming can be calculated. As an upper bound, assume that the altered climate occurs instantaneously and the ice cap does not move, then the rate of thickening in the center of the ice cap will be equal to the accumulation rate or 0.35 m/yr (water equivalent). Over 100 years, the total thickening would be 39 m (accounting for the density of ice). In this model this thickening is taken as uniform over the total accumulation area. As for ablation, the ablation rate at the ice margin for Warmer Case I would increase to 3.1 m/yr (water equivalent). Over 100 years, the total melt would be 344 m of ice. Ice of this thickness occurs about 4 km from the original ice margin. Thus, over a period of 100 years, an average retreat of 4 km would be expected.

If, on the other hand, it is assumed that the ice flows at the same rates in an altered climate as it does at present, then at the summit it sinks at a rate equal to the accumulation rate and rises at the margin at a rate equal to the ablation rate; this is a requirement of an equilibrium profile. In this case, then, the surface will rise at a rate equal to the increase in accumulation rate, 3.9 m/100 yr, and will thin in the ablation zone at the rate of 89 m/100 yr and retreat only 265 m. The major reason for these relatively small rates of marginal retreat is the very high slope at the surface near the margin and is a direct result of the parabolic profile assumed. For a wedge-shaped snout of angle θ, the retreat rate would be

$$\dot{x} = \dot{b} \cot \theta, \tag{18.11}$$

where $\dot{b}$ is the ablation rate (measured vertically) and $\dot{x}$ is the retreat rate.

To calculate a figure of total sea-level rise by the year 2100, assume a scenario in which there is no change in atmospheric warming from now to the year 2000, when the atmosphere warms at a rate that raises the equilibrium line 500 m (Warm Case I) by the year 2050, where it remains. The total change in sea level would be 0.10 m. If the equilibrium were raised 1000 m instead of 500 m (i.e., Warm Case II), the total rise would be 0.25 m.

DYNAMIC REPONSE TO CLIMATE CHANGE

The questions must now be asked: At what point will the changing geometry affect the flow of ice, and what will be the nature of this response both in the near and distant future?

For the perfectly plastic model posed here, the behavior of the ice is quite unrealistic. The ice motion stops when the shear at the base drops below the yield stress and flows at an infinite rate when the shear stress exceeds the yield stress. The ice sheet is always in equilibrium. For a more realistic nonlinear flow rheology, the flow rate depends on the product of surface slope and ice depth each raised to some power (usually between 2 and 5). In the Warm Case I considered above, the average slope over the entire ice cap length increased from 0.524° to 0.537°, or 2 percent over 100 years, while the average thickness decreased from 2167 to 2165 m or 0.1 percent over 100 years. These figures suggest that the dynamic response during the first 100 years following a warming would be slight. On the time scale of 1000 years, the ice cap will have time to adjust to this new climate. The initial response will result in thickening in the accumulation area and a retreat of the margin as described above. This will tend to increase ice velocities due to the increasing surface slope. Increasing velocities will increase the advection of ice from the central area of the ice cap. If this advection exceeds the thickening taking place in the accumulation zone, then the surface will lower. This effect could draw the accumulation zone below the equilibrium line converting it into an

ablation zone. If this were to happen, the ice cap would disappear irreversibly.

What is really needed is a simulation of this scenario using a dynamic model that takes into account the full nonlinear aspects of the ice-dynamic equations. Pioneering theoretical treatments by Nye (1960) showed that the compressive region (the ablation zone) of a glacier responded to an increase in accumulation rate unstably before the arrival of a kinematic wave from the tensile region (the accumulation zone) and caused an accelerating advance of the glacier terminus during the unstable period. No dynamic theory, however, can predict a retreat rate that exceeds the static case given in the previous section, since any ice motion will tend to advance the ice margin.

RAMIFICATIONS OF A POSSIBLE INCREASE OF CALVING

From studies of calving glaciers, Sikonia (1982) developed an empirical relationship between rate of calving and water discharge,

$$V_c = 1.092 \times 10^3 \, D^{0.5689} \, h_u^{2.175}, \qquad (18.12)$$

where V_c is the calving speed (km/yr), D is the water discharge (m^3/s), and h_u is the unsupported height of the ice column. If this relationship is used crudely to link the calving flux to the ablation flux, then for the warmer climate scenarios discussed in an earlier section, the fractional increase in calving flux should be 0.5689 times the fractional increase in ablation. If so, the calving flux would increase by 156 km^3/yr to 356 km^3/yr for Warm Case I and by 414 km^3/yr to 614 km^3/yr for Warm Case II. This would increase the magnitude of the net mass balance deficits to -617 km^3/yr and 1673 km^3/yr, or 1.7 mm/yr and 4.6 mm/yr of sea-level rise, respectively.

FINAL REMARKS

A simple model has been used to predict the response of the Greenland Ice Cap to future changes in climate. Given the limits to our knowledge of the areal distribution of the various mass-balance terms throughout the ice cap, the reduction of the ice cap to a single characteristic flowline is a useful first step to take in such a study. While the assumption of plasticity prevents a simulation of flow dynamics, the good fit of the model to present conditions lends credence to the technique used.

Therefore, it is worthwhile to repeat those results that are believed to be most valid and that are pertinent to the main purpose of this workshop.

- The Greenland Ice Cap is in approximate mass balance with the present climate.
- For conditions that cause a 500-m rise or a 1000-m rise in the average elevation of the equilibrium line, the ice cap will experience

a mass imbalance of -461 km^3/yr (1.3 mm/yr rise in sea level) and -1259 km^3/yr (or 3.5 mm/yr rise in sea level), respectively. These two cases bracket the predictions of equilibrated climate change for double the present amount of CO_2 in the atmosphere.

- Over the next 100 years, the rate of ice thickening or thinning will be primarily due to changes in the accumulation and ablation pattern. Retreat of the ice margin will be primarily due to increased melting, and any marked changes in ice flow will be limited to regions of outlet glaciers currently flowing rapidly.

REFERENCES

Ambach, W., 1982. Ansteig der CO_2--Konzentration in der atmosphare und klimaanderung: Mogliche auswirkungen auf den Gronlandischem Eisschild. Wetter und Leben, 32, 135-142.

Benson, C. S., 1962. Stratigraphic Studies in the Snow and Firn of the Greenland Ice Sheet. Research Report 70, U.S. Army Cold Regions Research and Engineering Laboratory, Corps of Engineers, Hanover, N.H., 93 pp.

Braithwaite, R. J., 1980. Regional Modelling of Ablation in West Greenland, Gronlands Geologiske Undersogelse, Report No. 98, 20 pp.

Flint, R. F., 1971. Glacial and Quaternary Geology. John Wiley & Sons, Inc., New York, 892 pp.

Hansen, J., A. Lacis, D. Rind, G. Russell, P. Stone, I. Fung, R. Ruedy, and J. Lerner, 1984. Climate processes and climate sensitivity. Geophysical Monograph, 29, American Geophysical Union, Washington, D.C., pp. 130-163.

Nye, J. F., 1960. The response of glaciers and ice sheets to seasonal and climatic changes. Proceedings of the Royal Society, Series A, 256, 559-583.

Orowan, E., and M. F. Perutz, 1949. The flow of ice and other solids. Journal of Glaciology, 1, 231-240.

Schlesinger, M. E., 1984. Atmospheric general circulation model simulations of the modern Antarctic climate. In Environment of West Antarctica: Potential CO_2-Induced Changes, Polar Research Board, National Research Council, National Academy Press, Washington, D.C., pp. 155-196.

Sikonia, W. G., 1982. Finite element glacier dynamics model applied to Columbia Glacier, Alaska. U.S. Geological Survey Professional Paper, 1258-B, 74 pp.

ATTACHMENT 19

A NUMERICAL SIMULATION OF CO_2-INDUCED TRANSIENT CLIMATE CHANGE WITH A COUPLED ATMOSPHERE-OCEAN GENERAL CIRCULATION MODEL

Michael E. Schlesinger
Department of Atmospheric Sciences and
Climatic Research Institute
Oregon State University

The CO_2-induced temperature change since the industrial revolution, and in the future, depends in part on the "climate response function," which measures the time lag between the actual response to a small step-function change in thermal forcing and the response that would occur if the climate system had no thermal inertia. The majority of the simulations of CO_2-induced climate change have been performed to determine the sensitivity of the climate system from the equilibrium warming resulting from an abrupt increase in CO_2. While these simulations are time dependent, their temperature evolution cannot be used to determine the climate response function because their treatment of the oceans was simplified for computational economy to enable equilibrium to be attained in as short a time as possible. In the past several years, however, simplified climate models with a variety of oceanic treatments have been applied to determine the characteristics of the climate response function. As shown in Table 19.1, two types of heating perturbation have been studied: a switch-on CO_2 increase, with either a doubling or quadrupling of the CO_2 concentrations, and an exponential increase of the CO_2 concentration in time. The temporal response of the climate system to the switch-on CO_2 increase can be partially characterized by an e-folding time τ_e, which is the time required to reach 63 percent of the equilibrium response, even though the actual response may not follow the "complementary" exponential function $1 - \exp(-t/\tau_e)$. The temporal response to the exponential CO_2 increase can be characterized by a lag L(t) defined implicitly by $\Delta T(t) = \Delta T_i(t - L)$, where ΔT is the actual temperature response and ΔT_i the temperature response that would occur if the climate system had zero thermal inertia. Table 19.1 shows that the estimates of $_e$ range from about 10 to 100 years.

The recent analytical study of Wigley and Schlesinger (1985) showed that the climate response function depends on the gain of the climate system (the change in surface temperature/the change in thermal forcing) and the rate at which heat is transported from the ocean surface downward into the interior of the ocean. Thus, it is likely that the climate response function simulated in these previous studies has been significantly influenced through the effects on the oceanic heat transports and climatic gain of the simplifications made in the models of the ocean and climate. Therefore, the objective of the present study

TABLE 19.1 Selected Climate Model Studies of Transient Climate Response

Study	Switch-on CO_2 Increase τ_e (Years)	Exponential CO_2 Increase Lag (Years)
Hunt and Wells (1979)	--	8 (at doubling)
Hoffert et al. (1980)	8-20	10-20 (1880-1980)
Cess and Goldenberg (1981)	--	20 28 (at doubling)
Schneider and Thompson (1981)	13	--
Bryan et al. (1982)	~25	--
Spelman and Manabe (1984)		
Hansen et al. (1984)	27 55 102	--
Bryan et al. (1984)	100	
Siegenthaler and Oeschger (1984)	~60	

is to investigate the characteristics of the climate response function with a global coupled atmosphere-ocean general circulation model (GCM).

The atmospheric component of the coupled model is basically the two-layer atmospheric GCM described by Schlesinger and Gates (1980, 1981) and documented by Ghan et al. (1982). The oceanic component of the coupled model is basically the six-layer oceanic GCM developed by Han (1984a, 1984b) and extended by him to include the Arctic Ocean. The coupled model predicts the temperatures and velocities of the atmosphere and ocean, the atmospheric surface pressure and water vapor, the oceanic salinity, the land-surface temperature and water content, the sea-ice thickness, the snow mass and clouds and includes both the diurnal and seasonal variations of solar radiation. The coupled model is global and has realistic continent/ocean geography and realistic land and ocean-bottom topographies. The coupled model is integrated synchronously, that is, both component models simulate the same period of time. Two simulations were performed with the coupled model, one with a CO_2 concentration of 326 ppm ($1 \times CO_2$) and the other with a doubled CO_2 concentration of 652 ppm ($2 \times CO_2$). Both simulations were started from the same initial conditions, and each was synchronously integrated for 20 years. The difference between the ($2 \times CO_2$) and ($1 \times CO_2$) simulations thus represents the climate change induced by an abrupt or switch-on CO_2 doubling.

The evolution of the change in global-mean temperature induced by the doubled CO_2 concentration is shown in Figure 19.1 in terms of the vertical distribution of monthly mean [($2 \times CO_2$) - ($1 \times CO_2$)]-temperature differences for the atmosphere and ocean. The top panel of Figure 19.1 shows an initially rapid and vertically uniform warming of

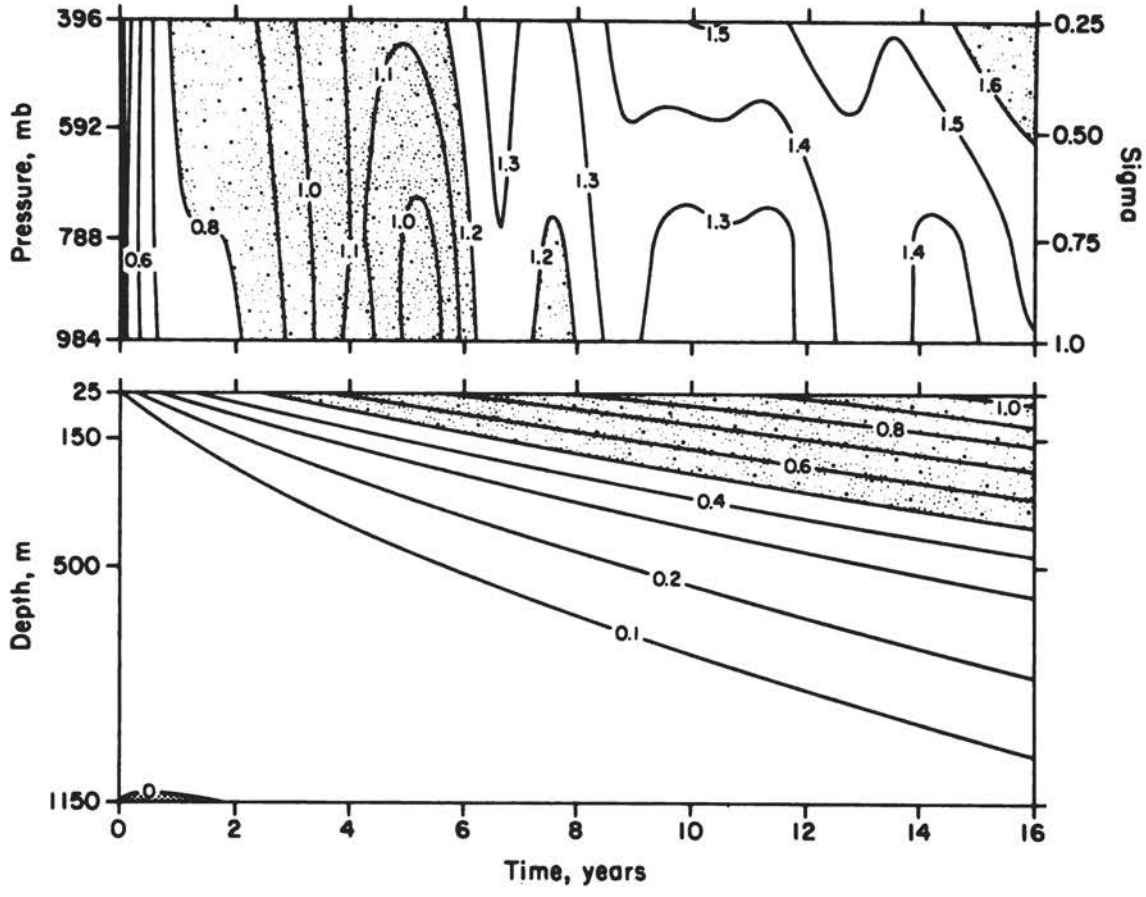

FIGURE 19.1 Time-vertical distribution of the [(2 x CO_2) - (1 x CO_2)] difference in monthly-mean global-mean temperatures (°C) of the atmosphere (above) and ocean (below). The temperature differences have been filtered using an asymmetric 12-pole, low-pass recursive filter with a 24-month cutoff period. Atmospheric warming between 0.8-1.2°C and larger than 1.6°C is indicated by light stipple, as is oceanic warming of 0.5-1.0°C, while oceanic cooling is shown by heavy stipple. (From Schlesinger et al. 1985).

the atmosphere followed by a progressively slowing atmospheric warming. The bottom panel of Figure 19.1 also shows an initially rapid warming of the sea surface followed by a progressively slowing warming. Figure 19.1 shows that the decrease in warming rate of the atmosphere and sea surface with time is the result of a downward transport and sequestering of heat into the interior of the ocean.

The temperature changes shown in Figure 19.1, when normalized by the equilibrium temperature change, define the climate response function for the global-mean temperature. Clearly, the present simulations are not of sufficient duration for the equilibrium change to have been attained, a result that was anticipated from the analytical study of Wigley and Schlesinger (1985). However, an estimate of the equilibrium

temperature change and the vertical transport characteristics of the ocean can be obtained from a representation of the time evolution of Figure 19.1 by simple one-dimensional climate/ocean models. An energy-balance climate/multibox ocean model gives an excellent representation of the evolution shown in Figure 19.1 with self-determined parameters for which the estimated equilibrium temperature change is 2.8°C. This estimate is near the mid-point of the values simulated by atmospheric GCM/interactive-ocean models (Schlesinger 1984). The effective ocean thermal diffusivity κ, by which all vertical heat transport is parameterized in the simple multibox ocean model, is 3.2 cm^2/sec at the 50-m level, 3.8 cm^2/sec at the 250-m level, and 1.5 cm^2/sec at the 750-m level. Values of κ for the deeper ocean levels cannot be determined because, as shown in Figure 19.1, the duration of the integrations was not long enough for the warming to penetrate below the 750-m level. The mass-averaged effective ocean thermal diffusivity of κ = 2.25 cm^2/sec is in agreement with the best estimate based on the value required by a box-diffusion ocean model to reproduce the observed penetration of bomb-produced radionuclides into the ocean (Broecker et al. 1980; Siegenthaler 1983). Moreover, an energy-balance climate/box-diffusion ocean model with κ = 2.25-2.50 cm^2/sec is successful in reproducing the evolution of the [(2 x CO_2) - (1 x CO_2)] differences in the surface air and ocean surface layer temperatures simulated by the coupled GCM. Consequently, it appears that the coupled model transports heat from the surface downward into the ocean at a rate that is commensurate with the rate observed for the downward transport of radionuclides.

The climate response function obtained from the energy-balance climate/multibox ocean model representation of the coupled model [(2 x CO_2) - (1 x CO_2)]-temperature evolution is shown in Figure 19.2, where a projection with the simple model has been made to year 200 after the switch-on CO_2 doubling. It is seen that the response function is not simply $1 - \exp(-t/\tau_e)$ as it would be if only the ocean mixed layer warmed without transporting heat to the thermocline and deeper ocean. Thus, the response function cannot be characterized by a single parameter such as τ_e. Nevertheless, the time to reach 63 percent of the equilibrium is useful for comparison with the earlier studies (Table 19.1). Figure 19.1 shows that such an e-folding time is about 75-100 years for the upper ocean. An estimate from the analytical study of Wigley and Schlesinger (1985) using the climatic gain and ocean thermal diffusivity estimated for the coupled GCM gives 108 years. This large e-folding time and the relationship between it and the lag for a time-dependent CO_2-increase have definite implications for the memory of the climate system and for the detection of a CO_2-induced climate change.

While the above discussion has focused on the global-mean climate response function, the results of the coupled GCM simulations show that the warming is geographically differentiated both at the Earth's surface and within the ocean. For example, the latitude-vertical distributions of the zonal-mean [(2 x CO_2) - (1 x CO_2)]-temperature differences are shown in Figure 19.3 for the atmosphere and ocean in terms of the annual mean over year 16. This figure shows that both the atmosphere and ocean warm as a result of the doubled CO_2. The oceanic warming

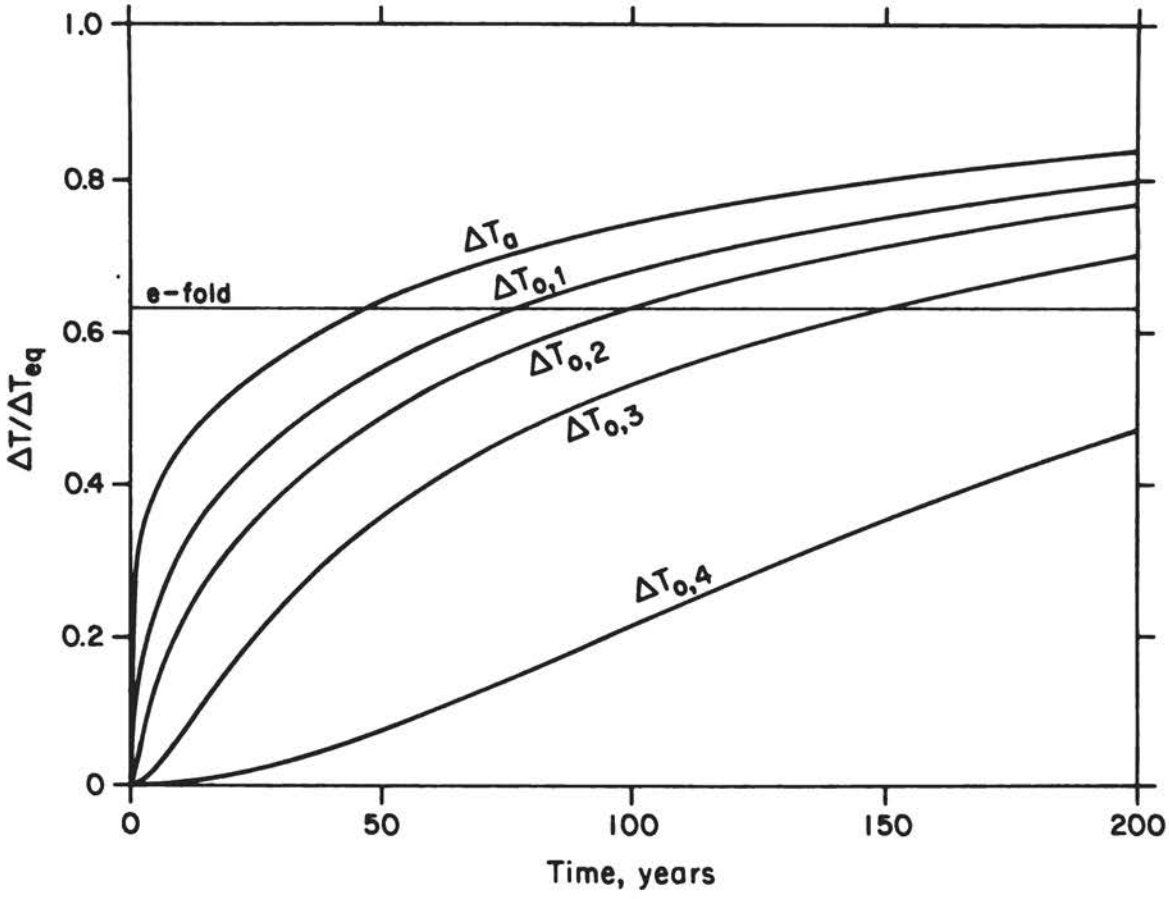

FIGURE 19.2 Energy balance climate multibox ocean model projection of the evolution of the $[(2 \times CO_2) - (1 \times CO_2)]$ difference in global-mean surface air temperature (ΔT_a) and ocean-layer temperature ($\Delta T_{0,k}$, $k = 1, 2, 3, 4$) for years 16-200 as a fraction of the equilibrium temperature difference (ΔT_{eq}). The horizontal line labeled e-fold indicates the level at which $\Delta T/\Delta T_{eq} = 1 - 1/e \simeq 0.63$. (From Schlesinger et al. 1985).

increases from the tropics toward the mid-latitudes of both hemispheres at the surface and penetrates to a greater depth in the subtropics and mid-latitudes than in the equatorial region. These features are similar to what is shown by the observed distribution of $\delta^{14}C$ in the ocean (Broecker et al. 1980). Large temperature increases are also evident in the 250-750 m ocean layer at 65°N and 60°S latitude. It is this deep penetration of heat into the ocean that results in a climate response function whose e-folding time is about 100 years.

From the viewpoint of physical oceanography it is fundamental to inquire by what pathways and through which physical processes the simulated ocean general circulation produces the penetration of CO_2-induced warming into the ocean. It is also of potential glaciological interest concerning the stability of the West Antarctic ice sheet to understand

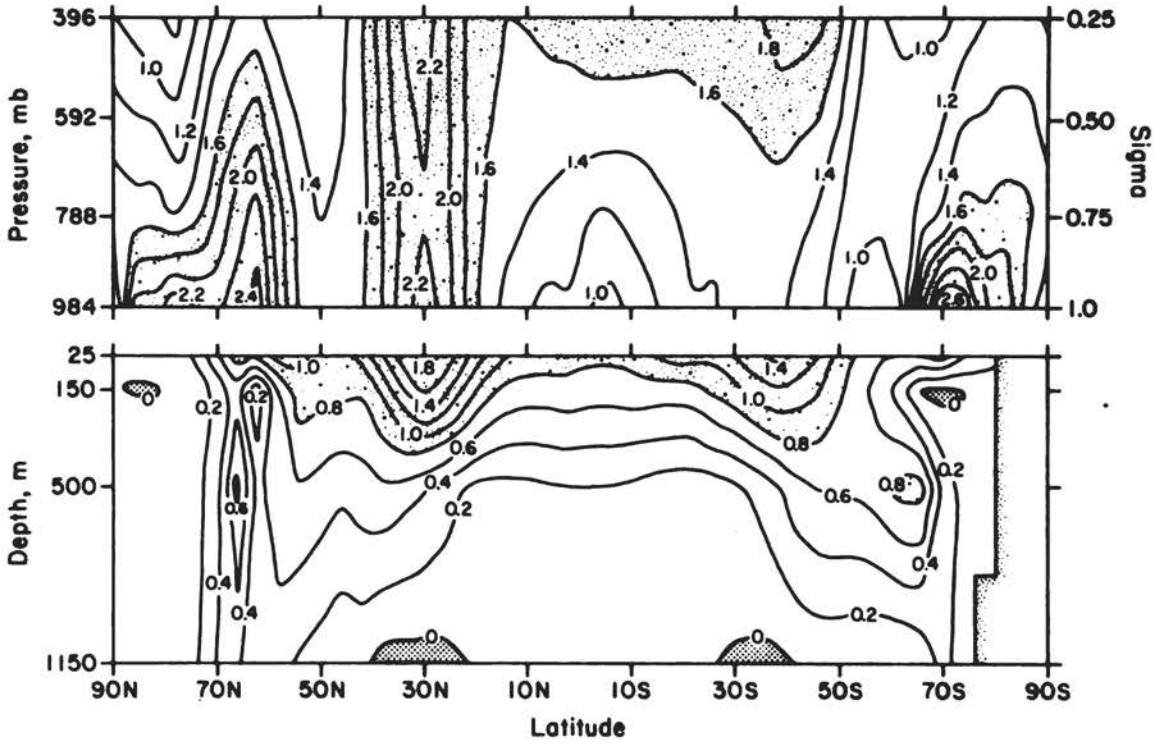

FIGURE 19.3 Latitude-vertical distribution of the [(2 x CO_2) - (1 x CO_2)] difference in the annual-mean, zonal-mean temperatures of the atmosphere (above) and ocean (below) for year 16. Atmospheric warming larger than 1.6°C is shown by light stipple, as is oceanic warming larger than 0.8°C, while oceanic cooling is indicated by heavy stipple. (From Schlesinger et al. 1985).

how the coupled model produces a considerable warming at depth in the vicinity of the Ross Ice Shelf. These inquiries can be made only through a time-dependent heat-budget analysis for the world ocean. Such a study is now in progress.

ACKNOWLEDGMENTS

I would like to acknowledge the collaboration of my colleagues W. Lawrence Gates and Young-June Han in this study. I would also like to thank Robert L. Mobley and William McKie for their management of the integration of the coupled GCM and their assistance in its analysis, Dean Vickers for his programming assistance with the energy-balance-model analysis, John Stark for drafting the figures, and Leah Riley for typing the manuscript. I also thank NCAR for the provision of the necessary time on their CRAY-1 computer. This research was supported by the National Science Foundation and the U.S. Department of Energy under grant ATM 8205992.

REFERENCES

Broecker, W. S., T.-H. Peng, and R. Engh, 1980. Modeling the carbon system. Radiocarbon, 22, 565-598.

Bryan, K., F. G. Komro, S. Manabe, and M. J. Spelman, 1982. Transient climate response to increasing atmospheric carbon dioxide. Science, 215, 56-58.

Bryan, K., F. G. Komro, and C. Roothe, 1984. The ocean's transient response to global surface temperature anomalies. In J. E. Hansen and T. Takahashi (eds.), Climate Processes and Climate Sensitivity, Maurice Ewing Series 5, American Geophysical Union, Washington, D.C., pp. 29-38.

Cess, R. D., and S. D. Goldenberg, 1981. The effect of ocean heat capacity upon the global warming due to increasing atmospheric carbon dioxide. Journal of Geophysical Research, 86, 498-502.

Ghan, S. J., J. W. Lingaas, M. E. Schlesinger, R. L. Mobley, and W. L. Gates, 1982. A documentation of the OSU two-level atmospheric general circulation model. Report No. 35, Climatic Research Institute, Oregon State University, Corvallis, 395 pp.

Han, Y.-J., 1984a. A numerical world ocean general circulation model, Part I. Basic design and barotropic experiment. Dynamics of the Atmosphere and Oceans, 8, 107-140.

Han, Y.-J., 1984b. A numerical world ocean general circulation model, Part II. A baroclinic experiment. Dynamics of the Atmosphere and Oceans, 8,, 141-172.

Hansen, J., A. Lacis, D. Rind, G. Russell, P. Stone, I. Fung, R. Ruedy, and J. Lerner, 1984. Climate sensitivity: Analysis of feedback mechanisms. In J. E. Hansen and T. Takahashi (eds.), Climate Processes and Climate Sensitivity, Maurice Ewing Series 5, American Geophysical Union, Washington, D.C., pp. 130-163.

Hoffert, M. I., A. J. Callegari, and C.-T. Hsieh, 1980. The role of deep sea storage in the secular response to climate forcing. Journal of Geophysical Research, 85, 6667-6679.

Hunt, B. G., and N. C. Wells, 1979. An assessment of the possible future climate impact of carbon dioxide increases based on a coupled one-dimensional atmospheric-oceanic model. Journal of Geophysical Research, 84, 787-791.

Schlesinger, M. E., 1984. Climate model simulations of CO_2-induced climatic change. In B. Saltzman (ed.), Advances in Geophysics 26, Academic Press, New York, pp. 141-235.

Schlesinger, M. E., and W. L. Gates, 1980: The January and July performance of the OSU two-level atmospheric general circulation model. Journal of Atmospheric Sciences, 37, 1914-1943.

Schlesinger, M. E., and W. L. Gates, 1981. Preliminary analysis of the mean annual cycle and interannual variability simulated by the OSU two-level atmospheric general circulation model. Report No. 23, Climatic Research Institute, Oregon State University, Corvallis, 46 pp.

Schlesinger, M. E., W. L. Gates, and Y.-J. Han, 1985. The role of the ocean in CO_2-induced climantic warming: Preliminary results from the OSU coupled atmosphere-ocean GCM. In Coupled Atmosphere-Ocean

Models (Proceedings of the 16th International Liège Colloquium), Elsevier, New York.

Schneider, S. H., and S. L. Thompson, 1981. Atmospheric CO_2 and climate: Importance of the transient response. Journal of Geophysical Research, 86, 3135-3147.

Siegenthaler, U., 1983. Uptake of excess CO_2 by an outcrop-diffusion model of the ocean. Journal of Geophysical Research, 88, 3599-3608.

Siegenthaler, U., and H. Oeschger, 1984. Transient temperature changes due to increasing CO_2 using simple models. Annals of Glaciology, 5, 153-159.

Spelman, M. J., and S. Manabe, 1984. Influence of oceanic heat transport upon the sensitivity of a model climate. Journal of Geophysical Research, 89, 571-586.

Wigley, T. M. L., and M. E. Schlesinger, 1985. The response of global mean temperature to changing carbon dioxide levels. Nature (submitted).

ATTACHMENT 20

THE "ICE PUMP," A MECHANISM FOR ICE-SHELF MELTING

E. L. Lewis
Institute of Ocean Sciences
Sidney, British Columbia, Canada

The freezing point of seawater is a function of pressure and decreases 7.5×10^{-3}°C for every 10 m of water depth. In the studies of conditions near the Filchner ice shelf, Foldvik and Kvinge (1974) pointed out that if water that had been in contact with ice at depth was, for any reason, raised then it would become supercooled in relation to the in situ freezing point as the pressure reduced and would provide a heat sink for ice growth within the water column. If upwelling were to occur, continuity demanded downwelling at some other location or time. The converse argument yields that waters so descending, after having been in contact with surface ice, will have sensible heat available to cause the melting of ice at depth. This constitutes an ice pump as described by Lewis and Perkin (1983), who applied the concept to freezing/melting processes near the surface of the pack-ice-covered Arctic Ocean. In that case downward water movement originating at a lead, where ice growth was taking place owing to heat loss into the atmosphere, would require a corresponding upwelling of water in contact with local pressure ridge keels so as to cause some melting from the keels and deposition of an equal amount of additional ice within the lead.

The whole process may be clarified by consideration of Figure 20.1. There a tank of seawater in an adiabatic enclosure has one of its walls made of ice, the ice-water interface being initially along the line AA. If the tank is taken to be a little more than 2 m deep the interface temperature at the bottom of the tank will be 0.008°C below that at the top of the tank. Suppose that infinitesimal melting occurs near the tank bottom. The reduction in density of the seawater immediately next to the interface will cause it to rise, and as it rises it will increasingly constitute an infinitesimal heat sink for ice growth. Should this growth occur near the top of the tank the full 0.008°C potential will have been utilized to move from the bottom to the top of the tank, and the salt rejected during the growth will cause a downward movement of water, which in turn will lead to more upwelling. A self-starting "ice pump" is in operation, and as time progresses the interface AA will tend to move through BB till eventually equilibrium is reached with the interface horizontal, in the CC position. The system has then reached its lowest energy state, and no further potential for ice pumping exists. If one applies this type of discussion to the

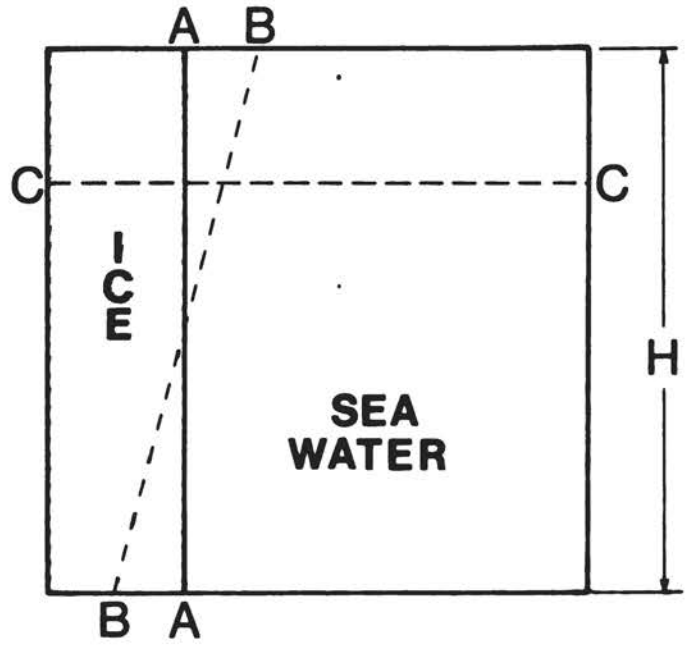

FIGURE 20.1 Schematic of a tank of seawater of depth H in an adiabatic enclosure. One wall of the tank is made of ice with the interface initially along the line AA. See text for discussion of the case for H ≈ 10 m.

floating ice shelves of Antarctica a potential of about 0.27°C exists to cause melting from the bottom of the 400-m-thick ice sheet and deposit of ice beneath the contiguous sea ice. However, the dynamics of most oceanic regimes provide a much stronger circulation to drive the pump than the "self-start" convection of Figure 20.1.

Melting by this mechanism at the bottom of the ice shelf will be augmented should circulation beneath the shelf bring in water from outside having significant sensible heat in relation to the depth freezing point, but it is important to realize that the described ice pump does not rely on an outside heat source to exist although its rate of operation can be greatly increased by greater water movement. Any heat flux from the water into the ice sheet in response to the latter's cold core will reduce the effects of the pump temperature. If this heat flux is the dominant factor there will be no melting and sea ice will grow beneath the ice sheet; the flux has been estimated to be about 0.2 w/m^2 or about 0.006 cm/day of sea-ice growth.

For a steady-state ice pump to work, water must be able to move up from beneath the floating ice sheet to the adjacent sea ice and there must be sufficient circulation so that the pump is not quenched by a stable layer of meltwater with low useful thermal content remaining in situ. The maximum pump rate is thus probably determined by the ability to transfer heat from the water to the ice through a planetary boundary layer, the formation of a density step being prevented by the slow upwelling of water from below.

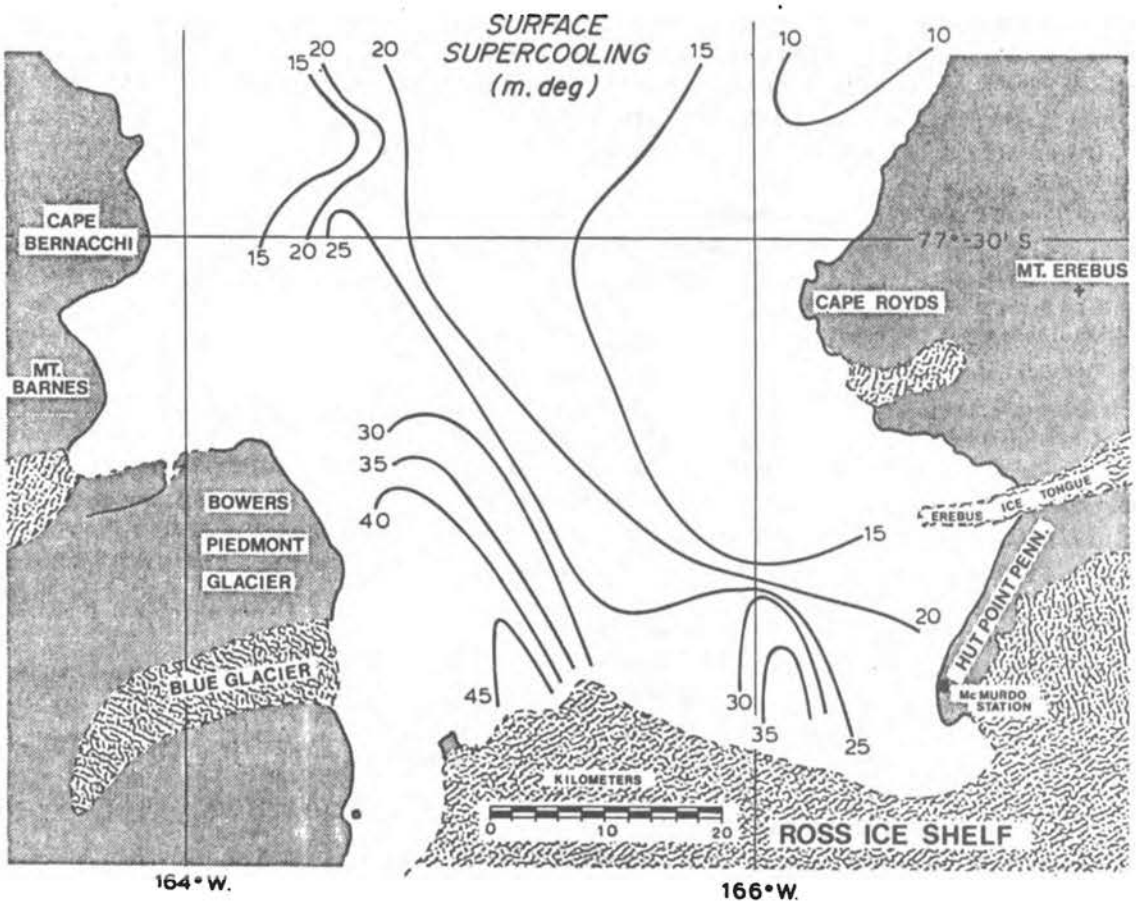

FIGURE 20.2 Contours of surface supercooling 2 m beneath the bottom of the sea-ice sheet in McMurdo Sound Antarctica. Such supercooling must be produced by water coming into contact with ice at depth then upwelling to the surface. The supercooling is relieved at the sea ice/water interface, with salt rejected into the water helping the vertical circulation.

Data on oceanographic conditions in the McMurdo Sound near the Ross Ice Shelf have been given by Lewis and Perkin (1985). Figure 20.2 shows the locations just below the sea-ice sheet of arrival of supercooled seawater from beneath the ice shelf. Two such foci for upwelling may be noticed from the figure; at these locations the supercooling is relieved within 2 m of the sea ice/water interface and owing to salt input the water column is unstable to a depth of 190 m so that resulting convection is capable of reaching a great depth. It is not known how far conditions in McMurdo Sound may be thought to typify those near the Ross Ice Shelf. There is a gradual reduction in the thickness of the shelf ice as one moves seaward in McMurdo, which contrasts with the ice cliff normally seen along the greater part of the Ross Ice Shelf front. Clearly in McMurdo Sound a lot of melting is taking place near the ice-shelf front and a sloping interface between shelf ice and seawater provides for easy exchange of bouyant water from beneath the shelf with

the surface waters of the Sound. Oceanographic profiles taken near the ice shelf/sea ice interface indicate that at a depth of 360 m (i.e., the bottom of a 400-m-thick shelf) the water is very close to its surface freezing point, that is, about 0.27°C above its in situ freezing point, and this potential is therefore available for ice melt. Suppose that this water were moving at a velocity of 5 cm/s beneath the ice shelf and that the freshwater produced by melting ice would be moved out of the system, then, using the planetary boundary-layer formulation of McPhee (1983), it may be shown that the melt rate would be of the order of 1.5 cm/day, dropping to 0.6 cm/day as the current dropped to about 2 cm/sec. It must be emphasized that this is a steady-state solution unlikely to be realized within nature except as an ensemble average. It assumes that, as stated above, there is a continual slope allowing sufficient drainage of meltwater from the location of melting up to the undersurface of the sea ice so that the tendency to form a density step is quenched. Far from the ice edge the drainage would be insufficient to allow these melt rates to be sustained, and the heat flow from the water would be limited by the circulation. The thickness of the ice sheet is variable and except near the ice edge will probably allow major "pooling" of meltwater to occur thus stopping further melting. The calculation also assumes that conditions in McMurdo Sound may be applied to the Ross Ice Sheet in general, which seems unlikely. In practice the ice pump will probably be limited by the opportunity for vertical water exchange rather than heat flow through the boundary layer, and the figure given above should be taken as typical of conditions near the ice-shelf front only.

How far "inland" from the ice-front edge is it realistic to assume a hydraulic connection between waters beneath and outside the ice shelf so that the needed flow can develop? Far more extensive oceanographic observations along and beneath the ice-shelf edge are needed. Should the logistics to make these measurements become available it is suggested that they should be augmented by a side-scan sonar imaging of the ice shelf/seawater interface. It may well be that an upside-down, river-valley-type drainage system develops in the ice-shelf edge with alternate downwelling and upwelling regions located in relation to the shelf-edge geometry.

REFERENCES

Foldvik, A., and T. Kvinge, 1974. Conditional instability of sea water at the freezing point. Deep Sea Research, 21, 160-174.

Lewis, E. L., and R. G. Perkin, 1983. Supercooling and energy exchange near the Arctic Ocean surface. Journal of Geophysical Research, 88, 7681-7685.

Lewis, E. L., and R. G. Perkin, 1985. The winter oceanography of McMurdo Sound. In S. Jacobs (ed.), Oceanology of the Antarctic Continental Shelf, American Geophysics Union, Washington, D.C.

McPhee, M. G., 1983. Turbulent heat and momentum transfer in the oceanic boundary layer under melting pack ice. Journal of Geophysical Research, 88, 2827-2835.

ATTACHMENT 21

ICE SHELVES AND ICE STREAMS: THREE MODELING EXPERIMENTS

J. L. Fastook
Institute for Quaternary Studies
University of Maine at Orono

ABSTRACT

Three fundamentally different modeling approaches are discussed and their implications concerning the near future are considered. The first is a finite-difference model that focuses on the marine instability. After applying the model to West Antarctica during retreat from 18,000 years before present (BP) to the present, the model was applied to continued retreat beginning in the Pine Island/Thwaites glacier region. Collapse of this region destablizes ice streams flowing into the Ross Ice Shelf and grounding-line retreat proceeds there also. The second is a plane-strain finite-element analysis of the stress distribution that occurs in an ice shelf due to the unbalanced hydrostatic forces at the front. This mechanism for iceberg calving, which leads to a tension maximum at the top surface about one half an ice thickness back from the ice front, appears only to be effective in the presence of sufficient meltwater to keep the opening crevasse filled to approximately sea level. The possibility of bottom crevasses coinciding with top crevasses and leading to calving can be ruled out in all but a few special cases owing to closing of the bottom crevasses as they move closer to the ice front. The effects of different shaped ice fronts (a submerged bulb and an undercut ice front) were investigated and found to have little effect on the formation of surface crevasses. The possibility of a second surface crevasse whose position depends on the shape of an undercut ice front is observed. The possibility of a bottom crevasse existing near the ice front is found in the case of the submerged-bulb ice front. The third is a fully time-dependent, finite-element flow-line reconstruction model. Based on the time-dependent continuity equation with ice velocity specified by a combination of flow and sliding laws, this model is used to investigate the formation of an ice stream in a region originally dominated by sheet flow. The time evolution of this process is discussed on various time scales, showing the changing basal traction as the ice stream forms as well as the changing mass outflow at the grounding line.

INTRODUCTION

Of major concern among those studying the problem of West Antarctic stability has been the effect of the anticipated climatic warming due to increased atmospheric concentration of CO_2. In model experiments increases of several degrees for worldwide average temperature are predicted, while for individual localities the increase may be greater. In particular, polar regions seem to experience a greater warming than the worldwide average, with some models suggesting as much as 6°C above present-day averages (Manabe and Wetherald 1975). A temperature warming of this magnitude in polar regions would certainly affect the stability, dynamics, and extent of the major ice sheets. In particular one might expect major irreversible changes in the possibly unstable marine-based West Antarctic Ice Sheet. In this paper the results of three different modeling experiments are discussed with particular emphasis on short-term (approximately 100 years) changes.

The first model experiment involves the marine instability first discussed by Weertman (1974) and further developed by Thomas and Bentley (1978) and Stuiver et al. (1981). The results presented here are discussed at length in Fastook (1984).

The second model experiment is a finite-element analysis of the calving process in an idealized ice shelf (Fastook and Schmidt 1982). This is done in an attempt to quantify the major unknown parameter used in the first model to control retreat of the grounding line, namely the extent of the buttressing ice shelf.

The third and final model experiment involves the use of a finite-element model to reconstruct flow-line profiles. This is in many ways similar to the finite-difference technique used in the first modeling experiment except that the finite-element model is explicitly time dependent so that the time response of the system to some change in its external or internal boundary conditions can be monitored. In particular, results concerning the formation of an ice stream (an area of anomalously low bed traction coupled with anomalously high ice velocities) in a region originally dominated by sheet flow are discussed. Transient events analogous to mountain-glacier surges are observed as the flow line adjusts to its new equilibrium configuration.

MARINE INSTABILITY

A marine-based ice sheet is one that, on removal of the ice and consequent isotatic rebound, will leave a bed predominantly below sea level. The importance of ice streams to the dynamic behavior of a marine ice sheet is evident from an examination of West Antarctica, the one remaining marine ice sheet. Examination of surface contours shows that fully 90 percent of the catchment area of West Antarctica drains through only 19 major ice streams (Hughes 1977). The importance of ice shelves is indicated by the fact that of these major ice streams 15 feed either into the Ross or the Filchner-Ronne Ice Shelves. Only two, Pine Island glacier and Thwaites glacier on the Amundsen Sea, flow into open sea with no major buttressing ice shelf. West Antarctica has only

small ablation zones so that the predominant mechanism for the removal of ice is calving from ice fronts. The relative movement of the calving front and the grounding line interact to provide the major negative feedback necessary to contain the otherwise unstable marine ice-sheet system (Fastook 1984).

Instability in a marine ice sheet is focused along the grounding line that separates the floating ice-shelf margin from the grounded interior dome (Weertman 1974). An expression can be obtained relating the movement of the grounding line to the change of thickness at the grounding line that will depend on the surface and bed slopes at the grounding line. This is discussed in detail in Fastook (1984).

The thinning rate at the grounding line can be expressed in terms of ice advection across the grounding line (dependent on ice velocity and surface and bed slopes), the creep thinning rate as described by a flow law (Glen 1955), and the local accumulation or ablation rate. The creep thinning term will contain a backstress term proportional to the extent of the buttressing ice shelf. There have been various parameterizations of this backforce, but a simple one involves the product of the shear stress with the length of the shear zone as the ice stream pushes through the buttressing ice shelf.

The velocity contained in the advection term is not a simple mass-balance velocity but must also account for the effects of thinning along the entire length of the flow line. Again there are several ways to deal with this problem but the method used in this modeling experiment involves the comparison of two equilibrium profiles differing only in thickness at the grounding line. While this can be criticized, it does at least give a reasonable approximation of the true behavior. Profiles are obtained from an improved CLIMAP reconstruction scheme (Hughes 1981), which is discussed at length in Fastook (1984).

While not central to the issue here it is worth noting that retreat and collapse of West Antarctic is driven in this model by rising sea level. This rise in sea level is triggered by melting along the terrestrial southern margin of the Laurentide and Eurasian ice sheets. As the marine margins in both the northern and southern hemispheres retreat this additional component of sea-level rise adds to the original sea level creating a positive feedback mechanism that greatly amplifies the effect of the local insolation variation, which produces the melting along the southern margin of the northern hemisphere ice sheets.

The extent of the buttressing ice shelf through its effect on the creep thinning rate at the grounding line has been used to moderate retreat and hence fit the retreat rate to the known geological data (Stuiver et al. 1981). Figure 21.1 shows surface elevation contours (dashed lines) and approximate calving front positions (hatched lines) at 10,000 BP. This is the conclusion of modeled retreat from a maximum configuration assumed at 18,000 BP (reported in detail in Fastook 1984). The margins have in generally reached their present positions. The ice-shelf extent shown on this figure is the ice-shelf buttressing needed to stabilize the grounding line at this position. Note the generally good agreement between the necessary ice shelf and the currently existing ice shelf. The only major discrepancy is in the Amundsen Sea, where an ice shelf of nearly 350 km is needed to halt retreat of Pine Island

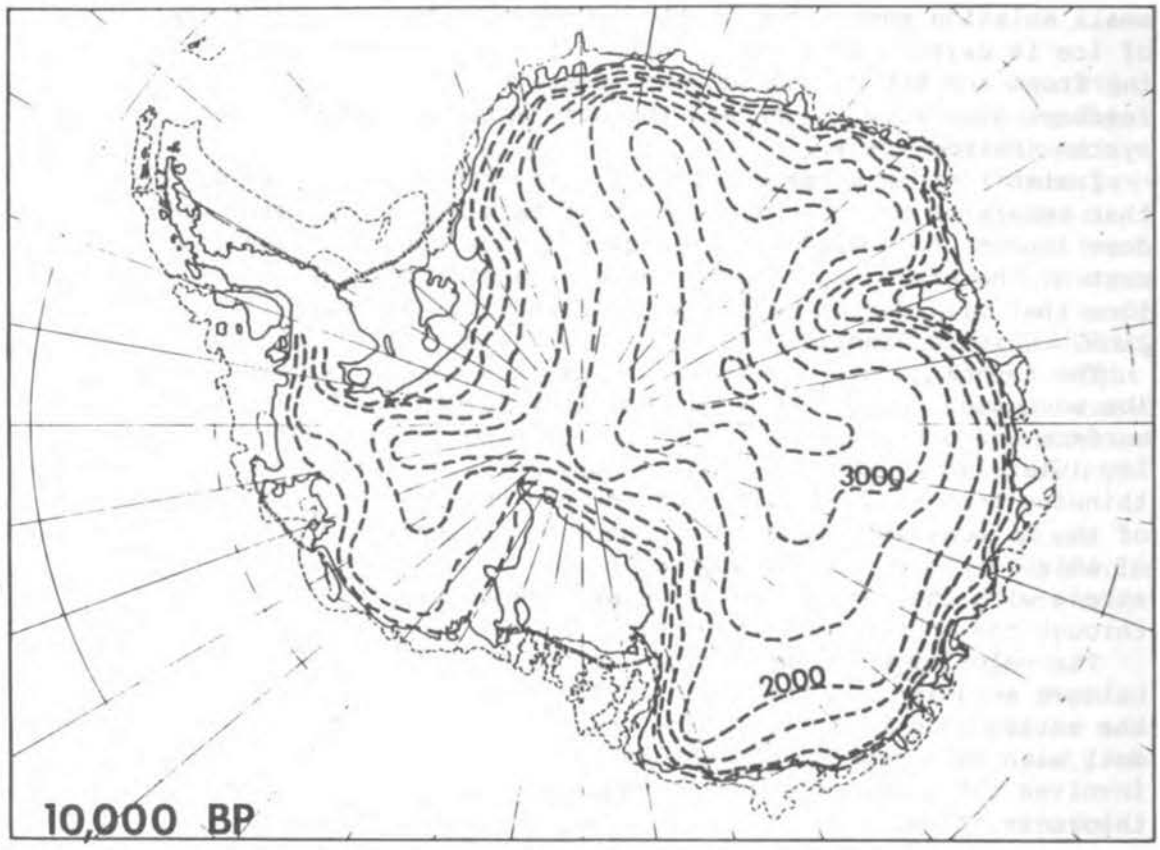

FIGURE 21.1 Surface elevation contours at 10,000 BP following the retreat modeled in Fastook (1984). The extent of the buttressing ice shelf in general agrees well with the current extent of the ice shelves, shown by the light hatched line. Note that in the Amundsen Sea a significant ice shelf is necessary to stablilize the grounding line at its current position.

and Thwaites glaciers. An ice shelf of this size would extend from Thurston Island on the west to Siple Island on the east, practically filling the Amundsen Sea out to the continental shelf. A possible explanation for this discrepancy is that until recently this ice shelf did exist and that its disappearance could be the first step in a second stage of retreat that could greatly reduce the extent of West Antarctica. Supporting evidence for this hypothesis can be seen in sediment records from cores taken near the edge of the continental shelf in the Amundsen Sea (Kellogg et al. 1982). The sparse diatom assemblages found in these cores may indicate ice shelf coverage of these areas as recently as 1000 years ago.

Figures 21.2-21.5 show the results of a modeling experiment where the shelf required to hold the grounding line at its present position for Pine Island and Thwaites glaciers is removed. Grounding-line positions are shown at 1000, 2000, 4000, and 6000 years after removal of the ice shelf. A conservative estimate of the extent of the buttressing

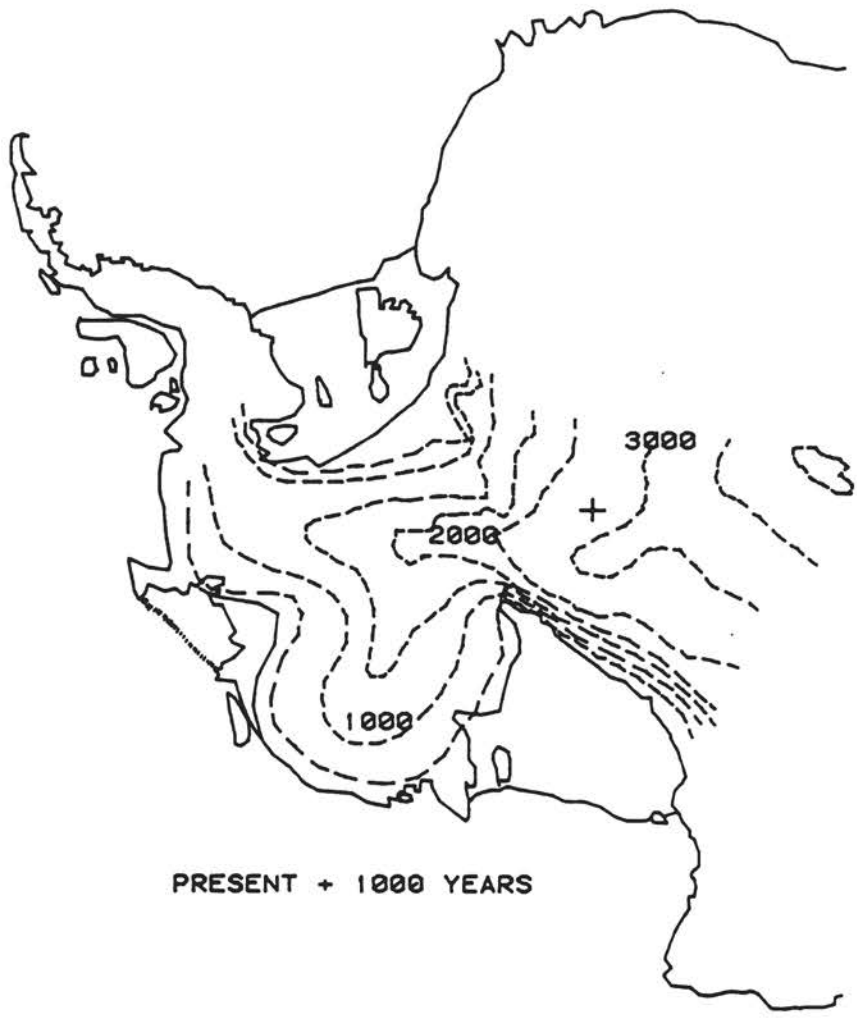

FIGURE 21.2 Map of West Antarctica showing surface elevation contours 1000 years after removing the hypothetical Amundsen Ice Shelf. A new ice shelf forms in essentially the same position, but the grounding line's movement into the deep Bentley subglacial trench causes retreat to continue.

ice shelf produced by the accelerated discharge of ice as grounding lines retreat is indicated by the hatched lines on the figures. Grounding-line retreat rates in this experiment are generally of the same order as those observed during grounding-line retreat from 18,000 to 10,000 BP. It should be stressed that should this ice shelf not reform, retreat into the interior of West Antarctica would proceed far more rapidly than is indicated by this modeling experiment. Experiments with no ice-shelf reforming retreat far into the Bentley subglacial trench in a few hundred years. An ancillary affect of massive retreat in the Amundsen Sea sector is to upset the equilibrium of the ice streams flowing into the Ross Ice Shelf. Migrating ice divides encroach upon

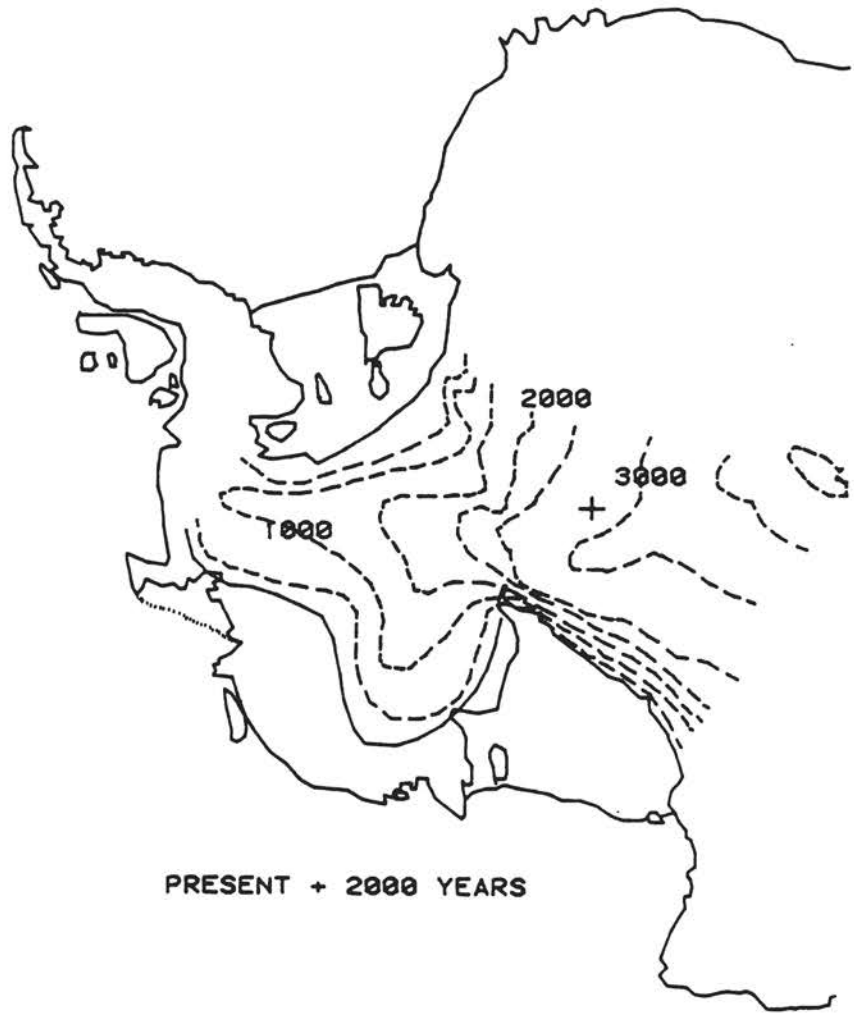

FIGURE 21.3 Surface elevation contours 2000 years after removal of the Amundsen Ice Shelf. The moving ice divide between the Amundsen Sea and the Ross Sea embayments has destabilized those ice streams flowing into the Ross Ice Shelf, and they too begin to retreat.

the catchment areas of flow lines on the opposite side of the divide, triggering grounding-line retreat as reduced grounding-line velocities result in thinning at the grounding line. This is shown in Figures 21.3-21.5 as the migrating ice divide reduces the catchment areas of ice streams D and E, causing the calving rate to exceed the ice flux across the grounding line, thereby reducing the backstress and allowing further retreat. The highly fractured surface of ice stream C, coupled with its anomalously low outlet velocity may indicate that such a process is already taking place.

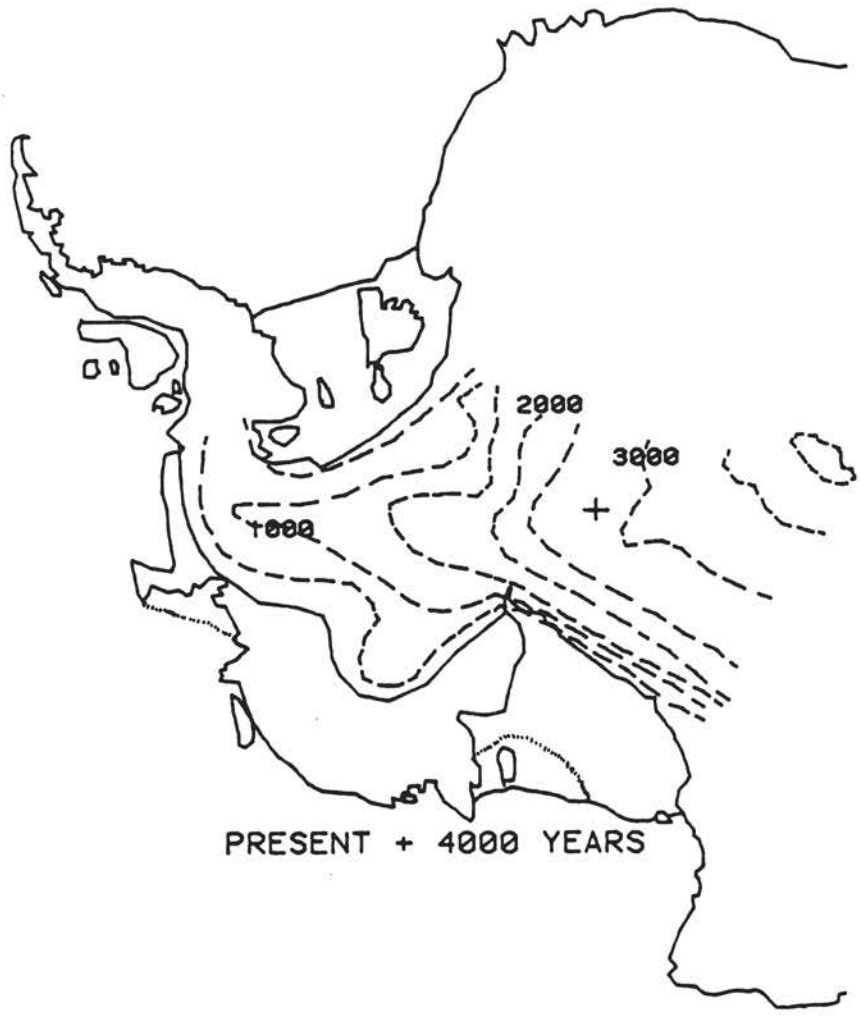

FIGURE 21.4 Surface elevation contours 4000 years after removal of the Amundsen Ice Shelf.

CREVASSE FORMATION

Loss of mass through calving from ice shelves and tidewater glaciers is though to be the dominant mechanism whereby ice is removed from Antarctica. Because of the postulated dependence of marine ice sheets such as West Antarctica on the existence of buttressing ice shelves it seems important to understand some of the processes that might control the calving process.

The analytical treatment of Reeh (1968) and Weertman (1973) is followed in that the primary driving force for calving is assumed to be the eccentric tension produced at the ice front by the unbalanced hydrostatic pressures in the ice and water columns. This treatment ignores the catastrophic mechanisms (e.g., storm surges, tidal waves) that may

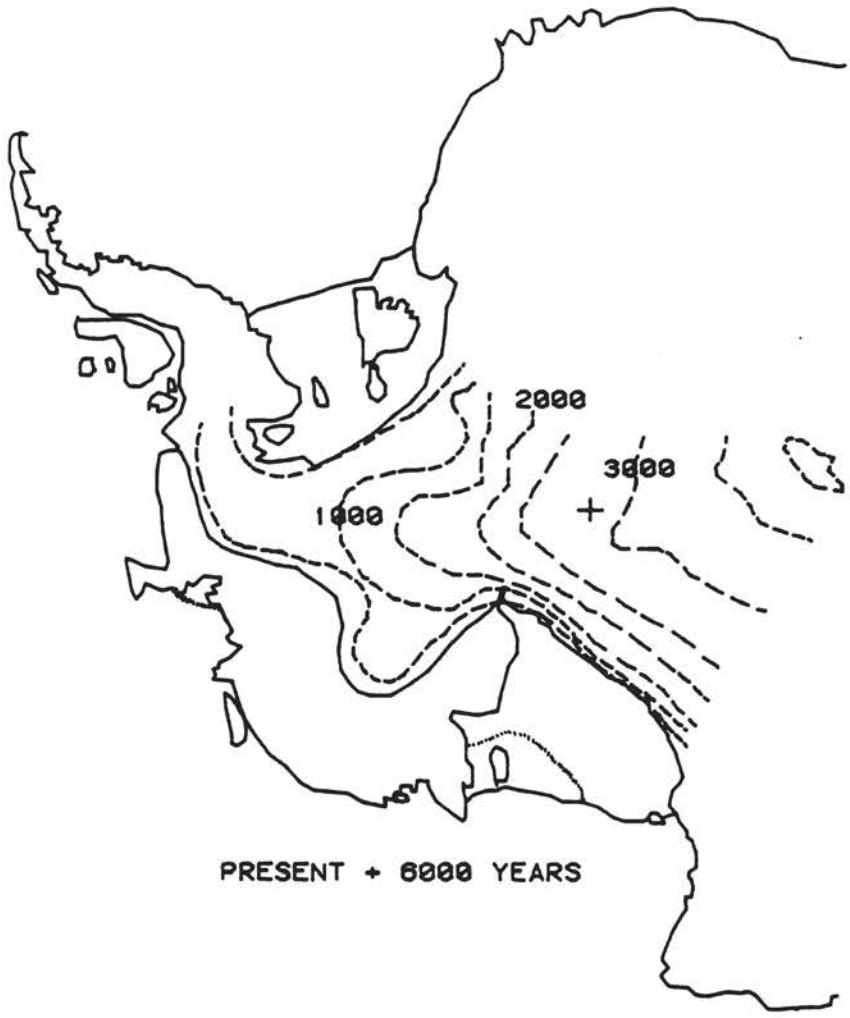

FIGURE 21.5 Surface elevation contours 6000 years after the removal of the Amundsen Ice Shelf.

be responsible for the formation of very large icebergs. The following treatment is discussed in greater detail in Fastook and Schmidt (1982).

The form of the eccentric tension at the ice front is obtained from the balance of hydrostatic pressures in the ice and water columns. The ice, being less dense, needs a longer column to provide the same pressure at the base of the ice column. Pressures within each column are proportional to the density and the depth and must be equal at the base. Since the ice extends above the water surface there is an unsupported face where the tension increases from zero at the top surface to a maximum value at the sea level. At sea level, the hydrostatic pressure of the water begins to counteract the hydrostatic pressure of the ice and the tension decreases to zero at the base of the ice column. The magnitude of the tension depends on the relative densities of the ice and water as well as on the thickness of the ice column. Typically the

average tension on an ice shelf 600 m thick with a density of 917 kg/m^3 in seawater with a density of 1030 kg/m^3 will be 3 bars, with a maximum value at sea level of 6 bars.

It is this tension that is responsible for the thinning of floating ice, but the fact that this tension acts with a maximum at the water level produces a bending torque that causes the ice shelf to arch over. This bending produces a tension maximum some distance back from the ice front. It is at this location that a crevasse is assumed to form. None of the analytic treatments nor this treatment has arrived at an adequate criteria for the fracture of ice. Stress and strain-rate distribution, as well as the past history of the ice in question, seem to affect the formation of crevasses (Holdsworth 1969; Hambrey and Muller 1978) and estimates of the critical values for the fracture of ice range over orders of magnitude. Hughes (1984) has attempted to quantify a fracture criteria, but it is not incorporated in this treatment. Instead a simple criteria that a crevasse forms at the point of maximum tensions is used. Propagation of the crack into the body of the ice shelf depends on the continued existence of tension immediately below the crack. In addition, the crack should not be closing at any level within the crack.

In the present model, this process is investigated using a finite-element model (Zienkiewicz 1971; Schmidt 1977) to obtain an approximate solution to the equations of slow creeping Newtonian flow with velocity and pressure as independent variables. The finite-element technique allows the specification of acceptable ice configurations including cracks and spatially variable material properties as well as realistic (i.e., nonlinear) equations of state without the constraints imposed by an analytic solution. Most importantly one can look at the time evolution of the system as it responds to the changing stress configuration created by the development and propagation of the crack.

Figure 21.6 shows the material configuration used to model the floating ice shelf. The hatched area represents a highly viscous material with a density of 917 kg/m^3, a flow law constant of 3.14 bars/yr, and

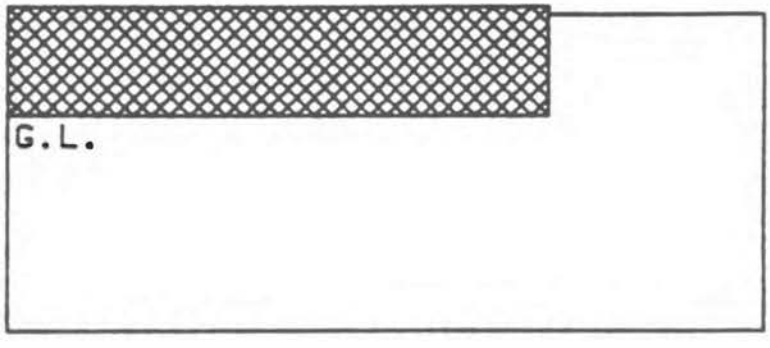

FIGURE 21.6 Material configuration used to model a floating ice shelf. The unhatched region is a low-viscosity waterlike material, while the hatched region is a higher-viscosity icelike material. The point marked G.L. represent the grounding line and is constrained not to move.

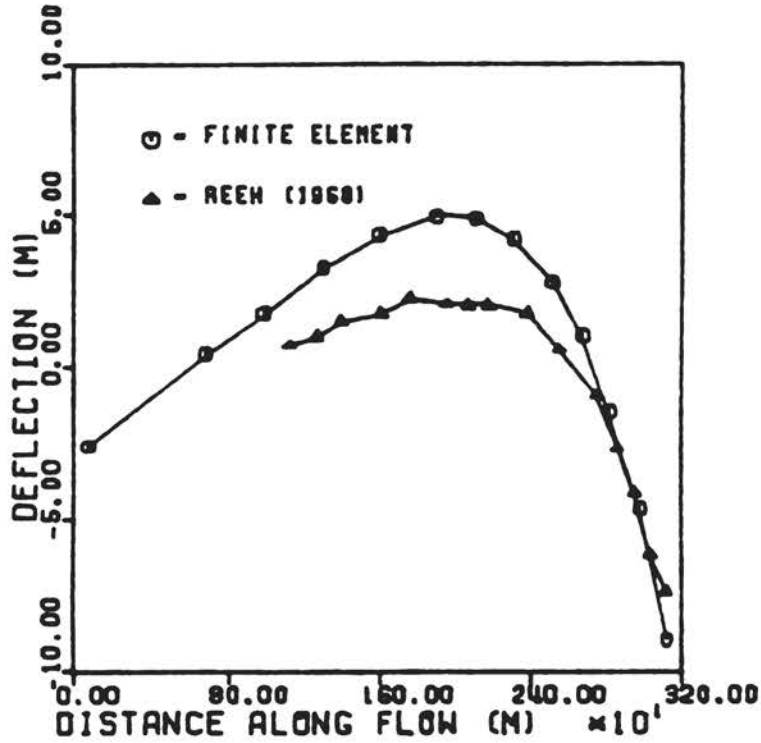

FIGURE 21.7 Comparision of deflections after 0.325 year has elapsed predicted by the viscous-beam approximation of Reeh (1968) and by the finite-element method.

an exponent of 1 [these values correspond to an ice shelf 600 m thick at a temperature of -4°C (Reeh 1968)]. The unhatched area represents the supporting seawater with a density of 1030 kg/m^3 and a flow law constant two orders of magnitude lower than the ice. Although not the actual viscosity of water, this value produces realistic results while avoiding a difference in viscosities between water and ice. The use of water elements to support the ice eliminates the need to calculate the unbalanced tension at the ice front since this is performed internally by the model.

Figure 21.7 shows a comparison of Reeh's (1968) beam analysis with the results of the finite-element analysis. Qualitatively the results are similar. The arching and bending of the ice shelf produce a non-uniform distribution of tensions along the top surface with a maximum tension of 3.44 bars about 300 m back from the ice front. This distribution is shown in Figure 21.8, as are the distributions that occur when a 10-m-wide crack 30 and 60 m deep is introduced into the ice shelf. The presence of the crack seems to have little effect elsewhere. Tension exists below the crack for depths up to 115 m, although such a crack would tend to close off at an intermediate depth near sea level. The deepest crack that one could obtain from this analysis, which displayed tension below it and was opening along its entire depth, was approximately 60 m, which compares favorably with Weertman's (1973)

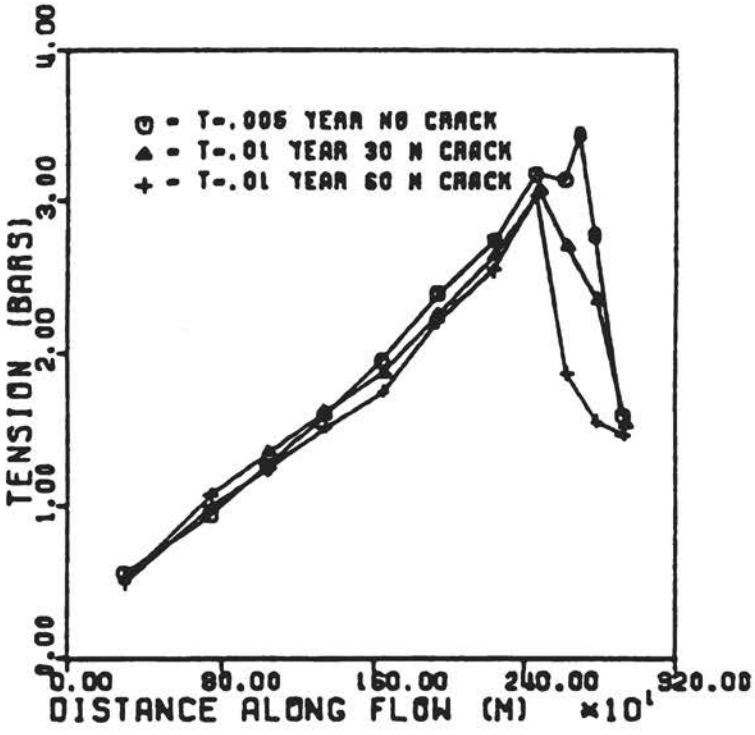

FIGURE 21.8 Normal stress at the centroids of elements along the surface of the floating ice for no crack and for cracks of different depths. The grounding line is to the left, and the calving front to the right.

prediction of 52 m for an ice shelf with a uniform tension of 3 bars. The basic conclusion of this analysis is that such a crevasse would not produce calving, since the crevasse can only penetrate a fraction of the total ice thickness. It is possible, however, that nonuniformities in the ice might skew the direction of propagation of the crack so that a large section of the ice front (300 m back from the ice front and extending perhaps 50 m below sea level) might flake off, producing an underwater bulb similar to those described by Swithinbank and Zumberge (1965). More will be said about nonrectangular fronts later.

Weertman (1973) provided an analytic expression for the depth of propagation of a crack filled to various depths with water. The finite-element method yields general agreement with the analytic solution predicting a depth of 126 m for a crack two thirds full of water and the finite-element method predicting a depth of 138 m.

Up to this point little has been done that could not be performed equally well with the analytic formulations. One of the strengths of the finite-element method lies in continuing the analysis in time beyond the point where the assumptions necessary for the analytic solution have broken down. Figure 21.9 shows the tensions at different levels within the element directly below the crack bottom as a function of time. One can readily note a general trend of increasing tension in the element

as time progresses. Assuming a linear variation of stress within the element, one can obtain a measure of the depth of the level of zero tension (Figure 21.9). Because of thinning and other deformation of the ice shelf with time, the zero tension level is displayed relative to sea level, relative to the crack bottom, and relative to the top surface. For clarity the curves are displaced, the slope being the important characteristic to observe. For this particular crack depth of 108 m one finds the level of zero tension moving downward at a rate of between 0.41 and 0.30 m/day depending on the reference point chosen. A similar analysis for cracks of different depths (Figure 21.10) shows rates of zero-tension level movement as a function of crack depth for a crack filled two thirds full of water. As the crack becomes progressively deeper, the rate of movement of the zero tension level increases. Indeed, an extreme example not shown on Figure 21.10 for a crack 530 m

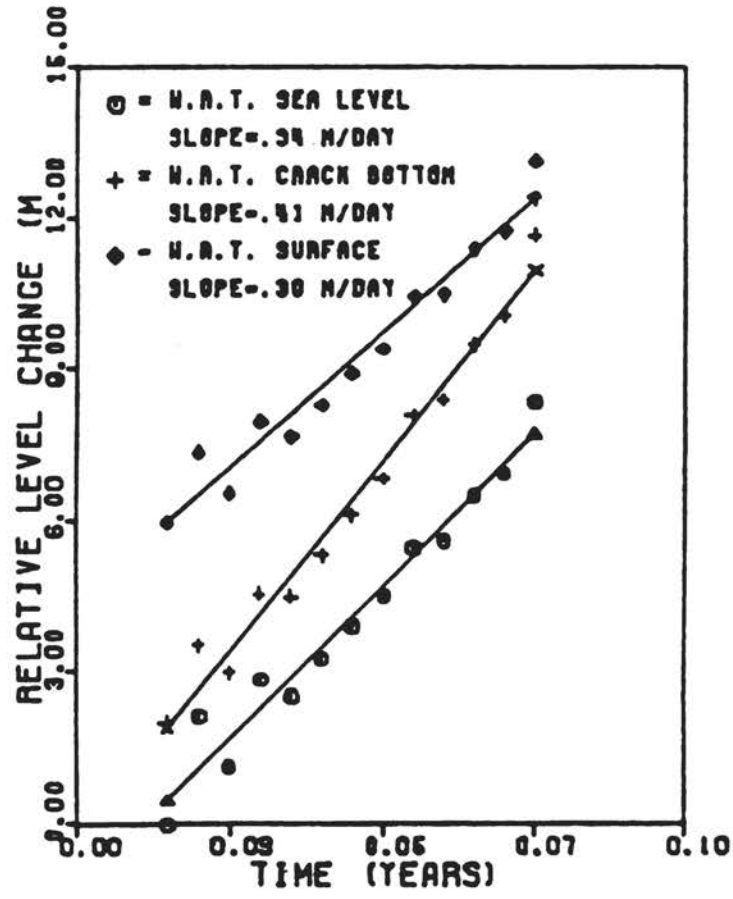

FIGURE 21.9 Movement of the level of zero tension below a crack, initially 10 m wide and 44 m deep, filled two thirds full of water, as a function of time taken with respect to sea level, the crack bottom, and the ice surface. Least-squares fits are shown by the straight lines.

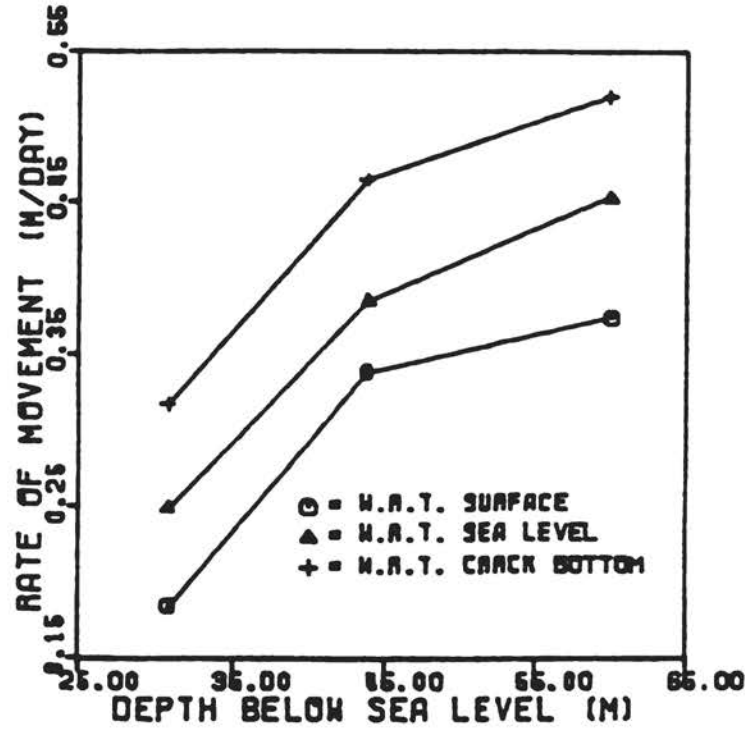

FIGURE 21.10 Rate of movement of the level of zero tension for cracks two thirds full of water and differing bottom depth below sea level. Zero-tension-level movement is measured with respect to the ice surface, sea level, and the crack bottom.

deep (90 percent of the ice thickness) filled with water to approximately sea level shows movement of the zero tension level as high as 10 m/day.

Based on the preceding analysis one can postulate a probable calving scenario as follows. After the calving of an iceberg the ice front deflects downward at the same time that the ice surface more than one ice thickness from the front arches upward. This produces a tension maximum on the surface about one-half ice thickness from the ice front. Fracture is assumed to occur in this region. In the absence of meltwater this crevasse can only propagate to approximately sea level, producing either no calving or only small icebergs, leaving a submerged bulb for the ice-front configuration. If sufficient meltwater is present to maintain the water level in the crack just above sea level, the crack can propagate downward into the ice. Presumably the crack propagates rapidly to approximately the zero tension level and then stops. As the ice shelf continues to deform with time, the zero tension level moves downward, allowing the crack to propagate further into the ice. This movement of the zero tension level accelerates as the crack depth increases. As this mechanism depends heavily on the presence of copious meltwater, one would expect it to be strongly seasonal in character, although once the crack has propagated to a sufficient depth the pre-

sence of seawater that may infiltrate through microcracks will be capable of maintaining the crevasse.

Weertman (1980) described a process whereby bottom crevasses can extend up to 78 percent of the total ice thick into the ice shelf. The possibility of a top and bottom crevasse joining and producing calving is then a possibility. Pol (1984), using a similar finite-element technique, suggested that this is unlikely because a bottom crevasse can only remain open far from the ice front (the situation considered in Weertman's analysis). As the bottom crevasse approaches the ice front where the surface crevasses can exist it begins to close. Pol also considered the case of an overhanging front and a submerged bulb (see Swithinbank and Zumberge 1965). Pol's conclusions are that for an overhanging front the possibility exists for a second top-surface creavasse to form at a position dependent more on the shape of the overhang than on its distance from the ice front. The secondary crevasse seems to form where the ice shelf thickens considerably, although this result may be an artifact of the abrupt change in thickness used to model the overhang. The significant result of his analysis of the submerged bulb configuration is a strong tendency for bottom crevasses to remain open much closer to the ice front, hence producing the possibility of a top and bottom crevasse coinciding and producing calving.

TIME-DEPENDENT FINITE-ELEMENT MODEL

There are important drawbacks of the two modeling techniques discussed in the previous two sections.

The finite-difference scheme used to reconstruct profiles for calculation of the grounding-line position as controlled by the marine instability uses a steady-state profile. While this is acceptable on the time scales dealt with in that modeling exercise, for more rapid change, or to model accurately the state of a system as it changes in response to changing boundary conditions, one must include the full time-dependent continuity equation as a starting point. This is difficult to do in the finite-difference scheme because of the stepwise nature in which this modeling technique obtains profiles.

The second model suffers from similar drawbacks in that the solution obtained is also a steady-state solution so that one cannot observe the effects of changing boundary conditions. In addition the requirement that one specify the configuration of the boundary as well as all the forces acting on that boundary makes this modeling technique less useful in situations where the configurations is unknown (as when attempting to reconstruct a given flow-line profile).

The modeling technique described here combines the best points of the previous two models while addressing the above-mentioned drawbacks.

Finite-elements analysis is especially appropriate for modeling situations in which a quantity identifiable as a flux is proportional to the derivative of some state variable for which one wishes to solve. In the problem under consideration the flux, σ, given by

$$\sigma = uwH \tag{21.1}$$

is simply the product of u (velocity), w (width of the flowband), and H (ice thickness at any given point), while the state variable of interest is taken to be the ice-surface elevation at that point. Velocities can be expressed analytically as some linear combination of sliding and flow, where the different components are given by integrating appropriate sliding and flow laws. In this model Weertman's (1964) sliding law and Glen's (1955) flow law have been used. Any constitutive relationship that relates either velocity or strain rate to applied stress could as easily be used in this formulation. The continuity equation for a flow line is given by

$$(\partial h/\partial t) = \dot{a} - (d\sigma/dx)/w, \tag{21.2}$$

where h is the surface elevation, $\dot{a}$ is the accumulation rate, x is the distance along the flow line with the origin at the margin, and t is time. The continuity equation is then solved using a variational-principle approach (Becker et al. 1981) that takes advantage of the fact that over appropriately small regions (i.e., finite elements) within the area being modeled, such variable factors as width, accumulation, flow-law constant, and sliding law constant can be taken as constant with respect to the integration variable (in this case the distance along the flow line). In addition the state variable (surface elevation) is approximated by a linear combination of simple quadratics (termed shape functions) that can be integrated exactly in any arbitrary element. The problem reduces to an algebraic problem of solving for the coefficients of the linear combinations of shape functions. Combination of these coefficients yields the solution over the entire region under consideration.

The procedure above yields a matrix equation of the form

$$\bar{\bar{K}}h + \bar{\bar{C}}\,(dh/dt) = f, \tag{21.3}$$

where h and dh/dt are the vector and the time derivative of the vector of surface elevations that make up the boundaries of the set of elements used to approximate the flow line, $\bar{\bar{K}}$ is the stiffness matrix obtained from the flux derivative term equation, $\bar{\bar{C}}$ is the capacitance matrix obtained from the surface-elevation-time derivative, and f is the load vector obtained from this equation by solving the h with the time derivative equal to zero.

$$h = \bar{\bar{K}}^{-1}f. \tag{21.4}$$

For the full time-dependent solution one can use a backward-difference scheme where

$$(dh_{n+1}/dt) = (h_{n+1} - h_n)/\Delta t; \tag{21.5}$$

here Δt is the time step and n is the number of the time steps taken. Combining Eqs. (21.3) and (21.5) and solving for h_{n+1} one obtains

$$h_{n+1} = (\bar{\bar{I}} + \bar{\bar{C}}^{-1}\bar{\bar{K}}\,t)^{-1}\,(h_n + \bar{\bar{C}}^{-1}f_{n+1}\Delta t), \tag{21.6}$$

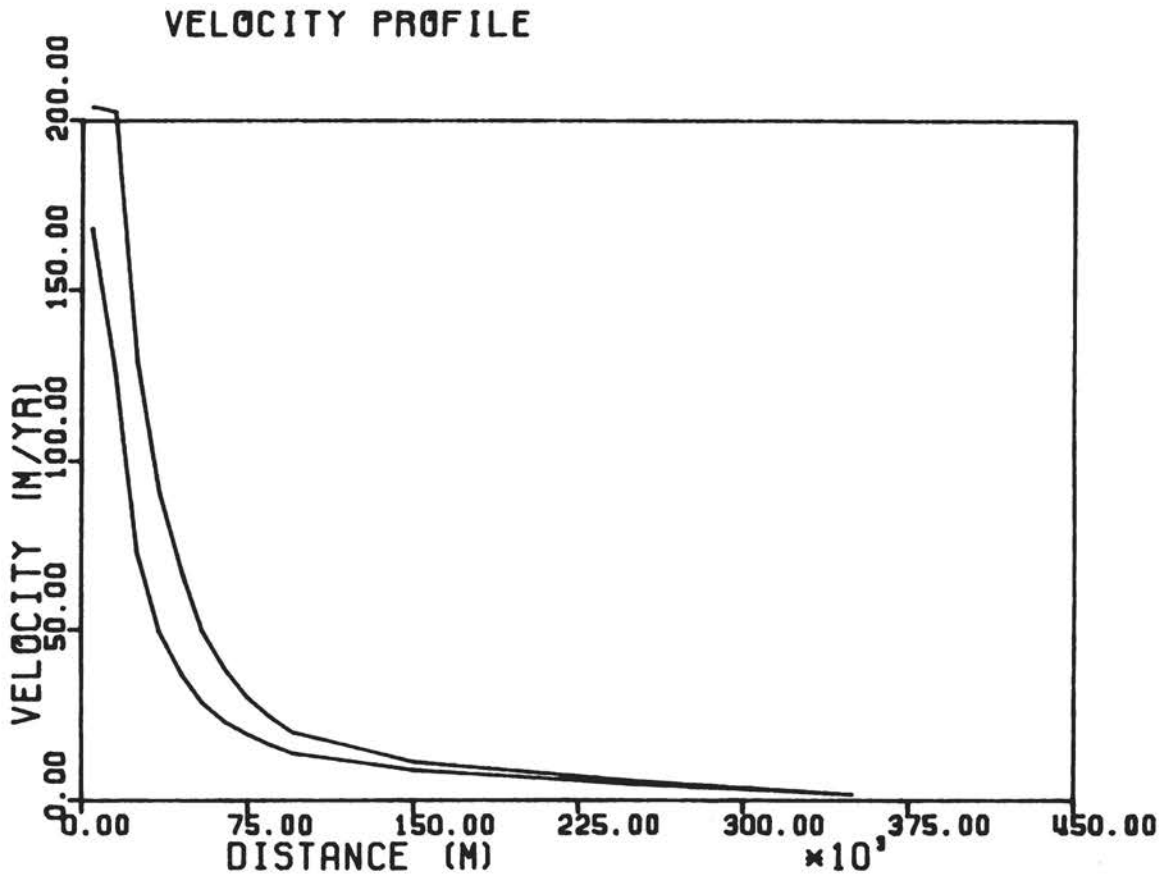

FIGURE 21.11 Equilibrium velocity for a flat-bed, marine-based flow line, with and without an ice stream.

where $\bar{\bar{I}}$ is the identity matrix, h_n and h_{n+1} are the surface elevation vectors at time steps n and n + 1, and f_{n+1} is the new load vector.

The following is an example of what can be done with this type of model, as well as to show what sort of changes one might expect to observe in the surface profile of a glacier that has undergone a sudden change in boundary conditions. A flat-bed marine-based flow line 400 km long undergoes a sudden decoupling of the bed that increases progressively from a point 100 km inland of the grounding line until at the grounding line the ice is completley decoupled from the bed. Assuming a thawed bed along the length of the flow line, one can interpret this in context of Weertman's (1964) sliding law as a progressive drowning of the controlling obstacles as one moves inland from the grounding line. The equilibrium profiles that are obtained by solving Eq. (21.4) for the two different sets of boundary conditions are shown as dashed lines on Figure 21.12. The grounding line is at the left, and flow is from right to left with the flux across the right-hand boundary equal to zero. The upper profile presents a typical sheet flow profile, while the lower uncoupled bed profile displays the concave surface often

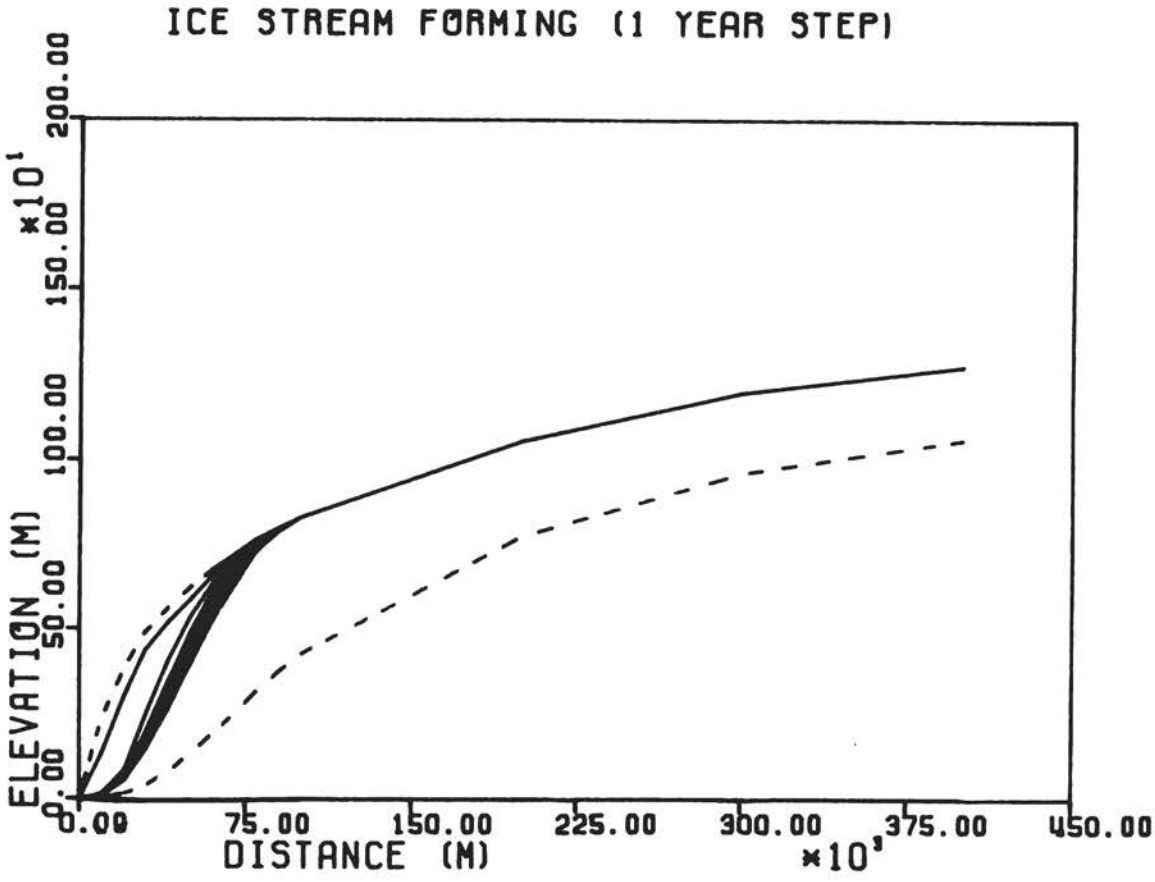

FIGURE 21.12 Ice-stream forming, the first 10 years, time step equals 1 year. Dashed lines indicate equilibrium surface elevation profiles for a flat-bed, marine-based flow line, with and without an ice stream 100 km long.

associated with ice streams. The basal shear stresses obtained for these two equilibrium profiles are shown as dashed lines on Figure 21.15. Note the very low stresses associated with the uncoupled ice stream portion of the profile. Figure 21.11 shows velocity profiles for the same two flow lines. Again note the higher velocities along the ice stream profile. Figures 21.12-21.14 show the results of this model experiment. The upper dashed line is the original profile, and the lower dashed line is the equilibrium profile of the new boundary conditions. Intermediate solid lines show the surface response as a function of time for varying time steps. In Figure 21.12 the first 10 years of response are shown at 1-year intervals. Note the spreading effect of the ice stream that now extends well beyond the 100 km directly affected by the changing boundary conditions. Figure 21.14 shows the long term response of the flow line with 1000-year intervals showing the clear convergence of the time-dependent solution toward the equilibrium profile obtained for the new boundary conditions. Figure 21.15 shows for 10-year intervals the response of the basal shear stress

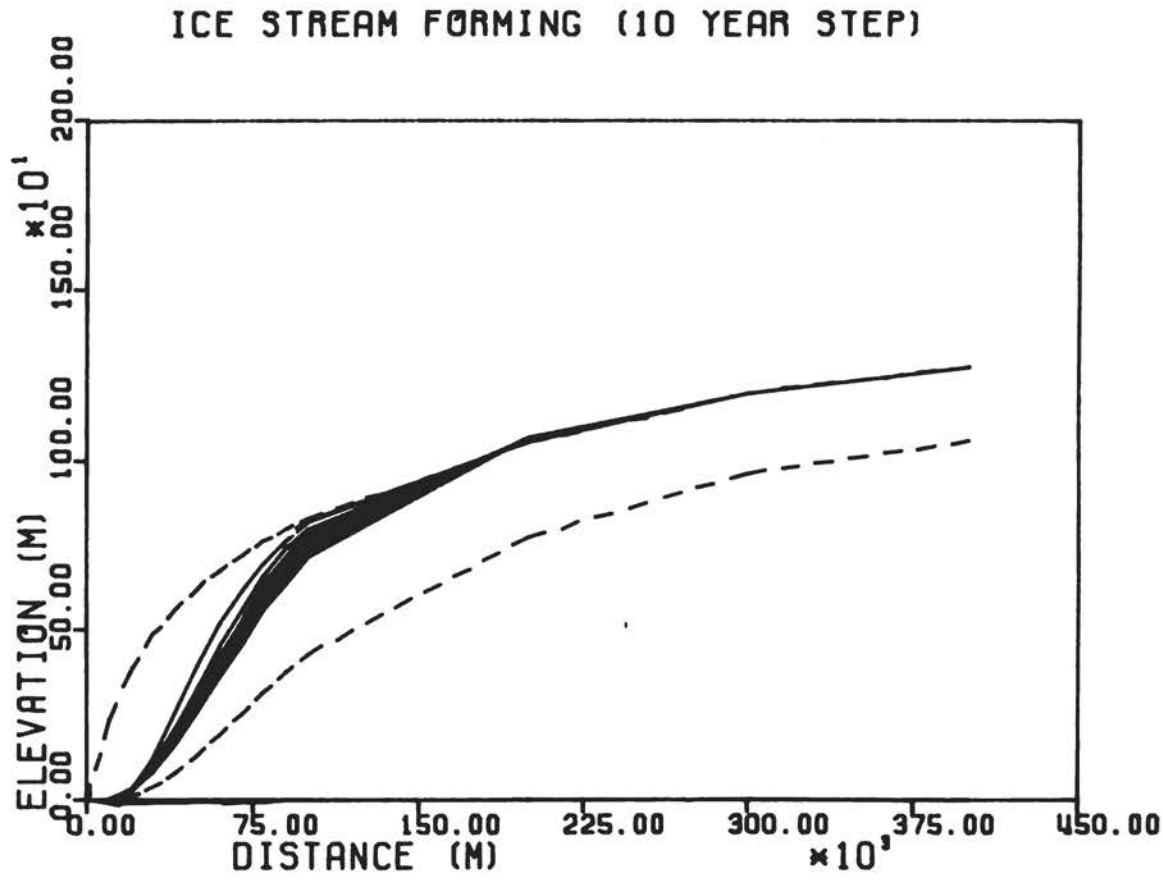

FIGURE 21.13 Ice-stream forming, the first 100 years, time step equals 10 years.

as the ice stream forms. Note that even though the bed is becoming progressively decoupled through the drowning of the controlling obstacles the effect is for the basal shear stress to increase locally in and above the ice stream region as the ice stream forms. Finally, Figure 21.16 shows the calculated grounding-line flux as a function of time. The equilibrium flux is shown as a horizontal dashed line. The flux initially increases to a high value when the bed is decoupled and then displays exponential decay to its equilibrium value as time progresses.

While the use of a step function for the change in boundary conditions is at best artificial, this model serves to demonstrate the power of this technique, as well as displaying some of the short-term effects that one might expect to observe in the formation of an ice stream in a region originally dominated by sheet flow. More realistic changes in boundary conditions are not difficult to implement; linear rams, sinusoidal variations, and others all being possible to introduce through Eq. (21.6). In this model one is not limited to varying the bed coupling. One can also vary accumulation rates (in response to changing

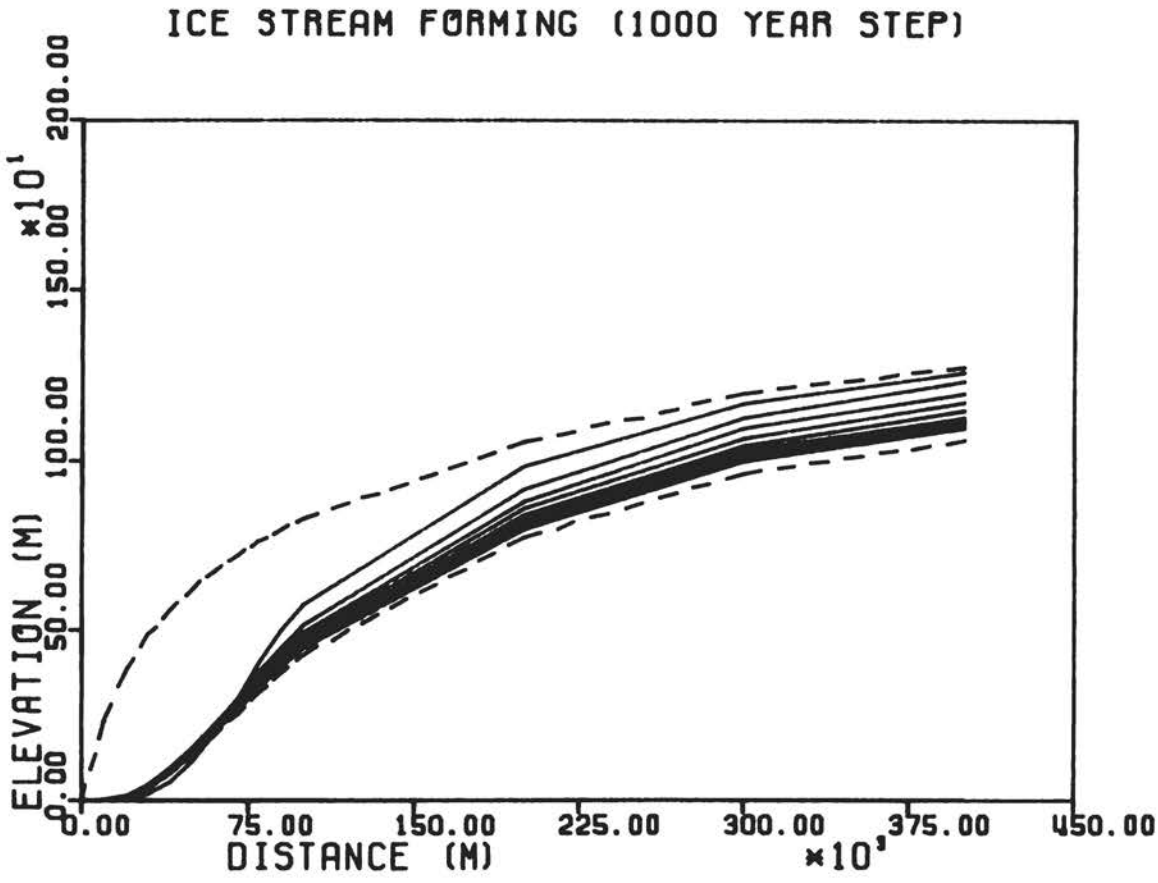

FIGURE 21.14 Ice-stream forming, the first 9000 years, time step equals 1000 years.

climate), catchment areas (in response to changes in the neighboring flowlines), flow- or sliding-law constants (in response to changing temperature), or bedrock profiles (in response to isostatic adjustments).

ACKNOWLEDGMENTS

I would like to acknowledge the National Science Foundation, whose grants DPP8017071, DPP8107668, and DPP8209311 supported this research. I am also indebted to Terry Hughes and George Denton for valuable discussions and assistance.

REFERENCES

Becker, E. B., G. F. Carey, J. T. Oden, 1981. Finite Elements, An Introduction, Prentice-Hall, Inc., Englewood Cliffs, New Jersey, pp. 40-87.

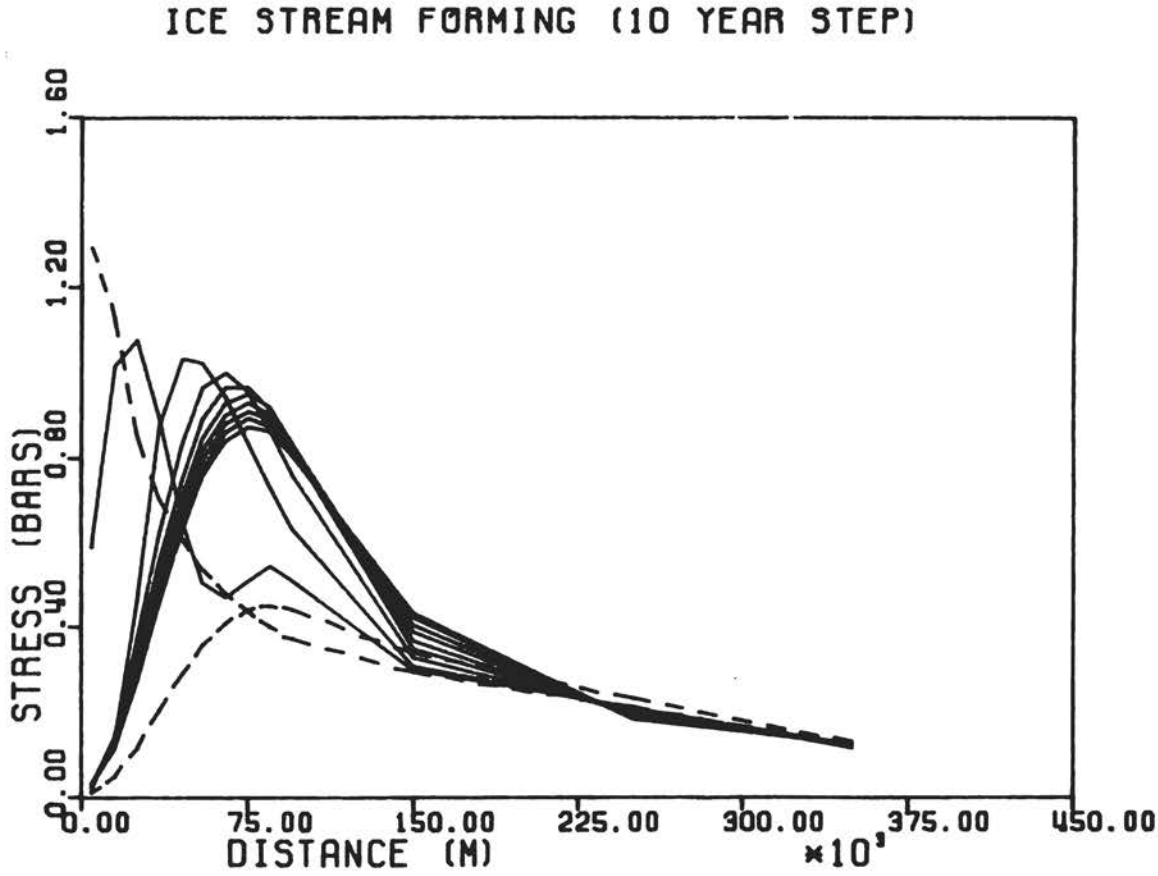

FIGURE 21.15 Basal-shear-stress distribution for the first 100 years corresponding to Figure 21.13. Dashed lines indicate the equilibrium basal-shear-stress profiles for a flat-bed, marine-based flow line, with and without an ice stream 100 km long.

Fastook, J. L., 1984. West Antarctica, the sea-level controlled marine instability: Past and future. In J. E. Hansen and T. Takahashi (eds.), Climate Processes and Climate Sensitivity, American Geophysical Union, Washington, D.C., pp. 275-287.

Fastook, J. L., and W. Schmidt, 1982. Finite-element analysis of calving from ice fronts. Annals of Glaciology, 3, 103-106.

Glen, J. W., 1955. The creep of polycrystalline ice. Proceeding of the Royal Society of London, 228, 519-538.

Hambrey, M. J., and F. Muller, 1978. Structure and ice deformation in the White Glacier, Axel Heiberg Island, Northwest Territorities, Canada, Journal of Glaciology, 20, 41-66.

Holdsworth, G., 1969. Primary transverse crevasses. Journal of Glaciology, 8, 107-129.

Hughes, T. J., 1977. West Antarctic ice streams. Review of Geophysics and Space Physics, 15, 1-46.

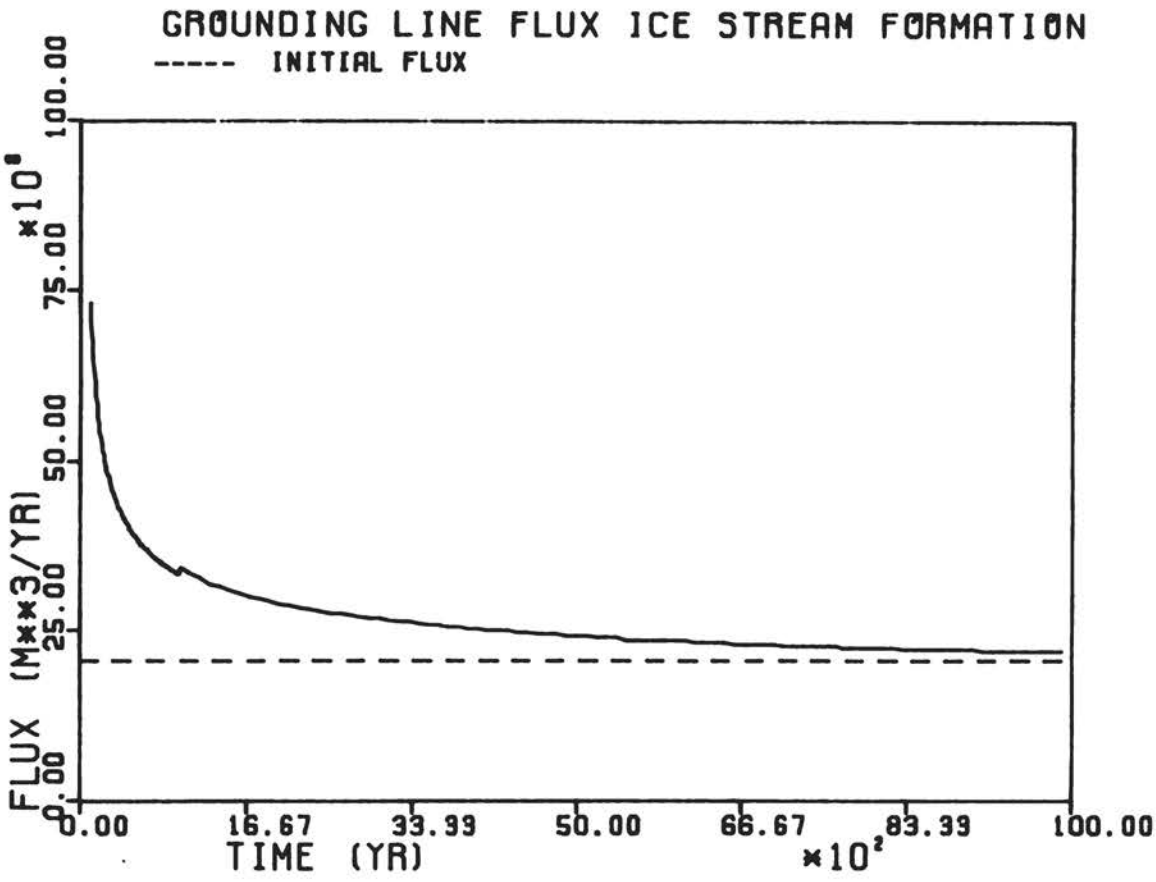

FIGURE 21.16 Grounding-line flux as a function of time (solid line) showing the exponential decay to equilibrium (dashed line).

Hughes, T. J., 1981. Numerical reconstruction of paleo ice sheets. In G. H. Denton and T. J. Hughes (eds.), The Last Great Ice Sheets, Wiley-Interscience, New York, pp. 221-261.

Hughes, T. J., 1984. On the disintegration of ice shelves: The role of fracture. In press.

Kellogg, T. B., D. E. Kellogg, and J. B. Andersen, 1982. Preliminary results of microfossil analysis of Amundsen Sea sediment cores. Antarctic Journal, 17, 125-126.

Manabe, S., and R. T. Wetherald, 1975. The effect of doubling the CO_2 concentration on the climate of a general circulation model. Journal of Atmospheric Science, 32, 3-15.

Pol, S. A., 1984. Finite element analysis of calving from ice fronts. Master's Thesis, University of Maine at Orono.

Reeh, N., 1968, On the calving of ice from floating glaciers and ice shelves. Journal of Glaciology, 7, 215-234.

Schmidt, W. F., 1977. Finite element analysis of planar creeping flow. Department of Mechanical Engineering Report, 77-1, University of Maine.

Stuiver, M., G. H. Denton, T. J. Hughes, and J. L. Fastook, 1981.

History of the marine ice sheet in West Antarctica during the last glaciation: A working hypothesis. In G. H. Denton and T. J. Hughes (eds.), The Last Great Ice Sheets, Wiley-Interscience, New York.

Swithinbank, C. W., and J. H. Zumberge, 1965. The ice shelves. In T. Hatherton (ed.), Antarctica, Methuen, London, pp. 199-220.

Thomas, R. H., and C. R. Bentley, 1978. Model for the Holocene retreat of the West Antarctic Ice Sheet. Quaternary Research, 10, 150-170.

Weertman, J., 1964. The theory of glacier sliding. Journal of Glaciology, 5, 287-303.

Weertman, J., 1973. Can a water-filled crevasse reach the bottom surface of a glacier? In International Association of Scientific Hydrology Publication 95 (Symposium of Cambridge 1969 - Hydrology of Glaciers), pp. 139-145.

Weertman, J., 1974. Stability of the junction of an ice sheet and an ice shelf. Journal of Glaciology, 13, 3-11.

Weertman, J., 1980. Bottom crevasses. Journal of Glaciology, 25, 185-188.

Zienkiewicz, O. C., 1971. The Finite Element Method in Engineering Science, McGraw-Hill, London.

ATTACHMENT 22

RESPONSES OF THE POLAR ICE SHEETS TO CLIMATIC WARMING

Robert H. Thomas
National Aeronautics and Space Administration
Washington, D.C.

INTRODUCTION

This document presents an assessment of possible responses by the Antarctic ice sheet to a climate warming associated with increasing concentrations in the atmosphere of greenhouse constituents such as CO_2 and methane. This has been a cooperative effort with the Goddard Institute of Space Studies (GISS) climate modeling group under J. Hansen.

Increased ice drainage from West Antarctica is generally identified as the most probable cause for a major increase in sea level if global climate becomes appreciably warmer. Potential outlets for the ice are the Pine Island and Thwaites glaciers and the great embayments containing the Ross and Filchner/Ronne Ice Shelves. In addition, parts of the East Antarctic ice sheet grounded more than 0.5 km below sea level (Figure 22.1) may also be vulnerable to increased discharge. A quantitative assessment of these responses over the next century is hindered by lack of both data and understanding of the physical processes that might operate. Nevertheless, I attempt here to formulate a simple model to describe the initial response of Antarctic outlet glaciers and ice streams to warming climate, and I shall use this model to estimate upper limits to increased ice discharge during the next century.

RATIONALE FOR A MODEL DESCRIBING ENHANCED ICE DISCHARGE

Most of the large Antarctic glaciers and ice streams drain into ice shelves--in marked contrast to those in Greenland, which flow directly into the ocean where they calve to form comparatively small icebergs. The Antarctic ice shelves impose a backpressure on ice flowing into them, and the magnitude of the backpressure is determined by how difficult it is to push the ice shelf seaward. Large, embayed ice shelves containing grounded ice rises, such as the Amery, Filchner-Ronne, and Ross Ice Shelves, impose very large backpressures--up to several bars--on their tributary glaciers. As a rough rule of thumb, the backpressure can be approximated as 1 bar for every 200 m by which the grounding-line thickness exceeds 400 m. Thus, where the Ronne Ice Shelf approaches 1400 m in thickness, the backpressure is about 5 bars.

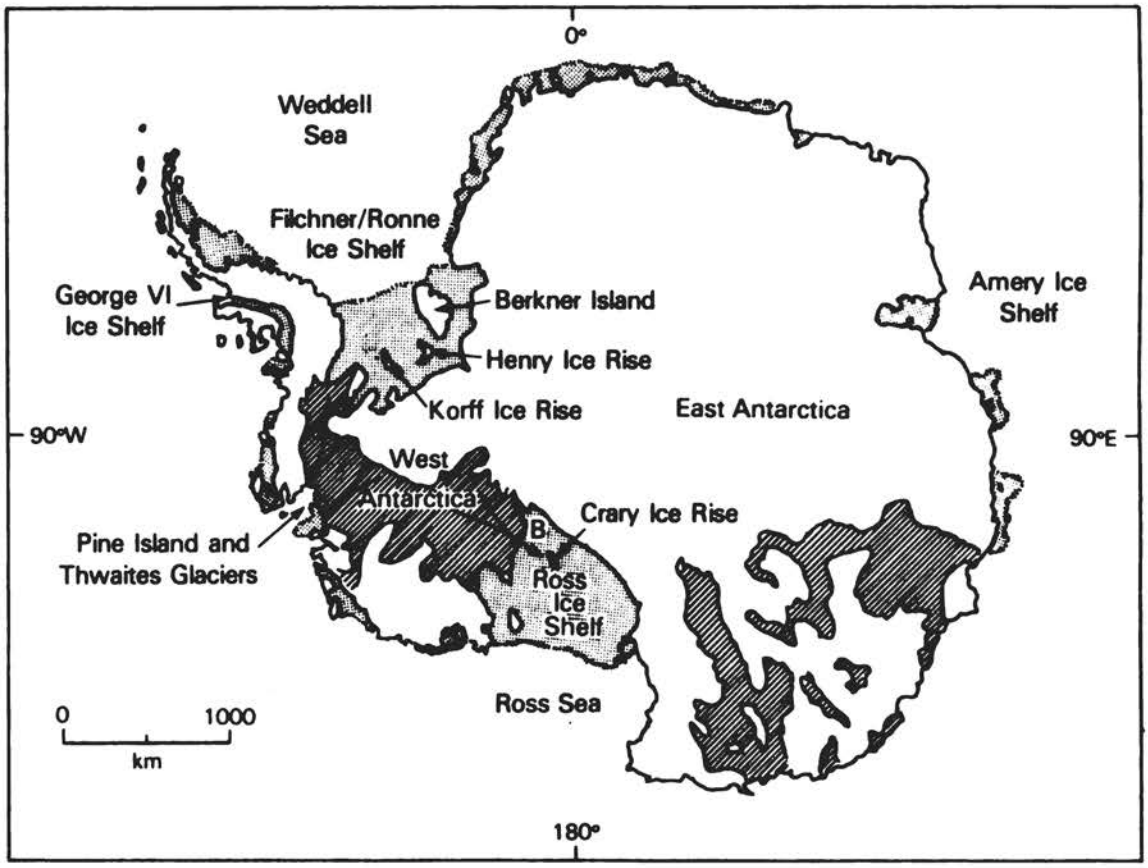

FIGURE 22.1 Antarctica. The floating ice shelves are shaded. The hachured regions are "marine-based" portions of the ice sheet resting on bedrock more than 500 m below sea level.

The effect of this backpressure is to limit creep rates in the ice shelf and for some distance upstream in tributary glaciers. The upstream distance over which the glacier "feels" the presence of the ice shelf is determined by how easily it slides over its bed. Backpressure is transmitted over the greatest distance for wide, rapidly sliding glaciers with low basal shear stresses (and therefore low surface slope). A climatic warming sufficient to cause ice-shelf thinning and/or accelerated calving would result in a reduction in backpressure, since the ice-shelf thickness in contact with the margins and ice rises would be reduced. This, in turn, would permit accelerated creep in the upstream portions of the ice shelf and for some distance upstream tributary glaciers. The net result would be accelerated discharge into the ice shelves.

This is the basis upon which I shall formulate two models describing increased ice discharge. The first model (A) is simple and contains no physics. I assume that the increased ice discharge exactly balances ice lost from the ice shelves by increased melting. Note, however, that the ice shelves would nevertheless become progressively thinner, because

additional ice would be lost by enhanced calving at the seaward ice fronts to balance the increased ice-shelf speed. I include this model to provide a datum against which to compare results from the second, more elaborate model (B). In the second model, I calculate ice-stream acceleration consistent with progressive ice-shelf weakening due to enhanced melting, and I include the negative-feedback effects of the increased ice discharge on ice-shelf thinning. First, to illustrate the importance of the ice shelves, I shall consider the effects of their complete removal on a large tributary ice stream.

THE DYNAMIC ROLE OF ICE SHELVES

The thick, broad ice streams that drain West Antarctic ice into the Ross and Filchner/Ronne Ice Shelves have anomalously low surface slopes. Driving stresses balancing shear at the bed and ice-stream sides are typically 0.1 to 0.2 bar. If shear stresses at the ice/ice marginal interfaces are approximatley 1 bar, basal shear stresses may be less than 0.1 bar within the faster-moving lower reaches of these ice streams--extending 200 km or more inland from the ice-shelf grounding line. This suggests that the ice is sliding readily over a slurry of water-saturated glacial drift. Moreover, these portions of the inland ice can be regarded almost as extensions of the ice shelf, with negligible shear within vertical planes. The rate at which the ice stream accelerates as it moves seaward is then determined by longitudinal tensile stresses, and expressions for these can be derived using ice-shelf theory (Thomas 1973). Referring to Figure 22.2, the ice-stream longitudinal strain rate at P is

$$\dot{E}_{xx} = \left\{ \frac{(1 + \alpha + \alpha^2)^{n-1/2n}}{\bar{B}\,(2 + \alpha)} \left[\frac{\rho_i g H}{2} - \frac{F_s + F_{is}}{WH} \right] \right\}^n \qquad (22.1)$$

and $\alpha = \dot{E}_{yy}/\dot{E}_{xx}$, where $\dot{E}_{yy}$ is the lateral strain rate; H is the ice thickness at P; W is the ice stream width at P; F_s is the total force due to shear between the ice stream and its sides and bed downstream of P; F_{is} is the total compressive force between the ice stream and ice shelf at the grounding line; B is a temperature-dependent ice hardness parameter, averaged over depth; and n is the ice-flow law exponent, generally assumed to be approximately 3. The term $(\rho_i g H)/2$ is the weight-induced spreading stress (σ_e), and the term $(F_s + F_{is})/WH$ is the retarding stress (σ_r). (Note that a more generalized expression can be written for an ice stream with nonhorizontal bed, but it becomes more complex and does not alter our final result.)

With this relationship, we can now examine the influence of ice-shelf weakening on ice-stream velocity. Some of the ice streams draining into the Ross and Filchner/Ronne Ice Shelves have thicknesses close to 1 km at the point where they enter the ice shelves. For these thick portions of ice shelf to survive as equilibrium features, thinning rates due to creep must be balanced by thickening rates due to snow accumulation and advection of thicker ice from upstream. These thickening effects gen-

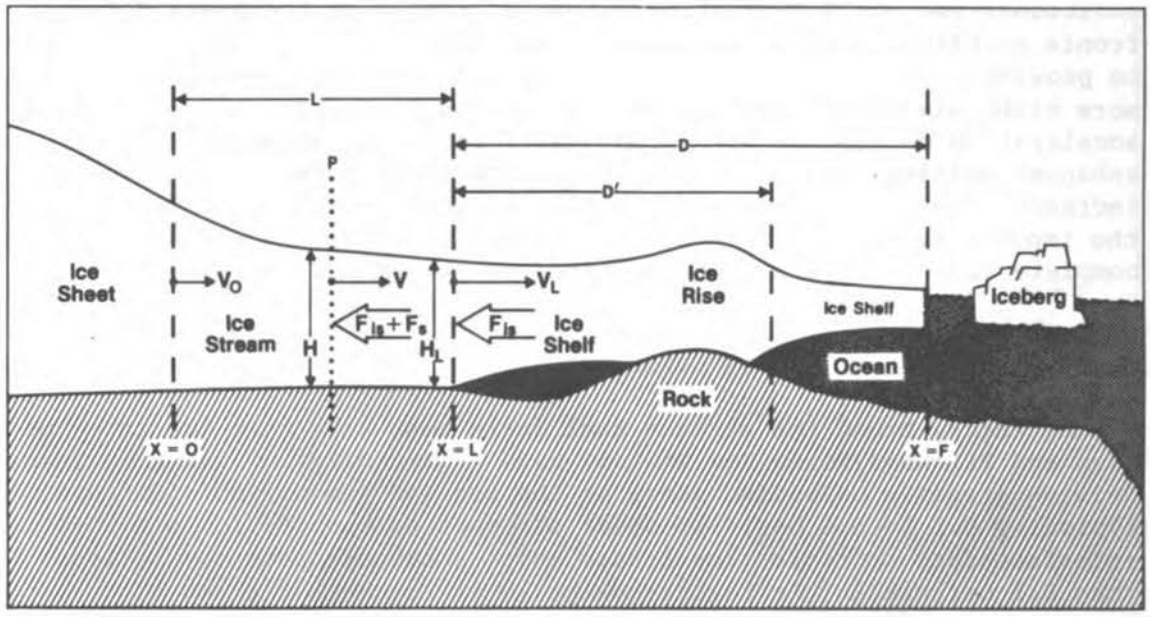

FIGURE 22.2 A typical Antarctic ice-drainage system. The ice stream pushes the ice shelf seaward past its margins and around the grounded ice rises, and there is a comprehessive force (F_{is}) at the grounding line between ice stream and ice shelf. This compressive force is transmitted for some distance (L) upstream of the grounding line, and there is an additional force (F_s) due to shear between the ice stream and its sides and bed.

erally are very small. Consequently, creep rates must also be small, implying that the retarding stress (σ_r) in Eq. (21.1) is almost equal to the weight-induced spreading stress (σ_e). Any weakening of the ice shelf sufficient to decrease F_{is} could cause a significant increase in the horizontal creep rate ($\dot{E}_{xx}$).

To illustrate the point, consider a 1000-m-thick ice stream entering a parallel-sided ice shelf at a speed of V_L = 500 m/yr. For an accumulation rate (A) of 0.2 m of ice equivalent per year and a thickness gradient in the direction of flow ($\partial H/\partial x$) of -10^{-3}, the value of horizontal creep rate necessary to maintain flow is

$$\dot{E}_{xx} \sim (\dot{A} - V_L \frac{\partial H}{\partial x})/H_L = 7 \times 10^{-4}\ \text{yr}^{-1}.$$

Then, with $\bar{B} \simeq 6$ bars $\text{yr}^{1/3}$ and $\alpha = 0$ (since $\dot{E}_{yy} = 0$),

$$\sigma_e = \rho_i g H/2 \simeq 46 \text{ bars}$$

and

$$\sigma_r\ (=F_{is}/WH_L) = \sigma_e - 2B\dot{E}_{xx}^{1/3} \simeq 45 \text{ bars}. \qquad (22.2)$$

If the ice shelf were removed completely, σ_r would not decrease to

zero; it would become the water pressure on the ice stream averaged over total thickness

$$\sigma_{r0} = \rho_i g H_L (\rho_i/\rho_w)/2 \sim 41 \text{ bars.} \qquad (22.3)$$

Thus, in this example, the ice shelf transmits a backpressure ($\sigma_p = \sigma_r - \sigma_{r0}$) of 4 bars, representing the cumulative effects of shear past its sides and interaction with ice rises. Without the ice shelf, the net spreading stress at the ice-stream grounding line would increase from 1 bar to 5 bars, and $\dot{E}_{xx}$ would increase by a factor of 5^3 to 8.7×10^{-2} yr^{-1}.

Clearly, a slow climatic warming will not remove the big ice shelves quickly. Even with increased melting rates, ice shelves will remain anchored to the ice rises until they thin sufficiently to float free of the shoaling seabed.

THE IMPORTANCE OF ICE RISES

The flow of both Ross and Filchner/Ronne Ice Shelves is strongly influenced by large ice rises that have formed where seabed shoals have locally grounded the ice-shelf land arrested its forward motion. Ice flows predominantly around these obstructions and is, to some extent, dammed up behind them. This is clearly illustrated by the contrasting thicknesses of ice upstream and downstream from the ice rises. This damming effect requires that backpressure transmitted by the ice shelf be proportional to ice-shelf thickness integrated over distance between the grounding line and ice front. We must also consider the possibility that some of the ice rises may be removed by the effects of increased melting.

ICE-SHELF THINNING SUFFICIENT TO PERMIT FLOTATION OF ICE RISES

If ice-shelf thinning sufficient to permit flotation were to happen, the ice-rise damming effect would be removed, permitting upstream thinning and a major increase in ice-stream velocity. However, the increased speed would also increase the advection of thick ice from the ice stream, and this would delay total ungrounding of the ice rise.

In the Ross Ice Shelf, ungrounding of Crary Ice Rise would have the most pronounced effect on ice-stream drainage rates. However, Crary Ice Rise is grounded on seabed with a minimum depth of approximately 300 m below sea level and, because of the effects of increased advection described above, anticipated upper values of enhanced melting will not be sufficient to unground the ice during the next century. In the Filchner/Ronne Ice Shelf, the ice of Berkner Island is securely grounded on very shallow bedrock. More vulnerable are the Korff and Henry Ice Rises further south, and I have tried to assess their viability by comparing creep-thinning of the ice shelf leeward of the ice rises with thickening due to advection and snow accumulation. I assumed that ice shelf to the east of Korff Ice Rise and to the north of Henry Ice Rise

is dragged seaward by faster-moving, thicker ice shelves on each side. If this is correct, the creep of ice shelf leeward of the ice rises is restricted solely by seawater pressure. Then for zero lateral strain, creep rates can be estimated using Weertman's (1957) equations for two-dimensional ice-shelf creep. Thickening effects of advection are calculated assuming that basal ice on the ice rises is below the melting point.

This analysis provides estimates of maximum depth to bedrock beneath the ice rises for continued survival in their present form. Calculated maximum depth beneath the northeast part of Korff Ice Rise lies between 250 and 300 m below sea level; equivalent values for Henry Ice Rise are 235 and 315 m. The range in values is determined partly by uncertainty in snow accumulation rate and partly by differences in ice-rise width. If the seabed beneath the ice rises lies at greater depths, then the leeward grounding lines of these ice rises are probably already retreating. A stage in such a retreat is degeneration of the ice rise into ice rumples--when the ice shelf upstream is pushed over the shoaling seabed.

IGY data indicate that Korff Ice Rise is grounded on bedrock less than 200 m below sea level but that bedrock beneath Henry Ice Rise is about 600 m below sea level (Behrendt 1962). Thus, Henry Ice Rise may already be collapsing, and the partly grounded ice rumples between Korff and Henry Ice Rises may represent the remains of an earlier ice rise. Total ungrounding of Henry Ice Rise and the nearby rumples would permit increased thinning of the ice shelf upstream and accelerated drainage down Foundation Ice Stream and the ice stream to the west. If this process is already under way, it could respond rapidly to climatic warming. However, its effect would probably be less pronounced than, for example, removal of Crary Ice Rise, because the neighboring inland ice rests on more highly elevated bedrock (Figure 22.1).

A MODEL RELATING ENHANCED ICE DISCHARGE TO INCREASED RATES OF ICE-SHELF MELTING AND CALVING

In order to formulate a model describing ice-stream discharge into an ice shelf undergoing increased rates of melting and calving, I shall make several simplifying assumptions and approximations. These will generally be biased to yield upper estimates of ice discharge under prescribed conditions in order to satisfy the goals of this study.

Initial assumptions are as follows:

1. The lower reaches of the ice stream affected by ice-shelf back-pressure has length L, and within this region the ice stream is parallel sided, and longitudinal strain rate $\dot{E}_{xx}$ is independent of position.
2. As ice-stream velocities increase, ice-stream length (L) and ice thickness at the grounding line remain constant.
3. As the ice stream accelerates, V_0, F_s, $\bar{B}$, and the thickness profile remain constant.

In order for those assumptions to be satisfied, as ice velocities at the grounding line increase, the entire ice stream must retreat inland maintaining a constant active length (L). In reality, L almost certainly would decrease. A more realistic analysis will require a careful study of conditions at the "inflexion line" of an ice stream--the inland limit of the active portion.

With these assumptions, the velocity at the grounding line prior to the increase in melting rate is

$$V_L = V_0 + L\dot{E}_{xx}.$$

As melting rates increase, the ice shelf weakens, σ_p decreases by $\Delta\sigma_p$, $\dot{E}_{xx}$ increases to $\dot{E}'_{xx}$, and V_L increases to

$$V'_L = V_L + \Delta V_L = V_0 + L\dot{E}'_{xx}.$$

But, from Eq. (22.1),

$$(\dot{E}'_{xx})^{1/3} = (\dot{E}_{xx})^{1/3} + \Delta\sigma_p/2\bar{B},$$

so

$$\left(\frac{V'_L - V_0}{L}\right)^{1/3} = \left(\frac{V_L - V_0}{L}\right)^{1/3} + \Delta\sigma_p/2\bar{B}. \qquad (22.4)$$

To proceed further, we make this additional assumption:

4. At any time t, σ_p is proportional to the average thickness of the ice shelf and to its seaward extent.

Then at the seaward end (f) of the active ice-stream zone [using Eqs. (22.2) and (22.3)]

$$\sigma_p = k \int_L^f H dx$$

and

$$\sigma_p = \frac{\rho_i g H}{2}(1 - \rho_i/\rho_w) - 2\bar{B}\left(\frac{V_L - V_0}{L}\right)^{1/3}, \qquad (22.5)$$

and the decrease in backpressure ($\Delta\sigma_p$) associated with a decrease (ΔH) in ice-shelf thickness is

$$\Delta\sigma_p = k\Delta\int_L^f H dx,$$

which, using Eq. (22.5), becomes

$$\Delta\sigma_p = \frac{\Delta\int_L^f H dx}{\int_L^f H dx}\left[\frac{\rho_i g H_L(1 - \rho_i/\rho_w)}{2} - 2\bar{B}\left(\frac{V_L - V_0}{L}\right)^{1/3}\right]. \qquad (22.6)$$

and, from Eq. (22.4)

$$\Delta\sigma_p = 2\bar{B}\left[\left(\frac{V'_L - V_o}{L}\right)^{1/3} - \left(\frac{V_L - V_0}{L}\right)^{1/3}\right]. \qquad (22.7)$$

Given expressions for the two integrals in Eq. (22.6), we can solve these equations for V_L. The integral of Hdx between L and f can readily be calculated from the present-day thickness profile of the ice shelf; evaluation of the change in the integral is more difficult. In principle, numerical techniques could be used to take account of changes in melting rates and ice-shelf velocities and creep rates—all changing with both x and t. However, in our present state of ignorance concerning future behavior of these parameters, such an approach might be considered an example of overkill. Instead, I shall retain simplicity by making these additional assumptions:

5. Increase in melting rate ($\Delta\dot{M}$) is independent of x, but changes with time.
6. Although ice-shelf velocity changes with time, the longitudinal velocity gradient is not time dependent.
7. Time-dependent changes in the ice-shelf thickness profile are caused by increases in melting and calving rates modulated by increases in ice velocity.
8. Thickness profiles of present-day ice shelves are in equilibrium with prevailing tributary glacier discharge rates, accumulation rates, creep rates, and basal-melting rates.

We can now express the change in the ice-thickness integral in terms of the increase in melting rates ($\Delta\dot{M}$) and enhanced calving that causes the ice-shelf seaward front to retreat from x = f to x = f',

$$\Delta\int_L^f Hdx = \int_L^{f'} \Delta H dx + \int_{f'}^{f} Hdx. \tag{22.8}$$

The final integral in Eq. (22.8) represents the additional amount of ice removed by enhanced calving. To evaluate the other term on the right-hand side of Eq. (22.8), let basal-melting rates start to increase at t = 0. Then, at t less than the time (t_c) taken for ice that was at the grounding line at t = 0 to reach the ice front,

$$\int_L^{f'} Hdx \sim (D' - d')\int_0^t \Delta\dot{M}dt + \frac{d'}{2}\int_0^t \Delta\dot{M}dt = (D' - d'/2)\int_0^t \Delta\dot{M}dt, \tag{22.9}$$

where D' = f' - L' and d' is the distance moved during time t by ice that was at the grounding line at t = 0. Here, I shall make the approximation

$$d' \sim \int_0^t V_L dt \sim \left(\frac{V_L - V_L'}{2}\right) t, \tag{22.10}$$

which provides a lower bound for d', consistent with our goal of estimating upper limits for increased ice discharge.

At $t \geq t_c$,

$$\int_{L}^{f'} H dx \sim 0.5\, D' \int_{t'_c}^{t} \dot{\Delta M} dt, \qquad (22.11)$$

where t'_c is the time taken for ice to travel from the grounding line in order to reach the ice front at time t.

Finally, t_c can be approximated as

$$t_c \sim 4D'/(V_L + V'_L + V_f + V'_f). \qquad (22.12)$$

For a given ice-stream/ice-shelf system undergoing a prescribed sequence of enhanced melting and/or calving we can now solve Eqs. (22.6) and (22.7) to give V'_L at time t using Eqs. (22.8), (22.9), and (22.10), or Eqs. (22.8) and (22.11), depending on the value of t. I shall apply these equations to ice-stream B flowing into the Ross Ice Shelf, but first we must prescribe scenarios of melting and calving that provide upper bounds for conditions over the next 100 years.

INCREASED MELTING AND CALVING ASSOCIATED WITH CLIMATIC WARMING

GISS simulations currently under way should improve our assessment of Antarctic surface melting in a doubled CO_2 climate. Meanwhile, I shall assume that most enhanced melting is from beneath the ice shelves. Today, basal-flux ranges from freezing of a few centimeters per year to melting of a few meters per year, depending on ocean properties, local climate, and ice-shelf thickness. The most extensively studied ice shelves are the Ross and George VI, and melting predominates beneath both of these. It probably averages a few tens of centimeters per year beneath the Ross Ice Shelf (Jacobs et al. in preparation) and between 2 and 3 m/yr beneath George VI Ice Shelf (Bishop and Walton 1981).

Melting rates appear to be controlled principally by ocean temperature beneath the ice shelves. Water passing beneath the Ross, the Filchner/Ronne, and probably most other ice shelves is cooled significantly during its passage across the continental shelf. In contrast, circumpolar deep water is cooled only slightly before reaching George VI Ice Shelf (Jacobs et al. 1985). Further research is urgently required to explain these markedly different ocean behaviors. Meanwhile, I shall consider two basal-melting scenarios that might be associated with climatic warming.

For the purposes of this study I assume that a doubled CO_2 climate will be achieved by the year 2050. This is at the fast-response end of current estimates, but it is in keeping with out goal of providing upper limits for possible sea-level rise during the next century. I also assume that in the year 2000, basal melting rates start to increase linearly to reach a maximum value ($\dot{\Delta M}_{max}$) in 2050. Thereafter, they remain constant.

In the first scenario, ocean water continues to cool significantly before passing beneath the ice shelves and $\dot{\Delta M}_{max}$ = 1 m/yr. This is an upper bound consistent with A. Gordon's (Columbia University, personal communication, 1984) estimated ocean warming around Antarctica

following a CO_2 doubling and MacAyeal's (1984) analysis of the dependence of basal melting on ocean temperature.

In the second scenario, I assume that circumpolar deep water is able to reach the ice shelves without major cooling, permitting melting rates to increase to values similar to those beneath George VI Ice Shelf. For this situation, I set $\Delta\dot{M}_{max}$ = 3 m/yr. The two melting scenarios are illustrated in Figure 22.4A.

Surface melting on the ice shelves may also increase significantly. However, much of the meltwater will initially be refrozen at depth in the porous firn. Later it will flow into surface crevasses, overdeepening them and thus weakening the ice shelf in readiness for premature calving. Consequently, I shall consider two contrasting calving scenarios. In the first, calving exactly balances increased forward motion to keep the seaward ice fronts in the positions that they occupy today. In the second, there are major calving events in the 2050s that cause the ice fronts to retreats to a line linking neighboring areas of grounded ice.

In principle, we could apply the model formulated earlier to the various combinations of these calving and melting scenarios and estimate increased discharge rates from all the major Antarctic glaciers. I have chosen not to do this, partly because of time constraints imposed by the publication schedule of this report, but mainly because we lack sufficient data from most of the glaciers to solve the relevant equations. Instead, I shall apply the model to Ice Stream B flowing from West Antarctica into the Ross Ice Shelf (Figures 22.1 and 22.3). Currently, the flow of this ice stream is strongly regulated by the Ross Ice Shelf, particularly by the presence of Crary Ice Rise within the ice shelf. Consequently, Ice Stream B is likely to respond sensitively to weakening of the ice shelf. Finally, I shall assume that ice discharge from the entire ice sheet will respond in the same way. The resulting estimates of total ice discharge should represent reasonable upper limits from which to calculate maximum probable sea-level rise due to accelerated flow of the Antarctic ice sheet.

RESULTS

I shall consider four combinations of basal melting and calving:

Case 1: $\Delta\dot{M}$ increasing from zero in 2000 to $\Delta\dot{M}_{max}$ = 1 m/yr in 2050 and remaining constant thereafter. Seaward ice fronts remain at present-day positions.

Case 2: Same as Case 1, but with ice fronts calving back to a line linking adjacent areas of grounded ice in the 2050s.

Case 3: Same as Case 1, but with $\Delta\dot{M}_{max}$ = 3 m/yr.

Case 4: Same as Case 2, but with $\Delta\dot{M}_{max}$ = 3 m/yr.

Model A

For the first model, increased ice discharge equals enhanced melting from the total area (A) of Antarctic ice shelves. The corresponding

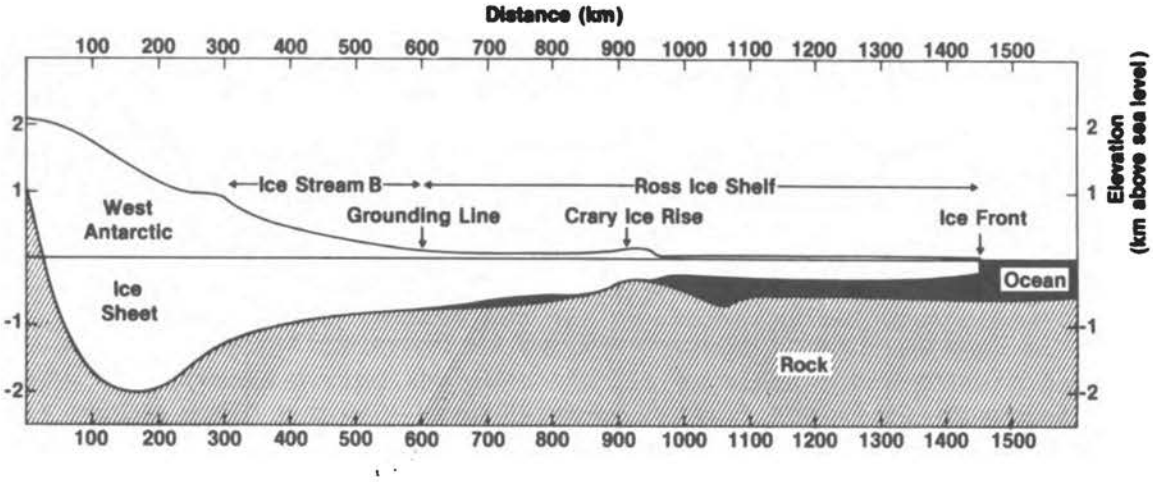

FIGURE 22.3 Ice Stream B, flowing from West Antarctica into the Ross Ice Shelf (see Figure 22.1).

rise in sea level t years after the year 2000 is defined by the scenario

$$\Delta S = \frac{A}{A_0} \Delta \dot{M}_{max}(R + Q), \qquad (22.13)$$

where A_0 = total area of the global oceans, $R = t^2/100$ yr, and $Q = 1$ for $t < 50$ years; $R = 0$ and $Q = (t - 25$ years) for $t \geq 50$ years.

Results are shown in Figure 22.4C. Note that if we assume that the increased ice discharge is sufficient to balance both increased melting and calving, and thus to prevent the ice-shelf thinning, sea-level rise would be approximately double the values shown in Figure 22.4C.

Model B

For Ice Stream B, measurements indicate that $V_L \sim 600$ m/yr, $H_L \sim 900$ m, $D \gtrsim 850$ km, $D' \sim 350$ km, $B \sim 5$ bars $yr^{1/3}$, $\int_L^t Hdx \sim 4 \times 10^8$ m^2, and $\int_t^{t'} Hdx \quad 1.7 \times 10^8$ m^2, and I assume that $V_0 \sim 100$ m/yr and $L \sim 200$ km.

With $t = 0$ at the year 2000, solution of Eqs. (22.6)-(22.10) gives the values of V_L' shown in Figure 22.4B for Cases 1 through 4 at $t = 10$, 30, 50, 55, 70, 85, and 100 years. In order to transform these results into estimates of sea-level rise, I assume that all Antarctic outlet glaciers respond to climatic warming in the same way as Ice Stream B. Further, if present-day annual ice discharge balances the average Antarctic snow accumulation of about 15 cm/yr water equivalent, it represents a layer of water over the entire ocean approximately 5 mm thick. Consequently, a doubling of the ice-discharge rate will cause a sea-level rise of approximately 5 mm/year. Sea-level rise rates can then be calculated for each estimate of velocity for Ice Stream B shown in Figure 22.4B. Integration over time of the calculated sea-level rise rates gives the increase in sea level at any prescribed time, and this is shown in Figure 22.4C.

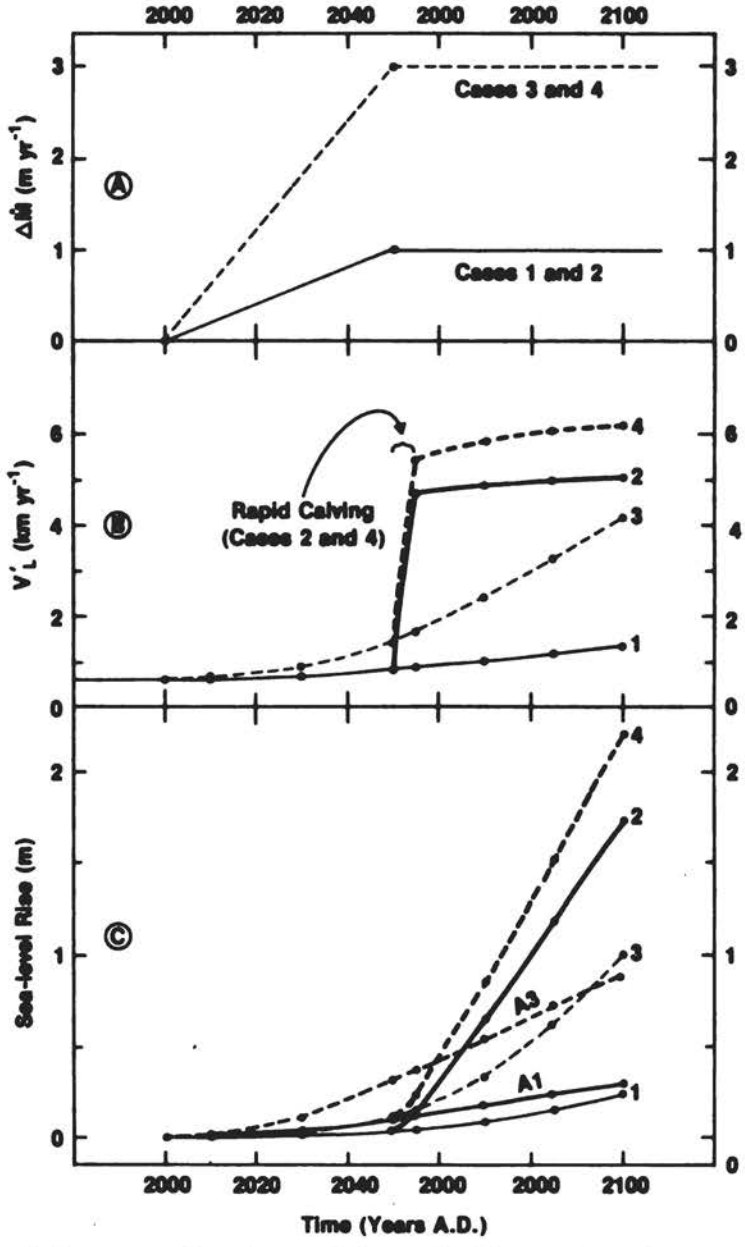

FIGURE 22.4 (A) Assumed enhanced ice-shelf basal-melt rates (ΔM) due to CO_2-induced climatic warming during the next century. In cases 1 and 3, ice-shelf seaward fronts are assumed to remain in present-day positions. In cases 2 and 4, they are assumed to calve back in the 2050s to a line joining major ice rises (e.g., Crary Ice Rise in Figure 22.3). (B) Speed (V_L') of Ice Stream B at the grounding line calculated using model B for the four different melting and calving scenarios. (C) Sea-level rise due solely to increased ice discharge assuming all Antarctic outlet glaciers respond in the same way as Ice Stream B in Figure 22.4B. Cases A1 and A3 depict sea-level rise derived using Model A in which enhanced ice discharge exactly balances increased ice-shelf melting.

DISCUSSION

The results shown in Figure 22.4C clearly reveal the sensitive response of ice-discharge rates to enhanced melting and calving from the Antarctic ice shelves. Associated estimates of total sea-level rise for Cases 1 through 4 during the next century vary by a factor of 10. Although we cannot make reliable predictions, we can indicate which of the four cases is most likely, based on current understanding. I suggest that present glaciological and oceanographic consensus favors $\Delta\dot{M}_{max} \sim 1$ m/yr as representing the maximum enhanced melting during the next century. This would be unlikely to cause major retreat of the seaward ice fronts during the next 100 years, since total melting during this period would not cause excessive thinning. Therefore, based on existing knowledge, I believe that Case 1 is most likely with a total associated sea-level rise during the next century of 24 cm. Assumptions made in deriving all the estimates were biased toward providing upper limits for each prescribed scenario. Consequently, ice-front retreat that does occur, particularly on the fringing ice shelves of East Antarctica, is unlikely to cause increased ice discharge sufficient to raise the Case 1 estimate of sea-level rise much above 24 cm.

It is important to stress that much remains to be learned about ocean behavior near Antarctica. We cannot rule out the possibility that a climatic change of the magnitude predicted for CO_2 doubling could radically alter ocean circulation. In particular, if circumpolar deep water is able to reach the major ice shelves without suffering major cooling, then $\Delta\dot{M}_{max}$ could rise toward the 3 m/yr of Cases 3 and 4. If this were to occur, the ice shelves could thin enough to be vulnerable to massively enhanced calving. This would probably occur later than the 2050 assumed here, suggesting that probable associated sea-level rise would be closer to the 1 m of Case 3 than the 2.2 m of Case 4. Clearly, we need to learn more about ocean behavior near Antarctica.

The model used to calculate enhanced ice discharge is based on the simple premise that the stress field in the lower reaches of tributary glaciers is affected by the presence of an ice shelf. Controversy arises over prescribing the distance (L) over which the glacier "feels" the ice shelf. Here, I have set L = 200 km, consistent with the size of the "ice-shelf-like" lower reaches of West Antarctic ice streams flowing into the Ross Ice Shelf. For some ice streams, L may be larger, but for most, it is probably less than 200 km. Moreover, if ice-stream grounding lines retreat during ice-sheet thinning, L probably decreases with time. This is unlikely to have a large effect on results presented here--covering the period up to 2100--but extrapolation beyond this date would require incorporation of a time-dependent L in the model.

Meanwhile, we should be aware of how sensitive the present results are to the assumed value of L. Table 22.1 shows total sea-level rise for Cases 1 through 4 for values of L = 100, 200, and 300 km. For L = 100 km, the value of V_0 is probably greater than 100 m/yr, and Table 22.1 includes a set of results with V_0 = 300 m/yr. It can be seen that results are strongly dependent on L but only weakly dependent on V_0--as might be expected from the equations used in the model. For the major Antarctic ice streams, L probably lies between 100 and 200 km,

TABLE 22.1 Sea-Level Rise during the Next Century Calculated Using Model B with Different Assumed Values of L and V_0 and Different Scenarios for Enhanced Melting and Calving

$\Delta\dot{M}_{max}$	Enhanced Calving	L (km)	V_0 (m/yr)	Total Rise (cm) by the Year 2100
1	No	100	300	13
1	Yes	100	300	92
3	No	100	300	55
3	Yes	100	300	121
1	No	100	100	16
1	Yes	100	100	100
3	No	100	100	62
3	Yes	100	100	130
1	No	200	100	24
1	Yes	200	100	174
3	No	200	100	100
3	Yes	200	100	220
1	No	300	100	30
1	Yes	300	100	239
3	No	300	100	130
3	Yes	300	100	295

which reduces the Case 1 and 3 estimates of sea-level rise to about 0.2 m and 0.8 m, respectively. Our present understanding of ocean/ice interactions leads me to favor the lower estimate, and even this could be too high, since the assumed value of $\Delta\dot{M}_{max}$ = 1 m/yr may not be realized beneath the interior regions of the Ross and Filchner/Ronne Ice Shelves.

RECOMMENDATIONS FOR FUTURE RESEARCH

There are several areas of research that would help to improve our ability to predict ice-sheet response to future climate. Here, I shall list only those that, I believe, are likely to provide major improvements.

- GCM simulations in the polar regions that include effects due to sea ice, the ocean, albedo, and ice-sheet topography. In particular, we need better estimates of accumulation, surface metling, and air temperature.
- Ocean circulation in polar regions. We need a better understanding of present conditions, particularly around Antarctica. In particular, differences between processes operating in the Bellingshausen compared with those in the Weddell and Ross Seas should be investigated.
- Basal melting and iceberg calving from ice shelves. This requires measurement of basal-melting rates and ocean characteristics via ice-shelf drill holes. First requirements for calving studies are recon-

naissance surveys to monitor iceberg calving and to identify ice-shelf characteristics where calving occurs.

- Field studies on ice streams to examine (a) the stress and velocity distribution upstream of the grounding line; (b) the regions of intense shear at the sides of the glacier; (c) the "inflexion-line" region where the glacier starts to accelerate into a "fast" mode; and (d) zones of intense convergence, such as on the Byrd and Pine Island glaciers. This work should be attempted on several glaciers with contrasting characteristics. Some of this work has already been started--on the Byrd, Rutford, and Jacobshavn glaciers and on the adjacent, but very different, Ice Streams B and C entering the Ross Ice Shelf. In addition, analysis of the remarkable data set from Columbia Glacier will cast light on some of these problems.
- Field studies on surging glaciers to investigate the transition from "slow" to "fast" glacier motion. The extensive sets of measurements on Varigated Glacier, which has recently surged, will prove particularly valuable.
- Reconnaissance work on poorly surveyed coastal regions of Antarctica. In particular, we need surveys of ice-margin position, surface elevation, ice thickness, and ice velocity to identify potentially vulnerable ice streams and measure basic characteristics of fringing ice shelves and their ice rises.
- More detailed work on Crary Ice Rise in the Ross Ice Shelf, and Henry Ice Rise in the Ronne Ice Shelf.
- Finally, we need to establish an ice-sheet monitoring program. Prime requirements are repeated measurements of (a) surface elevation, (b) ice-margin position, (c) melt zones on the ice sheet, (d) surface temperature, and (e) imagery (visible and/or synthetic aperture radar) of coastal regions and the major outlet glaciers.
- Over the surrounding ocean, sea-ice cover and iceberg populations should be measured routinely.

All of this monitoring program can be achieved from satellites; parts of it are already under way. During the next decade, satellites carrying all the relevant sensors will fly, primarily for purposes other than polar monitoring. There is an urgent need for a strong advocacy to ensure that these satellites will be used effectively over the polar regions and that acquired data are processed to a form that is useful for polar research. The various space agencies that will acquire the data generally do not have a vested interest in satisfying peripheral research applications. Consequently, a clear case must be made to the space agencies to justify acquisition and processing of the data and to the research agencies to justify funding of research using satellite data.

SUMMARY

If global climate becomes significantly warmer during the next century, sea level will be affected, to some extent, by increased ice discharge from Antarctica and Greenland. The major contribution will pro-

bably be from Antarctica, where most outlet glaciers flow into floating ice shelves that have a strong influence on glacier dynamics. Removal, or weakening, of the ice shelves would permit increased ice discharge.

A simple model relating enhanced ice drainage to ice-shelf melting rate during the next century provides estimates of associated global sea-level rise for several combinations of increased melting and iceberg calving. Our present understanding suggests that, during the next century, the increase in ice-shelf melting is unlikely to exceed 1 m/yr, and ice-shelf seaward fronts will probably remain in approximatley their present-day positions.

If this is correct, the model indicates that sea-level rise due to increased ice discharge from Antarctica will be approximately 0.2 m by the year 2100. However, climate-induced changes in ocean circulation may induce considerably greater melting--perhaps 2 or 3 m/yr greater than today. Under these conditions, ice discharge could increase sufficiently to raise sea level by as much as 0.8 m by the year 2100.

REFERENCES

Behrendt, J. C., 1962. Geophysical and glaciological studies in the Filchner Ice Shelf area of Antarctica. Journal of Geophysical Research, 67, 221-234.

Bishop, J. R., and J. L. Walton, 1981. Bottom melting under George VI Ice Shelf, Antarctica. Journal of Glaciology, 27, 429-447.

Jacobs, S. S., R. G. Fairbanks, and Y. Horibe, 1985. Origin and evolution of water masses near the Antarctic continental margin: Evidence from $H_2{}^{18}O/H_2{}^{16}O$ ratios. In Oceanology of the Antarctic Continental Shelf, Antarctic Research Series, vol. 43, American Geophysical Union, Washington, D.C., in press.

MacAyeal, D. R., 1984. Thermohaline circulation below the Ross Ice Shelf: A consequence of tidally induced vertical mixing and basal melting. Journal of Geophysical Research, 89, 597-606.

Thomas, R. H., 1973. The creep of ice shelves: Theory. Journal of Glaciology, 3, 45-53.

Weertman, J., 1957. Deformation of floating ice shelves. Journal of Glaciology, 3, 38-42.

ATTACHMENT 23

A MODEL OF A POLAR ICE STREAM, AND FUTURE SEA-LEVEL RISE DUE TO POSSIBLE DRASTIC RETREAT OF THE WEST ANTARCTIC ICE SHEET

Craig S. Lingle
University of Colorado

INTRODUCTION

Numerical modeling experiments simulating the response of an ice stream in the Ross Sea sector of West Antarctica to changes in the Ross Ice Shelf and in the accumulation rate have been described by Lingle (1984). The model ice stream was found to be more sensitive to changes in the Ross Ice Shelf than to changes in the accumulation rate. Analyses of field data obtained during the Ross Ice Shelf Glaciological and Geophysical Survey (RIGGS) (Thomas and Bentley 1978a; Greischar and Bentley 1980; Thomas and MacAyeal 1982; Jezek and Bentley 1985) and numerical modeling experiments of ocean circulation below the Ross Ice Shelf (MacAyeal 1984) permit a judgment to be made as to which of the scenarios modeled by Lingle (1984) are most probable. In this paper a brief review of field results from RIGGS is given. The analyses based on field measurements are interpreted in terms of the probable future behavior of the West Antarctic ice sheet upglacier (northeast) from Roosevelt Island (Figure 23.1). This interpretation is based on an assumption that climatic warming caused by increasing carbon dioxide in the atmosphere will not significantly alter the state of the Ross Ice Shelf as measured during RIGGS. Modeling results indicating the possibility of grounding-line retreat in the event that climatic warming causes increased basal melting below the Ross Ice Shelf are also described. A minimum time is suggested for drastic retreat of the West Antarctic ice sheet in the event that warming is sufficient to cause extreme thinning of the ice shelf. An estimate for the corresponding rate of sea-level rise is given.

FUTURE CHANGES IN THE ROSS ICE SHELF

In a flow on the Ross Ice Shelf that included discharge from ice stream E (Figure 23.1) Thomas and Bentley (1978a) concluded that the ice shelf is thickening at a rate of 0.15 $\pm$ 0.06 m/yr of ice minus the basal melt rate, which was unknown. Thomas and MacAyeal (1982) found that the basal melt rate is approximately 0.7 m/yr near the ice shelf front, decreasing to roughly $\pm$ 0.1 m/yr 100 km upglacier. Combining this with the result of Thomas and Bentley (1978a) gives a net thicken-

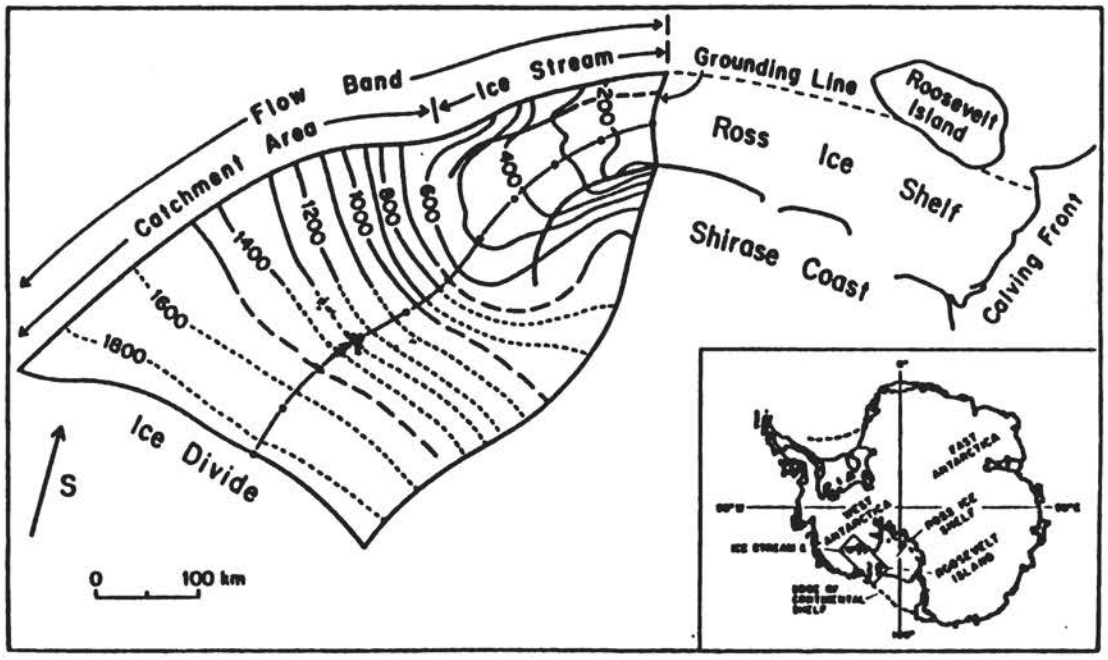

FIGURE 23.1 Ice Stream E and catchment area, West Antarctica. Insert shows location. Solid elevation contours, upper boundary of flow band, boundaries defining ice stream and location of grounding line are from Rose (1979). Contours consisting of long dashes at 1000 and 1500 m are from the American Geographical Society map of Antarctica. Contours consisting of short dashes are extrapolated from Rose (1979) and also estimated from Drewry et al. (1982). Dashed contours are less accurate than solid contours. Backpressure at the grounding line of the ice stream (discussed in text) is caused by shear stress acting between the Ross Ice Shelf and the NE side of Roosevelt Island and also between the Ross Ice Shelf and Shirase Coast.

ing rate of 0.15 $\pm$ 0.16 m/yr for the Roosevelt Island sector of the Ross Ice Shelf. This implies that the ice shelf is either in equilibrium or that it will thicken by about 10 percent in 160 to 330 years (since the average thickness of the ice shelf in this area is roughtly 500 m).

Greischar and Bentley (1980) found that continuing uplift of the seafloor in the future should cause a substantial area of the eastern Ross Ice Shelf (which adjoins West Antarctica) to ground, because the subglacial water layer is relatively thin on the eastern side of the ice shelf. Advance of the grounding line would not continue indefinitely, however, because the subglacial water depth increases substantially toward the west. Northeast of Roosevelt Island where Ice Stream E discharges into the Ross Ice Shelf (Figure 23.1), Greischar and Bentley (1980) predicted a maximum grounding-line advance of about 100 km on a time scale of several thousand years owing to continuing uplift of the seafloor.

Thomas and MacAyeal (1982) found that the ice shelf has been approximately in steady state for the past 1500 to 2500 years, upglacier from

five widely spaced drill holes. (The drill hole at Little America V was located within the flow band discharging Ice Stream E.) They emphasized, however, that this conclusion could not necessarily be applied to the entire ice shelf.

Jezek and Bentley (1985) recalculated the mass balance of a flow band in the southeastern sector of the ice shelf, which Thomas and Bentley (1978a) found to be thickening at 0.34 $\pm$ 0.15 m/yr plus the rate of basal freezing. After taking a previously unsuspected ice rise into account and using indirect methods to estimate the maximum of basal freezing, they found that the flow band is approximately in equilibrium. Citing a comparison between flow lines indentified from radar returns and flow lines mapped from surface velocity measurements (Jezek 1980) and geological evidence from the Trans-Antarctic Mountains (Mercer 1968a), Jezek and Bentley (1985) suggested that the ice shelf thinned somewhat between 1000 and a few hundred years ago, then stabilized, and that in the future thickening will occur owing to an apparent positive mass balance over the Ross Sea sector of the inland West Antarctic ice sheet.

MacAyeal (1984) found that the bottom melt/freeze regime below the Ross Ice Shelf is stabilized by the formation of cold, high-salinity shelf water beneath the large area of sea ice that forms seaward of calving front of the Ross Ice Shelf each winter. The basal melting regime was found to be impervious to the effects of climatic warming, unless warming is sufficient to eliminate the production of cold, high-salinity shelf water. MacAyeal (1984) suggested that this could conceivably happen if climatic warming caused by increasing CO_2 in the atmosphere is of sufficient magnitude to eliminate the growth of winter sea ice in the Ross Sea.

PROBABLE FUTURE CHANGES IN THE INLAND ICE SHEET NORTHEAST OF ROOSEVELT ISLAND

The data analyses summarized above indicate that the Ross Ice Shelf is either in equilibrium or thickening slowly in the Roosevelt Island sector (Figure 23.1), as well as in other sectors. Modeling results from Lingle (1984) corresponding to a state of dynamic equilibrium between Ice Stream E and the Ross Ice Shelf are shown in Figure 23.2. The position of the ice-shelf front was held stationary. This case was judged a close approximation to reality, because the backpressure required to hold the model grounding line in dynamic equilibrium was found to be within 8 percent of backpressure mapped from surface strain-rate data near the grounding line of Ice Stream E by Thomas and MacAyeal (1982). Backpressure is caused by shear stress along the sides of a confined ice shelf and by pinning points where the bottom of the ice shelf is in contact with the seafloor. It is the difference between the theoretical driving stress that would cause the ice shelf to spread if it were unconfined and unpinned (Weertman 1957) and the real driving stress causing the confined ice shelf to spread. It is thought to play an important role in the stabilization of ice streams grounded below sea level and in the dynamics of ice shelves (e.g., Budd 1969; Thomas 1973,

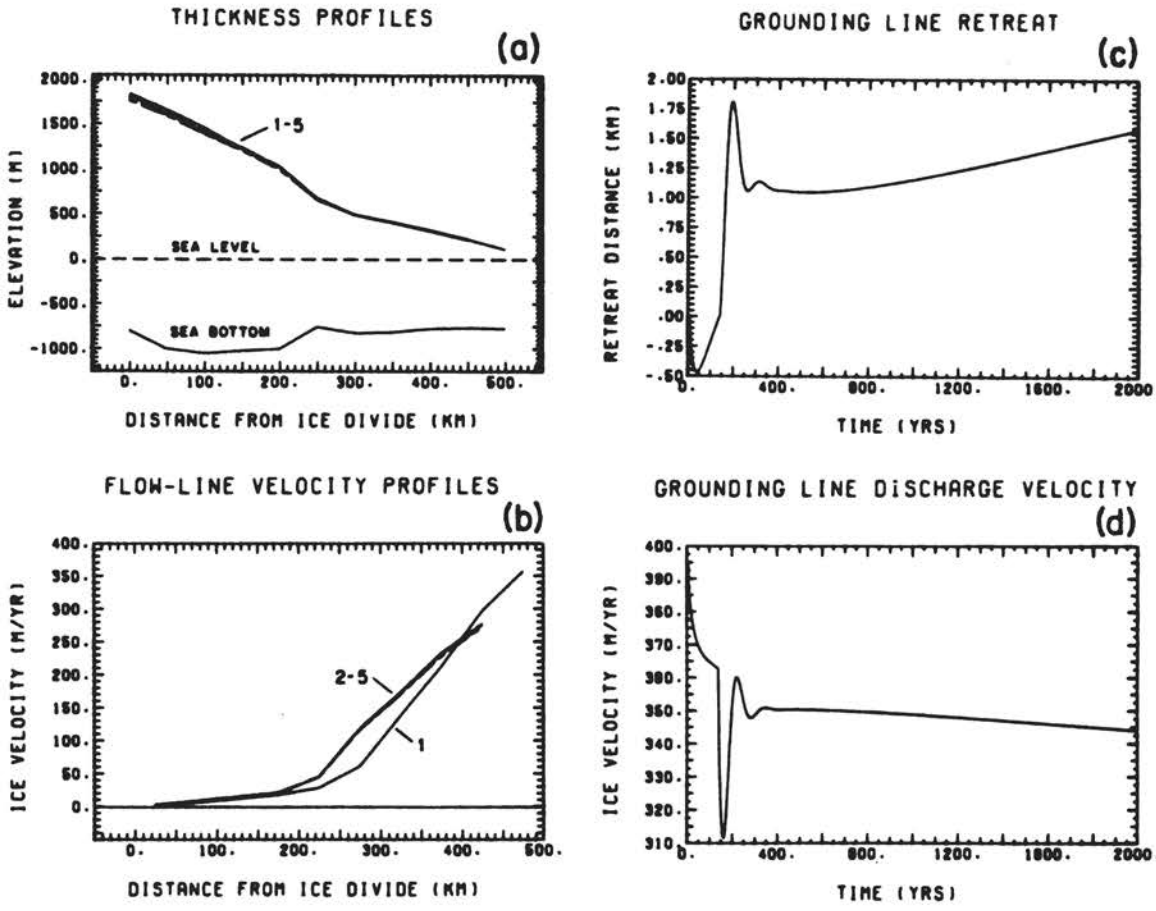

FIGURE 23.2 Model applied to ice stream with equilibrium backpressure at grounding line at start of run. Flow band remained in approximate mass balance, with only minor thinning discernible on the upper flow band [(a) and (b)]. Grounding line maintained a state of dynamic balance, remaining within 2 km of its present position throughout the 2000-year test period (c). Profiles 1-5 are 0, 500, 1000, 1500, and 2000 years, respectively. In all model runs shown in Figure 23.2 and through 23.5, the position of the calving front of the ice shelf was constant.

1977, 1979; Thomas and Bentley 1978b; Sanderson 1979; Stuiver et al. 1981; Thomas and MacAyeal 1982). Figure 23.2 show that almost no change can be expected in the thickness profile along the central flow line of Ice Stream E, if backpressure from the ice shelf remains constant and if the ice stream and its catchment area are approximately in mass balance. Backpressure can be expected to remain constant if the geometry of the ice shelf does not change and if sea depth below the ice shelf does not decrease.

Ice stream E and its catchment area were found to be approximately in mass balance by Rose (1979) and Lingle (1984). Using older data, Hughes (1973) also calculated a balance discharge velocity near the

grounding line that is within 8 percent of the nearest measured velocity on the Ross Ice Shelf (Thomas and MacAyeal 1982). Accumlation data over the entire Ross Sea sector of the inland West Antarctic ice sheet are very sparse, however, and detailed field measurements of ice discharge velocity have not yet been made. Thus, the conclusion that Ice Stream E is approximately in mass balance must be regarded as preliminary.

Figure 23.3 shows modeling results computed with backpressure from the Ross Ice Shelf increased initially by 10 percent, from the equilibrium backpressure used to compute the results shown in Figure. The position of the ice-shelf front was held stationary. This case is equivalent to an instantaneous 10 percent increase in the average thickness of the model ice shelf. For the real ice shelf, this would be equivalent to an increased shear resistance along the sides of a thicker ice shelf combined, perhaps, with increased pinning caused by an isostatically rising seabed. The 160- to 330-year time delay estimated above for a 10 percent increase in the thickness of the Ross Sea Shelf is not taken into account, so Figure 23.3 should be viewed as the most rapid possible response to a 10 percent increase in backpressure.

Figure 23.3(c) shows that a 35-km advance of the grounding line occurred during 2000 model years, with about 19 km of advance occurring during the first 100 years. Subsequently the rate of advance decreased because the ice-shelf front was constrained to remain stationary. This caused the ice shelf to grow progressively shorter, and backpressure at the grounding line was correspondingly decreased. The grounding line thus restablized at an advanced position. Figure 23.3(a) shows that slight thickening on the lower and central flow band occurred.

Simulations of the response of Ice Stream E to a doubling of accumulation rates were also described by Lingle (1984). (Increased accumulation rates might occur if air temperatures become warmer over West Antarctica.) When the ice-shelf front was constrained to remain stationary a 5-km advance of the grounding line occurred during the first 100 years, followed by an eventual 36-km advance after 4000 model years. When the ice-shelf front was constrained to advance at the same rate as the grounding line a-13 km advance occurred during the first 100 years, followed by an eventual 100-km advance after 2000 model years. Thickening of the ice stream and its catchment area occurred in both cases, but thickening was greater when the ice-shelf front advanced at the same rate as the grounding line. Present accumulation rates over the Ross Sea sector of the inland West Antarctic ice sheet are poorly known, however, and the potential effect of increasing CO_2 in the atmosphere is even more poorly known. Thus, the model scenarios corresponding to increased accumulation rates must be considered more speculative. These results are not shown here.

POSSIBLE GROUNDING-LINE RETREAT DUE TO FUTURE THINNING OF ROSS ICE SHELF

If increasing CO_2 in the atmosphere causes substantial warming in the polar regions, recent field measurements may not be indicative of future changes in the Ross Ice Shelf. For instances, MacAyeal (1984) suggested that if air and sea-surface temperatures warm sufficiently to

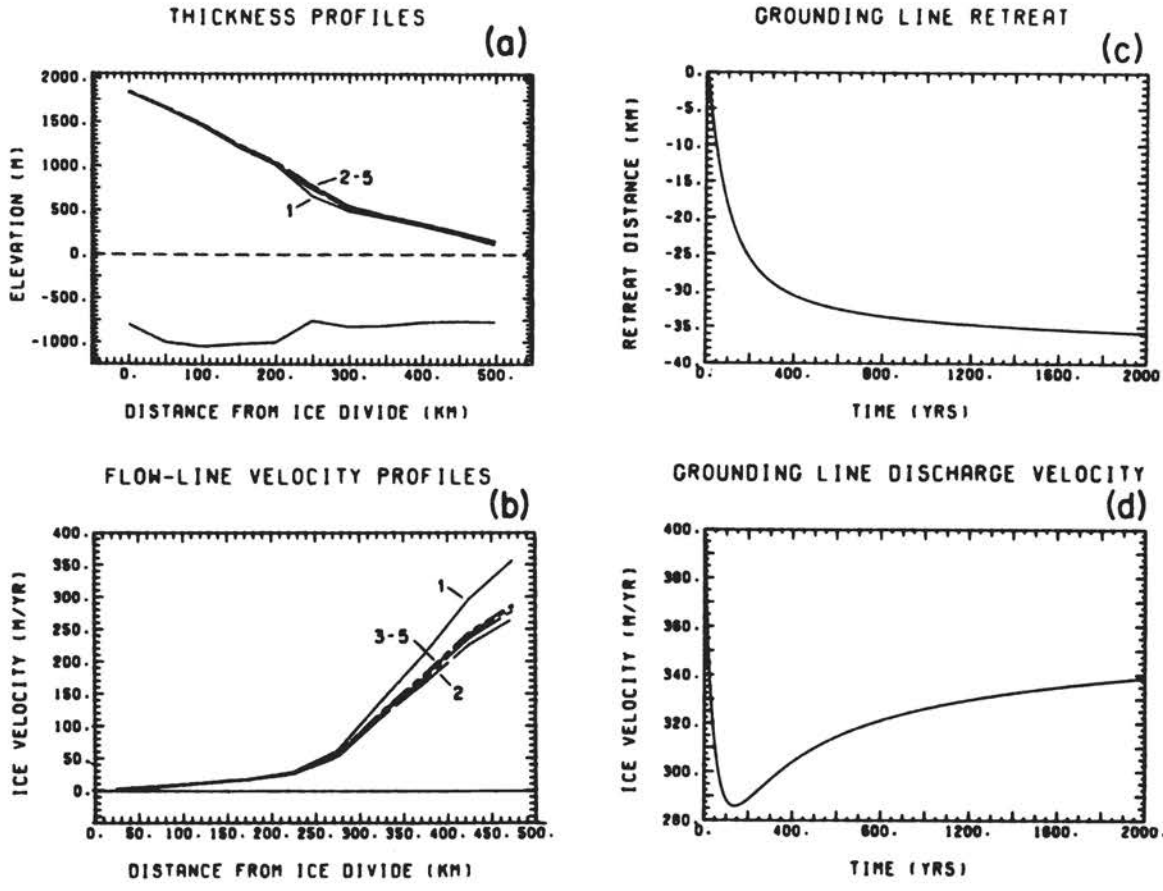

FIGURE 23.3 Model applied to ice stream with backpressure at grounding line increased by 10 percent from equilibrium value at start of run. The grounding line advanced by 36 km during the 2000-year test period, and slight thickening of the flow band occurred. Profiles 1-5 are 0, 500, 1000, 1500, and 2000 years, respectively.

suppress the growth of winter sea ice north of the calving front of the Ross Ice Shelf, cold, high-salinity shelf water (which now forms below the sea ice) would no longer buffer the ice shelf against increases in the bottom melt rate. The ice shelf would then become thinner. This, in turn, would probably cause backpressure to decrease (that is, the ice-shelf buttressing effect would probably decrease) at ice-stream grounding lines. Grounding lines could then be expected to retreat.

Figure 23.4 shows a 2000-year model run with backpressure at the grounding line decreased by 10 percent from the equilibrium backpressure used to compute the results shown in Figure 23.2. This is equivalent to instantaneously decreasing the average thickness of the equilibrium ice shelf by 10 percent at the start of the model run. The position of the ice shelf front was held stationary. Thinning of the flow [Figure 23.4(a)] was accompanied by a substantial increase in the velocity profile after 500 years [Figure 23.4(b)] during rapid retreat of the

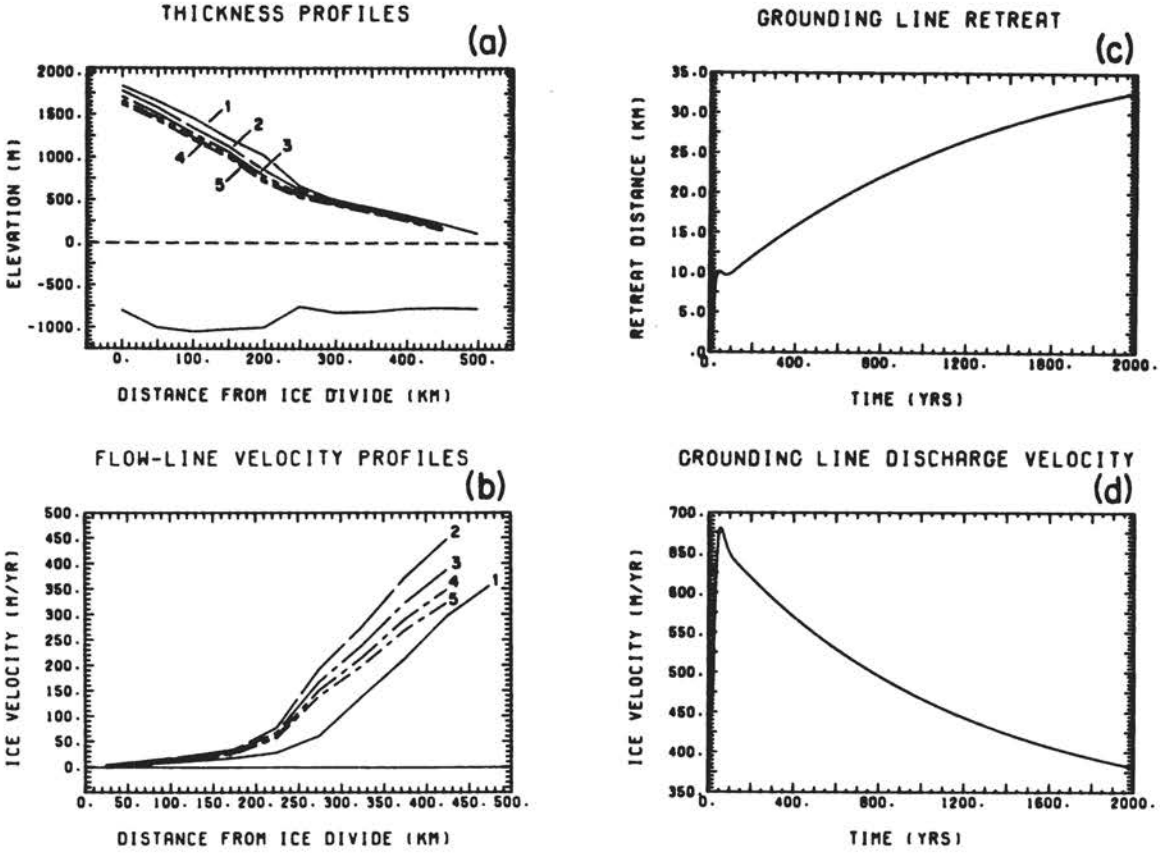

FIGURE 23.4. Model applied to ice stream with backpressure at grounding line decreased by 10 percent from equilibrium backpressure at start of run. This is equivalent to decreasing the mean ice-shelf thickness by 10 percent from the mean thickness during the equilibrium run shown in Figure 23.2. (a) Significant thinning of the flow band occurred, (b) the velocity profile increased as the retreat rate peaked, (c) the grounding-line retreated 33 km, and (d) the discharge velocity peaked at 680 m/yr during initial retreat of the grounding line. Profiles 1-5 are 0, 500, 1000, 1500, and 2000 years, respectively.

grounding line. The velocity profile then decreased, however, as the rate of grounding-line retreat decreased [Figure 23.4(c)]. The retreat rate decreased because of the greater stabilizing influence of the lengthening ice shelf. Ten kilometers of retreat occurred during the initial 100-year period. After 2000 model years the grounding line retreated 33 km and (apparently) approached a new position of equilibrium. This result, together with the model results shown in Figure 23.3, suggests that if the calving front of the Ross Ice Shelf remains stationary the grounding lines of ice streams in the Ross Sea sector may be stable with respect to small perturbations, such as changes in the average thickness of the Ross Shelf on the order of $\pm$10 percent or less.

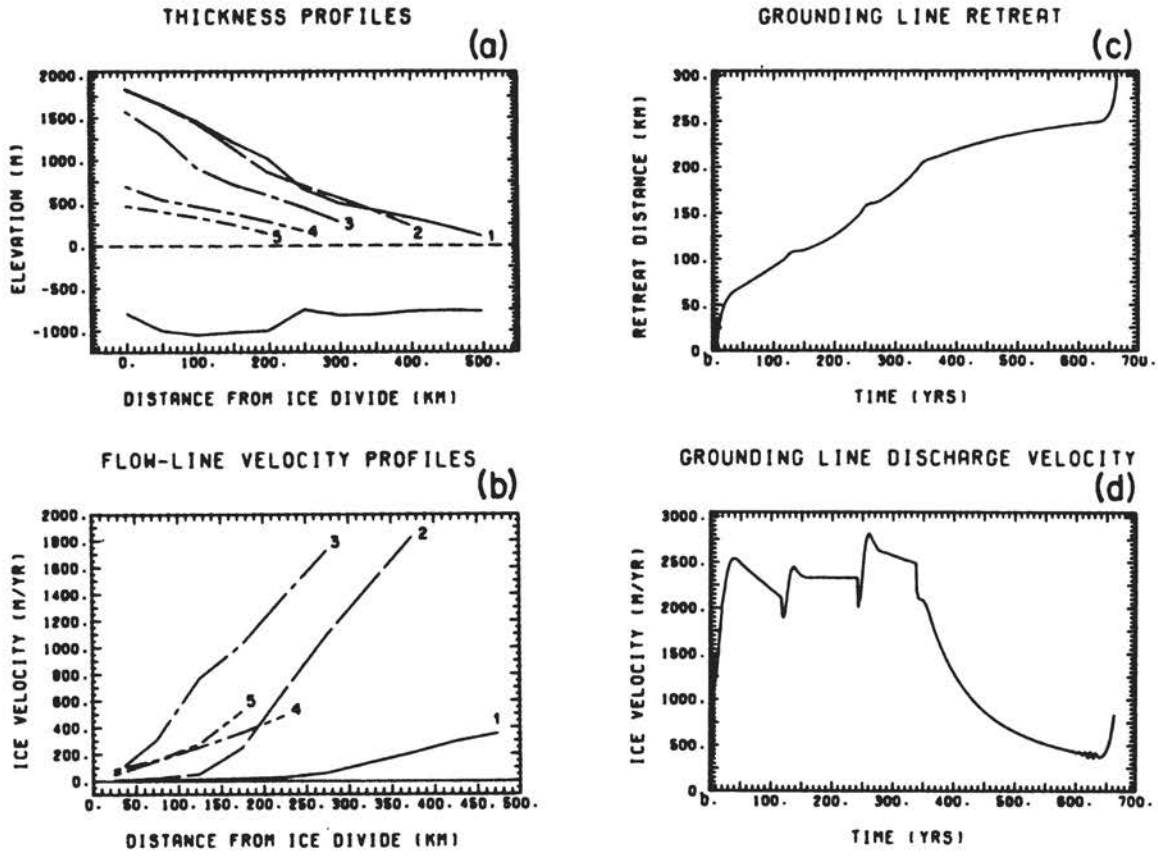

FIGURE 23.5 Model applied to ice stream with backpressure at the grounding line decreased by 50 percent (at the start of the run) from equilibrium backpressure. This is equivalent to decreasing the mean ice-shelf thickness by 50 percent from the mean thickness during the equilibrium run shown in Figure 23.2. (a) The flow band thinned rapidly, (b) the velocity profile peaked as the flow band acquired maximum surface slope, (c) rapid and sustained retreat of the grounding line occurred, and (d) the discharge velocity peaked between 0 and 350 years as ice was brought out from the interior at rates far in excess of the rate of replenishment over the catchment area. Profiles 1-5 are 0, 39, 251, 487, and 664 years, respectively.

Figure 23.5 shows a model run with backpressure at the grounding line decreased by 50 percent from the equilibrium backpressure used to compute the results shown in Figure 23.2. This is equivalent to instantaneously decreasing the average thickness of the equilibrium ice shelf by 50 percent at the start of the model run. The position of the ice-shelf front was again held stationary. Major thinning of the flow band [Figure 23.5(a)] accompanied rapid and sustained retreat of the grounding line [Figure 23.5(c)]. The velocity profile rose dramatically [Figure 23.5(b)] as surface slopes increased and ice was discharged at rates far in excess of the rate of replenishment over the catchment area. [The sharp dips in the discharge velocity curve—Figure 23.5(d)—

between 120 and 260 years were caused by retreat of the grounding line across points of the finite difference grid, and have no physical significance.] The model run was stopped after 300-km retreat, which occurred after 600 years. At that point the catchment area had disappeared, the ice-stream channel extended to the ice divide, and the flow band was considered to have collapsed.

The model results shown in Figure 23.5 indicate that ice-stream grounding lines in the Ross Sea sector should be unstable with respect to a large perturbation consisting of a 50 percent reduction in the average thickness of the Ross Ice Shelf. Qualitatively, this is in accordance with the suggestions of Mercer (1968b, 1978), Thomas et al. (1979), and Stuiver et al. (1981) that the West Antarctic ice sheet would not survive a major thinning of the Ross and Filchner-Ronne Ice Shelves.

MINIMUM TIME FOR DRASTIC RETREAT OF WEST ANTARCTIC ICE SHEET

Thomas et al. (1979) found that Ice Streams B and E in the Ross Sea sector would retreat irreversibly if the melt rate below the Ross Ice Shelf increased to one or more meters per year. They predicted that the grounding lines of Ice Streams B and E would retreat 300 km in 200 and 300 years, respectively, if the bottom melt rate increased to 1 m/yr. Their model predicted faster retreat rates for higher bottom melt rates. Hughes (1983) argued that irreversible retreat of the West Antarctic ice sheet has already begun in the Pine Island Bay sector and will proceed to completion in about 200 years.

Bentley (1983) argued that it would be physically impossible for the West Antarctic ice sheet to disintegrate in 200 years and that 500 years is a more reasonable minimum estimate. Lingle (1984) (Figure 23.5) found that the grounding line of Ice Stream E would retreat 300 km in 660 years, if the Ross Ice Shelf thinned by 50 percent instantaneously and the ice-shelf front remained stationary. Fastook (1984) found that a major retreat via the Pine Island Bay sector might take as long as 6000 years if a confined ice shelf formed during retreat. (He emphasized, however, that retreat could proceed much more rapidly if a confined ice shelf did not form.)

The variation in the above estimates is partly accounted for by differing treatments of the physics of ice-stream motion. It is also accounted for a large degree by differing assumptions about the behavior of the Ross Ice Shelf and whether an ice shelf would form during retreat of grounding lines in the Pine Island Bay Sector.

FUTURE SEA-LEVEL RISE DUE TO POSSIBLE DRASTIC RETREAT OF WEST ANTARCTIC ICE SHEET

The following worst-case scenario is based on an assumed sequence of events in the Ross Sea, where the grounding line of Ice Stream E appears close to dynamic equilibrium at present (Lingle, 1984). The possibility of present grounding-line retreat in the Pine Island Bay sector of West

Antarctica is regarded as hypothetical and is not considered here, because the field measurements necessary to substantiate this have not yet been made. The following events are assumed. (1) A doubling of CO_2 in the atmosphere will cause average air temperatures around Antarctica to increase about 5°C by 2030, as indicated by general circulation models. (2) The 5°C warming will cause the extent of winter sea ice in the Ross Sea to be reduced by about 50 percent, as modeled by Parkinson and Bindschadler (1984). (3) The 50 percent sea-ice reduction will be sufficient to permit an increased flux of circumpolar deep water across the continental shelf and into the sub-ice shelf cavity, increasing the average bottom melt rate to 1 m/yr. (This assumption is speculative.) (4) During the ensuing 70 years (2030 to 2100) the Ross Ice Shelf will thin by about 50 m or 10 percent, because the present ice shelf is close to dynamic equilibrium (Thomas and Bentley 1978a; Jezek and Bentley in press) with an average bottom melt rate of about 0.25 m/yr (Jacobs 1979). A melt rate of 1 m/yr would thus cause 0.75 m/yr of thinning if other factors (such as the rate of advection of thicker ice across grounding lines from the inland ice sheet) remain constant. (5) A relatively minor retreat of ice stream grounding lines will occur during 2030 to 2100, as shown by Figure 23.4(c). (6) After 2100, grounding lines will begin to retreat rapidly. Sustained thinning will cause the average thickness of the Ross Ice Shelf to be reduced by about 50 percent within 330 years after 2030, and thinning will continue. Retreat will proceed to completion within 660 years after 2100, i.e., by 2760, as suggested by Figure 23.5. (Note that the retreat behavior of Ice Stream E as shown in Figure 23.5 is assumed to be representative of the entire West Antarctic Ice Sheet. Note also that the position of the ice-shelf front is assumed to remain constant.)

The amount of sea-level rise likely to be caused by a 10 percent thinning of the Ross Ice Shelf between 2030 and 2100 can be estimated from the difference between profiles 1 and 2 in Figure 23.4(a). Five hundred years after the instantaneous 10 percent decrease in the average thickness of the Ross Ice Shelf at the start of the model run, the average thinning along the entire length of the central flow line was 64.5 m. The average above-sea-level ice thickness was thus 0.07. If the same fractional thinning occurred over the entire area of the West Antarctic ice sheet, and if the rate of thinning between the start of the model run and 500 years is approximated as linear, the sea-level rise after 70 years (i.e., between 2030 and 2100) would be about 50 mm.

An alternative estimate can be made by applying the method described by Thomas (this volume, Attachment 22). The entire West Antarctic ice sheet is assumed to be in mass balance, and the average accumulation rate is assumed equal to the average over the entire continent, about 0.17 m/yr (Dolgushin et al. 1962; Paterson 1981, p. 56). Both the total volume input and outflow rates, at present, are thus equal to the average accumulation rate multiplied by the 1,809,706 km^2 area (Drewry et al. 1982) of the West Antarctic ice sheet, that is, about 308 km^3/yr. The fractional increase in volume flux across the grounding line of Ice Stream E during the 70-year period after the instantaneous 10 percent thinning of the Ross Ice Shelf shown in Figure 23.4 was estimated from Figure 23.4(d). The same fractional increase was assumed to apply to

all of West Antarctica. [This assumption was judged reasonable because approximately 90 percent of the discharge flux from West Antarctica is via marine ice streams terminating in the ocean (Hughes 1972, pp. 31-32). The response of these ice streams to ice-shelf thinning may be at least roughly similiar to the response of Ice Stream E.] Application of this method yields an estimated 11,040 km^3 of excess ice discharged into the ocean (beyond what would be discharged if the West Antarctic ice sheet remained in mass balance). This is equivalent to a sea-level rise of about 30 mm by 2100.

In summary, this sequence of events would result in 0 contribution to eustatic sea-level rise from West Antarctica between the present and 2030, and a contribution of 0.4 to 0.7 mm/yr between 2030 and 2100. The total sea-level rise at 2100 would be about 30 to 50 mm. After 2100 the average contribution from West Antarctica would be 7.6 mm/yr, and the eventual sea-level rise, corresponding to disappearance of the West Antarctic ice sheet, would be approximately 5 m by 2760 (i.e., 780 years from the present).

It is reasonable to suppose that at least two negative feedback mechanisms would tend to cause grounding-line retreat to proceed more slowly than predicted by existing numerical models of polar ice streams in the event that drastic retreat of the West Antarctic ice sheet actually begins. (1) As ice-stream grounding lines retreat into thicker ice, ice should converge into ice-stream channels and toward the retreating grounding lines. The resulting transverse compressive strain rates should tend to counteract the large longitudinal extensive strain rates caused by the retreat of ground lines into deeper water. This would probably cause net vertical thinning rates and retreat rates to be less than predicted because ice-stream models do not (at present) take transverse strain rates at grounding lines into account. (2) Large discharge velocities from ice streams during rapid retreat should cause velocity gradients along the sides of the Ross Ice Shelf and around ice rises to increase. This, in turn, would cause shear to increase. The result would probably be increased backpressure at ice-stream grounding lines. This also should cause retreat to proceed more slowly than predicted, because numerical models of ice streams do not (at present) include the regulatory role of changing velocity gradients along the sides of ice shelves.

If the above negative feedback mechanisms are arbitrarily assumed to increase the time required for drastic retreat of the West Antarctic ice sheet by a factor of 2, the contribution to eustatic sea-level rise from this source would be 0 between the present and 2030, 20 to 50 mm (at 0.4 to 0.7 mm/yr) between 2030 and 2100, and about 5 m between 2100 and 3420. The average rate of rise between 2100 and 3420 would be 3.8 mm/yr. The total time required for drastic retreat in this case would be about 1400 years.

A best-case scenario, of course, would be for sufficient winter sea ice to form around Antarctica despite climatic warming to keep the Ross Ice Shelf and other ice shelves adequately buffered against increases in the bottom melt rate that might otherwise be caused by elimination of the high-salinity shelf water that now forms below the winter sea ice (MacAyeal 1984). In this case, the only contribution to eustatic

sea-level rise from West Antarctica would be runoff from surface melting, if warming is sufficient to force low-altitude areas near the ocean into the ablation zone.

It is worth noting that relative sea-level rise caused by retreat of the West Antarctic ice sheet will not be uniformly distributed over the world ocean. Clark and Lingle (1977) showed that if this ice sheet thinned instantaneously and uniformly by 1 m, the relative sea-level rise (i.e., the increase in separation between the surface and the bottom) at Hawaii, New York, and in the North Sea would be 125, 115, and 110 percent of the average global rise, respectively. After 1000 years relative sea-level rise would be 117, 107, and 103 percent of the average global rise, respectively, at these three locations. The immediate nonuniform distribution of relative sea-level change is caused by the elastic response of the Earth to the change in ice and water loading and associated distortion of the gravitational potential field. The altered distribution of sea-level change after 1000 years is caused by time-dependent flow of rock within the Earth's mantle and associated distortion of the gravitational potential field.

ACKNOWLEDGMENTS

The numerical modeling study described here was done at the Geophysical and Polar Research Center, University of Wisconsin--Madison. Support was provided by National Science Foundation Grants DPP-7920736 and DPP-8119989 to Charles R. Bentley. Preparation of this paper was supported by Department of Energy contract DE-AC02-84ER60197 to Uwe Radok at the Cooperative Institute for Research in Environmental Sciences, University of Colorado/NOAA, Boulder, Colorado.

REFERENCES

Bentley, C. R., 1983. The West Antarctic ice sheet: Diagnosis and prognosis. In Carbon Dioxide, Science and Consensus, Proceedings: Carbon Dioxide Research Conference, U.S. Department of Energy, pp. IV.3-1V.50.

Budd, W. F., 1969. The dynamics of the Amery Ice Shelf. Journal of Glaciology, 6, 335-358.

Clark, J. A., and C. S. Lingle, 1977. Future sea-level changes due to West Antarctic ice sheet fluctuations. Nature, 269-209, 1977.

Drewry, D. J., S. R. Jordan, and E. Jankowski, 1982. Measured properties of the Antarctic ice sheet: Surface configuration, ice thickness, volume and bedrock characteristics. Annals of Glaciology, 3, 83-91.

Dolgushin, L. D., S. A. Yevteyev, and V. M. Kotlyakov, 1962. Current changes in the Antarctic Ice Sheet. International Association of Scientific Hydrology Publication 58, pp. 286-294.

Fastook, J. L., 1984. West Antarctica, the sea-level controlled marine instability: Past and future. In J. E. Hansen and T. Takahashi

(eds.), Climate Processes and Climate Sensitivity, American Geophysical Union, Washington, D.C., pp. 275-287.

Greischar, L. L., and C. R. Bentley, 1980. Isostatic equilibrium grounding line between the West Antarctic inland ice sheet and the Ross Ice Shelf. Nature, 283, 651-654.

Hughes, T. J., 1972. Scientific justification, ISCAP Bull. 1, Inst. of Polar Studies, Ohio State Univ., Columbus.

Hughes, T. J., 1973. Is the West Antarctic ice sheet disintegrating? Journal of Geophysical Research, 78, 7884-7910.

Hughes, T. J., 1982. On the disintegration of ice shelves: The role of thinning. Annals of Glaciology, 3, 146-151.

Hughes, T. J., 1983. The stability of the West Antarctic ice sheet: What has happened and what will happen. In Carbon Dioxide, Science and Consensus, Proceedings: Carbon Dioxide Research Conference, U.S. Department of Energy, pp. IV.51-IV.73.

Jacobs, S. S., 1979. Circulation and melting beneath the Ross Ice Shelf, Science, 203, 439-443.

Jezek, K. C., 1980. Radar investigations of the Ross Ice Shelf, Antarctica. Ph.D. dissertation, Univ. of Wisconsin, Madison, 214 pp.

Jezek, K. C., and C. R. Bentley, 1985. A reconsideration of the mass balance of a portion of the Ross Ice Shelf, Journal of Glaciology, 30(106), 381-384.

Lingle, C. S., 1984. A numerical model of interactions between a polar ice stream and the ocean: Application to Ice Stream E, West Antarctica. Journal of Geophysical Research, 89, 3523-3549.

MacAyeal, D. R., 1984. Thermohaline circulation below the Ross Ice Shelf: A consequence of tidally induced vertical mixing and basal melting, Journal of Geophysical Research, 89(C1), 597-606.

Mercer, J. H., 1968a. Glacial geology of the Reedy Glacier area, Antarctica, Geological Society of America Bulletin, 79, 471-486.

Mercer, J. H., 1968b. Antarctic ice and Sangamon sea level, International Association of Scientific Hydrology Publication 79, pp. 217-225.

Mercer, J. H., 1978. West Antarctic ice sheet and CO_2 greenhouse effect: A threat of disaster, Nature, 271, 321-325.

Parkinson, C. L., and R. A. Bindschadler, 1984. Response of Antarctic sea ice to uniform atmospheric temperature increases. In J. E. Hansen and T. Takahashi (eds.), Climate Processes and Climate Sensitivity, American Geophysical Union, Washington, D.C., pp. 254-264.

Paterson, W. S. B., 1981. The Physics of Glaciers, Pergamon, New York.

Rose, K. E., 1979. Characteristics of ice flow in Marie Byrd Land, Antarctica. Journal of Glaciology, 24, 63-75.

Sanderson, T. J. O., 1979. Equilibrium profile of ice shelves. Journal of Glaciology, 22, 435-460.

Stuiver, M., G. H. Denton, T. J. Hughes, and J. L. Fastook, 1981. History of the marine ice sheet in West Antarctica during the last glaciation: A working hypothesis. In G. H. Denton and T. J Hughes (eds.), The Last Great Ice Sheets, Wiley-Interscience, New York, pp. 319-436.

Thomas, R. H., 1973. The creep of ice shelves: Theory. Journal of Glaciology, 12, 45-53.

Thomas, R. H., 1977. Calving-bay dynamics and ice-sheet retreat up the St. Lawrence valley system. Geographic Physique Quaternaire, 31, 347-456.

Thomas, R. H., 1979. The dynamics of marine ice sheets. Journal of Glaciology, 24, 167-177.

Thomas, R. H., and C. R. Bentley, 1978a. The equilibrium state of the eastern half of the Ross Ice Shelf. Journal of Glaciology, 20, 509-518.

Thomas, R. H., and C. R. Bentley, 1978b. A model for Holocene retreat of the West Antarctic ice sheet. Quaternary Research, 10, 150-170.

Thomas, R. H., and D. R. MacAyeal, 1982. Derived characteristics of the Ross Ice Shelf, Antarctica, Journal of Glaciology, 28, 397-412.

Thomas, R. H., T. J. O. Sanderson, and K. E. Rose, 1979. Effect of climatic warming on the West Antarctic ice sheet. Nature, 227, 355-358.

Weertman, J., 1957. Deformation of floating ice shelves, Journal of Glaciology, 3, 38-42.